



Universidad de Concepción
Dirección de Postgrado
Facultad de Ciencias Químicas
Programa Doctorado en Ciencias Geológicas

**Taxonomía y paleoecología de los mamíferos Neógenos de la
Formación Cura-Mallín de la Laguna del Laja (37°S) y Lonquimay
(38°S), Chile. Implicaciones en la evolución tectónica de los
Andes centro-sur**

*(Taxonomy and paleoecology of the Neogene mammals from the
Cura-Mallín Formation from Laguna del Laja (37°S) and
Lonquimay (38°S), Chile. Implications for the tectonic evolution of
the central-south Andes)*

Tesis para optar al grado de Doctor en Ciencias Geológicas

ANDRÉS DANILO SOLÓRZANO BARRETO
CONCEPCIÓN-CHILE
2021

Profesor Guía: Alfonso Encinas Martín
Dpto. de Ciencias de la Tierra, Facultad de Ciencias Químicas,
Universidad de Concepción

AGRADECIMIENTOS

A la Universidad de Concepción (Udec) y la Agencia Nacional de Investigación y Desarrollo (ANID) por el apoyo académico, logístico y financiero (ANID–PCHA/Doctorado Nacional/2018–21180471 y FONDECYT regular 1151146) que permitió el desarrollo y culminación de esta tesis. Al Consejo de Monumentos Nacionales (CMN) por su autorización para la prospección paleontológica de la Formación Cura-Mallín.

A mi profesor guía, Alfonso Encinas, por su confianza, por haberme brindado la oportunidad de trabajar por primera vez con la interesante fauna extinta de vertebrados de Chile, así como por todos los conocimientos, consejos y anécdotas compartidas. A los profesores del Departamento de Ciencias de la Tierra (Udec), especialmente Sylvia Palma, Alfonso Encinas, Verónica Oliveros, Andrés Tassara, Joaquín Cortes y José Luis Palma, por su constante apoyo en diversas actividades, así como por todos los conocimientos impartidos a lo largo de estos últimos años. A Enrique Rodríguez, Cristian Hernández, Oscar Inostroza y Danielle Silvestro por “abrirme los ojos” ante nuevos ámbitos dentro de la paleontología, y por su apoyo y colaboración. A Gerardo Flores y Andrés Tassara por facilitarme el acceso al Museo Geológico Udec y la compra de equipos imprescindibles para la culminación de esta tesis. A María Esperanza Aravena por su enorme colaboración y buenas vibras.

A tod@s mis compañer@s de la Cabina cuatro por su amistad y por todos los excelentes momentos compartidos que hicieron más llevaderos estos últimos años. A Mónica Núñez, Maximiliano Reyes, Andrés Cáceres, Patricia Iturrieta, Ignacio Huenupi, Paz Butikofer, German Montoya, Francisca Riffo, Gabriel Arriagada, Hernán Arriagada, Aníbal Anavalón, Eduardo Rosselot, y especialmente a Gabriel Carrasco por su apoyo y camaradería durante las actividades de terreno. A David Rubilar (MNHN), Katherine Cisterna (MHNC), Laura Chornogubsky (MACN), Martín Ezcurra (MACN) y Marcelo Reguero (MLP) por facilitarme el acceso a las colecciones paleontológicas bajo su cuidado.

A mis coautores, Alfonso Encinas, Alejandro Kramarz, René Bobe, Gabriel Carrasco, Germán Montoya, y Mónica Núñez por sus valiosos comentarios y sugerencias que incrementaron la calidad de los artículos publicados. A los evaluadores Enrique Rodríguez (Udec) y Sergio Vizcaíno (Universidad de La Plata)

por sus sugerencias y críticas constructivas que permitieron mejorar la versión final de esta tesis. Al Centro de Microscopia Avanzada, CMA BIO-BIO de la Udec, y en especial a Paul San Martín por el apoyo en la toma de fotografías SEM.

A mis padres (María Elizabeth y Alfredo) y a mi "*little-brother*" (César), pilares fundamentales en mi vida, por siempre brindarme su apoyo, cariño y motivación y por soportar la distancia que nos ha separado físicamente durante estos cuatro años. A Mónica, el amor de mi vida, sin importar lo que nos depare el futuro te estaré eternamente agradecido por el amor, apoyo y motivación que me has brindado durante estos últimos 11 años. Finalmente, a todas aquellas personas que de una u otra forma colaboraron en la realización de esta tesis doctoral, de corazón, ¡muchas gracias!



RESUMEN

Durante las últimas décadas, nuestro conocimiento de la biodiversidad de mamíferos continentales extintos de Chile ha mostrado un progreso significativo. Pero a pesar de estos esfuerzos, ésta sigue siendo poco conocida, como lo ilustran los informes taxonómicos preliminares de varias de las localidades más diversas con decenas de nuevos taxones no descritos y/o taxones en nomenclatura abierta. Esto hace necesario renovar los esfuerzos de muestreo y refinar la taxonomía de faunas poco conocidas, como las de la Formación Cura-Mallín, una unidad volcánico-sedimentaria del Oligoceno Superior al Mioceno Superior depositada en ambientes continentales y que aflora en la Cordillera de los Andes en Chile y Argentina entre los 36° y 39°S. Aunque se han reportado, desde la década de 1980, mamíferos miocenos en dos localidades principales (Lonquimay y Laguna del Laja) esta Formación, la composición taxonómica de dichas faunas sigue siendo poco conocida, lo que limita nuestra comprensión de su relevancia bioestratigráfica, biogeográfica y paleoambiental.

En la presente tesis doctoral, proporcionamos estudios detallados de dichas faunas y avanzamos en los temas mencionados anteriormente. Se identificaron al menos 23 taxones diferentes, se describieron dos nuevas especies y se reportaron cuatro taxones por primera vez para Chile. La mayor diversidad de especies se encontró en estratos del Mioceno temprano tardío (Santacrucense SALMA) de la Laguna del Laja (17 spp.). Además, a partir de la combinación de información geocronológica y bioestratigráfica, se reconoció por primera vez la existencia de dos faunas cronológicamente distintivas en el área de Lonquimay, con edades Mioceno temprano (Colhuehuapiense a Santacrucense SALMAs) y Mioceno medio tardío (Mayoense SALMA). Las faunas de Lonquimay y Laguna del Laja muestran fuertes afinidades con las diversas localidades contemporáneas de la Patagonia Argentina. Las faunas Miocenas analizadas probablemente vivieron en hábitats relativamente templados y húmedos, en bosques y zonas abiertas y ambientes fluviales. Si bien la Formación Cura-Mallín probablemente fue depositada en condiciones sinorogénicas desde los 18 Ma, las condiciones ambientales relativamente homogéneas inferidas a través de múltiples evidencias sugieren que la región de Lonquimay, hoy ubicada en la Cordillera Principal, alcanzó elevaciones superiores a los 1000 metros solo después de los 12 Ma.

Finalmente, se ha argumentado que los cambios en el ambiente físico promovidos por el alzamiento de los Andes tuvieron un efecto importante en la evolución de la fauna sudamericana. Sin embargo, pocos trabajos han examinado

esta hipótesis utilizando el registro fósil como la principal línea de evidencia. Aquí, encontramos que la hipsodoncia, en los notoungulados, es significativamente mayor hacia la región occidental del sur de Sudamérica, coincidiendo espacialmente con el orógeno andino. Por lo tanto, proveemos evidencia inédita del significativo rol de los procesos superficiales asociados a la tectónica Andina en la evolución de uno de los grupos más diversos de mamíferos nativos en los ecosistemas cenozoicos del sur de América del Sur.



ABSTRACT

During the last decades, our understanding of Chile's extinct continental mammalian biodiversity has shown significant progress. Despite these efforts, this remains poorly known, as illustrated by the preliminary taxonomic reports from several of the most diverse localities with dozens of new undescribed taxa and/or taxa in open nomenclature. This situation makes it necessary to renew sampling efforts and refine the taxonomy of poorly known faunas, like those of the Cura-Mallín Formation, an Upper Oligocene to Upper Miocene volcanic-sedimentary unit deposited in continental settings that crop out in the Andean Cordillera of Chile and Argentina, between 36° and 39°S. Since the 1980s, Miocene mammals have been reported from this Formation. Specifically, from two prominent localities (Lonquimay and Laguna del Laja). However, the taxonomic composition of these faunas remains poorly known. Then, limiting our understanding of their biostratigraphic, biogeographic, and paleoenvironmental significance.

In the present doctoral dissertation, we provide detailed studies of such faunas and further advance on the above topics. Briefly, we recognized at least 23 different taxa, two new species were described, and four taxa were reported for the first time for Chile. The higher species diversity was found in the late early Miocene (Santacrucian SALMA) beds of the Laguna del Laja (17 spp.). Additionally, combining geochronological and biostratigraphic information, we recognized the existence of two chronologically distinctive faunas in the Lonquimay area of early Miocene (Colhuehuapian to Santacrucian SALMAs) and late Middle Miocene (Mayoan SALMA) ages. The fauna of Lonquimay and Laguna del Laja shows strong affinities with the diverse contemporaneous localities from the high latitudes of Argentina. The analyzed faunas probably lived on relatively temperate and humid forested to open habitats with premontane fluvial environments during the Miocene. Although the Cura-Mallín Formation was probably deposited under synorogenic conditions since ~18 Ma, the relatively homogeneous environmental conditions inferred through multiple evidence suggest that the study area, today located in the Main Cordillera, reached elevations greater than 1000 meters only after 12 Ma.

Finally, it has been argued that the changes in the physical environment promoted by the rise of the Andes had an important effect on the evolution of the South American fauna. However, few papers have examined this hypothesis using

the fossil record as the primary line of evidence. Here, we found that notoungulate hypsodony is significantly higher towards the western region of southern South America, spatially coinciding with the Andean orogen. Therefore, supporting that the surface processes related to the Andean orogen drive the long-term evolution of one of the most diverse groups of native mammals in southern South America's Cenozoic ecosystems.



ÍNDICE DE CONTENIDO

AGRADECIMIENTOS _____	ii
RESUMEN _____	iv
ABSTRACT _____	vi
ÍNDICE DE CONTENIDO _____	viii
ÍNDICE DE FIGURAS _____	xii
ÍNDICE DE TABLAS _____	xv
CAPÍTULO I. Introducción general _____	1
1.1 Introducción _____	1
1.2 Formulación del problema _____	9
1.3 Unidades sedimentarias del Mioceno en la Cordillera Andina entre los 36° y los 39° S y trabajos previos en la región _____	10
1.3.1 Contexto geológico y estratigráfico general _____	10
1.3.2 Contexto tectónico asociado a la sedimentación de la Formación Cura-Mallín _____	17
1.3.3 Trabajos estratigráficos/paleontológicos previos en la Cuenca de Cura-Mallín _____	17
1.4 Ubicación del área de estudio y vías de acceso _____	23
1.5 Topografía, clima y vegetación actual en el área de estudio _____	25
1.6 Hipótesis _____	26
1.7 Objetivos _____	26
1.7.1 Objetivo general _____	26
1.7.2 Objetivos específicos _____	27
1.8 Organización de los resultados _____	27
1.9 Metodología _____	30
1.9.1 Autorización para la colección de vertebrados fósiles en Chile _____	30
1.9.2. Revisión bibliográfica _____	30
1.9.3 Trabajo de campo _____	30
1.9.4 Trabajo de Laboratorio _____	32
CAPÍTULO II. The Early to late Middle Miocene mammalian assemblages from the Cura-Mallín Formation, at Lonquimay, southern Central Andes, Chile (~38°S): Biogeographical and paleoenvironmental implications _____	33
Highlights _____	34

Abstract	34
2.1 Introduction	35
2.2 Geological, paleontological and geographical background	38
2.3 Material and methods	45
2.4 Systematic paleontology	46
2.5 Discussion	63
2.5.1 A reassess of the biochronological affinities of the Lonquimay Neogene mammals	64
2.5.2 Paleobiogeographical considerations	67
2.5.3 Paleoenvironmental significance	69
2.6 Conclusions	74
CAPÍTULO III. Late early Miocene caviomorph rodents from Laguna del Laja (~37° S), Cura-Mallín Formation, south-central Chile	77
Highlights	78
Abstract	78
3.1 Introduction	79
3.2 Geological and geographical settings	81
3.3 Brief paleontological background	83
3.4 Material and methods	84
3.5 Systematic paleontology	84
3.6 Discussion	96
3.7 Conclusions	100
CAPÍTULO IV. Late early Miocene mammals from the Laguna del Laja, Cura-Mallín Formation, south central Chile (~37°S) and their biogeographical, and paleoenvironmental significance	103
Highlights	104
Abstract	104
4.1. Introduction	105
4.2. Geological and geographical setting	106
4.3. Brief paleontological background	109
4.4. Materials and Methods	110
4.4.1. Abbreviations	111
4.4.2. Institutional abbreviations	111
4.6. Discussion	127

4.7. Conclusions _____	134
CAPÍTULO V. Evolutionary trends of body size and hypsodonty in Notoungulates and their probable drivers _____	137
Highlights _____	138
Abstract _____	138
5.1 Introduction _____	139
5.2 Methods _____	143
5.2.1 Fossil occurrence database _____	143
5.2.2 Body mass estimations in notoungulates _____	143
5.2.3 Hypsodonty in notoungulates _____	145
5.2.4 Dealing with potential bias in the lifespan of individual species _____	146
5.2.5 Correlations between body size and hypsodonty with origination and extinction rates _____	147
5.2.6 Body mass and hypsodonty evolution through time _____	148
5.2.7 Potential mechanisms driving the historical dynamics of body size and hypsodonty in notoungulates in the south of South America _____	149
5.2.8 Spatial patterns of body size and hypsodonty in notoungulates _____	150
5.3 Results _____	151
5.3.1 Body mass in notoungulates _____	151
5.3.2 Hypsodonty in notoungulates _____	155
5.3.3 Lifespan of individual species _____	155
5.3.4 Correlation between traits and speciation/extinction rates _____	155
5.3.5 Describing the body size and hypsodonty macroevolutionary patterns in notoungulates _____	156
5.3.6 Potential mechanisms driving the historical dynamics of body size and hypsodonty in SSA _____	161
5.3.7 Body size and hypsodonty in through space and time _____	162
5.4 Discussion _____	162
5.4.1 Body mass estimations in notoungulates _____	162
5.4.2 The evolution of the body size in notoungulates _____	163
5.4.3 The evolution of the hypsodonty in notoungulates _____	166
5.4.4 Drivers of the body size and hypsodonty evolution in SSA notoungulates _____	167
5.4.5 Spatial patterns in notoungulate body size and hypsodonty _____	170

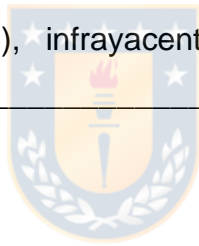
5.5 Conclusions_____	171
CAPÍTULO VI. Síntesis y Discusión_____	177
6.1 Paleodiversidad de la Formación Cura-Mallín y su contexto temporal ___	177
6.1.1 Lonquimay_____	177
6.1.2 Laguna del Laja_____	181
6.2 Afinidades biogeográficas de los mamíferos Neógenos de la Formación Cura-Mallín_____	186
6.3 Paleoambientes durante la sedimentación de la Formación Cura-Mallín	189
6.4 Implicaciones tectónicas _____	193
CAPÍTULO VII. Conclusiones _____	204
REFERENCIAS_____	207
ANEXO 1. Publicaciones resultantes de esta tesis doctoral_____	240
ANEXO 2. Materiales suplementarios asociados a cada una de las publicaciones resultantes de esta tesis doctoral_____	286
Electronic supplementary materials for: The Early to late Middle Miocene mammalian assemblages from the Cura-Mallín Formation, at Lonquimay, southern Central Andes, Chile (~38°S): biogeographical and paleoenvironmental implications _____	287
Electronic supplementary materials for: Late early Miocene caviomorph rodents from Laguna del Laja (~37° S), Cura-Mallín Formation, south-central Chile.	290
Electronic supplementary materials for: Late early Miocene mammals from the Laguna del Laja, Cura-Mallín Formation, south-central Chile (~37°S) and their biogeographical and paleoenvironmental significance _____	291
Electronic supplementary materials for: Evolutionary trends of body size and hypsodonty in notoungulates (Mammalia: Notoungulata) and its probable drivers. _____	296

ÍNDICE DE FIGURAS

Figura 1.1. Relaciones entre las fases orogénicas de creación de montañas y los procesos biológicos. _____	2
Figura 1.2. Mapa de ubicación de las localidades y regiones donde se han encontrado restos de mamíferos en rocas cenozoicas pre-pleistocénicas (terciarias) en Chile. _____	5
Figura 1.3. Ubicación geográfica regional de los afloramientos de las unidades incluidas en Cuenca de Cura-Mallín en la Cordillera Principal de Chile y Argentina entre los 36° y 39°S, así como de las dos localidades principales dentro de la Cuenca. _____	7
Figura 1.4. Mapa geológico regional de la Cordillera Principal comprendida entre los 36° y 39°S en Chile y Argentina. _____	12
Figura 1.5. Esquemas estratigráficos propuestos por diversos autores para agrupar las diferentes unidades incluidas en la Cuenca de Cura-Mallín y que afloran en las regiones de la Laguna del Laja y Lonquimay, Cordillera Principal, Chile. _____	15
Figura 1.6. Mapa de ubicación geográfica de las principales localidades prospectadas durante el desarrollo de la presente tesis doctoral. _____	24
Figura 1.7. Fotografías de algunos de los afloramientos de la Formación Cura-Mallín prospectados durante el desarrollo de la presente tesis doctoral. _____	31
Figure 2.1. Geographical settings of the fossil-bearing localities (star) mentioned in the text. _____	41
Figure 2.2. Schematic (not in scale) chronostratigraphic framework of the fossil mammal-bearing localities among the Cura-Mallín Formation cropping out in the surroundings of Lonquimay, based on radiometric ages and biochronologic correlation. _____	43
Figure 2.3. <i>Parastrapotherium</i> sp. (SGO.PV.4003) from the Río Quepuca, Río Guapítrio Member, Cura-Mallín Formation (Early Miocene), Chile. _____	47
Figure 2.4. <i>Theosodon</i> sp. (SGOP.4000) from the Cerro Rucañanco locality, Río Pedregoso Member, Cura-Mallín Formation (late Middle Miocene; Serravallian), Chile. _____	50
Figure 2.5. Notoungulates from Cura-Mallín Formation (Río Pedregoso Member) recovered in the surroundings of Lonquimay, Chile. _____	56

Figure 2.6. Cingulata remains from the Cura-Mallín Formation (Río Pedregoso Member) in the surroundings of Lonquimay, Chile. _____	61
Figure 2.7. Scanning electron microscopy photograph of the lower molar of the putative Platyrrhini monkey from the Cerro Rucañanco locality. _____	63
Figure 3.1. Geographic and stratigraphic provenance of the caviomorph remains described in the present study from the Laguna del Laja region. _____	82
Figure 3.2. <i>Maruchito</i> sp. nov? (SGO.PV.1400) from late early Miocene beds of the Cura-Mallín Formation, Laguna del Laja, Chile; left maxilla with dP4-M3 in occlusal (A) and lingual (B) views. _____	85
Figure 3.3. Cavioid rodents from late early Miocene beds of the Cura-Mallín Formation, Laguna del Laja, Chile. _____	90
Figure 4.1. Geographic and stratigraphic provenance of the mammals remains described in the present study from the late early Miocene of the Cura-Mallín Formation at the south of the Laguna del Laja (Biobío Province, south-central Chile). _____	108
Figure 4.2. Sparassodonts, palaeothenids, and caviomorphs rodents from late early Miocene (Santacrucian) beds of the Cura-Mallín Formation, Laguna del Laja, Chile. _____	118
Figure 4.3. Litoptern and notoungulates from late early Miocene (Santacrucian) beds of the Cura-Mallín Formation, Laguna del Laja, Chile. _____	118
Figure 4.4. Boxplot comparing the M1/M3 length proportion in the <i>Pachyrukhos</i> from the Laguna del Laja (<i>Pachyrukhos</i> sp. nov.?), and others Neogene Pachyrukhinae taxa. _____	123
Figure 4.5. Xenarthrans from early Miocene beds of the Cura-Mallín Formation, Laguna del Laja, Chile. _____	125
Figure 4.6. Geographic location of Santacrucian as well as other early and middle Miocene fossiliferous localities in middle and high latitudes of South America _____	132
Figure 5.1. Body mass and hypsodonty in Notoungulates. _____	153
Figure 5.2. Distribution of frequency of the Log10 of the body mass of toxodonts and tytotherians. _____	153
Figure 5.3. Temporal patterns of body size evolution in notoungulates and subordinate clades. _____	158

Figure 5.4. Temporal patterns of hypsodonty evolution in notoungulates and subordinate clades. _____	160
Figure 5.5. Paleolatitudinal distribution of notoungulates through time grouped according to body size classifications described in the main text. _____	170
Figura 6.1. Proporción del número de taxones de mamíferos (por orden) del Mioceno temprano tardío reconocidos durante el desarrollo de esta tesis doctoral en la Formación Cura-Mallín en la Laguna del Laja, Chile. _____	183
Figura 6.2. A, Restos de madera fosilizada encontrados en el tope del Cerro Campamento (Formación Cura-Mallín; Mioceno temprano tardío), al sur de la Laguna del Laja. B. restos de hojas carbonizadas encontradas en niveles Tcm ₄ , Estero Trapa-Trapa Este, Sur de la Laguna del Laja. _____	185
Figura 6.3. Mapa de ubicación de localidades Santacrucenses, así como otras localidades importantes del Mioceno temprano y medio, en el sur de Sudamérica _____	188
Figura 6.4. Estratos de crecimiento observados en el Cerro Campamento (Tcm ₃ ; Mioceno temprano tardío),* infrayacentes a los niveles portadores de mamíferos fósiles. _____	194



ÍNDICE DE TABLAS

Table 2.1. Summary of the age and mammals from each of the recognized mammal-bearing localities from the Cura-Mallín Formation at the Lonquimay area (Chile).	76
Table 3.1. Measurements (in mm) of the materials collected in the late early Miocene of the Cura-Mallín Formation at Laguna del Laja, Chile.	102
Table 4.1. Ecological attributes of the late early Miocene mammals (Tcm ₃) from the Laguna del Laja.	136
Table 5.1. Summary of BM and hypsodonty estimated for each of the clades analyzed (families and suborder as a whole).	174
Table 5.2. Summary of the best mode of trait (BM and hypsodonty) evolution in notoungulates and lower taxonomic hierarchies.	175
Table 5.3. Summary of best-fitting GLS multiple regression models for predicting mean body mass (BM in natural log scale) and hypsodonty in notoungulates, tyotherians, and toxodonts considering an autocorrelation structure for age parameter.	175
Table 5.4. Results of the OLS analyses dealing with the spatial patterns of the body mass (BM in kg) and hypsodonty in the SSA notoungulates.	176
Table 5.5. Comparisons among the body mass reported in the literature from a selected sample of notoungulates and those estimated by us in the present contribution.	176
Tabla 6.1 Comparación entre la diversidad (y edad) de los mamíferos fósiles reconocidos en la Formación Cura-Mallín durante el desarrollo de esta tesis doctoral, y aquella mencionada en trabajos previos.	179

CAPÍTULO I. Introducción general

1.1 Introducción

La superficie de la Tierra, modelada por la compleja interacción entre la tectónica y el clima, es una zona extremadamente dinámica donde operan numerosos ciclos biogeoquímicos y donde la vida ha evolucionado (Schrag y Hoffman, 2001; Lowe y Tice, 2007; Allen, 2008; Lyons et al., 2014). No obstante, la relación entre los procesos geodinámicos superficiales y la evolución de la vida que habita sobre el planeta es compleja (Morrone, 2015). Por ejemplo, hoy en día las zonas geológicamente activas (i.e., márgenes convergentes) alrededor del mundo mantienen una proporción sustancial de la biodiversidad del planeta, comprendiendo casi el doble de especies de mamíferos terrestres por unidad de área en comparación con regiones adyacentes de menor topografía (i.e., en el retroarco) (Badgley, 2010; Antonelli et al., 2018). Para entender por qué surge éste patrón es importante comprender cómo se origina y mantiene la biodiversidad, y cómo los procesos de construcción del relieve influyen sobre ésta (Hoorn et al., 2010; Eronen et al., 2015; Silvestro y Schnitzler, 2018; Antonelli et al., 2018).

La compleja interacción entre la tectónica, el clima y la erosionabilidad de las rocas controlan el desarrollo del relieve topográfico, y la formación de montañas se produce cuando la erosión es superada por el alzamiento impulsado por la tectónica (Molnar y England, 1990; Whipple, 2009; Molnar, 2018). Los cambios en las condiciones tectónicas de una región tienen el potencial de transformar los paisajes de baja elevación, bajo relieve, clima homogéneo y vegetación espacialmente continua en paisajes de alto relieve con zonaciones climáticas y cobertura vegetal fragmentada, generando además nuevos hábitats (Badgley, 2010; Antonelli et al., 2018). El incremento en los gradientes ambientales (e.g., climáticos, topográficos) asociados puede dar lugar a: *i*) la extinción local de algunos organismos, *ii*) generar barreras topográficas que promueven la generación de nuevas especies (especiación), *iii*) permitir que algunos linajes se adapten y persistan a pesar de estos cambios topográficos, *iv*) favorecer la colonización de nuevas especies presentes en zonas “bajas” adyacentes, *v*) ocasionar una selección de especies, o *vi*) simplemente gatillar cambios evolutivos en la fauna y flora circundante (Figura

1.1) (Badgley, 2010; Antonelli et al., 2018; Huang et al., 2019). El efecto combinado de estos procesos (e.g., especiación, extinción, dispersión) pueden resultar, a lo largo del tiempo, en faunas progresivamente más diversas (o incluso endémicas), y/o favorecer el sucesivo recambio faunístico asociado a características ecológicas intrínsecas (Ortiz-Jaureguizar y Cladera, 2006; Huang et al., 2019). Por ejemplo, especies con distribuciones geográficas restringidas, a veces endémicas, son comunes en regiones montañosas (Badgley, 2010; Antonelli et al., 2018).

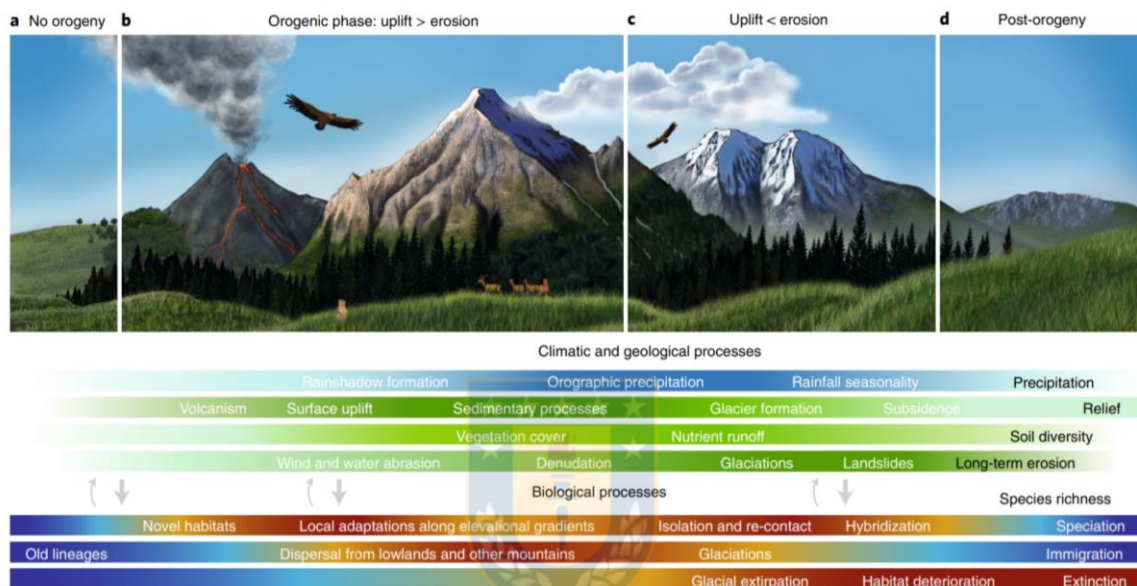


Figura 1.1. Relaciones entre las fases orogénicas de creación de montañas y los procesos biológicos. a – d, variables climáticas (barra azul) y geológicas (barras verdes) influyen en la riqueza de especies a través de la especiación, inmigración y extinción (barras inferiores) durante diferentes fases orogénicas. Los colores más oscuros/cálidos y más claros/fríos en las barras indican cotas altas y bajas, respectivamente. Como indican las flechas, los procesos climáticos y geológicos ejercen los efectos más importantes sobre la riqueza de especies, pero existe cierta retroalimentación (como plantas que colonizan rocas desnudas y aumentan la erosión, y animales que afectan los suelos a través de excavaciones). Tomado de Antonelli et al. (2018).

La construcción de montañas también puede afectar indirectamente la evolución de los organismos, al por ejemplo modificar los patrones de drenaje; de esta forma los ríos pueden actuar como puentes o barreras geográficas, modificando las tasas de dispersión, especiación y extinción (Hoorn et al., 2010, 2013). Además, puede modificar la circulación atmosférica o simplemente reorganizar los patrones de precipitación a escala regional (Hoorn et al., 2013; Eronen et al., 2015). Así, es posible formar una lluvia orográfica en el lado de barlovento del orógeno y crear una sombra de lluvia su lado de sotavento (Blisniuk et al., 2005; Siler et al., 2012; Antonelli et al., 2018).

Lo antes expuesto sugiere que la construcción de relieve, impulsado por la tectónica, tiene el potencial de generar cambios climáticos y paisajísticos, gradientes ecológicos, heterogeneidad ambiental y nuevos hábitats, los cuales finalmente influirán sobre la evolución de la biota local y regional. Esto hace necesario utilizar aproximaciones interdisciplinarias, combinando información tectónica, sedimentológica, ecológica, biogeográfica, neontológica y paleontológica para comprender el rol de los procesos de construcción de relieve sobre la evolución de la vida sobre el planeta (Antonelli et al., 2018; Rahbek et al., 2019; Huang et al., 2019). Considerando las estrechas relaciones entre la geosfera y la biosfera, la integración de los procesos geodinámicos superficiales junto con datos del registro fósil podría permitir, por ejemplo, evaluar diferentes hipótesis relacionadas con el momento de levantamiento de los cinturones montañosos (Lieberman, 2005; Picard et al., 2008; Mulch, 2016; Antonelli et al., 2018; Rahbek et al., 2019). De igual forma, el registro sedimentario debe contener evidencia de los procesos biológicos evolutivos de largo plazo que han dado forma a la biosfera actual de la Tierra y, por lo tanto, pueden permitir poner a prueba cómo los cambios ambientales (e.g., alzamiento de superficie) han afectado la evolución y distribución de los organismos (Lieberman, 2005; Eronen et al., 2015; Favre et al., 2015; Lagomarsino et al., 2016).

Los Andes, un cinturón montañoso que se extiende por más de 8.000 km desde el Mar Caribe (~11°N) en el norte hasta Tierra del Fuego (~54°S) en el sur, con alturas promedio de ~4.000 m.s.n.m. y elevaciones máximas de hasta ~7.000 m.s.n.m, puede ser considerado como un accidente geográfico de primer orden en Sudamérica (Ramos, 2009). A lo largo de su larga historia geológica la parte oeste de Sudamérica ha sido testigo de eventos de acreción, colisiones de terrenos y la subducción de diferentes tipos de corteza oceánica, que han generado la compleja segmentación del orógeno andino, mostrando además como los procesos tectónicos, magmáticos y sedimentarios asociados a su génesis fueron heterogéneos a través del tiempo y el espacio (Tassara and Yáñez, 2003; Ramos, 2009, 2010; Martinod et al., 2010; Armijo et al., 2015; Horton, 2018b, 2018a). Trabajos previos han propuesto que la compleja formación de los Andes ejerció una fuerte influencia sobre la singular biota sudamericana, la cual evolucionó (*in situ*) en relativo aislamiento geográfico de otros continentes durante gran parte del Cenozoico (Simpson, 1980; Ortiz-Jaureguizar y Cladera, 2006; Hoorn et al., 2010;

Strömberg et al., 2013; Madden, 2014; Kohn et al., 2015; Antoine et al., 2016; Lagomarsino et al., 2016). En este sentido, la región de los Andes es una buena zona de estudio para investigar el impacto de los procesos tectónicos sobre la evolución de la vida sobre el planeta a través del espacio y tiempo (Hoorn et al., 2010; Madden, 2014; Lagomarsino et al., 2016).

Los mamíferos (Clase Mammalia), un grupo monofilético de vertebrados cuyo origen se remonta al Jurásico, pueden ser un buen modelo de estudio ya que exhiben una gran diversidad de morfologías, tamaños corporales, hábitos ecológicos, y comportamientos (Luo, 2007; Benton, 2014; Patton et al., 2015). Se han reconocido abundantes restos fósiles de este grupo en los ecosistemas cenozoicos de Sudamérica (Simpson, 1980; Prevosti y Forasiepi, 2018a; Croft et al., 2020). Sin embargo, para llevar a cabo la compleja tarea de discernir el impacto de la tectónica andina sobre la evolución de los mamíferos cenozoicos sudamericanos es necesario, en primer lugar, reducir el déficit linneano (incertidumbre en el número de especies y división taxonómica de un grupo) y wallaceano (incertidumbre en el conocimiento sobre la distribución geográfica de un grupo) presente (Núñez-Flores et al., 2019), especialmente en zonas poca estudiadas, o poco comprendidas desde el punto de vista de su diversidad taxonómica, tal como ocurre en Chile (Canto et al., 2010).

Se ha sugerido que el registro fósil sudamericano se conoce menos que el de otros continentes (Smith et al., 2004; Goin et al., 2016), debido, entre otras cosas, a que históricamente los trabajos realizados, especialmente en mamíferos, se han concentrado en las zonas más meridionales del subcontinente, particularmente en Argentina (e.g., Rincón et al., 2016; Antoine et al., 2016; Antoine y Pujos, 2017). En contraste, la diversidad de mamíferos extintos de Chile permaneció casi desconocida hasta el año 1980, cuando se inició un mayor interés por su registro fósil (Canto et al., 2010), estudiándose inicialmente faunas del Cuaternario y, más recientemente, faunas del Cretácico, Eoceno, Oligoceno y Mioceno (Flynn et al., 1995, 2002a, 2005; Croft et al., 2004, 2008; Hitz et al., 2006; McKenna et al., 2006; Bertrand et al., 2012; Shockey et al., 2012; Bostelmann et al., 2013; Woodburne et al., 2014; Bradham et al., 2015; Wyss et al., 2018; McGrath et al., 2018, 2020; Engelman et al., 2018, 2020).

En Chile, las principales localidades con mamíferos fósiles Paleógenos y Neógenos se ubican, de norte a sur, en la Precordillera de Arica-Iquique (localidad

de Caragua), Cordillera Occidental de Arica-Iquique (localidad de Chucal), Franja costera de la región de Caldera, Cordillera Principal de Chile central (entre las hoyas superiores de los ríos Maipo y Bio-Bío), Sector del Río Cisnes, Región de Aysén, Meseta Guadal- Cosmelli, Región de Aysén, y en diversos sectores de la Región de Magallanes (Figura 1.2) (Charrier et al., 2015).

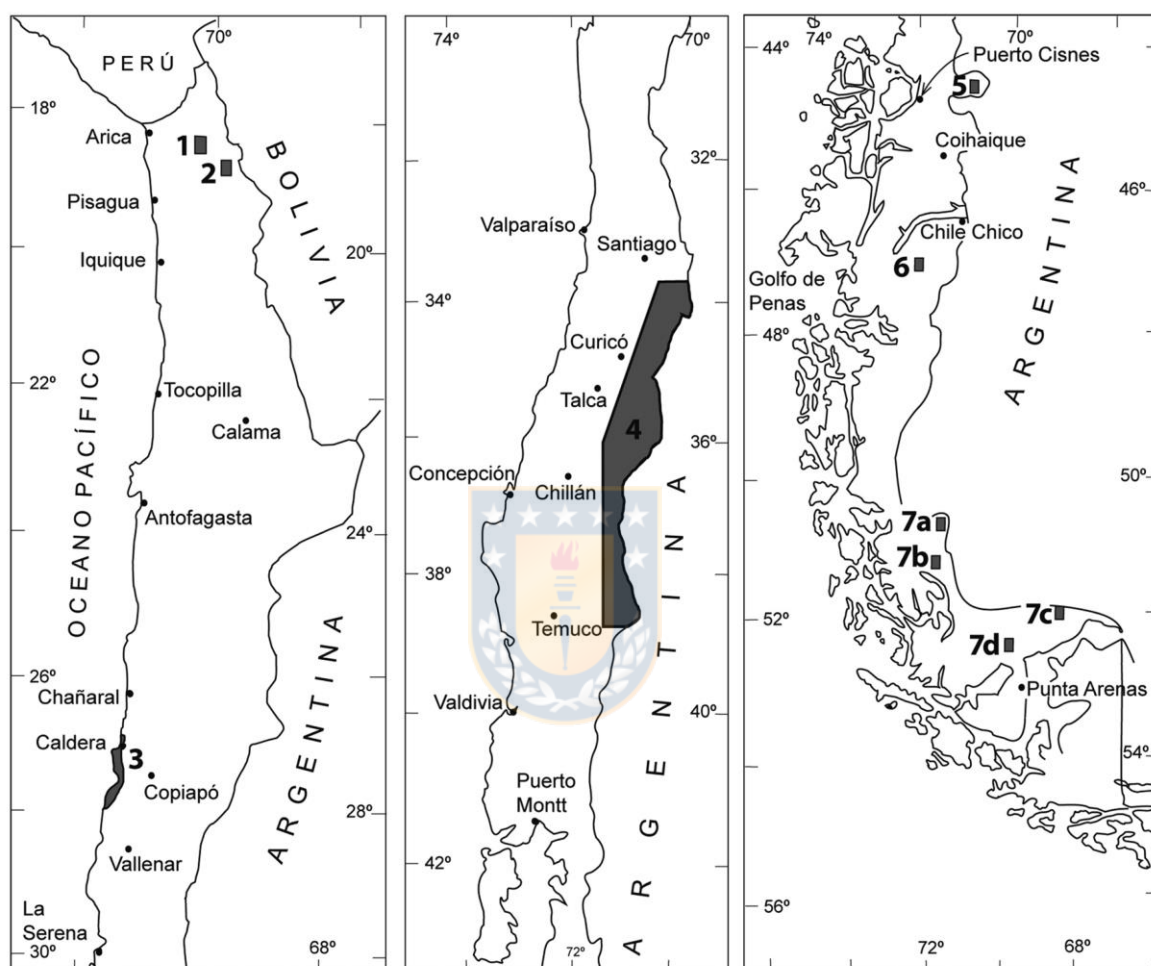


Figura 1.2. Mapa de ubicación de las localidades y regiones donde se han encontrado restos de mamíferos en rocas cenozoicas pre-pleistocénicas (terciarias) en Chile: 1. Caragua en la Precordillera oriental de Arica, 2. Chucal, en la parte oriental de la Cordillera Occidental de Arica, 3. Franja costera de la región de Caldera, Región de Atacama, 4. Cordillera Principal de Chile central, 5. Río Cisnes, en la región fronteriza de Aysén, 6. Pampa Castillo en la Meseta Guadal-Cosmelli, al sur del Lago General Carrera, Aysén, 7. Región de Magallanes: a. Alto río Baguales, b. Lago Toro, c. Cueva de Fell, y d. Sector de Laguna Blanca. Tomado de Charrier et al. (2015).

Los mamíferos más antiguos de Chile son *Magallanodon baikashkenke* (Gondwanatheria), y *Orretherium tzen* (Meridiolestida), descritos recientemente a partir de restos dentales recuperados en estratos de edad Campaniense – Maastrichtiense de la Formación Dorotea, Región de Magallanes, sur de Chile (Goin et al., 2020; Martinelli et al., 2021). Sin embargo, la mayor diversidad de

mamíferos fósiles en Chile se reconoce en formaciones geológicas cenozoicas que afloran en su gran mayoría sobre la cordillera de los Andes (Canto et al., 2010; Charrier et al., 2015). Dentro de ellas resalta la fauna de la Formación Abanico con afloramientos ubicados en la cordillera principal entre los 33,5° y 35,5°S. En esta Formación se han mencionado más de 12 localidades fosilíferas, y se han colectado más de 1.500 especímenes de roedores, marsupiales, armadillos, perezosos, notoungulados, peces teleósteos, aves, tortugas y primates con edades comprendidas entre el Eoceno al Mioceno temprano (Flynn et al., 1995, 2003; Croft et al., 2008; Charrier et al., 2015; Wyss et al., 2018; Engelman et al., 2020). La asociación de mamíferos mejor conocida de la Formación Abanico es la denominada Fauna de Tinguiririca. Esta fauna consiste en más de 25 especies, muchas de ellas nuevas para la ciencia (Flynn et al., 1995, 2003; Hitz et al., 2006; McKenna et al., 2006), que exhiben una composición taxonómica singular, y vivieron durante un intervalo temporal (33,6–31,3 Ma) desconocido previamente en otras regiones de Sudamérica. Es por ello que ésta fauna permitió reconocer una nueva Edad Mamífero Sudamericana (SALMA por sus siglas en inglés), denominada Tinguiririquense (Flynn et al., 2003).

Pese a los esfuerzos realizados, la paleodiversidad de mamíferos en Chile está aún infraestimada (=alto déficit linneano) a juzgar por los listados taxonómicos preliminares presentes en algunas de las localidades más diversas, las cuales mencionan docenas de taxones potencialmente nuevos para la ciencia y/o en nomenclatura abierta (Flynn et al., 2002b, 2003, 2008; Wertheim, 2007; Canto et al., 2010; Charrier et al., 2015; Luna, 2015). Entonces, es necesario realizar nuevos esfuerzos de muestreo en zonas poco exploradas, y refinar la taxonomía y sistemática, especialmente en faunas poco conocidas (Canto et al., 2010). Tal es el caso de la fauna descrita en dos de las unidades sedimentarias incluidas dentro de la Cuenca de Cura-Mallín (Flynn et al., 2008), objeto de estudio de esta investigación y que representan una de las pocas mencionadas en la Cordillera Principal Andina centro-sur (Flynn et al., 2008).

La Cuenca de Cura-Mallín aflora entre los 36° y 39°S y presenta una de las secuencias mejor expuestas del Oligoceno(?)–Mioceno en los Andes sur-centrales de Argentina y Chile (Figura 1.3) (Jordan et al., 2001; Radic et al., 2002; Burns et al., 2006). La Cuenca contiene hasta 4 km de estratos sedimentarios y volcanoclásticos depositados en ambientes continentales fluviales, aluviales y

lacustres, bajo la influencia de volcanismo explosivo, con tres unidades geológicas tradicionalmente bien diferenciadas: formaciones Cura-Mallín, Trapa-Trapa y Mitrauquén (Suárez y Emparan, 1995, 1997; Burns et al., 2006; Radic, 2010; Rosselot et al., 2019a). Estas unidades geológicas se sedimentaron en varios depocentros cuyas transiciones laterales son poco entendidas debido a que la configuración paleogeográfica original fue modificada durante la deformación y elevación del Cenozoico tardío de los Andes y, además, algunas de las zonas intermedias están cubiertas por rocas volcánicas más jóvenes (Radic, 2010; Rosselot et al., 2019a). Dos de las localidades con mejores afloramientos de las unidades litoestratigráficas que conforman la Cuenca se ubican en los alrededores de Lonquimay (~38°S) y la Laguna del Laja (~37°S) (Figura 1.3).

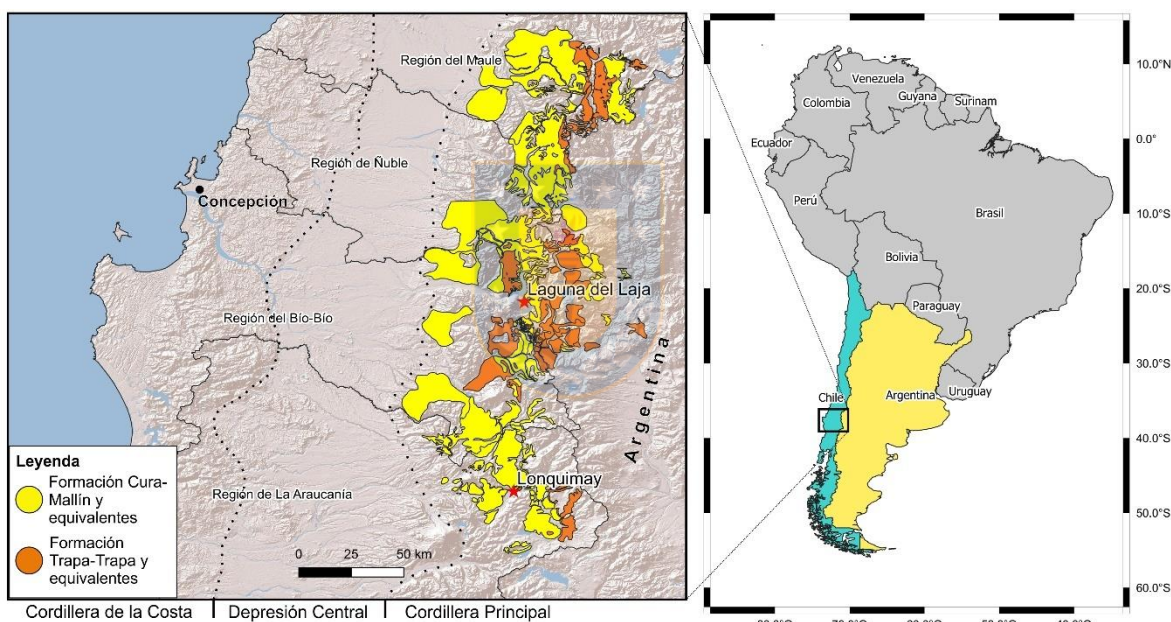


Figura 1.3. Ubicación geográfica regional de los afloramientos de las unidades incluidas en Cuenca de Cura-Mallín en la Cordillera Principal de Chile y Argentina entre los 36° y 39°S (Rosselot et al. 2019b), así como de las dos localidades principales dentro de la Cuenca (denotadas con estrellas rojas). Note, además, la disposición espacial de las distintas unidades fisiográficas longitudinales presentes en la región (líneas punteadas).

La Formación Cura-Mallín, la unidad basal dentro de la cuenca homónima, se caracteriza por presentar un miembro volcánico y un miembro sedimentario, que generalmente sobreyace a éste, con facies características de ambientes aluviales, fluviales, lacustres y deltáicos (Suárez y Emparan, 1995, 1997; Jordan et al., 2001; Radic et al., 2002; Pedroza et al., 2017). Dataciones K-Ar y U-Pb (en circones detríticos) indican una edades comprendidas entre 19,9–10,7 Ma y 19,8–14,5 Ma (Mioceno Inferior a Mioceno Superior) para los estratos de la Formación Cura-Mallín

encontrados en Lonquimay y la Laguna del Laja, respectivamente (Suárez y Emparan, 1995; Herriott, 2006; Flynn et al., 2008; Pedroza et al., 2017; Rosselot et al., 2019b).

La Formación Cura-Mallín es la unidad fosilífera más importante dentro de la cuenca homónima. En Lonquimay, se ha reportado la presencia de notoungulados, litopternos, xenarthros, astrapotherios y roedores (Marshall et al., 1990; Suárez et al., 1990; Croft et al., 2003; Buldrini y Bostelmann, 2011; Bostelmann et al., 2014; Buldrini et al., 2015), además de peces, anuros, aves continentales e invertebrados de agua dulce (Rubilar, 1994; Alvarenga, 1995; Azpelicueta y Rubilar, 1997; Arratia, 2015; Guevara et al., 2018). Se ha sugerido que estos diferentes taxones provienen principalmente de estratos depositados durante el Mioceno temprano (Croft et al., 2003; Buldrini et al., 2015). Aunque trabajos más recientes indican que algunos de ellos podrían provenir del Mioceno medio (Pedroza et al., 2017; Rosselot et al., 2018).

En la región de la Laguna del Laja se ha reportado una sucesión sedimentaria con asociaciones de mamíferos dominadas, en términos de riqueza y abundancia, por roedores caviomorfos y notoungulados, aunque también se han reconocido astrapoterios, marsupiales y xenartros (Wertheim, 2007; Flynn et al., 2008; Shockey et al., 2012; Luna, 2015). Estas faunas, encontradas principalmente en la Formación Cura-Mallín y en menor medida en la Formación Trapa-Trapa, representan un registro fosilífero relativamente continuo comprendido entre los 20 y 8 Ma (Flynn et al., 2008). Además, se ha mencionado la existencia de un elevado grado de endemismo local basados en la existencia de al menos 29 taxones potencialmente nuevos para la ciencia, considerando solamente roedores caviomorfos y notoungulados (Wertheim, 2007; Luna, 2015). Sin embargo, ninguno de éstos ha sido formalmente publicado. Este elevado endemismo local es particularmente interesante considerando la cercanía geográfica (~150 km) de localidades paleontológicas contemporáneas (e.g., Cañadon del Tordillo, Argentina) que exhiben una importante diversidad (Flynn et al., 2008; Luna, 2015).

Datos previos sugieren una marcada diferencia en cuanto a los grupos taxonómicos representados en cada localidad, así como a su tamaño corporal, con taxones relativamente pequeños a medianos (hasta ~50 kg) en Laguna del Laja (Wertheim, 2007; Luna, 2015), y mucho más grandes (hasta 800 kg) en Lonquimay (Croft et al., 2003). Estas diferencias taxonómicas y ecológicas podrían

corresponder a discrepancias en la intensidad del muestreo, al efecto de diferentes procesos tafonómicos, o a variaciones ambientales marcadas entre ambos sectores (separadas por solo ~120 km) durante el Mioceno. Sin embargo, estas posibles diferencias aún no se comprenden bien.

1.2 Formulación del problema

La mayoría de los especímenes colectados en la Cuenca de Cura-Mallín en Lonquimay y en la Laguna del Laja no han sido previamente identificados ni descritos en detalle (salvo algunas excepciones, Croft et al., 2003; Shockey et al., 2012). Esta situación limita nuestro entendimiento sobre la paleodiversidad de mamíferos Neógenos de Chile, las relaciones biogeográficas de las faunas dentro de la formación y su relación con otras faunas coetáneas de Sudamérica, las posibles causas del elevado nivel de endemismo de los mamíferos de la Laguna del Laja, y las condiciones paleoambientales en donde habitaron estas faunas.

Por otra parte, el inicio de la contracción regional durante el Mioceno ocasionó el alzamiento de los Andes Patagónicos y el subsecuente aumento progresivo de la aridez en las cuencas de retroarco y antepaís conocido como efecto de sombra de lluvia (i.e., fuerte disminución de la precipitación en el sotavento de las cordilleras) (Blisniuk et al., 2005), lo cual tuvo efectos sustanciales en la flora y fauna del sur de Sudamérica (Gregory-Wodzicki, 2000; Ortiz-Jaureguizar y Cladera, 2006). Por ejemplo, el registro fósil muestra que la fauna y flora de altas y medias latitudes de Sudamérica sufrió adaptaciones, como el incremento en la altura de la corona de los dientes de los mamíferos herbívoros, a ambientes más abiertos y secos durante el Mioceno medio (~16-14 Ma), relacionadas al alzamiento Andino y subsecuente efecto de sombra de lluvia (Blisniuk et al., 2005; Ortiz-Jaureguizar y Cladera, 2006; Dunn et al., 2015). En este sentido, el registro fósil tiene una importancia fundamental en la evaluación de modelos tectónicos, proporcionando edad y restricciones geográficas (Hoorn et al., 2013; Huang et al., 2019; Benton y Harper, 2020).

Entonces, el estudio de las sucesivas asociaciones de mamíferos de la Laguna del Laja, que representan un registro fosilífero relativamente continuo comprendido entre los 20 y 8 Ma (Flynn et al., 2008), podría brindar novedosas líneas de evidencia para comprobar alguna de las hipótesis existentes respecto al

contexto tectónico asociado a la sedimentación de las unidades incluidas en la Cuenca de Cura-Mallín (ver detalles sección 1.3.2). Además, el estudio detallado estas faunas podría permitir reconocer cambios sucesivos en su diversidad taxonómica, e inferir posibles cambios ambientales (quizás gatillados por la tectónica) durante el Neógeno en la región.

Por otra parte, aunque, en general, se ha considerado que la evolución tectónica de los Andes ha ejercido una importante influencia en la evolución de la biota sudamericana (Ortiz-Jaureguizar y Cladera, 2006; Hoorn et al., 2010; Madden, 2014; Kohn et al., 2015; Lagomarsino et al., 2016), existen pocos casos de estudio en esta región que han comprobado este vínculo utilizando información del registro fósil, un marco de trabajo regional y métodos estadísticos que permitan la comparación de hipótesis alternativas. En este sentido, en la presente tesis doctoral se investigó, además, el posible impacto del desarrollo del orógeno Andino y otros factores abióticos (e.g., cambios climáticos globales) sobre la evolución de dos rasgos ecomorfológicos (tamaño corporal e hipsodoncia) en un grupo diverso de mamíferos nativos de Sudamérica, los notoungulados. Para ello se utilizaron datos tomados de la literatura, en conjunto con los nuevos datos generados a partir del estudio de la fauna de la Formación Cura-Mallín.

1.3 Unidades sedimentarias del Mioceno en la Cordillera Andina entre los 36° y los 39° S y trabajos previos en la región

1.3.1 Contexto geológico y estratigráfico general

La Cordillera de los Andes representa uno de los mejores ejemplos de un orógeno activo formado por la convergencia entre una placa oceánica y otra continental (Ramos, 2009, 2010; Laznicka, 2010; Folguera et al., 2011; Horton, 2018b). Aunque la Cordillera de los Andes es un sistema montañoso continuo sobre el margen occidental de Sudamérica, es posible reconocer variaciones longitudinales marcadas en su topografía, tectónica, volcanismo, estructura litosférica profunda, geometría de subducción e historia geológica (Tassara y Yáñez, 2003; Ramos, 2010; Martinod et al., 2010; Horton, 2018b). De tal forma, es posible distinguir a lo largo de los Andes diferentes segmentos que presentan una evolución geodinámica particular. Tassara y Yáñez (2003) proponen dividir la

Cordillera de los Andes en cuatro grandes segmentos de primer orden: Andes del norte (5°N – 15°S), Andes centrales (15° – $33,5^{\circ}\text{S}$), Andes del sur ($33,5^{\circ}$ – 47°S) y Andes australes (47° – 56°S). Además, reconocen los siguientes segmentos de segundo orden: Altiplano (15° – 23°S), Puna (23° – 28°S) y Cordillera Frontal (28° – $33,5^{\circ}\text{S}$) en los Andes centrales, y Cordillera Principal ($33,5^{\circ}$ – 39°S) y Cordillera Patagónica (39° – 47°S) en los Andes del sur (Tassara y Yáñez, 2003).

Por otra parte, en el extremo occidental de Sudamérica, entre los 36° y 39°S , y en territorio chileno, se pueden identificar diferentes unidades fisiográficas longitudinales: la Cordillera de la Costa, la Depresión Central y la Cordillera Principal (SERNAGEOMIN, 2003; Figura 1.3). Además, a estas latitudes, pero en territorio argentino se puede reconocer una serie de cuencas de antepaís. Siguiendo la propuesta de Tassara y Yáñez (2003), la sección de la Cordillera Principal entre los 36° y 39°S corresponde a la sección de norte de los Andes del sur. Aunque otros autores consideran a esta sección (36° – 39°S) una zona de transición entre el sur de los Andes centrales y el norte de los Andes Patagónicos (= Andes del sur) (Rojas Vera et al., 2016; Horton, 2018b). Independientemente de esta situación, en esta región de la cordillera andina (en Chile) es donde se ubica geográficamente nuestra área de estudio (Figura 1.3).

Las secuencias mesozoicas y cenozoicas expuestas en la Cordillera Principal están depositadas sobre un basamento Pérmico-Triásico (Rosselot et al., 2019a). Estas unidades se han deformado por contracción en dos fases principales de edad Cretácico temprano a Eoceno(?), y Neógeno (Rojas Vera et al., 2015, 2016; Horton y Fuentes, 2016; Rosselot et al., 2019a). Estos eventos compresivos fueron interrumpidos por un evento extensional de escala regional que ocurrió desde el Eoceno?–Oligoceno hasta el Mioceno, formando diferentes cuencas a lo largo de los Andes Centrales y del Sur (Jordan et al., 2001; Radic et al., 2002; Charrier et al., 2002; Burns et al., 2006; Radic, 2010; Orts et al., 2012; Encinas et al., 2019). Esta evolución tectónica está bien ilustrada por la diversidad de edades y litologías de las unidades que afloran sobre la Cordillera Principal entre los 36° y 39°S (Figura 1.4). Debido a que en la literatura existen descripciones detalladas de las unidades ígneas, metamórficas y sedimentarias presentes en esta región (e.g., Gonzalez y Vergara, 1962; Niemeyer y Muñoz, 1983; Suárez y Emparan, 1997; Carpinelli, 2000; SERNAGEOMIN, 2003; Melnick et al., 2006), en adelante nos enfocaremos en proveer mayores detalles de las unidades litoestratigráficas que

afloran sobre la Cordillera Principal y que están incluidas en la Cuenca de Cura-Mallín.

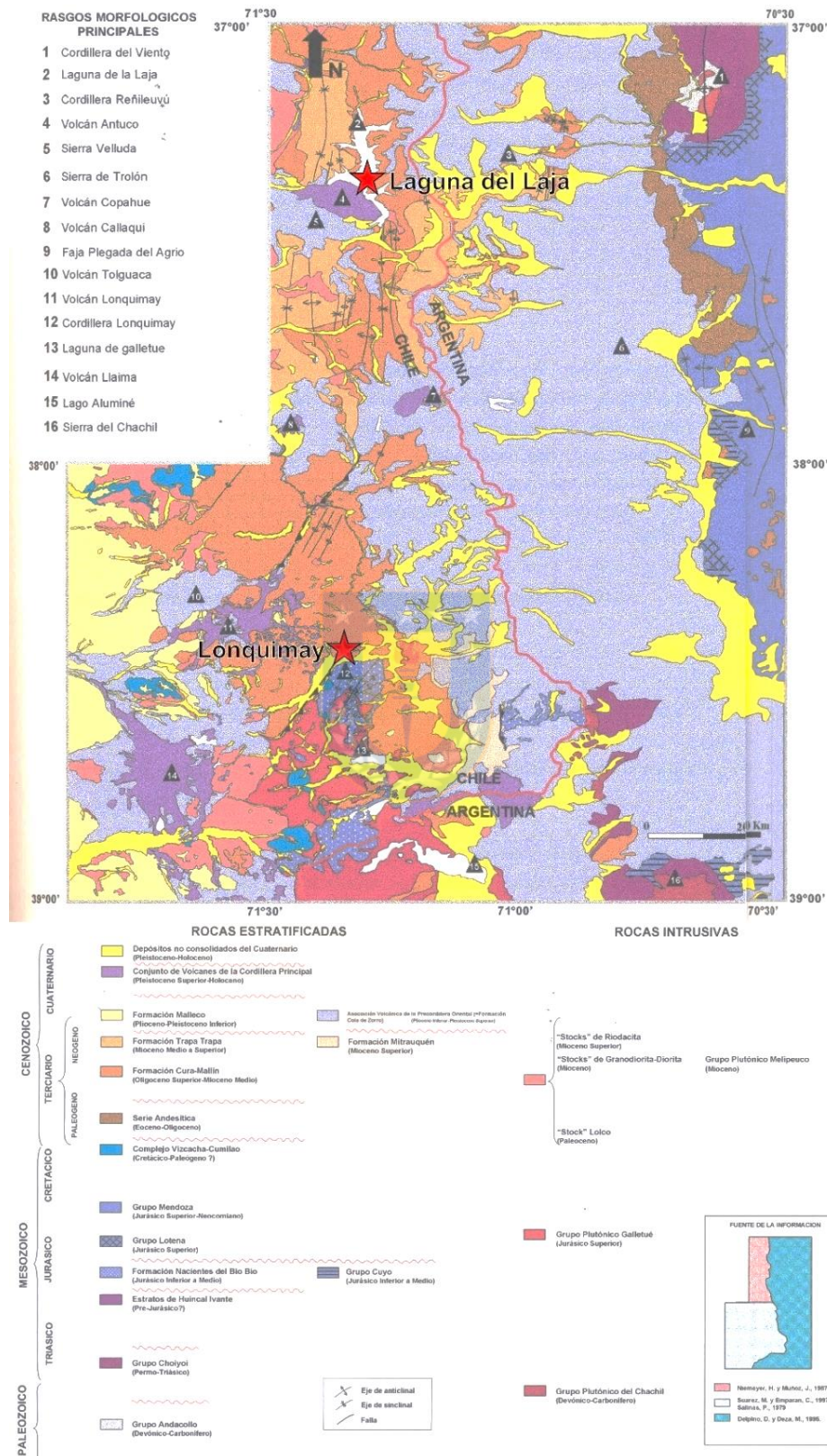


Figura 1.4. Mapa geológico regional de la Cordillera Principal comprendida entre los 36° y 39°S en Chile y Argentina. Tomado de Carpinelli (2000).

La Cuenca de Cura-Mallín se ubica actualmente en la Cordillera Principal de los Andes, entre los 36° y 39°S en Argentina y Chile, y corresponde a una depresión elongada en dirección norte-sur rellena por aproximadamente 4.000 metros de sedimentos continentales de origen volcánico y sedimentario cuyas edades oscilan entre Oligoceno tardío y el Mioceno tardío (Niemeyer y Muñoz, 1983; Suárez y Emparan, 1995, 1997; Carpinelli, 2000; Jordan et al., 2001; Radic et al., 2002; Burns et al., 2006; Utge et al., 2009; Radic, 2010; Pedroza et al., 2017; Rosselot et al., 2019a). La Cuenca consiste en un sistema de al menos tres subcuencas diacrónicas e independientes, denominadas subcuenca Chillán, subcuenca Lileo y subcuenca Lonquimay (Carpinelli, 2000; Radic et al., 2002; Melnick et al., 2006; Radic, 2010; Rosselot et al., 2019a). El relleno de esta cuenca corresponde a las formaciones Cura-Mallín, Trapa Trapa y Mitrauquén (Gonzalez y Vergara, 1962; Niemeyer y Muñoz, 1983; Suárez y Emparan, 1997), las cuales serán descritas brevemente a continuación.

Formación Cura-Mallín (Oligoceno Superior-Mioceno Medio). La Formación Cura-Mallín fue definida originalmente a partir de la secuencia de sedimentos continentales con influencia volcánica que aflora en el estero homónimo ubicado al sur de la Laguna de la Laja, en Chile hacia los 37° S (Gonzalez y Vergara, 1962). Trabajos posteriores la redefinieron y extendieron su área de distribución geográfica en Chile (Niemeyer y Muñoz, 1983; Suárez y Emparan, 1995, 1997). Tradicionalmente se ha reconocido que la formación puede ser subdividida en dos miembros. Un miembro volcánico, compuesto esencialmente por depósitos de caída y flujos de piroclastos y subordinadamente lavas andesíticas y cuerpos hipabisales; y un miembro sedimentario (que generalmente sobreyace al primero, pero que en ciertos sectores se interdigitan), compuesto por areniscas, areniscas conglomerádicas, conglomerados de ambientes aluvio-fluviales y deltaicos, además de fangolitas, areniscas, calizas y algunos horizontes carbonosos depositados en un ambiente lacustre (Niemeyer y Muñoz, 1983; Suárez y Emparan, 1995, 1997; Carpinelli, 2000; Pedroza et al., 2017). Dependiendo de la latitud donde afloran, cada miembro recibe un nombre diferente: Río Queuco (volcánico) y Malla Malla (sedimentario) en la región de la Laguna del Laja, y Guapítrio (volcánico) y Río Pedregoso (sedimentario) en la región de Lonquimay (Niemeyer y Muñoz, 1983; Suárez y Emparan, 1995, 1997).

En la región de Lonquimay se propuso, recientemente, redefinir la formación Cura-Mallín como un grupo y elevar sus miembros Guapitrío y Río Pedregoso al rango de formaciones (Pedroza et al., 2017). Sin embargo, no está claro si ésta nomenclatura es también apropiada para la sucesión reconocida en la Laguna del Laja (Niemeyer y Muñoz, 1983). Tampoco está claro si las rocas volcánicas y sedimentarias asignadas a esta formación son realmente contemporáneas e indicativas de variación lateral en el estilo deposicional (Suárez y Emparan, 1995, 1997) o si corresponden a dos secuencias diferentes donde las primeras son más antiguas que las segundas, tal como sugiere Utgé et al. (2009). Es por ello que, a la espera de una revisión integral de la estratigrafía de esta región, en adelante se utilizará el nombre de Formación Cura-Mallín para referirse a la sucesión sedimentaria continental del Mioceno temprano a medio que aflora en la Cordillera de los Andes chilenos entre los 36° y 39°S.

Por otra parte, trabajos más recientes en la región de la Laguna del Laja parecen indicar que los miembros originalmente propuestos para la Formación Cura-Mallín en dicha región no son consistentemente mapeables (Herriott, 2006; Flynn et al., 2008). Por el contrario, estos autores subdividieron la sucesión sedimentaria de esta formación que aflora al sur de la Laguna del Laja en cinco unidades mapeables: Tcm₁, Tcm₂, Tcm₃, Tcm₄ y Tcm₅ (Herriott, 2006). Las unidades Tcm₁, Tcm₃ y Tcm₅ están constituidas principalmente por areniscas y lutitas volcánicas, teniendo Tcm₅ una mayor proporción de sedimentos de grano fino (Herriott, 2006). La unidad Tcm₂ es una ignimbrita que separa los estratos litológicamente similares Tcm₁ y Tcm₃, considerándose como un estrato guía (Herriott, 2006). La unidad Tcm₄ es litológicamente distintiva por contener clastos de granitoides y cuarcita de tamaño guijarro (Herriott, 2006). En la presente tesis doctoral, se estudiaron mamíferos fósiles colectados en la unidad Tcm₃. Las unidades suprayacentes a la Formación Cura-Mallín, corresponden a las Formaciones Trapa-Trapa y Mitrauquén, con afloramientos en la Laguna del Laja, y Lonquimay, respectivamente.

Dataciones K-Ar y U-Pb (en circones detríticos) indican edades comprendidas entre 19,9–10,7 Ma, y 19,8–14,5 Ma (Mioceno Inferior a Mioceno Superior) para los estratos de la Formación Cura-Mallín encontrados en Lonquimay y la Laguna del Laja, respectivamente (Suárez y Emparan, 1995; Herriott, 2006; Flynn et al., 2008; Pedroza et al., 2017; Rosselot et al., 2019b). Este marco

geocronológico relativamente bien definido nos permitió asignar los diferentes vertebrados fósiles colectados a una edad particular. Un resumen de los diferentes esquemas estratigráficos propuestos por diferentes autores para la Formación Cura-Mallín y sus unidades neógenas suprayacentes, así como las edades radiométricas reportadas para cada sector se muestra en la Figura 1.5.

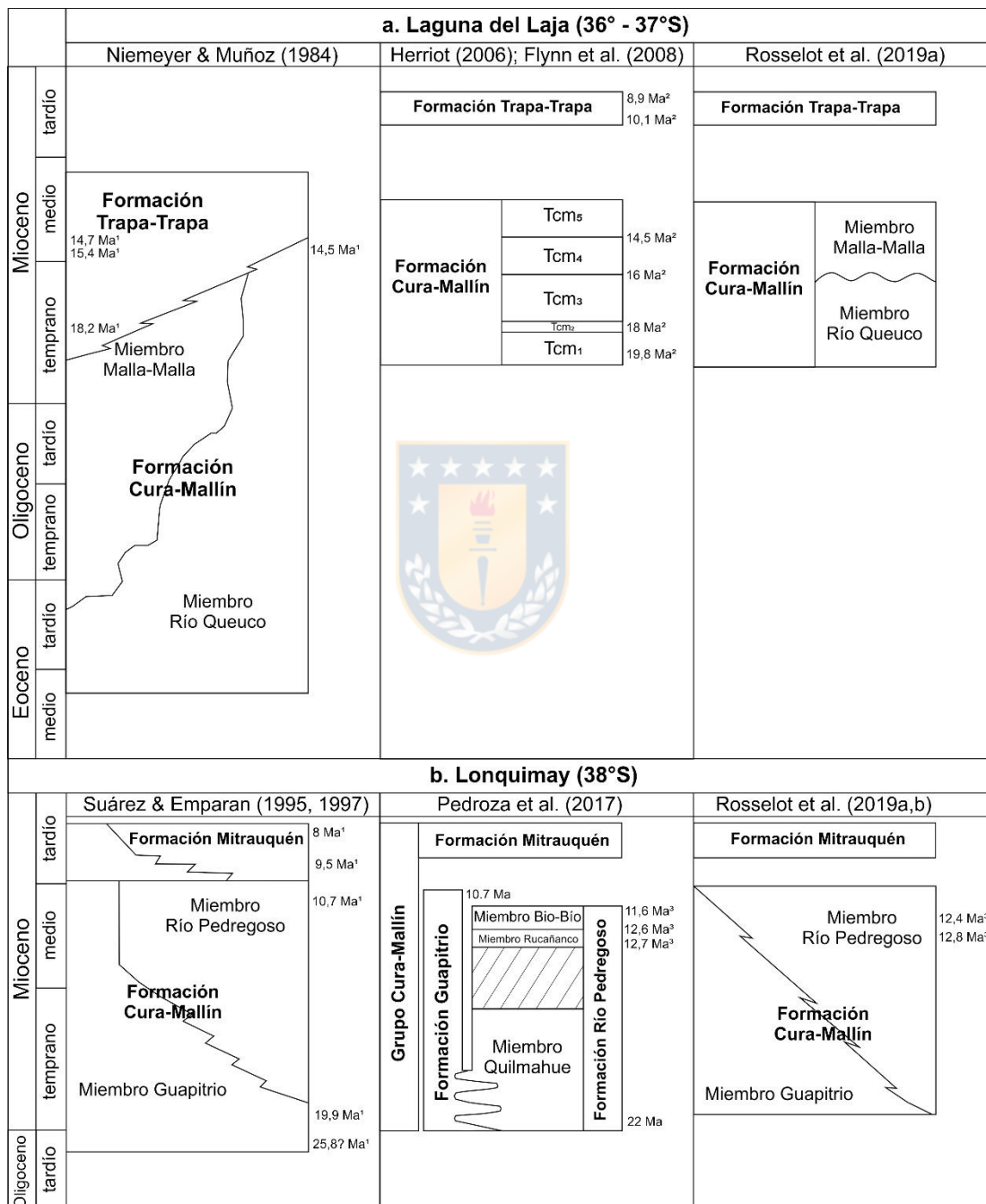


Figura 1.5. Esquemas estratigráficos propuestos por diversos autores (Niemeyer y Muñoz, 1983; Suárez y Emparan, 1995; Herriott, 2006; Flynn et al., 2008; Pedroza et al., 2017; Rosselot et al., 2019a,b) para agrupar las diferentes unidades incluidas en la Cuenca de Cura-Mallín y que afloran en las regiones de la Laguna del Laja y Lonquimay, Cordillera Principal, Chile. Edades radiométricas obtenidas por los métodos K/Ar¹, Ar/Ar² y U/Pb³.

Los estratos de la Formación Cura-Mallín en la región de la Laguna del Laja fueron depositadas en llanuras aluviales o en ambientes principalmente fluviales con facies menores indicativas de fases lacustres de corta duración, todo esto en una región de volcanismo activo (Carpinelli, 2000; Herriott, 2006; Flynn et al., 2008). Un ambiente similar (i.e., predominancia de ambientes fluvio-lacustres en asociación con estratovolcanes) ha sido propuesto para esta Formación en la región de Lonquimay (Suárez y Emparan, 1995; Pedroza et al., 2017). Por otro parte, el espesor de la formación es variable, alcanzado hasta 2.500 metros (Carpinelli, 2000; Radic, 2010). Las unidades infrayacentes a la Formación Cura-Mallín son variables e incluyen rocas sedimentarias marinas jurásicas (Formación Nacientes del Bío-Bío), rocas ígneas de edad cretácica (Intrusivos de la Cordillera Andina, Complejo Plutónico Galletué) y rocas sedimentarias y volcánicas de edad cretácica superior-terciaria inferior (Niemeyer y Muñoz, 1983; Suárez y Emparan, 1997; Carpinelli, 2000; Radic, 2010).

Formación Trapa-Trapa (Mioceno Superior). Esta formación, definida originalmente por Niemeyer y Muñoz (1983), corresponde a una sucesión expuesta entre los 36° y 37°S de andesitas, andesitas basálticas, tobas, brechas y, en menor proporción, dacitas, basaltos, areniscas y conglomerados, de espesores variables entre 300 y ~1.500 (Niemeyer y Muñoz, 1983; Muñoz y Niemeyer, 1984; Carpinelli, 2000). Las rocas de la Formación Trapa-Trapa sobreyacen en transición, concordancia o discordancia de bajo ángulo, a aquellas de la Formación Cura-Mallín, y están cubiertas, en marcada discordancia de erosión, por rocas volcánicas plio-pleistocénicas (Niemeyer y Muñoz, 1983; Muñoz y Niemeyer, 1984; Carpinelli, 2000). Dataciones radiométricas K-Ar de la Formación Trapa-Trapa (en Chile) indican edades comprendidas entre los $14,7 \pm 0,7$ y $18,2 \pm 0,8$ Ma, apoyando una edad Mioceno Inferior a Medio (Niemeyer y Muñoz, 1983; Muñoz y Niemeyer, 1984). Sin embargo, trabajos posteriores, utilizando dataciones Ar/Ar, obtienen edades de $10,1 \pm 0,2$ Ma, $9,1 \pm 0,1$ Ma y $8,9 \pm 0,1$ Ma (Herriott, 2006; Flynn et al., 2008), lo que le otorgaría una edad Mioceno Superior a esta formación.

Formación Mitrauquén (Mioceno Superior). La formación, definida originalmente por Suárez y Emparan (1997), está expuesta a lo largo de una franja ubicada al este del río Biobío, en los alrededores de Lonquimay (38°S). Se pueden distinguir

dos miembros dentro de esta formación. Uno esencialmente conglomerático, con intercalaciones de ignimbritas dacíticas y lavas, y uno volcánico, compuesto de lavas andesíticas, tobas dacíticas de caída e ignimbritas (Suárez y Emparan, 1997; Carpinelli, 2000; Melnick et al., 2006). La Formación Mitrauquén sobreyace en leve discordancia angular, o de forma concordante, a los estratos de la Formación Cura-Mallín (Suárez y Emparan, 1997; Carpinelli, 2000; Melnick et al., 2006). Dataciones radiométricas (K-Ar) realizadas en tobas de esta unidad, indican edades que varían desde $9,5 \pm 2,8$ Ma a $8,0 \pm 0,5$ Ma (Mioceno Superior) (Suárez y Emparan, 1997).

1.3.2 Contexto tectónico asociado a la sedimentación de la Formación Cura-Mallín

Existen diversas interpretaciones con respecto al contexto tectónico en el que se formó la Cuenca de Cura-Mallín. Suárez y Emparan (1995) sugieren que la cuenca en el sector de Lonquimay podría corresponder a una cuenca de tipo *pull-apart* relacionada con la falla de rumbo Liquiñe-Ofqui. Trabajos posteriores consideran que el relleno de la cuenca se inició en un régimen extensional, y que luego este relleno fue sometido a una inversión tectónica (e.g., Jordan et al., 2001). Sin embargo, el momento en que se inicia la inversión de la Cuenca de Cura-Mallín ha sido objeto de controversia (Cobbold et al., 2008). Al respecto, existen dos hipótesis sobre el momento temporal en que se inicia esta inversión. La primera sugiere que la sedimentación de la Formación Cura-Mallín se produjo completamente en un contexto extensional, y las primeras facies sinorogénicas ocurrieron durante los 12–9 Ma, con la sedimentación de los depósitos volcánicos y conglomeráticos de las formaciones Mitrauquén y Trapa-Trapa (Jordan et al., 2001; Burns et al., 2006; Melnick et al., 2006; Radic, 2010). La segunda hipótesis sugiere que únicamente los estratos basales de la Formación Cura-Mallín son sinextensionales, mientras que los niveles sedimentarios superiores de esta formación, y sus unidades suprayacentes (formaciones Mitrauquén y Trapa-Trapa), son sinorogénicas, y se depositaron en cuencas de antepaís o intermontanas relacionadas con el alzamiento de los Andes a partir de los ~18 Ma (Spikings et al., 2008; Utge et al., 2009; Rosselot et al., 2019a).

1.3.3 Trabajos estratigráficos/paleontológicos previos en la Cuenca de Cura-Mallín

Estratigrafía. A continuación, se presentará un breve resumen de los trabajos estratigráficos previos más relevantes (en orden cronológico) realizados en la Cuenca de Cura-Mallín entre los 36° y 39°S (Chile). Para mayores detalles ver el trabajo de Carpinelli (2000).

González y Vergara (1962) realizaron un reconocimiento de las unidades geológicas que afloran sobre la Cordillera Principal de Chile. Estos autores definen la Formación Cura-Mallín a partir de estratos aflorantes en el estero homónimo, ubicado en las nacientes del río Queuco, afluente del Bio-Bío. Le asignaron una edad tentativa Jurásico superior a Cretácico inferior a esta formación.

Niemeyer y Muñoz (1983) caracterizaron las unidades litoestratigráficas presentes en la Hoja Laguna del Laja. Estos autores, entre otras cosas, redefinen la antigua Formación Malla-Malla, como el Miembro Superior de la Formación Cura-Mallín.

Suárez y Emparan (1995) analizaron la estratigrafía, geocronología y paleofisiografía de la cuenca continental de intra-arco que aflora en la Cordillera Principal entre los 38° y 39°S. Proporcionaron 23 dataciones K-Ar con edades comprendidas entre los 19,9 y 10,7 Ma que indican una edad Mioceno Inferior a Medio-Superior para la Formación Cura-Mallín. Las rocas piroclásticas y flujos de lava presentes en el Miembro Guapitrío indican la existencia de estratovolcanes. Además, sugieren la presencia (entre 17,5 y 13,0 Ma) de una gran cuenca lacustre (>100 km de largo), representada por algunas facies del Miembro Río Pedregoso.

Suárez y Emparan (1997) caracterizaron las unidades litoestratigráficas presentes en la Hoja Curacautín. Estos autores redefinen algunas formaciones, tratando de agrupar de manera más ordenada todas aquellas secuencias definidas en trabajos previos en el área. Indican que, en esta región, la Cuenca de Cura-Mallín esta rellena con 2.600 m de rocas volcánicas y volcanoclásticas asignadas al intervalo Mioceno temprano – Mioceno tardío.

Herriott (2006) llevo a cabo un mapeo geológico detallado de la región ubicada al sur de la Laguna del Laja, reconociendo las formaciones Cura-Mallín y Trapa-Trapa. Este autor presentó 14 nuevas dataciones radiométricas $^{40}\text{Ar}/^{39}\text{Ar}$ de la Formación Cura-Mallín que indican que la sedimentación de esta secuencia ocurrió entre los $19,80 \pm 0,40$ Ma y los $14,50 \pm 0,50$ Ma. Adicionalmente, proveen tres nuevas dataciones $^{40}\text{Ar}/^{39}\text{Ar}$ de la Formación Trapa-Trapa ($10,10 \pm 0,20$ Ma; $9,10 \pm 0,10$ Ma; and $8,90 \pm 0,1$ Ma). Estas edades fueron publicadas formalmente

en el trabajo de Flynn et al. (2008). Además, Herriott (2006) indica que los miembros originalmente propuestos para la Formación Cura-Mallín en dicha región no son consistentemente mapeables, y en contraste reconoce cinco facies (Tcm₁, Tcm₂, Tcm₃, Tcm₄ y Tcm₅) en el área ubicada al sur de la Laguna del Laja.

A partir de trabajos en terreno y dataciones U-Pb en circones detríticos, Pedroza et al. (2017) propone redefinir las unidades Neógenas aflorantes en los alrededores de Lonquimay como Grupo Cura-Mallín. Dentro de este Grupo estarían incluidas la Formación Guapitrío (volcano-sedimentaria; 20,37–10,7 Ma), la Formación Río Pedregoso (predominantemente sedimentaria) y la Formación Mitrauquén (volcano-sedimentaria). Además, dividen la Formación Río Pedregoso en tres subunidades: Miembro Quilmahue (22–16 Ma), Miembro Rucañanco (12,7–12,6 Ma) y Miembro Bío-Bío (12,6–11,6 Ma).

Rosselot et al. (2019a) realizaron una revisión de los datos geocronológicos, estructurales, geoquímicos, termocronológicos y de subsidencia disponibles para la Formación Cura-Mallín. A partir de estos datos reconocieron dos etapas en su evolución tectono-sedimentaria: 1) un período Oligoceno tardío a Mioceno temprano caracterizado por depósitos sin-extensionales en una corteza atenuada, y 2) un período Mioceno medio a tardío que coincide con la exhumación y compresión regionales reveladas por datos termocronológicos y sedimentación sin-contraccional.

Paleontología. En la Cuenca de Cura-Mallín se ha reportado una importante diversidad de animales y plantas. A continuación, se presentará un breve resumen de los trabajos paleontológicos previos más relevantes (en orden cronológico) realizados en dicha cuenca entre los 36° y 39° S (Chile).

Felsch (1915) menciona por primera vez restos de invertebrados de agua dulce, así como restos de peces en la zona de Lonquimay. Posteriormente, Parodiz (1969) le asignó una edad Paleoceno superior a la asociación de invertebrados de agua dulce mencionada por Felsch (1915).

Chang et al. (1978) describe, a partir de restos colectados en Lonquimay, la primera especie de pez fósil de la región, *Percichthys lonquimayiensis*, reconociendo que este taxon tiene claras afinidades con la fauna de peces moderna de Chile. Estos autores asignaron esta especie al Paleoceno superior.

Salinas (1979) reportó la presencia de hojas de myrtaceas, una familia con representantes modernos en Chile comúnmente encontrados en bosques húmedos, en afloramientos de la Formación Lolco (=Formación Cura-Mallín) ubicados en el Estero Los Azules (15 km al sur de Lonquimay).

Arratia (1982) realizó una revisión de peces percoideos (Perciformes: Percoidea) de agua dulce de Sudamérica (actuales y extintos) y describió una nueva especie de *Percichthys*, *P. sandovali*, a partir de material recuperado en Lonquimay.

Palma-Heldt (1983) analizó el contenido palinológico de muestras colectadas en la Formación Cura-Mallín en los alrededores de Lonquimay. Esta autora reconoció al menos 31 morfoespecies que indicarían edades comprendidas entre el Oligoceno y Mioceno. Además, interpreta que esta flora es indicativa de bosques húmedos, en parte pantanoso, y temperaturas templadas a frías (Palma-Heldt, 1983).

Palma-Heldt y Rondanelli (1990) estudiaron una asociación de hojas fósiles colectadas en el Cerro Rucañanco (Formación Cura-Mallín, Lonquimay) y reconocen las especies *Nothofagus pumillo*, *Nothofagus antarctica* y *Boquilla trifoliolata*.

Rubilar y Abad (1990) describieron una tercera especie de *Percichthys*, *P. sylviae*, a partir de materiales colectados en Cerro La Mina (Ralco), en estratos del miembro Malla-Malla de la Formación Cura-Mallín. Rubilar and Wall (1990) reportaron el primer Siluriforme fósil de Chile, a partir de restos de una región cefálica y vértebras aisladas colectados en las cercanías del Cerro Rucañanco (Lonquimay).

Durante el año 1990 se dieron los primeros reportes de mamíferos fósiles en la Formación Cura-Mallín. Marshall et al. (1990) describieron restos de *Astrapotherium* sp. (*Astrapotheria*) colectados en el Río Quepuca 50 km al norte de Lonquimay. Además, Suárez et al. (1990) mencionaron el hallazgo de restos de macrauchenidos indeterminados (*Litopterna*), cf. *Protypotherium* (*Notoungulata*), un gliptodonte indeterminado (*Cingulata*), roedores caviomorfos, y un posible mesotherido (*Notoungulata*) en los alrededores de Lonquimay. En ambos trabajos, estos mamíferos fósiles se asignaron al Mioceno temprano (Marshall et al., 1990; Suárez et al., 1990).

Rubilar (1994) realizó una revisión de la diversidad ictiológica de la Formación Cura-Mallín, y sugiere la presencia de dos familias no reportadas (como fósiles) anteriormente en Chile: Characidae (Actinopterygii: Characiforme), y Atherinidae (Actinopterygii: Atheriniformes), a partir de restos colectados en Cerro La Mina y Cerro Rucañanco, miembros Malla-Malla y Río Pedregoso, respectivamente.

Alvarenga (1995) describió una nueva especie y género de ave continental, *Megahinga chilensis* (Suliformes: Anhingidae) utilizando como holotipo un tarsometatarso casi completo colectado en el Cerro Rucañanco (Lonquimay), Formación Cura-Mallín, al cual asigno una edad Mioceno temprano.

Una espina pectoral, identificada como perteneciente a un Siluroidei indeterminado, fue descrita por Azpelicueta y Rubilar (1997). Posteriormente, Azpelicueta y Rubilar (1998) describieron una nueva especie de bagre fósil, *Nematogenys cuivi* (Siluriformes: Nematogenyidae) a partir de restos colectados en los depósitos fluviolacustres continentales de la Formación Cura-Mallín en los alrededores de Lonquimay.

Croft et al. (2003) reportaron el hallazgo de un toxodóntido (Notoungulata) de gran tamaño, *Nesodon conspiratus*, en afloramientos fluvio-lacustres de la Formación Cura-Mallín en el Cerro Tallón (Lonquimay). Le asignaron a este fósil una edad Mioceno temprano (Santacrucense).

En su tesis doctoral (no publicada), Wertheim (2007) reconoció la presencia de dasypróctidos, eocárdidos, lagostóminos y echímidos, en estratos del Mioceno temprano y medio de la Formación Cura-Mallín presentes al sur de la Laguna del Laja. A partir del análisis detallado de los restos de roedores encontrados en esta región, la autora propone la presencia de 20 nuevas especies y 10 nuevos géneros.

Flynn et al. (2008) reconocieron una sucesión de mamíferos fósiles en la región de la Laguna del Laja, incluyendo fósiles encontrados en las formaciones Cura-Mallín y Trapa-Trapa con edades comprendidas entre 20 y 8 Ma. Esta fauna está dominada en términos de riqueza y abundancia por roedores caviomorfos y notoungulados, aunque también reconocieron astrapoterios, marsupiales y xenarthros (Flynn et al., 2008).

Buldrini y Bostelmann (2011) reanalizaron un cráneo de interatérido encontrado por Suarez et al. (1990) en el Puente Tucapel (Lonquimay) y lo

asignaron a *Protypotherium* cf. *australe*. Además, asignaron a estos restos una edad Mioceno temprano (Santacrucense).

Shockey et al. (2012) describieron un nuevo notoungulado leontínido, *Colpodon antucoensis*, a partir de restos colectados en los estratos más basales de la Formación Cura-Mallín aflorando en la Laguna del Laja (19,53–19,25 Ma; Colhuehuapiense).

Nuevos restos fósiles, entre los que destaca un coracoides y fragmento distal de un húmero derecho, fueron asignados a *Meganhinga chilensis* por Soto-Acuña et al. (2013).

Bostelmann et al. (2014) revisaron el material colectado en el Río Quepuca, originalmente asignado a *Astrapotherium* sp., y concluyeron que el mismo debería ser incluido en el género *Parastrapotherium*.

Buldrini et al. (2015) revisaron el material mandibular de interatérido colectado por Suarez et al. (1990), en el Puente Tucapel (Lonquimay), y lo asignan a *Protypotherium* sp.

En su tesis doctoral (no publicada), Luna (2015) llevo a cabo una revisión detallada de los ungulados presentes en la Formación Cura-Mallín en la Laguna del Laja. Este autor reconoció la posible presencia de cinco nuevos géneros de typotherios, además de *Protypotherium praerutilum* y *Astrapothericulus iheringi*.

Arratía (2015) realizó una revisión y evaluación del registro fósil de peces osteíctios de Chile desde el Paleozoico (Pérmico tardío) hasta el Neógeno (Mioceno), incluyendo los encontrados en la Formación Cura-Mallín. Esta autora indicó que el estudio exhaustivo de los peces de esta formación aportará antecedentes significativos para comprender la evolución de grupos de peces actuales de aguas continentales, al tratarse de los registros más antiguos de especies recientes.

Pedroza et al. (2017) mencionaron la presencia de restos de “*Macrauchenia litopterna*” en la localidad de Puente Tucapel (Lonquimay). Además, basados en dataciones radiométricas, estos autores sugirieron, por primera vez, que algunos de los mamíferos fósiles encontrados en la Formación Cura-Mallín, en la región de Lonquimay, pueden tener una edad Mioceno medio tardío (Laventense).

Guevara et al. (2018) mencionaron la presencia de un anuro (bufónido) en la Formación Cura-Mallín, a partir de restos postcraneales recuperados en el Cerro Rucañanco (Lonquimay).

1.4 Ubicación del área de estudio y vías de acceso

Los sectores estudiados se sitúan en la Cordillera de los Andes y administrativamente ocupan parte de las regiones del Biobío y la Araucanía, Chile.

La mayor parte de los ejemplares fósiles descritos en esta tesis doctoral fueron colectados por nuestro equipo de investigación durante un periodo de cuatro años (2017-2021), durante prospecciones geológicas y paleontológicas realizadas en afloramientos de la Formación Cura-Mallín ubicados al sur de la Laguna del Laja, Comuna de Antuco, Provincia de Biobío, Región del Biobío, Chile.

Hay dos localidades principales donde estos fósiles fueron colectados, Cerro Campamento (Estero Trapa-Trapa Oeste) y Estero Trapa-Trapa Este (Figura 1.6a). Las coordenadas geográficas de estas localidades son las siguientes: Estero Trapa-Trapa Este, 37.60°S, 71.23°W; Cerro Campamento, 37.57°S, 71.26°W. La zona estudiada se ubica al sur del Parque Nacional Laguna del Laja (fuera del área del parque), y a aproximadamente 20 km al sureste del volcán Antuco.

Para acceder a las localidades ubicadas al sur de la Laguna del Laja, desde Concepción, es necesario tomar la Ruta 146 hasta Cabrero. Luego se debe tomar la ruta Q-97 hasta Yungay, para luego dirigirse por la ruta N-59 hasta el sector Canteras, y de allí tomar a la ruta Q-45 para dirigirse al pueblo de Antuco y la entrada al Parque Nacional Laguna del Laja. Los caminos mencionados anteriormente se encuentran asfaltados. Desde la entrada del Parque se debe continuar hacia el este, por un camino de tierra de regular estado (ruta Q-45), que bordea el volcán Antuco y la sección sur de la Laguna del Laja y que se dirige hasta el paso internacional de Pichachén. Tres kilómetros antes de llegar a la aduana del paso Pichachén se dobla al sur y se continua por un camino de tierra por 5 km hasta llegar a un valle de orientación norte-sur donde fluye el Estero Trapa-Trapa.

Adicionalmente, se estudiaron especímenes de mamíferos colectados (por investigadores previos) en múltiples localidades (Figura 1.6b) de la Formación Cura-Mallín en la región de Lonquimay (Comuna de Lonquimay, Provincia de Malleco, Región de la Araucanía, Chile). Aunque la proveniencia geográfica precisa de estas las localidades no se conoce con precisión. Las coordenadas geográficas aproximadas de cada una de ellas son: Cerro Rucañanco, 38.64°S, 71.15°W; Puente Tucapel, 38.58°S, 71.14°W; Cerro Tallón, 38.50°S, 71.22°W; Río Quepuca, 37.99°S, 71.44°W; Piedra Parada, 38.46°S, 71.22°W.

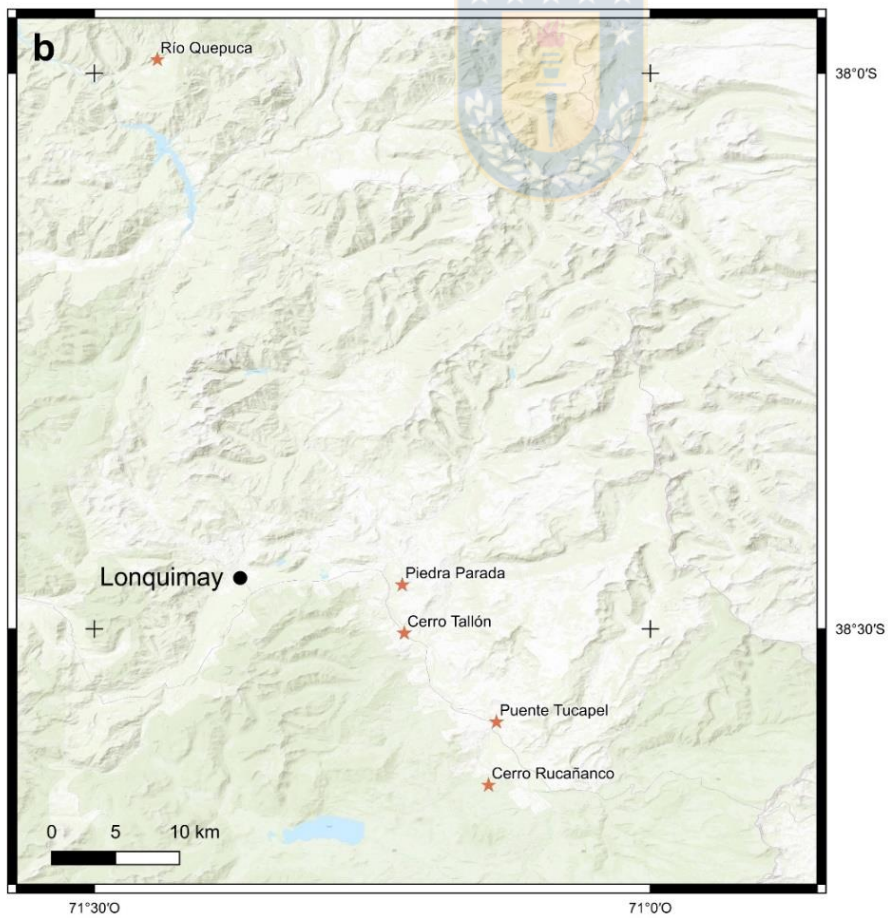
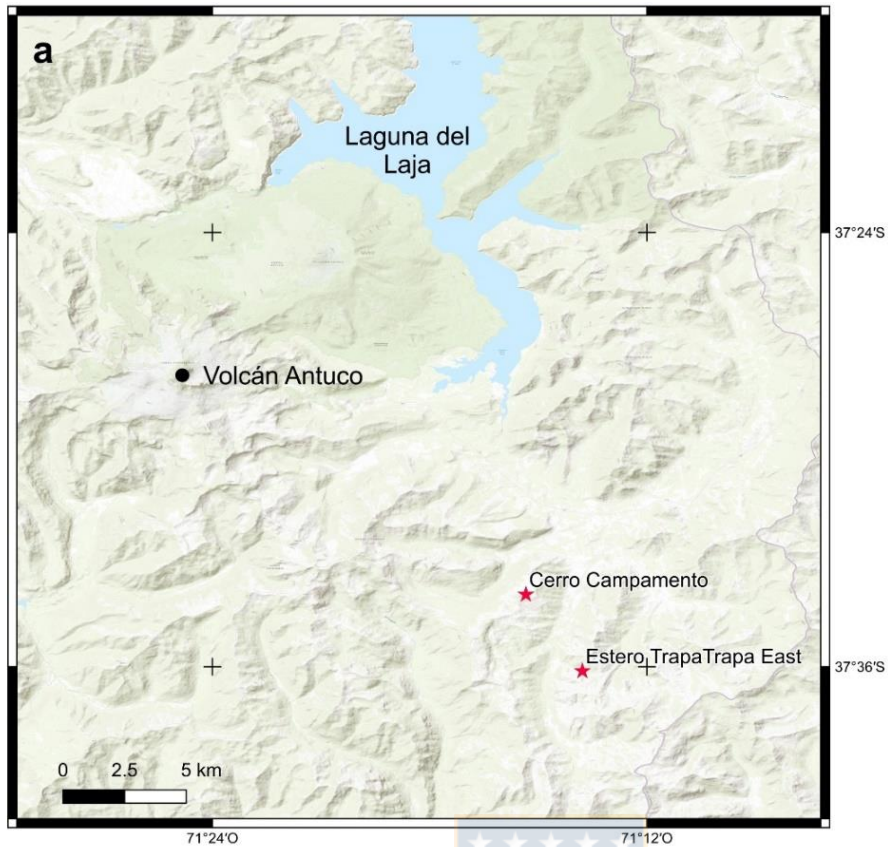


Figura 1.6. Mapa de ubicación geográfica de las principales localidades prospectadas durante el desarrollo de la presente tesis doctoral en las regiones de Lonquimay (a) y la Laguna del Laja (b).

Para acceder a las localidades ubicadas en los alrededores de la población de Lonquimay, desde Concepción, es necesario tomar la Ruta 146, hasta alcanzar la Ruta 5 Sur para luego dirigirse, por esta última, hasta la ciudad de Victoria, pasando por las ciudades de Los Ángeles, Mulchén y Collipulli. Desde Victoria, acceder a la ciudad de Lonquimay por la Ruta 181 atravesando las ciudades de Curacautín, Manzanar y Malalcahuello. Las tres rutas mencionadas anteriormente se encuentran pavimentadas. Desde Lonquimay, para llegar a las localidades Cerro Rucañanco, Piedra Parada, Puente Tucapel y Cerro Tallón se debe seguir por la Ruta 181 (ruta pavimentada) en dirección al paso fronterizo Pino Hachado. Por su parte, para llegar al punto en el Cerro Rucañanco es necesario tomar la ruta R-959 por 4 km hacia el sur hasta llegar a la Ruta R-939 por donde se recorren 2 km hasta llegar a los pies del Cerro. Las rutas R-959 y R-939 son caminos de tierra.

1.5 Topografía, clima y vegetación actual en el área de estudio

La región comprendida entre los 37° y los 38° de latitud sur, corresponde a un relieve montano, donde la mayoría de las cumbres no sobrepasan los 2.500 metros. Sólo cuatro cumbres se ubican cerca de los 3.000 metros y corresponden a los edificios volcánicos de Sierra Velluda (3.385 m), Volcán Antuco (2.987 m), Volcán Copahue (2.969 m) y Volcán Callaqui (3.080 m). El relieve decrece y se allana paulatinamente hacia la vertiente argentina de los Andes, hasta encontrarse con el frente occidental de la Cordillera del Viento y la Faja plegada del Agrio que constituyen los sistemas montañosos más orientales desarrollados a estas latitudes (Carpinelli, 2000). Al sur de los 38°, los relieves más elevados corresponden a los sistemas volcánicos Tolhuaca (2.806 m), Lonquimay (2.726 m), Sierra Nevada (2500 m) (inactivo) y Llaima (3.125 m), ubicados en el extremo occidental del área en estudio. Hacia el oriente, las alturas varían entre 1500–1900 metros en el Cordón de los Tres Pinos, Cordillera General o de Huisa y más al sur en las Cordilleras Lonquimay, Lolén, Pedregoso, Litrancura y Galletué y los cordones Quillén, Paule y Pacunto. Al este de esta zona montañosa, en territorio argentino, el relieve se convierte en una extensa meseta basáltica con suave pendiente en dirección este disectada por cursos fluviales y valles glaciares (Carpinelli, 2000).

La región se caracteriza por presentar dos tipos de clima según la clasificación de Köppen (1931). Bajo los 1.700 m el clima corresponde al tipo templado cálido,

con menos de cuatro meses secos, mientras que, las regiones más altas, se caracterizan por un clima de hielo por efecto de altura (Carpinelli, 2000). Durante el invierno, gran parte del territorio se cubre de nieve, mientras durante los meses de verano se tienen temperaturas superiores a los 20°C durante el día (Carpinelli, 2000). La amplitud térmica diaria es elevada y variable entre 8° y 14 °C. Las precipitaciones medias anuales son variables entre 1000 y 2500 mm (Carpinelli, 2000).

La zona de estudio se caracteriza por una densa cubierta vegetal, constituida por ejemplares típicos de selva austral (Carpinelli, 2000). En las partes más bajas se reconocen coigües, lengas, olivillos y, en las partes altas, ñirres. Al sur de los 37,6°S predominan los bosques de araucarias ocupando los cordones de cerros más altos, mientras que entre los arbustos destacan la murtilla, el maqui y el parrille (Carpinelli, 2000).

1.6 Hipótesis

La ocurrencia de sucesivas asociaciones de mamíferos Neógenos abarcando un periodo de ~11 Myr, dentro de una misma área geográfica (Laguna del Laja), es extremadamente inusual en el registro fósil de Sudamérica. Considerando, además, que durante el Mioceno se dieron importantes cambios en los ecosistemas del sur de Sudamérica potencialmente asociados al alzamiento andino es posible proponer la siguiente hipótesis:

Las sucesivas asociaciones de mamíferos de la zona de estudio muestran adaptaciones eco-morfológicas (e.g., incremento de la hipsodoncia) hacia ambientes progresivamente más abiertos y secos y presentan un aumento en el nivel de endemismo local como consecuencia del alzamiento de los Andes durante el Mioceno.

1.7 Objetivos

1.7.1 Objetivo general

Determinar la taxonomía y paleoecología de las asociaciones de mamíferos de la Formación Cura-Mallín en los alrededores de la Laguna del Laja (37°S) y Lonquimay (38°S), Chile, y evaluar estos resultados dentro del contexto tectónico y

climático que caracterizó a esta región del sur de la Cordillera Central Andina durante el Mioceno.

1.7.2 Objetivos específicos

1. Determinar la riqueza de especies y abundancia de los mamíferos presentes en la Formación Cura Mallín dentro del área de estudio.
2. Establecer similitudes y diferencias entre las distintas localidades con mamíferos dentro de la Formación, así como con otras localidades fosilíferas del Mioceno del sur de Sudamérica.
3. Determinar, dentro de un contexto temporal, las condiciones paleoambientales y paleoclimáticas en las que habitaron los mamíferos de la Formación.
4. Establecer el rol del alzamiento andino del Mioceno sobre los patrones evolutivos de los mamíferos en el sur de Sudamérica.

1.8 Organización de los resultados

Durante el desarrollo de esta tesis doctoral se colectaron decenas de restos de vertebrados fósiles en las regiones de Lonquimay y la Laguna del Laja. En la zona de Lonquimay la mayoría de éstos corresponden a fragmentos articulados y desarticulados de peces óseos, así como a huesos aislados de aves continentales. Sin embargo, también fue posible estudiar los mamíferos colectados en Lonquimay en los años 90 por autores previos. Por otra parte, en la región de Laguna del Laja, se colectaron restos principalmente craneales y dentales de mamíferos en afloramientos del Mioceno Inferior de la Formación Cura-Mallín. Desafortunadamente y, a pesar de importantes esfuerzos de prospección paleontológica en la zona, no se encontraron mamíferos fósiles en los estratos del Mioceno Medio y Superior de la Formación Cura-Mallín o las formaciones Trapa-Trapa y Mitrauquén. En este sentido, los restos de mamíferos fósiles del Mioceno temprano de la Formación Cura-Mallín fueron el objeto de estudio principal de este trabajo de investigación.

Los resultados de la presente investigación están desglosados en siete capítulos, descritos brevemente a continuación. Los capítulos II–V están escritos en inglés y en formato de revistas ISI, cada uno con su propia estructura general

(i.e., Introducción, Materiales y Métodos, Resultados y Discusión). Estos capítulos abordan diferentes temáticas que en conjunto permitieron cumplir con los objetivos planteados inicialmente. Es importante mencionar que los capítulos II–IV tienen un foco a nivel local (i.e., taxonomía, sistemática y paleoecología de la fauna de la Formación Cura-Mallín), mientras que el capítulo V tiene un foco a nivel regional (ver detalles más adelante).

En el capítulo I se presenta una visión introductoria al tema y objeto de estudio, la problemática detectada, el marco geológico general enfocado en las unidades Miocenas aflorantes en la Cordillera de los Andes entre los 36°–39° S, una síntesis de los trabajos paleontológicos y estratigráficos previos realizados en la región, así como los objetivos planteados, la hipótesis de trabajo y un resumen de las metodologías utilizadas durante el desarrollo de la presente tesis doctoral.

En el capítulo II se abordó el estudio detallado de una pequeña, pero significativa, colección de mamíferos fósiles recuperados en afloramientos de la Formación Cura-Mallín ubicados en los alrededores de la población de Lonquimay. La mayor parte de estos mamíferos fueron colectados a finales del siglo XX y todos ellos fueron inicialmente referidos al Mioceno temprano (Suárez et al., 1990; Buldrini y Bostelmann, 2011; Buldrini et al., 2015). En este capítulo se realizó una reevaluación de las afinidades taxonómicas de esta fauna, así como una revisión de las edades radioisotópicas reportadas en las localidades que las contienen. Esto con el fin de clarificar tanto su diversidad taxonómica como contexto geocronológico.

El capítulo III abarca el estudio de una pequeña asociación de roedores que fueron colectados por nuestro equipo de investigación, entre 2018 y 2019, en rocas del Mioceno Inferior de la Formación Cura-Mallín que afloran al sur de la Laguna del Laja. Estudios previos sugieren que las asociaciones de mamíferos del Mioceno temprano a tardío de la localidad fosilífera de Laguna del Laja (formaciones Cura-Mallín y Trapa-Trapa), comprenden decenas de taxones no descritos (Flynn et al., 2008). Es necesaria una mejor comprensión de las afinidades taxonómicas de estas asociaciones, ya que representan una de las pocas faunas conocidas en la cordillera principal Andina centro-sur. En este capítulo, se describen en detalle varios especímenes de roedores caviomorfos recuperados recientemente en rocas del Mioceno temprano tardío de la Formación Cura-Mallín en Laguna del Laja,

incluyendo una especie nueva y se proporciona una breve discusión de su importancia cronológica, biogeográfica y paleoambiental.

En el capítulo IV se estudiaron en detalle todos los mamíferos fósiles recuperados durante nuestras campañas de terreno en la zona de Laguna del Laja en estratos del Mioceno temprano tardío (17,7–16,4 Ma) de la Formación Cura-Mallín y se proporciona una breve discusión de su significancia bioestratigráfica, biogeográfica y paleoambiental.

En el capítulo V se hace un cambio de enfoque, desde uno “local” concentrado en el estudio de la fauna de la Formación Cura-Mallín, a un enfoque más regional al evaluar el efecto de los cambios ambientales globales y regionales sobre la evolución de la fauna sudamericana. La idea surge a partir de la “generalización” de la hipótesis central de esta tesis. Es posible proponer que las sucesivas asociaciones de mamíferos de Sudamérica mostraron adaptaciones ecomorfológicas hacia ambientes progresivamente más áridos, como consecuencia del alzamiento de los Andes durante el Cenozoico. Algunas de las adaptaciones ecomorfológicas más importantes mostradas por estas faunas pudieron ser el incremento de la hipsodoncia o el tamaño corporal, rasgos potencialmente estimables para los mamíferos Cenozoicos extintos de Sudamérica. Para poner a prueba la hipótesis antes mencionada se utilizó una aproximación macroevolutiva y macroecológica y se utilizaron los mamíferos del Orden Notoungulata como modelo de estudio. Los notoungulados son un clado de mamíferos herbívoros nativos del subcontinente (hoy extintos) que presentan una importante diversidad taxonómica y ecomorfológica, siendo dominantes en los ecosistemas terrestres de Sudamérica durante la mayor parte del Cenozoico (Simpson, 1980; Croft et al., 2020). Durante el desarrollo de este capítulo se recopiló una extensa base de datos de ocurrencias de notoungulados (incluyendo nuevos datos generados a partir del análisis de la fauna de la Formación Cura-Mallín, así como datos obtenidos de la *Paleobiology Database*) y estimaciones del tamaño corporal e hipsodoncia con los objetivos de caracterizar el modo evolutivo de estos rasgos fenotípicos a lo largo del tiempo, e investigar en qué medida diversos factores (e.g., desarrollo de ambientes abiertos) han influenciado estos rasgos a lo largo del tiempo, y si la selección de especies (en un sentido amplio) actuó sobre estos rasgos mediante tasas de especiación o extinción diferenciadas.

En el capítulo VI se presenta una síntesis y discusión general sobre los principales resultados de los artículos publicados. Finalmente, en el Capítulo VII se presentan las conclusiones obtenidas en esta tesis.

1.9 Metodología

Para el logro de los objetivos planteados, se realizaron distintas actividades que se describen brevemente a continuación.

1.9.1 Autorización para la colección de vertebrados fósiles en Chile

La colección de fósiles en Chile está sujeta a la Ley N° 17.288 sobre Monumentos Nacionales. Por lo tanto, cualquier trabajo de prospección con intervención y/o excavación paleontológica, en terrenos públicos o privados, debe contar con la autorización previa del Consejo de Monumentos Nacionales (CMN). Durante el desarrollo de la presente tesis doctoral se obtuvo dicha autorización del CMN especificada con la orden 5612 de fecha 20/11/2017.

1.9.2. Revisión bibliográfica

Se realizó un estudio bibliográfico de los trabajos sedimentológicos, estratigráficos y paleontológicos realizados en las unidades que conforman la Cuenca de Cura-Mallín (ver detalles en sección 1.3.3).

1.9.3 Trabajo de campo

Un fósil en sí mismo solo provee una información limitada (principalmente taxonómica). Es por ello que el estudio de los restos fósiles siempre debe estar asociado al contexto estratigráfico donde fue encontrado. En este sentido, en el marco del proyecto FONDECYT 1151146 (*“Tectonosedimentary evolution of the mid-Cenozoic basins in the forearc and Main Andean Cordillera of south-central Chile (~36°–43°S)”*) se realizó el levantamiento geológico de superficie de las diferentes secciones de la Formación Cura-Mallín en las localidades de Lonquimay y la Laguna del Laja (Figura 1.7). De tal forma, todos los ejemplares fósiles coleccionados tienen un nivel estratigráfico de proveniencia relativamente bien determinado. Una vez encontrado algún ejemplar fósil, se tomó el dato de

proveniencia geográfica utilizando un GPS. Los restos fósiles fueron envueltos cuidadosamente en papel de embalaje y debidamente rotulados (especificando localidad de colecta, fecha y descripción preliminar), para su transporte al Laboratorio.



Figura 1.7. Fotografías de algunos de los afloramientos de la Formación Cura-Mallín prospectados durante el desarrollo de la presente tesis doctoral en **(a)** Lonquimay (vista de los afloramientos lacustres presentes en la base del Cerro Tallón), y **(b)** la Laguna del Laja (tope del Cerro Campamento, y vista al Estero Trapa-Trapa Este).

1.9.4 Trabajo de Laboratorio

En el laboratorio, se procedió a la limpieza y preparación de los fósiles colectados durante el desarrollo de esta investigación. Para la limpieza de éstos se utilizó etanol, agujas y excavadores curvos. Cuando el fósil se encontró adherido a la roca caja (generalmente una roca volcániclastica competente) se utilizaron martillos neumáticos (*PaleoTools*), modelos “ME-9100 Series” y “Micro Jack Series” para separar el fósil de la roca o para remover sedimento y poder observar los elementos óseos/dentales diagnósticos de material. Estas actividades se llevaron a cabo en el Museo Geológico, de la Universidad de Concepción.

Una vez que los ejemplares fósiles fueron preparados se procedió a su identificación taxonómica hasta el nivel más bajo posible. Para realizar las descripciones e identificación se utilizó la nomenclatura anatómica actualizada acorde a cada grupo taxonómico analizado (ver detalles en los capítulos subsiguientes). Las medidas de los ejemplares descritos se tomaron, en milímetros (mm), utilizando un vernier digital. Además, se revisaron materiales depositados en colecciones paleontológicas de Chile (Museo Nacional de Historia Natural de Santiago, MNHN) y Argentina (Museo Argentino de Ciencias Naturales “Bernardino Rivadavia”, Buenos Aires, y Museo de La Plata, La Plata) con fines de comparación. Los holotipos a partir del cual se describieron nuevas especies fueron depositados en el MNHN. Los nuevos especímenes colectados durante el desarrollo de esta investigación (especialmente en la Laguna del Laja) fueron depositados en la colección de paleontología del Museo de Historia Natural de Concepción (MHNC), Concepción, Chile. De algunos de los especímenes de menor tamaño se tomaron imágenes con Microscopio Electrónico (SEM) en el Centro de Microscopía Avanzada (CMA, Biobío) de la Universidad de Concepción (Concepción) y en la Unidad de Microscopía Avanzada de la Universidad Católica de Chile (Santiago).

En general, las inferencias realizadas sobre las características paleobiológicas y paleoecológicas de las especies de mamíferos encontrados en la Formación Cura-Mallín fueron obtenidas de la literatura (e.g., Croft y Anderson, 2007; Townsend y Croft, 2008; Cassini et al., 2012; Kay et al., 2012a, 2021; Candela et al., 2013b; Bargo et al., 2013; Cuitiño et al., 2019). Finalmente, para investigar el rol del alzamiento andino en la evolución de la hipsodoncia y el tamaño corporal en los notoungulados del Sur de Sudamérica se utilizó la metodología detallada en la sección 5.2 del Capítulo V.

CAPÍTULO II. The Early to late Middle Miocene mammalian assemblages from the Cura-Mallín Formation, at Lonquimay, southern Central Andes, Chile (~38°S): Biogeographical and paleoenvironmental implications



¹**Solórzano A**, Encinas A, Bobé R, Reyes M, Carrasco G. (2019). The early to late middle Miocene mammalian assemblages from the Cura-Mallín Formation, at Lonquimay, southern Central Andes, Chile (~38°S): Biogeographical and paleoenvironmental implications. *Journal of South American Earth Sciences*, 96, 102319.

¹Artículo publicado en 2019, disponible en <https://doi.org/10.1016/j.jsames.2019.102319>

**The Early to late Middle Miocene mammalian assemblages from the Cura-Mallín Formation, at Lonquimay, southern Central Andes, Chile (~38°S):
biogeographical and paleoenvironmental implications**

Solórzano Andrés^{1*}, Encinas Alfonso², Bobe René³, Reyes Maximiliano², Carrasco Gabriel⁴

¹Programa de Doctorado en Ciencias Geológicas, Facultad de Ciencias Químicas, Universidad de Concepción, Víctor Lamas 1290, Concepción, Chile.

²Departamento de Ciencias de la Tierra, Facultad de Ciencias Químicas, Universidad de Concepción, Víctor Lamas 1290, Concepción, Chile

³School of Anthropology, University of Oxford, UK

⁴Servicios Científicos Educativos y Turismo Científico Chile, Pedro León Ugalde 254, San Bernardo, Chile

*Corresponding author: solorzanoandres@gmail.com

Highlights

- Two chronological distinctive mammalian assemblages are recognized in the Cura-Mallín Formation at Lonquimay area.
- The lower assemblage is of Early Miocene age; the upper assemblage is late Middle Miocene age (Serravallian).
- A new species of Interatheriinae is described: *Protyotherium conceptionensis*.
- Both assemblages suggest mostly temperate and forested habitats.
- The area (~38°S) likely did not reach enough paleoaltitudes to cause an important rain shadow at least after 12 Ma.

Abstract

The Cura-Mallín Formation consists of a series of upper Oligocene to Upper Miocene volcanic and sedimentary rocks deposited in continental settings that crop out in the Andean Cordillera in Chile and Argentina between ~37°–39°S. Since the 1990s few fossil mammals have been recovered from this unit in the surroundings of Lonquimay, south-central Chile (38.5°S), and all of them were assigned to the Early Miocene. After a reassessment of the taxonomic affinities of the fauna so far recovered from the Cura-Mallín Formation in the Lonquimay area, and based on the

radioisotopic ages of the fossil-bearing localities, here we recognized two chronological distinctive mammalian assemblages: one of Early Miocene age (probably Colhuehuapian–Santacrucian SALMA), which includes *Nesodon imbricatus* and *Parastrapotherium* sp.; and a second one of late Middle Miocene age (12.8–11.6 Ma; Serravallian; Mayoan SALMA), which includes glyptodonts (Glyptodontidae indeterminate), armadillos (Eutatini indeterminate), macraucheniids (*Theosodon* sp.), a new interatheriid species (*Protypotherium concepcionensis* sp. nov.), and a likely platyrrhine monkey. Therefore, in contrast with previous interpretations, the fauna from Lonquimay is not uniquely restricted to the Early Miocene. The fossil mammals and plants recognized from the area indicate the persistence of mostly temperate and forested habitats with permanent bodies of water during the Early to latest Middle Miocene. This suggests that this part of the Andean Cordillera (38°–39°S) did not reach enough paleoaltitudes (>1000 m) to cause an important orographic rain shadow effect in the foreland basins at least after the late Middle Miocene (c. 12 Ma). However, the role of Neogene South Hemisphere climatic changes in triggering, or reinforcing, the foreland desertification along the south-central Andes is an additional factor that cannot be discarded.

Keywords. Cura-Mallín Formation, Miocene, fossils mammals, rain-shadow effect, *Protypotherium concepcionensis*.

2.1 Introduction

During the last decades our understanding of the extinct continental mammalian biodiversity from Chile has shown significant progress, with the discovery of many new localities and the description of several new taxa, especially from the late Paleogene and Neogene (Flynn et al., 2003, 2005, 2008; McKenna et al., 2006; Hitz et al., 2006; Croft et al., 2007, 2008; Canto et al., 2010; Bertrand et al., 2012; Shockey et al., 2012; Bostelmann et al., 2013; Charrier et al., 2015; Montoya-Sanhueza et al., 2017; Wyss et al., 2018). Despite these efforts, the paleobiodiversity of Chilean mammals remains poorly known, as illustrated by the preliminary taxonomic reports from several of the most diverse localities with dozens of new undescribed taxa and/or taxa in open nomenclature (Flynn et al., 2002a, 2002b, 2008; Croft et al., 2007; Bostelmann et al., 2013; Charrier et al., 2015). This

makes necessary to renew sampling efforts and to refine the taxonomy of poorly known faunas (Canto et al., 2010). The latter is needed for the mammalian remains reported from distinct localities of strata referred to the Cura-Mallín Formation (Marshall et al., 1990; Suárez et al., 1990; Suárez and Emparan, 1995; Flynn et al., 2008).

The Cura-Mallín Formation consists of a series of Upper Oligocene to Upper Miocene volcanic and sedimentary rocks deposited in continental settings that crop out in the Andean Cordillera in Chile and Argentina between 36°–39°S (Suárez and Emparan, 1995; Burns et al., 2006; Flynn et al., 2008; Utge et al., 2009; Radic, 2010). In Chile, some of the best exposures of the Cura-Mallín Formation are located in the surroundings of Laguna del Laja (37–38°S) and Lonquimay (38–39°S) (Niemeyer and Muñoz, 1983; Suárez and Emparan, 1995, 1997; Pedroza et al., 2017). Miocene mammals have been reported from both localities (Marshall et al., 1990; Suárez et al., 1990; Croft et al., 2003; Flynn et al., 2008; Shockey et al., 2012). The first record of mammals from the Cura-Mallín Formation derives from geological and paleontological prospections carried out in 1988–1991 in multiple localities around the Lonquimay town (Marshall et al., 1990; Suárez et al., 1990). These initial works allowed for the recognition of *Astrapotherium* sp. (*Astrapotheria*; Marshall et al., 1990), an indeterminate *Macraucheniidae* (*Litopterna*), cf. *Protypotherium* (*Notoungulata*: *Interatheriidae*), an indeterminate *Glyptodontidae* (*Xenarthra*: *Cingulata*), caviomorphs (*Rodentia*), and a possible mesotheriid (*Notoungulata*) (Suárez et al., 1990); which together were assigned to the Early Miocene (Santacrucian SALMA; Marshall et al., 1990; Suárez et al., 1990). Subsequent works dealing with the Lonquimay mammal fauna have refined or confirmed the taxonomic identity of some of these taxa, increased the number of taxa recognized, and provided a better chronostratigraphic context to this fauna. Croft et al. (2003) provided the first record of a large notoungulate from the Lonquimay area (Cerro Tallón locality) with the report of *Nesodon conspurcatus*, an age-diagnostic taxon of the Santacrucian SALMA (Croft et al., 2003). Though, the taxonomic validity of the last taxon has been questioned as its morphology falls within the range of variability of other *Nesodon* species (Hernández Del Pino, 2018; Cuitiño et al., 2019). Bostelmann et al. (2014) suggest that the astrapothere recovered by Marshall et al. (1990) from the Rio Quepuca must be included in the genus *Parastrapotherium*, a taxon relatively common in the Late Oligocene and Early Miocene (Kramarz and

Bond, 2010). Buldrini et al. (2015) and Buldrini and Bostelmann (2011) confirmed the presence of *Protypotherium* in the Cura-Mallín Formation after finding near the Puente Tucapel locality and suggested a lower Miocene age ('Pinturan' – Santacrucian SALMA) for the remains. However, excepting for *Parastrapotherium* and *Nesodon*, an Early Miocene age for the additional taxa reported from the Lonquimay surroundings are not well-supported by biochronological correlations nor geochronology data.

Recent stratigraphic work and U/Pb radiometric dates by Pedroza et al. (2017) and Rosselot et al. (2019b) in the Cura-Mallín Formation cropping out in the Lonquimay area have challenged some of the ages previous inferred for these taxa (Marshall et al., 1990; Suárez et al., 1990; Buldrini and Bostelmann, 2011). For example, the *Protypotherium* specimen recovered from Puente Tucapel must have a late Middle Miocene or younger age as detrital zircon dates indicate maximum ages of 12.5 and 12.7 Ma for this fossil-bearing stratigraphic section (Pedroza et al., 2017). This raised the question of how many temporally distinctive mammal assemblages are recorded in the Cura-Mallín Formation in the Lonquimay area. Moreover, according to Pedroza et al. (2017), the Macraucheniidae remains (incorrectly identified as '*Macrauchenia litopterna*') also comes from the Puente Tucapel locality. However, Suárez et al. (1990) clearly stated that the Macraucheniidae comes from the south bank of the BioBío river, at the NE foot of Cerro Rucañanco. These cases exemplify the uncertainties in the stratigraphic and geographic provenance of some of the mammalian fossils recovered from Lonquimay. This situation is further exacerbated as the fossils come from an area with discontinuous outcrops. Some of the reported materials have not been described in detail, and sometimes not even illustrated, limiting our understanding of the taxonomic diversity as well as the biochronological and paleoenvironmental significance of the fauna.

During the summers of 2017 and 2018 we conducted geological and paleontological prospections in the Lonquimay area, with special emphasis on the fossiliferous localities mentioned by previous authors (Suárez et al., 1990; Rubilar, 1994; Suárez and Emparan, 1995; Pedroza et al., 2017). Unfortunately, we did not find any new mammal specimens. In order to evaluate the significance of this fauna, here we review all the mammalian specimens recovered from the Cura-Mallín Formation (in the traditional sense of Suarez and Emparan, 1995) in the Lonquimay

area (38°S), now stored in the Museo Nacional de Historia Natural (MNHN in Santiago, Chile), and assess their biostratigraphic, biogeographical and paleoenvironmental significance. We also place our findings within the complex tectonostratigraphic framework of the Cura-Mallín Basin deposition.

2.2 Geological, paleontological and geographical background

The Cura-Mallín basin is part of a chain of basins that formed within the Andean volcanic arc and the foreland of Chile and Argentina between 33° and 43°S between the Upper Oligocene and Upper Miocene (Suárez and Emparan, 1995; Jordan et al., 2001; Burns et al., 2006; Flynn et al., 2008; Utge et al., 2009; Pedroza et al., 2017). The Cura-Mallín basin contains up to 4 km of volcanic and sedimentary rocks with three traditionally well-differentiated geological units, the Cura-Mallín, Trapa-Trapa, and Mitrauquén formations (Niemeyer and Muñoz, 1983; Suárez and Emparan, 1995, 1997; Burns et al., 2006). These geological units were deposited into several sub-basins (Rosselot et al., 2019a) whose lateral transitions are poorly understood because the original paleogeographic configuration was modified during the late Cenozoic deformation and uplift of the Andes, and some of the intervening zones are covered by younger volcanic rocks (Burns et al., 2006).

The Cura-Mallín Formation is the basal unit in the homonymous basin and it is characterized by a predominant volcanic member (with intercalations of sedimentary strata), and a predominant sedimentary member (with intercalations of volcanic strata), which generally overlies it and was deposited in alluvial, fluvial, lacustrine and deltaic environments (Suárez and Emparan, 1995; Burns et al., 2006; Radic, 2010; Pedroza et al., 2017). Different names have been applied locally to these members. Niemeyer and Muñoz (1983) defined the volcanic Río Queuco lower member and the sedimentary Malla-Malla upper member in the Laguna del Laja area. Suárez and Emparan (1995) defined the predominantly volcanic Guapítrio member and the sedimentary Río Pedregoso member in the Lonquimay region. Although traditionally, it has been considered that the sedimentary members of the Cura-Mallín Formation are younger than the volcanic ones (Utge et al., 2009), in the sector of Lonquimay it has been proposed that both members interdigitate and are partially coeval (Suárez and Emparan, 1995; Pedroza et al., 2017). The coeval sedimentation of lithological distinctive members has been also interpreted

as the result of their dissimilar location respect to the Miocene main active volcanic sources (i.e., distal facies being predominantly clastic, and proximal facies being predominantly volcanic; Burns et al., 2006). However, Salinas (1979) had previously considered the sedimentary rocks present in the Guapitrío Member (*sensu* Suárez and Emparan, 1995), to be younger than the volcanic rocks and correlative with the Río Pedregoso Member (*sensu* Suárez and Emparan, 1995). Volcanic and sedimentary rocks included in the Cura-Mallín Formation typically crop out in separate areas, so their correlation has been inferred from their overlapping radiometric ages (Suárez and Emparan, 1995, 1997; Burns et al., 2006). However, some of these ages are dubious since they were obtained by the K-Ar method. Radiometric dates (K-Ar and U-Pb) suggest a Lower to earliest Upper Miocene age (22–10.7 Ma) for the Cura-Mallín Formation strata cropping out in the Lonquimay region (Suárez and Emparan, 1995; Pedroza et al., 2017; Rosselot et al., 2019b, 2019a). In particular, the Guapitrío Member was dated between 22 ± 0.9 and 10.7 ± 1.1 Ma, and the Río Pedregoso Member between 17.5 ± 0.6 and 11.64 ± 0.13 Ma (Suárez and Emparan, 1995, 1997; Pedroza et al., 2017; Rosselot et al., 2019a, 2019b). These geochronological data allow to partially correlate the Cura-Mallín Formation with the Farellones (32° – 36° S) and the Ñirihuau (41° – 47° S) formations (Bechis et al., 2014; Giambiagi et al., 2016). The units overlaying the Cura-Mallín Formation correspond to the Trapa-Trapa and Mitrauquén formations, which crop out in the Laguna del Laja, and Lonquimay areas, respectively. Both formations are characterized predominantly by coarse-grained volcanoclastic deposits and volcanic rocks (Niemeyer and Muñoz, 1983; Suárez and Emparan, 1995, 1997; Pedroza et al., 2017). Radiometric dates (Ar-Ar and K-Ar) restrict both units to the Upper Miocene; 9.5 ± 2.8 and 8.0 ± 0.3 Ma for Mitrauquén Formation and 10.10 ± 0.20 and 8.9 ± 0.1 for Trapa-Trapa Formation (Suárez and Emparan, 1997; Herriott, 2006; Flynn et al., 2008). Both units are therefore correlative as proposed by Herriott (2006).

Pedroza et al. (2017) proposed a new stratigraphic scheme for the Cura-Mallín Formation in the Lonquimay area. They separated the traditionally recognized Cura-Mallín Formation (*sensu* Suárez and Emparan, 1995) into two units consisting of the mainly volcanic Guapitrío Formation (previously Guapitrío member), and the sedimentary Río Pedregoso Formation (previously Río Pedregoso member) that they divided (from base to top) in the Quilmahue, Rucañanco and Bío-Bío members.

Pedroza et al. (2017) also proposed to use the term Cura-Mallín Group, which includes their Guapitrío and Río Pedregoso 'formations'. However, Pedroza et al.'s (2017) interpretations could be biased by the complex stratigraphic scenario exhibited by the study area and exacerbated by the lack of continuous outcrops. In this sense, while waiting for a comprehensive stratigraphic revision of the belonging to the Cura-Mallín Basin, and for the sake of simplicity, we will use the name Cura-Mallín Formation in the traditional sense of Suárez and Emparan (1995).

There is some controversy regarding the tectonic context in which the geological units included in the Cura-Mallín Basin were deposited. There is a consensus that the fluvial deposits of the Upper Miocene Mitrauquén Formation (and the coeval Trapa-Trapa Formation) are syntectonic deposits based on the occurrence of conglomeratic facies and growth strata in this unit (Melnick et al., 2006). Early authors suggested that the Cura-Mallín Formation was deposited in a pull-apart basin related to the Liquiñe–Ofqui system fault (Suárez and Emparan, 1995). Subsequent authors agree that the Cura-Mallín Formation was deposited during the Upper Oligocene to Lower Miocene under an extensional regimen, later subjected to a tectonic inversion (Jordan et al., 2001; Burns et al., 2006). However, the time in which the basin inversion begins has been a matter of discussion, with two opposing models: 1) The sedimentation of the Cura-Mallín Formation took place under extensional conditions and the first synorogenic facies occurred after 9–8 Ma, giving rise to deposition of the overlying Mitrauquén and Trapa-Trapa Formations (Jordan et al., 2001; Burns et al., 2006; Melnick et al., 2006; Radic, 2010); 2) only the lowest strata of the Cura-Mallín Formation are synextensional, while their upper beds, as well as their overlying units (Mitrauquén and Trapa-Trapa Formations) are synorogenic and were deposited in intermontane basins likely related with the rise of the Andes since ~19–18 Ma (Spikings et al., 2008; Utge et al., 2009; Rosselot et al., 2018). After a recent extensive review on the available geochronological, structural, geochemical, thermochronological and basin subsidence evidence (see Rosselot et al., 2019a for details), it is more likely that at least the upper part of the Cura-Mallín Formation is related to compressional rather than extensional conditions. The Early Miocene beginning of the compressional regime at this latitudes is consistent with observations north and south of the Cura-Mallín Formation outcrop area (Charrier et al., 2002; Kay and Copeland, 2006; Echaurren et al., 2016; Cuitiño et al., 2016; Encinas et al., 2018; Folguera et al., 2018a, 2018b).

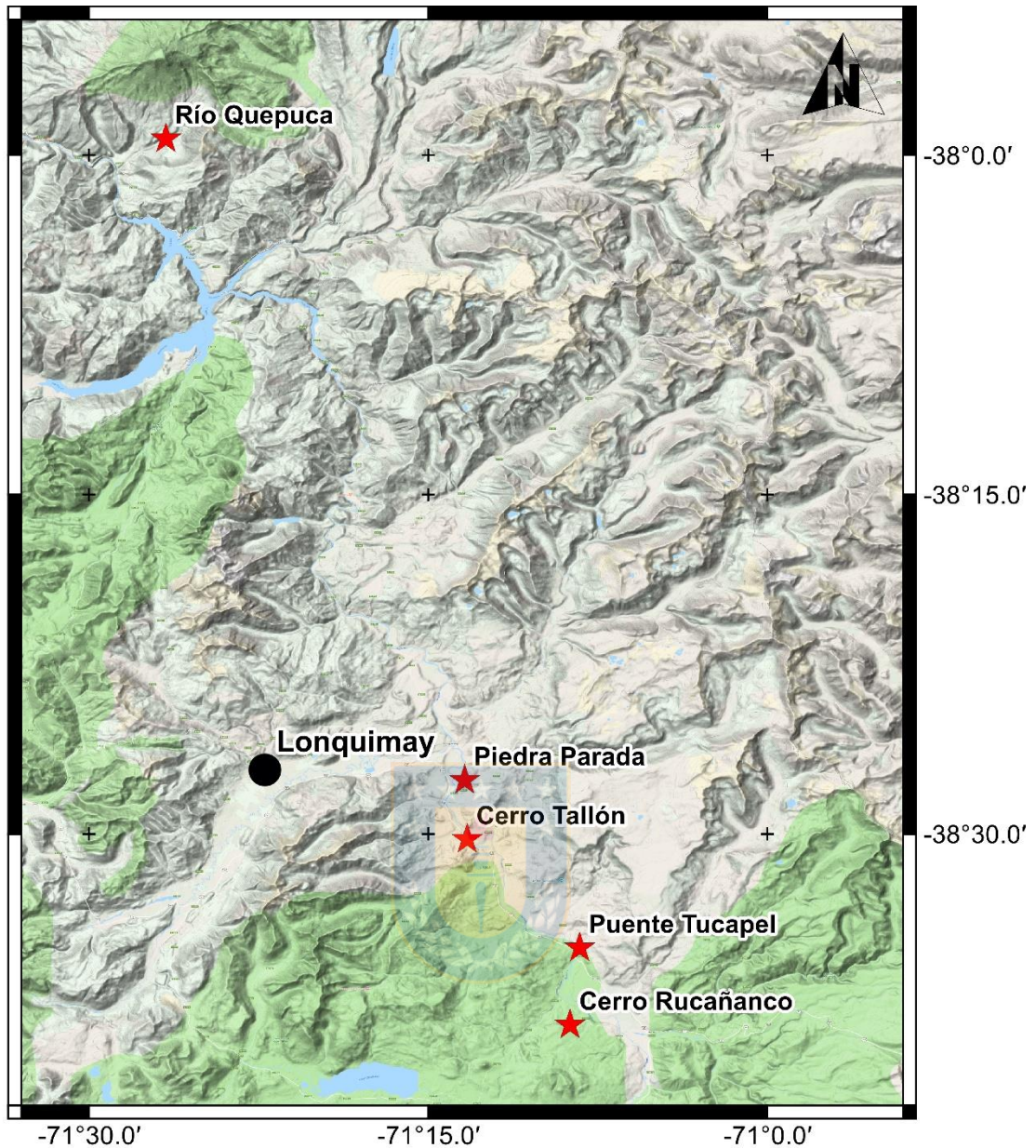


Figure 2.1. Geographical settings of the fossil-bearing localities (star) mentioned in the text.

As previously mentioned, several mammals have been recognized in distinct localities of the Cura-Mallín Formation in the Lonquimay region (Figure 2.1) (Marshall et al., 1990; Suárez et al., 1990; Croft et al., 2003; Buldrini and Bostelmann, 2011; Bostelmann et al., 2014; Buldrini et al., 2015). Additional taxa recognized in the area includes a continental bird (*Meganhinga chilensis*), an indeterminate Bufonidae (Anura), several plants (based in pollen and leaves) as well as freshwater fishes and invertebrates which are relatively common along the entire stratigraphic sequence (Salinas, 1979; Palma-Heldt, 1983; Palma-Heldt and

Rondanelli, 1990; Rubilar, 1994; Alvarenga, 1995; Azpelicueta and Rubilar, 1997; Arratia, 2015; Pedroza et al., 2017; Guevara et al., 2018).

Recent radiometric ages have improved the understanding about the stratigraphic relationships of the distinct sequences of the Cura-Mallín Formation cropping out in the Lonquimay area (Pedroza et al., 2017; Rosselot et al., 2019b). An updated schematic stratigraphic arrangement of the mammal-bearing localities in this area is provided in the Figure 2.2. The main difference with the proposal of Pedroza et al. (2017) is in the location of the Piedra Parada succession (see details below). In the following lines we provide a brief characterization of the Miocene mammal-bearing localities within the Lonquimay region.

Río Quepuca. The locality is along the Quepuca River, 50 km north of the Lonquimay town. It consists of a 14 m thick succession of crossbedded sandstones and black shales (Figure 2.1; Marshall et al., 1990). The black shale and crossbedded sandstone association was interpreted as having been deposited in a meandering river system, adjacent to an active volcano (Marshall et al., 1990). This levels are comparable to sedimentary strata exposed along the Guapitrío River (where the Guapitrío member takes its name Suárez & Emparan, 1995, 1997). Therefore, this locality is likely circumscribed to the Guapitrío member (Bostelmann et al., 2014). Although the Guapitrío Member yielded K/Ar ages between 22 and 10.7 Ma (Suárez and Emparan, 1995, 1997), radiometric ages are not available for the Río Quepuca locality. However, the fossil content (astrapothere) has been referred to the Santacrucian (Marshall et al., 1990) or the Colhuehuapian SALMA (Bostelmann et al., 2014).

Cerro Tallón. The locality is 15 km to the southwestern of the Lonquimay town in the western edge of the Biobio River (Figure 2.1). Deposits at the base of the Cerro Tallón in the banks of the Biobio river includes shales and carbonaceous shales with a high content of fish scales and spines are intercalated with fine-to medium-grained sandstones showing lower flow regime plane lamination, undulose stratification, and synsedimentary folds (Pedroza et al., 2017). Fresh-water fishes and a large notoungulate have been reported from this locality (Rubilar, 1994; Croft et al., 2003; Pedroza et al., 2017). The last being recovered from 5 m thick succession of fine to coarse grain montmorillonite-rich sandstone with tuffaceous intercalations (Croft et al., 2003). A single radiometric K-Ar dates from a level overlaying the recovered mammal yields an age of 17.5 ± 0.6 Ma (Suárez and Emparan, 1995; Croft et al.,

2003). In addition, the notoungulate recovered from this locality has been suggested as a taxon indicative of the Santacrucian SALMA (Croft et al., 2003). Therefore, both radiometric and biochronological evidence suggest a late Early Miocene (Santacrucian SALMA) age for the locality.

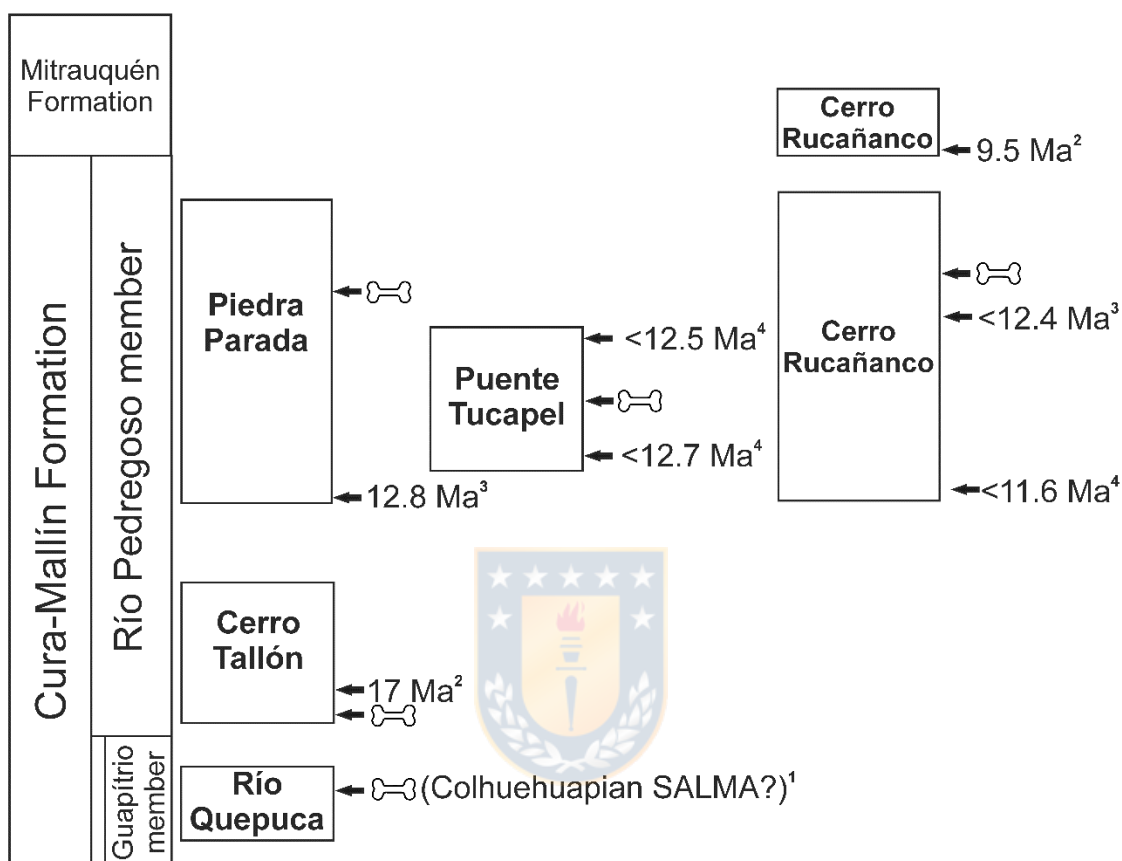


Figure 2.2. Schematic (not in scale) chronostratigraphic framework of the fossil mammal-bearing localities among the Cura-Mallín Formation cropping out in the surroundings of Lonquimay, based on radiometric ages (⁴Pedroza et al., 2017; ³Rosselot et al., 2019b; ²Suárez and Emparan, 1995) and biochronologic correlation (Bostelmann et al., 2014; ¹Kramarz and Bond, 2010). The bone symbol represents the approximate location of the fossil-bearing levels along each stratigraphic sequence.

Piedra Parada. The locality is 13 km to the southwestern of the Lonquimay town, in the eastern edge of the Biobio River (Figure 2.1). The stratigraphic succession is dominated by very fine-to medium-grained sandstones with numerous freshwater bivalve fossils, overlain by matrix-supported, polymictic conglomerates with poorly sorted, subrounded to angular clasts (Pedroza et al., 2017). Glyptodont osteoderms, fresh-water invertebrates, as well as wood and pollen have been recovered from this locality (Palma-Heldt, 1983; Suárez et al., 1990; Pedroza et al., 2017). Early K-Ar dates from the cliff of Piedra Parada indicated a Middle Miocene age (13 Ma)

(Suárez and Emparan, 1995). Recent U-Pb dates in a volcanic tuff from the base of the Piedra Parada section indicates a late Middle Miocene age (12.8 Ma; Rosselot et al., 2019b). Pedroza et al. (2017) had assigned this section to the Early Miocene based on stratigraphic interpretations but the cited radiometric ages indicate that this inference is erroneous.

Puente Tucapel. The 102 m thick succession crops out around 25 km to the south western of the Lonquimay town, in the eastern Biobio river margin (Figure 2.1). The succession is dominated by sandstones with minor mudrocks and conglomerates, interpreted as deposited in deltaic and fluvial environments (Pedroza et al., 2017). An interatheriid has been reported in this locality, being referred without definitive evidences to the 'Pinturan'–Santacrucian SALMAs (Suárez et al., 1990; Buldrini and Bostelmann, 2011; Buldrini et al., 2015). However, detrital zircons ages from the base and top of the Puente Tucapel succession yielded maximum ages of 12.7 ± 0.3 and 12.5 ± 0.3 Ma respectively (Pedroza et al., 2017).

Cerro Rucañanco. The locality is 29 km to the south western of the Lonquimay town, in the western Biobio river margin. In this area a 180 m thick succession of coarse-to-medium grained conglomerates, sandstones showing cross-bed stratification and inclined structures, with subordinate siltstones and channelized breccias, is exposed (Suárez and Emparan, 1995). The succession present facies associations typical of Gilbert-type deltas according to Suárez and Emparan, (1995) and Pedroza et al. (2017). The macraucheniid, bufonid, continental bird, as well as some freshwater fishes and invertebrates comes from this locality (Suárez et al., 1990; Alvarenga, 1995; Guevara et al., 2018). The coarse-grained succession of Cerro Rucañanco have been correlated with those of the Piedra Parada (Suárez and Emparan, 1995; Figure 2.2). Recent U-Pb dating of detrital zircons from the middle section of the Cerro Rucañanco yielded a maximum depositional age of 12.4 Ma (Rosselot et al., 2019b). A sample obtained from beds located in another section located in the Biobio banks at the base of Cerro Rucañanco yielded a detrital zircons age of 11.64 Ma (Pedroza et al., 2017). Pedroza et al. (2017) considered that the Biobio section is stratigraphically above that of the Cerro Rucañanco. However, we concur with Suárez and Emparán (1995) that the Biobio section underlies the latter as it is located in a lower topographic position and strata in both sections are almost horizontal.

It is important to note that the Piedra Parada, Puente Tucapel, and Cerro Rucañanco sections show similar facies that, from base to top, consist of tuffs (only present at the base of the Piedra Parada section, dated in 12.8 Ma by Rosselot et al., 2019b), finely laminated lacustrine siltstones and sandstones, and coarse-grained sandstones and conglomerates. Therefore, these sections can be also correlated based in facies similarities (Figure 2.2). The Mitrauquén Formation crops out at the top of the Cerro Rucañanco, overlying a covered area between this unit and the Cura Mallín Formation. Therefore, the age of the Cura-Mallín Formation at the Puente Tucapel, Piedra Parada and Cerro Rucañanco sections is constraint between 12.8 Ma (late Middle Miocene, Serravallian; the age of the tuff at the base of the succession; Rosselot et al., 2019b) and 9.5 Ma (early Middle Miocene, Tortonian; the oldest age for the Mitrauquén Formation; Suárez and Emparan, 1997). However, the fossil-bearing sections of Piedra Parada, Puente Tucapel, and Cerro Rucañanco probably have ages close to 12.8–11.64 Ma (Serravallian; Figure 2.2), because the available detrital zircons maximum ages could be interpreted as near-sedimentation ages. The similar age range for the radiometric dates (Pedroza et al., 2017; Rosselot et al., 2019b) is also consistent with this idea.

2.3 Material and methods

The original geographic provenance and collector labels for all the specimens deposited in the MNHN was reviewed in order to clarify this topic. All measurements are presented in millimeters (mm) and were made using a digital caliper. Dental terminology follows the convention of upper case for upper teeth (i.e., I, C, P, M) and lower case for lower teeth (i.e., i, c, p, m). For Cingulata osteoderm we follow the nomenclature of Croft et al. (2007) and González-Ruiz (2010). For macraucheniids, and interatheriids we follow the dental nomenclature of Soria and Hoffstetter (1985), and Reguero et al. (2003), respectively. Taxonomic nomenclature for higher categories follows McKenna and Bell (1997). However, we acknowledged the increasing body of literature (based in phylogenetic analyses on morphological and molecular data) highlighting different systematic hypothesis to those of McKenna and Bell (1997), especially regarding the arrangement within Cingulata (e.g. Delsuc et al., 2016; Gaudin and Wible, 2005; Mitchell et al., 2016). The use of traditional (McKenna and Bell 1997) over more recent systematic

hypotheses do not affect our general conclusions. The specimens used for comparison are included in the Electronic Supplementary Materials.

Institutional abbreviations. **SGO.PV**, Museo Nacional de Historia Natural de Santiago, Santiago, Chile.

2.4 Systematic paleontology

MAMMALIA Linnaeus, 1758
ASTRAPOTHERIA Lydekker, 1894
ASTRAPOTHERIIDAE Ameghino, 1887
PARASTRAPOTHERIUM Ameghino, 1895
Parastrapotherium sp.

Figure 2.3

Marshall et al., 1990: *Astrapotherium* sp.

Bostelmann et al., 2014: *Parastrapotherium* sp.

Revised materials. SGO.PV.4003; a fragment of right maxillary with P4–M3, and an isolated left M3, from a single individual.

Geographic and stratigraphic provenance. The specimen was collected by L. Marshall and P. Salinas in 1990 along the east bank of the Río Quepuca, southeast of Santa Bárbara, a tributary of the Biobío River, in Central Chile (38° 3'2.38"S; 71°24'35.88"W). The specimen comes from fluvial and lacustrine facies resembling those exposed along the Guapitrío River (Marshall et al., 1990) and might belong to the Guapitrío member (*sensu* Suárez and Emparan, 1995). Based in biochronological correlation with Patagonian faunas and the known radiometric ages for the Cura-Mallín Formation, the age of this specimen is likely Early Miocene (Colhuehuapian SALMA; Dunn et al., 2013; Kramarz and Bond, 2010, 2008).

Description. With half the size of M1, the P4 is the smallest of the preserved dental series (see ESM_2). The P4 has a single lingual cusp (protocone). Along the labial edge of the ectoloph there is a well-developed paracone fold and mesially directed parastyle (Figure 2.3a). The last two structures are positioned more mesially than the protocone. The protoloph is transversely more developed than the metaloph (Figure 2.3a), as in *Astrapotherium*, *Astrapothericulus*, *Parastrapotherium*, but unlike *Maddenia* (Kramarz and Bond, 2008, 2009; Kramarz, 2009). The

mesiodistally oriented central valley is posterolingually closed (Figure 2.3). In labial view, the P4 exhibit a labial fold broader at the base than in *Astrapotherium* and *Astrapothericulus* (Kramarz and Bond, 2008, 2010). The labial cingulum is absent at the base of the labial fold, while a well–development mesiolingual cingulum is present in lingual view.

In occlusal view, the M1 and M2 are similar in shape, both are nearly trapezoidal with a wider labial edge and exhibits a clearly folded ectoloph. In M1 the protoloph and metaloph exhibit a rather similar transverse development (Figure 2.3a) and the parastyle and paracone fold are slightly developed. The M2, larger than the M1, has a strongly folded ectoloph (parastyle and paracone fold are conspicuous), their protoloph is transversely more developed than the metaloph, and the mesial portion of the parastyle overlaps the metaloph of M1 (Figure 2.3a). In M1 and M2 a median fossette is absent (probably due to the advanced wear of the specimen), and the central valley is wide even in the advanced stages of wear of M1 (Figure 2.3a). The M3 is rather subtriangular in occlusal view due to the reduction of the metaloph and the lack of a hypocone (Figure 2.3b). The M3 also has a strongly folded ectoloph (conspicuous parastyle and paracone fold), and the mesial portion of the parastyle overlaps the metaloph of M2. Even considering the advance wear, the central valley of the upper molars remains wide but isolated on M1 (Figure 2.3a).



Figure 2.3. *Parastrapotherium* sp. (SGO.PV.4003) from the Río Quepuca (Figure 2.1), Río Guapitrio Member, Cura-Mallín Formation (Early Miocene), Chile. A fragment of right maxillary with P4–M3 in occlusal view (a); isolated left M3 in occlusal view (b). Scale bar = 20 mm.

Remarks. The upper molar and premolars show an advanced stage of wear (Figure 2.3), thus SGO.PV.4003 represents an adult individual. The specimen represents a large astrapothere (like *Parastrapotherium*, *Astrapotherium*, *Xenastrapotherium*, and *Granastrapotherium*) as the M2 is larger than 40 mm long (Kramarz and Bond,

2009). The following character combination allows us to refer SGO.PV.4003 to the genus *Parastrapotherium*: upper premolars with labial fold broader at the base than in *Astrapotherium* and *Astrapothericulus*, upper molars without basal lingual cingulum, M3 hypocone absent (Kramarz and Bond, 2008, 2009). Thus, we agree with the interpretations of Bostelmann et al. (2014) about the taxonomic affinities of SGO.PV.4003.

In the genus *Parastrapotherium* there are circumscribed six valid species, with four species in the Deseadan SALMA, *Parastrapotherium holmbergi* Ameghino, 1895, *Parastrapotherium martiale* Ameghino, 1901, *Parastrapotherium crassum* Ameghino, 1902, and *Parastrapotherium? voghti* (Mercerat, 1891), and three species from the Colhuehuapian SALMA, *Parastrapotherium symmetrum* Ameghino, 1902, *Parastrapotherium herculeum* Ameghino, 1899, and *Parastrapotherium martiale* (also known from the Deseadan SALMA) (Kramarz and Bond, 2008, 2010). After the diagnosis of most of the species within *Parastrapotherium* are based on lower teeth and/or upper canines (Kramarz and Bond, 2008, 2010), we are unable to achieve a species level identification for the Rio Quepuca specimen. All these species were recognized from Argentina (Kramarz and Bond, 2008, 2010), whereas SGO.PV.4003 represent the first evidence of the genus in Chile, and represents together with those of the Early Miocene of Cerro Banderas (Kramarz et al., 2005) the northernmost record of the genus (Bostelmann et al., 2014).

LITOPTERNA Ameghino, 1889

MACRAUCHENIIDAE Gervais, 1855

'CRAMAUCHENIINAE' Ameghino, 1902

THEOSODON Ameghino, 1887

Included species. *Theosodon lydekkeri* Ameghino, 1887 (type species), *Theosodon lallemanti* Mercerat, 1891, *Theosodon fontanae* Ameghino, 1891, *Theosodon gracilis* Ameghino, 1891, *Theosodon patagonicum* Ameghino, 1891, *Theosodon karaikensis* Ameghino, 1904, *Theosodon. garretorum* Scott, 1910, *Theosodon pozzii* Kraglievich and Parodi, 1931, *Theosodon? frenguelli* Soria, 1981, and '*Theosodon*' *arozquetai* McGrath et al., 2018.

Geographic and Stratigraphic Distribution. Early Miocene to late Middle Miocene (Colhuehuapian–Laventan? SALMAs) of Argentina (Sarmiento, Pinturas, Santa

Cruz, and Collon Cura formations), Chile (Cura-Mallín, Pampa Castillo, Chucal, Río Negro, and Río Cisnes faunas), Bolivia (Quebrada Honda Fauna and Yecua Formation), Colombia (La Venta Fauna), and Peru (Fitzcarrald Arch) (Kramarz and Bond, 2005; McGrath et al., 2018).

Remarks. Several of the early species referred to this genus were based on fragmentary remains and/or ambiguous diagnoses (e.g. *T. fontanae*, *T. patagonicus* and *T. karaikensis*), hence the number of names proposed in the literature likely exceeds the actual number of taxa (Cifelli and Guerrero, 1997; McGrath et al., 2018). In addition, *T. ? frenguelli* have a reduced m3 entolophid (Soria, 1981), unlike other *Theosodon* spp., hence this taxa is not clearly referred to the genus (Cifelli and Soria, 1983). As several authors (Cifelli and Guerrero, 1997; Schmidt, 2013; McGrath et al., 2018) have pointed out, *Theosodon* is in need of comprehensive systematic revision, which is out of the scope of the present work.

Theosodon sp.

Figure 2.4

Suárez et al., 1990: *Macraucheniidae* gen. et sp. indet.

Pedroza et al., 2017: '*Macrauchenia litopterna*'

Revised materials. SGO.PV.4000; a right hemimandible, with a portion of the symphyseal region, comprising the p1–m3, and an associated posterior fragment of skull.

Geographic and stratigraphic provenance. The specimen was collected by R. Wall in 1990 in the south bank of the BioBío river, at the northern foot of the Cerro Rucañanco in lacustrine facies of the Rio Pedregoso Member (Suárez et al., 1990), late Middle Miocene (Serravallian) age (Pedroza et al., 2017; Rosselot et al., 2019b; Figure 2.2).

Description. The mandible is relatively thin and gracile (mandible height of 25 mm below the m1 and 29.6 mm below the m3). The mandibular symphysis extends posteriorly to the level of the anterior edge of p2 (Figure 2.4a,b). Posterior to the symphysis, the horizontal ramus is slightly thicker dorsoventrally (ca. 21 mm between p2 and p3, ca. 26 mm below the midpoint of m3). Although partially broken, in the labial side of the mandible is possible to recognize one mental foramina located below the anterior portion of the p3 (Figure 2.4b). The angle and coronoid process of the mandible are partially broken, but them broadly resembles those of

other macraucheniiids (McGrath et al., 2018). In the mandible, there is the p1–m3 series in situ. These teeth show little wear and the series does show deciduous teeth, indicating that the specimen is a young adult individual.

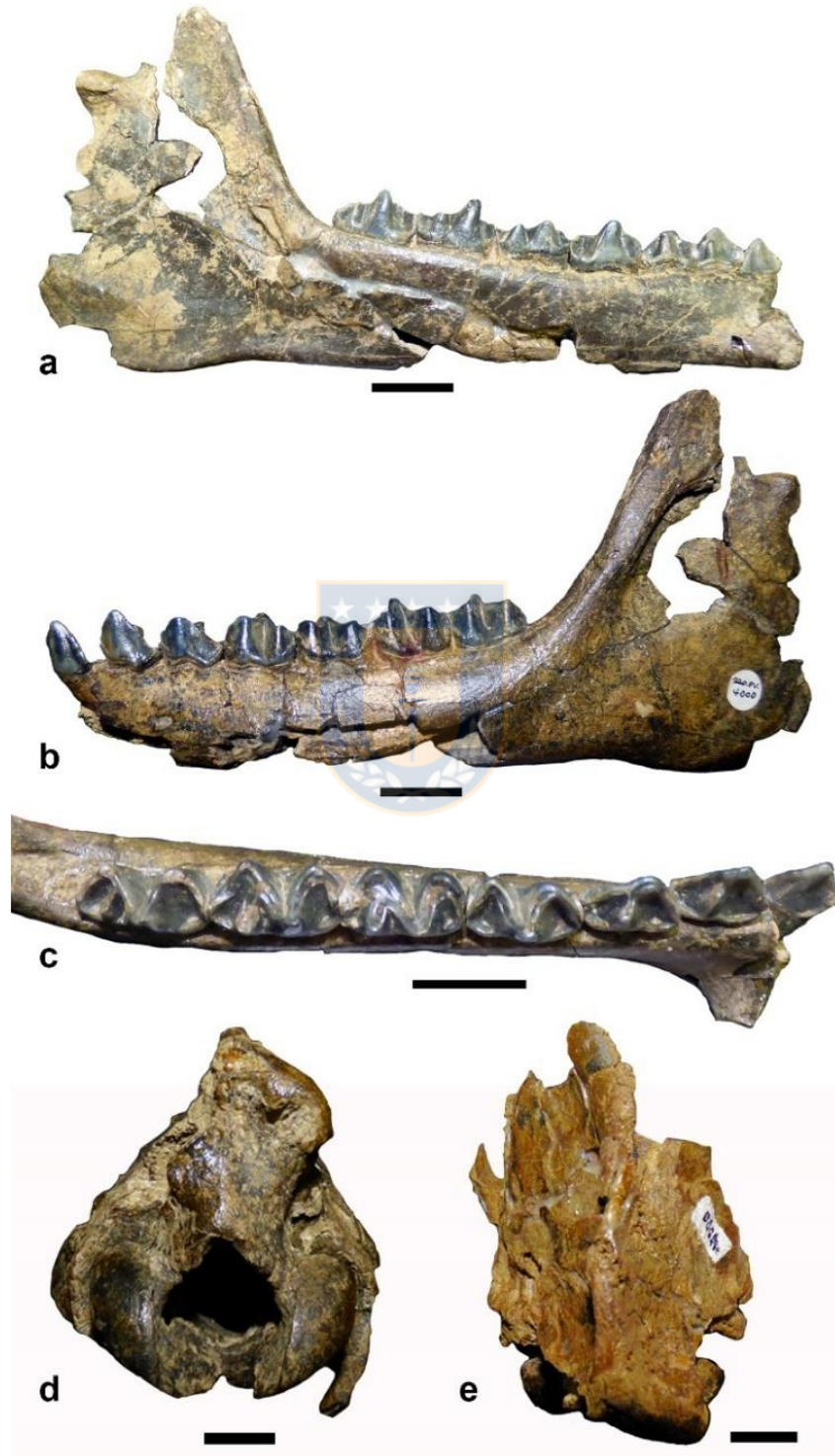


Figure 2.4. *Theosodon* sp. (SGOP.4000) from the Cerro Rucañanco locality, Río Pedregoso Member, Cura-Mallín Formation (late Middle Miocene; Serravallian), Chile. Mandible in lingual (a), labial (b) and occlusal (c) views; a fragment of skull in posterior (d) and dorsal (e) views. Scale bar = 20 mm.

The p1–p3 are relatively simple (caniniform–like) with a single major cuspid (protoconid). The talonid and trigonid of p1–p3 are similar in size. The p1 is the smaller premolar, while the posterior ones progressively increasing in size and complexity. A small diastema separates the p1 and p2. In the posterolingual side of p2 and p3 are a columnar metaconid (absent in p1). The metaconid of p3 is larger than those of p2; p3 lacks a paraconid (unlike *Cramauchenia* and *Pternoconius*). The protocristid of p1–p3 is not completely aligned with the mandible axis (there are rather slightly imbricated), that is the reasons for why these premolars are partially overlapping in lateral and medial views (Figure 2.4c). In p1–p3 the preprotocristid is rather straight and mesiolingually directed. A lingual cingulum is present in the mesiolingual margin of p1, and it is relatively continuous along the lingual side of p2 and p3, being less–development in the lingual portion of the metaconid. A labial cingulum is also present in the anterior-most side of the p3, less developed in p2, and absent in p1. The p4, larger than p3, is molariform with a selenedont and bicrescent pattern resembling most *Macraucheniidae* (Soria and Hoffstetter, 1985). The p4 lacks entolophid and distinctive paraconid and entoconid (Figure 2.4c). The hypolophulid is shorter than paralophid, unlike *Cramauchenia* (Schmidt, 2013; Schmidt and Ferrero, 2014). The trigonid is anteroposteriorly wider than the talonid, but in advances stages of wearing this feature likely disappear, generating a talonid–trigonid of a rather similar size. The metaconid is the higher cuspid in the lingual edge. In the labial edge, the hipoconid and protoconid are the most elevated cuspid. Both are mesiodistally separated by a wide and deep ectoflexid. In fact, the p4 ectoflexid is wider than those of m1 and m2, being comparable in width to the m3 (Figure 2.4c).

The m1 is slightly larger than the p4, unlike *T. gracilis* and *T.? frenguellii* in which the p4 is larger than the m1 (ESM_3). The m2 and m3 are of similar size. In m1 and m2 the trigonid is reduced with respect to the talonid, and the opposite occurs in the m3 (Figure 2.4c). However, as previously mentioned this pattern probably is not observable in advances stages of wear. The lower molars (m1–m3) present a distinct entoconid, connected mesiolabially to the middle portion of the oblique cristid (anteriorly to the metaconid; Figure 2.4c), forming a relatively long crest (entolophid). This large entolophid reaches the medial edge of the m1–m3 (Figure 2.4c). In m1–m3 the paraconid and hypolophulid are indistinct and merged into the

paralofid and hypolophulid, respectively. The hypolophulid is larger and better developed than the paralofid. In m1–m2 the paralofid reach the lingual side (Figure 2.4c). In m3 the paralofid reach the lingual side. The entoconid of m1–m3 is large and mediolaterally opposed to the hypolophulid. In p4–m3 a labial cingulum is present in the paralofid and hypolophulid, but not in the ectoflexid, and two lingual cingula are present on either side of the metaconid. The p4–m3 series is mesiodistally aligned. The skull fragment is narrow, with a slender braincase and prominent sagittal crest clearly observed in dorsal view (Figure 2.4d,e). In lateral view, the occipital condyles do not protrude at the level of the nuchal crest.

Remarks. Size is a relevant feature for distinguishing among Macraucheniidae genera, and the Cura-Mallín specimen is more similar in size to several *Theosodon* species, being definitely larger than other ‘Cramaucheniinae’ (Cheme–Arriaga et al., 2016; Forasiepi et al., 2016; McGrath et al., 2018; Soria, 1981), and smaller than several Macraucheniinae (Schmidt, 2013).

A well–developed m3 entolophid attached to the obliquid crista is present in SGO.PV.4000, *Theosodon*, *Coniopternium*, *Scalabrinitherium*, *Paranauchenia*, differing from *Cramauchenia*, *Oxydontherium*, *Xenorhinotherium*, *Macrauchenia*, *Macrauchenopsis*, in which the m3 entolophid is absent (Soria, 1981; Cifelli and Soria, 1983; Soria and Hoffstetter, 1985; Schmidt, 2013; Schmidt and Ferrero, 2014; Forasiepi et al., 2016); *Cullinia*, *Promacrauchenia*, *Lullataruca*, in which the m3 entolophid is reduced (Schmidt, 2013; Forasiepi et al., 2016; McGrath et al., 2018); and *Pternoconius* in which the m3 entolophid is attached to the hypoconulid (Soria and Hoffstetter, 1985). In SGO.PV.4000, *Coniopternium*, *Scalabrinitherium* and *Theosodon* the entoconid on m1–m2 reaches the lingual level of metaconid, while in *Paranauchenia* it does not (Schmidt, 2013; Forasiepi et al., 2016). In SGO.PV.4000, *Theosodon* and *Scalabrinitherium* the paralofid in m1–m2 is developed (terminates on the lingual side), while in *Coniopternium* it is less developed, terminating in an anterior medial position (Schmidt, 2013; Schmidt and Ferrero, 2014; Forasiepi et al., 2016). In dorsal view, the SGO.PV.4000 skull fragment shows a prominent sagittal crest (Figure 2.4d), similar to those of *Theosodon* (Scott, 1910), but unlike *Scalabrinitherium* and others Macraucheniinae (Schmidt, 2013; Forasiepi et al., 2016). This allows us to refer with confidence the Cura-Mallín macraucheniid to the *Theosodon* genus.

The Cura-Mallín *Theosodon* represents a young adult individual slightly smaller than others referred to Santacrucian (*T. lallemani*, *T. gracilis*, *T. lydekkeri*, *T. garretorum*, *T. pozzii*, *T. patagonicus*) and Laventan (*T. arozquetai*, *Theosodon* sp.) species (Ameghino, 1897, 1889; Cifelli and Guerrero, 1997; McGrath et al., 2018; Scott, 1910; Soria, 1981; ESM_3). These size differences are especially evident by their reduced anteroposterior length of premolars and width of molar and premolars (ESM_3). SGO.PV.4000 is rather similar in size to *?T. frenguellii* (Soria, 1981). Besides size differences, morphological traits also allow us to differentiate the Cura-Mallín specimen from some of the *Theosodon* spp. better known and illustrated. The specimen here described differs from the Colhuehuapian *?T. frenguellii* in having a larger entolophid in m3, from *T. gracilis* in having a p4 smaller than the m1 (Scott, 1910; Soria, 1981; ESM_3), and from *T. lydekkeri* in having an m1 entolophid reaching the labial side (Ameghino, 1894). Despite these differences and taking into account the uncertainty surrounding the taxonomic status of the putative species included in the genus, we prefer to use a conservative taxonomic approach and just refer the specimen from Lonquimay to the taxon *Theosodon* until a thorough revision of genus has been conducted.

Theosodon has been previously recorded in Chile in the Rio Cisnes Fauna ('Friasian' SALMA), as well from the Pampa Castillo (Colhuehuapian to 'Friasian' SALMAs) and Chucal faunas (Santacrucian SALMA) (Flynn et al., 2002a, 2002b; Croft et al., 2004). With a well-constrained late Middle Miocene age (Serravallian) SGO.PV.4000 represents the youngest record (ca. 12 Ma) of the genus in Chile, and the south of South America (see Discussion section).

NOTOUNGULATA Roth, 1903

TYPOTHERIA Zittel, 1893

INTERATHERIIDAE Ameghino 1887

INTERATHERIINAE Ameghino, 1887

PROTYPOTHERIUM Ameghino, 1885

Included species. *P. antiquum* Ameghino, 1885 (type species); *P. attenuatum* Ameghino, 1887a; *P. praerutilum* Ameghino, 1887a; *P. australe* Ameghino, 1887b; *P. diastematum* (Ameghino, 1891); *P. distinctum* Cabrera and Kraglievich, 1931; *P. minutus* Cabrera and Kraglievich, 1931; *P. sinclairi* Kramarz et al., 2015, *P.*

endiadys (Roth, 1899), *P. colloncurensis* Vera et al., 2017 and *P. concepcionensis* sp. nov.

Geographic and Stratigraphic Distribution. Early to Late Miocene, Patagonia (Chile and Argentina), central Argentina, and Bolivia.

Remarks. According to recent phylogenetic analyses (Vera et al., 2017, 2019), the genus *Protypotherium* is not monophyletic.

Protypotherium concepcionensis sp. nov.

Figure 2.5a–d

Suárez et al., 1990: cf. *Protypotherium* sp.

Buldrini and Bostelmann, 2011: *Protypotherium* cf. *australe*

Buldrini et al., 2015: *Protypotherium* sp.

Holotype. SGO.PV.21000; well-preserved skull bearing all the teeth.

Tentatively referred materials. SGO.PV.4004; fragmented left dentary, with well-preserved p3, p4 and m1. SGO.PV.4005; anterior portion of the mandibular symphysis, with fragmented portions of i1, i2, i3 and c, and partial p1.

Diagnosis. Large size interatherine (similar in size to *P. australe* and *P. colloncurensis*) with the following unique character combinations: I1 subequal in size to I2–I3; P1 does not overlapped by P2 and C; P1 shape different from canine and P2; M1-M2 protocone more developed than hypocone and lingually protruding (especially in M1); deep parastylar sulcus on M1, but little evident parastylar sulcus in M2; single and vertical lingual sulcus on M1–2; upper molars imbricated and decrease in size from M1 to M3; lack of a posteriorly projected metastyle in the M3; moderately developed descending process of the maxilla; maxillary bone exposed along the laterodorsal surface of the skull and extended dorsally over the orbit; absence of a sliver of frontal anteriorly projected.

Etymology. In honor to the Universidad de Concepción (Concepción, Biobío region, Chile), an institution commemorating in 2019 its 100th foundation anniversary.

Type locality. The holotype (SGO.PV.21000) was collected in the surrounding of the Puente Tucapel locality, Araucanía Region, Chile (Figure 2.1). The tentatively referred specimens SGO.PV.4004 and SGO.PV.4005 comes from the east bank of the Biobío River, in outcrops located 1 km north of the Puente Tucapel, Araucanía Region, Chile.

Type horizon. late Middle Miocene (Serravallian; Mayoan SALMA, Figure 2.2), Rio Pedregoso member, Cura-Mallín Formation.

Description. The SGO.PV.21000 specimens is a nearly complete (but slightly deformed) skull with left and right I1–M3, but some of the incisors, canines, and premolars are partially damaged and/or covered by sediments (Figure 2.5a,b,c). The jugals and the basioccipital bones are not preserved. The rostrum is relatively short (basicranium is much mesiodistally longer), with a high maxilla and wide nasals (Figure 2.5b). The maxillary bone is exposed along the laterodorsal surface of the skull and largely extended dorsally over the orbit, as occurs in *P. endiadys*, but unlike *P. australe* (Vera et al., 2017). Besides, also resembling *P. endiadys* any anterior process of the frontal bone is observed between the nasals (Vera et al., 2017). The root of the zygomatic arch is well-expanded, as in *P. australe*. The sagittal crest is well-developed. The palate is rather curved (concave). In lateral view, the parietal is considerably elevated, therefore, the upper profile of the skull slopes forward and backward gradually. This feature, unlikely to be the result of post-mortem distortion, is much more marked in SGO.PV.21000 than in *P. endiadys* and *P. australe* (Sinclair, 1908; Vera et al., 2017). The antorbital foramen is large and circular and placed above the P4 (Figure 2.5c).

The upper incisors are poorly preserved. However, several features can be distinguished. In occlusal view (Figure 2.5a), the I1–I3 are rather similar in size (ESM_4), elongated, transversally flattened, and they appear to be slightly narrowing mesially. All the incisors are of similar mesiodistal length. The C is rather subtriangular, labiolingually compressed, with a wider mesial section. The P1 is wider than the C, and a diastema between both is lacking (Figure 2.5a). The P1 is different in shape from canine and P2, as in *P. australe* and *P. endiadys* (Vera et al., 2017, 2019). P1 is longer than wide, with the longer axis mesiodistally oriented, lacks a parastyle, and does not overlaps with none P2 or C (Figure 2.5a). The P2–P4 are completely differentiated from molars. As partially covered by sediment, details of the occlusal surface of P2-P4 are obscured, however, the broad outline of these premolars indicates that the P3 and P4 are rather similar in size (slightly wider than longer; ESM_4), while the P2 is nearly as long as wide (ESM_4). P2–4 have a folded ectoloph, which is more clearly marked in the P4 (Figure 2.5a).

The upper tooth-row is gently curved. Upper molars are strongly imbricated (a feature clearly observed in P4–M2), lack permanent fossettes, decrease in size

markedly from M1 to M3 (ESM_4), and exhibit a single transversely straight and wide lingual sulcus dividing the lingual wall in anterior and posterior lobes. The M1 and M2 exhibit a more developed area of the protocone than area of the hypocone, and the area of the protocone is lingually protruding, especially in the M1 (Figure 2.5a). M1 has a well-developed and forwardly extended parastyle with a rather deep parastylar sulcus, unlike *P. australe* and *P. praerutilum* in which the parastyle is moderate and/or little evident (Sinclair, 1908; Vera et al., 2019). The M2 has a shallow parastylar sulcus (Figure 2.5a). The M3 parastyle is much less developed than in M1 and M2. The M3 does not exhibit a posteriorly projected metastyle. Distally, the parastyle and paracone fold become progressively less prominent than in premolars (Figure 2.5a).

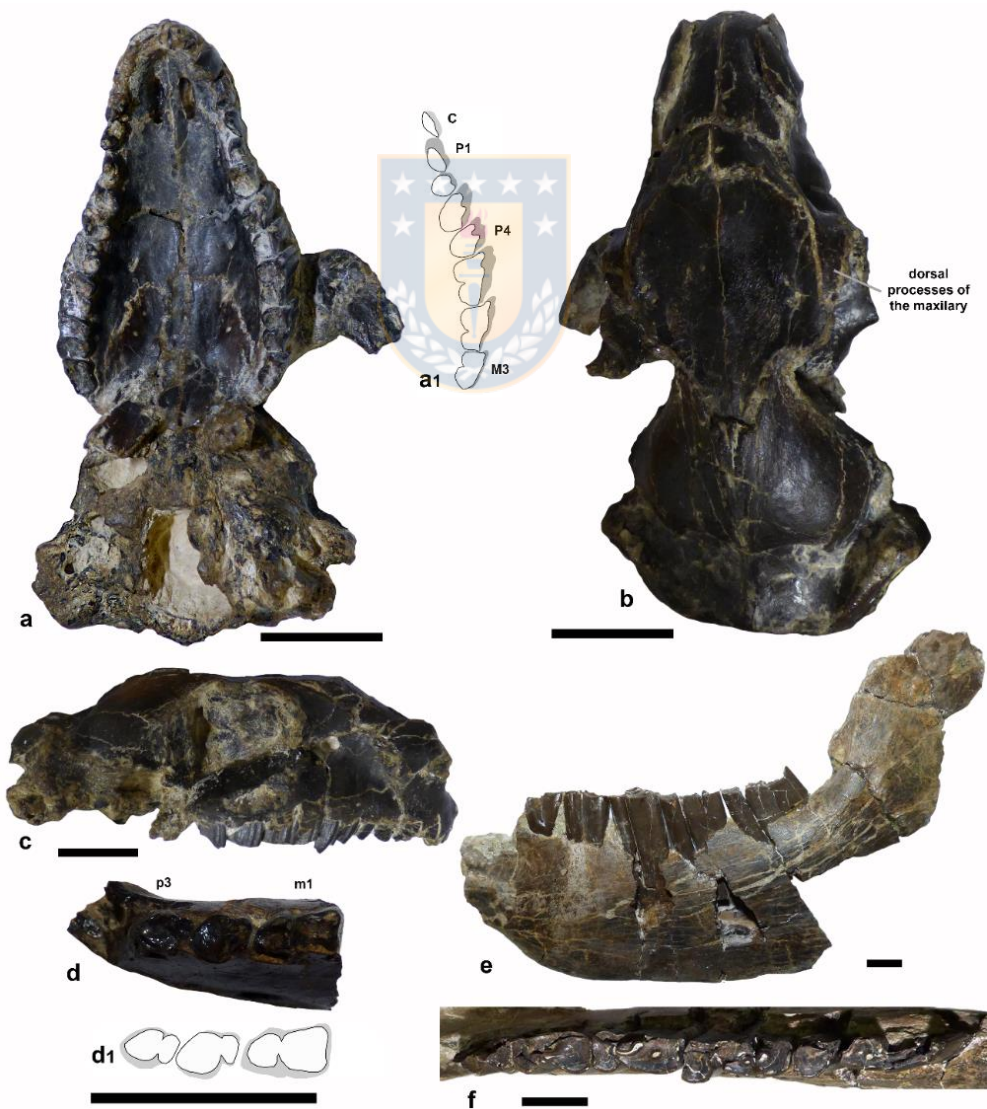


Figure 2.5. Notoungulates from Cura-Mallín Formation (Río Pedregoso Member) recovered in the surroundings of Lonquimay, Chile. *Protyotherium concepcionensis* sp. nov. (Puente Tucapel

locality, late Middle Miocene; Serravallian): skull (SGO.PV.21000; holotype) in ventral (a), dorsal (b) and lateral (c) views, and mandible fragment (SGO.PV.4004; tentative referred material) in dorsal view (d). *Nesodon imbricatus* (Cerro Tallón, Early Miocene; Santacrucian SALMA), a partial left mandible (SGO.PV.5226) in lingual view (e) and a detail of the occlusal view (f). Scale bar = 20 mm.

The two referred specimens likely represent a single individual. SGO.PV.4004 is a right fragment of the anterior region of the mandible preserving parts of the i1–p1 (see Buldrini et al., 2015; fig 2f–i). The i1–i3 display a similar oval shape, with the longer axis labiolingually oriented. The i1 lacks any groove, unlike *P. australe* in which the i1 is bifid (Vera et al., 2019). The incisors become distally larger (i.e., $i3 > i2 > i1$). The lower canine is larger than the i3. There is no space (diastema) among i3, c and p1. The p1 is oval in shape with the longer axis mesiodistally oriented and lacks a differentiated talonid (caniniform-like). SGO.PV.4005 is a fragment of the left mandible bearing the p3–m1 (Figure 2.5d). The height of the mandible below the m1 is 18.7 mm. The p3–p4 are not molariform. Despite its poor preservation, premolars have a visible very shallow lingual and labial sulcus dividing the anterior (trigonid) and posterior (talonid) lobes (Figure 2.5d). The p3 and p4 talonid are much more mesiodistally short and transversally narrower than the trigonid, giving to the teeth a pear-like shape. The m1 has two lobes separated by the hypoflexid and lingual fold, the anterior lobe is mesiodistally shorter and transversally wider than the posterior one. The m1 is larger than the premolars.

Remarks. The holotype and referred materials were recovered from the surroundings of the Puente Tucapel (Figures 2.1, 2.2), but they likely represent two different individuals. However, as the size of upper and lower teeth are rather congruent, we tentatively classify all these materials as belonging to the same new taxon. The presence of P/p3–P/p4 completely differentiated from molars, mesial sulcus on P/p3–4, and smaller talonid than trigonid on p3–4 supports their assignment to the genus *Protypotherium* (Schmidt, 2013; Vera et al., 2017).

Protypotherium concepcionensis differs from several of the species so far recognized; *P. attenuatum* has a highly curved upper tooth-row, and a shallow notch in the distal-most edge of the M3; *P. distinctum* has upper molars with bifid lingual sulcus and a roughly equally developed area of the hypocone/protocone in M1–M2; *P. minutus* has upper molars with a single and mesially oriented lingual sulcus, and a posterior lobe of M3 with more triangular contour in occlusal view; *P. praeutilum* has a shallow notch in the distal-most edge of the M3; *P. endiadys* has nearly

equally-sized upper molars and a well-developed parastylar sulcus in M2 (Tauber, 1996; Vera et al., 2017); *P. endiadys*, *P. praerutilum*, *P. attenuatum*, and *P. diastematum* are significant smaller than *P. concepcionensis* in tooth size (Sinclair, 1908; Tauber, 1996; Vera et al., 2017). Unlike *P. colloncurensis*, *Protypotherium concepcionensis* has a P1 different in size from canine and P2; P1 does not overlap with C or P2; P2–3 with a low length/width ratio; M1 with a deep parastylar sulcus; single and vertical lingual sulcus on M1–2. Previous work on the Lonquimay's protypotheres suggests close affinities with *P. australe* (Buldrini and Bostelmann, 2011; Buldrini et al., 2015). However, *P. concepcionensis* differs from the later in several features: I1 subequal in size to I2; M1-M2 with area of the protocone more developed than area of hypocone and lingually protruding; M1 with a deep parastylar sulcus; maxillary bone exposed along the laterodorsal surface of the skull and extended dorsally over the orbit; absence of a sliver of frontal anteriorly projected; and lack of a third lobe (posteriorly projected metastyle) in the M3. Few species within *Protypotherium* (*P. antiquum* and *P. sinclairi*) were described upon mandibular remains limiting comparisons with the skull SGO.PV.21000. The tentatively referred material (mandible fragment bearing the p3-m1; SGO.PV.4004; Figure 2.5d) provides differences with these species. *Protypotherium sinclairi* (Colhuehuapian SALMA), a species similar in size to *P. australe* and SGO.PV.21000, has transversely larger talonids and deeper lingual and labial sulcus in p3–p4 (Kramarz et al., 2015); while *P. antiquum* (Huayquerian SALMA) exhibits a lingually displaced talonid in p4 (Schmidt, 2013; Fernández et al., 2018). Therefore, the unique character combination (mentioned in the diagnosis) of the holotype, as well those of the tentatively referred material, are distinct from those of other intherateriine species and warrants their attribution to a new species.

In Chile, *Protypotherium* remains appears to be common. It has been reported in Early Miocene localities of the Cura-Mallín Formation at Laguna del Laja (Flynn et al., 2008), and the Santa Cruz Formation, in Pampa Castillo, and Pampa Guadal (Buldrini et al., 2015); in early Middle Miocene of the Río Frías Formation in the upper Río Cisnes (Bostelmann et al., 2012; Encinas et al., 2016); and now in the late Middle Miocene of the Cura-Mallín Formation. Additional remains potentially referable to *Protypotherium* were collected at Río Oscuro, Aysén in Mayoan SALMA age strata (Buldrini et al., 2015).

TOXODONTIDAE Gervais, 1847

NESODONTINAE Murray, 1866

NESODON Owen 1846

Nesodon imbricatus Owen 1847

Figure 2.5e,f

Croft et al., 2003: *Nesodon conspurcatus*

Revised materials. SGO.PV.5226; a partial left mandible preserving the base of the third incisor and nearly complete p3–m3, as well as a portion of the coronoid process.

Geographic and stratigraphic provenance. The specimen was collected by J.P. Radic and E. Zurita toward the north of the Cerro Tallón locality, Río Pedregoso Member, in beds with an age slightly older than 17.5 Ma and younger than 20 Ma (Croft et al., 2003; Pedroza et al., 2017). Therefore, the specimen could be referred to the Early Miocene (Santacrucean SALMA; Figure 2.2).

Description. The specimen SGO.PV.5226 was previously described in details by Croft et al. (2003).

Remarks. Based mostly on their size, SGO.PV.5226 was initially referred to *N. conspurcatus* (Croft et al., 2003). Nevertheless, after a recent review of the Santacrucean nesodontids, Hernández Del Pino (2018) suggested that *N. conspurcatus* is a junior synonymous of *N. imbricatus*.

XENARTHRA Cope, 1889

CINGULATA Illiger, 1811

GLYPTODONTIDAE Gray, 1869

Glyptodontidae gen. et sp. indet.

Figure 2.6a,b

Suárez et al., 1990: Glyptodontidae gen. et sp. indet.

Revised materials. SGO.PV.4006a, SGO.PV.4006b; two isolated (but associated) fixed osteoderms.

Geographic and stratigraphic provenance. The identification label of the MNHN indicates that the osteoderms were collected by L. Marshall and P. Salinas in 1989 at Piedra Parada locality, 2 km to the N–NE of Puente Lolén, BioBio river (Figure 2.1), Río Pedregoso Member. However, the specimen was collected by one of us

(GC) in the same locality. In the present work, we assign these specimens to the late Middle Miocene (Serravallian; see discussion below and Figure 2.2).

Description. Fixed osteoderms of hexagonal contour and small size (SGO.PV.4006a = 19.4 x 20.8 mm; SGO.PV.4006b = 20 x 22.7 mm). They have an enlarged sub-circular principal figure positioned along the posterior edge of each osteoderm, occupying most of the dorsal surface of the osteoderm (Figure 2.6a,b). The principal figure reaches the posterior edge of the osteoderm. There are four reduced peripheral figures located only in the anterior-most osteoderm edge; two to any peripheral figures in the lateral edges; lacking peripheral figures in the posterior edge (Figure 2.6a). The principal and peripheral figures are separated by a shallow peripheral groove (U-shaped). Conspicuous dorsal foramina (=piliferous pits) occur at the intersections of the principal and peripheral groove. Dorsally the osteoderms are flat to gently convex, and the principal and peripheral figures are rather similar in height. The osteoderms are relatively thick (9–10 mm) in relation to their dorsal area. Dorsal osteoderm sculpturing is quite faint, as occurs in glyptatelines and propalaehoplophorines (Croft et al., 2007; González–Ruiz, 2010). The ventral portion of the osteoderm is much more sculpted, and there are several (2–5) pits.

Remarks. The most relevant features displayed by the Piedra Parada glyptodont are their large principal figure located close to the posterior edge of the osteoderm, without posterior peripheral figures and reduced lateral peripheral figures. These features are present in most portions of the carapace of glyptatelines and *Parapropalaehoplophorus septentrionalis* Croft et al., 2007, some dorsal osteoderm of *Eonaucum colloncuranum* Scillato–Yané and Carlini, 1998, the anterodorsal osteoderms of *Paraeucinepeltus raposeirasi* González-Ruiz et al., 2011, and in some lateral osteoderms of Propalaehoplophorinae and Hoplophorinae Hoplophorini (Croft et al., 2007; González–Ruiz, 2010; González–Ruiz et al., 2011; Scillato–Yané and Carlini, 1998). As the osteoderms from Cura-Mallín are rather hexagonal they likely represent dorsal ones (Ameghino, 1889; Croft et al., 2007). In this sense, their morphology appears to be more closely related with the Glyptatelineae and the three Glyptodontidae *incertae sedis*, *Eonaucum*, *Parapropalaehoplophorus*, and *Paraeucinepeltus*. The Piedra Parada glyptodont differs from the Glyptatelineae (*Glyptatelus fractus*, *Glyptatelus tatusinus*, and *Clypeotherium magnum*) in which the principal and peripheral figures are convex and rounded (except in *Clypeotherium* where they are flat), and the grooves that

delimit the figures are deep (Ameghino, 1897; Scillato–Yané, 1977b; Zurita et al., 2015). It differs from *Parapropalaehoplophorus* in its smaller size, because *Parapropalaehoplophorus* largest dorsal osteoderm is 42 mm long×34 mm wide, but also by its more conspicuous piliferous pits (Croft et al., 2007). The anterodorsal osteoderms of *Paraeucinepeltus* are slightly larger than those of the Cura-Mallín glyptodont, and have larger peripheral figures (González–Ruiz et al., 2011). *Eonaucum* is a small size glyptodont (as SGO.PV.4006), but it shows a larger number and size of the peripheral figures than those observed in the Piedra Parada osteoderms (Scillato–Yané and Carlini, 1998). Glyptodont taxonomy is one of the most complex among fossil mammal groups in South America (e.g. González–Ruiz, 2010; Toriño and Perea, 2018). Further, the limited and fragmentary materials show some degree of erosion, which undoubtedly hinders the anatomical study of the material. Therefore, we are unable to perform any precise taxonomic arrangement of Piedra Parada glyptodont.

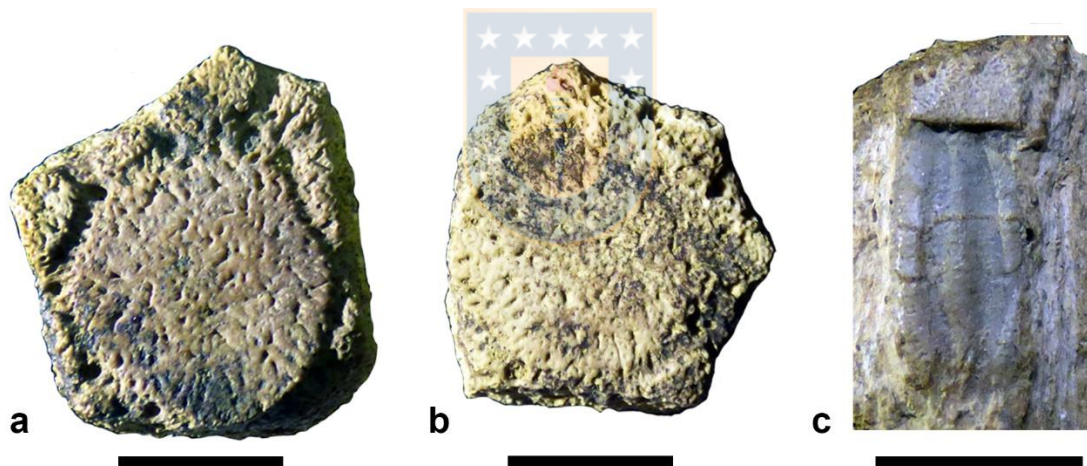


Figure 2.6. Cingulata remains from the Cura-Mallín Formation (Río Pedregoso Member) in the surroundings of Lonquimay, Chile. Glyptodontidae gen. et sp. indet. (SGO.PV.4006a and SGO.PV.4006b), from the Piedra Parada locality (late Middle Miocene; Serravallian), osteoderm in dorsal view (a, and b respectively). Eutatini gen. et sp. indet. (SGO.PV.22476) from the Cerro Rucañanco locality (late Middle Miocene; Serravallian), osteoderm in dorsal view (c). Scale bar = 10 mm.

DASYPODOIDEA Gray, 1821

DASYPODIDAE Gray, 1821

EUPHRACTINAE Winge, 1923

EUTATINI Bordas, 1933

Eutatini gen. et sp. indet.

Figure 2.6c

Revised materials. SGO.PV.22476; a moveable band osteoderm.

Geographic and stratigraphic provenance. The specimen was collected by L. Marshall in 1991, along the NE of Cerro Rucañanco, Rio Pedregoso Member, Cura-Mallín Formation, late Middle Miocene (Serravallian; Pedroza et al., 2017; Rosselot et al., 2019b; Figure 2.2)

Description. Rather small (20 mm length, 5 mm width) and smooth osteoderm composed of a principal figure separated by two wide and shallow transverse grooves from two lateral figures (Figure 2.6c). The principal figure is broader toward the middle portion of the osteoderm (being wider than the lateral figures), and narrower toward the distal and proximal edges. The lateral figures are undivided by lateral grooves (Figure 2.6c). The lateral and principal figures are of similar height (=elevation) along the entire osteoderm. Over the transversal groove (dorsal surface) there are few and inconspicuous piliferous pits. The caudal margin of the osteoderm is not well preserved but appears to contain at least one large foramen. In the anterior-most osteoderm edge, there is the quadrangular region for the overlap between moveable band osteoderms.

Remarks. The moveable band osteoderm SGO.PV.22476 lacks distinctive pits on its dorsal surface, as occurs in the tribe Eutatini (Croft et al., 2007; Scillato-Yané, 1977a; Scillato-Yané et al., 2010). Members of Eutatini also display a row of three-four large piliferous pits along the caudal margin of moveable band osteoderms (Croft et al., 2007; Ciancio et al., 2017). Yet, due to the poor preservation of the osteoderm caudal margin, we are unable to confirm whether this last feature is present in the Cura-Mallín material.

At least 11 genera, ranging from ?late Eocene to the late Pleistocene, are grouped within Eutatini (McKenna and Bell, 1997; Croft et al., 2007). During the Neogene, several Eutatini genera could be recognized (Croft et al., 2007; González-Ruiz, 2010; Scillato-Yané et al., 2010; Scott, 1903). Many of them (e.g. *Proeutatus*, *Paraeutatus*, *Doellotatus* and *Paraeutatus*) are characterized by moveable band osteoderms with a lageniform central figure (Ciancio and Carlini, 2016; Dozo et al., 2014; González-Ruiz, 2010; Scillato-Yané et al., 2010), unlike that of SGO.PV.22476 (Figure 2.6c). In this sense, the Cura-Mallín Eutatini mostly resembles *Stenotatus*, a late Oligocene to Middle Miocene genus that includes five named species, as well as two potentially undescribed species (Croft et al., 2009, 2007; González-Ruiz, 2010). The specimen SGO.PV.22476 is in the range of size

of *Stenotatus patagonicus* Ameghino, 1887, and *S. planus* Scillato-Yané and Carlini 1998 (Croft et al., 2009; González–Ruiz, 2010; Scott, 1903). However, taking into account the scarcity of available material, we are unable to achieve a reliable genus level identification for the Cura-Mallín armadillo.

2.5 Discussion

The few specimens so far collected from the Lonquimay area (38° S) allow us to recognize at least six taxa including a primitive toxodont (*Nesodon imbricatus*), astrapotheres (*Parastrapotherium* sp.), glyptodonts (Glyptodontidae indeterminate), armadillos (Eutatini indeterminate), macraucheniids (*Theosodon* sp.), and new interatheriine species (*Protypotherium concepcionensis* sp. nov.). The last three taxa are for the first time recognized in the area. Contrasting with previous interpretations (Marshall et al., 1990), after our surveys of the MNHN collections we are unable to recognize any specimen referable to mesotheriid nor to caviomorph. Thus, their record from the Lonquimay area could not be confirmed, albeit does not mean that they did not could exist there. We acknowledge the presence of a seventh taxon, which likely corresponds to a small Platyrrhini monkey represented by a worn lower molar (SGO.PV.22204; Figure 2.7) recovered from the Cerro Rucañanco locality (late Middle Miocene, Serravallian; Cura-Mallín Formation; Figure 2.2), but whose taxonomic status is still under study. Whether their taxonomic assignation is confirmed the specimen SGO.PV.22204 could correspond to the first record of a monkey in the Cura-Mallín Formation.

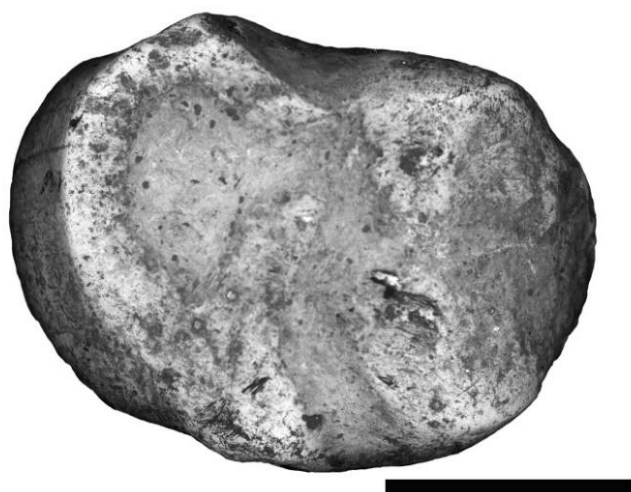


Figure 2.7. Scanning electron microscopy photograph of the lower molar (SGO.PV.22204; in occlusal view) of the putative Platyrrhini monkey recovered from the Cerro Rucañanco locality (late Middle Miocene, Serravallian; Río Pedregoso Member; Cura-Mallín Formation).

2.5.1 A reassess of the biochronological affinities of the Lonquimay Neogene mammals

The Cura-Mallín mammalian assemblages found in the surroundings of Lonquimay town were initially assigned to the Early Miocene (Marshall et al., 1990; Suárez et al., 1990). Successive works (Croft et al., 2003; Bostelmann et al., 2014; Buldrini et al., 2015) reinforced an Early Miocene age for this fauna. The *Nesodon* indicated a Santacrucian (~18.2 to ~15.6 Ma *sensu* Cuitiño et al., 2016) SALMA (Croft et al., 2003), the *Protypotherium* was tentatively assigned to the 'Pinturan' (19.0–18.0 Ma *sensu* Cuitiño et al., 2016) – Santacrucian SALMA (Buldrini and Bostelmann, 2011), whereas the *Parastrapotherium* was referred to the Colhuehuapian (20–21 Ma *sensu* Dunn et al., 2013) SALMA (Bostelmann et al., 2014). At the genus levels, these interpretations were considered reliable because these notoungulates as well the macraucheniid genera are typical (although not exclusive) from the Santacrucian SALMA (e.g. Cassini et al., 2012), and *Parastrapotherium* is known from the Deseadan to the Colhuehuapian SALMA (Kramarz and Bond, 2008, 2010). However, new stratigraphic information and U-Pb dating have challenged some of these ideas (Pedroza et al., 2017; Rosselot et al., 2019b), with the *Protypotherium* recovered from the Puente Tucapel being referred to the Laventan SALMA (13.5–11.8 Ma; Pedroza et al., 2017). These contradictions illustrate the needed of a reassessing of the biochronological affinities of the Lonquimay Neogene mammals.

A review of the stratigraphic interpretations, published radioisotopic dates, the original geographic provenance of the fossil specimens (Pedroza et al., 2017; Rosselot et al., 2019b; Suárez et al., 1990; Suárez and Emparan, 1995; Figure 2.2), as well as preliminary field observations, allows us to recognize two distinctive chronological mammalian assemblages in the Lonquimay area of Early Miocene (likely Colhuehuapian–Santacrucian SALMA), and late Middle Miocene (Serravallian) ages. The former includes the mammals recovered from Cerro Tallón and Rio Quepuca localities, while the latter contains those recovered from Piedra Parada, Cerro Rucañanco, and Puente Tucapel localities (Table 2.1; Figures 2.1, 2.2). Although the maximum depositional ages from Puente Tucapel and Cerro Rucañanco localities (Pedroza et al., 2017; Rosselot et al., 2019b) might be interpreted as near-sedimentation ages, slightly younger (early Late Miocene;

Tortonian) ages for these localities are also plausible and cannot be completely discarded.

The Early Miocene assemblage includes the large taxa *Nesodon* and *Parastrapotherium*. As previously mentioned, *Parastrapotherium* is a taxon so far only known from the Deseadan–Colhuehuapian SALMAs (Kramarz and Bond, 2008, 2010). However, due to the lack of radiometric data in the sampling locality, we cannot definitively assign an age for this specimen rather than likely Early Miocene (likely Colhuehuapian SALMA) based on biostratigraphic correlation. On the other hand, *N. imbricatus* comes from the Cerro Tallón locality from which K-Ar radioisotopic dating yields an age of 17.5 ± 0.6 Ma (Croft et al., 2003; Suárez and Emparan, 1995; Figure 2.2). Yet, the K-Ar method has limited accuracy and the age must be taken with caution. In spite of this, the age is broadly consistent with those of *N. imbricatus* in Early Miocene (Santacrucian SALMA) faunas from the Santa Cruz Formation, where this taxon is very common and abundant (Cassini et al., 2012; Hernández Del Pino, 2018).

The late Middle Miocene assemblage is the more diverse and includes the protypothere, macrauchenid, armadillo, glyptodont, and the presumable platyrrhini. The *Protypotherium* specimens from Lonquimay were found in loose blocks on the Puente Tucapel hillside, making their geochronological assignment doubtful (Suárez et al., 1990). However, a nearly autochthonous provenance is inferred. Recent U-Pb dates of detrital zircons from the base and top of Puente Tucapel section yielded maximum ages of 12.7 ± 0.3 and 12.5 ± 0.3 (late Middle Miocene; Pedroza et al., 2017). Hence, the new taxon *Protypotherium concepcionensis* must be of late Middle Miocene age (Figure 2.2). The armadillo, macraucheniid and putative platyrrhini were recovered from the Cerro Rucañanco surroundings (Figure 2.2). There are recent U-Pb dating of detrital zircons from the basal(?) and middle sections of this locality that yielded a maximum depositional ages of 11.64 and 12.4 Ma respectively (Pedroza et al., 2017; Rosselot et al., 2019b). In this sense, the putative Platyrrhini from the Cerro Rucañanco would be one of the younger records of monkeys in the south of South America, likely indicating continuous presence of the clade in Chile from the Early to late Middle Miocene (after *Chilecebus* and Rio Cisnes Platyrrhini) (Flynn et al., 1995; Tejedor, 2003; Bobe et al., 2015). The presence of *Theosodon* in the late Middle Miocene is of particular interest because most of *Theosodon* specimens and all named species come from the Early Miocene

(Scott, 1910; McGrath et al., 2018). While the younger (Serravallian) records of the genus are restricted to low and middle latitudes in La Venta (Colombia), Quebrada Honda (Bolivia) and Fitzcarrald (Peru) (Cifelli and Guerrero, 1997; Tejada-Lara et al., 2015; McGrath et al., 2018). Therefore, here we illustrate the persistence of *Theosodon* in the Chilean Andes until ca. 12 Ma.

The glyptodont was recovered from Piedra Parada outcrops. Early K-Ar dates from the cliff of Piedra Parada hill indicated a Middle Miocene age (13 Ma) (Suárez and Empanan, 1995). Nonetheless, based on stratigraphical interpretations this locality was later referred to the Early Miocene (22–17 Ma; *sensu* Pedroza et al., 2017). Recent U-Pb dating of a volcanic tuff at the base of the Piedra Parada section indicates an age of 12.8 Ma (Rosselot et al., 2019a) confirming a late Middle Miocene (Serravallian) age for this locality. These findings also raise the question about the general reliability of Pedroza et al.'s (2017) interpretations and reinforce the idea of a complex stratigraphic scenario in the area exacerbated by the lack of continuous outcrops. In any case, the age of the glyptodont from Lonquimay must be slightly younger than 12.8 Ma (late Middle Miocene; Figure 2.2) because it was recovered from a bed overlying the dated tuff.

As previously mentioned, Pedroza et al. (2017) assign the *Protypotherium* remains from Puente Tucapel locality to the Laventan SALMA. The U-Pb radiometric ages of 12.8 to 11.6 Ma (Figure 2.2; Table 2.1) indicate a late Middle Miocene age for the upper mammal assemblages from the Cura-Mallín Formation, and agrees with the proposed interval of the Laventan SALMA (13.5–11.8 Ma) which was erected based on the locality of La Venta (~3°N) in Colombia (Madden et al., 1997). However, recent faunal comparison between localities coeval with La Venta, as Quebrada Honda (~22°S, Bolivia) for example, demonstrates the relative paucity of taxa shared between them. Therefore SALMAs may not be useful for biocorrelation between low-latitude faunas and those from elsewhere in South America as previously proposed by Croft (2007). Here, we argued that the age range (12.8–11.6 Ma) of the upper mammalian assemblage of the Cura-Mallín Formation is also consistent with the Mayoan SALMA. Fossils considered Mayoan comes typically from the Río Mayo Formation a continental sequence mainly characterized by sandstones, tuffs, tuffites, pelites and conglomerates, which crops out in several localities in south-western Chubut and northwestern Santa Cruz provinces, Argentina (Dal Molin et al., 1998; De Iuliis et al., 2008; González Ruiz et al., 2017;

Vera et al., 2019). Additional Mayoan fossils also have been recovered in the underlying El Portezuelo and El Pedregoso formations (Scillato-Yané and Carlini, 1998; De Iuliis et al., 2008; Folguera et al., 2018b). Early works suggested, without the aid of radiometric ages, an early Late Miocene age (10.0–11.8 Ma) for the Mayoan fauna (Flynn and Swisher, 1995). However, recent radiometric data acquired from the El Pedregoso, El Portezuelo, and Río Mayo formations (with faunas typically ascribed to the Mayoan) indicates ages between 13.5–11.8 Ma (De Iuliis et al., 2008; Folguera et al., 2018b; Vera et al., 2019). Consequently, the updated chronostratigraphic framework indicates that the Mayoan SALMA (defined in the high latitudes, ~46°S) is, at least partially (González Ruiz et al., 2017), temporally superposed with the Laventan SALMA (defined in low latitudes, ~3°N; Madden et al., 1997). Thus, the differences between both Laventan and Mayoan faunas are probably linked to different environmental and ecological conditions in both regions of South America, rather than to temporally distinctive evolutionary stages, and deserve further scrutiny as discussed in the present contribution. New fossil collections under strict stratigraphic control will be necessary to corroborate and/or refine the validity and position of the Mayoan mammal association (González Ruiz et al., 2017). Despite the fauna analyzed here does not bear typical 'Mayoan' taxa, here we tentatively correlate the upper mammalian assemblage from the Cura-Mallín Formation cropping out in Lonquimay with the Mayoan SALMA based in geochronological correlations.

2.5.2 Paleobiogeographical considerations

Some of the specimens analyzed here could not be identified at the species level due to their fragmentary state of preservation, limited sampling, and the uncertainty surrounding the taxonomy of some genera (e.g., *Theosodon* needing taxonomic revision). However, it is possible to establish the broad biogeographical relationships of the Lonquimay mammal assemblages with those from other coeval localities.

The Lonquimay fauna encompasses one of the few well-documented occurrences of *Nesodon imbricatus* outside of high latitude localities (e.g. Croft et al., 2004, 2003), as well as the unique report of *Parastrapotherium* from Chile (Bostelmann et al., 2014). Both indicated Early Miocene biogeographic connections with the classic high latitude Patagonian faunas (~50°S) in both Argentina and Chile

(Kramarz and Bond, 2008, 2010; Cassini et al., 2012; Bostelmann et al., 2013; Hernández Del Pino, 2018). Prior to the present work, the geographic distribution of *Theosodon* during the late Middle Miocene (Serravallian) was limited to La Venta (3°N; Colombia), and to Quebrada Honda (22°S; Bolivia) (Cifelli and Guerrero, 1997; McGrath et al., 2018). Consequently, our work corroborates a significant southern extension of the geographic distribution of this taxon during the late Middle Miocene, extending from the cited localities to the Lonquimay area (38°S). *Protypotherium concepcionensis* (Cura-Mallín Formation, Chile), contributed to increase the biodiversity of the genus in the Serravallian. Two additional late Middle Miocene taxa are known, *P. colloncurensis* (Collon Cura, ~41°S and Rio Mayo, ~46°S formations, Argentina), and *P. endiadys* (Collon Cura formation, ~41°S). Both are recognized in the Colloncuran SALMA and likely in younger Mayoan SALMA beds (Vera et al., 2018, 2017). This suggest that protypotheres were more widespread along the late Middle Miocene (Serravallian) intra-arc and foreland basins in the central south Andes than previously thought.

Considering the limited sampling of mammals so far recorded from the Lonquimay region, taxonomic comparison with relatively close geographic paleontological localities in both Chile and Argentina must be considered preliminary. Three taxa (*Nesodon*, *Theosodon*, and *Protypotherium*) are shared with the Early Miocene Pampa Castillo fauna (~47°S), and that of the early Middle Miocene Río Frías Formation (~45°S) in southern Chile (Flynn et al., 2002b; Bostelmann et al., 2012; Charrier et al., 2015; Encinas et al., 2016), and also with the Santa Cruz Formation (~51°S) in Argentina (Cassini et al., 2012). Two taxa (*Nesodon* and *Theosodon*) are shared with the early Miocene Chucal fauna, Chile (~19°S; Charrier et al., 2015; Croft et al., 2004). One genus (*Protypotherium*) is shared with the early Miocene Cerro Bandera fauna of Neuquen, Argentina (Kramarz et al., 2005). So far no taxon is shared with the early to middle Miocene fauna from the Aisol Formation, Argentina (~34.5°S; Forasiepi et al., 2015, 2011), nor with the late Miocene of Caragua, Chile (~18°S; Bostelmann et al., 2018).

Is necessary to note the paucity of shared taxa between the two mammalian faunas of the Cura-Mallín Formation in Chile, Lonquimay (38°S) and Laguna del Laja (~37.5°S). This could be due to the combination of several factors including poor taxonomic resolution, few fossil findings, and differences in age. The lower mammalian assemblage from Lonquimay might temporally correlate with the Tcm₁

(19.8–18 Ma) and Tcm₃ (17.8–16.4 Ma) levels of the Laguna del Laja, cropping out in the Estero Trapa-Trapa (Herriott, 2006; Flynn et al., 2008), but none shared taxa between both have been so far reported. The upper mammalian assemblage from Lonquimay area might temporally correlate with the fossil-bearing horizons reported from the Trapa-Trapa Formation (cropping out in the Laguna del Laja area), which appears to be mid-late Miocene, possibly Colloncuran or Mayoan SALMA, in age (Flynn et al., 2008). The Trapa-Trapa Formation only include a record of an interatheriid referred to cf. *Interatherium* sp. (Flynn et al., 2008). The upper mammalian assemblage from Lonquimay also include an interatheriid but included in the *Protypotherium* genus (Figure 2.5). Indeterminate *Protypotherium* remains have been also reported from Early Miocene (Tcm₁ and Tcm₃) levels in the Laguna del Laja (Herriott, 2006; Flynn et al., 2008). Therefore, *Protypotherium* is the only taxa shared between the Lonquimay and Laguna del Laja faunas so far. Futures studies dealing with the taxonomy and systematic of the Laguna del Laja fauna, as well as increasing sampling efforts could certainly provide a better framework for further comparisons between these two geographically close localities within the Cura-Mallín Basin.



2.5.3 Paleoenvironmental significance

Even though the Lonquimay taxa described here may not have necessarily coexisted, as they were recovered from different outcrops (Figure 2.2), they provide ecological information about the depositional environment of the study area. The macraucheniid *Theosodon* would likely have inhabited mainly closed-canopy habitats, with the larger species having more mixed–feeding habits than the smaller ones, which would have had more browsing habits (Cassini et al., 2012). Several lines of evidence, including paleobiology (Cassini et al., 2012; Cassini, 2013), taphonomy (common occurrence in stream–channel sediments or associated with aquatic fauna), and microanatomical features (Houssaye et al., 2016), are consistent with the astrapothere specialization for graviportal, semi-aquatic, and closed-habitat foraging. Using a microwear approach, Townsend and Croft (2008) described *Nesodon imbricatus* as a leaf browser focused more on hard browsing, and *Protypotherium* as a browser on both soft browse and soft fruits. However, other authors used paleobiological evidence to indicate that *Nesodon* was a taxon adapted foraging on grass and leaves depending on the availability in mixed habitats

(Cassini et al., 2012; Cassini, 2013). *Protypotherium* has been interpreted as a generalized terrestrial mammal tending toward cursoriality (Croft and Anderson, 2007) living in open habitats and foraging on grass (Cassini et al., 2012; Cassini, 2013). The armadillos, essentially fossorial and occupants of burrows, naturally avoid the environments in which these can be overflown (Scillato-Yané et al., 2013). Due to their small size, both the armadillo and glyptodont from the Lonquimay area likely inhabited mixed to closed habitats (Vizcaíno et al., 2011, 2012). The platyrrhine monkey would suggest forested environments, as modern platyrrhines are mostly adapted to such habitats in tropical to subtropical conditions (Lynch Alfaro et al., 2015; Silvestro et al., 2019b), and the same has been acknowledge for some Miocene platyrrhines (Kay et al., 2012a).

The knowledge about taxonomic diversity of the mammals from the Lonquimay area is low, and micromammals are likely underrepresented due to the scarce fossiliferous content of the Cura-Mallín Formation in the area. Then, additional lines of evidence must be necessary for a more reliable paleoenvironmental reconstruction (Kay et al., 2012b). Previous work dealing with the fossil pollen and leaves imprints recovered from the CMF in the Lonquimay area allows for the recognition of a diverse flora suitable to complement the paleoenvironmental reconstruction based on mammals. For example, Palma-Heldt and Rondanelli (1990) report the presence of *Nothofagus pumillo*, *Nothofagus antarctica* and *Boquilla trifoliolata* from the Cerro Rucañanco section (late Middle Miocene). These *Nothofagus* species are indeed extant ones and indicate (if a niche conservatism is accepted) a microthermal climate with a mean annual temperature of $\sim 7^{\circ}\text{C}$ ($11.6\text{--}2.5^{\circ}\text{C}$), and mean of annual precipitation of ~ 1200 mm (Hinojosa et al., 2016). Salinas (1979) reports Myrtaceae leaves, a family with extant representatives in Chile commonly found in humid rainforests or flooded environments (Kausel, 1944), from the Lolco Formation (a former name for the Guapitrío Member) at the Estero Los Azules ($38^{\circ}14'30.49''\text{S}$; $71^{\circ}26'13.16''\text{W}$). On the other hand, palynomorphs recovered from several stratigraphic levels along Lonquimay area, including the older (Early Miocene) levels of the Cura-Mallín Formation at Paso Rahue area and the younger levels outcropping in Cerro Rucañanco, suggest the persistence of humid and partly marshy forests in temperate to cold temperatures (Palma-Heldt, 1983). The freshwater fishes and invertebrates commonly found in along the Rio Pedregoso member advocate fluviolacustrine environments (Rubilar, 1994). Finally,

the presence of serrasalmids remains in the Cerro Rucañanco (Rubilar, 1994) is indicative of tropical affinities, as they are common in ichthyological assemblages from Neotropics (Freeman et al., 2007). However, additional work is necessary in order to refine the taxonomic affinities of those serrasalmids remains.

Putting all this paleoecological information into a temporal framework (Table 2.1; Figure 2.2) it is possible to recognize an Early Miocene environment mainly characterized by the existence of semi-aquatic and forested habitats, and a late Middle Miocene environment with a microthermal climate with closed canopy and permanent bodies of water. Yet, the presence of *Protypotherium* in the last assemblage might advocate the existence of open habitats in their surroundings. In any case, though restricted, the information provided by the fossil biota (mammals, freshwater-fishes, and flora) reveals a rather homogeneous forested, humid and temperate environment during the deposition of the Cura-Mallín Formation (Early to late Middle Miocene).

Today, the Andean Cordillera exhibits a lower topography (up to 3500 m) between the 37°–39°S than in northern parts of this range (Rojas Vera et al., 2016). Even though, these relatively low altitudes constitutes a topographic barrier to atmospheric circulation, and causes a 'rain-shadow effect'—the sharp decline in precipitation often observed on the leeward side of mountain ranges— (Hijmans et al., 2005; Siler et al., 2012). Based on regional scale land cover and global annual mean precipitation data are possible to characterize the present-day broad scale setting of the Andes Cordillera around the 37–39°S (Hijmans et al., 2005; Zhao et al., 2016). The western-most (windward side) portion of the Andes has high precipitation rates (>1500 mm/year), with the dominance of forested environments (Figure 2.8). In the eastern portion of the Andes (leeward side), where the Lonquimay fossiliferous localities are located, there is a progressive decrease in the precipitation rates (reaching ~1000 mm/year), and a progressive dominance of grasslands and shrublands toward the east (Figure 2.8).

Finally, the foreland (east of the Andean Cordillera) exhibits a very low mean annual precipitation rate (<500 mm/year), with predominant grassland and barren land (Figure 2.8). Therefore, at the latitudes of our work (37–39°S) the foreland is strongly affected by the rain-shadow effect, but the intermontane basins emplaced in the eastern portion of the Andes main Cordillera also exhibit a rain-shadow effect, even if not extreme.

The combination of Andean uplift (and the subsequent rain-shadow effect in the foreland) and global climatic oscillations cause a significant impact in the southern South American Neogene biota (Zachos et al., 2001; Ortiz-Jaureguizar and Cladera, 2006; Palazzesi and Barreda, 2012; Horton, 2018a). Neogene mammals exhibit a pattern of progressive reduction of browsers and frugivorous taxa, which were abundant in the Early Miocene and successive less common in the Late Miocene, with grazers showing the inverse pattern (Ortiz-Jaureguizar and Cladera, 2006). The Patagonian (46°–50°S) floral change from an Early Miocene highly diverse forested ecosystem to a markedly different community of lower diversity dominated by arid-adapted shrubs by Late Miocene (Palazzesi and Barreda, 2012; Barreda and Palazzesi, 2014). But the possible existence of environmental changes during the Miocene related to the rain-shadow effect is not well-documented at the 38°–39°S latitude.

The rather homogenous paleoenvironmental conditions suggested by the fossil biota of the Cura-Mallín Formation recovered from the Lonquimay area indicate that during the late Middle Miocene forested, temperate, and humid conditions persist at this latitude. This environmental interpretation contrast with the present day setting of the Lonquimay area, where is noted the predominance of grasslands and shrublands (Figure 2.8). Therefore, even when contractional conditions in the CMB could be established since the Early Miocene (Rosselot et al., 2019a), we suggest that this portion of the Andes did not reach sufficient paleoaltitudes (>1000 m) to cause an important orographic rain shadow effect, with the subsequent increase in the aridity in the eastern foreland, at least until after the late Middle Miocene (ca. 12 Ma). This scenario is consistent with previous works at the latitude of our study area (~38°–39°S), because after the Late Miocene there is a significant increase in crustal shortening (Rojas Vera et al., 2014), exhumation rates (Spikings et al., 2008), the occurrence of synorogenic deposits (Melnick et al., 2006), and seasonally wet and dry conditions in the foreland (Le Roux, 2012). Our interpretation is also consistent with the diverse, humid and forested vertebrate fauna reported in the Middle Miocene (Langhian) Collon Cura Formation (37°–40°S), which also includes platyrrhine monkeys (Pardiñas, 1991; Vucetich et al., 1993). However, we acknowledge that in similar time spans (~12 Ma) the southern extra-Andean Patagonia regions already exhibited vegetational, and faunal changes toward cooler and more arid climate likely driven by an important orographic rain

shadow effects due to the uplift of the Patagonian Andes (45–47°S) (Blisniuk et al., 2005; Ortiz-Jaureguizar and Cladera, 2006; Palazzesi and Barreda, 2012; Folguera et al., 2018b). On the other hand, it has been argued that the Neogene Andean uplift (and the associated rain shadow effect) may not be the sole determinant force for Patagonian desertification, because global climatic changes affecting the Southern Hemisphere could be another important factor (Palazzesi et al., 2014; Trayler et al., 2019). Thus, an alternative climatically driven scenario is also plausible because both (tectonic and climatic) triggers are virtually indistinguishable with the available data. Future paleoecological analysis of the still poorly known Early to Late Miocene mammalian assemblages cropping out in the Laguna del Laja area (Cura-Mallín and Trapa-Trapa Formations; Flynn et al., 2008) certainly could shed more light in this regard.

2.6 Conclusions

The review of the taxonomic and chronological affinities of the Lonquimay fauna (Cura-Mallín Formation) allows us to recognize two chronological distinctive mammalian assemblages (Table 2.1). The lower assemblage is Early Miocene (likely Colhuehuapian–Santacrucian SALMA) in age and includes *Nesodon imbricatus* and *Parastrapotherium* sp.; while the upper assemblage is late Middle Miocene in age (12.8–11.6 Ma) and includes glyptodonts (Glyptodontidae indeterminate), armadillos (Eutatini indeterminate), macraucheniids (*Theosodon* sp.), a new protypothere species (*Protypotherium concepcionensis* sp. nov.) and likely a platyrrhini monkey. In this sense, contrasting with previous interpretations (Marshall et al., 1990; Suárez et al., 1990; Alvarenga, 1995; Buldrini and Bostelmann, 2011; Bostelmann et al., 2013; Buldrini et al., 2015; Diederle, 2015) the fauna from Lonquimay is not uniquely confined to the Early Miocene. As a consequence, the continental bird *Meganhinga chilensis* from the Cerro Rucañanco (Alvarenga, 1995) must be of late Middle Miocene age.

Despite their very low species richness, and only based in the age of their sediment-bearing fauna, the upper levels from the Cura-Mallín Formation in Lonquimay area must be putatively assigned to the Mayoan SALMA. Biogeographically, the lower Lonquimay fauna (Early Miocene) is clearly of Patagonian affinities. At the genus level *Theosodon* is shared with other coeval

localities in Colombia, and Bolivia, highlighting the wider geographic late Middle Miocene (Serravallian) distribution of this macraucheniid along the Andes.

Even when limited, the information provided by the fossil biota (mammals, freshwater-fishes, and flora) recovered from the Lonquimay area reveals a rather homogeneous environment during the deposition of the Cura-Mallín Formation along the Early to late Middle (Figure 2.2), with a predominance of rather temperate, humid and forested habitats with permanent bodies of water. At the time, our finding suggests that the Andean Cordillera of south-central Chile (38°S) did not reach a sufficient elevation to cause an important orographic rain shadow effect in late Middle Miocene, and the increased aridity in the eastern foreland basins was likely developed at this latitude only after c. 12 Ma. However, considering the contrasting degrees of Neogene crustal shortening and exhumation noted in the immediately northern latitudes (Spikings et al., 2008; Rojas Vera et al., 2014, 2016), we prefer not to generalize our interpretations to the entire Cura-Mallín basin. Given the scarcity of fossils mammals in the area, future studies involving independent proxies such as oxygen isotopic analyses of fish tooth/bone bioapatite and mollusk/gastropod shells (Wang et al., 2008) undoubtedly will provide valuable information to test our paleoenvironmental interpretations.

Acknowledgments. We wish to thank the Consejo de Monumentos Nacionales (CMN, Chile) the authorization for fossil prospections and to the Corporación Nacional Forestal (CONAF). To David Rubilar (MNHN, Santiago) for granting access to the vertebrate paleontological collections under his care, and Yuanyuan Zhao (Tsinghua University, China) for providing access to the land cover original data. We thank the reviewer A.G. Kramarz, and an anonymous reviewer for valuable suggestions and comments that greatly improved the manuscript. This research was funded by Conicyt, Fondecyt project n°1151146 (AE); and Conicyt–PCHA/Doctorado Nacional/2018–21180471 (AS).

Table 2.1. Summary of the age and mammals from each of the recognized mammal-bearing localities from the Cura-Mallín Formation at the Lonquimay area (Chile). References from ages: ^aRosselot et al. (2019b), ^bPedroza et al. (2017), ^cSuárez and Emparan (1995), ^dKramarz and Bond (2008).

Locality	Age (Ma)	Epoch	Dating method	Mammals recovered
Cerro Rucañanco	12.4 ^a – 11.64 ^b	late Middle Miocene	U/Pb in detrital zircons (maximum age)	Platirrini indet., Eutatini indet. <i>Theosodon</i> sp.
Puente Tucapel	12.5 – 12.7 ^b	late Middle Miocene	U/Pb in detrital zircons (maximum age)	<i>P. concepcionensis</i> sp. nov.
Piedra Parada	13.0 ^c	late Middle Miocene	K-Ar (whole-rock) in brecciated andesite	Glyptodontidae indet.
	12.8 ^a	late Middle Miocene	U/Pb in detrital zircons	
Río Quepuca	-	Early Miocene ^d	Biochronological correlation	<i>Parastrapotherium</i> sp.
Cerro Tallón	17.5 ^c	Early Miocene	K-Ar (biotite) tuff	<i>Nesodon imbricatus</i>



CAPÍTULO III. Late early Miocene caviomorph rodents from Laguna del Laja (~37° S), Cura-Mallín Formation, south-central Chile



²**Solórzano A**, Encinas A, Kramarz A, Carrasco G, Montoya-Sanhueza G, Bobe R. (2020). Late early Miocene caviomorph rodents from Laguna del Laja (~ 37° S), Cura-Mallín Formation, south-central Chile. *Journal of South American Earth Sciences*, 102658.

²Artículo publicado en 2020, disponible en <https://doi.org/10.1016/j.jsames.2020.102658>

Late early Miocene caviomorph rodents from Laguna del Laja (~37° S), Cura-Mallín Formation, south-central Chile

Andrés Solórzano^{1,*}, Alfonso Encinas², Alejandro Kramarz³, Gabriel Carrasco⁴, Germán Montoya-Sanhueza⁵, René Bobe⁶

¹Programa de Doctorado en Ciencias Geológicas, Facultad de Ciencias Químicas, Universidad de Concepción, Víctor Lamas, 1290, Concepción, Chile

²Departamento de Ciencias de la Tierra, Facultad de Ciencias Químicas, Universidad de Concepción, Víctor Lamas, 1290, Concepción, Chile

³Sección Paleontología de Vertebrados, Museo Argentino de Ciencias Naturales Bernardino Rivadavia, Av. Ángel Gallardo 470 (C1405DJR), Ciudad Autónoma de Buenos Aires, Argentina.

⁴Servicios Científicos Educativos y Turismo Científico Chile, Pedro León Ugalde 254, San Bernardo, Chile

⁵Department of Biological Sciences, University of Cape Town, Cape Town, South Africa

⁶School of Anthropology, University of Oxford, UK

* Corresponding author: solorzanoandres@gmail.com

Highlights

- A late early Miocene rodent assemblage of the Cura-Mallín Formation at Laguna del Laja (Chile) is here analyzed.
- A new species of caviomorph rodent is described: *Luantus sompallwei*.
- *Phanomys mixtus* Ameghino is for the first time reported in Chile.
- The rodent assemblage here studied might be related to the Santacrucian SALMA.

Abstract

Despite recent efforts, the paleodiversity of the Neogene mammals in Chile remains poorly known, with several putative new species awaiting description. For example, previous studies suggest that the early to late Miocene mammalian assemblages from the Laguna del Laja fossiliferous locality (Cura-Mallín and Trapa-Trapa formations), which crop out in the Andean Cordillera of Chile (~37°), comprise dozens of undescribed taxa. A better understanding of the taxonomic affinities of the Laguna del Laja faunas is needed, as it represents one of the few faunas known from the early to late? Miocene of the south-central Andean main range. Several specimens of caviomorphs recently recovered in late early Miocene beds of the

Cura-Mallín Formation at Laguna del Laja are here described in detail, and a brief discussion of their chronological, biogeographical, and paleoenvironmental significance is also provided. Based on fragments of mandible, maxilla and isolated teeth five taxa were recognized, *Phanomys mixtus* Ameghino, *Prolagostomus* sp., *Neoreomys* sp., *Maruchito* nov. sp.?, and *Luantus sompallwei* nov. sp. The radiometric ages of the fossil-bearing horizons, constrained between 17.7 and 16.4 Ma, as well as the common species (*P. mixtus*) and genera (*Prolagostomus* and *Neoreomys*) indicate that the fauna here reported belongs to the Santacrucian SALMA. Finally, our finding preliminary suggests the predominance of rather open habitats in the Cura-Mallín Formation during this time, but also a widely distributed late Early Miocene caviomorph fauna along the southern Andes, in both intra-arc and foreland basins.

Keywords: Santacrucian SALMA, Neogene fossils rodents, echimyids, dasyproctids, “eocardiids”, lagostomines, early Miocene paleoenvironments.

3.1 Introduction

Caviomorpha is a taxonomically and ecomorphologically diverse clade of hystricognath rodents endemic to the Americas and Caribbean islands that comprises nearly 250 extant species distributed among 52 genera and 10 families (Álvarez et al., 2011; Patton et al., 2015; Upham and Patterson, 2015). Caviomorphs have a long evolutionary history, and their representation in the South American fossil record begins in the late middle Eocene deposits of Contamana, Peru (Antoine et al., 2012; Boivin et al., 2017). Slightly younger assemblages indicate an early diversification of the group since the late Eocene? and early Oligocene as exemplified by the Santa Rosa (Peru), Tinguiririca (Chile) and La Cantera (Argentina) faunas (Frailey and Campbell Jr, 2004; Vucetich et al., 2010b; Bertrand et al., 2012; Álvarez et al., 2017; Arnal et al., 2019a). Early Miocene caviomorphs were also diverse with 36 genera recognized in the Colhuehuapian and Santacrucian SALMA faunas, mostly recognized in several localities in the Argentinean Patagonia (Ameghino, 1889, 1894; Scott, 1905; Kramarz and Bellosi, 2005; Kramarz et al., 2010; Vucetich et al., 2010a, 2015a; Arnal et al., 2019b). However, in contrast with neighboring geographical areas such as Argentina, work focused on Chilean caviomorph paleodiversity is still scarce. Recent findings

indicate the presence of several distinctive early Miocene rodent assemblages in Chile (Flynn et al., 2002a, 2002b; Croft et al., 2008; Bostelmann et al., 2012, 2013; Charrier et al., 2015), but some of them are poorly studied. This is the case of the rodent assemblages of the Cura-Mallín Formation in south-central Chile.

The Cura-Mallín Formation consists of a series of upper Oligocene to middle Miocene volcanic and sedimentary rocks deposited in continental settings that crop out in the Andean Cordillera of Chile and Argentina between 36°–39°S (Suárez and Emparan, 1995; Burns et al., 2006; Flynn et al., 2008; Utge et al., 2009; Radic, 2010; Pedroza et al., 2017; Solórzano et al., 2019). In Chile, some of the best exposures of the Cura-Mallín Formation are located near Laguna del Laja (37–38°S) and Lonquimay (38–39°S) (Suárez et al., 1990; Flynn et al., 2008; Pedroza et al., 2017; Solórzano et al., 2019). Miocene mammals including caviomorphs have been reported from both localities. Suárez et al. (1990) reported an indeterminate rodent in the Lonquimay area in putative early Miocene beds. However, the only specimen stored in the collections of the Museo Nacional de Historia Natural in Santiago (Chile) labeled as “Rodentia” likely belongs to a platyrrhine monkey of late middle Miocene age (Solórzano et al., 2019). Therefore, the presence of caviomorph rodents in the Cura-Mallín Formation at Lonquimay could not be confirmed (Solórzano et al., 2019).

Flynn et al. (2008) reported multiple fossiliferous horizons of the Cura-Mallín and Trapa-Trapa formations cropping out in the surroundings of Laguna del Laja, with ages ranging from early to late Miocene. The preliminary faunal lists provided indicates that these faunas are dominated, in terms of diversity, by caviomorph rodents and notoungulates (Flynn et al., 2008; Shockey et al., 2012). Interestingly, the former group appears to include several undescribed species of octodontids, dinomyids, dasyproctids, “eocardiids”, lagostomines, and echimyids (Flynn et al., 2008). Some of these forms show affinities with Patagonian taxa at the genus level, but most likely represent new genera and species (Flynn et al., 2008). In this sense, the Laguna del Laja rodents may be distinct from their Patagonian contemporaries in Argentina (Flynn et al., 2008). This is noteworthy given the geographic location of Laguna del Laja in the northern edge of modern Patagonia (Flynn et al., 2008). This proposed uniqueness could be related to habitat heterogeneity and environmental fragmentation caused by the surrounding volcanoes, geographic isolation probably linked to Andean uplift, and differences in age with contemporaneous faunas (Flynn

et al., 2008). In any case, as none of these putative new caviomorph rodent taxa have been formally described, the relatively high endemism could not be assessed and confirmed. Therefore, a better understanding of the taxonomic affinities of the Laguna del Laja faunas is needed, as it represents one of the few early to late? Miocene faunas from the south-central Andean main range (Charrier et al., 2015).

Recent paleontological surveys of the lower beds of the Cura-Mallín Formation south of Laguna del Laja (Chile) allowed us to collect few informative new rodent specimens within a relatively well-constrained chronostratigraphic framework (Herriott, 2006; Flynn et al., 2008). The main goal of this work is to describe these specimens, which include a new taxon, and to discuss the chronological and biogeographical affinities of the assemblage.

3.2 Geological and geographical settings

The Cura-Mallín Formation is the basal unit in the homonymous basin and is characterized by a predominant volcanic member (with intercalations of sedimentary strata), and a sedimentary member, which generally overlies it and was deposited in alluvial, fluvial, lacustrine and deltaic environments (Suárez and Emparan, 1995; Burns et al., 2006; Radic, 2010; Pedroza et al., 2017). Different names have been applied locally to these members. Niemeyer and Muñoz (1983) defined the volcanic Río Queuco lower member and the sedimentary Malla-Malla upper member in the Laguna del Laja area (Chile). Suarez and Emparan (1995) defined the volcanic Guapítrio member and the sedimentary Río Pedregoso member in the Lonquimay region (Chile) but considered both members to be coeval. However, based on lithostratigraphic data, Herriott (2006) and Flynn et al. (2008) could not recognize the volcanic (Río Queuco) and sedimentary (Malla-Malla) members within the southeast of Laguna del Laja.

In contrast, they subdivided the southeast the Laguna del Laja area into five mappable units: Tcm₁, Tcm₂, Tcm₃, Tcm₄, and Tcm₅. The Tcm₁, Tcm₃, and Tcm₅ are volcanoclastic sandstone and mudstone, with Tcm₅ having a greater component of fine-grained strata; the Tcm₂ is an ignimbrite that separates the lithologically similar Tcm₁ and Tcm₃ strata, being considered a well-marker bed; Tcm₄ is lithologically distinctive in containing pebble-sized clasts of granitoid and quartzite (Herriott, 2006). Herriott (2006) and Flynn et al. (2008) also provides Ar/Ar

radiometric dates for the rock cropping out in Laguna del Laja and indicates that deposition of the Cura-Mallín Formation in this area started in 19.80 Ma and continued until at least 14.50 Ma. The bracket age of the defined mappable units is 18–19.8 Ma for Tcm₁, 17.84–18 Ma for Tcm₂, ~16–17.84 Ma for Tcm₃, 14.5– ~16 Ma for Tcm₄ and younger than 14.5 Ma and older than 10 Ma for Tcm₅ (Herriott, 2006; Flynn et al., 2008; Shockey et al., 2012). In the Laguna del Laja, the predominantly volcanic conglomerates and breccias, intermediate to mafic lavas, and rare to minor beds of finer-grained volcanoclastic deposits of the late Miocene (8.9 ± 0.1 and 10.10 ± 0.20 Ma) Trapa-Trapa Formation overly the Cura-Mallín Formation (Niemeyer and Muñoz, 1983; Herriott, 2006; Flynn et al., 2008).

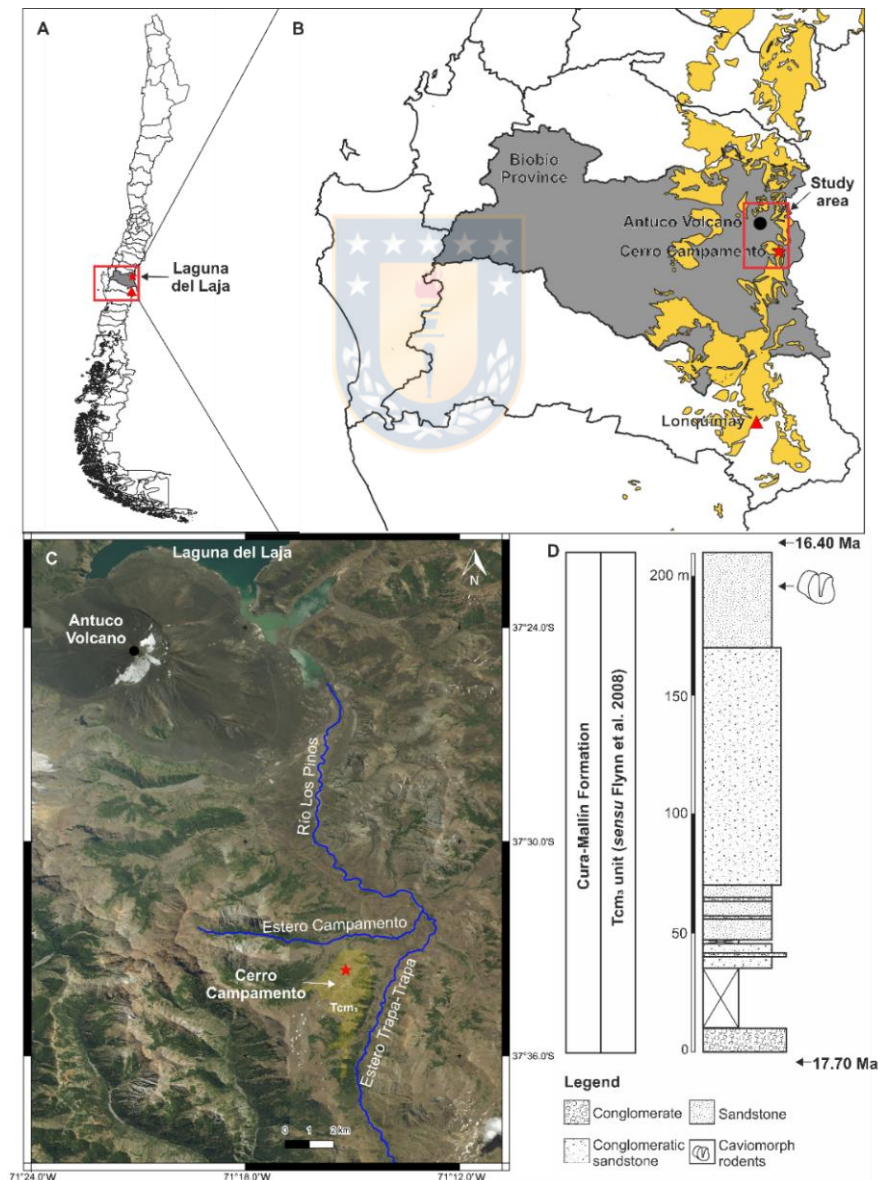


Figure 3.1. Geographic and stratigraphic provenance of the caviomorph remains described in the present study from the Laguna del Laja region (late early Miocene of the Cura-Mallín Formation;

Cerro Campamento, west of the Estero Trapa-Trapa; Biobío Province, south-central Chile). A and B) geographic location of the study area; C) aerial view of the Laguna del Laja region showing details about the location of the fossiliferous sampled levels (denoted by a red star); D) generalized stratigraphic profile of the Cerro Campamento. The grey region in A and B, denotes the location of the Biobío Province, Chile. The yellow polygons in B indicate the geographic extension of the Oligocene to Miocene volcano-sedimentary units, which must mainly correspond (at this latitudes) with the units included in the Cura-Mallín Basin (SERNAMEG, 2003). The pale-yellow polygon in C, denotes the extension of the Tcm3 unit over the Cerro Campamento (west of the Estero Trapa-Trapa). The geographic and chronological extension of Tcm3 unit is based on Flynn et al. (2008) and Herriott (2006).

In the present work, we follow the lithostratigraphic framework previously described (Herriott, 2006; Flynn et al., 2008; Shockey et al., 2012). The rodents here reported were recovered from surface picking along few subhorizontal volcanoclastic grey sandstones cropping out at the top of the Cerro Campamento, at the west of the Estero Trapa-Trapa, south of the Laguna del Laja (Biobío Province, Chile; Figure 3.1). Volcanoclastic sandstone and conglomerate are the dominant lithologies over the upper section of the Cerro Campamento, which belongs to the Tcm₃ unit (Flynn et al., 2008). The age of these fossil-bearing horizons is constrained to the late early Miocene, between 17.70 and 16.40 Ma (Fig. 3.1).

3.3 Brief paleontological background

Flynn et al. (2008) provide a preliminary faunal list for the distinct localities and stratigraphic levels cropping out in the Laguna del Laja area. The mammals so far reported from the early Miocene Tcm₁–Tcm₃ levels include notoungulates (*Paedotherium minor*, *Colpodon antucoensis*, cf. *Protyotherium* sp., ?*Hegetotherium* sp., Toxodontidae indet., Typotheria indet. and Interatheriinae indet.), caviomorphs rodents (?*Neoreomys* sp., *Maruchito* sp. nov., *Protacaremys* sp. nov., *Prostichomys* sp. nov. I, *Prostichomys* sp. nov. II, *Luantus* sp. nov., *Acarechimys* sp. nov., *Scleromys* sp. nov., *Prolagostomus* sp. nov., gen. et sp. nov. aff. *Prostichomys*, gen. et sp. nov. aff. *Protacaremys*, gen. et sp. nov. aff. *Incamys*, gen. et sp. nov. aff. *Maruchito*, gen. et sp. nov. aff. *Prospaniomys* and gen. et sp. nov. aff. *Alloiomys*), marsupials (*Sipalocyon* sp. and Abderitidae indet.), astrapotheres (Astrapotheriidae indet.), armadillos (Dasypodidae indet.), and sloths (*Nematherium* cf. *N. angulatum* or sp. nov.) (Flynn et al., 2008; Shockey et al., 2012). However, just few of these taxa have been illustrated (Flynn et al., 2008), and excepting *Colpodon antucoensis* (Shockey et al., 2012), none of them have

been described. Therefore, the Laguna del Laja paleodiversity remains poorly known.

3.4 Material and methods

The specimens described here are housed at the Museo de Historia Natural de Concepción, Concepción, and the Museo Nacional de Historia Natural de Santiago, Chile. All measurements are in millimeters and were taken with a digital caliper. Comparisons of taxa described here are mainly with closely related taxa in Argentina (see Electronic Supplementary Material 1). Nomenclature of the lower and upper cheek teeth of caviomorph rodents follows Boivin and Marivaux (2018), Marivaux et al. (2004) and Rasia and Candela (2019).

Abbreviations. Upper case letters are used for the upper dentition (P: for premolar, M: for molar) and lower case letters for the lower dentition (p: for premolar, m: for molar); dP/dp: deciduous premolar, SALMA, South American Land Mammal Age; APL, anteroposterior length; AW, anterior width; PW, posterior width.

Institutional abbreviations. **SGOPV**, Museo Nacional de Historia Natural de Santiago, Santiago, Chile; **MHNC**, Museo de Historia Natural de Concepción, Concepción, Chile; **MACN**, Museo Argentino de Ciencias Naturales “Bernardino Rivadavia”, Buenos Aires, Argentina; **MLP**, Museo de La Plata, La Plata, Argentina.

3.5 Systematic paleontology

Order RODENTIA Bowdich, 1821

Suborder HYSTRICOGNATHI Tullberg, 1899

Superfamily OCTODONTOIDEA Waterhouse, 1839

Family ECHIMYIDAE Gray, 1825

Genus *MARUCHITO* Vucetich et al., 1993

Type and only species. *Maruchito trilofodonte* Vucetich et al., 1993.

Geographic and Stratigraphic Distribution. Late early Miocene, Cura-Mallín Formation, Biobío Province, Chile, and middle Miocene, Collón Curá Formation, Neuquén Province, Argentina (Vucetich et al., 1993; Flynn et al., 2008).

Maruchito nov. sp.?

Figure 3.2

Referred material. SGO.PV.1400, a fragment of left maxilla with dP4-M3.

Geographic and stratigraphic provenance. Estero Trapa-Trapa west, Laguna del Laja (Chile), Tcm₃ unit, Cura-Mallín Formation, early Miocene.

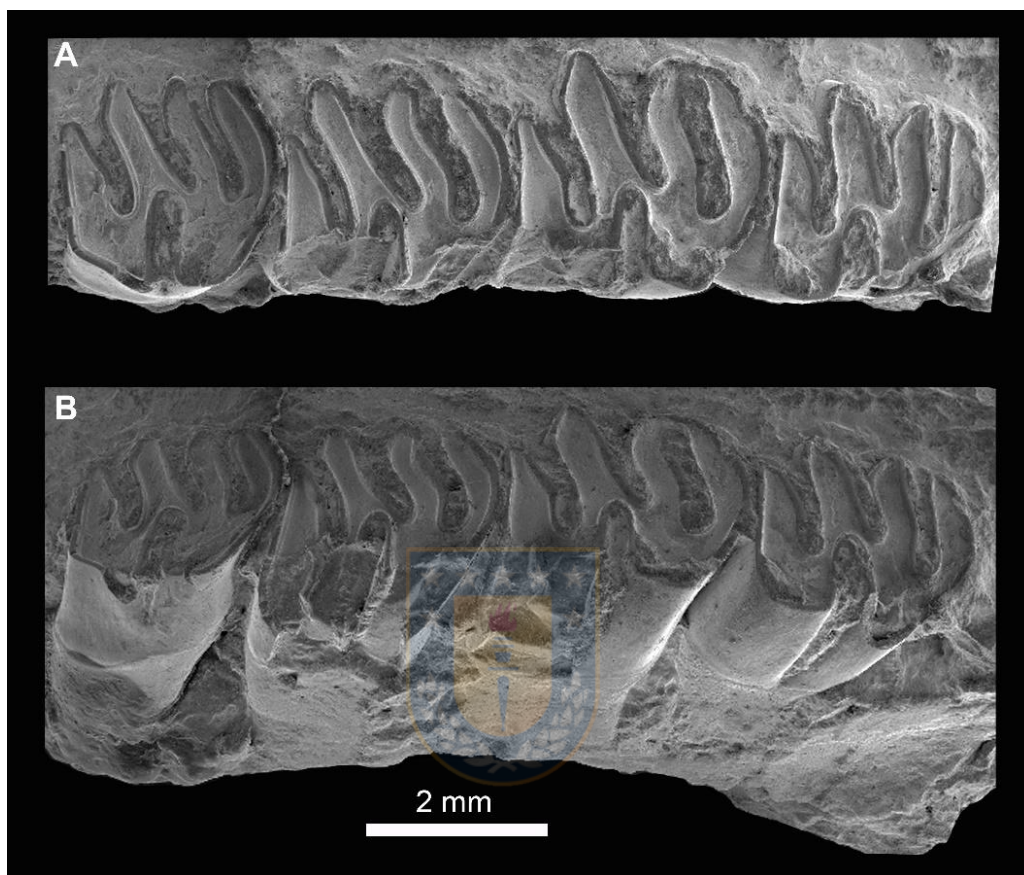


Figure 3.2. *Maruchito* sp. nov? (SGO.PV.1400) from late early Miocene beds of the Cura-Mallín Formation, Laguna del Laja, Chile; left maxilla with dP4-M3 in occlusal (A) and lingual (B) views.

Description. The tooth row is straight and preserves rectangular, mesodont (crown height/anteroposterior length on M3 = 0.60), and tetralophodont upper molariforms (dP4-M3), with crests broader than flexi (Fig. 3.2), and cusps entirely subsumed in their associated crests. The enamel layers are relatively narrow and surround the entire molariforms. The mesiodistal length of the dP4-M3 series is 13.32 mm.

The dP4, slightly (4%) larger than the M1 (Table 3.1), has a short anteroloph (not reaching the labial end of the protoloph, suggesting that the labial end of the anteroloph is located more lingual than the paracone and metacone areas), while the other crests (protoloph, metaloph and posteroloph) are similar in length (Figure 3.2A). The crests are oblique, forming around 60° with the mesiodistal tooth axis,

with labial ends broadly pointed (this feature is better exemplified in the protoloph; Figure 3.2A). Labial flexi of approximately similar length, but paraflexus is the most penetrating one. The hypoflexus is relatively short (reaching less than half of the occlusal surface), transverse (forming around 90° with the lingual tooth wall), and slightly mesiodistally wider than the labial flexi. The mesiolingual angle is typically obtuse (~110°); the distal teeth wall is broadly concave.

The upper molars are broadly similar to the dP4. The major differences are in the obliquity of the crests and flexi (Figure 3.2A), with a progressive reduction in the obliquity from M1 to M3: in M1 the crest forms an angle around 60° with the mesiodistal tooth axis, 75° in M2, and nearly 90° in the M3. The mesiolingual angle is nearly 90° (this feature is especially clear in the M3; Figure 3.2A). In M1, the protoloph and mesolophule have a similar labial extension; while in the M2 and M3, the protoloph extends more labially than the remaining crests, suggesting that the paracone area is located more labial than the metacone area and the labial end of the anteroloph. The hypoflexus in the M1–M3 series is transverse and persistently reaches less than half of the occlusal surface. In M1 and M2 the paraflexus is the most penetrating labial flexus (Figure 3.2A). The M2 is the largest tooth of the series, being slightly (~5%) larger than the M1 and M3 (Table 3.1). In M2, the mesolophule and posteroloph are connected in the lingual margin, enclosing the posterior-most fossette (Figure 3.2A). In M3, the posteroloph is transversally shorter than in M1 or M2 (Figure 3.2A), the area of the protocone appears to be mesiodistally shorter than the area of the hypocone (unlike other upper molariforms), the paraflexus is less penetrating with respect to M2, being the posteroflexus the most penetrating labial flexus, but, it does not reach the lingual margin. The wear trajectory of the upper molars suggests that the posteroloph becomes less penetrating in advanced stages of wear, while the paraflexus becomes more penetrating with wear (Figure 3.2A).

A direct examination of the labial wall of the molars of the specimen was not possible (Figure 3.2A). However, in the dP4 and M1 the metastrria must be deeper than in M2, because the metastrria persists even with greater wear (Figure 3.2A). The labial ends of dP4-M3 crest are acuminate (Figure 3.2A). In lingual view, variable depth of the hypostria was noted likely suggesting differences in wear (Figure 3.2B): hypostria becomes progressively deeper distally (i.e., in the dP4 the hypostria did not reach the base of the tooth, while in the M3 the hypostria almost reach the 95% of the tooth base).

Remarks. The material from Laguna del Laja (SGO.PV.1400) shares several dental characters with the middle Miocene echimyid *M. trilofodonte*, including size, crown height, rather narrow and straight hypoflexus, and transverse crests and labial flexi in some of the upper molars (Vucetich et al., 1993). These similarities suggest that they might belong to the same genus.

A preliminary revision of a sample of upper molariforms referred to *M. trilofodonte* (from the Collón Curá Formation, Argentina; see Electronic Supplementary Material 1) indicates the wide ontogenetic variability of this taxon. In this sense, an assessment of this variability is in need. Unlike SGO.PV.1400, *M. trilofodonte* has dP4 with a marked rectangular outline (mesiodistal length >> transverse length) in most stages of wear (e.g. MLP 91-IX-1-33, MLP 91-IX-1-23), upper molars with a transversely more penetrating posterior-most fossette (even in a very advanced stage of wear), and acuminate labial ends of crest only in early stages of wear, which become rounded and thicker with wear. Considering the limited sample of *Maruchito* from Laguna del Laja, as well as the unclear ontogenetic variability of the type species, the identity of SGO.PV.1400 cannot be determined with certainty. Based on the differences previously mentioned, SGO.PV.1400 could represent a new species of *Maruchito* as previously proposed (Flynn et al., 2008). Nevertheless, additional materials, especially lower molars, are necessary to refine its taxonomic affinities.

Superfamily CAVIOIDEA (Fischer de Waldheim, 1817)

Family "EOCARDIIDAE" Ameghino, 1891

Genus *LUANTUS* Ameghino, 1899

Included species. *Luantus propheticus* Ameghino, 1899 (type species), *Luantus initialis* Ameghino, 1902, *Luantus toldensis* Kramarz, 2006, *Luantus minor* Pérez et al., 2010 and *Luantus sompallwei* sp. nov.

Geographic and Stratigraphic Distribution. Early Miocene (Colhuehuapian SALMA) of the Sarmiento Formation (Colhue Huapi Member), Chubut Province, Argentina; early Miocene (Santacrucian SALMA) of Pinturas (Santa Cruz Province, Argentina), Santa Cruz (Santa Cruz Province, Argentina) and Cura-Mallín formations (Biobío Province, Chile) (Kramarz and Bellosi, 2005; Kramarz, 2006a; Flynn et al., 2008; Pérez et al., 2010).

Luantus sompallwei nov. sp.

Figure 3.3A–F

Holotype. SGO.PV.1401, a fragment of right mandible with the base of incisor, incompletely erupted unworn p4, and moderately worn m1.

Tentatively referred material. SGO.PV.1402, isolated m1 or m2.

Diagnosis. Similar in size to *L. propheticus*, and *L. toldensis*, but 20% larger than *L. minor* (based in dental measurements, Table 3.1). Cheek teeth lower crowned than *L. initialis*, but higher crowned than in *L. propheticus*, with large discontinuities of the enamel covering on the base of the cheek teeth (resembling *L. toldensis*). Differs from *L. propheticus*, and *L. toldensis* in having a p4 with a persistent (even in advance stage of wear) and well-developed mesially projected lophid (“anteroconid”) attached to the metaconid area, and two ephemeral flexids on the mesial wall in early stages of wear, which are lost in later stages.

Etymology. *Sompallwe*, refers a mermaid shaped mythological entities of the Mapuche cosmovision which inhabit and protect their lakes, as the Laguna del Laja.

Geographic and stratigraphic provenance. Estero Trapa-Trapa west, Laguna del Laja, Chile, Tcm₃ unit, Cura-Mallín Formation, late early Miocene (Santacrucian SALMA).

Description and comparison. The mandible of the holotype is poorly preserved and shows no relevant characters. The incisor extends posteriorly beyond the m1. The base of the incisor is rather transversally compressed, at least in the exposed portion above the m1 (Figure 3.3A, B). The cheek teeth are high crowned but rooted (protohypsodont).

The unworn, and not fully erupted, p4 has two asymmetrical lobes with the mesial being mesiodistally larger and transversely narrower than the distal (Figure 3.3C). These lobes are labially separated by the rather sub-triangular hypoflexid, which is located opposite to the mesofossettid, extends more than half of the tooth width, and lacks cement (at least in this stage of wear). The p4 also exhibits three lingual flexids forming a tetralophodont (molariform-like) occlusal pattern. Two flexids (anteroflexid and mesoflexid) are located in the mesial lobe, while the metaflexid is on the distal one. The anteroflexid and mesoflexid open lingually, with the former being labiolingually larger and mesiodistally narrower than the latter. The metaconid area is well-developed and has a mesially projected lophid, that could be equivalent to the element described as “anteroconid” in premolars of other

caviomorphs with lower crowned cheek teeth (e.g. *Cephalomys*; see Wood and Patterson, 1959). The last feature is retained even in advanced stages of wear because it persists toward the base of the tooth (Figure 3.3D). In occlusal view, there is columnar element on the mesial wall of the tooth, between the metaconid and protoconid areas, likely derived from the metalophulid I. The flexids separating this column from the adjacent cuspids are ephemeral, and thus the column becomes indistinct in advanced stages of wear, and the labial edge of the “anteroconid” would form roughly right angle with the mesiolabial aspect of the tooth (metalophulid I). The second transverse lophid (metalophulid II?) connects the lingual aspect of the protoconid area with the small cuspid in the lingual margin of the tooth between the metaconid and the entoconid areas. The marginal cuspid (mesostylid?) is smaller than the adjacent cuspids and would become indistinct with moderate wear. The posterior lobe of the tooth is rather triangular, with a very large, labiolingually elongate, and lingually open metaflexid separating the hypolophid from the posterolophid (Figure 3.3C). The protoconid area is slightly lingually positioned with respect to the hypoconid area, and thus the trigonid is distinctly narrower than the talonid.

The m1 of the holotype is bilobed, with a lingual wall straight, and wide, transversally elongated, and persistent fossettids (Figure 3.3C). The mesial lobe has two fossettids: the anterofossettid and the mesofossettid. The former is labiolingually elongate and distolingually oblique, while the latter is smaller, transverse, more posteriorly placed, and opposite the hypoflexid (Figure 3.3C). The distal lobe is slightly transversally larger than the mesial one and exhibits a very labiolingually elongate metafossettid. The posterolophid occupies more than 50 % of the occlusal surface of the distal lobe (Figure 3.3C). The hypoflexid is triangular, with “V” shaped apex extending more than halfway the crown width and lacks cement (at least in this stage of wear). The enamel is rather continuous along the occlusal surface of the tooth but appears to be thinner toward the lingual margin and in the mesiolingual and distolingual corners. Two vertical bands of exposed dentine are present on the lingual wall, reaching more than half of the preserved crown height (Figure 3.3A).

The isolated m1 or m2 (SGO.PV.1402) (Figure 3.3E-F) is almost identical to the m1 of the holotype, although it is slightly larger (Table 3.1). In this molar, two

vertical bands of exposed dentine are also present on the lingual wall, reaching 75% the preserved height of the crown (Figure 3.3E).

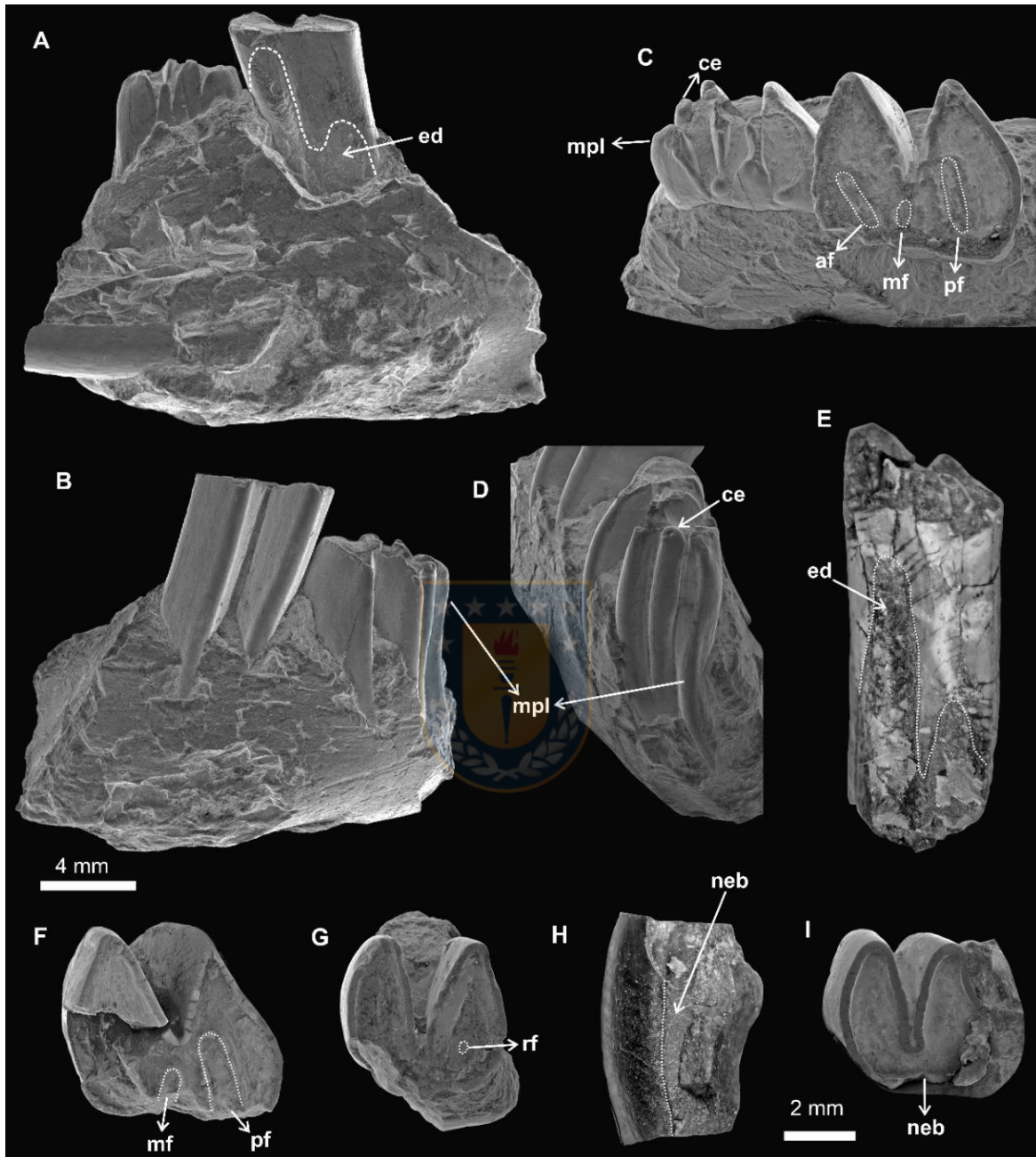


Figure 3.3. Cavioid rodents from late early Miocene beds of the Cura-Mallín Formation, Laguna del Laja, Chile. A–F, *Luantus sompallwei* sp. nov.: fragment of right dentary bearing the p4, m1 and the base of the lower incisor (Holotype: SGO.PV.1401) in lingual (A), labial (B), occlusal (C) and mesial (D) views; isolated m1 or m2 (SGO.PV.1402) in lingual (E) and (F) occlusal views. G–I, *Phanomys mixtus*: right isolated upper M1 or M2 (MHNC 38.0038) in occlusal (G) and distolabial (H) views; right isolated M1 or M2 (MHNC 38.0037) in occlusal view (I). Note the lack of enamel in the lingual face of the tooth in G. A and B are in the same scale (4 mm); C–I are in the same scale (2 mm). Abbreviations: ed, exposed dentine; neb, no enamel band; af, anterofofsette; mf, mesofossette; pf, posterior-most fossette; mpl, mesially projected lophid (= “anteroconid”); ce, columnar element on mesial p4 wall; rf, relictuall fossette.

Remarks. The specimens described here show the diagnostics feature of the genus *Luantus*, e.g. protohypsodont cheek teeth, hypoflexid with triangular contour, large and transversally elongated fossettids which persist in at least moderate ontogenetic stages (Kramarz, 2006a; Pérez et al., 2010). The Laguna del Laja specimens differ from the Colhuehuapian *L. initialis* in having higher crowned teeth and more molarized p4 (Kramarz, 2006a; Vucetich et al., 2010b), and from *L. minor* (Colhuehuapian) by their larger size and more penetrating hypoflexids (Pérez et al., 2010).

The configuration of the p4 from the Laguna del Laja specimen differs from those observed in named *Luantus* species in which this tooth is known (Kramarz, 2006a; Pérez et al., 2010). After a revision of a large sample of *L. propheticus*, Kramarz (2006a) reports intraspecific variability within the mesial lobe of p4, particularly the varying presence and degree of development of a mesial projection of the metaconid (which likely might include an “anteroconid”) and an ephemeral flexid on the anterior wall. However, when present the mesial projection of the metaconid of *L. propheticus* (e.g. MACN- PV SC3617; MACN-Pv SC2235) is much less developed and persistent than in the Laguna del Laja specimen (Figure 3.3D). The p4 of *L. toldensis* has a comparatively larger mesiodistal diameter than in *L. propheticus*, and the anterolingual projection of the tooth is more pronounced than in the former (Kramarz, 2006a). Unlike *L. sompallwei*, the p4 of *L. toldensis* has a simpler trigonid with a rather straight mesial wall or with a single and more superficial mesial flexid (Kramarz, 2006a). After a revision of several isolated p4 from the Pinturas Formation referred to *L. toldensis*, we conclude that the distinctive p4 morphology of SGO.PV.1401 exceeds the known range of intraspecific variability of *L. toldensis*, reinforcing the notion that both represent distinct species. Moreover, although the specimens from Laguna del Laja exhibits an unique trait combination (mentioned in the diagnosis) they appear to be closely related to *L. toldensis*, because both share relatively high crowned tooth and vertical bands of exposed dentine (in the lingual wall) that reach nearly half the height of the tooth crown (Kramarz, 2006a).

Genus PHANOMYS Ameghino, 1887

Included species. *Phanomys mixtus* Ameghino, 1887 (type species), and *Phanomys vetulus* Ameghino, 1891.

Geographic and chronological distribution. Late early Miocene of Pinturas, Jeinemení and Santa Cruz formations (Santacrucian SALMA), Santa Cruz Province, Argentina, and Cura-Mallín Formation (Santacrucian SALMA), BioBío Province, Chile (Kramarz, 2006a; Pérez and Vucetich, 2012).

Phanomys mixtus Ameghino, 1887b

Figure 3.3G–I

Referred materials. MHNC 38.0038, right isolated M1 or M2; MHNC 38.0037, right isolated M1 or M2.

Geographic and stratigraphic provenance. Estero Trapa-Trapa west, Laguna del Laja (Chile), Tcm₃ unit, Cura-Mallín Formation, early Miocene (Santacrucian SALMA).

Description. The specimens represent isolated upper molars (M1 or M2). These molars are high crown (protohypsodont) and deeply bilobated, with the mesial lobe slightly labiolingually narrower than the distal one. In the distal lobe of MHNC 38.0038 (Figure 3.3G) there is a relictual fossette, while MHNC 38.0037 lacks fossettes over the occlusal surface (Figure 3.3I). The hypoflexus is roughly funnel-shaped, with a “U” shaped apex, extends transversely more than the half of the tooth, and shows cement in its more labial portion. Most of the labial wall of the teeth lack enamel, while the remaining walls of the teeth show a relatively thick enamel coverage (Figure 3.3H, I).

Remarks. The specimens display all the recognized diagnostics features of the genus *Phanomys*, as protohypsodont molariforms; enamel interrupted along labial walls of the upper teeth; fossettes less persistent during ontogeny than in any other protohypsodont species of Caviioidea; hypoflexus narrow, extending transversely more than half of the crown and bearing cement since early ontogenetic stages (Pérez and Vucetich, 2012). There are only two species recognized within the genus, *P. mixtus* and *P. vetulus*, and size is the main difference between both taxa, with the former being larger than the latter (Pérez and Vucetich, 2012). The size of the molars recovered from the Laguna del Laja falls into the range size reported for *P. mixtus*, and is decidedly larger than those known for *P. vetulus* (Pérez and Vucetich, 2012). Therefore, Laguna del Laja specimens can be referred to *P. mixtus*. The genus *Phanomys*, was previously recognized only in southern Argentina (Pérez and Vucetich, 2012). Therefore, *Phanomys* is reported here for the first time in Chile.

Family DASYPROCTIDAE Smith, 1842

Genus *NEOREOMYS* Ameghino, 1887

Included species. *Neoreomys australis* Ameghino, 1887 (type species), *Neoreomys huilensis* Fields, 1957 and *Neoreomys pinturensis* Kramarz, 2006b.

Geographic and chronological distribution. Late early Miocene of Pinturas Formation and Santa Cruz formations, Santa Cruz and Chubut provinces, Argentina; late early Miocene of Cura-Mallín Formation, Biobío Province, Chile; middle Miocene (Colloncuran SALMA) of Collón Curá Formation, Río Negro and Neuquén provinces, Argentina; late middle Miocene (Laventan SALMA) of La Victoria Formation, Colombia (Fields, 1957).

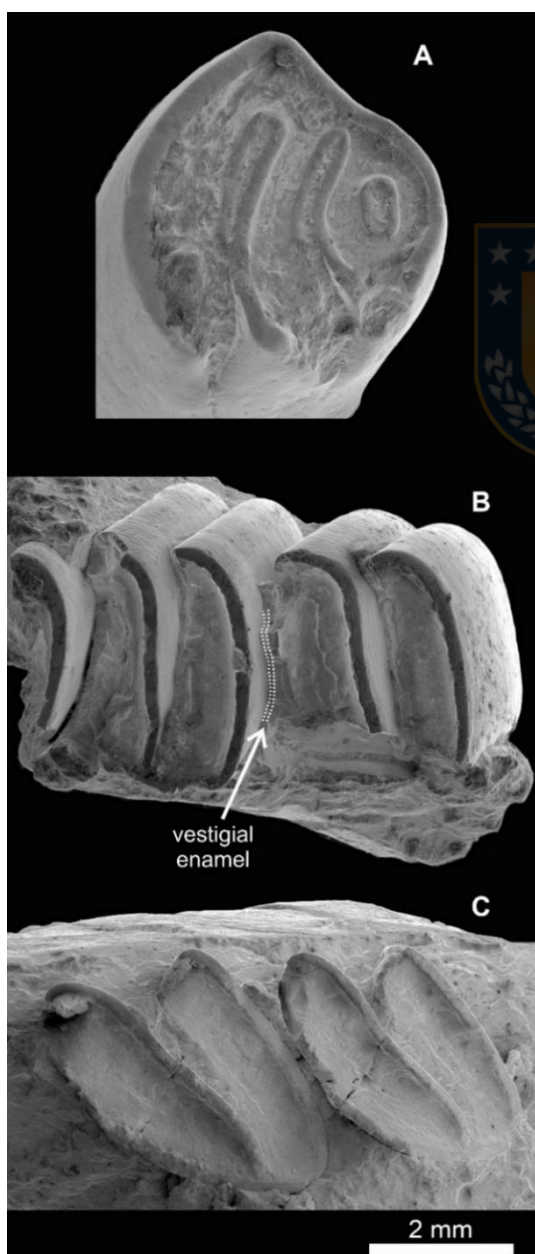


Figure 3.4. Dasyproctid and chinchillid rodents from late early Miocene beds of the Cura-Mallín Formation, Laguna del Laja, Chile. *Neoreomys* sp.: isolated P4 (MHNC 38.0039) in occlusal view (A). *Prolagostomus* sp.: left maxillary fragment with M1, M2 and a mesial portion of the M3; MHNC 38.0040) in occlusal view (B), right mandibular fragment with m2 and m3 (MHNC 38.0041) in occlusal view (C).

Neoreomys sp.

Figure 3.4A

Revised specimen. MHNC 38.0039; isolated right P4.

Geographic and stratigraphic provenance. Estero Trapa-Trapa west, Laguna del Laja, Chile, Tcm₃ unit, Cura-Mallín Formation, early Miocene.

Description. Tetralophodont and protohypodont upper premolar, with a distinctive bell-shape crown outline (in occlusal view), wide crests and thick enamel layers. The tooth is slightly wider than long (Figure 3.4A). The paraflexus and mesoflexus are very narrow. The paraflexus is rather straight and subparallel to the mesial edge of the tooth (Figure 3.4A). The mesoflexus is distally more penetrating than the paraflexus and curved along the occlusal tooth surface. The posteroloph and mesolophule enclosed a short and elliptical posterior-most fossette. While the most lingual portion of protoloph is almost parallel to the paraflexus, the protoloph becomes markedly curved distally toward the central surface of the tooth (Figure 3.4A). Hypoflexus absent.

Remarks. Among Miocene taxa referred to Dasyproctidae, the absence of a hypoflexus over the lingual side of the P4 plus a wide enamel layer is known in *Neoreomys*, *Alloiomys*, and *Australoprocta* (Kramarz, 1998). The upper premolar from Laguna del Laja rather resembles the general morphology of the former. It differs from *Australoprocta* in being much larger and higher crowned and in having a more simplified occlusal pattern by lacking a distinctive mesoloph (Kramarz, 1998, 2006b); while the P4 of *Alloiomys* has a rather subtriangular contour, and has only three transverse lophs (at least in a similar stage of wear) (Vucetich, 1977). The P4 from Laguna del Laja is in the size range of the *N. australis* (Santacrucian) and is decidedly larger than *N. huilensis* (Laventan) (Fields, 1957; Kramarz, 2006b). Even when the P4 of *N. pinturensis* is unknown, this taxon differs from *N. australis* by their lower crowned cheek teeth (Kramarz, 2006b). However, as the only P4 available from Laguna del Laja is broken toward its base the crown height cannot be estimated, making it unreliable to provide more details at the species level and its affinities with other species.

Superfamily CHINCHILLOIDEA Bennett, 1833

Family CHINCHILLIDAE Bennett, 1833

Subfamily LAGOSTOMINAE Pocock, 1922

Genus *PROLAGOSTOMUS* Ameghino, 1887

Included species. *Prolagostomus pusillus* Ameghino, 1887 (type species), *Prolagostomus divisus* Ameghino, 1887; *Prolagostomus profluens* Ameghino, 1887; *Prolagostomus imperialis* Ameghino, 1887; *Prolagostomus lateralis* (Ameghino, 1889); *Prolagostomus primigenius* (Ameghino, 1889); *Prolagostomus obliquidens* Scott, 1905 and *Prolagostomus rosendoi* Vucetich, 1984.

Geographic and chronological record. Late early to late middle Miocene of Pinturas and Santa Cruz formations (Santacrucian SALMA), south of Patagonia, Argentina, Collón Curá Formation (Colloncuran SALMA), north of Patagonia, Argentina, Cerro Boleadoras Formation (Santacrucian SALMA), Patagonia, Argentina, Rio Frias Formation (“Friasian” SALMA), Western Patagonia, Chile, Cura-Mallín Formation (Laguna del Laja; Santacrucian to Laventan? SALMA) South Central Chile, Galera Formation (Pampa Castillo; Santacrucian to “Friasian”), South of Chile, and Honda Group (Quebrada Honda; Laventan SALMA), Bolivia (Kramarz, 2002; Croft et al., 2011).

Prolagostomus sp.

Figure 3.4B,C

Referred materials. MHNC 38.0040, a fragment of left maxilla with M1-M2 and the mesial-most edge of M3; MHNC 38.0042, right isolated M1 or M2, with portions of the maxillary; MHNC 38.0041, a fragment of right mandible with m2 and m3.

Geographic and stratigraphic provenance. Estero Trapa-Trapa west, Laguna del Laja, Chile, Tcm₃ unit, Cura-Mallín Formation, early Miocene.

Description. The M1 and M2 are euhypsodont and bilaminated (formed by two laminae connected by a narrow labial isthmus). The mesial and distal laminae has an enamel layer in its mesial and lingual walls (Figure 3.4B). However, a vestigial enamel layer on the backside of the M1 is present, but it is not clearly observed in the partially eroded M2 (Figure 3.4B). The M1 and M2 are quite similar, with the mesial lamina slightly labially projected. In the distal lamina, the labial wall is mesiodistally more elongated than the lingual wall. The mesial wall is slightly curved, and the distal wall is straight. The hypoflexus is very narrow and penetrating (almost reaching the labial edge), slightly sinuous, and filled with cementum. The laminae are slightly oblique (the labial and mesial wall form an angle of around 80°).

The lower molars have two oblique laminae. The boundary between lingual and mesial walls is curved, forming a 120° angle (Figure 3.4C). The distal lamina is mesiodistally wider than the mesial. The mesial lamina wedges toward the lingual wall, while the distal one is rather rectangular (Figure 3.4C). The enamel covers the mesiolingual and distal wall of the anterior lamina and distal wall of the distal lamina (Figure 3.4C).

Remarks. The specimens here described display the diagnostic features of the genus *Prolagostomus* (Vucetich, 1984), and differ from *Lagostomus* and *Pliolagostomus* in having rounded molariform walls (Croft et al., 2011). *Prolagostomus* is the most common taxon found in the sampled beds of the Tcm₃ unit on the Estero Trapa-Trapa west. Contrasting with previous findings (Flynn et al., 2008), *Prolagostomus* remains are the most common rodent in the analyzed stratigraphic levels.

Several species have been historically assigned to *Prolagostomus*, and some of them are mostly recognized by size differences (Scott, 1905; Vucetich, 1984; Kramarz, 2002; Croft et al., 2011). However, the actual number of valid species is likely overestimated because it is unclear how to confidently distinguish among ontogenetic, intraspecific, and interspecific variation (Kramarz, 2002; Croft et al., 2011). The rather distinctive feature of the Laguna del Laja *Prolagostomus* is the presence of a vestigial enamel layer in the distal wall of the upper molars. This feature is absent in other *Prolagostomus* species recognized on upper molars (e.g. *P. pusillus*, *P. divisus* and *P. profluens*) (Kramarz, 2002). However, several *Prolagostomus* specimens recovered from the middle and upper levels of the Pinturas Formation (Argentina), appears to display the same putative ancestral feature and may represent an unnamed taxon (Kramarz, 2002). In this sense, even when we agree with the complex taxonomic status of some species within *Prolagostomus*, the Laguna del Laja specimens are likely more closely related to forms from the upper beds (Santacrucian SALMA) of the Pinturas Formation (Kramarz and Bellosi, 2005).

3.6 Discussion

The study of a restricted collection of mandibular and maxillary fragments, and isolated teeth of caviomorph rodents recovered from beds of relatively well-

constrained late early Miocene age from the Laguna del Laja region (Cura-Mallín Formation) allows to the recognizing of five taxa, *Phanomys mixtus*, *Prolagostomus* sp., *Neoreomys* sp., *Luantus sompallwei* nov. sp., and *Maruchito* nov. sp.? One of these taxa is new to science and increases the paleodiversity of Miocene mammals in southern South America. The early to middle Miocene has been regarded as the time period with the highest known mammal paleodiversity in Chile with more than 54 taxa (Canto et al., 2010). However, the available preliminary taxonomic lists from the most diverse localities in the country reporting dozens of new undescribed taxa and/or taxa in open nomenclature (Flynn et al., 2002a, 2002b, 2008; Bostelmann et al., 2013; Charrier et al., 2015), indicate that much more work is necessary to assess the ancient diversity of the Miocene of Chile. Therefore, our study provides a new step in this regard.

The Tcm₁ and Tcm₃ units are the most prolific source of fossils in the Laguna del Laja area (Flynn et al., 2008). The five rodent taxa here reported come from the middle section of the Tcm₃ unit (*sensu* Flynn et al., 2008), with a relatively well-constrained ⁴⁰Ar/³⁹Ar ages of 17.70 – 16.40 Ma. Flynn et al. (2008) suggested that the successive faunas from the Laguna del Laja, which include materials recovered from the Cura-Mallín and Trapa-Trapa formations, might represent as many as six SALMAs, including the Colhuehuapian, Santacrucian, Colloncuran, Laventan, Mayoan, and Chasicoan. Other authors (Kramarz et al., 2010), suggested that the Laguna del Laja fauna could be referred, at least in part, to the “Pinturan” fauna (likely representing the earliest part of the Santacrucian SALMA) due to the presence of the octodontoid rodent *Prostichomys* (Flynn et al., 2008). In fact, there are two putative and undescribed new species of *Prostichomys* from Laguna del Laja, both recovered from the lower-most Tcm₃ levels with a ⁴⁰Ar/³⁹Ar radiometric age of ~17.9 Ma (Flynn et al., 2008). These remains are therefore broadly consistent with the age of the “Pinturan” faunas (19.0 – 18.0 Ma) in Argentina (Cuitiño et al., 2016). However, the incomplete taxonomic record of the successive mammalian faunas of Laguna del Laja limits our attempts to use biochronologic correlations. The rodent assemblage here reported comes from levels with radiometric ages consistent with the late early Miocene Santacrucian SALMA (Cuitiño et al., 2016). The presence of the exclusive Santacrucian species (e.g. *Phanomys mixtus*) associated with typical (but not exclusive) Santacrucian genera (*Prolagostomus*,

Neoreomys), also support that the fauna reported here belongs to this SALMA (e.g. Arnal et al., 2019b).

Prolagostomus was a widespread taxon during the early to middle Miocene, with records in Argentina, Chile, and Bolivia (Vucetich, 1984; Croft et al., 2011). In two Chilean localities the genus has been reported, Pampa Castillo (Santacrucian to “Friasian” (Flynn et al., 2002b)), and Laguna del Laja (Flynn et al., 2008). *Neoreomys* is also a widely distributed taxon being known in the late early Miocene faunas of Pinturas and Santa Cruz formations (Santacrucian SALMA), the Early Miocene Pampa Castillo fauna, Chile, as well as in the middle Miocene Collón Curá (Colloncuran SALMA; Río Negro and Neuquén provinces) and La Victoria (Laventan SALMA) formations in Argentina and Colombia (Fields, 1957; Flynn et al., 2002b, 2008; Kramarz, 2006b; Cuitiño et al., 2019). *Luantus* was recognized in the Sarmiento Formation (43°– 46°S; Colhuehuapian SALMA), Chubut Province, the lower, middle and upper beds of the Pinturas Formation (47°– 51°S; Santacrucian SALMA), and the late Early Miocene of the Cura-Mallín Formation at Laguna del Laja (Kramarz, 2006a; Flynn et al., 2008; Pérez et al., 2010). *Phanomys* was previously known only from the Santa Cruz, Río Jeinemení and Pinturas formations (Pérez and Vucetich, 2012), but here its geographic distribution is extended to the east, thus representing a shared taxon between the Santacrucian faunas of Laguna del Laja and Patagonia.

The *Prolagostomus* and *Luantus* forms from the Laguna del Laja are likely closely related to forms from upper levels of the Pinturas Formation which bear mammals with Santacrucian SALMA affinities (Kramarz, 2002; Kramarz and Bellosi, 2005). *Phanomys mixtus* and *Neoreomys* are also present in the upper levels of the Pinturas Formation (Kramarz and Bellosi, 2005). Therefore, the rodent assemblage here reported is closely allied with the western Santacrucian faunas of the upper levels of the Pinturas Formation.

Previous to the present work, the only confirmed records of *Maruchito* comes from the Collón Curá Formation (40°S; Colloncuran SALMA) (Vucetich et al., 1993). Here, we confirm the presence of *Maruchito* into the late early Miocene of the Cura-Mallín Formation at Laguna del Laja, representing the unequivocal oldest record of the genus, and expanding its biochron from the late early (Santacrucian) to middle Miocene (Colloncuran) in southern Andean Cordillera (Vucetich et al., 1993). In addition, a species closely related to *M. trilofodonte*, yet undescribed, has been

recognized in the Río Frías Formation (44°S; “Friasian” SALMA) (Vucetich et al., 1993). Nevertheless, it should be noted that we could not confirm the presence of *Maruchito*, or some related form nearby, in the Río Frías Collection at MLP. The Collón Curá and Río Frías formations are slightly younger than classic deposits of the Santa Cruz Formation in Southern Patagonia (Folguera et al., 2018b). However, radiometric ages in the Santa Cruz Formation suggest some chronological overlap with the base of the formers formations (Cuitiño et al., 2016), with several taxa shared among these faunas (e.g. Marshall, 1990). That is why some authors have been advised that taxonomic differences within Santacrucian, Colloncuran and “Friasian” faunas might reflect ecological or geographic, rather than temporal, differences (Cuitiño et al., 2016). Despite this situation, which deserves further scrutiny (and is out of the scope of the present contribution), the presence of a putative new species of *Maruchito* in early Miocene levels of the Cura-Mallín Formation tentatively suggests their relationships with early middle Miocene western Patagonian localities (e.g. Collón Curá and Río Frías formations). Therefore, the rodents described here consist of a mosaic of taxa, which indicates a widely distributed late early Miocene caviomorph fauna along the south of the Andes, in both intra-arc and foreland basins.

The paleoenvironmental affinities of the fauna described here are difficult to assess, mostly because several aspects of their paleobiology based on postcranial elements, areas of origin and insertion of masticatory muscles and locomotor modes are barely known for most of the present taxa, even at the genus levels. *Neoreomys*, a common and abundant Miocene rodent with protohypsodont teeth, has been interpreted as a cursorial taxon that probably inhabited relatively warm forested areas, probably associated with water bodies (Kramarz and Bellosi, 2005; Candela et al., 2013b). In their type locality, *Maruchito* inhabit relatively warm and humid environments (Vucetich et al., 1993). *Luantus* and *Phanomys* have protohypsodont cheek teeth, which may indicate abrasive diets and/or living in more open habitats such as grassland (Eronen et al., 2010). However, it must be noted that some euhyposodont Miocene caviomorph could be mixed feeders (Candela et al., 2013a). This is likely the case for the euhyposodont *Prolagostomus* which has been interpreted as a mixed feeder, depending on food availability (Rasia, 2016). Based on the limited available evidence the late early Miocene rodent fauna of the Laguna del Laja tentatively advocates the occurrence of warm and rather open habitats.

This generalized paleoenvironmental interpretation disagrees with the temperate and forested habitats with permanent bodies of water inferred for the Lonquimay fauna (also belonging to the Cura-Mallín Formation) during the late early Miocene (Solórzano et al., 2019). However, considering the limited studied taxa, this paleoenvironmental interpretation fauna must be taken with caution. Additional sampling efforts and future taxonomic assessments on the Laguna del Laja Neogene mammals will provide a better framework to evaluate this hypothesis.

The multiple fossiliferous horizons previously reported from the Laguna del Laja (early to late Miocene), appears to include several putative undescribed species of octodontids, dinomyids, dasyproctids, “eocardiids”, lagostomines and echimyids, suggesting an important distinctiveness of the Laguna del Laja rodents relative to Patagonian contemporaries deposits (*sensu* Flynn et al., 2008). Several potential explanations have been mentioned to account for the proposed uniqueness of the Laguna del Laja rodents, including unusual environments or elevation, topographic or other geographic barriers, and/or temporal distinctions (Flynn et al., 2008). One (but probably two) of the five taxa reported here represent new taxa, supporting, in part, the apparent uniqueness of the late Early Miocene fauna of Laguna del Laja. Nevertheless, given the limited sample of the caviomorph rodents described, the proposed pronounced local endemism must remain in question until additional materials from Laguna del Laja will be collected and properly described.

3.7 Conclusions

The study of a restricted collection of rodents from late early Miocene beds of the Cura-Mallín Formation at the Laguna del Laja area allowed us to illustrate the presence of five taxa belonging to echimyids, dasyproctids, “eocardiids”, and lagostomines, including a new taxon, *Luantus sompallwei* sp. nov. Additionally, *Phanomys mixtus* is reported in Chile for the first time, while the presence of *Maruchito* (likely represented by a new species) into the late early Miocene (Santacrucian) is confirmed, representing the unequivocal oldest record of the genus. This fauna has biostratigraphical and geochronological affinities with the Santacrucian SALMA formations of Argentina and especially resembles that reported in the temporal equivalent beds of upper levels of the Pinturas Formation.

Our findings support a widely distributed late early Miocene caviomorph fauna along the south of South America and suggest the predominance of warm and open habitats in the Cura-Mallín Formation during this time period, yet the recovery of additional Laguna del Laja early Miocene mammals will provide a better framework to evaluate this hypothesis.

Acknowledgments. We wish to thank the Consejo de Monumentos Nacionales (CMN, Chile) and the Corporación Nacional Forestal (CONAF) for the authorization of paleontological prospecting in the Laguna del Laja area. To David Rubilar (MNHN), Katherine Cisterna (MHNC), Laura Chornogubsky (MACN), Martín Ezcurra (MACN) and Marcelo Reguero (MLP) for granting access to the vertebrate paleontological collections under their care; to Mónica Núñez-Flores, Maximiliano Reyes, Paz Butikofer, Francisca Rizzo, Gabriel Arriagada, Hernán Arriagada and Aníbal Anavalón for their help and camaraderie during the field trips at Laguna del Laja; and to Paul San Martín (CMA Biobío), and Verónica Oliveros (Udec) for their assistance and support in obtaining pictures of the studied materials. We thank to María Encarnación Pérez (Museo Paleontológico Egidio Feruglio) and an anonymous reviewer for their valuable comments and suggestions that greatly improved the early version of the manuscript. This research was funded by Conicyt, Fondecyt project n°1151146 (AE), and Conicyt–PCHA/Doctorado Nacional/2018–21180471 (AS).

Table 3.1. Measurements (in mm) of the materials collected in the late early Miocene of the Cura-Mallín Formation at Laguna del Laja, Chile. Abbreviations: **MDL**, mesiodistal length; **MW**, mesial width; **DW**, distal width; **W**, width.

Lower tooth

Taxa	Specimen	p4			m1			m2			m3			m1 or m2		
		MD	M	D	M	M	D	M	M	D	M	M	D	M	M	D
		L	W	W	D	W	W	D	W	W	D	W	W	D	W	W
					L			L			L			L		
<i>L. sompallwei</i> sp. nov.	SGO.PV.1401 (holotype)	4.5	2.	3.	4.	3.	3.	-	-	-	-	-	-	-	-	-
		1	98	23	26	59	73									
<i>L. sompallwei</i> sp. nov.	SGO.PV.1402	-	-	-	-	-	-	-	-	-	-	-	-	4.	3.	3.
														55	80	75
<i>Prolagostomus</i> sp.	MHNC 38.0041	-	-	-	-	-	-	2.	3.	3	2.	3.	3	-	-	-
								5	2		43	3				

Upper tooth

Taxa	Specimen	P4		dP4		M1		M2		M3		M1 or M2		
		MD	W	MD	W	MD	W	MD	W	MD	W	MD	AW	PW
		L		L		L		L		L		L		
<i>Maruchito</i> sp. nov.?	SGO.PV.1400	-	-	3.2	2.9	3.1	2.9	3.3	3.1	3.1	3.0	-	-	-
				4	8	2	5	4	5	5	2			
<i>Phanomys mixtus</i>	MHNC 38.0038	-	-	-	-	-	-	-	-	-	-	4.3	4.5	4.3
												9	0	7
<i>Phanomys mixtus</i>	MHNC 38.0037	-	-	-	-	-	-	-	-	-	-	4.3	4.5	4.4
												5	5	1
<i>Neoreomys</i> sp.	MHNC 38.0039	4.7	4.8	-	-	-	-	-	-	-	-	-	-	-
		6	4											
<i>Prolagostomus</i> sp.	MHNC 38.0040	-	-	-	-	2.3	3.0	2.2	2.9	-	-	-	-	-
						8	0	0	5					

CAPÍTULO IV. Late early Miocene mammals from the Laguna del Laja, Cura-Mallín Formation, south central Chile (~37°S) and their biogeographical, and paleoenvironmental significance



³**Solórzano A**, Encinas A, Kramarz A, Carrasco G, Montoya-Sanhueza G, René Bobe (submitted, 2021). Late early Miocene mammals from the Laguna del Laja, Cura-Mallín Formation, south-central Chile (~37°S) and their biogeographical, and paleoenvironmental significance.

³Artículo enviado en 2021 al *Journal of South America Earth Sciences*.

Late early Miocene mammals from the Laguna del Laja, Cura-Mallín Formation, south-central Chile (~37°S) and their biogeographical and paleoenvironmental significance

Andrés Solórzano^{a,*}, Alfonso Encinas^b, Alejandro Kramarz^c, Gabriel Carrasco^d, Germán Montoya-Sanhueza^e, René Bobe^f

^aPrograma de Doctorado en Ciencias Geológicas, Facultad de Ciencias Químicas, Universidad de Concepción, Víctor Lamas, 1290, Concepción, Chile

^bDepartamento de Ciencias de la Tierra, Facultad de Ciencias Químicas, Universidad de Concepción, Víctor Lamas, 1290, Concepción, Chile

^cSección Paleontología de Vertebrados, Museo Argentino de Ciencias Naturales Bernardino Rivadavia, Av. Ángel Gallardo 470 (C1405DJR), Ciudad Autónoma de Buenos Aires, Argentina

^dServicios Científicos Educativos y Turismo Científico Chile, Pedro León Ugalde 254, San Bernardo, Chile

^eDepartment of Zoology, Faculty of Science, University of South Bohemia. Branišovská 1760, České Budějovice 37005, Czech Republic.

^fSchool of Anthropology, University of Oxford, UK

*Corresponding author: solorzanoandres@gmail.com

Highlights

- A late early Miocene mammal assemblage of the Cura-Mallín Formation at Laguna del Laja (Chile) is analyzed.
- At least 17 taxa, including some potential new ones, were recognized.
- The mammal assemblage here studied might be related to the Santacrucian SALMA.
- Some of the recognized taxa were previously found only in older and younger ages SALMAs.
- The studied assemblage supports the presence of mixed forested and open habitats.

Abstract

Despite recent efforts, the Neogene mammal's diversity in Chile remains poorly known, with several presumed new taxa awaiting description. For example, previous studies have suggested that the early to late Miocene mammalian

assemblages from the Laguna del Laja fossiliferous locality (Cura-Mallín and Trapa-Trapa formations), in the Andean Cordillera of south-central Chile (~37°), comprise dozens of undescribed taxa. Therefore, a better understanding of the Laguna del Laja faunas' taxonomic affinities is needed, as it represents one of the few known localities from early to late Miocene in Chile. Dozens of mammal specimens recently recovered in late early Miocene beds of the Cura-Mallín Formation at Laguna del Laja are described and illustrated, and a discussion of their biogeographical and paleoenvironmental significance is provided. We recognized the presence of at least 17 taxa, including some potential new ones (e.g., *Pachyrukhos* sp. nov.?) and others recognized in Chile for the first time (e.g., *Galileomys*). Geochronological (17.7–16.4 Ma) and biostratigraphical data indicate that this fauna correlates well with the Santacrucian SALMA, contributing to filling the gap in the taxonomic composition of Santacrucian mammalian assemblages in Chile and the southwestern of South America. However, it is striking our finding in the Laguna del Laja of some taxa previously found only in older (Colhuehuapian) and younger (Colloncuran) ages. Finally, the assemblage recognized supports mixed forested and open habitats, likely with the predominance of the former, in the Laguna del Laja region during the late early Miocene and a widely distributed Santacrucian fauna throughout southern South America in both intra-arc and foreland basins.

Keywords. Neogene mammals, Chile paleodiversity, Santacrucian, late early Miocene paleoenvironments.

4.1. Introduction

The paleodiversity of Cenozoic Chilean continental mammals remains barely known compared with neighboring geographical areas such as Argentina or Bolivia. Despite the increased number of paleontological studies in the last decade in the country (e.g., Engelman et al., 2020, 2018; Montoya-Sanhueza et al., 2017; Shockey et al., 2012; Solórzano et al., 2020a, 2019; Wyss et al., 2018) dozens of new taxa from several of the most-diverse localities remain undescribed and/or in open nomenclature (Flynn et al., 2002a, 2002b, 2008; Croft et al., 2007; Bostelmann et al., 2013; Charrier et al., 2015). Therefore, it is

necessary to renew sampling efforts and taxonomic studies of poorly known faunas, like those from the Laguna del Laja (Flynn et al., 2008).

Multiple mammal-bearing horizons have been reported from distinct early to late Miocene beds in the Cura-Mallín and Trapa-Trapa formations at the Laguna del Laja locality in the Andean Cordillera of south-central Chile (Flynn et al., 2008). It represents one of the longest succession of directly superposed mammalian assemblages in South America and documents the Neogene mammalian evolution of the region (Flynn et al., 2008). The preliminary faunal lists provided for the Laguna del Laja indicates the predominance, in terms of diversity, of caviomorph rodents and notoungulates, although xenarthrans, marsupials, and astrapotheriids have also been mentioned (Flynn et al., 2008; Shockey et al., 2012; Solórzano et al., 2020a). Nevertheless, only a few of the taxa so far reported have been described in detail (Shockey et al., 2012; Solórzano et al., 2020a), limiting accurate interpretations regarding the biostratigraphic and paleoenvironmental significance of these faunas.

New paleontological prospections in the lower (late early Miocene) beds of the Cura-Mallín Formation cropping out in the south of Laguna del Laja allowed us to collect new mammalian specimens into a relatively well-constrained chronostratigraphic framework. We described a late early Miocene mammalian fossil assemblage from the Laguna del Laja and analyzed its biogeographic and palaeoecological affinities based on these new fossil collections. The study of these fossil remains improves our understanding of the Neogene continental vertebrate records from the central Andean Cordillera, an area so far barely sampled (Flynn et al., 2008; Shockey et al., 2012; Solórzano et al., 2020a).

4.2. Geological and geographical setting

Between 36° and 39° S and along the Chile-Argentina international border, the Oligo-Miocene continental deposits are grouped in the Cura-Mallín Formation (Niemeyer and Muñoz, 1983; Suárez and Emparan, 1995, 1997; Burns et al., 2006; Flynn et al., 2008; Utge et al., 2009; Radic, 2010; Rosselot et al., 2019a). The Cura-Mallín Formation is the basal unit in the homonymous basin and is characterized by pyroclastic deposits and volcanic flows interbedded with continental sediments deposited in alluvial, fluvial, lacustrine, and deltaic

environments (Suárez and Emparan, 1995, 1997; Burns et al., 2006; Radic, 2010; Pedroza et al., 2017; Rosselot et al., 2019a). Radiometric dates (K-Ar and U-Pb) suggest a Lower to earliest Upper Miocene age (22–10.7 Ma) for the Formation (Suárez and Emparan, 1995, 1997; Flynn et al., 2008; Pedroza et al., 2017; Rosselot et al., 2019a). Volcanic and sedimentary rocks included in the Cura-Mallín Formation typically crop out in separate areas, so their correlation has been inferred from their overlapping radiometric ages (e.g., Burns et al., 2006; Radic, 2010; Suárez and Emparan, 1995, 1997).

The fossils described below come from two Cura-Mallín Formation outcrops located south of Laguna del Laja in the Andean Cordillera of south-central Chile (37° S; Fig. 4.1a, b). The Cura-Mallín succession at Laguna del Laja is >1 km thick and consists primarily of sandstone, mudstone, conglomerate, and subordinate levels of ignimbrite (Herriott, 2006; Flynn et al., 2008; Solórzano et al., 2020a). $^{40}\text{Ar}/^{39}\text{Ar}$ radiometric dates for this succession range between ~19.80 Ma in the basal part and 14.50 Ma in the upper part (Herriott, 2006; Flynn et al., 2008; Shockey et al., 2012). In the region, volcanic conglomerates and breccias, intermediate to mafic lavas, and rare to minor beds of finer-grained volcanoclastic deposits of the late Miocene (8.9 ± 0.1 and 10.10 ± 0.20 Ma) Trapa-Trapa Formation overly the Cura-Mallín Formation (Niemeyer and Muñoz, 1983; Flynn et al., 2008). The Cura-Mallín and Trapa-Trapa formation strata at the south of the Laguna del Laja are moderately deformed (Niemeyer and Muñoz, 1983; Flynn et al., 2008).

Herriott (2006) and Flynn et al. (2008) divided the Cura-Mallín Formation in the Laguna del Laja area into five informal units: Tcm₁, Tcm₂, Tcm₃, Tcm₄, and Tcm₅. Tcm₁, Tcm₃, and Tcm₅ are volcanoclastic sandstone and mudstone, with Tcm₅ having a significant fine-grained strata component. Tcm₂ is an ignimbrite that constitutes a marker bed. Tcm₄ is lithologically distinctive from similar units because it contains pebble-sized clasts of granitoid and quartzite (Herriott, 2006; Flynn et al., 2008).

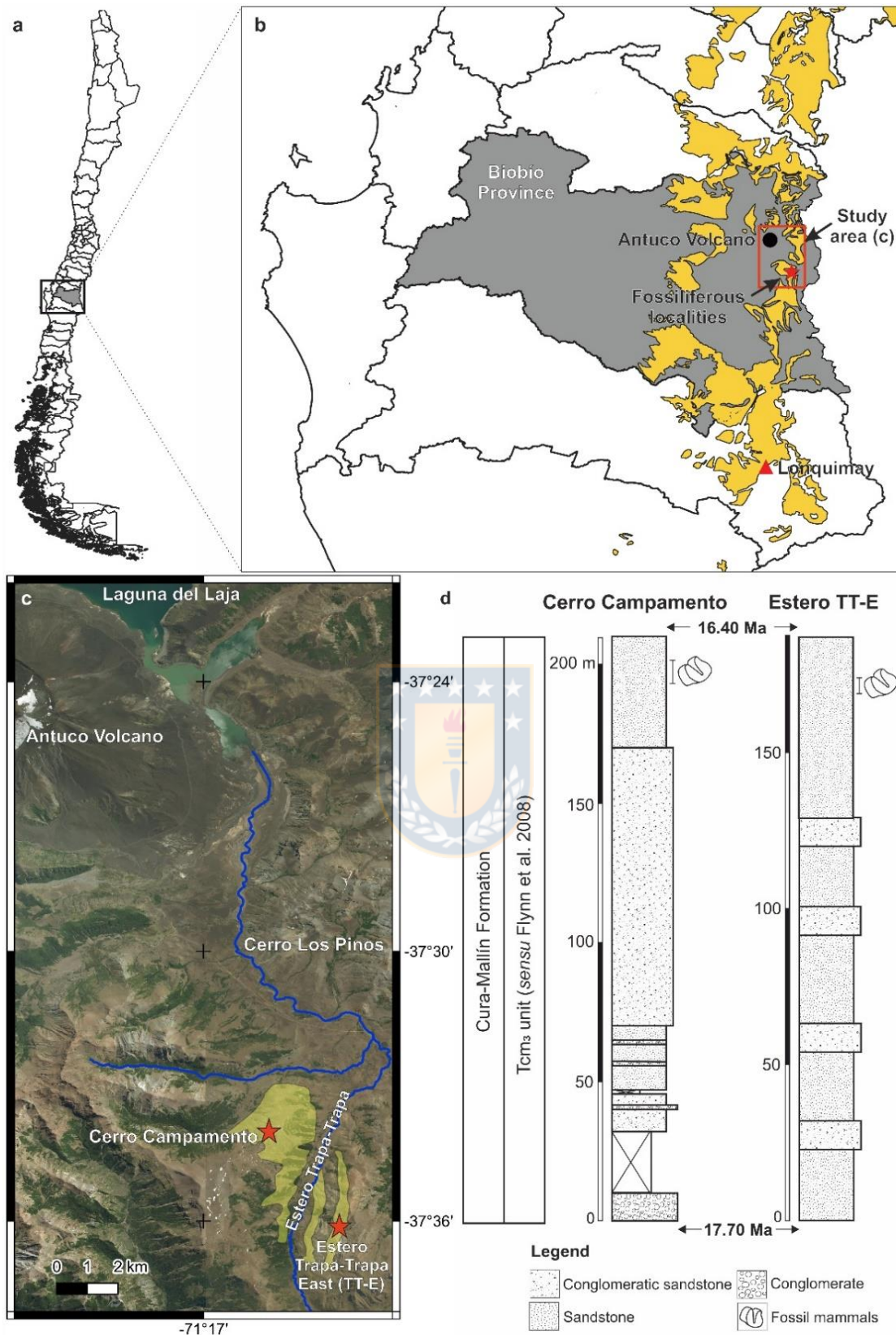


Figure 4.1. Geographic and stratigraphic provenance of the mammals remains described in the present study from the late early Miocene of the Cura-Mallín Formation at the south of the Laguna del Laja (Biobío Province, south-central Chile). **a–b**, regional geographic location of the study area; **c**, aerial view at the south of Laguna del Laja showing the location of the fossiliferous sampled levels (denoted by a red star); **d**, stratigraphic profiles of the Tcm₃ unit in Cerro Campamento and Estero Trapa-Trapa East (TT-E), at Laguna del Laja, showing the

levels in which the fossils described here were recovered. The grey region in **a** and **b**, denotes the location of the Biobío Province, Chile. The yellow polygons in **b** indicate the geographic extension of the Oligocene to Miocene volcano-sedimentary units, which must mainly correspond (at this latitudes) with the geological units included in the Cura-Mallín Basin (SERNAGEOMIN, 2003). The pale-yellow polygons in **c**, denotes the extension of the Tcm₃ unit over Cerro Campamento and Estero Trapa-Trapa East. The geographic and chronological extension of the Tcm₃ unit is based on Flynn et al. (2008) and Herriott (2006).

The fossils described here were recovered from surface picking in two localities of the Cura-Mallín Formation, Cerro Campamento (west of Estero Trapa-Trapa) and Estero Trapa-Trapa East (Fig. 4.1c). The first, Cerro Campamento, is the most fossil-rich site and consists of volcanoclastic grey sandstone, while the second, Trapa-Trapa East, consists of volcanoclastic sandstones. Both fossil-bearing localities belong to the Tcm₃ unit (Fig. 4.1d), with constrained radiometric (⁴⁰Ar/³⁹Ar) ages between 17.70–16.40 Ma (late early Miocene) (Flynn et al., 2008; Solórzano et al., 2020a).

4.3. Brief paleontological background

Flynn et al. (2008) provide a preliminary faunal list from several localities corresponding to different stratigraphic levels from the Cura-Mallín and Trapa-Trapa formations at Laguna del Laja. The fossil mammals reported from Flynn et al. (2008) from the early Miocene Tcm₃ unit of the Cura-Mallín Formation include notoungulates (*Paedotherium minor*, New taxon cf. *Protypotherium* sp., *?Hegetotherium* sp., Toxodontidae indet., Typotheria indet. and Interatheriinae indet.), caviomorphs rodents (*Maruchito* sp. nov., *Protacaremys* sp. nov., cf. *Protacaremys* sp. nov., *Prostichomys* sp. nov. I, *Prostichomys* sp. nov. II, *Luantus* sp. nov., *?Luantus* sp. nov., *Acarechimys* sp. nov., *Scleromys* sp. nov., *Prolagostomus* sp. nov. and unident., gen. et sp. nov. (aff. *Incamys*), gen. et sp. nov. (aff. *Alloiomys*), gen. et sp. nov. (aff. *Prostichomys*), gen. et sp. nov. (aff. *Protacaremys*), gen. et sp. nov. (aff. *Prospaniomys*)), marsupials (*Sipalocyon* sp. and Abderitidae indet.), astrapotheres (Astrapotheriidae indet.), and armadillos (Dasypodidae indet.). However, just a few of these taxa have been illustrated (Flynn et al., 2008), and with some exceptions (Shockey et al., 2012; Solórzano et al., 2020a), they have not been described in detail. Although five rodent taxa have been recently described in late early Miocene beds of Cerro Campamento

(Tcm₃) (Solórzano et al., 2020a), a taxonomic and systematic assessment of the Laguna del Laja mammalian paleodiversity is much needed.

In addition to the mammals described in the following sections, we also found fragmentary postcranial elements of birds in early Miocene beds (Tcm₃) at Cerro Campamento (west of Estero Trapa-Trapa; Cura-Mallín Formation), and few undetermined and poorly preserved teleostid fish remains were observed on loose blocks at west Estero Trapa-Trapa foothills of uncertain age. Nevertheless, none of these remains display diagnostic features. Consequently, they are not described here but mentioned hoping that additional fieldwork will provide more diagnostic materials. We also report the finding of Equisetaceae remains in the lower strata of the Cerro Los Pinos succession, in middle Miocene beds (Tcm₄; ca. 14.5 Ma; Flynn et al., 2008), large wood remains in early Miocene beds (Tcm₃) at the top of the Cerro Campamento (but not in association with mammal remains), and few carbonized and poorly preserved leaves in the upper strata of the Estero Trapa-Trapa East section (Tcm₄).

4.4. Materials and Methods



The specimens described here are housed at the Museo de Historia Natural de Concepción (Concepción) and the Museo Nacional de Historia Natural (Santiago de Chile), Chile. All measurements are in millimeters (mm) and were obtained with a digital caliper. The comparison of the taxa here described was mainly made with other closely related taxa from Argentinean localities (Supplementary File 1). We performed a preliminary palaeoecological analysis of the fauna recorded in Laguna del Laja, following a general protocol based on body mass, diet, and substrate preference and use (Kay et al., 2012b, 2021; Vizcaíno et al., 2016). These features were taken from the literature (Cassini et al., 2012; Kay et al., 2012b; Vizcaíno et al., 2012; Candela et al., 2013b; Prevosti et al., 2013; Solórzano and Núñez-Flores, 2021). Also, we estimated the body mass (in kg) of some caviomorphs taxa for the first time using the Hystricomorpha equation ($Ln_{BM} = 2.81 * Ln_{LTRL} - 0.91$) of Hopkins (2008) based on measurements of lower tooth row length (LTRL; in mm) taken from the literature (Vucetich et al., 1993; Kramarz, 2006a; Pérez and Vucetich, 2012; Arnal and Vucetich, 2015),

4.4.1. Abbreviations

Upper-case letters are used for the upper dentition (P: for premolar, M: for molar), and lower-case letters for the lower dentition (p: for premolar, m: for molar); dP/dp: deciduous premolar; mf, molariform; cf, caniniform; SALMA, South American Land Mammal Age; HI, Hypsodonty index.

4.4.2. Institutional abbreviations

SGOPV, Museo Nacional de Historia Natural de Santiago, Santiago, Chile; **MHNCCL (=MHNC)**, Museo de Historia Natural de Concepción, Concepción, Chile; **MACN**, Museo Argentino de Ciencias Naturales “Bernardino Rivadavia”, Buenos Aires, Argentina; **MLP**, Museo de La Plata, La Plata, Argentina.

4.5. Systematic Paleontology

Infraclass METATHERIA Huxley, 1880

Order SPARASSODONTA Ameghino, 1894

Family HATHLIACYNIDAE Ameghino, 1894

Genus *SIPALOCYON* Ameghino, 1887

cf. *Sipalocyon* sp.

Revised material. MHNCCL PALEO-CS 65, isolated right lower molar (likely an m1).

Geographic and stratigraphic provenance. Estero Trapa-Trapa East, Laguna del Laja, Chile; Tcm₃ levels, Cura-Mallín Formation, late early Miocene.

Comments. The recovered lower molar has two roots. The crown bears three main mesiodistally aligned structures, paraconid, protoconid, and talonid (Fig. 4.2a), typical of sparassodonts. The protoconid and talonid are partially broken, and only their labial view is visible. Size has been considered a relevant feature for the taxonomic identification of sparassodonts (Marshall, 1981). MHNCCL PALEO-CS 65 represents a small-sized taxon as the hathliacynids, *Pseudonotictis* Marshall 1981, *Perathereutes* Ameghino 1891, and *Sipalocyon* (Marshall, 1981). The m1 talonid of the Laguna del Laja sparassodont is proportionately more extensive and higher than in *Pseudonotictis* and *Perathereutes*, but it is undifferentiated from those of *Sipalocyon* (Marshall, 1981). However, the mesiodistal length of MHNCCL PALEO-CS 65 (3.9 mm) is

15% smaller than the lower size range of the species included in *Sipalocyon* (Marshall, 1981; Prevosti and Forasiepi, 2018b). Given the fragmentary nature, and a limited sample of the Laguna del Laja material achieves a better taxonomic identification, other than cf. *Sipalocyon*, is unreliable. This genus has been previously identified in the early Miocene (Colhuehuapian and Santacrucian) of Argentina (Prevosti and Forasiepi, 2018 and references therein), early Miocene beds at the Laguna del Laja (Flynn et al., 2008), and “Friasian” beds of the Rio Cisnes, Chile (Marshall, 1990).

Supercohort MARSUPIALIA Illiger, 1811

Order PAUCITUBERCULATA Ameghino, 1894

Superfamily PALAEOTHENTOIDEA Goin, Candela, Abello & Oliveira, 2009

Family PALAEOTHENTIDAE Sinclair, 1906

Genus *PALAEOTHENTES* Ameghino, 1887

Palaeotherentes intermedius Ameghino, 1887

Revised material. MHNCCCL PALEO-CS 66, left mandibular fragment bearing the p3–m4 series.

Geographic and stratigraphic provenance. Cerro Campamento, west of Estero Trapa-Trapa, Laguna del Laja, Chile; Tcm₃ levels, Cura-Mallín Formation, late early Miocene.

Comments. Although poorly preserved, the material preserved the diagnostic character of the family Palaeotherentidae: the oblique (anterolabial-posterolingual) postparacristid in m2 (Abello, 2013). Their double-rooted p3 (posterior root larger than anterior root), m1 with an anterior crest in the trigonid, straight protocristid, and oblique cristid, very posteriorly placed metaconid with respect to protoconid, paraconid, and metaconid very distant from each other and V-shaped gap between metaconid and entocristid (in medial view) (Fig. 4.2b, c), as well as size (Supplementary File 2), allowed us to refer this material to the genus *Palaeotherentes* (Marshall, 1980; Bown and Fleagle, 1993; Abello, 2013; Rincón et al., 2015). Based on their low cuspids, paracristid subparallel to the dentary axis, as well as m1 and m1–m4 length, we assigned the Laguna del Laja specimen to the Santacrucian *Palaeotherentes intermedius* (Bown and Fleagle, 1993; Abello, 2007; Chornogubsky et al., 2019). This taxon has been previously recognized in Chile from Santacrucian and “Friasian” beds at Pampa Castillo and Rio Cisnes,

respectively (Marshall, 1990; Flynn et al., 2002b), but also in several Santacrucian localities of the Pinturas and Santa Cruz formations, Argentina (Abello, 2007 and references therein).

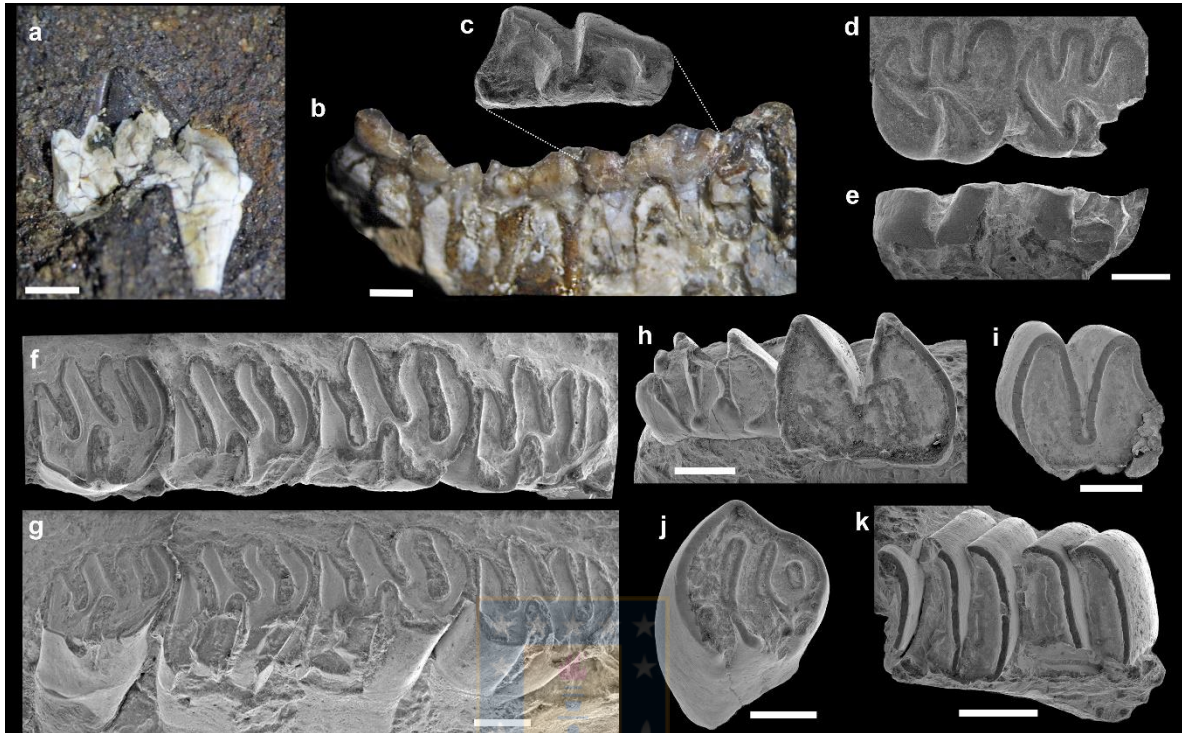


Figure 4.2. Sparassodonts, palaeotheniids, and caviomorphs rodents from late early Miocene (Santacrucian) beds of the Cura-Mallín Formation, Laguna del Laja, Chile. **a**, cf. *Sipalocyon* sp. (MHNCCCL PALEO-CS 65): isolate m1? in labial view. **b–c**, *Palaeothenes intermedius* (MHNCCCL PALEO-CS 66): left mandibular fragment bearing the p3–m4 series in lingual view (**b**), and detail of the m1 in occlusal view (**c**). **d–e**, *Galileomys antelucanus* (MHNCCCL PALEO-CS 67): fragment of left mandible bearing the m1 and m2 in occlusal (**d**) and lingual (**e**) views. **f–g**, *Maruchito* sp. nov? (SGO.PV.1400): left maxilla with dP4-M3 in occlusal (**f**) and lingual (**g**) views. **h**, *Luantus sompallwei* (SGO.PV.1401): a fragment of right dentary bearing the p4 and m1 in occlusal view. **i**, *Phanomys mixtus* (MHNC 38.0037): right isolated M1 or M2 in occlusal view. **j**, *Neoreomys* sp. (MHNC 38.0039): isolated P4 in occlusal view. **k**, *Prolagostomus* sp. (MHNC 38.0040): left maxillary fragment with M1, M2, and a mesial portion of the M3 in occlusal view. Scale bar = 1 mm.

Infraclass EUTHERIA Huxley, 1880

Order RODENTIA Bowdich, 1821

Suborder HYSTRICOGNATHI Tullberg, 1899

Superfamily OCTODONTOIDEA Waterhouse, 1839

Family ACAREMYIDAE Wood, 1949

Genus *GALILEOMYS* Vucetich and Kramarz, 2003

Galileomys antelucanus Vucetich and Kramarz, 2003

Revised material. MHNCCCL PALEO-CS 67, fragment of left mandible bearing the m1, m2, and an incisor fragment.

Geographic and stratigraphic provenance. Estero Trapa-Trapa East, Laguna del Laja, Chile; Tcm₃ levels, Cura-Mallín Formation, late early Miocene.

Comments. The somewhat worn lower molars exhibit a morphology that broadly resembles taxa included in Acaremyidae (Vucetich and Kramarz, 2003; Kramarz, 2004). MHNCCCL PALEO-CS 67 molars have a short posterolophid, unlike *Sciamys*, *Changquin*, and *Acaremys*, but similar to *Galileomys* (Vucetich and Kramarz, 2003; Kramarz, 2004). The genus *Galileomys* is represented by four species recognized in Desedean to Colloncuran localities in Argentina, *G. baios*, *G. antelucanus*, *G. eurygnathus* and *G.? colloncurensis*. The Laguna del Laja material differs from *G.? colloncurensis* (Colloncuran SALMA) in having molars with a larger second transverse lophid, and from *G. baios* by its larger size and narrower incisor (Fig. 4.2d) (Vucetich and Kramarz, 2003; Kramarz, 2004; Vucetich et al., 2015b). The studied molars indeed are similar in morphology and size (see Supplementary File 2) to those of *G. antelucanus* (Colhuehuapian SALMA) and *G. eurygnathus* (“Pinturan” SALMA), two taxa differentiated by their mandibular traits and incisor width (Kramarz, 2004). The mesiodistal incisor length (i_{APL}) of the Laguna del Laja specimen is 2.02 mm, much narrower than in *G. eurygnathus* (i_{APL} of 2.65–2.75 mm; Kramarz, 2004), but comparable to the holotype of *G. antelucanus* (i_{APL} of 2.04 mm; Vucetich and Kramarz, 2003). Therefore, the last trait supports the taxonomic assignment of MHNCCCL PALEO-CS 67 to *G. antelucanus*, a taxon previously only known from the Lower Fossil Zone of the Colhue Huapi Member of the Sarmiento Formation at Gran Barranca, Argentina (Vucetich and Kramarz, 2003; Vucetich et al., 2010a), the type locality of the Colhuehuapian SALMA.

Family ECHIMYIDAE Gray, 1825

Genus *MARUCHITO* Vucetich et al., 1993

Maruchito sp. nov.?

Revised material. SGO.PV.1400, fragment of left maxilla with dP4-M3.

Geographic and stratigraphic provenance. Cerro Campamento, west of Estero Trapa-Trapa, Laguna del Laja, Chile; Tcm₃ levels, Cura-Mallín Formation, late early Miocene.

Comments. The material (SGO.PV.1400), previously described by Solórzano et al. (2020a), shares several dental characters with the middle Miocene

(Colloncuran; Collón Cura Formation, Argentina) echimyid *M. trilofodonte*, including size, crown height, relatively narrow and straight hypoflexus, and transverse crests and labial flexi in some of the upper molars (Vucetich et al., 1993; Solórzano et al., 2020a) (Fig. 4.2f, g). Unlike SGO.PV.1400, *M. trilofodonte* has dP4 with a marked rectangular outline (mesiodistal length \gg transverse length) in most stages of wear, upper molars with a transversely more penetrating posterior-most fossette (even in a very advanced stage of wear), and acuminate labial ends of crest only in early stages of wear, which become rounded and thicker with wear (Solórzano et al., 2020a). Although SGO.PV.1400 presents morphological differences with the upper teeth referred to *M. trilophodonte*, we cannot determine whether it corresponds to a different species because *M. trilophodonte* was defined on lower teeth.

Superfamily CAVIOIDEA (Fischer de Waldheim, 1817)

Family "EOCARDIIDAE" Ameghino, 1891

Genus *LUANTUS* Ameghino, 1899

Luantus sompallwei Solórzano et al., 2020

Hypodigm. SGO.PV.1401, fragment of right mandible with incisor base, incompletely erupted unworn p4, and moderately worn m1 (Holotype; Fig. 4.2h); SGO.PV.1402, isolated m1 or m2.

Geographic and stratigraphic provenance. Cerro Campamento, west of Estero Trapa-Trapa, Laguna del Laja, Chile; Tcm₃ levels, Cura-Mallín Formation, late early Miocene.

Comments. The specimen on which *L. sompallwei* was erected shows the diagnostic features of the genus *Luantus* (Kramarz, 2006a; Pérez et al., 2010). The Laguna del Laja specimens differ from the Colhuehuapian species *L. initialis* in having higher crowned teeth and more molarized p4 (Kramarz, 2006a; Vucetich et al., 2010b), from *L. minor* (Colhuehuapian) by their larger size and more penetrating hypoflexids (Pérez et al., 2010) and from *L. propheticus* in having large discontinuities of the enamel covering on the base of the cheek teeth and a much less developed and persistent mesial projection of the metaconid in the p4 (Kramarz, 2006a; Solórzano et al., 2020a). *Luantus sompallwei* also differs from *L. toldensis* (Pinturas Formation, Argentina) since the p4 has a simpler

trigonid with a relatively straight mesial wall or a single and more superficial mesial flexid (Kramarz, 2006a).

Genus *PHANOMYS* Ameghino, 1887

Phanomys mixtus Ameghino, 1887

Revised material. MHNC 38.0038, right isolated M1 or M2; MHNC 38.0037, right isolated M1 or M2 (Fig. 4.2i).

Geographic and stratigraphic provenance. Cerro Campamento, west of Estero Trapa-Trapa, Laguna del Laja, Chile; Tcm₃ levels, Cura-Mallín Formation, late early Miocene.

Comments. The specimens display all the recognized diagnostics features of the genus *Phanomys*, such as protohypsodont molariforms, enamel interrupted along labial walls of the upper teeth, less persistent fossettes during ontogeny compared to any other protohypsodont genera of Caviodea, and hypoflexus narrow, extending transversely more than half of the crown and bearing cement since early ontogenetic stages (Pérez and Vucetich, 2012). There are two species recognized within the genus, *P. mixtus* and *P. vetulus*, and size is the main difference between both taxa, with the former being larger than the latter (Pérez and Vucetich, 2012). The size of the molars recovered from the Laguna del Laja falls into the range size reported for *P. mixtus* (Supplementary File 2) and is markedly larger than those known for *P. vetulus* (Pérez and Vucetich, 2012; Solórzano et al., 2020a). Therefore, Laguna del Laja specimens can be referred to *P. mixtus* (Solórzano et al., 2020a), a Santacrucian taxon previously only known from the Pinturas, Santa Cruz and Río Jeinemení formations in Argentina (Pérez and Vucetich, 2012; Arnal et al., 2019b).

Family DASYPROCTIDAE Smith, 1842

Genus *NEOREOMYS* Ameghino, 1887

Neoreomys sp.

Revised material. MHNC 38.0039; isolated right P4 (Fig. 4.2j).

Geographic and stratigraphic provenance. Cerro Campamento, west of Estero Trapa-Trapa, Laguna del Laja, Chile; Tcm₃ levels, Cura-Mallín Formation, late early Miocene, 17.70–16.40 Ma.

Comments. The isolated upper premolar from Laguna del Laja resembles the general morphology of *Neoreomys* (Solórzano et al., 2020a), being in the size range of the *N. australis* (Santacrucian) and decidedly larger than *N. huilensis* (Laventan) (Fields, 1957; Kramarz, 2006b; Supplementary File 2). Even when the P4 of *N. pinturensis* is unknown, this taxon differs from *N. australis* by their lower crowned cheek teeth (Kramarz, 2006b). However, as the only P4 available from Laguna del Laja is broken toward its base, the crown height cannot be estimated, making it unreliable to provide more details at the species level and its affinities with other species. *Neoromys* have been previously recognized in the late early Miocene of the Chinchas, Pinturas, and Santa Cruz formations (Argentina), the late early Miocene of Pampa Castillo and Laguna del Laja (Chile), the middle Miocene (Colloncuran) of the Collón Curá Formation (Argentina), and the late middle Miocene (Laventan) of the La Victoria Formation, Colombia (Fields, 1957; Flynn et al., 2002b, 2008; Kramarz, 2006b; López et al., 2011; Arnal et al., 2019b). Finally, although we cannot assess the taxonomic status of the material figured by Flynn et al. (2008: SGOPV 3834, Figure 4c) without accessing their collection materials, there is little doubt that this material is co-generic with the specimen described here.

Superfamily CHINCHILLOIDEA Bennett, 1833

Family CHINCHILLIDAE Bennett, 1833

Subfamily LAGOSTOMINAE Pocock, 1922

Genus *PROLAGOSTOMUS* Ameghino, 1887

Prolagostomus sp.

Revised material. MHNC 38.0040, fragment of left maxilla with M1-M2 and the mesial-most edge of M3 (Fig. 4.2k); MHNC 38.0042, right isolated M1 or M2, with portions of the maxillary; MHNC 38.0041, fragment of right mandible with m2 and m3.

Geographic and stratigraphic provenance. Cerro Campamento, west of Estero Trapa-Trapa, Laguna del Laja, Chile; Tcm₃ levels, Cura-Mallín Formation, late early Miocene.

Comments. The specimens, previously described by Solórzano et al. (2020a), display the diagnostic features of the genus *Prolagostomus* (Vucetich, 1984) and differ from *Lagostomus* and *Pliolagostomus* in having rounded molariform walls

(Croft et al., 2011). *Prolagostomus* is the most common rodent found in the sampled beds of the Tcm₃ unit on the Estero Trapa-Trapa West. While several species have been historically assigned to the genus (Scott, 1905; Vucetich, 1984; Kramarz, 2002; Croft et al., 2011), the actual number of valid species is likely overestimated because it is unclear distinguish among ontogenetic, intraspecific, and interspecific variations (Kramarz, 2002; Croft et al., 2011; Arnal et al., 2019b). The presence of a vestigial enamel layer in the distal wall of the upper molars of the Laguna del Laja *Prolagostomus*, resembles the *Prolagostomus* specimens recovered from the middle and upper levels of the Pinturas Formation (Argentina) (Kramarz, 2002; Solórzano et al., 2020a).

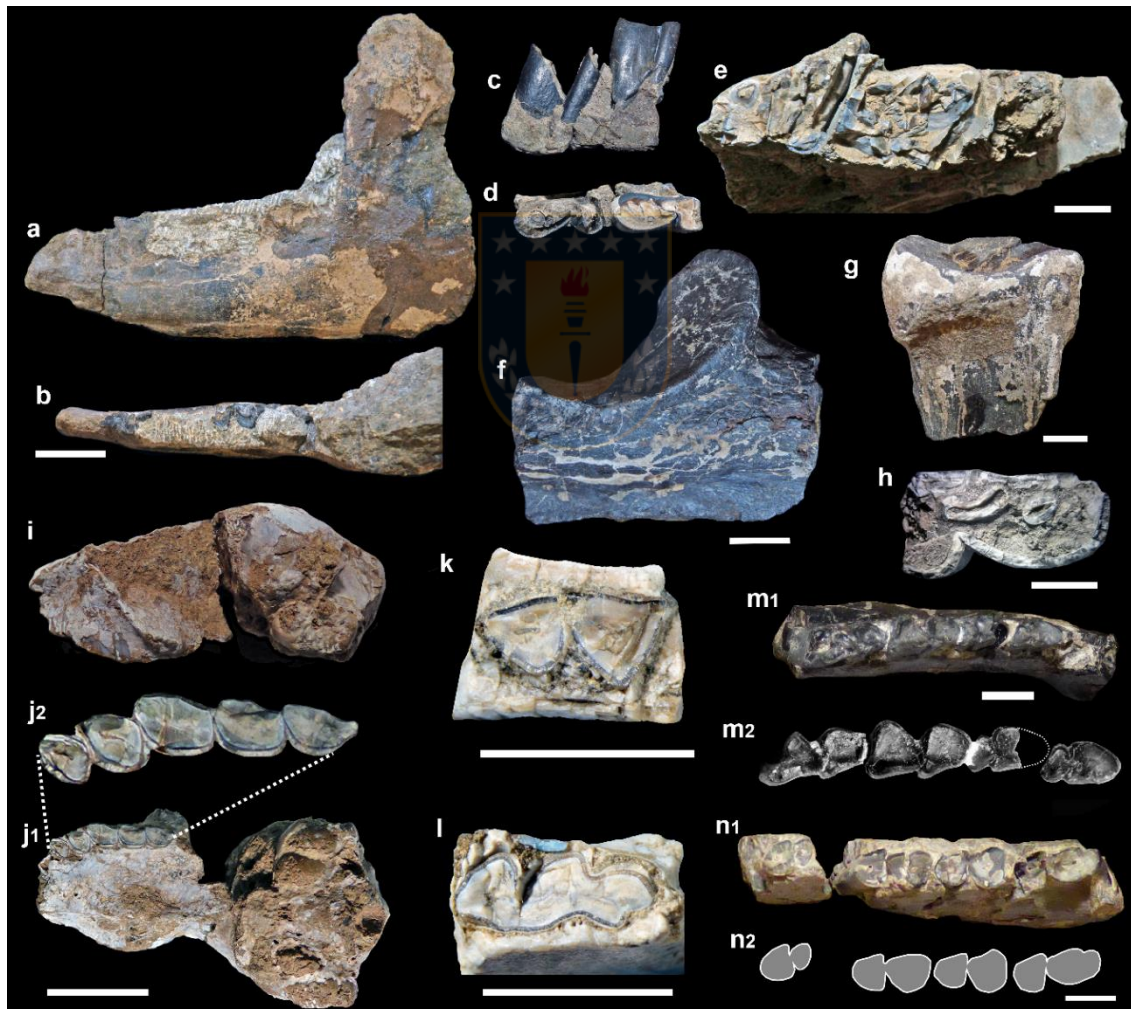


Figure 4.3. Lithoptern and notoungulates from late early Miocene (Santacrucian) beds of the Cura-Mallín Formation, Laguna del Laja, Chile. **a–b**, *Diadiaphorus majusculus* (MHNCCCL PALEO-CS 68): fragment of left mandible bearing the m3, and portions of m1 trigonid and p4 talonid in lateral (**a**) and occlusal (**b**) views. **c–g**, *Nesodon* sp.: associated fragments of the mandible and maxillary with m1–m2 (MHNCCCL PALEO-CS 71a) in labial (**c**) and occlusal (**d**) views and right M1–M3 in occlusal view (**e**); associated proximal ulna (**f**) and proximal radius fragments (**g**) (MHNCCCL PALEO-CS 71b). **h**, *Adinotherium* sp. (MHNCCCL PALEO-CS 70),

isolated m1 in occlusal view. **i–m**, *Pachyrukhos* nov. sp.?: a partial skull with the left P3–M3 series (MHNCCCL PALEO-CS 72) in lateral (**i**) and ventral (**j**) views; fragment of the mandible with m1 or m2 (MHNCCCL PALEO-CS 76) in occlusal view (**k**); fragment of the mandible with m3 (MHNCCCL PALEO-CS 75) in occlusal view (**l**). **m**, *Protypotherium* cf. *sinclairi* (MHNCCCL PALEO-CS 81): fragment of left mandible bearing the p3–m2 in occlusal view. **n**, *Protypotherium* sp. (MHNCCCL PALEO-CS 82): associated fragments of left mandible bearing with p3 and m1–m3 in occlusal view. Scale bar_{a–g, i–j} = 2 cm, Scale bar_{h, m–n} = 0.5 cm. Note that a–b, c–e, and i–j are on the same scale.

Order LITOPTERNA Ameghino, 1889

Family PROTEROTHERIIDAE Ameghino, 1887

Genus *DIADIAPHORUS* Ameghino, 1887

Diadiaphorus majusculus Ameghino, 1887

Revised material. MHNCCCL PALEO-CS 68, fragment of left mandible bearing the m3, and portions of m1 trigonid and p4 talonid (Fig. 4.3a, b); MHNCCCL PALEO-CS 69, left mandibular fragment bearing a deeply worn m1? talonid, and m2? trigonid.

Geographic and stratigraphic provenance. Cerro Campamento, west of Estero Trapa-Trapa, Laguna del Laja, Chile; Tcm₃ levels, Cura-Mallín Formation, late early Miocene.

Comments. MHNCCCL PALEO-CS 68 shows the diagnostic characters of the genus *Diadiaphorus*, like their relatively large size and m3 with indistinct entoconid and without the tendency to form a third lobe (Fig. 4.3a–b) (Soria, 2001; Schmidt et al., 2019). The tooth size and the dentary robustness of the second Litoptern specimen (MHNCCCL PALEO-CS 69) recovered from the same stratigraphic levels are very similar to those of the MHNCCCL PALEO-CS 68 (Supplementary File 2), likely suggesting the presence of a second (but ontogenetically much older) *Diadiaphorus* individual in the locality. Among the described species of the genus, *D. eversus* is only known by scarce and fragmentary upper teeth from the late Miocene of Argentina (Schmidt, 2015), limiting comparisons with the Laguna del Laja specimen. *Diadiaphorus? caniadensis* (Pinturas Formation, Argentina) differs from *D. majusculus* in having a large entoconid (Kramarz and Bond, 2005). MHNCCCL PALEO-CS 68 is indistinguishable from the contemporaneous *Diadiaphorus majusculus*, a taxon previously known from the late early Miocene of the Santa Cruz Formation, Argentina (Soria, 2001 and reference therein).

Order NOTOUNGULATA Roth, 1903
Family TOXODONTIDAE Owen, 1845
Subfamily NESODONTINAE Murray, 1866
Genus *NESODON* Owen, 1847

Nesodon sp.

Revised materials. MHNCCL PALEO-CS 71a, associated fragments of the mandible with left and right m2, the base of an m1, left p2?, and a portion of the palate with right M1–M3 and base of left M3 (Fig. 4.3d–e); MHNCCL PALEO-CS 71b, associated fragments of ulna and radio (Fig. 4.3f–g).

Geographic and Stratigraphic provenance. Cerro Campamento, west of Estero Trapa-Trapa, Laguna del Laja, Chile; Tcm₃ levels, Cura-Mallín Formation, late early Miocene.

Comments. The examined materials are characterized by their relatively large size (Supplementary File 2), hypsodont and rooted cheek teeth, reduction of enamel along the antero and postero-lingual walls of the lower molars, lower molars with two lingual folds plus an accessory fossetid, upper molars with lingual folds that become completely isolated as fossettes (Fig. 4.3d–e), all of these representing typical features of nesodontines (Scott, 1912; Nasif et al., 2000; Croft et al., 2004). Three genera were included among nesodontines, *Proadinothorium*, *Adinothorium*, and *Nesodon* (Scott, 1912; Nasif et al., 2000; Croft et al., 2004). The MHNCCL PALEO-CS 71a tooth size is larger than those of *Adinothorium* and *Proadinothorium*, but within the size range of *Nesodon* (Scott, 1912; Croft et al., 2004; Forasiepi et al., 2015). Even when fragmentary, the recovered forearm bones are quite massive. The ulna has a sigmoid notch (Fig. 4.3f) indistinguishable from early Miocene nesodontines (Scott, 1912; Croft et al., 2004). The ulna width from Laguna del Laja at sigmoid notch is 57 mm, almost twice as the reported for *Adinothorium*, but within the range of size of *Nesodon imbricatus* (Scott, 1912). Therefore, the molar size and crown height and the shape and size of the recovered materials allowed us to recognize the presence of *Nesodon* in the Tcm₃ fauna. *Nesodon* is a relatively common taxon found in Santacrucian localities of Argentina and Chile (Flynn et al., 2002b; Croft et al., 2003, 2004; López et al., 2011; Bostelmann et al., 2013; Forasiepi et al., 2015; Fernández and Muñoz, 2019; Solórzano et al., 2019; Cuitiño et al., 2019),

but also reported in “Friasian” and Colloncuran localities in Argentina (Marshall, 1990; Kramarz et al., 2011).

Genus *ADINOTHERIUM* Ameghino, 1887

Adinotherium sp.

Revised materials. MHNCCCL PALEO-CS 70, heavily eroded p4 and isolated m1 (Fig. 4.3h).

Geographic and stratigraphic provenance. Cerro Campamento, west of Estero Trapa-Trapa, Laguna del Laja, Chile; Tcm₃ levels, Cura-Mallín Formation, late early Miocene.

Comments. The isolated molar shows typical traits of nesodontines, such as one lingual fold plus two accessory fossettids (Scott, 1912; Nasif et al., 2000; Croft et al., 2004). The m1 is smaller than those of *Nesodon* (Supplementary File 2) but within the size range of *Adinotherium* (Scott, 1912; Croft et al., 2004; Forasiepi et al., 2015). Although the m1 base is broken, the examined molar has a higher crown ($HI \gg 1$) than *Proadinotherium* (with HI between 0.5–1 *sensu* Croft et al., 2003). Thus, molar size and crown height support its referral to *Adinotherium*. This genus is also common during the Santacrucian, with several records in Argentina and Chile (Flynn et al., 2002b; Croft et al., 2004; Bostelmann et al., 2013; Fernández and Muñoz, 2019). However, it has also been mentioned in younger ages (e.g., “Friasian”) in Argentina and Chile (Marshall, 1990; Bostelmann et al., 2012) and tentatively in the middle to late Miocene of Venezuela (Rincón et al., 2016).

Suborder TYPOTHERIA Zittel, 1893

Family HEGETOTHERIIDAE Ameghino, 1894a

Subfamily PACHYRUKHINAE Kraglievich, 1934

Genus *PACHYRUKHOS* Ameghino, 1885

Pachyrukhos sp. nov.?

Revised materials. MHNCCCL PALEO-CS 72, partial skull with the left P3–M3 series and the bases of right P3–M3 (Fig. 4.3i–j); MHNCCCL PALEO-CS 73, skull fragment with left M1–M3 and right M1–M2; MHNCCCL PALEO-CS 74, mandible fragment with p3–p4; MHNCCCL PALEO-CS 75, mandible fragment with m3 (Fig. 4.3l); MHNCCCL PALEO-CS 76, mandible fragment with m1 or m2 (Fig. 4.3k);

MHNCCL PALEO-CS 77, isolate upper premolar (P3?); MHNCCL PALEO-CS 78, maxillary fragment with P4–M1; MHNCCL PALEO-CS 79, maxillary fragment with P4–M1; MHNCCL PALEO-CS 80, skull fragment with the left and right P4–M3 series.

Tentatively referred material. SGOPV 3805, partial palate with a complete right dentition (I1, P2–M3) and a portion of the left dentition (I1, P2–P4) (Flynn et al., 2008).

Geographic and stratigraphic provenance. Cerro Campamento, west of Estero Trapa-Trapa, Laguna del Laja, Chile; Tcm₃ levels, Cura-Mallín Formation, late early Miocene.

Comments. The revised materials, which include upper and lower molars (Fig. 4.3i–l), display a suite of characteristic traits of *Pachyrukhos*, such as the absence of I2–C–P1, tooth size (see Supplementary File 2), m3 trilobated with a rounded distal lobe, and M3 larger than M2 (Ameghino, 1889; Seoane and Cerdeño, 2019). However, the proportion M1 mesiodistal length / M3 mesiodistal length of the Laguna del Laja *Pachyrukhos* (mean = 1.35; ranging from 1.29–1.40) does not superpose with those previously reported for *Pachyrukhos moyani* (mean = 1.11; ranging from 1.05–1.19), or even *Paedotherium* or *Tremacyllus* (Fig. 4.4) (Cerdeño et al., 1998; Seoane and Cerdeño, 2019). Figure 4 illustrates that the studied materials display a relatively large M1 and small M3 compared with *Pachyrukhos* specimens from Santa Cruz and Collon Cura formations studied by Seoane and Cerdeño (2019). The Laguna del Laja *Pachyrukhos* also shows a distinctive enamel layer invariably present in upper and lower teeth and rather subtriangular upper premolars (Fig. 4.3j–l), contrasting with the thin or absent enamel observed and the more quadrangular upper premolars present in *Pachyrukhos moyani* (Seoane and Cerdeño, 2019). The last features suggest that the Laguna del Laja *Pachyrukhos* might not belong to the contemporaneous *P. moyani* (Seoane and Cerdeño, 2019). The second valid species of the genus, the Colhuehuapian *Pachyrukhos politus*, is only distinguishable by the relative size between p2–p3, elements so far unknown in Laguna del Laja specimens. Therefore, the studied materials might represent a new *Pachyrukhos* species, although we cannot dismiss the possibility that they represent the youngest record of *P. politus*.

Previous work in the Laguna del Laja region has mentioned the pachyrukhine, *Paedotherium minor*, based on the specimen SGOPV 3805 (Flynn et al., 2008). However, SGOPV 3805 exhibits an M3 smaller than the M2, unlike those observed in the species encompassed in *Paedotherium* (Cerdeño et al., 1998; Seoane and Cerdeño, 2019). Consequently, the presence of *Paedotherium* in the Laguna del Laja fauna is unsupported, and this specimen is more likely to belong to *Pachyrukhos*. Indeed, the rather subtriangular upper premolars and the proportion of the M1/M3 length exhibited by SGOPV 3805 agrees well with the remains briefly described here.



Figure 4.4. Boxplot comparing the M1/M3 length proportion in the *Pachyrukhos* from the Laguna del Laja (*Pachyrukhos* sp. nov.?), and others Neogene Pachyrukhinae taxa. *Pachyrukhos* sp. includes specimens without specific identification listed by Seoane and Cerdeño (2019).

Family INTERATHERIIDAE Ameghino, 1897

Subfamily INTERATHERIINAE Ameghino, 1887

Genus *PROTYPOTHERIUM* Ameghino, 1885

Protypotherium cf. *sinclairi* Kramarz, Bond & Arnal, 2015

Revised material. MHNCCL PALEO-CS 81, fragment of left mandible bearing the p3–m2.

Geographic and stratigraphic provenance. Cerro Campamento, west of Estero Trapa-Trapa, Laguna del Laja, Chile; Tcm₃ levels, Cura-Mallín Formation, late early Miocene.

Comments. The specimen is referred to *Protypotherium* by having p₃–p₄ completely differentiated from molars, talonids of p₃–p₄ shorter (mesiodistally) than the trigonid, and P-shaped trigonid and triangular talonid on m₁–2 (Sinclair, 1908; Kramarz et al., 2015; Vera et al., 2017, 2019). The more distinctive feature of MHNCCCL PALEO-CS 81 is their transversely larger p₃–p₄ talonids that are almost as wide as the trigonids (Fig. 4.3m) (i.e., the talonid width of p₄ and p₃ is >85% the trigonid width). The last trait resembles *P. sinclairi*, a taxon described and previously only known from the early Miocene of the Cerro Bandera Formation and the Trelew member of the Sarmiento Formation, Argentina (Kramarz et al., 2015).

Protypotherium sp.

Revised material. MHNCCCL PALEO-CS 82, associated fragments of left mandible bearing the base of p₃ and m₁–m₃; MHNCCCL PALEO-CS 83, maxillary fragment with the base of two molars (M₁–M₂?); MHNCCCL PALEO-CS 84, mandible fragment with two lower molars (m₂–m₃?); MHNCCCL PALEO-CS 85, fragment of eroded mandible partially covered of sediments with p₃–m₁.

Geographic and stratigraphic provenance. Cerro Campamento, west of Estero Trapa-Trapa, Laguna del Laja, Chile; Tcm₃ levels, Cura-Mallín Formation, late early Miocene.

Comments. MHNCCCL PALEO-CS 82 differs from *P. cf. sinclairi* in having a p₃ talonid mesiodistally narrow than the trigonid (Fig. 4.3n), and it is similar in size to *Protypotherium praerutilum* and *Protypotherium colloncurensis* (Vera et al., 2017). The other poorly preserved specimens are in the size range of *P. praerutilum* (MHNCCCL PALEO-CS 84) and *Protypotherium attenuatum* (MHNCCCL PALEO-CS 85; Supplementary File 2). Thus, the differences in size and the lower premolar morphology indicate at least one additional *Protypotherium* species than *P. cf. sinclairi*, but the materials are too fragmentary to achieve reliable species-level identifications.

Suborden FOLIVORA Delsuc, Catzefflis, Stanhope & Douzery, 2001

Superfamily MEGATHERIOIDEA Gray, 1821

Genus *HAPALOPS* Ameghino, 1887

Hapalops sp.

Revised material. MHNCCCL PALEO-CS 86, anterior fragment of dentary with the bases of a caniniform and three molariforms (Fig. 4.5a–c).

Geographic and stratigraphic provenance. Cerro Campamento, west of Estero Trapa-Trapa, Laguna del Laja, Chile; Tcm₃ levels, Cura-Mallín Formation, late early Miocene.

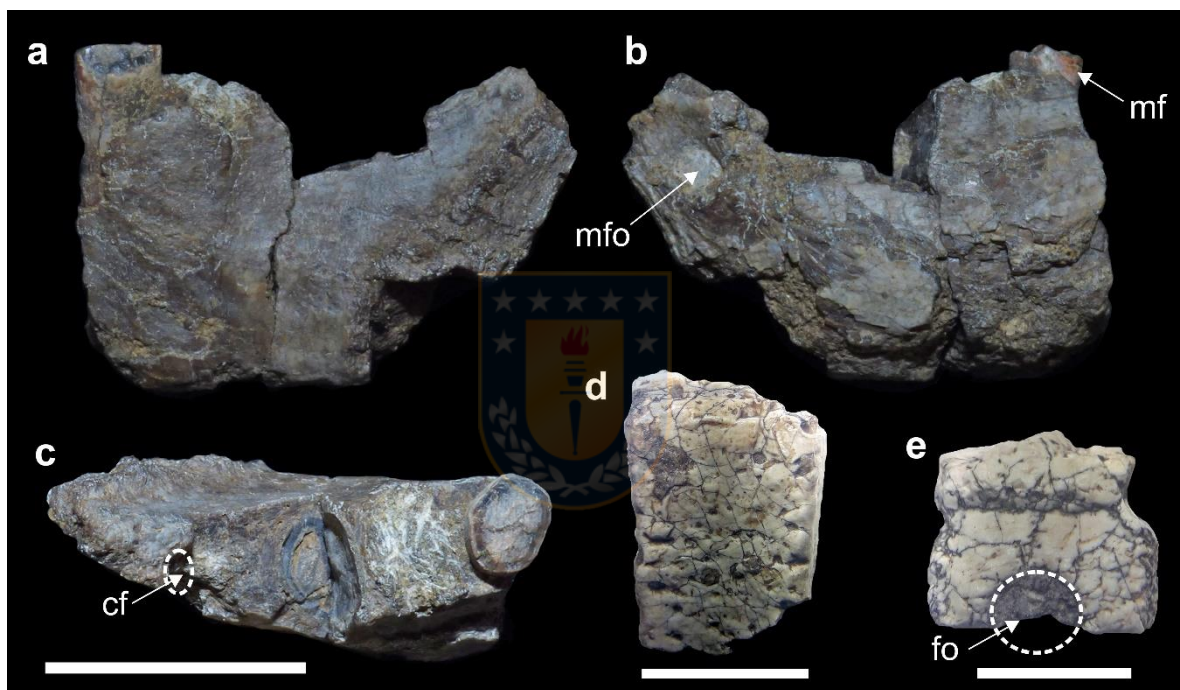


Figure 4.5. Xenarthrans from early Miocene beds of the Cura-Mallín Formation, Laguna del Laja, Chile. **a–c**, *Hapalops* sp. (MHNCCCL PALEO-CS 86): anterior fragment of dentary with four molariforms in medial (**a**), lateral (**b**), and occlusal (**c**) views. **d**, *Prozaedyus* sp. (MHNCCCL PALEO-CS 87), fragment of mobile osteoderm. **e**, Peltephilidae gen. et sp. indet. (MHNCCCL PALEO-CS 88), fragment of fixed osteoderm. Abbreviations: cf, caniniform; mf, molariform; mfo, mental foramen; fo, foramen piliferous. Scale bar_{a–c} = 1 cm; Scale bar_{d–e} = 0.5 cm.

Comments. The dentary is robust (dentary height at mf1 level is 24 mm), with the anterior-most toothless section partially preserved. There is a large mental foramen (partially covered by sediments) near the tip of the spout (Fig. 4.5b). The mandibular symphysis is anteroposteriorly long and extends distally up to the mf1 level (Fig. 4.5a). The caniniform only preserved its base but is smaller than the molariforms (Fig. 4.5c). The caniniform and molariforms are oval, with their longer axis slightly oblique (Fig. 4.5c). A diastema is present between the caniniform

and the first molariform (Fig. 4.5c), as typically occurs in species of the genera *Hapalops* and *Analcimorphus* (Scott, 1905; Gaudin, 2004; Brandoni et al., 2016). The morphology of the dentary MHNCCCL PALEO-CS 86 resembles that reported for *Hapalops* (Naples and McAfee, 2014) and has a more prominent spout than *Eucholoeops* Ameghino, 1887 (de Iuliis et al., 2014). Dozens of species have been included in *Hapalops*, but only a few of these are proved to be valid (Scott, 1905; Bargo et al., 2013, 2019). MHNCCCL PALEO-CS 86 has a combination of the features (i.e., oval caniniform smaller than molariforms and somewhat elliptical molariforms) and molariform size (Supplementary File 2) similar to *Hapalops* species (Brandoni et al., 2016). However, the revised material is unfortunately too fragmentary to achieve a trustworthy species-level identification. *Hapalops* have been described in the early Miocene of the Chinchas, Santa Cruz, and Pinturas formations in Argentina, the early Miocene Pampa Castillo fauna, southern Chile, the early middle Miocene (“Friasian”) of Argentina, and tentatively in the late middle Miocene (Laventan) of La Venta, Colombia (Scott, 1905; Kraglievich, 1930; Hirschfeld, 1985; Flynn et al., 2002b; López et al., 2011; Bargo et al., 2013; Naples and McAfee, 2014; Brandoni et al., 2016).



Suborder CINGULATA Illiger, 1811

Superfamily DASYPODOIDEA Cabrera, 1929

Family DASYPODIDAE Bonaparte, 1838

Subfamilia EUPHRACTINAE Winge, 1923

Tribu EUPHRACTINI Winge, 1923

Genus *PROZAEDYUS* Ameghino (1891)

Prozaedyus sp.

Revised material. MHNCCCL PALEO-CS 87, fragment of mobile osteoderm (Fig. 4.5d).

Geographic and stratigraphic provenance. Cerro Campamento, west of Estero Trapa-Trapa, Laguna del Laja, Chile; Tcm₃ levels, Cura-Mallín Formation, late early Miocene.

Comments. The available fragment of mobile osteoderm is small (osteoderm width of 5.1 mm), and the central figure is eroded, but the osteoderm has denticulated margins typical of the genus *Prozaedyus* (Croft et al., 2009;

Barasoain et al., 2020). However, the remains are too fragmentary to further advance in their taxonomic affinities. *Prozaedyus* have been previously mentioned in several Deseadan to Mayoan SALMA localities in Argentina, “Friasian” to Laventan SALMA localities in Bolivia, and “Friasian” beds at Rio Cisnes, south of Chile (Croft et al., 2009 and references therein).

Family PELTEPHILIDAE Ameghino, 1894

Peltephilidae gen. et sp. indet.

Revised material. MHNCCCL PALEO-CS 88, fragment of fixed osteoderm (Fig. 4.5e).

Geographic and stratigraphic provenance. Cerro Campamento, west of Estero Trapa-Trapa, Laguna del Laja, Chile; Tcm₃ levels, Cura-Mallín Formation, late early Miocene.

Comments. The fragment of osteoderm shows diagnostic features of peltephilids, like a small overlap area with other osteoderms, a rough outer surface, one very conspicuous piliferous pit on the outer surface, and absence of figures on the outer surface (Fig. 4.5e) (Croft et al., 2007; González-Ruiz et al., 2012, 2013; Rincón et al., 2016). Nonetheless, given the scarce and fragmentary available material, more specific identification of this specimen is unfeasible. Peltephilids range from the early Eocene to late Miocene; however, most of the recognized species in the family are restricted to the late Oligocene to early Miocene of the southern and central South America (Croft et al., 2007; Kramarz et al., 2010; González-Ruiz et al., 2012, 2013; Rincón et al., 2016; Montoya-Sanhueza et al., 2017).

4.6. Discussion

The study of the specimens recently collected from late early Miocene beds of the Laguna del Laja allowed the recognition of at least 17 mammalian taxa, predominantly caviomorph rodents (6 spp.) and notoungulates (5 spp.). The small-sized notoungulates *Pachyrukhos* and *Protypotherium* are the most common taxa in the sampled beds, with a minimum number of individuals of 6 and 4, respectively. Armadillos (2 spp.), sloths (1 spp.), paucituberculates (1 sp.), sparassodonts (1sp.), and litopterns (1 sp.) were also recognized, but they are

less abundant and diverse in our sample. Several of these taxa are recognized for the first time in the Laguna del Laja, including *Hapalops*, palaeotheniids, proterotheriids, nesodontines, *Galileomys*, *Prozaedyus*, and peltephilids, others are reported for the first time in Chile (i.e., *Protypotherium* cf. *sinclairi*, *Galileomys antelucanus*, and *Diadiaphorus majusculus*), and others likely represent new taxa (e.g., *Pachyrukhos* nov. sp.?). We hope these potentially new species will be named formally after the recovery of more diagnostic materials.

As mentioned above, Flynn et al. (2008) listed several mammal taxa from Tcm₃ levels at the Laguna del Laja but provided figures and inventory numbers for only a few of them. Judging from the photos of the Tcm₃ specimens supplied by Flynn et al. (2008: fig. 4), SGOPV 5710 is an abderitid marsupial and confidently documents the occurrence of this metatherian clade in Tcm₃. SGOPV 3834 clearly belongs to a species of *Neoreomys*, although likely different from the type species *N. australis*. SGOPV 3901 was figured as *Protacaremys* sp. nov. by Flynn et al. (2008); however, these upper cheek teeth differ from those of *Protacaremys prior* and resemble *Prospaniomys priscus* by having: 1) short anteroloph that remains separated from the paracone at least up to moderate stages of wear, and 2) second and third transverse lophs mesially convex and diverging labially (especially on DP4 and M3). Thus, SGOPV 3901 more likely belongs to an octodontoid closer to the Colhuehuapian *Prospaniomys priscus*. Finally, as discussed above, SGOPV 3805 belongs more likely to *Pachyrukhos* than to *Paedotherium*. When the above-mentioned records are considered, the mammal diversity of the Tcm₃ levels can increase up to 19 taxa (see Table 4.1). In any case, the taxonomic list of the Laguna del Laja will undoubtedly further increase when the remaining specimens reported by Flynn et al. (2008) are formally described. Meanwhile, the claimed endemic and unique nature of the early Miocene fauna at the Laguna del Laja (Flynn et al., 2008) must remain in question.

All mammal remains reported here were recovered in the middle to upper section of the Tcm₃ unit, with a relatively well-constrained ⁴⁰Ar/³⁹Ar age of 17.70 – 16.40 Ma (Flynn et al., 2008; Solórzano et al., 2020a). Therefore, the age of the Tcm₃ assemblage reported here is consistent with the Santacrucian SALMA (Cuitiño et al., 2016, 2021). This inference is reinforced by the presence of the exclusive Santacrucian species (e.g., *Phanomys mixtus*, *Diadiaphorus*

majusculus) and typical (but not exclusive) Santacrucian genera (e.g., *Nesodon*, *Sipalocyon*, *Hapalops*, *Pachyrukhos*, *Adinotherium*, *Neoreomys*, *Prozaedyus*) (Ameghino, 1889; Scott, 1905, 1910, 1912).

Despite the limitations of our taxonomic determinations, it is possible to ascertain the broad biogeographical relationships of the late early Miocene Laguna del Laja mammal assemblage from Tcm₃, above described. The late early Miocene mammalian assemblage at Laguna del Laja is somewhat different in terms of diversity and taxonomic composition compared with broadly contemporaneous assemblages at northern and southern latitudes of Chile and Argentina (Scott, 1905; Flynn et al., 2002a; Kramarz and Bellosi, 2005; Kay et al., 2012b, 2021; Bostelmann et al., 2013; Charrier et al., 2015). Compared with contemporaneous Chilean localities, the Laguna del Laja (Tcm₃) and Chucal (~19°S) faunas differ in that the latter has mesotheriids, absence of sloths, lower diversity of small-sized typotherians, and a very different caviomorph composition (Flynn et al., 2002a; Charrier et al., 2015). Otherwise, the Laguna del Laja (Tcm₃) fauna is broadly similar to those of southern localities like Pampa Castillo (47°S; Santacrucian), and Rio Cisnes (44.5°S; “Friasian”) (Marshall, 1990; Flynn et al., 2002b; Bostelmann et al., 2012; Charrier et al., 2015), but has a much lower taxonomic diversity.

While most of the late early Miocene taxa reported here are broadly similar to those from coeval Santacrucian faunas from the Santa Cruz, Río Jeinemení formations, and especially with that from the Pinturas formations, Argentina (e.g., Cuitiño et al., 2019; Fernicola et al., 2019; Kramarz and Bellosi, 2005; Pérez and Vucetich, 2012), some taxa have been previously known in older and younger units and deserve further consideration. Our findings indicate the record of a taxon similar to *P. sinclairi* in Chile for the first time. *Protypotherium sinclairi* was previously only known from the early Miocene Cerro Banderas Formation (~39°S; 69.5°W; Neuquén Province, Argentina) and the Trelew Member of the Sarmiento Formation (Chubut Province, Argentina) (Kramarz et al., 2015). The mammal-bearing deposits of the Cerro Bandera Formation were initially assigned to the early Miocene Colhuehuapian SALMA (Kramarz et al., 2005). However, the record of additional taxa shared with older units has cast some doubts on this biochronological assessment (Kramarz et al., 2015). If further confirmed, the presence of *P. sinclairi* in Santacrucian deposits at the Laguna del Laja might

represent the youngest record of this taxon. A similar situation is detected for *Galileomys antelucanus*, described initially and only known from Colhuehuapian beds in Argentina (Vucetich and Kramarz, 2003). Therefore, its records in the Laguna del Laja fauna expand their chronological distribution to the Santacrucian. Moreover, the presence of *Maruchito* in Santacrucian levels of Laguna del Laja represents the oldest record of the genus (Solórzano et al., 2020a), previously known only from the middle Miocene Colloncuran SALMA in Argentina (Vucetich et al., 1993). The above-described findings might support previous ideas in which the current SALMA schemes, based on classical localities in southeastern Argentina, are of limited use in regional scales (Croft, 2007). Further sampling efforts with an accurate stratigraphic and geochronologic control, as well as continuous advances on the taxonomic composition of mammalian assemblages, are necessary for enhancing the SALMAs framework (e.g., Bucher et al., 2020; Cuitiño et al., 2016; Dunn et al., 2013; Prevosti et al., 2021).

The taxonomic differentiation between contemporaneous Santacrucian fossiliferous localities in Chile and Argentina might be related to geographic or environmental differences, but it is hard to discriminate against each other. From a broad regional point of view, the Santacrucian mammalian faunas of Chile located the western edge of the south of South America might represent a subsample of the richer Santacrucian faunas described in Argentina (Scott, 1905, 1910; Flynn et al., 2002b; Arnal et al., 2019b; Bargo et al., 2019; Chornogubsky et al., 2019; Fernicola et al., 2019; Schmidt et al., 2019; Solórzano et al., 2020a). Given their geographic location in the western border of the south of South America, the differences in species composition between the Tcm₃ fauna at the Laguna del Laja and the contemporaneous fossiliferous localities in Argentina might be a consequence of the topographic or climatic heterogeneity of the Laguna del Laja area related to Andean mountain-building processes (Hoorn et al., 2013; Silvestro and Schnitzler, 2018; Antonelli et al., 2018). This interpretation is consistent with the syncontractual sedimentation of the Cura-Mallín Formation strata, since ~18 Ma, proposed by Rosselot et al. (2019), which likely occurred in intra-arc or foreland basins related to Andean growth (Niemeyer and Muñoz, 1983; Suárez and Emparan, 1995; Flynn et al., 2008; Rosselot et al., 2019a).

Likewise, geographical and ecological regional differences might be further increased according to the distinct paleobotanical context in which the Laguna del Laja region is included, compared with the coastal localities of the Santa Cruz Formation (Fig. 4.6). The Laguna del Laja region belongs to the *Nothofagidites* Province (located in southwestern South America; Fig. 4.6), characterized by humid and temperate forests (Barreda et al., 2007). At the same time, the coastal Santacrucian localities are located in the Transitional Province (Fig. 4.6), characterized by alternating open coniferous forests, xerophilous groves, wooded and shrubby savannas, steppes with halophytic herbs, palm groves, and gallery forests (Barreda et al., 2007).

Currently, there are just a few interpretations about the prevailing environmental conditions during the sedimentations of the Cura-Mallín Formation at the Laguna del Laja region and are mainly based on stratigraphic and sedimentologic data. These interpretations pointed out to a floodplain deposition within a region of active volcanism (Carpinelli, 2000; Herriott, 2006) and predominantly-fluviatile volcanoclastic deposits (within which the vertebrate fossils occur most commonly), with minor facies indicative of short-lived lacustrine environments (Flynn et al., 2008). This depositional environment differs from those interpreted for penecontemporaneous localities in Argentina to a greater or lesser degree. For example, the paleoenvironment of the Santa Cruz Formation (Argentina) has been interpreted as low energy, floodplain-dominated fluvial system affected by episodic pyroclastic input with moderate to poorly developed paleosols and low gradient, oxygenated setting under elevated sedimentation rates (Raigemborn et al., 2015; Cuitiño et al., 2019, 2021). While the Pinturas Formation is a thin succession of pyroclastic rich deposits of aeolian origin, which appears to be accumulated over an irregular topography and limited watercourses, with mature paleosol development and several internal erosional unconformities (Bown and Larriestra, 1990; Kramarz and Bellosi, 2005; Cuitiño et al., 2019).

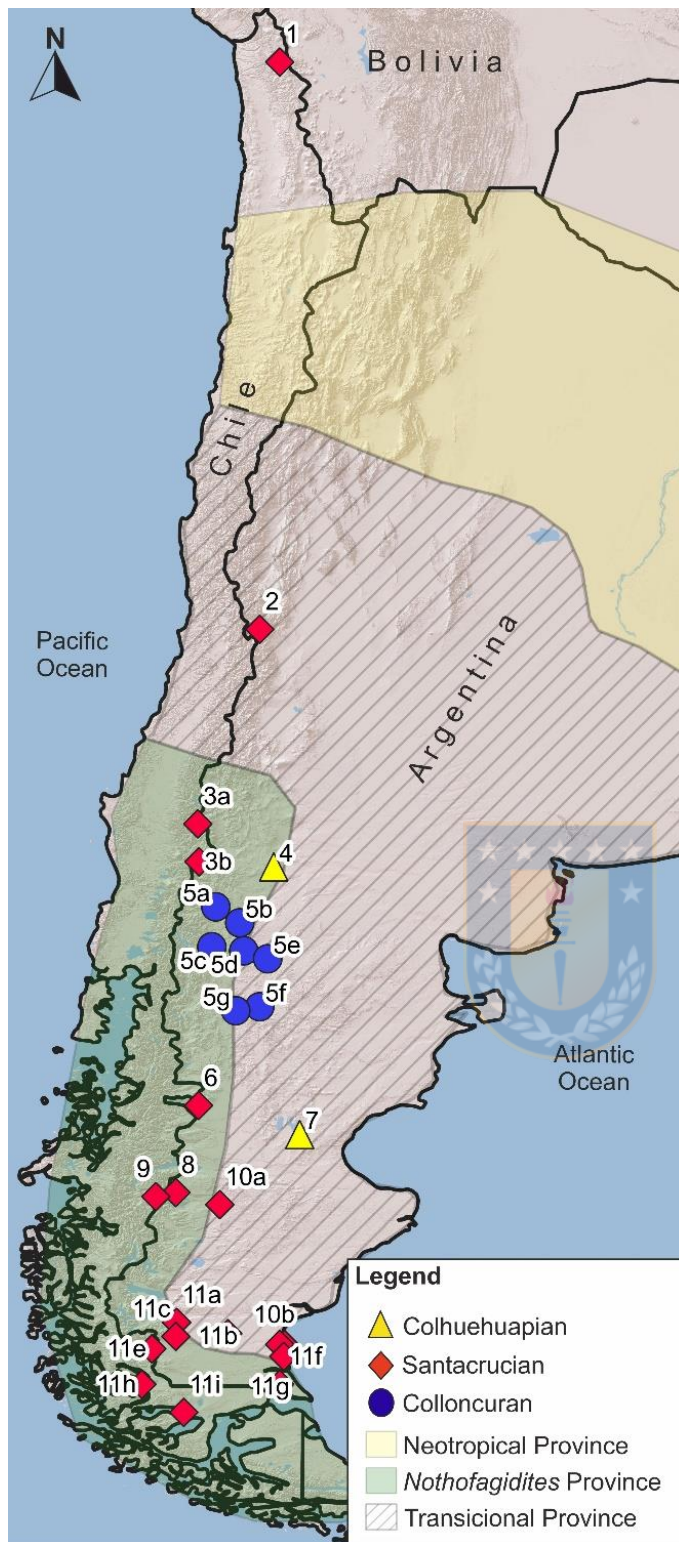


Figure 4.6. Geographic location of Santacrucian as well as other early and middle Miocene fossiliferous localities in middle and high latitudes of South America: 1, Chucal (Chile); 2, Chinchas Formation (Argentina); 3, Curamallín Formation (Chile): Laguna del Laja (3a) and Lonquimay (3b); 4, Cerro Bandera Formation (Argentina); 5, Collon Curá Formation (Argentina): Estancia Collón Cura and Collón Cura River (5a), Cañadón del Tordillo (5b), Pichileufú River (5c), Comallo (5d), Ingeniero Jacobacci (5e), Paso del Sapo (5f), Cerro Zeballos (5g); 6, Alto Río Cisnes (Chile); 7, Sarmiento Formation at Gran Barranca of Colhue Huapi lake (Argentina); 8, Río Jeinemení Formation (Argentina); 9, Pampa Castillo (Chile); 10, Pinturas Formation (Argentina): Valle del Río Pinturas (10a), Monte Observación (10b); 11, Santa Cruz Formation (Argentina and Chile), Karaiken (11a), Santa Cruz River valley (11b), Río Bote - Estancia Maria Elisa (11c), Cañadón de Las Vacas (11d), Sierra Baguales (11e), Cañadón Cerro Redondo (11f), Estancia Halliday (11g), Estancia Consuelo Ultima Esperanza (11h), Cañadon La Leona (11i). Note, furthermore, the early to middle Miocene palaeobotanical provinces in the south of South America (Barreda et al., 2007).

Although evidence of the ancient environment in the studied region is limited, extinct mammals can be a substantial source of information to reconstruct the environments in which they lived (e.g., Croft et al., 2018). Previous work focused on a reduced sample of late early Miocene rodents from the Laguna del

Laja preliminary suggested the predominance of open environments in the area (Solórzano et al., 2020a). However, after a broader taxonomic sampling, we can present a more compelling interpretation. A summary of the biological features, like body mass, diet, and preferred habitat (e.g., Cuitiño et al., 2019; Kay et al., 2021, 2012) previously inferred for the taxa represented in Tcm₃ is presented in Table 1. The scansorial, browser and frugivore taxa recorded indicate the predominance of forested habitats in the Laguna del Laja region during the early Miocene. The regional Neogene palaeobotanical composition in western Patagonia (Barreda et al., 2007; Palazzesi and Barreda, 2012; Palazzesi et al., 2014) and our local findings of large wood remains in (Tcm₃) beds stratigraphically below the deposits bearing most of the mammals here described it is also consistent with the presence of humid and temperate forests in the studied region during the late early Miocene. However, the occurrence of some mammals traditionally related to more open habitats (e.g., grazer mammals) also points out the existence of open environments in the region (Table 4.1). However, whether forested and open environments coexisted, with the first being likely predominant, or alternated through time in the study area, is hard to distinguish.

Kay et al. (2021, 2012) studied faunal assemblages of broadly comparable taxonomic composition to Tcm₃ levels at the Laguna del Laja from penecontemporaneous Santacrucian localities of southeastern Argentina. They estimated an ancient mean annual temperature between ~21°–25° C and ~1500–1800 mm/yr of mean annual precipitation and modest temperature seasonality. They also inferred the existence of mixed paleoenvironments, which primarily consisted of semi-deciduous forests ranging into savannas with gallery-forest components (Kay et al., 2012b, 2021). In contrast, the palynomorphs recovered in early Miocene beds of the Cura-Mallín Formation cropping out in the Lonquimay area (~120 km south of Laguna del Laja) indicate the predominance of humid and partly marshy forests in temperate to cold temperatures bracket in temperature ranges between 22° C and 11°C (Palma-Heldt, 1983; Solórzano et al., 2020a). Thus, the environment in the Laguna del Laja region during the late early Miocene would have been dominated by colder temperatures and more forested habitats than those above mentioned from the Atlantic coastal localities of the Santa Cruz Formation in Argentina. The last interpretation is also consistent with the fact that in the fauna recovered in the Pinturas Formation, the

unit with the more similar taxonomic composition concerning the Tcm₃ fauna, indicate the predominance of humid forested environments (Kramarz and Bellosi, 2005; see also this work for more details on the reasons for the possible contradictory paleoenvironmental interpretation provided by the sedimentological, paleopedological, and ichnological evidence compared with those based on the mammalian composition in this formation). Future palaeobotanical studies in the Laguna del Laja region based on the plant remains reported here may provide additional pieces of evidence in this regard.

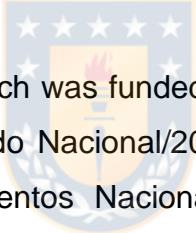
4.7. Conclusions

The study of new collections from the late early Miocene strata of the Cura-Mallín Formation at the Laguna del Laja area (Chile) allowed us to recognize at least 17 mammalian taxa, including putative new taxa. Some of these taxa, previously known only in Argentine localities, are reported in Chile for the first time, contributing to filling the gap in the Neogene mammalian paleodiversity of southwestern South America, an area much less sampled than those located in the southeastern of the continent. The assemblage described here is roughly like those previously reported in coeval localities located at southern latitudes in Argentina and Chile and primarily similar to those described from the Pinturas Formation (Argentina). Differences in taxonomic composition with these faunas could be due to different paleoenvironmental conditions along a longitudinal gradient in southern South America.

The paleoenvironment in which the Cura Mallin fauna from the Tcm₃ unit inhabited was one in which forested and open habitats likely coexisted in association with pedemontane fluvial environments on a region of syncontractual tectonism and active volcanism. Nevertheless, this fauna probably lived in a region with colder temperatures and more forested habitats than those inferred from the eastern Santacrucian localities in Argentina. The inferred environmental differences mentioned above are likely related to the significant topographic and climatic heterogeneity in southwestern South America driven by the Neogene Andean mountain-building processes. However, although the Andean orogeny has had a significant impact on the evolutionary dynamics of their native biota (e.g., Hoorn et al., 2010; Ortiz-Jaureguizar and Cladera, 2006;

Solórzano and Núñez-Flores, 2021; Strömberg et al., 2013), more studies are needed to test our hypothesis.

The available geochronological data indicate a late early Miocene age for the mammal assemblage described from the Laguna del Laja (Tcm₃), and the bulk of recognized taxa are consistent with an assignation to the Santacrucian SALMA. However, it is striking the presence of some taxa previously only known in older (Colhuehuapian) and younger (Colloncuran) ages. Therefore, our findings might support that the current SALMA schemes could be of limited use in regional scales. However, it also highlights the need to understand better the taxonomic composition of the early to middle Miocene faunas as an essential step to improve the SALMAs framework. Finally, the findings presented here endorse previous studies proposing that Santacrucian mammals were extraordinarily diverse and widely distributed in southern South American, improving our knowledge of this remarkable evolutionary period in the southwestern edge of South America.



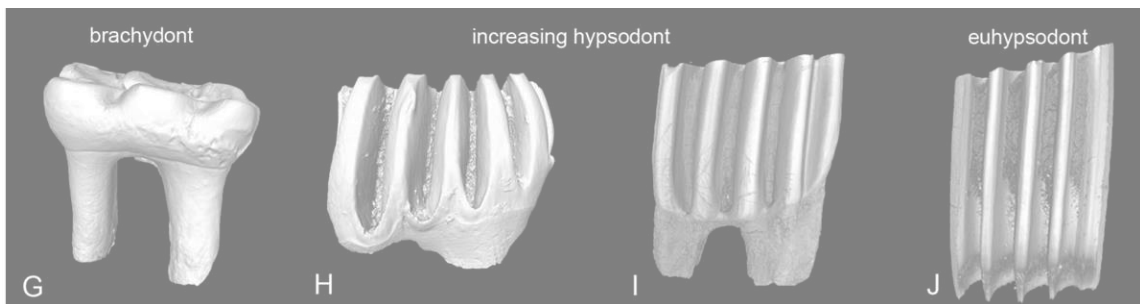
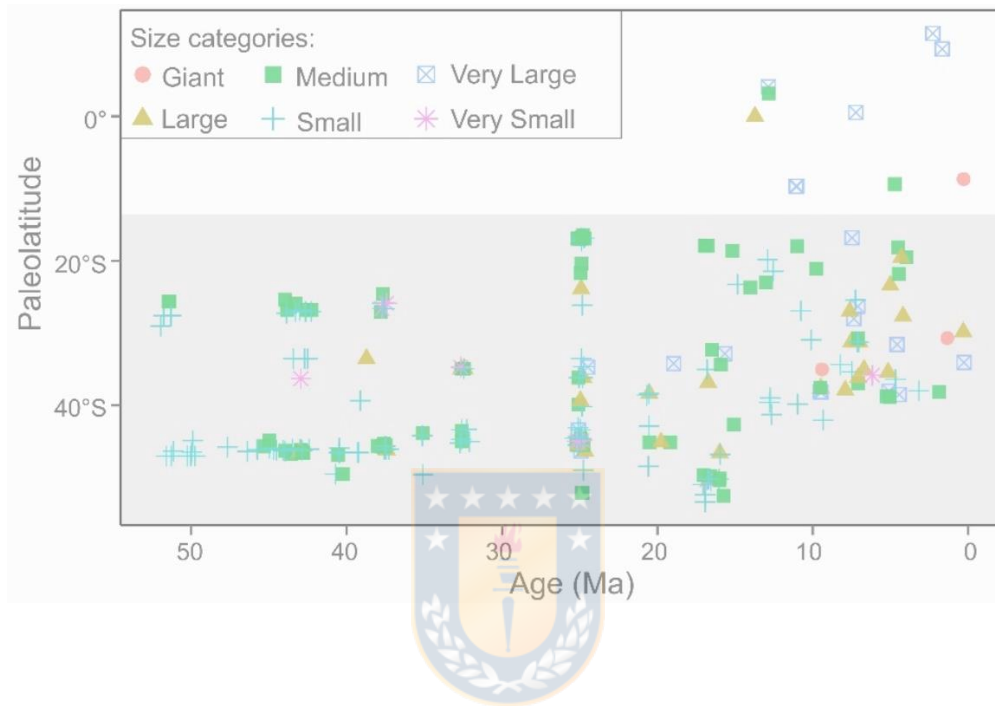
Acknowledgments. This research was funded by Fondecyt project n°1151146 (AE), and ANID–PCHA/Doctorado Nacional/2018–21180471 (AS). We wish to thank the Consejo de Monumentos Nacionales, the Corporación Nacional Forestal and the Gobernación Provincial del Bio-Bío for the authorization of paleontological prospections in the Laguna del Laja area. To David Rubilar (MNHN), Katherine Cisterna (MHNCCCL), Laura Chornogubsky (MACN), Martín Ezcurra (MACN) and Marcelo Reguero (MLP) for granting access to the vertebrate paleontological collections under their care; to Mónica Núñez-Flores, Maximiliano Reyes, Paz Butikofer, Francisca Riffo, Gabriel Arriagada, Hernán Arriagada, Andrés Cáceres, Ignacio Huenupi and Aníbal Anavalón for their assistance and camaraderie during the field trips at Laguna del Laja. We also extend our gratitude to the Centro de Microscopía Avanzada, CMA BIO-BIO (Proyecto CONICYT PIA ECM-12), and especially Paul San Martín, for their assistance and support in obtaining SEM images of the some of the studied materials.

Table 4.1. Ecological attributes of the late early Miocene mammals (Tcm₃) from the Laguna del Laja (Flynn et al., 2008; Vizcaíno et al., 2012; Cassini et al., 2012; Kay et al., 2012b, 2021; Shockey et al., 2012; Abello et al., 2013; Álvarez and Arnal, 2015; Fernicola et al., 2019; Cuitiño et al., 2019; Solórzano et al., 2020a; Solórzano and Núñez-Flores, 2021). Note that two additional mammals, than those described here, were included (Flynn et al., 2008) to provide a more compelling hypothesis about the late early Miocene paleoenvironments at Laguna del Laja.

	Taxa	SPr	BM (kg)	Diet	SPU
Rodentia					
	<i>Luantus sompallwei</i>	W	2.4* (III)	G?	?
	<i>Phanomys mixtus</i>	W	0.8 (II)	L	T(C)
	<i>Neoreomys</i> sp.	W	7 (III)	F(L)	T(C)
	<i>Prolagostomus</i> sp.	W	0.5–1.5 (II–III)	G/L	T(C)
	<i>Maruchito</i> sp. nov.?	W	0.8* (II)	G?	?
	<i>aff. Prospaniomys priscus</i> **	E	0.7* (II)	L(G)	?
	<i>Galileomys antelucanus</i>	E	0.4* (II)	L(G)?	?
Xenarthra					
	<i>Hapalops</i> sp.	W	30–50 (IV)	L	A(T)
	<i>Prozaedyus</i> sp.	W	0.75–2 (II–III)	S(I)	T(F)
	Peltephilidae gen. et sp. indet.	W	8–10 (III)	S(Tu)	T(F)
Notoungulata					
	<i>Adinotherium</i> sp.	W	50–100 (V)	G	T(A)
	<i>Nesodon</i> sp.	W	~250 (V)	G/L	T(A)
	<i>Pachyrukhos</i> sp. nov.?	W	~2 (III)	G	T(C)
	<i>Protypotherium</i> cf. <i>sinclairi</i>	W	7.9 (III)	G	T(C)
	<i>Protypotherium</i> sp.	W–E	2–9 (III)	G	T(C)
Litopterna					
	<i>Diadiaphorus majusculus</i>	W	92 (IV)	L	T(C)
Sparrasodonta					
	<i>Sipalocyon</i> sp.	E	1–3 (III)	V	A(T)
Paucituberculata					
	<i>Palaeothentes intermedius</i>	W	0.2 (II)	F(I)	T(A)
	Abderitidae gen. et sp. indet.**	W	0.25–0.5 (II)	F(I)	?

Body mass (BM) categories: II, 100 g to 1 kg; III, 1 to 10 kg; IV, 10 to 100 kg; V, 100 to 500 kg; VI, >500 kg. Diet: V, vertebrate prey; S(I), scavenging and insects; S(Tu), scavenging and tubers; S(L), scavenging and browse; F(L), fruit with leaves; F(I), fruit and invertebrates; L, leaves (=dicot leaves, buds shoots); G, grass stems and leaves (graze). SPU, Substrate Preference and Use: A(T), arboreal and terrestrial (scansorial); T(A), terrestrial and ambulatory; T(C), terrestrial and cursorial; T(F), terrestrial and fossorial. SPr, stratigraphic provenance in Laguna del Laja region: W, west of Estero Trapa-Trapa; E, east of Estero Trapa-Trapa. *body mass estimated here for the first time using the equation described in the materials and methods section. ** taxa mentioned from the Tcm₃ levels of the Laguna del Laja in previous a work, but not recognized during our surveys in the region.

CAPÍTULO V. Evolutionary trends of body size and hypsodonty in Notoungulates and their probable drivers



⁴**Solórzano A**, Núñez-Flores M. 2021. Evolutionary trends of body size and hypsodonty in notoungulates and their probable drivers. *Palaeogeography, Palaeoclimatology, Palaeoecology*, 568 (2021), 110306.

⁴ Artículo publicado en 2021. Disponible en <https://doi.org/10.1016/j.palaeo.2021.110306>

Evolutionary trends of body size and hypsodonty in notoungulates (Mammalia: Notoungulata) and their probable drivers

Solórzano Andrés^{1,*} and Núñez-Flores Mónica^{2,3}

¹Programa de Doctorado en Ciencias Geológicas, Facultad de Ciencias Químicas, Universidad de Concepción, Concepción, Chile.

²Programa de Doctorado en Sistemática y Biodiversidad, Facultad de Ciencias Naturales y Oceanográficas, Universidad de Concepción, Concepción, Chile.

³Programa de Doctorado en Biología Integrada, Facultad de Biología, Universidad de Sevilla, Sevilla, España

*Corresponding author: solorzanoandres@gmail.com

Highlights

- Notoungulates increased body sizes and hypsodonty throughout the last 50 Myr.
- Typotherians and toxodonts with low-crowned teeth had higher extinction rates.
- The body mass and the hypsodonty had a coupled long-term evolution.
- The Andean growth appears to be the main driver for the hypsodonty evolution.

Abstract

Members of the Order Notoungulata are among the most diverse and common mammals evolving in South America during the Cenozoic. Several lineages within notoungulates (e.g., suborders Typotheria and Toxodontia) show a tendency for increased body sizes and hypsodonty throughout the last 50 Myr. However, the timing, evolutionary mode, and drivers of such tendencies are not entirely understood. We use an extensive database of notoungulate fossil occurrences and body mass and hypsodonty estimations to characterize the evolutionary mode of these two phenotypic traits over time, test the extent to which several factors (e.g., development of open environments in the south of South America) have influenced it throughout time, and investigate whether large trait values were selected through elevated origination or reduced extinction rates. Our results suggest that most of the major clades within notoungulates

evolved toward larger body sizes (up 1.5. ton) and higher tooth crown, from a small sized and low-crowned tooth ancestor, in a punctuated mode. We also show that body mass and the hypsodonty in typotherians and toxodonts had a coupled evolutionary history. Species sorting was a relevant macroevolutionary process in some notoungulates clades, as taxa with high teeth crown and body mass had lower extinction rates. Finally, the Cenozoic Andean mountain building processes, which might increase volcanic and other terrigenous particles' availability to be removed or transported, appear to be the more likely driver for the long-term evolutionary dynamics of the hypsodonty in notoungulates.

Keywords: macroevolution; species sorting; Typotheria; Toxodontia; South America.

5.1 Introduction

During most of the Cenozoic, South America (SA) witnessed the evolution of several groups of mammals in relative geographic isolation (Simpson, 1980). One of the most diverse and common Cenozoic mammals evolving in this continent was the notoungulates (Order Notoungulata), achieving an impressive taxonomic diversity (with at least 154 genera so far recognized, but without leaving a single extant representative) and morphologic disparity, and filling a wide variety of ecological niches (Reguero and Prevosti, 2010; Reguero et al., 2010; Croft et al., 2020; Scarano et al., 2021). Their relationships within placental mammals remained elusive for more than a century, but recent ancient collagen and protein analyses have recovered notoungulates, together with other South American native ungulates like litopterns (Order Litopterna), as the sister taxon of Perissodactyla (Buckley, 2015; Welker et al., 2015). The phylogenetic relationships within notoungulates have supported their monophyly and the existence of two relatively well-defined suborders Toxodontia and Typotheria, and two early-diverging families, Henricosborniidae and Notostylopidae (Billet, 2011; Croft et al., 2020).

High-crowned (hypsodont) teeth are widely found among extant and extinct mammalian herbivores (Janis and Fortelius, 1988; Damuth and Janis, 2011; Kaiser et al., 2013). Notoungulata is one of the clades of SA mammals that evolved high-crowned or hypsodont teeth (Ortiz-Jaureguizar and Cladera, 2006;

Madden, 2014; Croft et al., 2020). The development of such kinds of tooth in SA appears precocious concerning other continents (Patterson and Pascual, 1968; Pascual and Odreman-Rivas, 1971). This precocity was first evident as early as the end of the Paleocene. Independently of its body size, it was during the Late Oligocene when many families of notoungulates acquired protohypsodont to hypselodont cheek-teeth (Pascual and Odreman-Rivas, 1971; Pascual and Jaureguizar, 1990; Ortiz-Jaureguizar and Cladera, 2006), and the Tinguirirican (Early Oligocene) South American fauna is the world's oldest fauna dominated by hypsodont herbivores (Flynn et al., 2003). Recent evidence suggests the existence of several periods of relatively intense evolutionary change in hypsodonty in South American mammals (Strömberg et al., 2013; Madden, 2014), and a general trend for an increased hypsodonty throughout the last 40 Myr has been noted in several notoungulates clades (Reguero et al., 2010; Strömberg et al., 2013). Increased hypsodonty appears to be synchronous across several lineages of tyotherians by the Tinguirirican SALMA (Reguero et al., 2010). In contrast, hypselodont (i.e., ever-growing teeth) appears to have originated among notoungulates in two pulses: Divisaderan SALMA (late Eocene) in hegetotheriids and mesotheriids and Deseadan SALMA (late Oligocene) in interatheriids and toxodontids (Reguero et al., 2007). Nevertheless, some authors have noted that relatively large errors in hypsodonty estimations are present, and consequently, the feasible bias in some of the estimated temporal trends cannot be ruled out (Dunn et al., 2015).

The causes of the development of a precocious hypsodonty in SA notoungulates are not entirely understood, as they might be very complex (Reguero et al., 2010; Strömberg et al., 2013; Madden, 2014; Dunn et al., 2015). Its development was initially linked to adaptive shifts given grassland/open habitats expansion (Flynn et al., 2003), consisted with the idea that most modern ungulate clades developed hypsodont teeth in drier and more open habitats (Janis, 1990; Raia et al., 2010; Damuth and Janis, 2011). Recent works found that grasses only were common in SA after the Miocene, being relatively rare during the Eocene, making it unclear whether hypsodonty evolved in forested or in open but grass-free habitats (Raia et al., 2010; Strömberg et al., 2013; Dunn et al., 2015). In any case, the relevance of exogenous grit or soil's ingestion has driven the necessity to deal with tooth abrasion has been claimed and now are

considered a plausible mechanism for hypsodonty evolution in ungulates (Damuth and Janis, 2011; Strömberg et al., 2013; Madden, 2014; Dunn et al., 2015; Semprebon et al., 2019). Indeed, the current view is that hypsodonty represents an adaptation to a worn effect that comprises both diet (e.g., phytoliths in grasses) and environment (dust or grit related to volcanism and erosion) (Damuth and Janis, 2011; Kaiser et al., 2013).

On the other hand, there are possible feedbacks among traits related to hypsodonty. For instance, hypsodont species could be larger-sized than non-hypsodont taxa because the resource that hypsodonty makes available to herbivores is a physiologically demanding one (Raia et al., 2011). Notungulates show high hypsodonty (brachyodont to hypselodont) and body size (~1–1,000 kg) disparity, which likely increases over time (Croft et al., 2020). Body size is one of the essential quantitative traits under evolutionary scrutiny because it influences nearly every aspect of an organism's biology (Peters, 1986). Body size exhibits prominent general trends in both space and time, as the tendency to evolve larger body sizes over evolutionary time (i.e., Cope's rule), or the pattern in which body size among closely related endothermic taxa tends to increase towards colder geographical regions (i.e., Berman's rule) (Ashton et al., 2000; Meiri and Dayan, 2003; Hone and Benton, 2005; McNab, 2010; Heim et al., 2015; Smith et al., 2016). However, none of these trends has been shown to apply generally across taxa (Ashton et al., 2000; Meiri and Dayan, 2003; Heim et al., 2015; Smith et al., 2016). The body size of organisms is often under selection pressure because it provides a direct way to adapt to several different environmental regimes (Kingsolver and Pfennig, 2004; Lyons and Smith, 2010; Smith et al., 2016). Thus, it seems likely that changes in the physical environment should exert a strong influence on the nature and directionality of body size evolution and other phenotypic traits (Hunt and Roy, 2006; Hunt et al., 2010, 2015; Clavel and Morlon, 2017). In general, both clade's biology and environment must be considered to understand trait evolution fully, and in general, macroevolutionary patterns. Accordingly, characterizing first-order patterns is essential for understanding the potential underlying causes that have shaped traits, like body size or hypsodonty, over evolutionary time (Hunt and Roy, 2006; Hunt et al., 2015; Smith et al., 2016). Characterizing the mode and tempo of the evolutionary change is a major theme in macroevolution since Simpson's earliest

days (Simpson, 1944). Nowadays, it is possible to characterize trait evolution based on the fossil record information, as each mode of evolution can be expressed as a statistical model (Hunt, 2006a). Three general models have become standard in attempts to understand the nature of evolutionary divergence in fossil lineages: directional change, unbiased random walk, and stasis, and although simplified, these modes of change are useful abstractions that distinguish fundamentally different kinds of evolutionary dynamics (Hunt, 2006a, 2007; Hunt and Rabosky, 2014; Hunt et al., 2015).

Even though the unique hypsodonty patterns exhibited by several lineages of notoungulates, to our knowledge, studies dealing with their evolutionary mode of trait evolution are still lacking, and the same situation is uncovered for the body size. Two primary drivers for evolutionary patterns of hypsodonty in notoungulates have been proposed, the tectonic evolution of the Andean orogen (as well as their concomitant complex volcanic history) and the development of open habitats through changes in the disposal of exogenous grit or soil (Madden, 2014; Kohn et al., 2015; Gomes Rodrigues et al., 2017). However, the few studies explicitly testing them have focused on the effects of the availability of open habitats over notoungulate hypsodonty (Strömberg et al., 2013). On the other hand, recently has been argued that the evolutionary patterns of body size in *Protypotherium*, a diverse genus of typotherians, could be correlated with global temperature trends (Scarano et al., 2021). Therefore, the potential drivers of the evolutive change of body mass and hypsodonty through time appear to be mostly related to abiotic or environmental changes. In contrast, additional potential drivers, including feedbacks among own-clade traits, have not been considered, and to our knowledge, no studies have examined multiple hypotheses simultaneously. The last is in need, given the complex interactions of biotic and abiotic factors driving long-term evolutionary patterns (Lehtonen et al., 2017; Fraser et al., 2020; Solórzano et al., 2020b).

In the present work, we compiled a comprehensive database of notoungulate fossil species occurrences, dental measurements (as a way to estimate the body mass of each species), and hypsodonty categories from the literature. Within a statistical framework, we analyzed these data to characterize the mode of evolution of phenotypic traits (body size and hypsodonty) over time. The more considerable diversity of notoungulates concentrates toward the south

of South America. Therefore, we also test the extent to which assorted environmental factors (e.g., paleobotanical changes) have influenced these traits (body size and hypsodonty). Given that both traits could fluctuate in both space and time, we also test the correlation between body size, hypsodonty, and geography (e.g., latitude, longitude as predictive variables). Moreover, although previous works have advocated an apparent increase of body size and hypsodonty in notoungulates through time (Reguero et al., 2010; Strömberg et al., 2013; Madden, 2014), it is necessary to distinguish whether these general trends are generated by a non-directional diffusive process or by an active directional evolutionary process due to selection for large body size or hypselodont species (McShea, 1994; Huang et al., 2017). Therefore, we also investigate whether large trait values (body size or hypsodonty) were selected through differential origination or extinction rates (Jablonski, 2008).

5.2 Methods

5.2.1 Fossil occurrence database

We collected data on fossil species occurrences over the entire evolutionary history of the Order Notoungulata, using mainly information in the Paleobiology Database (PBDB; <https://paleobiodb.org>). The data from the PBDB was taxonomically standardized by removing junior synonyms, outdated combinations, and *nomina dubia*. Some taxa were manually added to the dataset as they were absent from the PBDB. Each taxon's age was confirmed with the faunal list of the more diverse fossiliferous localities and updated accordingly to the recent advances in the South American Land Mammal Ages (hereafter SALMAs) (Reguero and Prevosti, 2010; Dunn et al., 2013; Prevosti and Forasiepi, 2018b; Croft et al., 2020). Each taxon was assigned to one of the traditionally recognized families. The final database comprises 1098 fossil occurrences representing 260 taxa (Supplementary File Table S1).

5.2.2 Body mass estimations in notoungulates

Several linear regression models have been developed to predict the body mass (BM) of extinct ungulates based on dental, cranial, and postcranial morphometric and body mass data from extant ungulates (e.g., Janis, 1990;

Mendoza et al., 2006). Three of the most widely employed, and also feasible to recover in the fossil record, dental measurements for body mass estimations in notoungulates are the lower molar series length (LMRL), second lower molar length (SLML), and second upper molar length (SUML) (Reguero et al., 2010; Elissamburu, 2012). After an extensive survey of the literature, we recover LMRL, SLML, SUML measurements for most (~90%) of the notoungulates species in our dataset (Supplementary File Tables S2, S3).

Craniodental body mass estimates appear to be inaccurate for large notoungulates, in part due to their relatively large head with ever-growing molars that are not closely similar to any extant ungulate (Croft et al., 2020). Therefore, body mass estimations in relatively large notoungulates based on ungulate craniodental variables (as LMRL, SLML, SUML) might result in overestimations (Croft et al., 2020). To circumvent this potential issue, we first use the database of LMRL, SLML, and SUML dental measurements (in mm) and body mass (in kg) of extant ungulates ($n = 138$) from Mendoza et al. (2006) (Supplementary File Table S4). Second regression models were fitted with segmented relationships (= piecewise linear regression) between the response (BM) and explanatory variables (LMRL, SLML, and SUML) using the package *segmented* (Muggeo, 2017) in the R environment (R Core Team, 2018). These allow us to find breaking points in the slope between the response and each of the explanatory variables at the following values: LMRL = 73.9; FLML = 19.2, and SUML = 20. The data of taxa in the dataset with lower values than these breakpoints ($n = 68$; BM ranging between 2–78.4 kg) were used to fit natural log-log ordinary linear regression (OLS) between the response (BM) and explanatory variables (LMRL, SLML, and SUML). For these models, we estimated their slope, interception, r^2 , Mean Absolute Error (MAE), percent Sum of Squares Error (%SSE), and percent Predicted Error (%PE). As tyotherians and other basal notoungulates include taxa smaller than 100 kg (Reguero et al., 2010; Elissamburu, 2012), we believe that estimations based on these new equations will provide an adequate approximation to their body mass. In cases in which more than a single dental measurement was available, we calculated these values' mean as a proxy of the BM in each taxon.

Given that relatively large notoungulates (i.e., members of Toxodontia) appear to have a relatively large head compared to extant ungulates, their BM

estimations may be severely biased. To diminish this bias, we use the above-resulting equations and estimate the 95% prediction intervals (which reflects the uncertainty around a single value) for the BM given each of the predictive variables (LMRL, SLML, SUML) in large notoungulates. Based on these prediction intervals, the lower BM values obtained for each taxon, even when more than a single dental measurement was available, was regarded as the most conservative BM estimation for members of the suborder Toxodontia and used in downstream analyses. Additionally, a summary of the BM calculations and their Log₁₀ frequency of distribution for all notoungulates and subordinate clades was provided. The last allows us to categorize the body size of notoungulates based on their BM (as well as their Log₁₀ BM) as follows: very small (<1 kg, or <0 in Log₁₀ space), small (BM between 1–10 kg, or 0–1 in Log₁₀ space), medium (BM between 10–100 kg, or 1–2 in Log₁₀ space), large (BM between 100–320 kg, or 2–2.5 in Log₁₀ space), very large (BM between 320–1000 kg, or 2.5–3 in Log₁₀ space) and giant taxa (BM between >1000 kg, or >3 in Log₁₀ space). Finally, we also estimate the body mass disparity (a measure of the range of morphologic variation in a sample of organisms) in each notoungulate family and suborder. While different methods and metrics for quantifying morphological disparity have been proposed (Erwin, 2007), the disparity is represented by the BM's standard deviation (kg).

5.2.3 *Hypsodonty in notoungulates*

Notoungulate taxa are hypsodont when a tooth crown's height exceeds its anteroposterior length, i.e., when hypsodonty index (hereafter HI), the ratio of first (or second) upper molar enamel crown height to anteroposterior or ectoloph length is over 1. The crown height in this group has been discussed in different ways (Madden, 2014). One approach is to express crown height measures in individual taxa as a hypsodonty index, which is generally measured on the best-preserved and least worn adult specimen available for each species, and the same value is assigned to the species (Madden, 2014). The last is a plausible measurement, as within an extant species, wear rates may not significantly differ among populations because individuals may vary little in dietary and habitat preferences (Damuth and Janis, 2011). Despite possible concerns regarding, among others, whether HI taken from upper or lower molars systematically differ

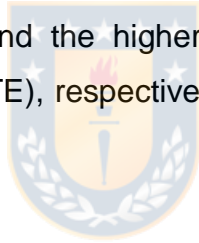
or not (Madden, 2014), this measurement has been provided for several notoungulates taxa (e.g., Reguero et al., 2010). A second approach is to express hypsodonty as an average of HI among the species, within a particular time-bin, at the family-level clade allowing the establishment of temporal evolutionary patterns of hypsodonty for each clade (Reguero et al., 2010; Strömberg et al., 2013; Madden, 2014). A third approach is to measure the percentage of faunal hypsodonty (i.e., the rate of herbivorous species with $HI > 1$). The last allows establishing the relative predominance of hypsodont taxa in different time-intervals (Madden, 2014; Dunn et al., 2015).

On the other hand, several categories could represent the distinct hypsodonty stages observed in herbivores molars, including brachydont ($HI < 1$), mesodont ($HI \sim 1$), hypsodont ($HI \geq 1 - 2.5$), and hypselodont (i.e., ever-growing teeth; $HI > 2.5$). We initially retrieved, from the literature, HI face values for 92 of the 260 notoungulate spp. (Supplementary File Tables S2, S3). Given the limited sample of HI values, as well as the apparent variability of ways in which it has been estimated (e.g., HI taken from upper vs. lower molars), we codify most of the studied taxa (259 spp.) in one of the hypsodonty stages above mentioned, following information from the literature. Specifically, taxa with brachydont, mesodont, hypsodont, and hypselodont dentition were coded as 0, 1, 2, and 3, respectively. These categorical values were used in downstream analyses (Supplementary File Tables S2, S3). We argue that this data can capture the broad long-term evolutionary dynamics of hypsodonty in notoungulates. Finally, it is noteworthy that we are interested in determining the relative hypsodonty changes through time rather than in their absolute amount of change.

5.2.4 Dealing with potential bias in the lifespan of individual species

The first and last appearances of a species in the fossil record are likely to underestimate the true extent of its life span (Liow and Stenseth, 2007). We envisioned that this could be an important issue in South American mammals as they are mainly known within the SALMAs framework, which has critical temporal gaps. Therefore, we estimate the speciation and extinction times for each lineage in our dataset, considering the uncertainties of the preservation process. For this task, we used the hierarchical Bayesian framework implemented in the software PyRate v2.0 (Silvestro et al., 2014a, 2014b, 2019a). From our original dataset of

notoungulates occurrences, we randomly resampled the ages of each fossil occurrence to generated ten datasets and ran the analyses on all replicates. To assess which of the preservation models implemented in PyRate (Non-homogeneous Poisson process of preservation (NHPP), Homogeneous Poisson process (HPP), or Time-variable Poisson process (TPP)) is best supported by our data, a maximum likelihood test was run in PyRate (Silvestro et al., 2019a). For the TPP model of preservation, we use the times that delimit the last stages of the International Chronostratigraphic Chart (v2020/03) with a duration of more than 2 Myr (Cohen et al., 2013). We ran 10,000,000 Reversible Jump Markov Chain Monte Carlo (RJMCMC) generations (sampling every 10,000), assuming a Gamma model to assess the heterogeneity in the preservation rate and the best-supported preservation model to estimate the expected number of fossil occurrences per lineage/Myr (Silvestro et al., 2019a). We inspected RJMCMC convergence (ESS>200) using Tracer software (Rambaut et al., 2018) and discarded the initial 10% iterations as burn-in. Finally, posterior estimates across replicates were summarized, and the higher and lower 95% HPD times in speciation (TS) and extinction (TE), respectively, were obtained, representing a plausible lifespan of each taxon.



5.2.5 Correlations between body size and hypsodonty with origination and extinction rates

PyRate also implements birth-death models in which speciation and extinction rates change in a lineage-specific fashion as a function of an estimated correlation with continuous or discrete traits (*covar* model) (Silvestro et al., 2014a; Piras et al., 2018). Therefore, we use this model to test whether large body size and hypsodonty were selected, at the suborder level, through elevated origination rate or reduced extinction rate. Our original dataset of notoungulates occurrences was split in two, focusing on the fossil's occurrence of the suborders Toxodontia and Typotheria. We randomly resampled the ages of each fossil occurrence to generated ten datasets and ran the analyses on all replicates for each of these. For each trait, using the *covar* model (setting -mCov 5), we ran 10,000,000 MCMC generations (sampling every 1,000), inspect MCMC convergence and discard the initial 10% iterations as burn-in. The correlations were considered statistically significant when 0 was not included within the 95% credibility interval

for $\alpha_{\text{speciation}}$ and $\alpha_{\text{extinction}}$ parameters, while the correlation was interpreted as positive or negative depending on whether $\alpha > 0$ or $\alpha < 0$, respectively (Silvestro et al., 2014a; Solórzano et al., 2020b).

5.2.6 Body mass and hypsodonty evolution through time

The lifespan (previously inferred) and the traits (BM and hypsodonty) calculated for each species were used to compute the mean and standard deviation of these traits values in 1 Myr time bins using the *paleoTS* package (Hunt, 2006b) implemented in the R environment (R Core Team, 2018). We used the “joint” parameterization of the *paleoTS* package to examine support across different simple statistical models of trait evolution: random walk (URW), directional evolution (GRW), Ornstein-Uhlenbeck (OU) model, and stasis (see details of the models in Hunt, 2008, 2006a). More complex models implying punctuations (number of punctuations ranging from 1–5) and changes among some of the simple models above mentioned (e.g., stasis to GRW) were also tested considering the minimum number of samples (= time-bins) within a segment as 6 ($\text{minb} = 6$). Some of the samples (= time-bins) could have very low N, and their variances are likely estimated imprecisely. Therefore, we replace the low N samples’ variances with the estimated pooled variance (Hunt, 2006b). The BM analyses were based on their natural logarithm, therefore considering the rate of proportional, rather than absolute, change and reducing the potential bias regarding trait estimations (Lyons and Smith, 2010; Cooper and Purvis, 2010).

Model support for the fitted evolutionary models was assessed by using the bias-corrected Akaike Information Criterion (AICc), which balances the goodness of fit (log-likelihood) with model complexity (the number of model parameters). For each trait, the model with the lowest AICc value and higher Akaike weights is the best supported. However, AICc cannot reject all candidate models even when they represent poor descriptions of the observed trait dynamics (Voje, 2018). Tests of model adequacy may help us avoid making meaningless interpretations of model parameters that do not describe the data well (Voje, 2018). We use the model adequacy tests for the best phyletic models implemented in the R package *adePEM* (Voje, 2018) to test whether the simple statistical models of trait evolution fitted in *paleoTs* describe the data well. The trait evolution analyses first were performed considering all Notoungulates and

repeated at the suborder and family levels when possible (i.e., number of time bins >20). Finally, we are interested in identifying whether BM and hypsodonty increase or not with time. Therefore, we performed generalized least squares (GLS), as described below, to identify possible correlations among mean, minimum, and maximum BM and hypsodonty with time and evaluate the relationship significance using the p values for the slope coefficient.

5.2.7 Potential mechanisms driving the historical dynamics of body size and hypsodonty in notoungulates in the south of South America

The larger diversity of notoungulates (250 of 260 spp. in our dataset) concentrates toward the south of South America (hereafter SSA, and defined as the area located south of the 15°S (Ortiz-Jaureguizar and Cladera, 2006)), making this region suitable to test whether regional or global environmental factors could be driving the evolution of body sizes and hypsodonty in notoungulates. To this task, we use four time-continuous global and regional (SSA) factors, including global mean temperature based on $\delta^{18}\text{O}$ values of deep-sea benthic fauna (Zachos et al., 2001), temporal patterns on the relative abundance of open habitats in SSA (Palazzesi and Barreda, 2012; Dunn et al., 2015), vegetation openness index in SSA (Dunn et al., 2015), and feedbacks among BM and hypsodonty.

To obtain a proxy on the broad paleobotanical changes in the SSA, we also use the Engauge Digitizer software (Mitchell et al., 2020) to digitalize the data of Palazzesi and Barreda (2012), which summarize the evolution of the wet-demanding (e.g., rainforest trees) and the arid-adapted (e.g., steppe elements) plants groups during the last 26 Ma in Patagonia, based on pollen records. We also compiled the data from Strömberg et al. (2013), which provides a high-resolution temporal succession of phytolith assemblages in Patagonia between 43–18 Ma. Even when the last works deals with different types of data (pollen vs. phytolith), we combined these two datasets to provide a broad approximation to the temporal patterns on the relative abundance of forest and open habitats in SSA. Dunn et al. (2015) developed the leaf area index (LAI) as a proxy for vegetation openness. We use the Engauge Digitizer software (Mitchell et al., 2020) to digitalize the data LAI values reported in SSA for a period restricted between 49–10 Ma (Dunn et al., 2015).

Correlations between our mean of BM (in natural log scale) and hypsodonty data through time and the proxies of the different factors mentioned above were implemented using generalized least squares (GLS) regressions with a first-order autoregressive model incorporated to avoid potential inflation of correlation coefficients created by temporal autocorrelation (Hunt et al., 2005; Mannion et al., 2015). To determinate the best combinations of explanatory variables explaining our data, stepwise regressions and the Akaike information criterion (AICc) were employed. The best model is the one with lower AICc values and few numbers of explanatory variables. We use the time-weighted mean of all the variables mentioned above for data points that fall within each time bin of 1 Myr (Table S9). As these explanatory variables are in distinct units, they were rescaled to have zero mean and unit variance before the analyses. GLS and model selection analyses were implemented in R (R Core Team, 2018) with the packages *nlme*, *MASS*, *rr2*, and *MuMIn* (Ives, 2019; Barton, 2020; Pinheiro et al., 2020; Ripley et al., 2020). The analyses were focused on a time-period restricted between 10–49 Ma because the factors investigated are well represented in this period and were implemented first in Notoungulates and repeated at the suborder level.

5.2.8 Spatial patterns of body size and hypsodonty in notoungulates

The main role of volcanic particles driving the evolution of high tooth crowns in notoungulates has been previously suggested (Strömberg et al., 2013; Madden, 2014). Therefore, we expect a major prevalence of hypsodonty taxa toward the western's longitudes associated with the Andean volcanic belt, as this is the only portion of the continent with an active tectonic margin in SA during the Cenozoic. On the other hand, it is also plausible to expect a positive relationship between body size and latitude (i.e., Bergman Rule) as this pattern appears to be general for mammals, even when it has not been extensively studied for fossil taxa. For these reasons, we test for possible correlation between the BM, hypsodonty, and geography (e.g., latitude, longitude as predictive variables) using ordinary least squares (OLS) regressions and evaluating the relationship significance using the p values for the slope coefficient. Data from paleogeographic coordinates were mostly retrieved from the PBDB. For fossil occurrence not included in PBDB, modern latitude and longitude of fossil

collection were introduced in the GPLates portal (Müller et al., 2018) to estimate their ancient latitude and longitude (paleocoordinates) considering the mean lifespan age of each taxon. Recent work has claimed that paleoclimatic information obtained from a particular location might require accurate knowledge of its paleolatitude defined relative to the Earth's spin-axis (van Hinsbergen et al., 2015). As ancient latitude is essential for the hypotheses here tested, we additionally estimated a second proxy for the paleolatitude (namely paleolatitude 2) relative to the Earth's spin-axis of each taxa considering the centroid of their current geographic coordinates of fossil collection and the mean of their lifespan, using the webpage <http://www.paleolatitude.org/> version 2.1 (van Hinsbergen et al., 2015). For taxa with more than a single fossil occurrence, the centroid of their reported geographic distribution was estimated and used for the analyses. The OLS analyses were performed in R (R Core Team, 2018) and were implemented first with SSA Notoungulates and repeated at the suborder level (only including SSA taxa).

Abbreviations. SALMA, South American Land Mammals Age; Myr, millions of years (as time interval); Ma, millions of years ago; SA, South America; BM, body mass; HI; hypsodonty index; LMRL, lower molar series length; SLML, second lower molar length; SUML, second upper molar length.

5.3 Results

5.3.1 Body mass in notoungulates

Table S5 (Supplementary File) summarized the results of the log-transformed bivariate ordinary least-squares regressions performed on LMRL, SLML, and SUML dental measurements and BM of extant ungulates with a body mass lower than 79 kg. The resulting equations have, in general, low error values (i.e., low %PE, %SEE, and MAE), which indicate an adequate power for predictive accuracy. The LMRL variable has low errors, and consequently, it is likely the best predictor of the BM in extinct taxa. However, the additional predictors (SLML and SUML) also display relatively low errors (Table S5) and can even predict the BM in extinct taxa. Based on these equations, we estimate the body mass of extinct Notoungulates. The full set of body mass estimations is

available in the Supplementary File (Table S6), but a summary is presented in Table 5.1 and Figure 5.1a,b. As previously mentioned, craniodental body mass estimates appear to be inaccurate for large notoungulates (e.g., Toxodontia) because of their relatively large head or longer limbs compared with extant ungulates (Croft et al., 2020). For this reason, body mass estimations of Toxodontia were based on the lower value of 95% prediction intervals for each of the variables.

Most of the earliest notoungulates were relatively small (BM between 1–10 kg) animals (Figure 5.1a), but their body masses increased rapidly with time, especially in Toxodontia, during the Casamayoran SALMA, a period in which appears the first medium (BM between 10–100 kg) and large (BM between 100–320) sized taxa (Figure 5.1a). The two main clades within Notoungulata, Typotheria, and Toxodontia achieve different body masses during the Casamayoran (Figure 5.1a,b), with the former being smaller than the latter. Toxodonts attain huge sizes, especially since the Miocene and three taxa probably achieve more than 1 ton in weight during the last 10 Myr (late Miocene to the late Pleistocene). In contrast, larger-sized typotherians were present during the Oligocene (Desedean) and especially in the late Miocene (Chapadmalalan, Montehermosan, and Huayquerian SALMAs) (Figure 5.1a).

The basal notoungulates, mainly included in Henricosborniidae and Notostylopidae, are divergent regarding their BM. Henricosborniidae, represented by 13 taxa, has a mean body mass of ~13 kg (ranging from 1–109 kg) and a high body mass disparity (SD = 29). However, Henricosborniidae were predominantly (76%) small-sized animals (BM: 1–10 kg). Notostylopidae, represented by 11 taxa, were mainly (63%) medium-sized taxa (BM: 10–100 kg) with a mean body mass of ~16 kg and a much lower body mass disparity than Henricosborniidae (SD = 12; Table 5.1).

The body mass of typotherians could range between 0.36–155 kg (mean BM = 15 kg), with *Punapithecus minor* and *Typotheriopsis internum* representing the smaller and largest taxon, respectively (Table 5.1). Regarding the frequency distribution of the body mass, it is clear that most (64%) typotherians were of small size (BM between 1–10 kg) and in a lower proportion of medium (BM between 10–100 kg; 26 %), very small (BM < 1 kg; 7%) or large (BM between 100–320 kg ; 3%) sizes (Figure 5.2a). Most of the families within typotherians

(Interatheriidae, Hegetotheriidae, Oldfieldthomasiidae, basal typtotherians, Archaeopithecidae) are mainly composed of small taxa, displaying body masses with a mean around 5 kg (Table 5.1). However, members of “Archaeohyracidae” and especially those of Mesotheriidae are in the upper range of the typtotherians size (Figure 5.1b; Table 5.1). The only typtotherians with estimated body masses over 100 kg (= large taxa) are from the Mesotheriidae family. The BM disparity of most of the families within typtotherians appears to be relatively low (SD between 0.5–10) (Table 5.1). The only exception is Mesotheriidae, which has a large BM disparity (SD = 45).

On the other hand, members of Toxodontia have a body mass ranging between 2.6–1464 kg (mean BM = 217 kg), with *Pampahippus secundus* and *Piauhytherium capivarae* representing the smaller and largest taxon, respectively.

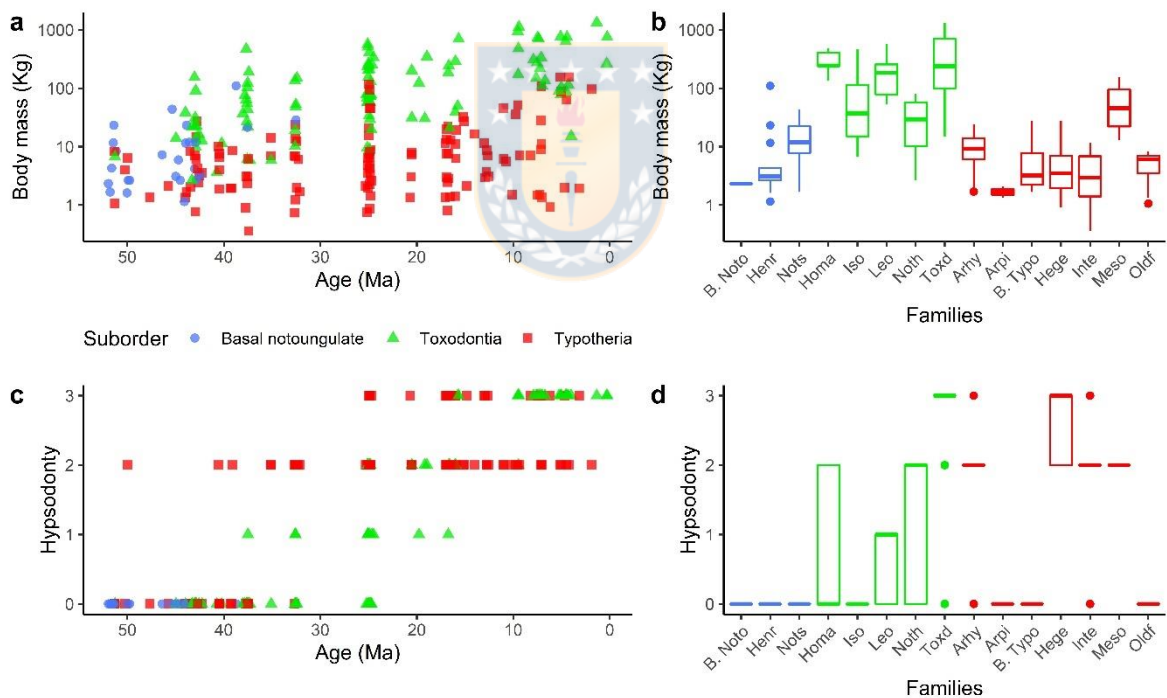


Figure 5.1. Body mass and hypsodontology in Notungulates. a, Notungulate BM (in kg) through time (in log10 scale); b, Box plot showing median (dark line), ranges (box range), and outliers (points) of BM for major notungulate families; c, Notungulate hypsodontology through time; d, Box plot showing median (dark line), ranges (box range), and outliers (points) of hypsodontology for major notungulate families. Colors in b and d represent suborders as in a and c. Abbreviations: Arhy, Archaeohyracidae; Arpi, Archaeopithecidae; B. Noto: basal notungulate; B. Typo, basal typtotherians; Hege, Hegetotheriidae; Henr, Henricosborniidae; Homa, Homalodtheriidae; Inte, Interatheriidae; Iso, Isotemnidae; Leo, Leontiniidae; Meso, Mesotheriidae; Noth, Notohippidae; Nots, Notostylopidae; Oldf, Oldfieldthomasiidae; Toxd, Toxodontidae.

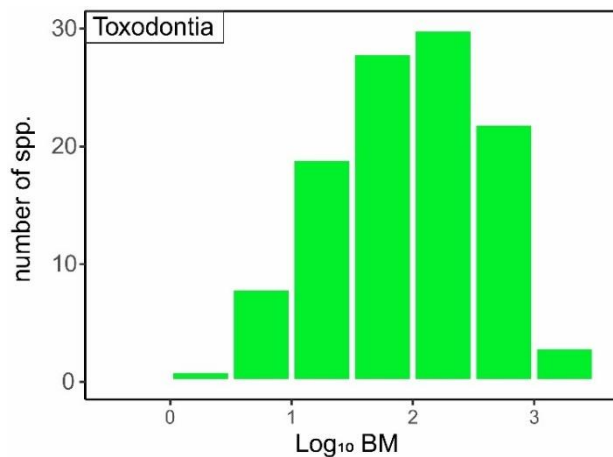
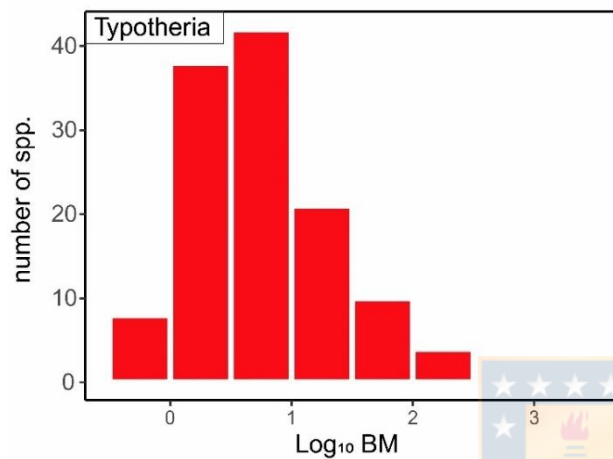


Figure 5.2. Distribution of frequency of the Log₁₀ of the body mass of toxodonts and typotherians. Note the predominance of relatively small to medium-sized typotherians and medium to very large-sized toxodonts (see further details in Figure 5.1).



Regarding the frequency distribution of the body mass, it is clear that most toxodonts were of medium size (BM between 10–100 kg; 42 %), but with a high proportion of large (BM between 100–320 kg; 27%) to very large (BM between 320–1000 kg; 20%) taxa (Figure 5.2b). In contrast, only a few members of Toxodontia were of small or giant size (8 and 3%, respectively) (Figure 5.2b). Notohippidae, represented by 29 spp., is the family with the lower mean BM (34 kg) as well BM disparity of the suborder, and groups predominantly (75%) medium-sized animals reaching up 80 kg (Table 5.1; Figure 5.1b). Isotemnidae, represented by 19 spp., exhibits wide BM disparity (SD =110), as includes predominantly 57% medium-sized taxa (yet small to very large taxa were noted), with a mean BM of 82 kg, and up 469 kg. Homalodtheriidae is a family with five large to very large representatives (mean BM of 300 kg), showing a large BM disparity (SD = 138) and reaching sizes up 476 kg. Leontiniidae, represented by 18 spp, exhibits wide BM disparity (SD = 150), as includes predominantly 50% large-sized taxa (yet small to very large taxa were noted), with a mean BM of 217 kg, and up 565 kg. Toxodontidae is the family with the high species richness (40

spp.) but also exhibits the more considerable body mass disparity (SD = 369) of any notoungulate family (i.e., the largest Toxodontidae has a BM one hundred times those of the smaller ones). They were predominantly very large (38%) and large (30%) animals (mean BM of 403 kg; reaching up 1,460 kg), including the largest notoungulates so far described, as *Piauhitherium capivarae* or *Toxodon platensis* (Table 5.1; Figure 5.1a,b). In fact, over time, the family Toxodontidae has ranged over three orders of magnitude in size.

5.3.2 Hypsodonty in notoungulates

The full set of HI values recovered from the literature (at face value) or even inferred based on hypsodonty degree categories (e.g., brachydont, mesodont, and hypsodont) from each notoungulate is available in the Supplementary File (Table S6). However, a summary of this information is presented in Table 5.1 and Figure 5.1c,d. Taken together, our results illustrate the temporal (Figure 5.1c) and within clade (Figure 5.1d) variations of the hypsodonty in notoungulates. The hypsodonty is different among the distinct notoungulate families and suborders. However, there is a general trend of increased hypsodonty with time in Typotheria, and Toxodontia. Besides, all the basal notoungulates have low crown heights (HI < 1; brachydont).

5.3.3 Lifespan of individual species

The maximum likelihood test results indicate that our data best supported the Time-variable Poisson process (TPP). The TPP model of preservation assumes that preservation rates are constant within a predefined time frame but can vary across time frames (e.g., geological epochs). These results are summarized in the Supplementary File (Table S6). The oldest species of notoungulate described (so far) appears to date from the early Eocene (~ 55 Ma), and the younger species go extinct at the end of the Pleistocene (or even the early Holocene). The mean lifespan of notoungulates species is ~5.4 Myr.

5.3.4 Correlation between traits and speciation/extinction rates

Neither speciation nor extinction rates were significantly correlated with body mass in typotherians. In toxodonts, higher body masses appear to be correlated with low extinction rates (mean $\alpha_{\text{extinction}} = -0.41$; 95% HPD interval = -

1.10 – 0.26) although the credible interval's upper bound falls slightly above zero. In another hand, higher crown teeth were significantly associated with very low extinction rates in tyotherians (mean $\alpha_{\text{extinction}} = -0.47$; 95% HPD interval = -0.84 – -0.19) and toxodonts (mean $\alpha_{\text{extinction}} = -0.290$; 95% HPD interval = -0.69– -0.09). Finally, either of the suborders showed a significant correlation between the traits examined (body size and hypsodonty) and preservation rate.

5.3.5 Describing the body size and hypsodonty macroevolutionary patterns in notoungulates

Body mass. The results of the mode of body-size evolution across notoungulates and lower taxonomic hierarchies are in the Supplementary File (Table S7), but a summary is presented in Table 5.2. When all notoungulates were analyzed, the directional evolution (GRW) outperforms other simple models and pass the adequacy tests (Table 5.2). This directionality is positive ($\mu_{\text{step}} = 0.054$; $\sigma^2_{\text{step}} = 0.020$), suggesting a relatively constant increase of BM in notoungulates through time. However, even when directional evolution might describe the data well, the more complex model with four punctuations (Punc-4) has a much better fit (dAICc=13.21; Table 5.2 and S7). The last model indicates several periods exhibiting stasis around one mean, which instantaneously shifts to stasis around a different mean. Notably, our data favored a scenario with four punctuations occurred in 40 (end of the Casamayoran), 30 (beginning of Deseadan SALMA), 19 (start of Santacrucian SALMA), and 11 Ma (Mayoan SALMA), which delimited five time periods (55–40 Ma, 40–30 Ma, 30–19 Ma, 19–11 Ma and 11–0.001 Ma) with dissimilar means BM values ($\mu_1 = 1.95$, $\mu_2 = 2.38$, $\mu_3 = 3.36$, $\mu_4 = 2.84$ and $\mu_5 = 3.92$, respectively in Log space; Figure 5.3). Interestingly, the Punc-4 model indicates that during the early to late Miocene (19–11 Ma) the mean body mass of notoungulates decreases ($\mu_4 = 2.84$) compared with the immediately early interval ($\mu_3 = 3.36$). The early to middle Eocene and late Miocene to late Pleistocene time intervals show the lowest ($\mu_1 = 1.95$) and the largest ($\mu_5 = 3.92$) mean BM values, respectively. The last results must indicate a general trend of the BM increase in notoungulates with time, yet this increase is not monotonic and was given in four main punctuations (Figure 5.3). On the other hand, the analysis of trait evolutionary mode at distinct taxonomic hierarchies (suborders and family levels) are summarized in Table 5.2 (see

details in the Supplementary File S7) and illustrated in Figures 5.3 and 5.4. These results reveal distinct ways of body mass evolution among the clades of notoungulates (Table 5.2).

The better-supported model of the body-size evolution of typotherians is the directional evolution (GRW), with a positive ($\mu_{\text{step}} = 0.020$; $\sigma^2_{\text{step}} = 0$) trend suggesting a relatively constant increase of BM in typotherians through time (Table 5.2). The slope of the BM increase in typotherians is 2.7 times slower than that exhibited by all notoungulates. However, it must be noted none of the simple models (including the GRW) pass the adequacy tests (Table S7). Within Typotheria the only families with enough data to implement the evolutionary models (above described) were Interatheriidae, Hegetotheriidae, Mesotheriidae, and Archaeohyracidae (Figure 5.3; Table 5.2). The BM evolution of interatheriids fits better with a directional evolution (GRW), with BM increasing with time ($\mu_{\text{step}} = 0.037$; $\sigma^2_{\text{step}} = 0$). The better-fitted model for hegetotheriids BM evolution is one with single punctuation that occurred at the end of the Miocene (~6 Ma), which delimited two broad periods (30–6 Ma, 6–0.001 Ma) with distinct mean BM values ($\mu_1 = 1.42$, $\mu_2 = 0.60$, respectively; in Log space). The last indicated that the mean BM of hegetotheriids was somewhat similar among the earliest forms and during a large portion of their evolutionary history (30–5 Ma) but much lower in their late (5–0.001 Ma) representatives. The best model describing the BM evolution of archaeohyracids is one with single punctuation, which occurred at 30 Ma, delineating two broad periods (43–30 Ma, 29–30 Ma) with dissimilar mean BM values ($\mu_1 = 2.03$, $\mu_2 = 2.89$, respectively; in Log space). The best model of mesotheriids BM evolution is those with two punctuations that occurred at the end Colhuehuapian (20 Ma) and the Laventan SALMAs (13 Ma), which delimited three broad periods (29–20 Ma, 20–13 Ma, and 13–2 Ma) with dissimilar mean BM values ($\mu_1 = 4.27$, $\mu_2 = 2.99$, $\mu_3 = 4.26$, respectively; in Log space). Mesotheriids highlight the drastic decrease of the mean BM during the early to middle Miocene (Figure 5.3), with a progressive increase exhibited by younger taxa.

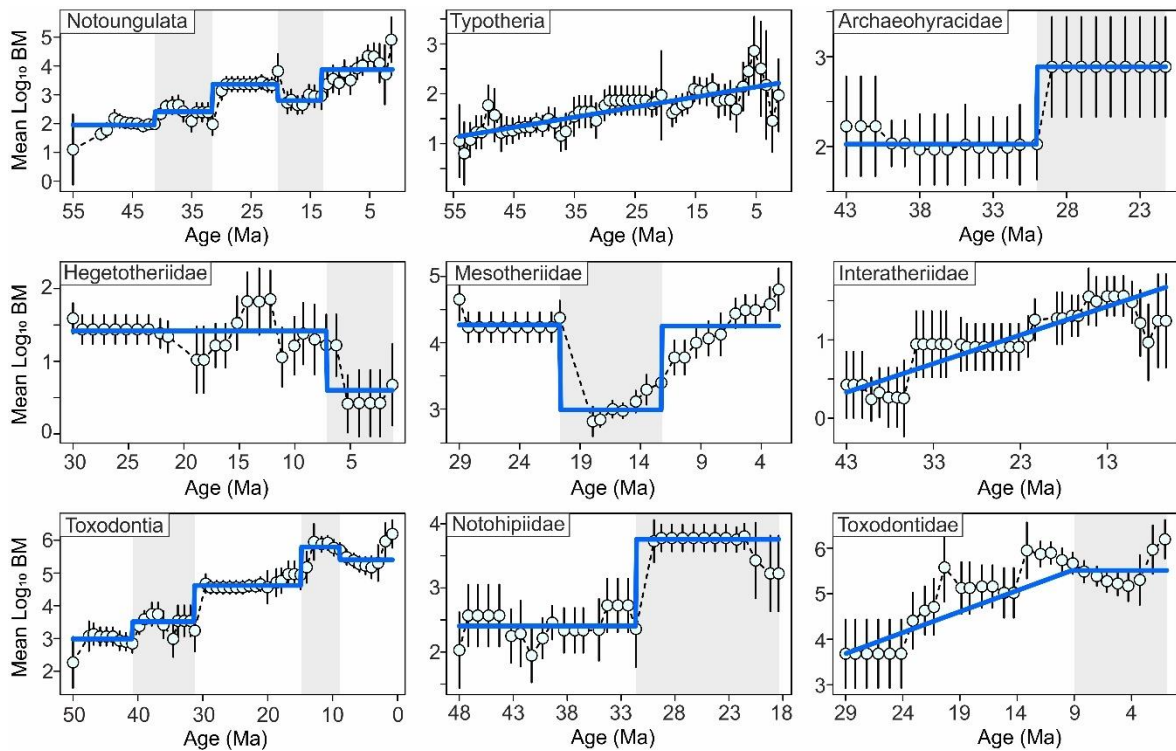


Figure 5.3. Temporal patterns of body size evolution in notoungulates and subordinate clades. The blue line denotes the best model parameters based on the trait evolution results performed with the PaleotS package. The circles represent the mean value in each time bin (1 Myr), and their associated vertical lines denote the variance around the mean. Time is in Ma. Note the predominance of punctuated changes in most clades.

The better-supported model of body-size evolution of toxodonts is a complex one with four punctuations (Punc-4), occurred during at 40, 30, 14, and 8 Ma, delimiting five periods (50–40, 40–30, 30–14, 14–8 and 8–0.001 Ma) of relative stasis with different means ($\mu_1 = 2.99$, $\mu_2 = 3.51$, $\mu_3 = 4.62$, $\mu_4 = 5.79$, $\mu_5 = 5.04$, respectively; in Log space). However, as occurs when all notoungulates were analyzed, the directional evolution (GRW) ($\mu_{\text{step}} = 0.062$; $\sigma^2_{\text{step}} = 0.016$) outperforms other simple models and is the only one passing the adequacy tests (Table S7). Therefore, it is evident a general trend of toxodont BM increases with time, but this increase occurs in four pulses. Within Toxodontia the families with enough data to implement the evolutionary models (above described) were Notohippiidae, and Toxodontidae (Table 5.2). For toxodontids, the best fit model of BM evolution is one complex with an early phase (29–10 Ma) of sustained positive directional evolution (GRW; $\mu_{\text{step}} = 0.12$; $\sigma^2_{\text{step}} = 0$), followed by a period (10–0.001 Ma) of relative stasis ($\mu = 5.45$). The best BM evolution model for notohippids is the one with single punctuation at 31 Ma, which separates two relative BM stasis periods. The first period (48–31 Ma) with somewhat lower BM

values ($\mu_1 = 2.41$) and a second one (31–17 Ma) with much larger values ($\mu_2 = 3.76$).

In tyrotherians, the minimum BM show a slightly yet non-significant increase with time (slope = -0.011 ; $p > 0.05$), while the mean and maximum BM significantly increase with time (slope = -0.01839 ; $p < 0.01$ and slope = -0.039 ; $p < 0.01$, respectively). In toxodonts, the minimum, maximum, and mean BM increase significantly with time (slopes varying between -0.061 – -0.0707 ; $p < 0.01$). Note that a negative slope implies an increase of body size towards the recent.

Hypsodonty. The results of the mode of hypsodonty evolution across notoungulates and lower taxonomic hierarchies are in the Supplementary File (Table S8), but a summary is presented in Table 5.2 and Figure 5.4. The directional evolution (GRW) outperforms other simple models and passes the adequacy tests when all notoungulates were analyzed (Table 5.2). This directionality is positive ($\mu_{\text{step}} = 0.06$; $\sigma^2_{\text{step}} = 0.01$), suggesting a relatively constant hypsodonty increase through time. However, even when directional evolution might describe well the data, the more complex model with five punctuations (Punc-5) has a much better fit (dAICc = 6.53; Table S8), indicating the existence of six periods exhibiting stasis around one mean which instantaneously shifts to stasis around a different mean. Remarkably, our data favored a scenario with five punctuations occurred in 37, 31, 25, 16 and 9 Ma, which delimited five time periods (55–37, 37–31, 31–25, 25–16, 16–9 and 9–0.001 Ma) with dissimilar means hypsodonty values ($\mu_1 = 0.05$, $\mu_2 = 0.18$, $\mu_3 = 1.37$, $\mu_4 = 1.65$, $\mu_5 = 2.32$, and $\mu_5 = 2.76$, respectively; Figure 5.4). Therefore, our results must indicate a general trend of the hypsodonty increase in notoungulates with time, with monotonic increases given in five main punctuations (Figure 5.4). The most significant increase in hypsodonty appears to occur at 31 Ma, during the Tinguirirican SALMA, when hypsodont taxa are dominant within the Order for the first time. The analyses of hypsodonty at distinct taxonomic hierarchies (suborders and family levels) are summarized in Table 5.2, revealing different ways of hypsodonty evolution among the clades within notoungulates (Figure 5.4).

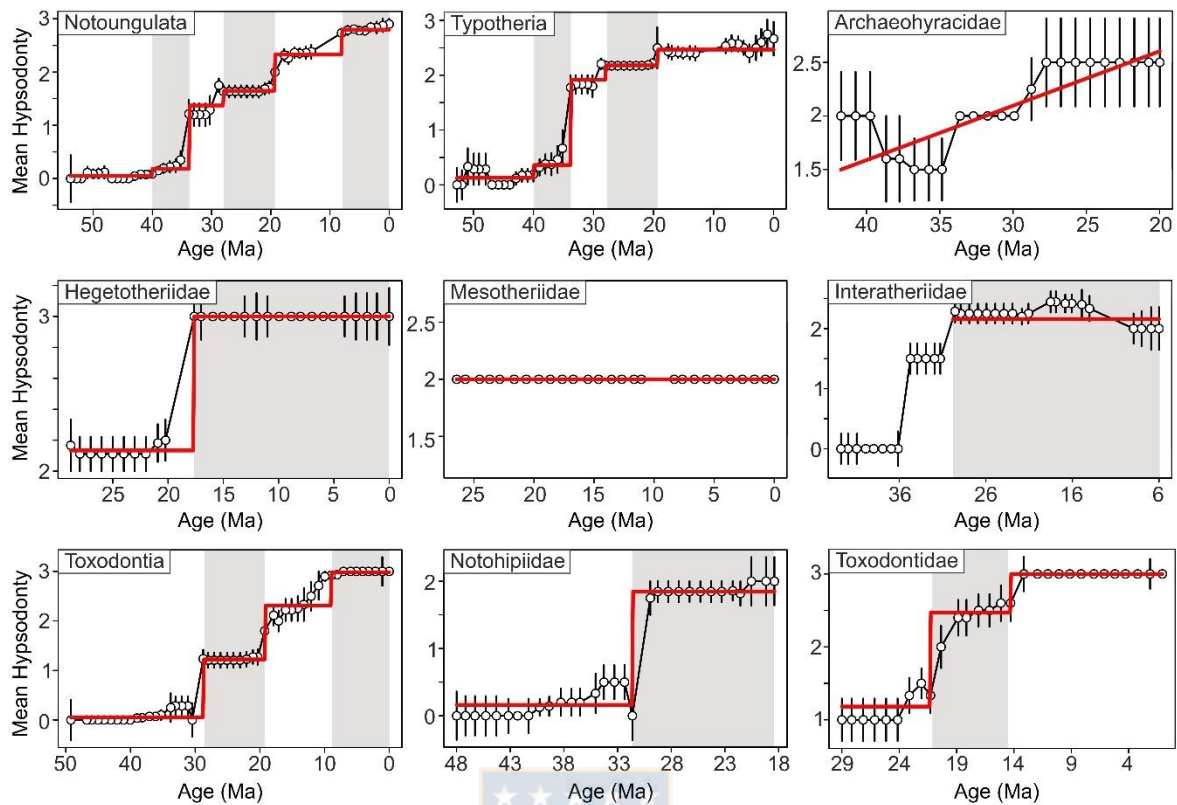


Figure 5.4. Temporal patterns of hypsodonty evolution in notoungulates and subordinate clades. The red line denotes the best model parameters based on the trait evolution results performed with the *PaleoTs* package. The circles represent the mean value in each time bin (1 Myr), and their associated vertical lines denote the variance around the mean. Time is in Ma. Note the predominance of punctuated changes in most clades.

The best model describing the hypsodonty evolution of typotherians is one of four punctuations (Punc-4, at 37, 31, 25 and 16 Ma), denoting five-time periods with dissimilar means hypsodonty values ($\mu_1 = 0.13$, $\mu_2 = 0.36$, $\mu_3 = 1.92$, $\mu_4 = 2.18$ and $\mu_5 = 2.47$, respectively; Figure 5.4). However, the GRW ($\mu_{\text{step}} = 0.05$; $\sigma^2_{\text{step}} = 0.01$) also appears to be an adequate model to explain our data. For archaeohyracids, the directional evolution (GRW; $\mu_{\text{step}} = 0.05$, $\sigma^2_{\text{step}} = 0$) is the best model for the hypsodonty evolution. However, this model fails the adequacy test. The evolutionary mode of hegetotheriids is better explained by a model with a single punctuation (Punc-1) occurred at 19 Ma (Early Miocene), which separate two time periods (30–19 and 19–0.001 Ma) of relatively little hypsodonty change ($\mu_1 = 2.13$, $\mu_2 = 3$). Nevertheless, the GRW ($\mu_{\text{step}} = 0.03$, $\sigma^2_{\text{step}} = 0.01$) also appears to be an adequate model explaining the hegetotheriid data. For interatheriids, the better fitter model of hypsodonty evolution is a complex one (URW-Stasis) with an initial phase of random walk ($\sigma^2_{\text{step}} = 0.11$), which changes at 30 Ma to a stasis

model ($\mu = 2.29$). Nevertheless, the GRW ($\mu_{\text{step}} = 0.06$, $\sigma^2_{\text{step}} = 0.04$) also appears to be an adequate model. Finally, the hypsodonty in mesotheriids did not vary significantly with time (Figure 5.4).

The best model describing the hypsodonty evolution of toxodonts is one of three punctuations (Punc-3), occurred at 30, 20, and 10 Ma, and indicating the presence of four-time intervals (50–30, 30–20, 20–12, and 10–0.01 Ma) with relative stasis around a mean hypsodonty value ($\mu_1 = 0.06$, $\mu_2 = 1.22$, $\mu_3 = 2.31$, and $\mu_4 = 2.98$, respectively). Nonetheless, the GRW ($\mu_{\text{step}} = 0.01$; $\sigma^2_{\text{step}} = 0.01$) also appears to be an adequate model to explain the toxodont data (Table 5.2). The hypsodonty evolution of notohippids fit better to a model with single punctuation at 30 Ma, indicating the presence of two-time intervals (48–30, and 30–17 Ma) of relative stasis around means of $\mu_1 = 0.16$ (predominantly brachyodont), and $\mu_2 = 1.85$ (predominantly hypsodont), respectively. For toxodontids, the better model of BM evolution is one complex two punctuations occurred at 20 and 13 Ma, indicating the presence of three-time intervals (29–20, 20–13, and 13–0.01 Ma) of relative stasis around means of $\mu_1 = 1.18$, $\mu_2 = 2.47$, and $\mu_3 = 3$, respectively (Figure 5.4). While the GRW ($\mu_{\text{step}} = 0.08$, $\sigma^2_{\text{step}} = 0.01$) could be also an adequate model for explain the data. Finally, the minimum, maximum, and mean hypsodonty increase significantly ($p < 0.01$) with time in both typotherians and toxodonts.

5.3.6 Potential mechanisms driving the historical dynamics of body size and hypsodonty in SSA

The GLS model fitting results shows that all notoungulates were considered, their mean body mass is positive and significantly correlated with the availability of open habitats; while none of the studied factors tracks, in a significant way, their mean hypsodonty patterns (Table 5.3). In typotherians, the best GLS model indicates that the mean body mass track the self-clade hypsodonty (and vice versa), with positive and significant relationships between both variables, and explaining a large portion of the data variance ($R^2_{\text{BM}} = 0.78$; $R^2_{\text{Hyp}} = 0.96$; Table 5.3). For toxodonts, the best GLS model reveals that a combination of global mean temperature and self-clade hypsodonty are the best predictor for the mean body mass evolution ($R^2_{\text{Hyp}} = 0.92$). Both factors had positive and significant effects on the response trait. Finally, the self-clade body

mass is the single best predictor of the mean hypsodonty in toxodonts ($R^2_{\text{Hyp}} = 0.96$) though positive effects (Table 5.3). Therefore, the coupled evolution of the body mass and hypsodonty in tyotherians and toxodonts (Table 5.3) is clear.

5.3.7 Body size and hypsodonty in through space and time

The OLS analyses performed with all notoungulates between the body mass, hypsodonty, and ancient latitude and longitude suggest that (Table 5.4): 1) the body mass significantly increase with latitude, but only when the “paleolatitude 2” proxy is employed ($p < 0.01$), and therefore it is not completely clear the generality of this trend; 2) the body mass shows a negative, yet non-significant ($p > 0.05$), relationships to longitude; 3) the hypsodonty significantly increase ($p < 0.01$) to western longitudes and lower latitudes.

5.4 Discussion

5.4.1 Body mass estimations in notoungulates

Previous work has claimed that craniodental and postcranial based body mass estimations appear to be inaccurate for large notoungulates because the use of these kinds of data might result in overestimations (Croft et al., 2020). The likely explanation is that large toxodonts have relatively large-headed ungulates with ever-growing premolars and molars, as well as short and stocky limbs, unlikely most extant ungulates (Croft et al., 2020). *Nesodon*, an early Miocene notoungulate, illustrates the claimed body mass overestimations. The body mass of this taxon has previously been estimated based on craniodental measurements and limb bone dimensions as ranging between 500–800 kg (Cassini et al., 2012; Elissamburu, 2012). However, these estimations contrast with those obtained on different proxies (e.g., head-body length), considered more reliable (Croft et al., 2020). Using the non-selenodont head-body length equation (Janis, 1990) and a head-body length estimate of 1.75 m (Scott, 1912), the body mass of this taxon was estimated as 247 kg (Croft et al., 2020), less than half that previously calculated. Based on available dental measurements of *Nesodon imbricatus* and the equations and methodology here developed, our body mass estimation on this taxon is 289 kg, in close agreement with those of Croft et al. (2020). Table 5.5 shows a selected sample of notoungulates with

several BM estimations available in the literature. Noteworthy, our BM estimations appear to be within the range of body mass values obtained by previous authors (Reguero et al., 2010; Cassini et al., 2012; Elissamburu, 2012; Gomes Rodrigues et al., 2017; Fernández-Monescillo et al., 2019). Even when our BM estimations appear to be reliable, given the above-described concerns regarding the potential dissimilarity between teeth and limb proportions of notoungulates relative to extant ungulates, we highlight it should be considered as provisional and consequently taken with some caution. The best way to circumvent the claimed problems in the notoungulate body mass estimation will be to use volumetric BM estimation methods based on whole articulated skeletons (Brassey, 2017). Of course, the application of such methods to the notoungulate fossil record could be limited by the paucity of well-preserved specimens.

5.4.2 The evolution of the body size in notoungulates

Our results illustrate that notoungulates had a large body size disparity because they include very small taxa of a rodent size (hundreds of grams) to large creatures of a rhino size (achieving nearly up 1.5 tons; Table 5.1; Figure 5.1). It is also possible to state that since a small-sized ancestor, notoungulates increased their body mass through time, ranging over 3.5 orders of magnitude in size (Table 5.1; Figure 5.1a). Nevertheless, when analyzed at lower taxonomic levels, each clade's body mass is distinctive, and it is noticeable that the two main suborders display different size ranges and unique evolutionary trends.

Toxodonts display a relatively active body mass increase during the last 50 Myr (McShea, 1994), as the mean BM increase is coupled with an increase in minimum and maximum BM of descendants (Figure 5.1a). Their body size trends were likely generated by species sorting for large bodies (McShea, 1994), as claimed for late Cenozoic artiodactyls and perissodactyls (Huang et al., 2017). The finding of correlations of body size with extinction rate (negatively) in toxodonts further supports the idea of a driven evolution towards larger body sizes through species sorting (McShea, 1994). The pattern exhibit by toxodonts is consistent with the expectations of the Cope's rule, a trend widely supported by the mammalian fossil record (Smith et al., 2004, 2016; Huang et al., 2017) but, to our knowledge, for the first time invoked for any extinct native south American

mammal clade. In contrast, the body mass evolution in tyotherians is best explained by a passive trend where the temporal patterns should mimic a diffusive process, perhaps asymmetrically bounded by a limit on the minimum size viable animal body (likely around 350 grams). This passive process can increase the maximum BM, and after enough time, increase the mean body size without raising the minimum (McShea, 1994; Smith et al., 2016; Huang et al., 2017).

Once we have supported the prevalence of distinct macroevolutionary processes generating the increasing body size through time observed in the two suborders within notoungulates (species sorting and diffusive process), it becomes necessary to characterize their predominant evolutionary modes. The likelihood-based models of evolution implemented (Hunt, 2006a, 2008; Hunt et al., 2015) allow us to recognize the prevalence of the directional (GRW) and punctuated (Punc) evolutionary modes as the best fitting models among both the traits under scrutiny and taxonomic groups (Table 5.2, Figure 5.3). Interestingly, these models are not the most commonly supported by the fossil record (Hunt et al., 2015). Besides, the predominance of complex punctuational models over the simple GRW model illustrates a stepwise, rather than gradual, evolution of the body size in most clades but also how the evolutionary reality is likely more complex than represented by simplified (though useful) models of trait change (Hunt and Rabosky, 2014; Hunt et al., 2015). These punctuational explanations exemplified intervals of accelerated evolution that differ qualitatively from “normal” evolutionary dynamics, and even when numerous mechanisms have been proposed to account for these two regimes of punctuation and stasis, what matters is that punctuations represent evolutionary changes governed by a different set of rules than those operating during stasis (Hunt, 2008). However, the causes of such punctuation are difficult to assess without further analyses, as ecophenotypic responses to environmental change and condensed stratigraphic intervals can produce patterns that mirror punctuated evolution within a lineage (Hunt, 2008). In any case, the variation in the timing of shifts in evolutionary dynamics emphasizes the complex nature of evolution here documented (Figure 5.3).

In toxodonts, there are a few time-intervals in which most of the rapid, and in several cases repeated, instances of evolutionary change of the BM appears

to occur (Table 5.2), middle Eocene (Bartonian; Barrancan; 40 Ma), early Oligocene (Rupelian; Deseadan; 30 Ma), and middle (Langhian; 14 Ma) and late Miocene (Tortonian; 8 Ma). The Bartonian is when the global temperature begins to decrease and coincides with the earliest stages of the Drake Passage opening (Zachos et al., 2008). Besides, an anomalously low $\delta^{13}\text{C}$ cluster in the Barrancan at ~39 Ma might represent a brief (c. 200 ka) interval of enhanced precipitation and wetter climates in Patagonia (Kohn et al., 2015). The analyses of $\delta^{18}\text{O}$ on teeth and bone reveals a dramatic drop in temperature, likely around 7–10° C, between 30–28 Ma (Deseadan) in high latitudes (~45°S) of South America, representing a short interval of drier climates in Patagonia likely due to regional (e.g., the uplift of the Patagonian Andes) rather than global reasons (Kohn et al., 2010). Besides, during the Early Oligocene, the Patagonian mammal fauna had experienced a significant turnover (termed as the “Patagonian Hinge”) associated with global climate cooling (Goin et al., 2010). Finally, the middle and late Miocene abrupt changes of the toxodonts BM coincides with the beginning of the middle Miocene Climatic Transition marked by the cooling of high and low latitudes and the stabilization of Antarctic ice sheets (Flower and Kennett, 1994), and with the enhanced seasonality, and restructuring of terrestrial plant and animal communities around the world (Palazzesi and Barreda, 2012; Herbert et al., 2016), respectively. Moreover, during the middle and late Miocene also essential environmental changes occurred in South America related to Andean uplift (e.g., reduced seasonal precipitation on the leeward side of the Andes mountains), impacting, among others, the trophic diversity of the mammalian communities in South America (Ortiz-Jaureguizar and Cladera, 2006; Hoorn et al., 2010).

In summary, the abrupt changes in BM in toxodonts appear to be likely a response related to the high extinction rate affecting small-sized species more strongly than large ones in the face of rapid changes in the regional environmental settings in SSA (Kohn et al., 2015). Attaching such large bodies sizes can contribute to resisting the extinction of toxodonts in several ways, including the increased capability of find suitable conditions due to longer dispersal distance and more extensive geographical ranges, providing a larger volume-to-surface ratio for preserving energy, and reducing the relative energy requirements (Peters, 1986; Ofstad et al., 2016; Huang et al., 2017). While on

the other hand, the overall body size trend of typotherians was generated by a bounded diffusive process rather than selecting large bodies (McShea, 1994). However, similar environmental drivers might also impact their passive trend of size increase over time.

5.4.3 *The evolution of the hypsodonty in notoungulates*

Notoungulates displayed a wide range of hypsodonty degrees, including brachydont to hypselodont taxa, with high crown forms (hypsodont and hypselodont) being increasingly common since the late Eocene (Strömberg et al., 2013; Dunn et al., 2015). Even when having a higher tooth crown represents different mechanisms that generated ecological and evolutionary advantages (Madden, 2014), the increased hypsodonty is shared by typotherians and toxodonts. Both suborders display an active trend of increased hypsodonty through time (including mean, minimum, and maximum). Therefore, it is also possible to hypothesize that this trait's long-term evolution was also driven by species sorting (McShea, 1994; Jablonski, 2008). Our results suggest that species sorting favored high-crown lineages within Toxodontia and Typotheria increase their survivorship during changes in the regional temperature or tectonic settings (Pascual and Jaureguizar, 1990; Ortiz-Jaureguizar and Cladera, 2006; Goin et al., 2010). These results are somewhat consistent with those observed in insular mammals, in which the acquisition of increased hypsodonty allowed them to delay senescence, extend reproductive lifespan, and increase fitness under environments with resource limitations (Jordana et al., 2012).

The current fossil record of notoungulates, and subordinate suborders, indicates that hypsodonty did not evolve gradually. Instead, we found rapid and repeated evolutionary change instances toward higher tooth crowns (Table 5.2), in broad agreement with previous interpretations (Kohn et al., 2015). When all notoungulates were considered, five main four punctuations were identified (at 37, 31, 25, 16, and 9 Ma), separating successive intervals of relative stasis (Table 5.2). Typotherians and toxodonts also display rapid and repeated evolutionary change instances toward higher tooth crowns, but with four and three punctuations, respectively (Table 5.2). The first punctuational increase in the mean hypsodonty occurs early in typotherians (at 37 Ma; Mustersan SALMA), but it was modest. In fact, since ~30 Ma (likely the earliest Deseadan) were the

toxodonts, which achieves for the first time mean hypsodonty values over 1. Besides, along with the Miocene distinct episodes of rapid hypsodonty increases in both tyotherians and toxodonts were recognized (Table 5.2). However, as mentioned above, the causes of such punctuations are difficult to assess without further analyses (Hunt, 2008) (but see details below).

5.4.4 Drivers of the body size and hypsodonty evolution in SSA notoungulates

Several GLS models were fitted to estimate the influence of some likely important variables on the mean evolution of the body mass and hypsodonty in SSA notoungulates using a maximum likelihood approach (Table 5.3). Our results supported that biotic (i.e., feedback among traits) and in less degree abiotic (global temperature) factors were important in driving the body mass and hypsodonty's temporal trends notoungulates, tyotherians, and toxodonts. However, as described above, the analyzed traits and suborders showed somewhat independent evolutionary histories. Therefore, let begin first with the main drivers in the evolution of their hypsodonty.

Previous works have hypothesized that increased hypsodonty in notoungulates must be related to the evolution of structural enhancements to prolong the functional longevity of the dentition given the landscape changes associated with the spread of grasslands, the climatic history of South America, and the tectonic evolution of the Andean orogen (and their concomitant complex volcanic history) (Flynn et al., 2003; Strömberg et al., 2013; Madden, 2014; Dunn et al., 2015; Kohn et al., 2015). Now, we examined each of these potential drivers in a separate way.

The initial expansion of open herbaceous communities in SSA begins in the Middle Eocene (~45 Ma), while the appearance of grassy habitats' likely occurs during the greenhouse to icehouse transition at the Eocene/Oligocene boundary (Bellosi and Krause, 2014). Although open-habitat grasses existed in southern South America since the middle Eocene, they were minor floral components in overall forested habitats until the early Miocene (Strömberg et al., 2013). Other authors have estimated a leaf area index (LAI) for the SSA extinct plant communities as a proxy of vegetation openness during the Eocene–late Miocene (Dunn et al., 2015). These authors suggested that the development of hypsodonty in notoungulates agrees relatively well with the increased availability

of open habitats (Dunn et al., 2015). Nevertheless, when the proportion of grasses and LAI were included as explanatory variables in our GLS analyses, none of these were significantly correlated with the mean hypsodonty evolution in notoungulates, and neither toxodonts nor tyotherians ($p>0.05$). Therefore, the hypotheses that the development of grasses or the increased open environments drive the long-term hypsodonty's evolution in notoungulates and subordinate suborders (Strömberg et al., 2013; Dunn et al., 2015) lacks statistical support.

South America's climatic history must respond to the tectonic changes in the subcontinent coupled with the global climate trends (e.g., Goin et al., 2010; Ortiz-Jaureguizar and Cladera, 2006). It has been suggested that the high tooth crowns in notoungulates likely evolved slowly and progressively over 20 Ma after the apparition of relatively dry environments through natural selection in response to dust ingestion favored by a cooled gradient of temperature and increases wind speeds across Patagonia (Kohn et al., 2015). While a proxy for wind speeds along the Cenozoic is lacking, we explicitly test whether the global temperatures drive hypsodonty changes using GLS regressions. We found that the global climate (Zachos et al., 2001) is not statistically correlated ($p>0.05$) with the trends of hypsodonty in notoungulates and subordinate suborders, denoting that significant changes in global temperature by himself did not drive the long-term trends in the evolution of this trait. Nevertheless, the global climate might be important in the evolution of some notoungulates lineages (Scarano et al., 2021).

The building of the Andes mountains can drove evolutionary changes in the Cenozoic mammals of South America in several ways. Mountain building creates topographic heterogeneity and new habitats where species evolve but also can provide nutrients to surrounding lowlands, increases sediment delivery (including volcanic particles) and heterogeneity of soil types, modified drainage patterns, and even alter the regional climate, generating climatic gradients along their slopes (Ehlers and Poulsen, 2009; Hoorn et al., 2010; Silvestro and Schnitzler, 2018; Antonelli et al., 2018; Huang et al., 2019). However, a proxy for the broad patterns in Cenozoic Andean uplift's is not yet available, mainly because their growth has been complex, involving fluctuations along time among three different tectonic regimes (shortening, extension, and neutral conditions, each of one reflecting contrasting degrees of mechanical coupling along the plate boundary between South America and the subducting oceanic slab), and along-

strike variability in deformation and crustal thickening (Ramos, 2010; Horton, 2018b). Therefore, it is likely that the uplift of the SSA Andes was heterogeneous in both time and space. For these reasons, we cannot include an SSA tectonic proxy in our analyses and cannot reject it as a potential driver for the hypsodonty's evolutionary patterns in notoungulates.

By fitting models describing the impact of several environmental factors driven macroevolution of the hypsodonty on our data, we can examine their relative importance, mainly because they are likely multicausal (Madden, 2014). For this reason, we fit GLS models looking for the best combination (if any) of variables explaining the evolution of the traits under scrutiny. Interestingly, our findings support that in tyotherians and toxodonts the body mass and the hypsodonty might have a coupled evolutionary history, unlike previous interpretations (Gomes Rodrigues et al., 2017), also challenging the view in which the main evolutionary changes in the hypsodonty in notoungulates were only driven by environmental factors (Strömberg et al., 2013; Dunn et al., 2015; Kohn et al., 2015). In any case, it remains unclear which of these traits (body mass and hypsodonty) were explanatory or response, although our data show that body mass increases in notoungulates predate increases in hypsodonty (Figures 5.3 and 5.4).

On the other hand, the main driver of the SSA notoungulates (as a whole) body size evolution is the availability of savanna grassland vegetation in this region (Palazzesi and Barreda, 2012; Strömberg et al., 2013), the single variable with a better fit to our data (Table 5.3). However, at the suborder level, this factor appears to be irrelevant. The increase of the body size through time in toxodonts is best explained by a combination of increased global temperature (Zachos et al., 2001) and hypsodonty in the clade. This finding partially supports the coupling between global temperatures and species body sizes generally observed in some mammals (Lovegrove and Mowoe, 2013; Martin et al., 2018). While the BM evolution of tyotherians is compatible with purely passive explanations for trends through time (McShea, 1994; Smith et al., 2016), the availability of savanna grassland vegetation and global temperatures are unlike drivers of their long-term mean fluctuations.

5.4.5 Spatial patterns in notoungulate body size and hypsodonty

Previous works have focused on the temporal patterns in the body mass and hypsodonty evolution in notoungulates (Reguero et al., 2010; Strömberg et al., 2013; Madden, 2014; Dunn et al., 2015). However, much less attention has been given to the spatial patterns of these traits. Today, the dominant mountain range of South America, located toward western longitudes, positively influence hypsodonty prevalence, and herbivores in the Andes are consistently more hypsodont (Madden, 2014). Here, we demonstrate a similar pattern in the fossil record, as there is a significant increase of hypsodonty in notoungulates toward the west of South America, close to the Andean mountains. This finding is highly congruent with the relevance of the Andean growth and its associated generation of volcanoclastic particles potentially driving the high crown tooth development in notoungulates, supporting previous interpretations (Strömberg et al., 2013; Madden, 2014). Therefore, it is likely that the surface processes related to the Andean orogen in South America drive the long-term evolution of some traits, like hypsodonty, in native mammal's lineages.

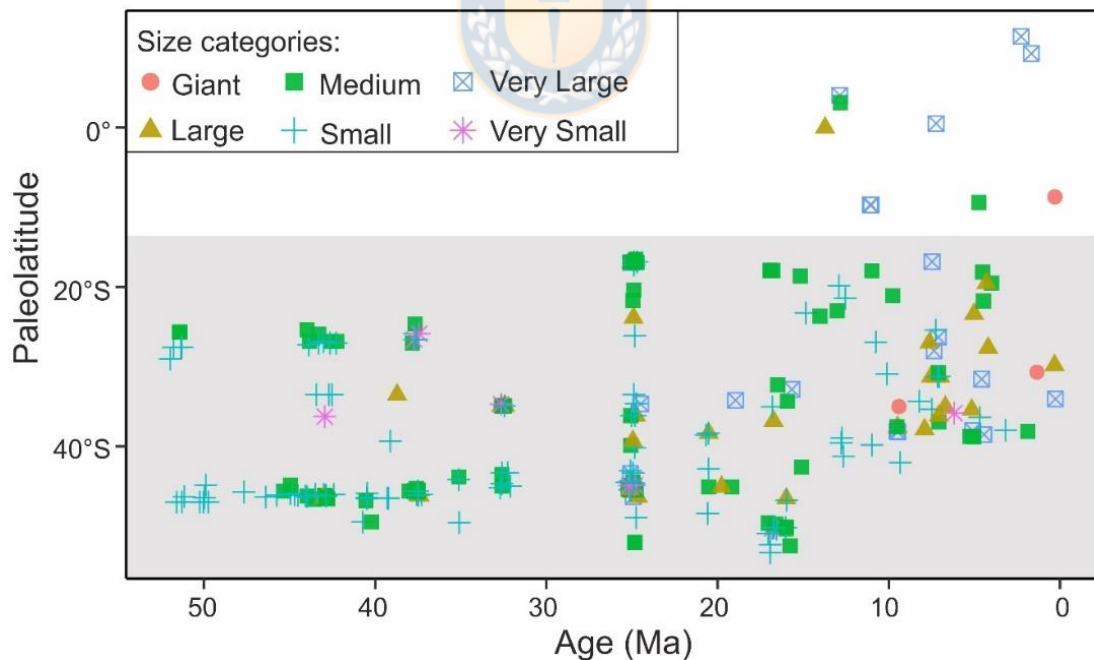


Figure 5.5. Paleolatitudinal distribution of notoungulates through time grouped according to body size classifications described in the main text. In grey is highlighted the location of taxa inhabiting the SSA.

On the other hand, our results also indicate an increase of BM toward tropical regions in SA, contrasting with Bergman's Rule's expectations (Ashton et

al., 2000). The spatial patterns in notoungulate body size did not trace the temperature (latitude), but whether it tracks other ecological important factors, as net primary production (Huston and Wolverton, 2011) or the availability and quality of resources (McNab, 2010; Saarinen, 2014), although likely, are not distinguishable with the available data. Nevertheless, these results may also be an artifact of fewer small-bodied species where species richness is low, as at lower latitudes (Figure 5.5). Inferring the macroevolutionary dynamics of completely extinct clades is challenging, mostly due to the fragmentary, distorted, and even biased nature of their fossil remains (Solórzano et al., 2020b). At present, the fossil record of notoungulates certainly reflects the absence or paucity of sampling from particular time intervals and geographic regions (Figure 5.5) (Croft et al., 2020). For example, the record of notoungulates is very poorly known in the neotropical area, as before the middle Miocene there is a lack of species reported in tropical regions (latitudes $<15^{\circ}\text{S}$), as well as a lack of notoungulates in higher latitudes ($>40^{\circ}\text{S}$) (Figure 5). Besides, it is also possible to note that these spatial biases might be related to BM, as there are just a few small-sized notoungulates in latitudes lower than 20°S (Figure 5.5). Whether this represents an absence of ecological opportunities for small-sized notoungulates, or a sampling bias needs to be further explored. However, we argue that further sampling effort for fossil data is unlikely to modify the broad patterns here described, as our analyses found neither body size nor hypsodonty associated with lower preservation rates in any of our suborders. Spatial heterogeneity in sampling is among the most pervasive biases of fossil data and might bias macroevolutionary analyses (Holland, 2016), and here we acknowledge that this kind of bias should be present in our data. Subsequently, our results might be improved or even challenged after the development of new proxies for the Cenozoic Andean building's timing, and after further advances in sampling efforts (especially towards lower latitudes) and taxonomy will be achieved.

5.5 Conclusions

We have compiled and analyzed a large dataset of notoungulates body mass and hypsodonty (>250 spp.) within statistical frameworks to assess these traits' evolutionary patterns through space and time and how environmental

changes (at a global and regional scale) and trait feedbacks have driven these patterns. Our results illuminate how these traits have emerged through space and time, providing further advances in understanding the long-term evolution of this intriguing and pervasive group of extinct South American mammals. Notoungulates and most low taxonomic hierarchies have mainly evolved from relatively small and lower-crowned ancestral forms after one or more abrupt positive and punctuated evolutionary changes in body mass and hypsodonty, denoting the complex nature of the evolution of these traits. Moreover, species sorting appears to be a crucial process in the macroevolutionary trends of the hypsodonty in notoungulates, and body mass in toxodons, primarily through extinction selectivity.

Here, we demonstrate for the first time that notoungulates have consistently evolved toward larger sizes and higher tooth crowns in a coupled way. Moreover, these increases were punctuated rather than gradual in most of the analyzed clades. The increases in hypsodonty must reflect repeated and quick instances of adaptive responses to the increase in volcanic and other terrigenous particles' availability to the removed or transported, within the broad context of the SSA Cenozoic Andean mountain building. The significant increase in hypsodonty toward the west of South America supports the last notion. Therefore, the Andean growth must be regarded as a more likely driver for the long-term hypsodonty evolution in notoungulates than the development of grasses, the increased availability of open environments, or even the global temperature. Nevertheless, rapid and punctuated body mass and hypsodonty changes may have been induced by short-term periods of high aridity, resource limitations, or volcanic activity. Whether the Andes growth and short-term environmental changes associated had a similar role in developing the hypsodonty (or other key traits) in other groups of South American mammals needs to be tested.

Acknowledgments. We want to express our gratitude to John Alroy and the entire PBDB team for their outstanding efforts in compiling and maintaining this database. We also thank Darin Croft and an anonymous reviewer for valuable comments and suggestions in an earlier manuscript version. The authors

acknowledge partial support from CONICYT–PCHA/Doctorado Nacional/2018–21180471 (to AS) and 2017–21170438 (to NFM).



Table 5.1. Summary of BM and hypsodonty estimated for each of the clades analyzed (families and suborder as a whole). The largest and smaller taxon in each clade is also provided.

Abbreviations: n, number of species in each clade; Min, minimum; Max, maximum; SD, standard deviation of the trait. Note that SD is considered a measure of morphological disparity.

Clade	# sp.	Body mass (kg)				Hypsodonty				Largest taxa	Smaller taxa
		Mean	Min	Max	SD	Mean	Min	Max	SD		
Basal notoungulate	26	14	1.15	109.8	22.6	0	0	0	0	<i>Acamana ambiguus</i>	<i>Peripantostylus minutus</i>
Henricosborniidae	13	13.3	1.15	109.8	29.6	0	0	0	0	<i>Acamana ambiguus</i>	<i>Peripantostylus minutus</i>
Notostylopidae	11	15.9	1.67	43.6	12.2	0	0	0	0	<i>Edvardotroues sartia sola</i>	<i>Homalostylops atavus</i>
Other basal notoungulates	2	2.3	2.33	2.3	-	0	0	0	0	-	-
Toxodontia	111	216.8	2.65	1464.1	281.9	1.45	0	3	1.26	<i>Piauhitherium capivarae</i>	<i>Pampahippus secundus</i>
Homalodtheriidae	5	300.7	135.43	476	137.7	0.80	0	2	1.10	<i>Chasicotherium rothi</i>	<i>Trigonolophodon elegans</i>
Isotemnidae	19	82.1	6.72	468.7	109.5	0	0	0	0	<i>Periphragmis circumflexus</i>	<i>Isotemnus ctalego</i>
Leontiniidae	18	216.9	52.55	565.4	150.3	0.67	0	1	0.49	<i>Leontinia gaudryi</i>	<i>Termastherium flacoensis</i>
Notohippidae	29	34.1	2.65	80	25.3	1.14	0	2	0.95	<i>Rhynchippus equinus</i>	<i>Pampahippus secundus</i>
Toxodontidae	40	402.9	15.1	1464.1	369.2	2.80	0	3	0.56	<i>Piauhitherium capivarae</i>	<i>Hypsitherium bolivianum</i>
Typotheria	123	15	0.36	155.2	27.9	1.69	0	3	1.06	<i>Typotheriopsis internum</i>	<i>Punapithecus minor</i>
Archaeohyracidae	14	10.4	1.7	23.8	6.8	1.93	0	3	0.62	<i>Archaeotypotherium propheticus</i>	<i>Protarchaeohyrax minor</i>
Archaeopithecidae	2	1.7	1.35	2.1	0.5	0	0	0	0	<i>Archaeopithecus rogeri</i>	<i>Teratopithecus elpidophoros</i>
Hegetotheriidae	25	5.5	0.92	27.9	5.6	2.64	2	3	0.49	<i>Hemihegetotherium achataleptum</i>	<i>Tremacyllus impressus</i>
Interatheriidae	41	4.1	0.36	11.5	3.3	1.78	0	3	0.97	<i>Protypotherium australe</i>	<i>Punapithecus minor</i>
Mesotheriidae	21	60.1	12.96	155.2	45.2	2.00	2	2	0	<i>Typotheriopsis internum</i>	<i>Rusconitherium mendocense</i>
Oldfieldthomasiidae	13	5.1	1.06	8.3	2.5	0.00	0	0	0	<i>Oldfieldthomasi anfractuosa</i>	<i>Itaboraiterium atavum</i>
Basal Typotheria	7	7.9	1.67	27.4	9.7	0	0	0	0	<i>Acoelohyrax complicatissimus</i>	<i>Campanorco inauguralis</i>
All notoungulates	260	101.4	0.36	1464.1	210.6	1.42	0	3	1.20	<i>Piauhitherium capivarae</i>	<i>Punapithecus minor</i>

Table 5.2. Summary of the best mode of trait (BM and hypsodonty) evolution in notoungulates and lower taxonomic hierarchies. The complete results of the model comparisons are in the Supplementary File. Together with the best model of evolution in each analyzed trait, we provide the age(s) of the change(s) in the complex models' evolutionary regimen. Abbreviations: BM, body mass; Hyp, hypsodonty; Punc-i, punctuational mode of evolution with i changes; GRW, directional evolution; URW, random walk, μ_i , mean of the i period; σ^2_{step} , variance of slope (for GRW models); μ_{step} , slope (for GRW models). In cases in which any of the simple evolutionary modes (e.g., GRW) were not the best model based on the AICc, but pass the adequacy test, they were also reported and denoted in parenthesis.

Clade	Time bins	The best model of trait evolution (<i>PaleoTs</i>)			
		BM _{Best model}	BM _{Parameters best model}	Hyp _{Best model}	Hyp _{Parameters best model}
Notoungulata	51	Punc-4: 40, 30, 19, 11 Ma (GRW)	$\mu_1 = 1.95, \mu_2 = 2.38, \mu_3 = 3.36, \mu_4 = 2.84, \mu_5 = 3.92$ ($\mu_{step} = 0.054; \sigma^2_{step} = 0.020$)	Punc-5: 37, 31, 25, 16, 9 Ma (GRW)	$\mu_1 = 0.05, \mu_2 = 0.18, \mu_3 = 1.37, \mu_4 = 1.65, \mu_5 = 2.32, \mu_6 = 2.76$ ($\mu_{step} = 0.055; \sigma^2_{step} = 0.008$)
Typtotheria	54	GRW	$\mu_{step} = 0.020; \sigma^2_{step} = 0$	Punc-4: 37, 31, 25, 16 Ma (GRW)	$\mu_1 = 0.13, \mu_2 = 0.36, \mu_3 = 1.92, \mu_4 = 2.18, \mu_5 = 2.47$ ($\mu_{step} = 0.05; \sigma^2_{step} = 0.01$)
Archaeohyracidae	23	Punc-1: 30 Ma	$\mu_1 = 2.03, \mu_2 = 2.89$	GRW	$\mu_{step} = 0.05, \sigma^2_{step} = 0$
Hegetotheriidae	27	Punc-1: 6 Ma	$\mu_1 = 1.42, \mu_2 = 0.60$	Punc-1: 19 Ma	$\mu_1 = 2.13, \mu_2 = 3$
Interatheriidae	37	GRW	$\mu_{step} = 0.037; \sigma^2_{step} = 0$	URW-Stasis: 30 Ma (GRW)	$\sigma^2_{step} = 0.11, \mu = 2.29$ ($\mu_{step} = 0.06, \sigma^2_{step} = 0.04$)
Mesotheriidae	27	Punc-2: 20, 13 Ma	$\mu_1 = 4.27, \mu_2 = 2.99, \mu_3 = 4.26$	-	-
Toxodontia	49	Punc-4: 40, 30, 14, 8 Ma (GRW)	$\mu_1 = 2.99, \mu_2 = 3.51, \mu_3 = 4.62, \mu_4 = 5.79, \mu_5 = 5.04$ ($\mu_{step} = 0.062; \sigma^2_{step} = 0.016$)	Punc-3: 30, 20, 10 Ma (GRW)	$\mu_1 = 0.06, \mu_2 = 1.22, \mu_3 = 2.31, \mu_4 = 2.98$ ($\mu_{step} = 0.07; \sigma^2_{step} = 0.01$)
Notohippidae	31	Punc-1: 31 Ma	$\mu_1 = 2.41, \mu_2 = 3.76$	Punc-1: 30 Ma	$\mu_1 = 0.16, \mu_2 = 1.85$
Toxodontidae	29	GRW-Stasis: 10 Ma	$\mu_{step} = 0.12, \sigma^2_{step} = 0; \mu_1 = 5.45$	Punc-2: 20, 13 Ma (GRW)	$\mu_1 = 1.18, \mu_2 = 2.47, \mu_3 = 3$ ($\mu_{step} = 0.08, \sigma^2_{step} = 0.01$)

Table 5.3. Summary of best-fitting GLS multiple regression models for predicting mean body mass (BM in natural log scale) and hypsodonty in notoungulates, typtotherians, and toxodonts considering an autocorrelation structure for age parameter. R^2 is a measure of the variance explained by each model (Ives, 2019). Note that the GLS models were fitted with data from 49–10 Ma.

Clade	Response	Parameters	Slope	p-value	R^2
Notoungulates	Body mass	Open habitats	0.25	<0.01	0.73
	Hypsodonty	-	-	-	-
Typtotheria	Body mass	Self-clade Hypsodonty	0.25	<0.01	0.78
	Hypsodonty	Self-clade body mass	0.63	<0.01	0.96
Toxodontia	Body mass	Global temperature	0.39	<0.01	0.92
		Self-clade Hypsodonty	0.81	<0.01	
	Hypsodonty	Self-clade body mass	0.38	<0.01	0.96

Table 5.4. Results of the OLS analyses dealing with the spatial patterns of the body mass (BM in kg) and hypsodonty in the SSA notoungulates.

Response	Parameters	Slope	SE	p-value
BM	Paleolongitude	-1.31	2.21	>0.05
	Paleolatitude	2.25	1.17	>0.05
	Paleolatitude 2	3.08	1.08	<0.01
HI	Paleolongitude	-0.09	0.01	<0.01
	Paleolatitude	0.02	0.01	<0.01
	Paleolatitude 2	0.04	0.01	<0.01

Table 5.5. Comparisons among the body mass reported in the literature from a selected sample of notoungulates and those estimated by us in the present contribution. Data from: ^IElissamburu (2012), ^{II}Cassini et al. (2012), ^{III}Reguero et al. (2010), ^{IV}Gomes Rodrigues et al. (2017), and others (*Fernández-Monescillo et al., 2019 and **Scarano et al., 2011).

Taxa	BM (kg)					
	I	II	III	IV	Others	Present work
<i>Asmodeus osborni</i>	-		-	400.70	-	406.21
<i>Asmodeus</i>	1785.70	-	-	-	-	325
<i>Adinotherium ovinum</i>	-	100.30	-	61.40	33.75 – 119.45*	31.4
<i>Adinotherium</i>	119.45	113.27	-	-	-	31.4
<i>Rhynchippus equinus</i>	99.67	-	-	-	77.87 – 99.67*	80.02
<i>Rhynchippus pumilus</i>	21.83	-	-	-	-	9
<i>Morphippus imbricatus</i>	97.80	-	-	31	-	57.2
<i>Nesodon imbricatus</i>	587.90	637.51	-	197	170.13 – 637.51*	289.42
<i>Interatherium robustum</i>	-	2.38	-	-	0.4 – 3.5*	1.42
<i>Interatherium</i>	3.33	-	-	-	-	1.64
<i>Protypotherium attenuatum</i>	-	3.80	-	-	2.59 – 3.1**	2.85
<i>Protypotherium australe</i>	-	7.30	2.82	-	2.81 – 7.73*; 3.79 – 7.39**	11.02
<i>Protypotherium praerutilum</i>	-	4.50	-	-	3.87 – 5.80**	7.58
<i>Protypotherium</i>	6.74	-	-	-	-	6.6
<i>Hegetotherium mirabile</i>	-	7.71	2.19	2.20	-	6.28
<i>Hegetotherium</i>	9.69	-	-	-	-	5.5
<i>Pachyrukhos moyani</i>	-	2.13	0.46	-	-	1.38
<i>Pachyrukhos</i>	1.77	-	-	-	-	1.36
<i>Trachytherus spegazzinianus</i>	-	-	40.75	29.50	136 – 408*	116.61
<i>Trachytherus alloxus</i>	-	-	-	21.70	18.56 – 120.45*	94.62
<i>Trachytherus</i>	408	-	-	-	-	
<i>Plesiotypotherium achirensense</i>	-	-	20.36	-	5.40 – 138*	35.91

CAPÍTULO VI. Síntesis y Discusión

La presente tesis doctoral se enfocó en el estudio de la fauna de mamíferos de la Formación Cura-Mallín, a partir de la colección de nuevos especímenes fósiles, así como la revisión de materiales depositados en museos. Esta fauna había sido poco comprendida previamente desde el punto de vista de su composición taxonómica, afinidades biogeográficas y paleoambientales, y distribución cronológica. Los nuevos avances obtenidos en estas temáticas se describen y discuten brevemente a continuación. Además, también se discutirá el rol de estos resultados dentro del contexto tectónico que caracterizó a la región del sur de la Cordillera Principal durante el Mioceno y cómo este contexto tectónico pudo influenciar la evolución de la biota del sur de Sudamérica (en adelante SSA y definida como la región ubicada al sur de los 15°S *sensu* Ortiz-Jaureguizar y Cladera, 2006).

6.1 Paleodiversidad de la Formación Cura-Mallín y su contexto temporal

Esta tesis doctoral se enfocó en el estudio de la paleodiversidad (y su contexto geocronológico) de los mamíferos de la Formación Cura-Mallín en dos áreas geográficas principales, Lonquimay y la Laguna del Laja. A continuación, se describen los principales resultados obtenidos en cada localidad.

6.1.1 Lonquimay

Paleodiversidad. La revisión de los materiales depositados en el Museo Nacional de Historia Natural de Santiago (MNHN, Chile) permitió reconocer, en la región de Lonquimay, al menos 7 especies de mamíferos distribuidas en dos asociaciones cronológicas distintivas: una del Mioceno temprano (probablemente Colhuehuapiense–Santacrucense), que incluye a *Nesodon imbricatus* y *Parastrapotherium* sp., y una de edad Mioceno medio a tardío (12,8–11,6 Ma; Mayoense), que incluye gliptodontes (Glyptodontidae indeterminado), armadillos (Eutatini indeterminado), macrauquénidos (*Theosodon* sp.), un probable mono platirrino, y una nueva especie de intheratérido (*Protyotherium concepcionensis* sp. nov.) (Tabla 6.1) (Solórzano et al., 2019). Durante la revisión

del material depositado en el MNHN no se encontró ningún espécimen asignable a Rodentia (Solórzano et al., 2019). Sin embargo, durante el último trabajo en terreno (febrero 2021) se colectó un incisivo aislado de caviomorfo en los estratos superiores del Cerro Rucañanco (en niveles estratigráficos similares a donde han sido previamente hallados huesos de aves y dientes de peces de agua dulce). Esto indica que nuevas prospecciones paleontológicas en el lugar, especialmente enfocadas en la búsqueda sistemática de micromamíferos podrían permitir recuperar taxones adicionales, incrementando la diversidad taxonómica de esta localidad (Cerro Rucañanco), y potencialmente en la Formación Cura Mallín.

Por primera vez se reportó *Theosodon* sp., Eutatini indeterminado y un primate platirrino para la Formación Cura-Mallín (Solórzano et al., 2019). Particularmente importante es el reporte del posible platirrino colectado en Cerro Rucañanco ya que, en general, los restos de platirrino son poco comunes en el registro fósil sudamericano y se conocen tan solo dos localidades con primates Miocenos en Chile: Las Leñas (Mioceno temprano) y Río Cisnes (Mioceno temprano a medio) (Flynn et al., 1995; Bobe et al., 2015). Con una edad de Mioceno medio a tardío (ca. 12 Ma), el molar colectado en el Cerro Rucañanco parece representar el registro más joven de primates platirrininos en Chile y en el sur de Sudamérica (Solórzano et al., 2019).

Aunque la presente tesis doctoral se enfocó particularmente en el estudio de los mamíferos fósiles de la Formación Cura-Mallín, también se tienen nuevos datos sobre otros grupos taxonómicos. En la región de Lonquimay se colectaron nuevos materiales de peces, aves e invertebrados de agua dulce. Respecto a los invertebrados de agua dulce, encontrados en el Cerro Rucañanco, éstos sugieren tentativamente la existencia de al menos cinco taxones algunos de ellos con claras afinidades con especies modernas de Chile (J.F. Araya, comunicación personal, 2020). Estos materiales aún están siendo objeto de estudio. Los nuevos restos de peces colectados fueron el objeto de estudio de una memoria de título (en Geología, Udec) (Munizaga, 2020). Finalmente, los fósiles de aves colectados parecen pertenecer a la especie *Macranhinga chilensis*, y a un segundo potencial taxon (de mayor talla) que aún está en estudio.

Tabla 6.1 Comparación entre la diversidad (y edad) de mamíferos fósiles de la Formación Cura-Mallín reconocidos durante el desarrollo de esta tesis doctoral (Solórzano et al., 2019, 2020a, 2021), y aquella mencionada en trabajos previos (Marshall et al., 1990; Suárez et al., 1990; Croft et al., 2003; Flynn et al., 2008; Buldrini y Bostelmann, 2011; Bostelmann et al., 2014; Buldrini et al., 2015).

Orden	Presente tesis doctoral	Trabajos previos
Laguna del Laja (Tcm₃)		
Rodentia	<i>Galileomys antelucanus</i> **; <i>Maruchito</i> sp. nov.? <i>Luantus sompallwei</i> *; <i>Phanomys mixtus</i> **; <i>Neoreomys</i> sp.; <i>Prolagostomus</i> sp.	<i>Maruchito</i> sp. nov.; <i>Protacaremys</i> sp. nov.; cf. <i>Protacaremys</i> sp. nov.; <i>Scleromys</i> sp. nov.; <i>Prostichomys</i> sp. nov. I; <i>Prostichomys</i> sp. nov. II; <i>Luantus</i> sp. nov.; ? <i>Luantus</i> sp. nov.; <i>Acarechimys</i> sp. nov.; <i>Prolagostomus</i> sp. nov. and unident; Gen. et sp. nov. (aff. <i>Incamys</i>); Gen. et sp. nov. (aff. <i>Alloiomys</i>); Gen. et sp. nov. (aff. <i>Prostichomys</i>); Gen. et sp. nov. (aff. <i>Protacaremys</i>); Gen. et sp. nov. (aff. <i>Prospaniomys</i>)
Notoungulados	<i>Nesodon</i> sp.***; <i>Adinotherium</i> sp.***; <i>Pachyrukhos</i> sp. nov.***; <i>Protypotherium</i> cf. <i>sinclairi</i> **; <i>Protypotherium</i> spp.	? <i>Hegetotherium</i> ; New taxon cf. <i>Protypotherium</i> sp.; <i>Paedotherium minor</i> ; Toxodontidae, unident; Interatheriinae, unident; Pachyrukhinae, unident.
Marsupiales	cf. <i>Sipalocyon</i> sp.; <i>Palaeothentes intermedius</i> ***	<i>Sipalocyon</i> ; Abderitidae, unident.
Xenartha	<i>Hapalops</i> sp.; <i>Prozaedyus</i> sp.; Peltephilidae gen. et sp. indet.	Dasypodidae indet.
Litopterna	<i>Diadiaphorus majusculus</i> **	-
Astrapotheria	-	Astrapotheriidae indet.
Lonquimay		
Caviomorfos	Caviomorpha gen. et sp. indeterminado***	-
Notoungulados	<i>Protypotherium concepcionensis</i> * ^{Mmt} ; <i>Nesodon imbricatus</i> ^{Mt}	<i>Protypotherium</i> cf. <i>australe</i> ^{Mt} ; <i>Nesodon conspurcatus</i> ^{Mt}
Cingulados	Glyptodontidae gen. et sp. indet. ^{Mmt} ; Eutatini gen. et sp. indet. ^{***, Mmt}	Glyptodontidae gen. et sp. indet. ^{Mt}
Primates	Primate gen. et sp. indeterminado***, Mmt	-
Litopterna	<i>Theosodon</i> sp. ^{***, Mmt}	Macraucheniidae gen. et sp. indet. ^{Mt}
Astrapotheria	<i>Parastrapotherium</i> sp. ^{Mt}	<i>Parastrapotherium</i> sp. ^{Mt}

*especie nueva, **primer registro en Chile, ***primera vez reportado en la localidad, ^{Mt}Mioceno temprano, ^{Mmt}Mioceno medio tardío.

Contexto temporal. Previamente se le había asignado una edad Mioceno temprano a la fauna colectada en afloramientos de la Formación Cura-Mallín en Lonquimay y sus alrededores (Suárez et al., 1990; Rubilar, 1994; Buldrini y Bostelmann, 2011; Soto-Acuña et al., 2013; Buldrini et al., 2015). Sin embargo, las edades radiométricas indican edades mucho más jóvenes para los niveles superiores de la Formación (ca. 12 Ma) (Pedroza et al., 2017; Rosselot et al.,

2019b; Solórzano et al., 2019). De tal forma nuestros resultados ayudan a refinar la distribución temporal de la fauna reportada en esta región.

La fauna de los niveles superiores de la Formación Cura-Mallín que afloran en la región de Lonquimay (12,8–11,6 Ma) pueden ser asignadas a la Edad Mamífero Mayoense y no a la Laventense, como habría sido sugerido previamente (Pedroza et al., 2017). Los fósiles asignados al Mayoense provienen típicamente de la Formación Río Mayo que aflora en varias localidades en el suroeste de Chubut y noroeste de las provincias de Santa Cruz, Argentina, aunque también se han recuperado fósiles Mayoenses en las formaciones subyacentes de El Portezuelo y El Pedregoso (Dal Molin et al., 1998; Scillato-Yané y Carlini, 1998; De Iuliis et al., 2008; González Ruiz et al., 2017; Folguera et al., 2018b; Vera et al., 2019). Inicialmente se le asignó a la fauna Mayoense, sin la ayuda de las edades radiométricas, una edad temprana Mioceno tardío (11.8–10.0Ma) (Flynn y Swisher, 1995). Sin embargo, datos radiométricos más recientes adquiridos en las formaciones El Pedregoso, El Portezuelo y Río Mayo (con faunas típicamente atribuidas al Mayoense) indican edades entre 13,5 y 11,8 Ma para estas unidades (De Iuliis et al., 2008; Folguera et al., 2018b; Vera et al., 2019). De esta forma, la Edad Mamífero Mayoense (definida en altas latitudes, ~46°S) está, al menos parcialmente, superpuesta temporalmente con la Edad Mamífero Laventense (definida en bajas latitudes, ~3°N) (Madden et al., 1997; González Ruiz et al., 2017; Solórzano et al., 2019). Las diferencias en composición taxonómica entre las faunas de Mayoense y Laventense probablemente estén más vinculadas a diferentes condiciones ambientales y ecológicas en ambas regiones de América del Sur que a estadios evolutivos distintivos (Solórzano et al., 2019). A pesar de que la fauna analizada aquí no presenta taxones típicos del Mayoense, la asociación superior de mamíferos de la Formación Cura-Mallín que aflora en Lonquimay puede ser correlacionable con dicha SALMA sobre la base de correlaciones geocronológicas. Aunque no existen, hasta el momento, taxones compartidos entre ambas faunas la nueva especie descrita de *Protypotherium* presenta, a la espera de una detallada revisión de las especies incluidas en el género y sus relaciones filogenéticas, similitudes morfológicas con aquellas especies reconocidas en el Colloncureense y Mayoense.

La clarificación de la edad de las principales localidades fosilíferas de la región de Lonquimay (Solórzano et al., 2019), permitió reconocer que también existen dos diferentes asociaciones temporales de peces, una de edad Mioceno temprano y otra del Mioceno medio-tardío (Munizaga, 2020). Ambas asociaciones de peces parecen mostrar diferencias en su composición taxonómica que podrían deberse a sesgos de muestreo, sesgos tafonómicos, o a cambios ambientales a lo largo del Mioceno (Munizaga, 2020). El registro fósil de peces de la Formación Cura-Mallín tiene una gran importancia en nuestro entendimiento de la fauna de peces nativos moderna del sur de Sudamérica, ya que es la única formación en Chile donde se han reportado peces de ambientes continentales (Rubilar, 1994; Azpelicueta y Rubilar, 1997; Arratia, 2015). A pesar de los avances realizados hasta la fecha, se hacen necesarios nuevos estudios en este grupo taxonómico. De particular interés es clarificar la taxonomía y sistemática de los molariformes previamente asignados a la subfamilia Serrasalminae, y que podrían pertenecer, entre otros, a los géneros *Colossoma*, o *Mylossoma*, taxones con representantes modernos, de hábitos frugívoros, que habitan en las regiones Neotropicales del norte de Sudamérica (Rubilar, 1994; Rincón et al., 2014; Munizaga, 2020). De confirmarse las afinidades taxonómicas de tales materiales podría sugerirse la existencia de conexiones hidrográficas entre la Cuenca de Cura-Mallín con cuencas argentinas ubicadas más al norte como la Cuenca de Paraná.

Por otra parte, es importante indicar que el ave continental *Macranhinga chilensis*, fue descrita a partir de especímenes colectados en estratos del Cerro Rucañanco que tienen una edad Mioceno medio a tardío (~12 Ma) (Pedroza et al., 2017; Solórzano et al., 2019), y no de edad Mioceno temprano como había sido sugerido previamente (Alvarenga, 1995; Soto-Acuña et al., 2013; Diederle, 2015). En este sentido, nuestros resultados ayudan a refinar el biocrón de este taxon, que aún parece ser el representante más antiguo de la familia Anhingidae en Sudamérica (Diederle, 2015).

6.1.2 Laguna del Laja

Paleodiversidad. Trabajos previos indicaron la presencia de una fauna relativamente diversa de mamíferos en la región de la Laguna del Laja, en afloramientos de las formaciones Cura-Mallín y Trapa-Trapa (Wertheim, 2007;

Flynn et al., 2008; Shockey et al., 2012; Luna, 2015). En esta región, Flynn et al. (2008) reportó la existencia de varias asociaciones de mamíferos, con edades comprendidas entre 20 y 9 Ma, dominadas en términos de diversidad por roedores y notoungulados, incluyendo más de 25 potenciales especies nuevas (Wertheim, 2007; Luna, 2015). Sin embargo, la gran mayoría de estos taxones no han sido descritos formalmente, limitando nuestro entendimiento de la paleodiversidad de la región.

La colección y estudio detallado de decenas de especímenes fósiles al sur de Laguna del Laja durante los años 2017–2021, contribuyó a subsanar esta interrogante (Solórzano et al., 2020a, 2021). Como resultado de este muestreo fue posible reconocer, en estratos pertenecientes a la Formación Cura-Mallín, la presencia de al menos 17 taxones (Tabla 6.1). La mayoría de éstos taxones fueron reportados por primera vez para esta localidad, incrementando y refinando la composición taxonómica de esta fauna (Solórzano et al., 2020a, 2021). La proporción entre el número de taxones reconocidos (durante el desarrollo de la presente tesis doctoral) por cada orden en la Laguna del Laja se ilustra en la Figura 6.1. De tal forma, los grupos con mayor número de taxones reconocidos en estos niveles corresponden a los roedores caviomorfos, notoungulados, y xenartros (Solórzano et al., 2020a, 2021).

Una comparación entre la fauna aquí descrita y aquella mencionada en trabajos previos (Flynn et al., 2008) para la unidad Tcm₃ se muestra en la Tabla 6.1. Comparativamente, hemos reportado una menor diversidad de caviomorfos, pero hemos reconocido por primera vez en la región perezosos (*Hapalops*), paleotentidos, proterotéridos, acarémidos, nesodontinos, *Prozaedyus*, y peltefílidos. Los resultados confirman, al menos parcialmente, que algunos de los caviomorfos presentes en la Laguna del Laja pueden representar especies nuevas (e.g., *Luantus* y *Maruchito*) (Solórzano et al., 2020a, 2021). De esta forma, se ha incrementado nuestro entendimiento de la paleodiversidad de esta localidad. Además, se describió formalmente una nueva especie de caviomorfo (*Luantus sompallwei*), aunque al menos dos taxones adicionales podrían también ser nuevos para la ciencia (e.g., *Maruchito nov. sp.?*, *Pachyrukhos nov. sp.?*) (Solórzano et al., 2020a, 2021). Sin embargo, se hacen necesarios especímenes mejor preservados para describirlos formalmente.

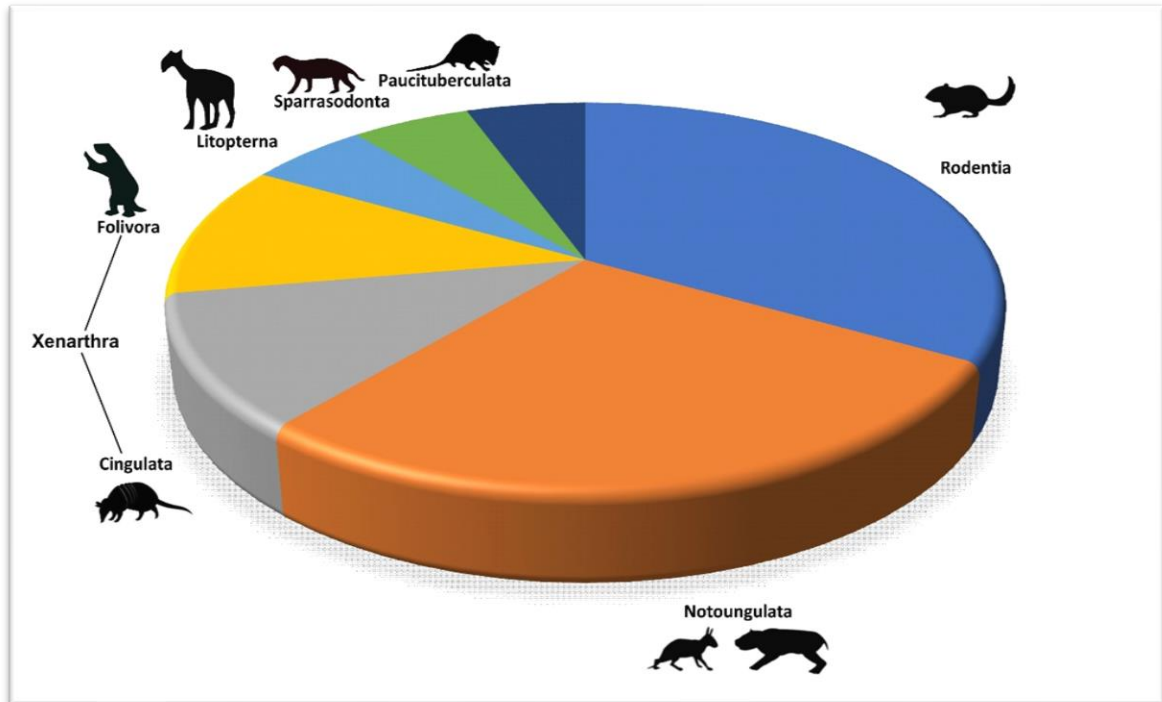


Figura 6.1. Proporción del número de taxones de mamíferos (por orden) del Mioceno temprano tardío reconocidos durante el desarrollo de esta tesis doctoral en la Formación Cura-Mallín en la Laguna del Laja, Chile (Solórzano et al., 2020a, 2021).

Una particularidad sugerida previamente para la fauna de mamíferos de la Laguna del Laja es la existencia de un marcado endemismo local (Wertheim, 2007; Flynn et al., 2008; Luna, 2015). Aunque la causa de este posible endemismo no ha sido determinada, se ha sugerido que puede deberse al aislamiento geográfico progresivo producto del inicio del levantamiento de los Andes a partir de los ~18 Ma (Wertheim, 2007), a un aislamiento geográfico parcial y heterogeneidad topográfica (Luna, 2015), a diferencias temporales entre las asociaciones de mamíferos de la Laguna del Laja y las Edades Mamíferos Continentales Sudamericanas (SALMAs) actualmente reconocidas (Croft et al., 2008), o incluso a una combinación de estos factores (Flynn et al., 2008). En cualquier caso, la fauna de Laguna del Laja parece no haber estado completamente aislada geográficamente, ya que algunos de los taxones encontrados a lo largo de la secuencia estratigráfica muestran claras afinidades con faunas contemporáneas de la Patagonia Argentina (Wertheim, 2007; Flynn et al., 2008; Luna, 2015).

Aquí se sugiere mantener en duda este “endemismo” (Solórzano et al., 2020a, 2021). La mayoría de las potenciales 26 especies nuevas de roedores y notoungulados mencionadas previamente para la fauna de Laguna del Laja

(Wertheim, 2007; Flynn et al., 2008; Luna, 2015) no han sido descritas formalmente. Además, solamente los caviomorfos parecen mostrar un mayor nivel de endemismo, especialmente hacia los estratos superiores de la Formación Cura-Mallín en este sector (Wertheim, 2007; Luna, 2015). Sin embargo, el material sobre el cual se proponen muchos de estos potenciales nuevos taxones (caviomorfos) es extremadamente fragmentario y escaso (ver materiales revisados por Wertheim, 2007 para más detalles), haciendo virtualmente imposible poder describir formalmente nuevos taxones a partir de este registro. Finalmente, aunque se ha sugerido que la aparente “endemidad” de taxones encontrada en la Laguna del Laja podría estar asociada a diferencias temporales respecto a las Edades de Mamíferos Continentales Sudamericanas (SALMAs) actualmente reconocidas (Croft et al., 2008), la calibración geocronológica y la bioestratigráfica (ver detalles más adelante) indica una clara superposición de la fauna estudiada con aquella mencionada en el Santacruceño (Solórzano et al., 2020a, 2021).

Asimismo, durante nuestras prospecciones paleontológicas al sur de la Laguna del Laja se colectaron fragmentos de elementos postcraneales de aves en niveles del Mioceno temprano (Tcm₃) del Cerro Campamento, y se observaron algunos restos mal conservados de peces teleósteos en bloques transportados (i.e., no *in situ*, edad incierta) en la estratificación este del Cerro Campamento (Solórzano et al., 2021). Siendo éstos los únicos restos de peces encontrados en esta zona. Desafortunadamente, la preservación fragmentaria de estos fósiles limita cualquier intento de identificación. También reportamos el hallazgo de restos de plantas similares a *Equisetum* en los estratos inferiores de la sucesión estratigráfica (Tcm₄; Mioceno medio, ca. 14.5 Ma) aflorando en Cerro Los Pinos, fragmentos de gran tamaño (hasta dos metros de largo) de madera fosilizada (Figura 6.2) en estratos de la unidad Tcm₃ ubicados en Cerro Campamento (pero no en asociación con mamíferos), y restos carbonizados de hojas en los estratos superiores de la unidad Tcm₄ en la zona este del Estero Trapa-Trapa (Solórzano et al., 2021). Todos estos nuevos datos permiten refinar la composición de la biota del Mioceno en la región.

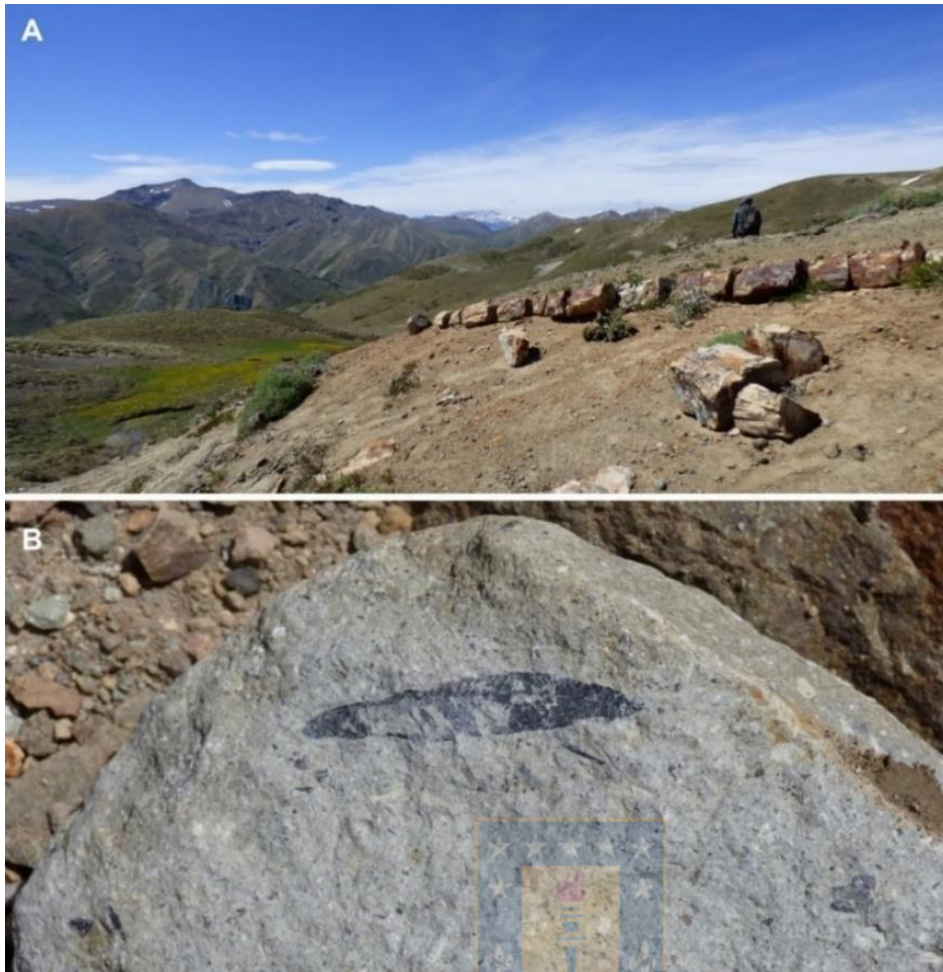


Figura 6.2.
 A, Restos de madera fosilizada encontrados en el tope del Cerro Campamento (Formación Cura-Mallín; Mioceno temprano tardío), al sur de la Laguna del Laja. B. restos de hojas carbonizadas encontradas en niveles Tcm₄, Estero Trapa-Trapa Este, Sur de la Laguna del Laja.

Contexto temporal. Todos los mamíferos fósiles recuperados al sur de la Laguna del Laja y aquí descritos, provienen de la sección media a superior de la unidad informal Tcm₃ la cual presenta edades ⁴⁰A/³⁹Ar restringidas entre 17.70 y 16.40 Ma (Flynn et al., 2008; Solórzano et al., 2020a, 2021). La edad de la asociación encontrada en Tcm₃ descrita en capítulos anteriores es consistente con la Edad Mamífero Santacrucense (Cuitiño et al., 2016). Además, el reconocimiento de especies exclusivas de Santacrucense (e.g., *Phanomys mixtus*, *Diadiaphorus majusculus*), así como géneros típicos (pero no exclusivos) de esta misma SALMA (e.g., *Nesodon*, *Sipalocyon*, *Hapalops*, *Pachyrukhos*, *Adinotherium*, *Neoreomys*, *Prozaedyus*) también son consistentes con esta noción (Arnal et al., 2019b; Fernicola et al., 2019; Schmidt et al., 2019; Solórzano et al., 2020a, 2021).

Sin embargo, es notable la presencia de algunos taxones que se han conocido previamente solamente en SALMAs más antiguas (Colhuehuapense) y más jóvenes (Colloncureense) (Solórzano et al., 2020a, 2021). Esto podría

reforzar interpretaciones previas en las que los esquemas SALMA actuales, propuestos sobre la base de localidades clásicas en el sureste de Argentina, podrían tener un uso limitado en escalas regionales (Croft, 2007). En cualquier caso, son necesarios más esfuerzos de muestreo con un control estratigráfico y geocronológico preciso y mejoras continuas en nuestro entendimiento de la composición taxonómica de las distintas asociaciones temporales de mamíferos (tales como los realizados en el marco de esta tesis) para abordar los potenciales problemas detectados en el marco de las SALMA, especialmente en los del Mioceno tardío temprano al medio (Marshall, 1990; Flynn and Swisher, 1995; Croft, 2007; Bostelmann et al., 2012; González Ruiz et al., 2017).

6.2 Afinidades biogeográficas de los mamíferos Neógenos de la Formación Cura-Mallín

En la Tabla 6.1 se ilustra la diversidad de mamíferos de la Formación Cura-Mallín, considerando las dos localidades estudiadas (Solórzano et al., 2019, 2020a, 2021). A partir de esta información, es posible indicar que: 1) la localidad de Laguna del Laja es la que exhibe la mayor riqueza de especies dentro de la Formación, 2) existen pocos taxones compartidos entre las faunas contemporáneas encontradas en Lonquimay y la Laguna del Laja. De hecho, *Nesodon*, un taxon común durante el Santacrucense (Hernández Del Pino, 2018), parece ser el único compartido entre faunas contemporáneas (Mioceno temprano) de la Formación Cura-Mallín analizadas, aunque es claro que la diversidad reconocida en la región de Lonquimay es escasa (Solórzano et al., 2019, 2021). El género *Protypotherium* también es reportado en ambas localidades, sin embargo, los fósiles encontrados provienen de estratos de edades disímiles (Mioceno temprano tardío en la Laguna del Laja y Mioceno medio tardío en Lonquimay), y la identidad taxonómica a nivel de especie también parece diferir. El reducido número de taxones (tan solo dos especies) encontrados en el Mioceno temprano de Lonquimay, y la ausencia de taxones del Mioceno medio tardío en la Laguna del Laja (Solórzano et al., 2019, 2020a, 2021), limita cualquier intento de realizar mayores comparaciones entre las faunas locales de mamíferos de la Formación Cura-Mallín. Sin embargo, contrario a interpretaciones previas, es posible que no exista una diferencia

significativa en cuanto a los tamaños corporales de los mamíferos identificados en cada localidad (Croft et al., 2003; Wertheim, 2007; Luna, 2015). Es probable que la ausencia de taxones pequeños en Lonquimay este más asociada a sesgos de preservación y/o muestreo de micromamíferos que a variaciones ambientales manifiestas entre ambos sectores (separados por solo ~120 km) durante el Mioceno.

Aunque algunos de los especímenes revisados durante el desarrollo de esta tesis doctoral no pudieron ser identificados hasta el nivel de especie, debido a su estado fragmentario de preservación, fue posible investigar, al menos de forma preliminar, las relaciones biogeográficas de la fauna de la Formación Cura-Mallín con respecto a localidades fosilíferas contemporáneas de Sudamérica (Solórzano et al., 2019, 2020a, 2021).

La fauna del Santacrucense de la Laguna del Laja comparte muchos taxones con localidades penecontemporáneas chilenas ubicadas más al sur como Rio Cisnes (44,5°S; "Friasiense") y Pampa Castillo (47°S; Santacrucense), pero exhibiendo una menor diversidad taxonómica (Flynn et al., 2002b; Bostelmann et al., 2012; Charrier et al., 2015; Solórzano et al., 2021). En contraste, esta fauna difiere de aquella de Chucal (~19°S), entre otras, por a la ausencia de mesotheridos y la presencia de perezosos (Flynn et al., 2002a; Charrier et al., 2015; Solórzano et al., 2021). Además, la fauna Santacrucense de la Laguna del Laja es, en general, similar en composición taxonómica a la encontrada en localidades contemporáneas en Argentina (Figura 6.3) (Arnal et al., 2019b; Bargo et al., 2019; Chornogubsky et al., 2019; Fernicola et al., 2019; Schmidt et al., 2019; Solórzano et al., 2020a, 2021). Mientras existen múltiples localidades con faunas del Santacrucense en el sur de Sudamérica (incluyendo la Laguna del Laja), éstas muestran variaciones taxonómicas locales que pueden reflejar la existencia de variaciones geográficas y/o ambientales (Cuitiño et al., 2016, 2019; Fernicola et al., 2019), aunque es complicado discernir entre ambas. Aunque en cualquier caso, la fauna estudiada de la Formación Cura-Mallín documenta por primera vez la presencia de múltiples taxones previamente mencionados tan solo en localidades clásicas ubicadas en las altas latitudes de la Patagonia de Argentina y Chile (Solórzano et al., 2019, 2020a, 2021).

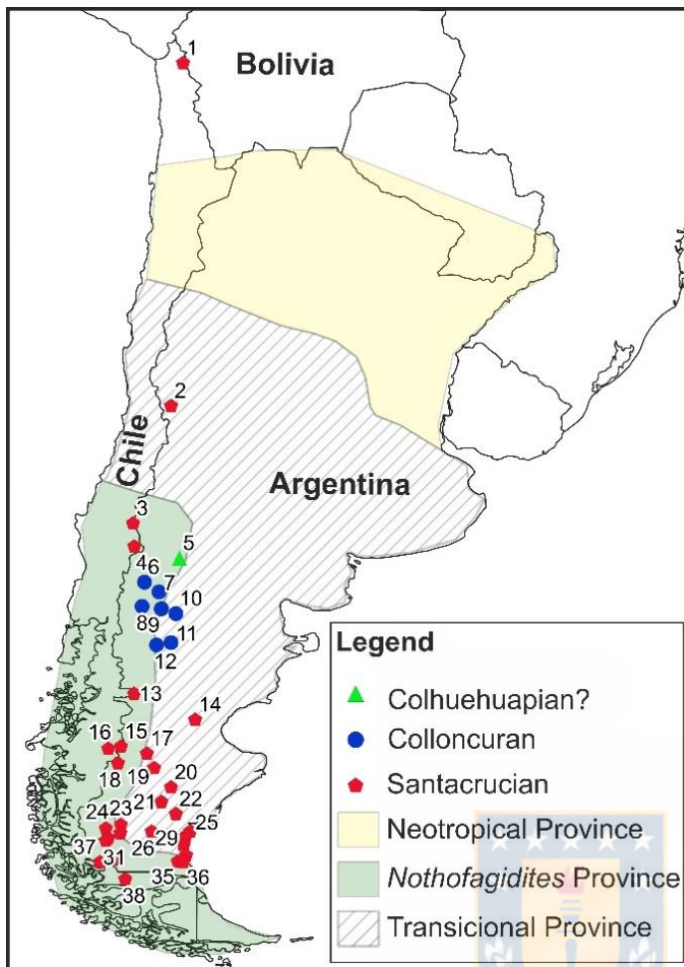


Figura 6.3. Mapa de ubicación de localidades Santacrucenses, así como otras localidades importantes del Mioceno temprano y medio, en el sur de Sudamérica (ordenadas por latitud): 1, Chucal, Chile; 2, Chinchas (Formación Chinchas), Argentina; **3, Laguna del Laja (Formación Cura-Mallín), Chile;** 4, Lonquimay (Formación Cura-Mallín), Chile; 5, Cerro Bandera (Formación Cerro Bandera), Argentina; 6, Estancia Collón Cura and Collón Cura River (Formación Collon Curá), Argentina; 7, Cañadón del Tordillo (Formación Collon Curá), Argentina; 8, Pichileufú River (Formación Collon Curá), Argentina; 9, Comallo (Formación Collon Curá), Argentina; 10, Ingeniero Jacobacci, Argentina; 11, Paso del Sapo (Formación Collon Curá), Argentina; 12, Cerro Zeballos (Formación Collon Curá), Argentina; 13, Alto Río Cisnes, Chile; 14, Gran Barranca of Colhue Huapi lake (Formación Sarmiento), Argentina; 15, Río Jeinemení, Argentina; 16, Pampa Guadal and Pampa Castillo, Meseta Cosmelli, Chile; 17, Valle del río Pinturas

(Formación Pinturas), Argentina; 18, Lago Pueyrredón and Lago Posadas, Argentina; 19, Estancia La Peninsular, Argentina; 20, Río Chico, Argentina; 21, Estancia La Bajada, Argentina; 22, Sehuén and Chalia River valleys, Argentina; 23, Karaiken, Argentina; 24, Lago Argentino, Argentina; 25, Monte León, Argentina; 26, Santa Cruz River valley, Argentina; 27, Río Bote - Estancia María Elisa, Argentina; 28, Cerro Centinela and Estancias Quién Sabe, La Josefina and Bon Accord, Argentina; 29, Cañadón de Las Vacas, Argentina; 30, Monte Observación, Argentina; 31, Sierra Baguales, Chile; 32, Cañadón Cerro Redondo, Argentina; 33, Monte Tigre-Cañadón Totoras, Estancia La Costa, Argentina; 34, Meseta Latorre, Argentina; 35, Felton's Estancia, Argentina; 36, Estancia Halliday, Argentina; 37, Estancia Consuelo, Ultima Esperanza, Chile; 38, Cañadón La Leona, Chile. Note, además, la distribución especial de las provincias paleobotánicas propuestas en el sur de Sudamérica durante el Mioceno temprano a medio (Barreda et al., 2007).

Desde una perspectiva regional, las faunas Santacrucenses de Chile (incluyendo la de la Laguna del Laja), ubicadas en el extremo oeste del sur de Sudamérica, representan (quizás con la excepción de las diversas faunas encontradas en la Patagonia Chilena) solo una submuestra de la elevada diversidad de mamíferos Santacrucenses encontrada en la Argentina (Arnal et al., 2019b; Bargo et al., 2019; Chornogubsky et al., 2019; Fernicola et al., 2019; Schmidt et al., 2019; Solórzano et al., 2020a, 2021). Las diferencias en la composición taxonómica entre la fauna de la Laguna del Laja, y aquellas

encontradas en altas latitudes de Sudamérica podrían estar además favorecida por las diferentes provincias paleobotánicas existentes durante el Mioceno temprano a medio en el SSA (Barreda et al., 2007). Por ejemplo, por su ubicación geográfica la región de Laguna del Laja debe pertenecer a la Provincia *Nothofagidites* (ubicada al suroeste de SSA), caracterizada por bosques húmedos y templados (Figura 6.3); mientras que la mayor parte de la fauna de la Formación Santa Cruz (y equivalentes Santacrucenses) se enmarcaron en la Provincia de Transición (ubicada en el centro y sureste argentino) caracterizada por alternancia de bosques abiertos de coníferas, bosques de galería, sabanas arboladas y arbustivas, estepas con hierbas halófitas y palmerales (Barreda et al., 2007). Los nuevos datos presentados en nuestro trabajo contribuyen a caracterizar la fauna extraordinariamente diversa del Santacrucense, apoyando la noción de que la misma estuvo ampliamente distribuida por todo el sur de Sudamérica (Flynn et al., 2002b, 2008; Charrier et al., 2015; Arnal et al., 2019b; Bargo et al., 2019; Solórzano et al., 2019, 2020a, 2021; Chornogubsky et al., 2019; Fernández y Muñoz, 2019; Fericola et al., 2019; Schmidt et al., 2019; Cuitiño et al., 2019).

Por otra parte, antes del desarrollo de la presente tesis doctoral, la distribución geográfica de *Theosodon* durante el Mioceno medio tardío se limitaba al norte de Sudamérica (entre 3°N y 22°S) (Cifelli y Guerrero, 1997; McGrath et al., 2018; Solórzano et al., 2019). En consecuencia, nuestros resultados soportan una importante extensión al sur (~38°S) en el rango de distribución geográfica de este taxón durante el Mioceno medio tardío (Solórzano et al., 2019). Por otra parte, la nueva especie de *Protypotherium* descrita en la región de Lonquimay, junto con aquellas previamente conocidas durante el Mioceno medio (Colloncurensis y Mayoense) de Argentina, *P. colloncurensis* (41°–46°S) y *P. endiadys* (~41°S), indica que los protypotherios estuvieron más ampliamente distribuidos a lo largo de las cuencas de intra-arco y de antepaís en los Andes centro-sur de lo que se pensaba anteriormente (Vera et al., 2017, 2019; Solórzano et al., 2019).

6.3 Paleoambientes durante la sedimentación de la Formación Cura-Mallín

Las evidencias sedimentológicas sugieren que los estratos de la Formación Cura-Mallín en la región de la Laguna del Laja fueron depositados en llanuras aluviales, o en ambientes principalmente fluviales con facies menores indicativas de fases lacustres de corta duración, todo esto en una región de volcanismo activo (Carpinelli, 2000; Herriott, 2006; Flynn et al., 2008). Un ambiente similar (i.e., predominancia de ambientes fluviolacustres) ha sido propuesto para esta Formación en la región de Lonquimay (Suárez y Emparan, 1995; Pedroza et al., 2017). Sin embargo, las observaciones realizadas durante las prospecciones paleontológicas realizadas en ambas regiones indican algunas diferencias. Por ejemplo, en Lonquimay parece existir una mejor expresión de ambientes lacustres, bien ilustrados por la presencia de abundantes restos de peces fósiles a lo largo de la sección estratigráfica (Pedroza et al., 2017; Munizaga, 2020). Por otra parte, la sección aflorante en la Laguna de Laja se caracteriza por presentar una importante cantidad de elementos volcánoclasticos (e.g., predominancia de areniscas y lutitas volcánoclasticas), mientras que en Lonquimay tales elementos solo tienen importancia local y restringida (Suárez y Emparan, 1997; Herriott, 2006). Finalmente, y en consonancia con lo sugerido recientemente (Herriott, 2006; Flynn et al., 2008), en la Laguna del Laja no fue posible discernir la existencia de los miembros Río Queuco (predominantemente volcánico) y Malla-Malla (predominantemente sedimentario), ya que la secuencia completa tiene una predominancia de rocas volcanosedimentarias (Niemeyer y Muñoz, 1983). Sin embargo, se reconoció la aparente separación entre miembros volcánicos y sedimentarios de la Formación Cura-Mallín reportada por autores previos en la zona de Lonquimay (Suárez y Emparan, 1997; Pedroza et al., 2017). Lo anteriormente expuesto sugiere que es posible que existieran ligeras variaciones latitudinales en cuanto a los ambientes de sedimentación, posiblemente debido a que las unidades se depositaron en múltiples subcuencas cuyas transiciones laterales son poco comprendidas (Radic, 2010; Rosselot et al., 2019a).

La integración de líneas de evidencia adicionales puede sin duda contribuir a mejorar nuestro entendimiento del ambiente donde se depositó la Formación Cura-Mallín, y el registro fósil ha sido durante mucho tiempo una fuente principal de información sobre los ecosistemas del pasado (Kay et al., 2012b; Croft et al., 2018; Benton y Harper, 2020). Esto se debe a que los mamíferos, por ejemplo, tienen algunos atributos como el tamaño corporal que tienen implicaciones en

una amplia variedad de características ecológicas (Peters, 1986). Aunque el tamaño corporal no puede ser, en general, directamente medido en organismos extintos, puede ser estimado utilizando relaciones alométricas obtenidas entre las dimensiones esqueléticas y/o dentales y la masa corporal de taxones modernos cercanamente relacionados (Mendoza et al., 2006; Lyons y Smith, 2010). Por otra parte, los dientes de los mamíferos poseen una variedad de formas debido tanto a su disposición en la mandíbula, como a la gran diversidad de interespecífica observada en especies modernas y extintas (Vizcaíno et al., 2016; Evans y Pineda-Munoz, 2018a; Green y Croft, 2018). La forma de éstos dientes provee indicios sobre las fuentes de alimentos típicas que consumen los mamíferos en una localidad fósil determinada (Vizcaíno et al., 2016), lo que a su vez proporciona información relevante sobre las condiciones ambientales generales y la estructura de la comunidad (Croft et al., 2018). Por ejemplo, una predominancia de mamíferos con dientes de corona alta (=hipsodontes) en una asociación dada, es usualmente asociado a la presencia de ambientes abiertos (Damuth y Janis, 2011; Semprebon et al., 2019). Además, la hipsodoncia puede ser considerada como un proxy de paleoprecipitación en escalas regionales amplias, y ha sido utilizada para inferir condiciones regionales de vegetación, y refinar modelos climáticos (Fortelius et al., 2002; Eronen et al., 2010).

Luego de analizar algunas características paleoecológicas inferidas para los mamíferos aquí descritos (Solórzano et al., 2019, 2020a, 2021), y complementarla con información adicional de otros taxones (e.g., polen y hojas), fue posible proponer novedosas interpretaciones sobre las condiciones paleoambientales y paleoclimáticas imperantes durante el Mioceno en algunas secciones de la Formación Cura-Mallín.

En Lonquimay, fue posible reconocer durante el Mioceno temprano la existencia de hábitats semiacuáticos y boscosos, mientras que durante el final del Mioceno medio se interpretó la presencia de vegetación boscosa y cuerpos de agua permanentes (Palma-Heldt, 1983; Palma-Heldt y Rondanelli, 1990; Rubilar, 1994; Solórzano et al., 2019; Munizaga, 2020). Aunque el hallazgo de *Protypotherium* en el Mioceno medio tardío podría indicar ambientes un poco más mixtos (Solórzano et al., 2019). Aunque la diversidad local de mamíferos es limitada, la información proporcionada por la biota de esta localidad (mamíferos, peces de agua dulce y flora) sugiere la existencia de ambientes

predominantemente boscosos, cuerpos de agua permanentes, y climas húmedos y templados (22–11°C) que fueron relativamente homogéneos durante la sedimentación (Mioceno temprano a medio tardío) de la Formación Cura-Mallín en la región de Lonquimay (Solórzano et al., 2019). Se hace notar que la recuperación de especímenes adicionales puede ser necesaria para soportar o no la interpretación ambiental aquí planteada, especialmente porque la misma difiere, al menos parcialmente, de aquellas dadas para localidades penecontemporáneas del sur de Sudamérica ubicadas más al este (Kay et al., 2012b, 2021; Trayler et al., 2020).

Los mamíferos recuperados en los niveles del Mioceno temprano tardío de la Laguna de Laja sugieren la existencia de ambientes mixtos de bosques y posibles sabanas (Solórzano et al., 2021). Asociaciones relativamente similares de mamíferos contemporáneos (Santacrucense) encontrados hacia el este de la Patagonia Argentina sugieren que éstos habitaron en una zona con temperatura media anual de 20°–25°C y una precipitación media anual de ~1500 mm (Kay et al., 2012b, 2021). Sin embargo, es plausible proponer temperaturas ligeramente más frías en la región de Laguna del Laja durante finales del Mioceno temprano. Esto debido a la presencia de un potencial mayor relieve topográfico asociado al inicio de la comprensión tectónica a partir de 18 Ma de esta región (Rosselot et al., 2019a), y además a las observaciones realizadas a partir de la biota de la zona de Lonquimay ubicada ~120 km al sur, que exhibe un rango de temperaturas más bajo (Palma-Heldt, 1983; Palma-Heldt y Rondanelli, 1990; Solórzano et al., 2019, 2021; Munizaga, 2020). Futuros estudios detallados del contenido paleobotánico presente en la región de Laguna del Laja podrían proporcionar mayor soporte a esta hipótesis. En cualquier caso, nuestros resultados son consistentes con la predominancia de ambientes mixtos en el sur de Sudamérica durante el Santacrucense (Kay et al., 2012b; Palazzesi y Barreda, 2012; Palazzesi et al., 2014; Cuitiño et al., 2019).

La interpretaciones generales aquí propuestas sobre la vegetación y clima reinante durante el Mioceno entre los 36° y 38°S podrían ser puestas a prueba utilizando métodos paleoecológicos adicionales tales como los análisis de cenogramas y estructura de tamaño corporal los cuales han sido ampliamente utilizados en localidades fosilíferas europeas y asiáticas (Legendre, 1986; Hernández Fernández et al., 2006; Menéndez et al., 2017; Kapur et al., 2020),

pero hasta ahora poco aplicados al registro fósil sudamericano (Croft, 2001; Kay et al., 2021). Sin embargo, antes de intentar aplicar tales métodos en esta región de la Cordillera Principal es necesario describir y caracterizar de mejor forma los especímenes colectados por Flynn et al. (2008), ya que parecen representar múltiples taxones no encontrados durante nuestras prospecciones paleontológicas en la Formación Cura-Mallín.

6.4 Implicaciones tectónicas

El contexto tectónico en el que se depositaron las sucesiones continentales Miocenas en la Cuenca de Cura-Mallín es controversial. Varios autores sostienen que la sedimentación de la Formación Cura-Mallín se produjo en un contexto extensional, mientras que los primeros depósitos sinorogénicos ocurrieron a partir de los 12–9 Ma y corresponderían a las formaciones Mitrauquén y Trapa-Trapa, constituidas por facies conglomeráticas y volcánicas (Carpinelli, 2000; Jordan et al., 2001; Radic et al., 2002; Burns et al., 2006; Radic, 2010). Las evidencias de que la Formación Cura-Mallín fuera depositada en condiciones extensionales no son del todo claras, y se basan principalmente en la interpretación de un perfil sísmico por Jordan et al. (2001). Dicha interpretación fue cuestionada por Cobbold et al. (2008), quien señaló que dicho perfil posee una mala resolución y carece además de control lito- y cronoestratigráfico. Cobbold et al. (2008) también señala la presencia de estratos de crecimiento a lo largo del valle del Río Lileo (Argentina; ~37°S) que interpretan como producto de una tectónica compresiva. Radic et al. (2002) y Radic (2010) proponen la existencia de dos hemigrábenes diacrónicos y de polaridad opuesta donde se habría depositado la Formación Cura Mallín sobre la base de variaciones de espesor de dicha unidad. Sin embargo, esta interpretación es cuestionable debido a la falta de afloramientos continuos de la Formación Cura-Mallín donde se pueda medir el espesor real de esta formación (Solórzano et al., 2019).

Otros autores sugieren que solamente los estratos basales de la Formación Cura-Mallín (facies volcánicas) de esta unidad son sinextensionales, mientras que las capas sedimentarias superiores de esta formación y sus unidades suprayacentes (formaciones Mitrauquén y Trapa-Trapa) son sinorogénicas, y se depositaron en cuencas de antepaís o intermontanas relacionadas con el

alzamiento de los Andes a partir de los ~19–18 Ma (Spikings et al., 2008; Utge et al., 2009).

En la región de la Laguna del Laja, en niveles estratigráficos infrayacentes a aquellos donde fueron recuperados restos de mamíferos fósiles (Cerro Campamento; Tcm₃), se observaron estratos de crecimiento (*growth strata*; Figura 6.4) que sugieren una sedimentación simultánea con la deformación (i.e., sinorogénica) (Vergés et al., 2002). La edad de estos estratos es Mioceno temprano tardío, y ya que se adelgazan hacia el tope de la sección estratigráfica parecen estar sugiriendo una sedimentación asociada a un régimen compresivo. Estas observaciones son congruentes con una revisión reciente de la evidencia geocronológica, estructural, geoquímica y termocronológica disponible entre los 36° y 39° S, donde se sugiere que la inversión de la Cuenca de Cura-Mallín se inició hacia los ~18 Ma (Rosselot et al., 2019a).



Figura 6.4. Estratos de crecimiento observados en el Cerro Campamento (Tcm₃; Mioceno temprano tardío), infrayacentes a los niveles portadores de mamíferos fósiles.

Por otra parte, a nivel regional, se ha establecido que luego de una fase Eocena-Oligocena de extensión, la Cuenca de Abanico (32°–36°S) fue invertida

tectónicamente entre los 21 y 16 Ma (Charrier et al., 2002; Giambiagi et al., 2016). Eventos de extensión pre-Mioceno temprano seguidos por una inversión tectónica que inicia alrededor de los 19–17 Ma también han sido documentados en cuencas de los Andes patagónicos. Entre los 41° y 47°S, luego de un evento de extensión regional (Eoceno/Oligoceno), se inició una fase de compresión tectónica a partir de los ~19 Ma, que resultó en la inversión de las cuencas extensionales, el inicio del alzamiento de los Andes patagónicos y la sedimentación de los depósitos sinorogénicos de las formaciones Ñirihuau, Cerro Plataforma y Santa Cruz (Lagabriele et al., 2009; Orts et al., 2012; Bechis et al., 2014; Cuitiño et al., 2016, 2021; Encinas et al., 2018, 2019; Folguera et al., 2018a; Fernández Paz et al., 2018). Además, análisis geoquímicos en rocas volcánicas de la cuenca de retroarco de Neuquén (36°–38°S; Argentina) sugieren que éstas fueron generadas durante los 19–15 Ma en un régimen compresivo (Kay y Copeland, 2006). Por lo tanto, la hipótesis de un inicio de la inversión tectónica de la Cuenca de Cura-Mallín durante el Mioceno temprano tardío (~18 Ma) (Rosselot et al., 2019a, 2019b) es congruente con nuestras observaciones, así como con las interpretaciones disponibles en cuencas penecontemporáneas ubicadas al norte, sur y este del área de estudio.

Por otra parte, aunque las fases iniciales de condiciones tectónicas compresivas y del alzamiento de los Andes (durante el Mioceno) en la región de estudio (~38°S) pudieron ocurrir a partir de ~18 Ma (Rosselot et al., 2019a), nuestros resultados indican que el alzamiento de superficie en la región no fue tan significativo sino hasta el Mioceno tardío (Solórzano et al., 2019).

En la actualidad, la Cordillera de los Andes presenta una topografía más baja (hasta 3500 m) entre los 37° y 39°S comparado con secciones más al norte (Rojas Vera et al., 2016). No obstante, aún estas altitudes relativamente bajas constituyen una barrera topográfica para la circulación atmosférica e inducen el llamado “efecto de sombra de lluvia” (i.e., una fuerte disminución de la precipitación que a menudo se observa en el lado de sotavento de las cadenas montañosas) (Hijmans et al., 2005; Siler et al., 2012). Actualmente la Cordillera de los Andes alrededor de los 37° y 39°S, exhibe una porción occidental (barlovento) con altas tasas de precipitación (>1.500 mm/año), con predominio de ambientes boscosos, y una sección oriental (sotavento) con una disminución progresiva hacia el este en la tasa de precipitación (alcanzando ~1.000 mm/año)

acoplado con un predominio progresivo de ambientes más abiertos y áridos (e.g., pastizales y matorrales; Hijmans et al., 2005; Zhao et al., 2016). Hacia la latitud del área estudio (37°–39°S) el antepaís se ve fuertemente afectado por el efecto de sombra de lluvia, pero las cuencas intermontanas emplazadas en la porción oriental de la Cordillera principal de los Andes también exhiben, aunque de forma incipiente, los efectos de la sombra de lluvia (Hijmans et al., 2005; Zhao et al., 2016; Solórzano et al., 2019).

Durante el Mioceno se ha sugerido la existencia de un efecto de sombra de lluvia en la Patagonia Argentina, utilizando distintas líneas de evidencia. Por ejemplo, cambios significativos, ocurridos hacia los 16,5 Ma, en la composición isotópica del oxígeno ($\delta^{18}\text{O}$) y carbono ($\delta^{13}\text{C}$) de carbonatos pedogenéticos de la Formación Santa Cruz (Argentina) han sido propuestos como evidencia del establecimiento o reforzamiento del efecto de sombra de lluvia asociado al alzamiento de los Andes patagónicos (47°–50°S) (Blisniuk et al., 2005). Por otra parte, se han observado cambios ecomorfológicos entre las asociaciones de mamíferos patagónicas del Mioceno temprano y Mioceno tardío (e.g., reducción progresiva de taxas ramoneadores frugívoros, y el incremento de taxas pastadores) (Ortiz-Jaureguizar y Cladera, 2006). Éstos cambios ocurren simultáneamente con el recambio botánico patagónico (46°–50°S) de ecosistemas boscosos diversos presentes en el Mioceno temprano a ecosistemas menos diversos dominados por arbustos adaptados a climas áridos durante el Mioceno tardío (Palazzesi y Barreda, 2012; Barreda y Palazzesi, 2014; Palazzesi et al., 2014). Los cambios en la composición botánica y características ecomorfológicas exhibidos por la fauna patagónica durante el Mioceno son congruentes con el inicio del efecto sombra de lluvia durante el límite Mioceno temprano a Mioceno medio (16–14 Ma) en la región (46°–50°S), asociado a un importante alzamiento de esta porción de los Andes (Ortiz-Jaureguizar y Cladera, 2006).

Sin embargo, la posible existencia de cambios ambientales durante el Mioceno relacionados con el efecto de sombra de lluvia no está bien documentada a la latitud de 37°–38°S. Las condiciones paleoambientales relativamente homogéneas sugeridas por la biota fósil de la Formación Cura-Mallín del área de Lonquimay (38°S), indican que durante el Mioceno medio tardío persisten condiciones boscosas, templadas y húmedas en esta región

(Solórzano et al., 2019). Estas interpretaciones ambientales contrastan con el escenario actual de la zona de Lonquimay (i.e., predominio de pastizales y matorrales). Por lo tanto, incluso cuando el inicio de un régimen técnico compresivo puede establecerse en el Mioceno temprano (~18 Ma) (Rosselot et al., 2019a), nuestros datos sugieren que esta porción de los Andes no alcanzó suficientes paleoaltitudes (>1000 m) para causar una importante sombra de lluvia orográfica con el consiguiente aumento de la aridez en el antepaís oriental, al menos hasta el Mioceno tardío (posterior a los 12 Ma) (Solórzano et al., 2019). Este escenario es consistente con algunos trabajos previos realizados en latitudes similares donde es a partir del Mioceno tardío cuando se reconocen aumentos significativos en el acortamiento cortical (Rojas Vera et al., 2014, 2016) y en la exhumación (Spikings et al., 2008). Sin embargo, es importante mencionar que diferentes autores han argumentado que el alzamiento andino Neógeno (y el efecto de sombra de lluvia asociado) puede no ser la única fuerza determinante de la desertificación patagónica, ya que los cambios climáticos globales que afectaron al hemisferio sur durante el Mioceno medio podrían ser otro factor significativo (Palazzesi et al., 2014; Trayler et al., 2019, 2020).

Es notable que entre los 36° y 39°S existe una gradiente norte-sur tanto en las tasas de acortamiento cortical como de exhumación durante el Mioceno, con mayores valores hacia el norte y una disminución progresivamente hacia el sur (Spikings et al., 2008; Rojas Vera et al., 2016; Rosselot et al., 2019a). Por ejemplo, el acortamiento inferido (en el retroarco) hacia los 36°S es de 30 km, y hacia los 38°S es de apenas 11 km (Rojas Vera et al., 2016). De tal forma, aunque nuestras interpretaciones sugieren que la región de Lonquimay (38°S) no sufrió elevaciones significativas durante el Mioceno temprano y parte del Mioceno medio, éstas no pueden ser generalizadas hacia latitudes ubicadas mucho más al norte (Solórzano et al., 2019).

Durante el desarrollo de esta tesis se propuso, inicialmente, establecer el potencial rol del alzamiento andino sobre los cambios en las condiciones paleoambientales y de patrones de riqueza de especies de los mamíferos fósiles de la Cuenca de Cura-Mallín. La idea, tal como estaba propuesta originalmente, estuvo basada en el supuesto que se podría muestrear la sucesión de faunas de mamíferos de distintas edades (entre ~20 y 8 Ma) reportada en trabajos previos en la zona de la Laguna del Laja (Flynn et al., 2008). Desafortunadamente, solo

en dos localidades se reconocieron y colectaron restos de mamíferos fósiles (Cerro Campamento y Estero Trapa-Trapa Este; ver detalles en el capítulo 4), y ambas localidades tienen una edad similar (Mioceno temprano tardío). Esta situación ocasionó que no se pudiese explorar, a partir de la fauna de la Laguna del Laja, la existencia de posibles cambios ambientales locales a través del tiempo utilizando información paleontológica (e.g., Capítulo II), limitando las interpretaciones sobre el rol del alzamiento andino en la evolución de esta fauna local y/o refinar el momento y magnitud del alzamiento de esta porción de los Andes. Para tratar de superar esta limitación, en el Capítulo 5 se utilizó una aproximación macroecológica y macroevolutiva a nivel regional y se exploró como los factores ambientales (e.g., temperatura global, tectónica Andina, cambios en la composición botánica regional) pudieron afectar la evolución de dos rasgos ecomorfológicos de un grupo nativo y diverso de mamíferos sudamericanos (Solórzano and Núñez-Flores, 2021).

Durante los últimos años se ha dado un renovado interés en comprender los efectos de los cambios tectónicos sobre la evolución de la vida (Finarelli y Badgley, 2010; Antonelli et al., 2018). Esto se debe a que por ejemplo el alzamiento de una cordillera puede dar lugar a la separación de poblaciones biológicas, lo que en última instancia resulta en la generación de nuevas especies (Lowe y Tice, 2007; Hoorn et al., 2013; Craw et al., 2016; Silvestro y Schnitzler, 2018; Antonelli et al., 2018). Sin embargo, la identificación de vínculos claros entre la construcción tectónica de cadenas montañosas y la evolución biológica está en parte limitado por la coexistencia de factores ambientales y ecológicos adicionales (Badgley, 2010; Finarelli y Badgley, 2010; Craw et al., 2016; Silvestro y Schnitzler, 2018; Huang et al., 2019; Solórzano y Núñez-Flores, 2021).

Aquí nos concentramos en determinar cuáles factores (incluyendo la tectónica andina) influyen la variación (temporal y espacial) en los rasgos morfológicos (*traits*) de las especies, lo que constituye un reto importante de la paleoecología y la biología evolutiva (Fritz et al., 2013). En este sentido, el registro fósil provee una importante fuente de datos para afrontar este reto, especialmente en taxones completamente extintos (Hunt, 2006b; Hunt et al., 2010; Hunt y Rabosky, 2014; Huang et al., 2017; Benson et al., 2018; Voje, 2018).

En Sudamérica, la mayoría de los trabajos enfocados en los efectos de la tectónica andina sobre la evolución biológica están principalmente concentrados en taxones modernos, utilizando filogenias moleculares (e.g., Muñoz-Ortiz et al., 2015; Lagomarsino et al., 2016), mientras que estudios concentrados en analizar el registro fósil sudamericano son más escasos (Hoorn et al., 2010), y en algunos casos no tienen un marco estadístico robusto que permita discernir entre hipótesis alternativas (Ortiz-Jaureguizar y Cladera, 2006; Strömberg et al., 2013; Madden, 2014). Por ejemplo, se ha propuesto que los cambios ecomorfológicos (e.g., hipsodoncia), observados en los mamíferos herbívoros de altas latitudes durante el Mioceno es evidencia de cambios ambientales potencialmente asociados a la tectónica Andina en la Patagonia durante el Mioceno medio (Ortiz-Jaureguizar y Cladera, 2006). En principio esta idea tiene sentido, ya que la construcción de la Cordillera de los Andes tiene el potencial de generar cambio evolutivo en la biota de múltiples formas. La generación de cinturones montañosos crea heterogeneidad topográfica y nuevos hábitats donde las especies evolucionan, pero también puede incrementar la disponibilidad de partículas sedimentarias y volcánicas, heterogeneidad en los tipos de suelo, modificar patrones de drenaje de ríos, y alterar el clima regional (Ehlers y Poulsen, 2009; Hoorn et al., 2010; Silvestro y Schnitzler, 2018; Antonelli et al., 2018; Huang et al., 2019). Sin embargo, durante el Mioceno medio también ocurrieron cambios en las condiciones climáticas globales (i.e., *middle Miocene Climate Transition*) incluyendo una disminución de la temperatura en latitudes altas y bajas, la estabilización de las capas de hielo de la Antártida, y una caída importante del nivel del mar (Flower y Kennett, 1994; Holbourn et al., 2013; Trayler et al., 2020; Methner et al., 2020). Esto complica la tarea de discernir entre el rol del alzamiento andino y el clima global en la evolución de la biota neógena Sudamericana (Finarelli y Badgley, 2010).

El desarrollo de molares de corona alta (hipsodoncia) es relativamente común en mamíferos herbívoros tanto modernos como fósiles (Janis y Fortelius, 1988; Damuth y Janis, 2011; Kaiser et al., 2013). El desarrollo de este tipo de molares ocurre más temprano en Sudamérica (final del Paleoceno) que en otros continentes, y los notoungulados (Mammalia: Notoungulata), un orden de mamíferos nativos taxonómicamente diversos y con amplia disparidad ecomorfológica, son un claro ejemplo de esto (Patterson y Pascual, 1968;

Pascual y Odreman-Rivas, 1971; Reguero et al., 2010; Welker et al., 2015; Croft et al., 2020). Los notoungulados incluyen diferentes clados que desarrollaron de forma independiente la hipsodoncia, y existe un patrón general de incremento a través del tiempo de este rasgo (Reguero et al., 2010; Strömberg et al., 2013; Gomes Rodrigues et al., 2017). El incremento de la hipsodoncia en notoungulados, evidenciado en el registro fósil sudamericano, podría estar relacionado con el desarrollo de mejoras estructurales para prolongar la longevidad funcional de la dentición ocasionados por cambios del paisaje asociados con: 1) la expansión de los pastizales, 2) la historia climática de Sudamérica, y 3) la evolución tectónica de los Andes así como su compleja historia volcánica concomitante (Flynn et al., 2003; Ortiz-Jaureguizar y Cladera, 2006; Reguero et al., 2010; Strömberg et al., 2013; Madden, 2014; Dunn et al., 2015; Kohn et al., 2015; Scarano et al., 2021). Ahora bien, no está claro cuál de estos tres factores es el que tiene mayor relevancia.

La recopilación de una extensa base de datos de ocurrencias de notoungulados (que incluyen todas las especies descritas a la fecha, así como los nuevos datos generados a partir del análisis de la fauna de la Formación Cura-Mallín) y estimaciones de tamaño corporal e hipsodoncia permitió, entre otras cosas, investigar en qué medida diversos factores bióticos y abióticos (incluyendo los mencionados previamente) han influenciado estos rasgos ecomorfológicos a lo largo del tiempo, mediante la comparación de hipótesis alternativas (Solórzano y Núñez-Flores, 2021). Considerando que la mayor porción del registro fósil del grupo esta espacialmente ubicada en el sur de Sudamérica (SSA), nuestra investigación se enfocó en esta región.

Nuestros resultados indican que, contrario a las interpretaciones previas, ni los cambios en la temperatura global (Zachos et al., 2001, 2008; Scarano et al., 2021), ni la abundancia relativa de los pastizales en SSA (Strömberg et al., 2013; Dunn et al., 2015) pueden explicar de forma significativa la evolución de la hipsodoncia en los notoungulados (Solórzano y Núñez-Flores, 2021). Descartando así dos de los tres factores previamente propuestos para explicar los patrones temporales de la hipsodoncia en los notoungulados. Debido a que aún no existe un proxy general para la evolución temporal del alzamiento andino cenozoico en SSA, no fue posible descartarlo como un impulsor potencial de los patrones evolutivos investigados (ver detalles más adelante).

Por otra parte, el incremento en disponibilidad de partículas volcánicas en los ecosistemas cenozoicos de SSA pudo impulsar la evolución de coronas dentales altas en notoungulados (Strömberg et al., 2013; Madden, 2014; Kohn et al., 2015). De tal forma, podría esperarse una prevalencia de taxones más hipsodontes hacia las longitudes occidentales asociadas con el cinturón volcánico andino, ya que esta es la única porción del continente con un margen tectónico activo en SSA durante el Cenozoico (Solórzano y Núñez-Flores, 2021). Al explorar, por primera vez, los patrones espaciales de la hipsodoncia en los notoungulados, se reconoció un incremento significativo de este rasgo hacia el oeste de SSA, cercano a la cordillera Andina (Solórzano y Núñez-Flores, 2021). De tal forma, los procesos superficiales asociados a la evolución del orógeno Andino, y especialmente la generación de partículas volcánicas, parecen ser significativos en la evolución a largo plazo de la hipsodoncia en los notoungulados (Solórzano y Núñez-Flores, 2021), apoyando interpretaciones previas (Madden, 2014). A pesar de esto, la implementación de modelos más complejos (i.e., analizando la distribución espacial de la hipsodoncia separada en intervalos temporales cortos) podrían indicar que este impacto no se dio de forma continua a lo largo de los últimos 50 Ma, sino que fue intensa únicamente en ciertos intervalos temporales en concordancia general con los modelos puntuados de evolución mostrados por los rasgos evaluados.

En una versión preliminar del capítulo 5 se consideró utilizar la evolución temporal del acortamiento (en km) de los Andes centrales (Figura 17 de Armijo et al., 2015) como un proxy general de la “tectónica andina”. Utilizando este proxy y la metodología descrita detalladamente en la Sección 5.2.7, se encontró una correlación significativa entre la evolución temporal de la hipsodoncia de los notoungulados (considerando taxones de toda Sudamérica) y la “tectónica Andina”. Sin embargo, considerando que la mayor cantidad de datos disponibles sobre los notoungulados provienen del SSA, es posible que existan importantes limitaciones para la búsqueda de posibles correlaciones entre variables espacialmente no superpuestas. Además, el acortamiento no necesariamente es correlacionable con el alzamiento, ya que se puede producir mucho acortamiento con fallas casi horizontales, y poco acortamiento con fallas de alto ángulo que supongan un alzamiento importante. En cualquier caso, estos resultados preliminares se mencionan aquí porque son congruentes con la evidencia

espacial obtenida (Solórzano y Núñez-Flores, 2021), y refuerzan la existencia de un link entre la tectónica andina y la evolución de la fauna y flora sudamericana del Cenozoico (Ortiz-Jaureguizar y Cladera, 2006; Hoorn et al., 2010; Strömberg et al., 2013; Madden, 2014; Palazzesi et al., 2014; Kohn et al., 2015).

Nuestros resultados sugieren, por primera vez, que el tamaño corporal y la hipsodoncia en los notoungulados evolucionaron de forma acoplada (Solórzano y Núñez-Flores, 2021), cambiando, al menos parcialmente, el paradigma donde los procesos de cambio evolutivo están meramente determinados por factores abióticos (Strömberg et al., 2013; Dunn et al., 2015; Kohn et al., 2015; Lehtonen et al., 2017; Solórzano et al., 2020b). Es probable que los notoungulados hipsodontes pudieron alcanzar mayores tamaños que los braquiodontes debido a que los recursos que permite disponer a los herbívoros la hipsodoncia son más demandantes fisiológicamente (Raia et al., 2011).

En resumen, la revisión del registro fósil de un grupo diverso de mamíferos sudamericanos y el uso de marcos de trabajo estadísticos permitió caracterizar los patrones evolutivos de rasgos ecomorfológicos importantes a través del espacio y el tiempo, y determinar cómo los factores abióticos (e.g., tectónica Andina) y bióticos (e.g. tamaño corporal) los han afectado (Solórzano y Núñez-Flores, 2021). Se ilustra, además, como los notoungulados evolucionaron a partir de formas ancestrales relativamente pequeñas y con dientes de corona baja (braquiodontes), que fueron seguidos por uno o más cambios evolutivos positivos “puntuados” en la masa corporal y la hipsodoncia (Solórzano y Núñez-Flores, 2021). Nuestros resultados sugieren que los procesos superficiales asociados al desarrollo del orógeno andino en SSA durante el Cenozoico tienen un mayor soporte estadístico como los impulsores (abióticos) de la evolución de la hipsodoncia a largo plazo en los notoungulados, comparado con el desarrollo regional de las gramíneas, la mayor disponibilidad de ambientes abiertos en SSA, y las variaciones en la temperatura global (Solórzano y Núñez-Flores, 2021). Finalmente, fue posible inferir que los notoungulados de mayores tamaños corporales y molares de coronas más altas mostraron significativamente menores tasas de extinción (Solórzano y Núñez-Flores, 2021).

Por otra parte, nuestro reconocimiento de taxones como *Maruchito*, un taxon previamente solo reconocido en el Mioceno medio de la Formación Collón Cura en el oeste de Argentina (Vucetich et al., 1993), en el Mioceno temprano

tardío de la Laguna del Laja (Formación Cura-Mallín) es consistente con que esta región de los Andes (~37°S) pudo actuar como una “cuna” (regiones con altas tasas de especiación) para algunos linajes de mamíferos sudamericanos los cuales se dispersaron posteriormente a otras regiones (e.g., Formación Collón Cura) (Bucher et al., 2020; Solórzano et al., 2021). Al mismo tiempo, esta región pudo actuar como un “museo” (regiones con bajas tasas de extinción), ya que la fauna estudiada representa el registro más joven de algunos mamíferos (e.g., *Galileomys antelucanus*; *Protypotherium sinclairi*) que previamente solo eran conocidos de cuencas de retroarco en la Patagonia Argentina (Vucetich y Kramarz, 2003; Kramarz et al., 2015). Todo esto es también congruente con una importante influencia de los procesos superficiales asociados a la construcción del orógeno andino en la evolución de la biota sudamericana, tal como ha sido sugerido previamente (Ortiz-Jaureguizar y Cladera, 2006; Hoorn et al., 2010; Strömberg et al., 2013; Madden, 2014).

El desarrollo de proxies regionales ilustrando la evolución temporal del alzamiento, e incluso la intensidad de la actividad volcánica en los Andes (Trumbull et al., 2006) podrían ser vitales para poner a prueba hipótesis macroevolutivas similares a la planteada en esta tesis doctoral pero a una escala regional especialmente enfocada en el SSA, la región con el mejor registro fósil de Sudamérica (Solórzano y Núñez-Flores, 2021). En este sentido, es además vital que las hipótesis sobre el impacto del alzamiento andino en la evolución de las faunas del Mioceno en SSA (e.g., modificando dinámicas de diversificación) deban ser explícitamente testeadas en un contexto de comparación entre hipótesis alternativas y considerando la incertidumbre inherente al registro fósil (Silvestro et al., 2014b, 2014a, 2019a; Lehtonen et al., 2017; Silvestro y Schnitzler, 2018; Solórzano et al., 2020b). Por ejemplo, si la heterogeneidad topográfica asociada al alzamiento andino tuvo un efecto sobre las dinámicas de diversificación de la biota en el SSA, deberíamos esperar un patrón espacial donde existan tasas de especiación y/o extinción diferenciales entre las regiones topográficamente complejas (áreas tectónicamente activas en el oeste de SSA) y las tierras bajas adyacentes (Badgley, 2010; Finarelli y Badgley, 2010; Badgley et al., 2017; Silvestro y Schnitzler, 2018).

CAPÍTULO VII. Conclusiones

A partir del estudio detallado de la fauna de mamíferos de la Formación Cura-Mallín en las localidades de Lonquimay y Laguna del Laja fue posible reconocer la presencia de al menos 23 taxones distintos, incluyendo cuatro que fueron reportados por primera vez para Chile. La mayor riqueza de especies se reconoció en estratos del Mioceno temprano tardío de la Laguna del Laja, con al menos 17 taxones. Además, durante el desarrollo de la tesis se describieron formalmente dos especies nuevas, mientras que otras, que también parecen representar nuevos taxones, permanecen en nomenclatura abierta a la espera de poder coleccionar especímenes mejor preservados, revisar sistemática de la variabilidad intraespecífica de los ejemplares más afines descritos en Argentina (*Maruchito* sp. nov.?) y obtener imágenes de tomografía 3D de algunos ejemplares disponibles (*Pachyrukhos* sp. nov.?). Estos nuevos avances constituyen una importante fuente de información para la comprensión de las relaciones filogenéticas y geográficas de varios taxones. Además, permiten reducir el déficit linneano y wallaceano existente en las faunas extra-patagónicas del SSA, lo que permitirá evaluar con mayor precisión diferentes hipótesis relativas al rol que jugó el alzamiento de los Andes y otros factores bióticos y abióticos en la evolución de la biota de esta región.

La combinación de información geocronológica y bioestratigráfica permitió refinar la edad de las distintas faunas de mamíferos neógenos de la Formación Cura-Mallín. De tal forma, en Lonquimay se reconoció por primera vez la existencia de dos faunas cronológicamente distintivas, de edades Mioceno temprano (Colhuehuapiense–Santacrucense) y Mioceno medio tardío (Mayoense). Mientras que la fauna de la Laguna del Laja aquí descrita puede ser asignada al Mioceno temprano tardío (Santacrucense). Además, la mayor parte de los taxones identificados muestran afinidades con aquellos pertenecientes a las clásicas localidades contemporáneas hiperdiversas ubicadas en altas latitudes de Argentina (e.g., formaciones Pinturas y Santa Cruz).

El análisis de algunos rasgos ecomorfológicos distintivos de las faunas de mamíferos identificadas en la Formación Cura-Mallín permite proveer nuevas

interpretaciones del ambiente donde estas faunas habitaron. La información proporcionada por la biota fósil (mamíferos, peces de agua dulce y flora) recuperada del área de Lonquimay (~38°S) revela un ambiente bastante homogéneo durante la sedimentación de la Formación Cura-Mallín a lo largo del Mioceno medio temprano al Mioceno medio tardío, con hábitats boscosos desarrollados en un clima relativamente templado y húmedo, asociados con cuerpos de agua permanentes. Por otra parte, el paleoambiente en el que habitó la fauna del Mioceno temprano tardío de la Laguna del Laja es interpretado como uno mixto donde probablemente coexistieron hábitats abiertos y boscosos, en asociación con ambientes fluviales pedemontanos. La paleotemperatura de esta región sin embargo fue posiblemente un poco más baja que las inferida previamente en localidades contemporáneas de Argentina (<20°C de temperatura media anual). En general, estos ambientes se desarrollaron bajo la influencia de un régimen tectónico compresivo y vulcanismo activo.

Nueva evidencia apoya hipótesis previas, indicando que la Formación Cura-Mallín se depositó en condiciones sinorogénicas a partir de, al menos, 18 Ma, en concordancia con lo propuesto previamente para otras unidades temporalmente equivalentes ubicadas entre los 32° y 45°S. A pesar de esto, las condiciones ambientales relativamente homogéneas inferidas a través de múltiples líneas de evidencia sugieren que al menos una porción de la zona de estudio (38°S), hoy emplazada en la Cordillera Principal, no alcanzó elevaciones mayores a los 1000 metros sino hasta después de los 12 Ma.

Diferentes autores han sugerido que los cambios en el medio físico promovidos por el alzamiento de los Andes tuvieron un importante efecto sobre la evolución de la fauna sudamericana. Sin embargo, pocos trabajos han examinado esta hipótesis en conjunto con hipótesis alternativas utilizando marcos de trabajo estadísticos y el registro fósil como línea primaria de evidencia. Como una contribución en este sentido, aquí nos enfocamos en caracterizar la evolución de dos rasgos ecomorfológicos (tamaño corporal e hipsodoncia) en los notoungulados, un grupo extremadamente diverso de mamíferos endémicos del sur de Sudamérica, para posteriormente evaluar el impacto de múltiples factores ambientales importantes en la evolución de estos rasgos. Encontramos que la hipsodoncia es significativamente mayor hacia la región oeste de SSA, coincidiendo espacialmente con el orógeno andino. El

mecanismo subyacente son los cambios en el paisaje, que incluyen la remoción y mayor disponibilidad de partículas sedimentarias erosionadas, y/o la adición de partículas volcánicas. De tal forma, proveemos evidencia inédita sobre el rol que jugó el orógeno Andino, durante el Cenozoico, en la evolución de uno de los clados de mamíferos nativos dominantes en los ecosistemas antiguos del SSA. Este es sin duda un área de investigación aun poco desarrollada en Sudamérica, especialmente utilizando el registro fósil como línea primaria de evidencia, pero con un potencial enorme de mejorar nuestro entendimiento de los drivers de la evolución biológica a grandes escalas espaciales y temporales.



REFERENCIAS

- Abello, M.A., 2013, Analysis of dental homologies and phylogeny of Paucituberculata (Mammalia: Marsupialia): *Biological Journal of the Linnean Society*, v. 109, p. 441–465, doi:10.1111/bij.12048.
- Abello, M.A., 2007, Sistemática y bioestratigrafía de los Paucituberculata (Mammalia: Marsupialia) del Cenozoico de América del Sur: Ph.d. thesis, Facultad de Ciencias Naturales y Museo, Universidad Nacional de la Plata, 456 p.
- Abello, M.A., Ortiz-Jaureguizar, E., and Candela, A.M., 2013, Paleocology of the Paucituberculata and Microbiotheria (Mammalia, Marsupialia) from the late Early Miocene of Patagonia, *in* *Early Miocene Paleobiology in Patagonia*, Cambridge University Press, p. 156–172, doi:10.1017/cbo9780511667381.011.
- Allen, P.A., 2008, From landscapes into geological history: *Nature*, v. 451, p. 274–276, doi:10.1038/nature06586.
- Alvarenga, H.M.F., 1995, A large and probably flightless anHINGA from the Miocene of Chile: *Courier Forschungsinstitut Senckenberg*, v. 181, p. 149–161.
- Álvarez, A., Arévalo, R.L.M., and Verzi, D.H., 2017, Diversification patterns and size evolution in caviomorph rodents: *Biological Journal of the Linnean Society*, v. 121, p. 907–922, doi:10.1093/biolinnean/blx026.
- Álvarez, A., and Arnal, M., 2015, First Approach to the Paleobiology of Extinct Prospaniomys (Rodentia, Hystricognathi, Octodontoidea) Through Head Muscle Reconstruction and the Study of Craniomandibular Shape Variation: *Journal of Mammalian Evolution*, v. 22, p. 519–533, doi:10.1007/s10914-015-9291-z.
- Álvarez, A., Pérez, S.I., and Verzi, D.H., 2011, Ecological and phylogenetic influence on mandible shape variation of South American caviomorph rodents (Rodentia: Hystricomorpha): *Biological Journal of the Linnean Society*, v. 102, p. 828–837, doi:10.1111/j.1095-8312.2011.01622.x.
- Ameghino, F., 1889, Contribución al conocimiento de los mamíferos fósiles de la República Argentina: *Actas de la Academia Nacional de Ciencias en Córdoba*, v. 6, p. 1–1027.
- Ameghino, F., 1894, Enumération Synoptique des espèces de mammifères fossiles des formations Éocènes de Patagonie: *Boletín de la Academia Nacional de Ciencias en Córdoba (República Argentina)*, v. 13, p. 259–452, doi:10.5962/bhl.title.77348.
- Ameghino, F., 1897, Mammifères crétacés de l'Argentine: 1. *Boletín del Instituto Geológico Argentino*, v. 18, p. 406–521.
- Antoine, P.O. et al., 2016, A 60-million-year Cenozoic history of western Amazonian ecosystems in Contamana, eastern Peru: *Gondwana Research*, v. 31, p. 30–59, doi:10.1016/j.jgr.2015.11.001.
- Antoine, P.-O. et al., 2012, Middle Eocene rodents from Peruvian Amazonia reveal the pattern and timing of caviomorph origins and biogeography: *Proceedings of the Royal Society B: Biological Sciences*, v. 279, p. 1319–1326, doi:10.1098/rspb.2011.1732.
- Antoine, P.O., and Pujos, F., 2017, Cenozoic Evolution of TRopical-Equatorial MAMMALS

- (TREMA)—an Introduction to the Symposium Proceedings Volume: *Journal of Mammalian Evolution*, v. 24, p. 1–3, doi:10.1007/s10914-016-9365-6.
- Antonelli, A. et al., 2018, Geological and climatic influences on mountain biodiversity: *Nature Geoscience*, v. 11, p. 718–725, doi:10.1038/s41561-018-0236-z.
- Armijo, R., Lacassin, R., Coudurier-Curveur, A., and Carrizo, D., 2015, Coupled tectonic evolution of Andean orogeny and global climate: *Earth-Science Reviews*, v. 143, p. 1–35, doi:10.1016/j.earscirev.2015.01.005.
- Arnal, M., Kramarz, A.G., Vucetich, M.G., Frailey, C.D., and Campbell, K.E., 2019a, New Palaeogene caviomorphs (Rodentia, Hystricognathi) from Santa Rosa, Peru: systematics, biochronology, biogeography and early evolutionary trends: *Papers in Palaeontology*, v. 6, p. 193–216, doi:10.1002/spp2.1264.
- Arnal, M., Pérez, M.E., and Deschamps, C.M., 2019b, Revision of the Miocene caviomorph rodents from the Río Santa Cruz (Argentinean Patagonia): *Publicación Electrónica de la Asociación Paleontológica Argentina*, v. 19, p. 193–229, doi:10.5710/PEAPA.25.09.2019.299.
- Arnal, M., and Vucetich, M.G., 2015, Revision of the fossil rodent *Acaremys* Ameghino, 1887 (Hystricognathi, Octodontoidea, Acaremyidae) from the Miocene of Patagonia (Argentina) and the description of a new acaremyid: *Historical Biology*, v. 27, p. 42–59, doi:10.1080/08912963.2013.863881.
- Arratia, G., 1982, A Review of Freshwater Percoids from South America (Pisces, Osteichthyes, Perciformes, Percichthyidae and Perciliidae) | NHBS Academic & Professional Books: *Abhandlungen der Senckenberg Gesellschaft für Naturforschung*, v. 540, p. 1–52.
- Arratia, G., 2015, Los peces osteíctios fósiles de Chile y su importancia en los contextos paleobiogeográfico y evolutivo: *Publicación Ocasional del Museo Nacional de Historia Natural, Chile*, v. 63, p. 35–83.
- Ashton, K.G., Tracy, M.C., and De Queiroz, A., 2000, Is Bergmann's rule valid for mammals? *American Naturalist*, v. 156, p. 390–415, doi:10.1086/303400.
- Azpelicueta, M. de las M., and Rubilar, A., 1997, A fossil siluriform spine (Teleostei, Ostariophysii) from the Miocene of Chile: *Andean Geology*, v. 24, p. 109–113, doi:10.5027/andgeov24n1-a07.
- Azpelicueta, D.L.M.M., and Rubilar, A., 1998, A miocene nematogenys (Teleostei: Siluriformes: Nematogenyidae) from south-central Chile: *Journal of Vertebrate Paleontology*, v. 18, p. 475–483, doi:10.1080/02724634.1998.10011075.
- Badgley, C. et al., 2017, Biodiversity and Topographic Complexity: Modern and Geohistorical Perspectives: *Trends in Ecology and Evolution*, v. 32, p. 211–226, doi:10.1016/j.tree.2016.12.010.
- Badgley, C., 2010, Tectonics, topography, and mammalian diversity: *Ecography*, v. 33, p. no-no, doi:10.1111/j.1600-0587.2010.06282.x.
- Barasoain, D., Contreras, V.H., Tomassini, R.L., and Zurita, A.E., 2020, A new pygmy armadillo (Cingulata, Euphractinae) from the late Miocene of Andean Argentina reveals an

- unexpected evolutionary history of the singular *Prozaedyus* lineage: *Journal of South American Earth Sciences*, v. 100, p. 102589, doi:10.1016/j.jsames.2020.102589.
- Bargo, M.S., De Iuliis, G., and Toledo, N., 2019, Early Miocene sloths (*Xenarthra*, *Folivora*) from the Río Santa Cruz valley (Southern Patagonia, Argentina): *Publicación Electrónica de la Asociación Paleontológica Argentina*, v. 19, p. 102–137, doi:10.5710/PEAPA.06.08.2019.297.
- Bargo, M.S., Toledo, N., and Vizcaíno, S.F., 2013, Paleobiology of the Santacrucian sloths and anteaters (*Xenarthra*, *Pilosa*), in Vizcaíno, S.F., Kay, R.F., and Bargo, S. eds., *Early Miocene Paleobiology in Patagonia*, Cambridge University Press, p. 216–242, doi:10.1017/cbo9780511667381.014.
- Barreda, V.D. et al., 2007, Diversificación y cambios de las angiospermas durante el Neógeno en Argentina: *Asociación Paleontológica Argentina*, v. 11, p. 173–191.
- Barreda, V.D., and Palazzesi, L., 2014, Response of plant diversity to Miocene forcing events: the case of Patagonia, in Stevens, W.D., Montiel, O.M., and Raven, P.H. eds., *Paleobotany and Biogeography: A Festschrift for Alan Graham in His 80th Year*, Missouri Botanical Garden Press, p. 1–25.
- Barton, K., 2020, MuMIn: multi-model inference. R package version 1.43.17., <https://ci.nii.ac.jp/naid/10030918982/> (accessed October 2020).
- Bechis, F., Encinas, A., Concheyro, A., Litvak, V.D., Aguirre-Urreta, B., and Ramos, V.A., 2014, New age constraints for the Cenozoic marine transgressions of northwestern Patagonia, Argentina (41°–43° S): Paleogeographic and tectonic implications: *Journal of South American Earth Sciences*, v. 52, p. 72–93, doi:10.1016/J.JSAMES.2014.02.003.
- Bellosi, E.S., and Krause, J.M., 2014, Onset of the Middle Eocene global cooling and expansion of open-vegetation habitats in central Patagonia: *Andean Geology*, v. 41, p. 29–48, doi:10.5027/andgeoV41n1-a02.
- Benson, R.B.J., Hunt, G., Carrano, M.T., and Campione, N., 2018, Cope's rule and the adaptive landscape of dinosaur body size evolution (P. Mannion, Ed.): *Palaeontology*, v. 61, p. 13–48, doi:10.1111/pala.12329.
- Benton, M.J., 2014, *Vertebrate Palaeontology: West Sussex, UK*, Blackwell Publishing Ltd, 506 p.
- Benton, M.J., and Harper, D.A.T., 2020, *Introduction to Paleobiology and the Fossil Record*, 2nd Edition | Wiley: West Sussex, John Wiley & Sons Ltd, 656 p.
- Bertrand, O.C., Flynn, J.J., Croft, D.A., and Wyss, A.R., 2012, Two new taxa (*Caviomorpha*, *Rodentia*) from the early Oligocene Tinguiririca fauna (Chile): *American Museum novitates*, v. 3750, p. 1–36.
- Billet, G., 2011, Phylogeny of the Notoungulata (Mammalia) based on cranial and dental characters: *Journal of Systematic Palaeontology*, v. 9, p. 481–497, doi:10.1080/14772019.2010.528456.
- Blisniuk, P.M., Stern, L.A., Chamberlain, C.P., Idleman, B., and Zeitler, P.K., 2005, Climatic and ecologic changes during Miocene surface uplift in the Southern Patagonian Andes: *Earth*

- and Planetary Science Letters, v. 230, p. 125–142, doi:10.1016/J.EPSL.2004.11.015.
- Bobbe, R., Bostelmann, E., Tejedor, M.F., Carrasco, G., Mancuso, A.C., Alloway, B. V., Bellosi, E., Ugalde, R., and Buldrini, K.E., 2015, Primates del Mioceno de Río Cisnes, Patagonia Chilena, *in* V Congreso Latinoamericano de Paleontología de Vertebrados, Colonia del Sacramento, Uruguay, p. 36.
- Boivin, M., and Marivaux, L., 2020, Dental homologies and evolutionary transformations in Caviomorpha (Hystricognathi, Rodentia): new data from the Paleogene of Peruvian Amazonia: *Historical Biology*, v. 32, p. 528–554, doi:10.1080/08912963.2018.1506778.
- Boivin, M., Marivaux, L., Orliac, M.J., Pujos, F., Salas-Gismondi, R., Tejada-Lara, J. V., and Antoine, P.O., 2017, Late middle eocene caviomorph rodents from Contamana, Peruvian Amazonia: *Palaeontologia Electronica*, v. 20, p. 19, doi:10.26879/742.
- Bostelmann, E. et al., 2013, Burdigalian deposits of the Santa Cruz Formation in the Sierra Baguales, Austral (Magallanes) Basin: Age, depositional environment and vertebrate fossils: *Andean Geology*, v. 40, p. 458–489, doi:10.5027/andgeoV40n3-a04.
- Bostelmann, E., Bobbe, R., Carrasco, G., Alloway, B. V., Santi-Malnis, P., Mancuso, A., Agüero, B., Allemseged, Z., and Godoy, Y., 2012, The Alto Río Cisnes fossil fauna (Río Frías Formation, early Middle Miocene, Friasian SALMA): A keystone and paradigmatic vertebrate assemblage of the South American fossil record., *in* III Simposio Paleontología en Chile, Punta Arenas, Chile, p. 42–45.
- Bostelmann, E., Buldrini, K.E., and Kramarz, A.G., 2014, A new generic assignment for the Quepuca River astrapothere (Mammalia, Astrapotheria), *in* IV Simposio Paleontología en Chile, Universidad Austral de Chile, Valdivia,.
- Bostelmann, E., Castro, N., Moreno, K., García, M., Fosdick, J., Campos-Medina, J., Croft, D.A., and Montoya-Sanhueza, G., 2018, Stratigraphy and paleontology of Caragua, Arica and Parinacota regions, Chile, part 2: biostratigraphy and geochronology of the late Miocene sedimentary sequence, *in* XV Congreso Geológico Chileno, Concepción, Chile, p. 1321.
- Bown, T.M., and Fleagle, J.G., 1993, Systematics, biostratigraphy, and dental evolution of the Palaeothentidae, later Oligocene to early-middle Miocene (Deseadan- Santacrucian) caenolestoid marsupials of South America: *Journal of Paleontology*, v. 67, p. 1–76, doi:10.1017/s0022336000062107.
- Bown, T.M., and Lariestra, C.N., 1990, Sedimentary paleoenvironments of fossil platyrrhine localities, Miocene Pinturas Formation, Santa Cruz Province, Argentina: *Journal of Human Evolution*, v. 19, p. 87–119, doi:10.1016/0047-2484(90)90013-2.
- Bradham, J., Flynn, J.J., Croft, D.A., and Wyss, A.R., 2015, New notoungulates (Notostylopidae and basal toxodontians) from the early Oligocene Tinguiririca fauna of the Andean Main Range, central Chile: *American Museum Novitates*, v. 3841, p. 1–21.
- Brandoni, D., Ruiz, L.G., Tejedor, M.F., Martín, G., and Fleagle, J.G., 2016, Megatherioidea (Mammalia, Xenarthra, Tardigrada) from the Pinturas Formation (Early Miocene), Santa Cruz Province (Argentina) and their chronological implications: *Palaontologische Zeitschrift*, v. 90, p. 619–628, doi:10.1007/s12542-016-0306-8.

- Brassey, C.A., 2017, Body-mass estimation in paleontology: a review of volumetric techniques: The Paleontological Society Papers, v. 22, p. 133–156, doi:10.1017/scs.2017.12.
- Bucher, J., Pérez, M.E., González Ruiz, L.R., D'Elía, L., and Bilmes, A., 2020, New middle Miocene (Langhian - Serravallian) vertebrate localities in northwestern Patagonia, Argentina: A contribution to high latitude south american land mammal ages sequence: Journal of South American Earth Sciences, p. 103024, doi:10.1016/j.jsames.2020.103024.
- Buckley, M., 2015, Ancient collagen reveals evolutionary history of the endemic south american 'ungulates': Proceedings of the Royal Society B: Biological Sciences, v. 282, doi:10.1098/rspb.2014.2671.
- Buldrini, K.E., and Bostelmann, E., 2011, A well preserved skull of *Protypotherium* cf. *P. australe* Ameghino 1887, (Mammalia, Notoungulata, Interatheriidae) from the Early Miocene of Chile: Ameghiniana, v. 48, p. R-149.
- Buldrini, K.E., Bostelmann, E., and Soto Acuña, S., 2015, Taxonomic identity of the Interatheriidae SGO.PV.4004 and SGO.PV.4005, and rectification of collection numbering of *Caraguatypotherium munozi* (Notoungulata; Mesotheriidae), in XIV Congreso Geológico Chileno, La Serena, Chile, p. 702–705.
- Burns, W.M., Jordan, T.E., Copeland, P., and Kelley, S.A., 2006, The case for extensional tectonics in the Oligocene-Miocene Southern Andes as recorded in the Cura Mallín basin (36°–38°S), in Special Paper 407: Evolution of an Andean Margin: A Tectonic and Magmatic View from the Andes to the Neuquén Basin (35°-39°S lat), Geological Society of America, p. 163–184, doi:10.1130/2006.2407(08).
- Candela, A.M., Cassini, G.H., and Nasif, N.L., 2013a, Fractal dimension and cheek teeth crown complexity in the giant rodent *Eumegamys paranensis*: Lethaia, v. 46, p. 369–377, doi:10.1111/let.12015.
- Candela, A.M., Rasia, L.L., and Pérez, M.E., 2013b, Paleobiology of Santacrucian caviomorph rodents: a morphofunctional approach, in Vizcaíno, S.F., Kay, R.F., and Bargo, S. eds., Early Miocene Paleobiology in Patagonia, Cambridge University Press, p. 287–305, doi:10.1017/cbo9780511667381.016.
- Canto, J., Yáñez, J., and Rovira, J., 2010, Estado actual del conocimiento de los mamíferos fósiles de Chile: Estudios Geológicos, v. 66, p. 255–284, doi:10.3989/egeol.39778.055.
- Carpinelli, A., 2000, Análisis estratigráfico, paleoambiental, estructural y modelo tectono-estratigráfico de la Cuenca de Cura-Mallín, VIII y IX Región, Chile, Provincia de Neuquén, Argentina: Memoria de Título, Departamento de Ciencias de la Tierra, Universidad de Concepción, Chile, 158 p.
- Cassini, G.H., 2013, Skull geometric morphometrics and paleoecology of Santacrucian (late early Miocene; Patagonia) native ungulates (Astrapotheria, Litopterna, and Notoungulata): Ameghiniana, v. 50, p. 193–216, doi:10.5710/AMGH.7.04.2013.606.
- Cassini, G.H., Cerdeño, E., Villafañe, A.L., and Muñoz, N.A., 2012, Paleobiology of Santacrucian native ungulates (Meridiungulata: Astrapotheria, Litopterna and Notoungulata), in Vizcaino, S.F., Kay, R.F., and Bargo, M.S. eds., Early Miocene Paleobiology in Patagonia,

- Cambridge, Cambridge University Press, p. 243–286, doi:10.1017/CBO9780511667381.015.
- Cerdeño, E., Cerdeño, E., and Bond, M., 1998, Taxonomic revision and phylogeny of *Paedotherium* and *Tremacyllus* (Pachyrhinae, Hegetotheriidae, Notoungulata) from the Late Miocene to the Pleistocene of Argentina: *Journal of Vertebrate Paleontology*, v. 18, p. 799–811, doi:10.1080/02724634.1998.10011108.
- Chang, A., Arratia, G., and Alfaro, G., 1978, *Percichthys lonquimaiensis* n. sp. from the Upper Paleocene of Chile (Pisces, Perciformes, Serranidae): *Journal of Paleontology*, v. 52, p. 727–736.
- Charrier, R., Baeza, O., Elgueta, S., Flynn, J.J., Gans, P., Kay, S.M., Muñoz, N., Wyss, A.R., and Zurita, E., 2002, Evidence for Cenozoic extensional basin development and tectonic inversion south of the flat-slab segment, southern Central Andes, Chile (33°–36°S.L.): *Journal of South American Earth Sciences*, v. 15, p. 117–139, doi:10.1016/S0895-9811(02)00009-3.
- Charrier, R., Flynn, J.J., Wyss, A.R., and Croft, D.A., 2015, Marco Geológico-tectónico, contenido fosilífero y cronología de los yacimientos cenozoicos pre-pleistocénicos de Mamíferos terrestres fósiles de Chile: *Publicación Ocasional del Museo Nacional de Historia Natural, Chile*, v. 63, p. 293–338.
- Cheme-Arriaga, L., Dozo, M.T., and Gelfo, J.N., 2016, A new *Cramaucheniinae* (Litopterna, *Macraucheniidae*) from the early Miocene of Patagonia, Argentina: *Journal of Vertebrate Paleontology*, v. 36, p. e1229672, doi:10.1080/02724634.2017.1229672.
- Chornogubsky, L., Abello, M.A., and Barmak, G., 2019, Los Metatheria Del Río Santa Cruz (Formación Santa Cruz, Mioceno Temprano–Medio, Argentina): *Historia Y Nuevos Registros: Publicación Electrónica de la Asociación Paleontológica Argentina*, v. 19, p. 62–84, doi:10.5710/PEAPA.04.10.2019.287.
- Ciancio, M.R., and Carlini, A.A., 2016, Identification of type specimens of *Dasypodidae* (Mammalia, Xenarthra) of the paleogene of Argentina: *Revista del Museo Argentino de Ciencias Naturales nueva serie*, v. 10, p. 221–237.
- Ciancio, M.R., Krmpotic, C.M., Scarano, A.C., and Epele, M.B., 2017, Internal Morphology of Osteoderms of Extinct Armadillos and Its Relationship with Environmental Conditions: *Journal of Mammalian Evolution*, p. 1–13, doi:10.1007/s10914-017-9404-y.
- Cifelli, R., and Guerrero, J., 1997, Litopterns, in Kay, R., Madden, R.H., Cifellii, R., and Flynn, J. eds., *Vertebrate paleontology in the Neotropics: the Miocene fauna of La Venta, Colombia*, Smithsonian Institution Press, Washington, D.C, p. 289–302.
- Cifelli, R.L., and Soria, M.F., 1983, Notes on Deseadan *Macraucheniidae*: *Ameghiniana*, v. 20, p. 141–153.
- Clavel, J., and Morlon, H., 2017, Accelerated body size evolution during cold climatic periods in the Cenozoic: *Proceedings of the National Academy of Sciences of the United States of America*, v. 114, p. 4183–4188, doi:10.1073/pnas.1606868114.
- Cobbold, P.R., Rossello, E.A., and Marques, F.O., 2008, Where is the evidence for Oligocene

- ripping in the Andes? Is it in the Loncopué Basin of Argentina?, *in* 7th International Symposium on Andean Geodynamics, p. 148–151.
- Cohen, K.M., Finney, S.C., Gibbard, P.L., and Fan, J.X., 2013, The ICS international chronostratigraphic chart: Episodes, v. 36, p. 199–204, doi:10.18814/epiiugs/2013/v36i3/002.
- Cooper, N., and Purvis, A., 2010, Body size evolution in mammals: complexity in tempo and mode.: *The American naturalist*, v. 175, p. 727–38, doi:10.1086/652466.
- Craw, D., Upton, P., Burrige, C.P., Wallis, G.P., and Waters, J.M., 2016, Rapid biological speciation driven by tectonic evolution in New Zealand.: doi:10.1038/NGEO2618.
- Croft, D.A., 2001, Cenozoic environmental change in South America as indicated by mammalian body size distributions (cenograms): *Diversity and Distributions*, v. 7, p. 271–287, doi:10.1046/j.1366-9516.2001.00117.x.
- Croft, D.A., 2007, The middle Miocene (Laventan) Quebrada Honda Fauna, southern Bolivia and a description of its notoungulates: *Palaeontology*, v. 50, p. 277–303, doi:10.1111/j.1475-4983.2006.00610.x.
- Croft, D.A., Anaya, F., Auerbach, D., Garziona, C., and MacFadden, B.J., 2009, New data on Miocene Neotropical provinciality from Cerdas, Bolivia: *Journal of Mammalian Evolution*, v. 16, p. 175–198, doi:10.1007/s10914-009-9115-0.
- Croft, D.A., and Anderson, L.C., 2007, Locomotion in the extinct notoungulate *Protypotherium*: *Palaeontologia Electronica*, v. 11, p. 1–20, doi:http://palaeo-electronica.org/2008_1/138/index.html.
- Croft, D.A., Chick, J.M.H., and Anaya, F., 2011, New Middle Miocene Caviomorph Rodents from Quebrada Honda, Bolivia: *Journal of Mammalian Evolution*, v. 18, p. 245–268, doi:10.1007/s10914-011-9164-z.
- Croft, D.A., Flynn, J.J., and Wyss, A.R., 2007, A new basal glyptodontid and other Xenarthra of the early Miocene Chucal Fauna, Northern Chile: *Journal of Vertebrate Paleontology*, v. 27, p. 781–797, doi:10.1671/0272-4634(2007)27[781:ANBGAO]2.0.CO;2.
- Croft, D., Flynn, J., and Wyss, A., 2008, The Tinguiririca Fauna of Chile and the early stages of “modernization” of South American mammal faunas: *Arquivos do Museu Nacional, Rio de Janeiro*, v. 66, p. 191–211.
- Croft, D. a, Flynn, J.J., Wyss, A.R., and Wyss, R., 2004, Notoungulata and Litopterna of the Early Miocene Chucal Fauna, Northern Chile: *Fieldiana, Geology*, v. 50, p. 1–52, doi:10.5962/bhl.title.5228.
- Croft, D.A., Gelfo, J.N., and López, G.M., 2020, Splendid Innovation: The Extinct South American Native Ungulates: *Annual Review of Earth and Planetary Sciences*, v. 48, p. 259–290, doi:10.1146/annurev-earth-072619-060126.
- Croft, D.A., Radic, J.P., Zurita, E., Charrier, R., Flynn, J.J., and Wyss, A.R., 2003, A Miocene toxodontid (Mammalia: Notoungulata) from the sedimentary series of the Cura-Mallín Formation, Lonquimay, Chile: *Revista geológica de Chile*, v. 30, p. 285–298, doi:10.4067/S0716-02082003000200008.

- Croft, D.A., Su, D.F., and Simpson, S.W., 2018, Introduction to paleoecological reconstruction, *in* Croft, D.A. ed., *Vertebrate Paleobiology and Paleoanthropology*, Springer, p. 1–5, doi:10.1007/978-3-319-94265-0_1.
- Cuitiño, J.I., Fernicola, J.C., Kohn, M.J., Trayler, R., Naipauer, M., Bargo, M.S., Kay, R.F., and Vizcaíno, S.F., 2016, U-Pb geochronology of the Santa Cruz Formation (early Miocene) at the Río Bote and Río Santa Cruz (southernmost Patagonia, Argentina): Implications for the correlation of fossil vertebrate localities: *Journal of South American Earth Sciences*, v. 70, p. 198–210, doi:10.1016/J.JSAMES.2016.05.007.
- Cuitiño, J.I., Raigemborn, M.S., Bargo, M.S., Vizcaíno, S.F., Muñoz, N.A., Kohn, M.J., and Kay, R.F., 2021, Insights on the controls on floodplain-dominated fluvial successions: a perspective from the early-middle Miocene Santa Cruz Formation in Río Chalfá (Patagonia, Argentina): *Journal of the Geological Society*, p. jgs2020-188, doi:10.1144/jgs2020-188.
- Cuitiño, J.I., Vizcaíno, S.F., Bargo, M.S., and Aramendía, I., 2019, Sedimentology and fossil vertebrates of the Santa Cruz Formation (early Miocene) in Lago Posadas, southwestern Patagonia, Argentina: *Andean Geology*, v. 46, p. 383–420, doi:10.5027/andgeov46n2-3128.
- Dal Molin, C., Márquez, M., and Maisonabe, B., 1998, Hoja Geológica 4571-IV Alto Río Senguerr, provincia del Chubut. 1. Escala: 250000.: SEGEMAR, p. 1–34.
- Damuth, J., and Janis, C.M., 2011, On the relationship between hypsodonty and feeding ecology in ungulate mammals, and its utility in palaeoecology: *Biological Reviews*, v. 86, p. 733–758, doi:10.1111/j.1469-185X.2011.00176.x.
- Delsuc, F. et al., 2016, The phylogenetic affinities of the extinct glyptodonts: *Current Biology*, v. 26, p. R155–R156, doi:10.1016/J.CUB.2016.01.039.
- Diederle, J.M., 2015, Los Anhingidae (Aves: Suliformes) del Neógeno de América del Sur: sistemática, filogenia y paleobiología: Phd. Thesis, Universidad de la Plata, 340 p.
- Dozo, M.T., Ciancio, M., Bouza, P., and Martínez, G., 2014, Nueva asociación de mamíferos del Paleógeno en el este de la Patagonia (provincia de Chubut, Argentina): Implicancias biocronológicas y paleobiogeográficas: *Andean Geology*, v. 41, p. 224–247, doi:10.5027/andgeoV41n1-a09.
- Dunn, R.E., Madden, R.H., Kohn, M.J., Schmitz, M.D., Stromberg, C.A.E., Carlini, A.A., Re, G.H., and Crowley, J., 2013, A new chronology for middle Eocene-early Miocene South American Land Mammal Ages: *Geological Society of America Bulletin*, v. 125, p. 539–555, doi:10.1130/B30660.1.
- Dunn, R.E., Strömberg, C.A.E., Madden, R.H., Kohn, M.J., and Carlini, A.A., 2015, Linked canopy, climate, and faunal change in the Cenozoic of Patagonia: *Science*, v. 347, p. 258–261, doi:10.1126/science.1260947.
- Echaurren, A., Folguera, A., Gianni, G., Orts, D., Tassara, A., Encinas, A., Giménez, M., and Valencia, V., 2016, Tectonic evolution of the North Patagonian Andes (41°–44° S) through recognition of syntectonic strata: *Tectonophysics*, v. 677–678, p. 99–114, doi:10.1016/J.TECTO.2016.04.009.
- Ehlers, T.A., and Poulsen, C.J., 2009, Influence of Andean uplift on climate and paleoaltimetry

- estimates: *Earth and Planetary Science Letters*, v. 281, p. 238–248, doi:10.1016/j.epsl.2009.02.026.
- Elissamburu, A., 2012, Estimación de la masa corporal en géneros del orden Notoungulata: *Estudios Geológicos*, v. 68, p. 91–111, doi:10.3989/egeol.40336.133.
- Encinas, A. et al., 2018, The Late Oligocene–Early Miocene Marine Transgression of Patagonia, *in* Folguera, A. et al. eds., *The Evolution of the Chilean-Argentinean Andes*, Springer, Cham, p. 443–474, doi:10.1007/978-3-319-67774-3_18.
- Encinas, A., Folguera, A., Litvak, V.D., Echaurren, A., Gianni, G., Fernández Paz, F., Bobe, R., and Valencia, V., 2016, New age constraints for the Cenozoic deposits of the Patagonian Andes and the sierra de San Bernardo between 43° and 46°S, *in* Primer simposio de tectónica sudamericana., Santiago, Chile, p. 140.
- Encinas, A., Folguera, A., Rizzo, R., Molina, P., Fernández Paz, L., Litvak, V.D., Colwyn, D.A., Valencia, V.A., and Carrasco, M., 2019, Cenozoic basin evolution of the Central Patagonian Andes: Evidence from geochronology, stratigraphy, and geochemistry: *Geoscience Frontiers*, v. 10, p. 1139–1165, doi:10.1016/j.gsf.2018.07.004.
- Engelman, R.K., Flynn, J.J., Gans, P.B., Wyss, A.R., and Croft, D.A., 2018, *Chlorocyon phantasma*, a late Eocene borhyaenoid (Mammalia, Metatheria, Sparassodonta) from the Los Helados locality, Andean Main Range, central Chile: *American Museum Novitates*, v. 3918, p. 22 p.
- Engelman, R.K., Flynn, J.J., Wyss, A.R., and Croft, D.A., 2020, *Eomakhaira molossus*, A New Saber-Toothed Sparassodont (Metatheria: Thylacosmilinae) from the Early Oligocene (?Tinguirirican) Cachapoal Locality, Andean Main Range, Chile: *American Museum Novitates*, v. 2020, p. 1, doi:10.1206/3957.1.
- Eronen, J.T., Janis, C.M., Chamberlain, C.P., and Mulch, A., 2015, Mountain uplift explains differences in palaeogene patterns of mammalian evolution and extinction between north America and Europe: *Proceedings of the Royal Society B: Biological Sciences*, v. 282, doi:10.1098/rspb.2015.0136.
- Eronen, J.T., Puolamäki, K., Liu, L., Lintulaakso, K., Damuth, J., Janis, C., and Fortelius, M., 2010, Precipitation and large herbivorous mammals II: Application to fossil data: *Evolutionary Ecology Research*, v. 12, p. 235–248, <http://www.helsinki.fi/science/now> (accessed October 2019).
- Erwin, D.H., 2007, Disparity: Morphological pattern and developmental context: *Palaeontology*, v. 50, p. 57–73, doi:10.1111/j.1475-4983.2006.00614.x.
- Evans, A.R., and Pineda-Munoz, S., 2018, Inferring mammal dietary ecology from dental morphology, *in* Croft, D.A., Su, D.F., and Simpson, S.W. eds., *Methods in Paleoecology Reconstructing Cenozoic Terrestrial Environments and Ecological Communities*, Springer, p. 37–51, doi:10.1007/978-3-319-94265-0_4.
- Favre, A., Päckert, M., Pauls, S.U., Jähmig, S.C., Uhl, D., Michalak, I., and Muellner-Riehl, A.N., 2015, The role of the uplift of the Qinghai-Tibetan Plateau for the evolution of Tibetan biotas: *Biological Reviews*, v. 90, p. 236–253, doi:10.1111/brv.12107.

- Felsch, J., 1915, Las pizarras betuminosas de Lonquimay: Boletín de la Sociedad Nacional de Minería, v. 27, p. 498–509.
- Fernández-Monescillo, M., Antoine, P.O., Pujos, F., Gomes Rodrigues, H., Mamani Quispe, B., and Orliac, M., 2019, Virtual Endocast Morphology of Mesotheriidae (Mammalia, Notoungulata, Typotheria): New Insights and Implications on Notoungulate Encephalization and Brain Evolution: *Journal of Mammalian Evolution*, v. 26, p. 85–100, doi:10.1007/s10914-017-9416-7.
- Fernández, M., Fernicola, J.C., Cerdeño, E., and Reguero, M.A., 2018, Identification of type materials of the species of *Protypotherium* Ameghino, 1885 and *Patriarchus* Ameghino, 1889 (Notoungulata: Interatheriidae) erected by Florentino Ameghino: *Zootaxa*, v. 4387, p. 473, doi:10.11646/zootaxa.4387.3.4.
- Fernández, M., and Muñoz, N.A., 2019, Notoungulata Y Astrapotheria (Mammalia, Meridiungulata) De La Formación Santa Cruz (Mioceno Temprano–Medio) A Lo Largo Del Río Santa Cruz, Patagonia Argentina: *Publicación Electrónica de la Asociación Paleontológica Argentina*, v. 19, p. 138–169, doi:http://dx.doi.org/10.5710/PEAPA.19.09.2019.288.
- Fernández Paz, L., Litvak, V.D., Echaurren, A., Iannelli, S.B., Encinas, A., Folguera, A., and Valencia, V., 2018, Late Eocene volcanism in North Patagonia (42°30'–43°S): Arc resumption after a stage of within-plate magmatism: *Journal of Geodynamics*, v. 113, p. 13–31, doi:10.1016/j.jog.2017.11.005.
- Fernicola, J.C., Vizcaíno, S.F., Bargo, M.S., Kay, R.F., and Cuitiño, J.I., 2019, Análisis De Las Asociaciones De Mamíferos Fósiles Del Mioceno Temprano–Medio Del Río Santa Cruz (Patagonia, Argentina): *Publicación Electrónica de la Asociación Paleontológica Argentina*, v. 19, p. 239–259, doi:10.5710/PEAPA.01.11.2019.309.
- Fields, R.W., 1957, Hystricomorph rodents from the late Miocene of Colombia, South America: A contribution from the University of California Museum of Paleontology, p. 273.
- Finarelli, J.A., and Badgley, C., 2010, Diversity dynamics of Miocene mammals in relation to the history of tectonism and climate, *in* *Proceedings of the Royal Society B: Biological Sciences*, Royal Society, v. 277, p. 2721–2726, doi:10.1098/rspb.2010.0348.
- Flower, B.P., and Kennett, J.P., 1994, The middle Miocene climatic transition: East Antarctic ice sheet development, deep ocean circulation and global carbon cycling: *Palaeogeography, Palaeoclimatology, Palaeoecology*, v. 108, p. 537–555, doi:10.1016/0031-0182(94)90251-8.
- Flynn, J.J., Charrier, R., Croft, D.A., Gans, P.B., Herriott, T.M., Wertheim, J.A., and Wyss, A.R., 2008, Chronologic implications of new Miocene mammals from the Cura-Mallín and Trapa Trapa formations, Laguna del Laja area, south central Chile: *Journal of South American Earth Sciences*, v. 26, p. 412–423, doi:10.1016/J.JSAMES.2008.05.006.
- Flynn, J.J., Croft, D.A., Charrier, R., Hérail, G., and Wyss, A.R., 2002a, The first Cenozoic mammal fauna from the Chilean Altiplano: *Journal of Vertebrate Paleontology*, v. 22, p. 200–206, doi:10.1017/S0016756897007061.

- Flynn, J.J., Croft, D.A., Wyss, A.R., Hérail, G., and García, M., 2005, New Mesotheriidae (Mammalia, Notoungulata, Typotheria), geochronology and tectonics of the Caragua area, northernmost Chile: *Journal of South American Earth Sciences*, v. 19, p. 55–74, doi:10.1016/J.JSAMES.2004.06.007.
- Flynn, J.J., Novacek, M.J., Dodson, H.E., Frassinetti, D., McKenna, M.C., Norell, M.A., Sears, K.E., Swisher, C.C., and Wyss, A.R., 2002b, A new fossil mammal assemblage from the southern Chilean Andes: Implications for geology, geochronology, and tectonics: *Journal of South American Earth Sciences*, v. 15, p. 285–302, doi:10.1016/S0895-9811(02)00043-3.
- Flynn, J.J., and Swisher, C.C., 1995, Cenozoic South American Land Mammal Ages: correlation to global geochronologies, *in* *Geochronology, Time Scales, and Global Stratigraphic Correlation*, SEPM (Society for Sedimentary Geology), p. 317–333, doi:10.2110/pec.95.04.0317.
- Flynn, J.J., Wyss, A.R., Charrier, R., and Swisher, C.C., 1995, An Early Miocene anthropoid skull from the Chilean Andes: *Nature*, v. 373, p. 603–607, doi:10.1038/373603a0.
- Flynn, J.J., Wyss, A.R., Croft, D.A., and Charrier, R., 2003, The Tinguiririca Fauna, Chile: biochronology, paleoecology, biogeography, and a new earliest Oligocene South American Land Mammal 'Age': *Palaeogeography, Palaeoclimatology, Palaeoecology*, v. 195, p. 229–259, doi:10.1016/S0031-0182(03)00360-2.
- Folguera, A. et al., 2018a, Neogene Growth of the Patagonian Andes, *in* *The Evolution of the Chilean-Argentinean Andes*, Springer, Cham, p. 475–501, doi:10.1007/978-3-319-67774-3_19.
- Folguera, A., Encinas, A., Echaurren, A., Gianni, G., Orts, D., Valencia, V., and Carrasco, G., 2018b, Constraints on the Neogene growth of the central Patagonian Andes at the latitude of the Chile triple junction (45–47°S) using U/Pb geochronology in synorogenic strata: *Tectonophysics*, v. 744, p. 134–154, doi:10.1016/J.TECTO.2018.06.011.
- Folguera, A., Orts, D., Spagnuolo, M., Vera, E.R., Litvak, V., Sagripanti, L., Ramos, M.E., and Ramos, V.A., 2011, A review of Late Cretaceous to Quaternary palaeogeography of the southern Andes: *Biological Journal of the Linnean Society*, v. 103, p. 250–268, doi:10.1111/j.1095-8312.2011.01687.x.
- Forasiepi, A.M., Cerdeño, E., Bond, M., Schmidt, G.I., Naipauer, M., Straehl, F.R., Martinelli, A.G., Garrido, A.C., Schmitz, M.D., and Crowley, J.L., 2015, New toxodontid (Notoungulata) from the Early Miocene of Mendoza, Argentina: *Palaontologische Zeitschrift*, v. 89, p. 611–634, doi:10.1007/s12542-014-0233-5.
- Forasiepi, A.M., MacPhee, R.D.E., Del Pino, S.H., Schmidt, G.I., Amson, E., and Grohé, C., 2016, Exceptional Skull of Huayqueriana (Mammalia, Litopterna, Macraucheniidae) From the Late Miocene of Argentina: Anatomy, Systematics, and Paleobiological Implications: *Bulletin of the American Museum of Natural History*, v. 404, p. 1–76, doi:10.1206/0003-0090-404.1.1.
- Forasiepi, A.M., Martinelli, A.G., de la Fuente, M.S., Dieguez, S., and Bond, M., 2011, Paleontology and stratigraphy of the Aisol (Neogene), San Rafael, Mendoza, *in* *Cenozoic Geology of the Central Andes of Argentina*, p. 135–154.

- Fortelius, M., Eronen, J., Jernvall, J., Liu, L., Pushkina, D., Rinne, J., Tesakov, A., Vislobokova, I., Zhang, Z., and Zhou, L., 2002, Fossil mammals resolve regional patterns of Eurasian climate change over 20 million years: *Evolutionary Ecology Research*, v. 4, p. 1005–1016.
- Friley, C.D., and Campbell Jr, K.E., 2004, Paleogene Rodents from Amazonian Peru: The Santa Rosa Local Fauna (K. E. Campbell, Ed.): *Science Series*, v. 40, p. 71–130.
- Fraser, D. et al., 2020, Investigating Biotic Interactions in Deep Time: *Trends in Ecology & Evolution*, v. 17, doi:10.1016/j.tree.2020.09.001.
- Freeman, B., Nico, L.G., Osentoski, M., Jelks, H.L., and Collins, T.M., 2007, Molecular systematics of Serrasalminae: Deciphering the identities of piranha species and unraveling their evolutionary histories: *Zootaxa*, v. 1484, p. 1–38, doi:10.11646/zootaxa.1484.1.1.
- Fritz, S.A., Schnitzler, J., Eronen, J.T., Hof, C., Bö Hning-Gaese, K., and Graham, C.H., 2013, Diversity in time and space: wanted dead and alive: *Trends in Ecology & Evolution*, v. 28, p. 509–516, doi:10.1016/j.tree.2013.05.004.
- Gaudin, T.J., 2004, Phylogenetic relationships among sloths (Mammalia, Xenarthra, Tardigrada): The craniodental evidence: *Zoological Journal of the Linnean Society*, v. 140, p. 255–305, doi:10.1111/j.1096-3642.2003.00100.x.
- Gaudin, T.J., and Wible, J.R., 2006, The Phylogeny of Living and Extinct Armadillos (Mammalia, Xenarthra, Cingulata): A Craniodental Analysis, *in* Carrano, M.T., Gaudin, T.J., Blob, R., and Wible, J.R. eds., *Amniote Paleobiology: perspectives on the evolution of mammals, birds, and reptiles*, University of Chicago Press, p. 153–198.
- Giambiagi, L. et al., 2016, Cenozoic Orogenic Evolution of the Southern Central Andes (32–36°S), *in* Folguera, A., Naipauer, M., Sagripanti, L., Ghiglione, Matías C. Orts, D.L., and Giambiagi, L. eds., *Growth of the Southern Andes*, Springer, Cham, p. 63–98, doi:10.1007/978-3-319-23060-3_4.
- Goin, F.J. et al., 2020, First mesozoic mammal from Chile: the southernmost record of a Late Cretaceous gondwanatherian: *Boletín del Museo de Historia Natural de Chile*, v. 69, p. 5–31.
- Goin, F.J., Abello, M.A., and Chornogubsky, L., 2010, Middle Tertiary marsupials from central Patagonia (early Oligocene of Gran Barranca): understanding South America's Grande Coupure, *in* Madden, R.H., Carlini, A.A., Vucetich, M.G., and Kay, R.F. eds., *The paleontology of Gran Barranca: evolution and environmental change through the middle Cenozoic of Patagonia*, Cambridge, Massachusetts, Cambridge University Press, p. 69–105.
- Goin, F., Woodburne, M., Zimicz, A.N., Martin, G.M., and Chornogubsky, L., 2016, A Brief History of South American Metatherians: Dordrecht, Springer Netherlands, Springer Earth System Sciences, doi:10.1007/978-94-017-7420-8.
- Gomes Rodrigues, H., Herrel, A., and Billet, G., 2017, Ontogenetic and life history trait changes associated with convergent ecological specializations in extinct ungulate mammals: *Proceedings of the National Academy of Sciences of the United States of America*, v. 114, p. 1069–1074, doi:10.1073/pnas.1614029114.

- González-Ruiz, L.R., 2010, Los Cingulata (Mammalia, Xenarthra) del Mioceno temprano y medio de Patagonia (edades Santacrucesense y "Friasense"). Revisión sistemática y consideraciones bioestratigráficas: Phd thesis, Universidad Nacional de La Plata, La Plata, Argentina, 471 p.
- González-Ruiz, L.R., Góis, F., Ciancio, M.R., and Scillato-Yané, G.J., 2013, Los Peltephilidae (Mammalia, Xenarthra) de la formación Collón Curá (Colloncurensis, Mioceno medio), Argentina: *Revista Brasileira de Paleontologia*, v. 16, p. 319–330, doi:10.4072/rbp.2013.2.12.
- González-Ruiz, L.R., Scillato-Yané, G.J., Krmpotic, C.M., and Carlini, A.A., 2012, A new species of Peltephilidae (Mammalia: Xenarthra: Cingulata) from the late Miocene (Chasicocoan SALMA) of Argentina: *Zootaxa*, v. 3359, p. 55–64, doi:10.11646/zootaxa.3359.1.5.
- González-Ruiz, L.R., Zurita, A.E., Scillato-Yané, G.J., Zamorano, M., and Tejedor, M.F., 2011, Un nuevo Glyptodontidae (Mammalia, Xenarthra, Cingulata) del Mioceno de Patagonia (Argentina) y comentarios acerca de la sistemática de los gliptodontes "friasenses": *Revista Mexicana de Ciencias Geológicas*, v. 28, p. 566–579.
- González Ruiz, L., Reato, A., Cano, M., and Martínez, O., 2017, Old and new specimens of a poorly known glyptodont from the Miocene of Patagonia and their biochronological implications: *Acta Palaeontologica Polonica*, v. 62, doi:10.4202/app.00280.2016.
- Gonzalez, O.L., and Vergara, M., 1962, Reconocimiento geológico de la Cordillera de los Andes entre los paralelos 35 y 38 sur: *Anales de la Facultad de Ciencias Físicas y Matemáticas*, v. 19, p. 19–121.
- Green, J.L., and Croft, D.A., 2018, Using dental mesowear and microwear for dietary inference: A review of current techniques and applications, in Croft, D.A., Su, D.F., and Simpson, S.W. eds., *Methods in Paleoecology Reconstructing Cenozoic Terrestrial Environments and Ecological Communities*, Springer, p. 53–73, doi:10.1007/978-3-319-94265-0_5.
- Gregory-Wodzicki, K.M., 2000, Uplift history of the Central and Northern Andes: A review: *Bulletin of the Geological Society of America*, v. 112, p. 1091–1105, doi:10.1130/0016-7606(2000)112<1091:UHOTCA>2.0.CO;2.
- Guevara, J.P., Alarcón-Muñoz, J., Soto-Acuña, S., Lara, F.S., Buldrini, K.E., Rubilar-Rogers, D., and Sallaberry, M., 2018, Primer registro de un Anuro fósil en el Neógeno de Chile, in *Resúmenes del I Congreso Paleontológico Chileno*, Punta Arenas, Chile, p. 313–316.
- Heim, N.A., Knope, M.L., Schaal, E.K., Wang, S.C., and Payne, J.L., 2015, Cope's rule in the evolution of marine animals: *Science*, v. 347, p. 867–870, doi:10.1126/science.1260065.
- Herbert, T.D., Lawrence, K.T., Tzanova, A., Peterson, L.C., Caballero-Gill, R., and Kelly, C.S., 2016, Late Miocene global cooling and the rise of modern ecosystems: *Nature Geoscience*, v. 9, p. 843–847, doi:10.1038/ngeo2813.
- Hernández Del Pino, S., 2018, Anatomía y sistemática de los Toxodontidae (Notoungulata) de la Formación Santa Cruz, Mioceno temprano, Argentina: Universidad de La Plata, Facultad de Ciencias Naturales y Museo., <http://sedici.unlp.edu.ar/handle/10915/65795> (accessed November 2018).

- Hernández Fernández, M., Alberdi, M.T., Azanza, B., Montoya, P., Morales, J., Nieto, M., and Peláez-Campomanes, P., 2006, Identification problems of arid environments in the Neogene-Quaternary mammal record of Spain: *Journal of Arid Environments*, v. 66, p. 585–608, doi:10.1016/j.jaridenv.2006.01.013.
- Herriott, T.M., 2006, Stratigraphy, structure, and $^{40}\text{Ar}/^{39}\text{Ar}$ geochronology of the southeastern Laguna del Laja area: Implications for the mid-late Cenozoic evolution of the Andes near 37.5°S , Chile: Unpublished Master's Thesis, Department of Earth Science, University of California, Santa Barbara, 110 p.
- Hijmans, R.J., Cameron, S.E., Parra, J.L., Jones, P.G., and Jarvis, A., 2005, Very high resolution interpolated climate surfaces for global land areas: *International Journal of Climatology*, v. 25, p. 1965–1978, doi:10.1002/joc.1276.
- Hinojosa, L.F. et al., 2016, Non-congruent fossil and phylogenetic evidence on the evolution of climatic niche in the Gondwana genus *Nothofagus*: *Journal of Biogeography*, v. 43, p. 555–567, doi:10.1111/jbi.12650.
- van Hinsbergen, D.J.J., de Groot, L. V., van Schaik, S.J., Spakman, W., Bijl, P.K., Sluijs, A., Langereis, C.G., and Brinkhuis, H., 2015, A Paleolatitude Calculator for Paleoclimate Studies (D. L. Royer, Ed.): *PLOS ONE*, v. 10, p. e0126946, doi:10.1371/journal.pone.0126946.
- Hirschfeld, S.E., 1985, Ground Sloths from the Friasian La Venta Fauna, with Additions to the Pre-Friasian Coyaima Fauna of Colombia, South America: *Geological Sciences (University of California)*, v. 28, p. 1–91.
- Hitz, R.B., Flynn, J.J., and Wyss, A.R., 2006, New basal Interatheriidae (Typotheria, Notoungulata, Mammalia) from the Paleogene of central Chile: *American Museum novitates*, v. 3520, p. 1–32.
- Holbourn, A., Kuhnt, W., Clemens, S., Prell, W., and Andersen, N., 2013, Middle to late Miocene stepwise climate cooling: Evidence from a high-resolution deep water isotope curve spanning 8 million years: *Paleoceanography*, v. 28, p. 688–699, doi:10.1002/2013PA002538.
- Holland, S.M., 2016, The non-uniformity of fossil preservation: *Philosophical Transactions of the Royal Society B: Biological Sciences*, v. 371, doi:10.1098/rstb.2015.0130.
- Hone, D.W.E., and Benton, M.J., 2005, The evolution of large size: How does Cope's Rule work? *Trends in Ecology and Evolution*, v. 20, p. 4–6, doi:10.1016/j.tree.2004.10.012.
- Horn, C. et al., 2010, Amazonia through time: Andean uplift, climate change, landscape evolution, and biodiversity.: *Science (New York, N.Y.)*, v. 330, p. 927–31, doi:10.1126/science.1194585.
- Horn, C., Mosbrugger, V., Mulch, A., and Antonelli, A., 2013, Biodiversity from mountain building: *Nature Geoscience*, v. 6, p. 154, doi:10.1038/ngeo1742.
- Hopkins, S.S.B., 2008, Reassessing the mass of exceptionally large rodents using toothrow length and area as proxies for body mass: *Journal of Mammalogy*, v. 89, p. 232–243, doi:10.1644/06-MAMM-A-306.1.

- Horton, B.K., 2018a, Sedimentary record of Andean mountain building: *Earth-Science Reviews*, v. 178, p. 279–309, doi:10.1016/J.EARSCIREV.2017.11.025.
- Horton, B.K., 2018b, Tectonic Regimes of the Central and Southern Andes: Responses to Variations in Plate Coupling During Subduction: *Tectonics*, v. 37, p. 402–429, doi:10.1002/2017TC004624.
- Horton, B.K., and Fuentes, F., 2016, Sedimentary record of plate coupling and decoupling during growth of the Andes: *Geology*, v. 44, p. 647–650, doi:10.1130/G37918.1.
- Houssaye, A., Fernandez, V., and Billet, G., 2016, Hyperspecialization in Some South American Endemic Ungulates Revealed by Long Bone Microstructure: *Journal of Mammalian Evolution*, v. 23, p. 221–235, doi:10.1007/s10914-015-9312-y.
- Huang, S., Eronen, J.T., Janis, C.M., Saarinen, J.J., Silvestro, D., and Fritz, S.A., 2017, Mammal body size evolution in North America and Europe over 20 Myr: Similar trends generated by different processes: *Proceedings of the Royal Society B: Biological Sciences*, v. 284, doi:10.1098/rspb.2016.2361.
- Huang, S., Meijers, M.J.M., Eyres, A., Mulch, A., and Fritz, S.A., 2019, Unravelling the history of biodiversity in mountain ranges through integrating geology and biogeography: *Journal of Biogeography*, v. 46, p. 1777–1791, doi:10.1111/jbi.13622.
- Hunt, G., 2006a, Fitting and comparing models of phyletic evolution: random walks and beyond: *Paleobiology*, v. 32, p. 578–601, doi:10.1666/05070.1.
- Hunt, G., 2008, Gradual or pulsed evolution: when should punctuational explanations be preferred? *Paleobiology*, v. 34, p. 360–377, doi:10.1666/07073.1.
- Hunt, G., 2006b, paleoTS: modeling evolution in paleontological time-series, Version 0.1–2.:
- Hunt, G., 2007, The relative importance of directional change, random walks, and stasis in the evolution of fossil lineages: *Proceedings of the National Academy of Sciences of the United States of America*, v. 104, p. 18404–18408, doi:10.1073/pnas.0704088104.
- Hunt, G., Cronin, T.M., and Roy, K., 2005, Species-energy relationship in the deep sea: a test using the Quaternary fossil record: *Ecology Letters*, v. 8, p. 739–747, doi:10.1111/j.1461-0248.2005.00778.x.
- Hunt, G., Hopkins, M.J., and Lidgard, S., 2015, Simple versus complex models of trait evolution and stasis as a response to environmental change.: *Proceedings of the National Academy of Sciences of the United States of America*, v. 112, p. 4885–90, doi:10.1073/pnas.1403662111.
- Hunt, G., and Rabosky, D.L., 2014, Phenotypic Evolution in Fossil Species: Pattern and Process: *Annual Review of Earth and Planetary Sciences*, v. 42, p. 421–441, doi:10.1146/annurev-earth-040809-152524.
- Hunt, G., and Roy, K., 2006, Climate change, body size evolution, and Cope's Rule deep-sea ostracodes: *Proceedings of the National Academy of Sciences of the United States of America*, v. 103, p. 1347–1352, doi:10.1073/pnas.0510550103.
- Hunt, G., Wicaksono, S.A., Brown, J.E., and Macleod, K.G., 2010, Climate-driven body-size trends in the ostracod fauna of the deep Indian Ocean: *Palaeontology*, v. 53, p. 1255–1268,

- doi:10.1111/j.1475-4983.2010.01007.x.
- Huston, M.A., and Wolverton, S., 2011, Regulation of animal size by eNPP, Bergmann's rule, and related phenomena: *Ecological Monographs*, v. 81, p. 349–405, doi:10.1890/10-1523.1.
- De Iuliis, G., Brandoni, D., and Scillato-Yané, G.J., 2008, New remains of *Megatheriulus patagonicus* Ameghino, 1904 (Xenarthra, Megatheriidae): Information on primitive features of megatheriines: *Journal of Vertebrate Paleontology*, v. 28, p. 181–196, doi:10.1671/0272-4634(2008)28[181:NROMPA]2.0.CO;2.
- de Iuliis, G., Pujos, F., Toledo, N., Bargo, M.S., and Vizcaíno, S.F., 2014, *Eucholoeops* Ameghino, 1887 (Xenarthra, Tardigrada, Megalonychidae) de la Formación Santa Cruz de Patagonie Argentine: Implications pour la systématique des paresseux santacruziens: *Geodiversitas*, v. 36, p. 209–255, doi:10.5252/g2014n2a2.
- Ives, A.R., 2019, R 2 s for Correlated Data: Phylogenetic Models, LMMs, and GLMMs: *Systematic Biology*, v. 68, p. 234–251, doi:10.1093/sysbio/syy060.
- Jablonski, D., 2008, Species Selection: Theory and Data: *Annual Review of Ecology, Evolution, and Systematics*, v. 39, p. 501–524, doi:10.1146/annurev.ecolsys.39.110707.173510.
- Janis, C.M., 1990, Correlation of cranial and dental variables with dietary preferences in mammals: a comparison of macropodoids and ungulates, in Damuth, J. and MacFadden B.J eds., *Body Size in Mammalian Paleobiology: Estimation and Biological Implications*, Cambridge University Press, p. 255–299.
- Janis, C.M., and Fortelius, M., 1988, On the means whereby mammals achieve increased functional durability of their dentitions, with special reference to limiting factors.: *Biological reviews of the Cambridge Philosophical Society*, v. 63, p. 197–230, doi:10.1111/j.1469-185x.1988.tb00630.x.
- Jordan, T.E., Burns, W.M., Veiga, R., Pángaro, F., Copeland, P., Kelley, S., and Mpodozis, C., 2001, Extension and basin formation in the southern Andes caused by increased convergence rate: A mid-Cenozoic trigger for the Andes: *Tectonics*, v. 20, p. 308–324, doi:10.1029/1999TC001181.
- Jordana, X., Marín-Moratalla, N., de Miguel, D., Kaiser, T.M., and Köhler, M., 2012, Evidence of correlated evolution of hypsodonty and exceptional longevity in endemic insular mammals: *Proceedings of the Royal Society B: Biological Sciences*, v. 279, p. 3339–3346, doi:10.1098/rspb.2012.0689.
- Kaiser, T.M., Müller, D.W.H., Fortelius, M., Schulz, E., Codron, D., and Clauss, M., 2013, Hypsodonty and tooth facet development in relation to diet and habitat in herbivorous ungulates: implications for understanding tooth wear: *Mammal Review*, v. 43, p. 34–46, doi:10.1111/j.1365-2907.2011.00203.x.
- Kapur, V. V., Yelo, B.A.G., and Morthekai, P., 2020, Cenogram analyses as habitat indicators for Paleogene-Neogene mammalian communities across the globe, with an emphasis on the early Eocene Cambay Shale mammalian community from India: *Journal of Iberian Geology*, v. 46, p. 291–310, doi:10.1007/s41513-020-00131-2.
- Kausel, E., 1944, Contribución al estudio de las Mirtáceas chilenas: *Revista Argentina de*

- Agronomía, v. 11, p. 320–327.
- Kay, S.M., and Copeland, P., 2006, Early to middle Miocene backarc magmas of the Neuquén Basin: Geochemical consequences of slab shallowing and the westward drift of South America, *in* Special Paper 407: Evolution of an Andean Margin: A Tectonic and Magmatic View from the Andes to the Neuquén Basin (35°–39°S lat), Geological Society of America, p. 185–213, doi:10.1130/2006.2407(09).
- Kay, R.F., Perry, J.M.G., Malinzak, M., Allen, K.L., Kirk, E.C., Plavcan, J.M., and Fleagle, J.G., 2012a, Paleobiology of Santacrucian primates, *in* Vizcaino, S.F., Kay, R.F., and Bargo, M.S. eds., Early Miocene Paleobiology in Patagonia, Cambridge, Cambridge University Press, p. 306–330, doi:10.1017/CBO9780511667381.017.
- Kay, R.F., Vizcaíno, S.F., and Bargo, M.S., 2012b, A review of the paleoenvironment and paleoecology of the Miocene Santa Cruz Formation, *in* Vizcaino, S.F., Kay, R.F., and Bargo, M.S. eds., Early Miocene Paleobiology in Patagonia, Cambridge, Cambridge University Press, p. 331–365, doi:10.1017/cbo9780511667381.018.
- Kay, R.F., Vizcaíno, S.F., Bargo, M.S., Spradley, J.P., and Cuitiño, J.I., 2021, Paleoenvironments and paleoecology of the Santa Cruz Formation (early-middle Miocene) along the Río Santa Cruz, Patagonia (Argentina): *Journal of South American Earth Sciences*, p. 103296, doi:10.1016/j.jsames.2021.103296.
- Kingsolver, J.G., and Pfennig, D.W., 2004, Individual-level selection as a cause of cope's rule of phyletic size increase: *Evolution*, v. 58, p. 1608–1612, doi:10.1111/j.0014-3820.2004.tb01740.x.
- Kohn, M.J., Strömberg, C.A.E., Madden, R.H., Dunn, R.E., Evans, S., Palacios, A., and Carlini, A.A., 2015, Quasi-static Eocene-Oligocene climate in Patagonia promotes slow faunal evolution and mid-Cenozoic global cooling: *Palaeogeography, Palaeoclimatology, Palaeoecology*, v. 435, p. 24–37, doi:10.1016/j.palaeo.2015.05.028.
- Kohn, M.J., Zanzatti, A., and Josef, J.A., 2010, Stable isotopes of fossil teeth and bones at Gran Barranca as monitors of climate change and tectonics, *in* Madden, R.H., Carlini, A.A., Vucetich, M.G., and Kay, R.F. eds., *The paleontology of Gran Barranca: evolution and environmental change through the middle Cenozoic of Patagonia*, Cambridge, Massachusetts, Cambridge University Press, p. 341–361.
- Köppen, W., 1931, *Grundriss der Klimakunde*: Berlin, Walter de Gruyter, 388 p.
- Kraglievich, L., 1930, La formación Friaseana del río Frías, río Fénix, Laguna Blanca, etc. y su fauna de mamíferos: *Physis*, v. 10, p. 127–161.
- Kramarz, A.G., 2009, Additions to the knowledge of *Astrapothericulus* (Mammalia, Astrapotheria): Craniodental anatomy, diversity and distribution: *Revista Brasileira de Paleontologia*, v. 12, p. 55–66, doi:10.4072/rbp.2009.1.05.
- Kramarz, A.G., 2006a, Eocardiids (Rodentia, Hystricognathi) from the Pinturas Formation, late early Miocene of Patagonia, Argentina: *Journal of Vertebrate Paleontology*, v. 26, p. 770–778, doi:10.1671/0272-4634(2006)26[770:ERHFTP]2.0.CO;2.
- Kramarz, A.G., 2006b, *Neoreomys* and *Scleromys* (Rodentia, Hystricognathi) from the Pinturas

- Formation, late Early Miocene of Patagonia, Argentina: *Revista del Museo Argentino de Ciencias Naturales*, v. 8, p. 53–62, doi:10.22179/revmacn.8.356.
- Kramarz, A.G., 2004, Octodontoids and erethizontoids (Rodentia, Hystricognathi) from the Pinturas Formation, Early - Middle Miocene of Patagonia, Argentina: *Ameghiniana*, v. 41, p. 199–216.
- Kramarz, A.G., 2002, Roedores chinchilloideos (Hystricognathi) de la Formación Pinturas, Mioceno temprano-medio de la provincia de Santa Cruz, Argentina: *Revista del Museo Argentino de Ciencias Naturales nueva serie*, v. 4, p. 167–180, <http://revista.macn.gov.ar/ojs/index.php/RevMus/article/view/9> (accessed April 2019).
- Kramarz, A.G., 1998, Un nuevo Dasyproctidae (Rodentia, Caviomorpha) del Mioceno inferior de Patagonia: *Ameghiniana*, v. 35, p. 181–192, <http://www.ameghiniana.org.ar/index.php/ameghiniana/article/view/2431> (accessed June 2019).
- Kramarz, A.G., and Bellosi, E.S., 2005, Hystricognath rodents from the Pinturas Formation, Early–Middle Miocene of Patagonia, biostratigraphic and paleoenvironmental implications: *Journal of South American Earth Sciences*, v. 18, p. 199–212, doi:10.1016/J.JSAMES.2004.10.005.
- Kramarz, A.G., and Bond, M., 2009, A new oligocene astrapothere (Mammalia, Meridiungulata) from Patagonia and a new appraisal of astrapothere phylogeny: *Journal of Systematic Palaeontology*, v. 7, p. 117–128, doi:10.1017/S147720190800268X.
- Kramarz, A.G., and Bond, M., 2010, Colhuehuapian Astrapotheriidae (Mammalia) from Gran Barranca south of Lake Colhue-Huapi, *in* Madden, R.H., Carlini, A.A., Vucetich, M.G., and Kay, R.F. eds., *The Paleontology of Gran Barranca: Evolution and Environmental Change through the Middle Cenozoic of Patagonia*, Cambridge, Cambridge University Press, p. 182–192.
- Kramarz, A.G., and Bond, M., 2005, Los Litopterna (Mammalia) de la Formación Pinturas, Mioceno Temprano-Medio de Patagonia: *Ameghiniana*, v. 42, p. 611–625.
- Kramarz, A.G., and Bond, M., 2008, Revision of *Parastrapotherium* (Mammalia, Astrapotheria) and other Deseadan astrapotheres of Patagonia: *Ameghiniana*, v. 45, p. 537–551.
- Kramarz, A.G., Bond, M., and Arnal, M., 2015, Systematic description of three new mammals (Notoungulata and Rodentia) from the early Miocene Cerro Bandera Formation, northern Patagonia, Argentina: *Ameghiniana*, v. 52, p. 585 – 597.
- Kramarz, A.G., Forasiepi, A.M., and Bond, M., 2011, Vertebrados Cenozóicos, *in* Leanza, H.A., Arregui, C., Carbone, O., Danieli, J.C., and Valles, J.M. eds., *Relatorio del XVIII Congreso Geológico Argentino. Geología y Recursos Naturales de la Provincia del Neuquén*, Neuquén, Argentina, p. 557–572.
- Kramarz, A.G., Forasiepi, A., Garrido, A., Bond, M., and Tambussi, C., 2005, Stratigraphy and vertebrates (Aves and Mammalia) from the Cerro Bandera Formation, Early Miocene of Neuquén Province, Argentina: *Revista Geologica de Chile*, v. 32, p. 273–291, doi:10.4067/S0716-02082005000200006.
- Kramarz, A.G., Vucetich, M.G., Carlini, A.A., Ciancio, M.R., Abello, M.A., Deschamps, C.M.,

- Gelfo, J.N., Madden, R.H., and Kay, R.F., 2010, A new mammal fauna at the top of the Gran Barranca sequence and its biochronological significance, *in* Madden, R.H., Carlini, A.A., Vucetich, M.G., and Kay, R. eds., *The Paleontology of Gran Barranca: Evolution and Environmental Change through the Middle Cenozoic of Patagonia*, Cambridge, p. 260–273.
- Lagabrielle, Y., Godd ris, Y., Donnadi u, Y., Malavieille, J., and Suarez, M., 2009, The tectonic history of Drake Passage and its possible impacts on global climate: *Earth and Planetary Science Letters*, v. 279, p. 197–211, doi:10.1016/j.epsl.2008.12.037.
- Lagomarsino, L.P., Condamine, F.L., Antonelli, A., Mulch, A., and Davis, C.C., 2016, The abiotic and biotic drivers of rapid diversification in Andean bellflowers (Campanulaceae): *New Phytologist*, v. 210, p. 1430–1442, doi:10.1111/nph.13920.
- Laznicka, P., 2010, Andean-type convergent continental margins (upper volcanic-sedimentary level), *in* *Giant Metallic Deposits*, Springer Berlin Heidelberg, p. 109–168, doi:10.1007/978-3-642-12405-1_6.
- Legendre, S., 1986, Analysis of mammalian communities from the late Eocene and Oligocene of Southern France: *Palaeovertebrata*, v. 16, p. 191–212.
- Lehtonen, S., Silvestro, D., Karger, D.N., Scotese, C., Tuomisto, H., Kessler, M., Pe a, C., Wahlberg, N., and Antonelli, A., 2017, Environmentally driven extinction and opportunistic origination explain fern diversification patterns: *Scientific Reports*, v. 7, p. 4831, doi:10.1038/s41598-017-05263-7.
- Lieberman, B.S., 2005, Geobiology and paleobiogeography: Tracking the coevolution of the Earth and its biota: *Palaeogeography, Palaeoclimatology, Palaeoecology*, v. 219, p. 23–33, doi:10.1016/j.palaeo.2004.10.012.
- Liow, L.H., and Stenseth, N.C., 2007, The rise and fall of species: implications for macroevolutionary and macroecological studies: *Proceedings of the Royal Society B: Biological Sciences*, v. 274, p. 2745–2752, doi:10.1098/rspb.2007.1006.
- L pez, G.M., Vucetich, M.G., Carlini, A.A., Bond, M., P rez, M.E., Ciancio, M.R., P rez, D.J., Arnal, M., and Olivares, A.I., 2011, New Miocene mammal assemblages from Neogene Manantiales Basin, Cordillera Frontal, San Juan, Argentina. *Cenozoic Geology of the Central Andes of Argentina (Salfity, JA; Marquillas, RA, 211-226.*, *in* Salfity, J.A. and Marquillas, R.A. eds., *Cenozoic Geology of the Central Andes of Argentina*, Salta, Argentina, SCS Publisher, p. 211–226.
- Lovegrove, B.G., and Mowoe, M.O., 2013, The evolution of mammal body sizes: responses to Cenozoic climate change in North American mammals: *Journal of Evolutionary Biology*, v. 26, p. 1317–1329, doi:10.1111/jeb.12138.
- Lowe, D.R., and Tice, M.M., 2007, Tectonic controls on atmospheric, climatic, and biological evolution 3.5-2.4 Ga: *Precambrian Research*, v. 158, p. 177–197, doi:10.1016/j.precamres.2007.04.008.
- Luna, D.A., 2015, Miocene ungulates from Laguna del Laja, Chile, and an assessment of the Laguna del Laja faunas: Ph.D. Thesis University of California, Santa Barbara, 287 p.
- Luo, Z.X., 2007, Transformation and diversification in early mammal evolution: *Nature*, v. 450, p.

- 1011–1019, doi:10.1038/nature06277.
- Lynch Alfaro, J.W., Cortés-Ortiz, L., Di Fiore, A., and Boubli, J.P., 2015, Special issue: Comparative biogeography of Neotropical primates: Molecular Phylogenetics and Evolution, v. 82, p. 518–529, doi:10.1016/j.ympev.2014.09.027.
- Lyons, T.W., Reinhard, C.T., and Planavsky, N.J., 2014, The rise of oxygen in Earth's early ocean and atmosphere: *Nature*, v. 506, p. 307–315, doi:10.1038/nature13068.
- Lyons, S.K., and Smith, F.A., 2010, Using macroecological approach to study geographic range, abundance and body size in the fossil record: *The Paleontological Society Papers*, v. 16, p. 117–141.
- Madden, R.H., 2014, *Hypsodonty in mammals: Evolution, geomorphology and the role of earth surface processes*: Cambridge and New York, Cambridge University Press, 1–423 p.
- Madden, R.H., Guerrero, J., Kay, R.F., Flynn, J.J., Swisher III, C.C., and Walton, A.H., 1997, The Laventan Stage and Age, *in* Kay, R.F., Madden, R.H., Cifelli, R.L., and Flynn, J.J. eds., *Vertebrate paleontology in the Neotropics: the Miocene fauna of La Venta, Colombia*, Smithsonian Institution Press, Washington, D.C, p. 499–519.
- Mannion, P.D., Benson, R.B.J., Carrano, M.T., Tennant, J.P., Judd, J., and Butler, R.J., 2015, Climate constrains the evolutionary history and biodiversity of crocodylians: *Nature Communications*, v. 6, p. 8438, doi:10.1038/ncomms9438.
- Marivaux, L., Vianey-Liaud, M., and Jaeger, J.J., 2004, High-level phylogeny of early Tertiary rodents: Dental evidence: *Zoological Journal of the Linnean Society*, v. 142, p. 105–134, doi:10.1111/j.1096-3642.2004.00131.x.
- Marshall, L.G., 1990, Fossil marsupials from the type Friasian Land Mammal Age (Miocene), Alto Río Cisnes, Aisen, Chile: *Andean Geology*, v. 17, p. 19–55, doi:10.5027/andgeov17n1-a02.
- Marshall, L.G., 1981, Review of the Hathlyacyninae, an extinct subfamily of South American “dog-like” marsupials: *Fieldiana Geology*, v. 7, p. 1–120.
- Marshall, L.G., 1980, Systematics of the South American marsupial family Caenolestidae: *Fieldiana: Geology*, v. 5, p. 1–145, doi:10.5962/bhl.title.3314.
- Marshall, L.G., Salinas, P., and Suarez, M., 1990, *Astrapotherium* sp. (Mammalia, Astrapotheriidae) from Miocene strata along the Quepuca river, central Chile: *Revista Geologica De Chile*, v. 17, p. 215–223.
- Martin, J.M., Mead, J.I., and Barboza, P.S., 2018, Bison body size and climate change: *Ecology and Evolution*, v. 8, p. 4564–4574, doi:10.1002/ece3.4019.
- Martinelli, A.G., Soto-Acuña, S., Goin, F.J., Kaluza, J., Bostelmann, J.E., Fonseca, P.H.M., Reguero, M.A., Leppe, M., and Vargas, A.O., 2021, New cladotherian mammal from southern Chile and the evolution of mesungulatid meridiolestidans at the dusk of the Mesozoic era: *Scientific Reports*, v. 11, p. 7594, doi:10.1038/s41598-021-87245-4.
- Martinod, J., Husson, L., Roperch, P., Guillaume, B., and Espurt, N., 2010, Horizontal subduction zones, convergence velocity and the building of the Andes: *Earth and Planetary Science Letters*, v. 299, p. 299–309, doi:10.1016/j.epsl.2010.09.010.
- McGrath, A.J., Anaya, F., and Croft, D.A., 2018, Two new macraucheniiids (Mammalia: Litopterna)

- from the late middle Miocene (Laventan South American Land Mammal Age) of Quebrada Honda, Bolivia: *Journal of Vertebrate Paleontology*, v. 38, p. e1461632, doi:10.1080/02724634.2018.1461632.
- McGrath, A.J., Flynn, J.J., and Wyss, A.R., 2020, Proterotheriids and macraucheniids (Litopterna: Mammalia) from the Pampa Castillo Fauna, Chile (early Miocene, Santacrucian SALMA) and a new phylogeny of Proterotheriidae: *Journal of Systematic Palaeontology*, v. 18, p. 717–738, doi:10.1080/14772019.2019.1662500.
- McKenna, M.C., and Bell, S.K., 1997, *Classification Of Mammals : above the species level*: New York, Columbia University Press, 631 p.
- McKenna, M.C., Wyss, A.R., and Flynn, J.J., 2006, Paleogene Pseudoglyptodont Xenarthrans from Central Chile and Argentine Patagonia: *American Museum Novitates*, v. 3536, p. 1–18, doi:10.1206/0003-0082(2006)3536[1:PPXFCC]2.0.CO;2.
- McNab, B.K., 2010, Geographic and temporal correlations of mammalian size reconsidered: A resource rule: *Oecologia*, v. 164, p. 13–23, doi:10.1007/s00442-010-1621-5.
- McShea, D.W., 1994, Mechanisms of large-scale evolutionary trends: *Evolution*, v. 48, p. 1747–1763, doi:10.1111/j.1558-5646.1994.tb02211.x.
- Meiri, S., and Dayan, T., 2003, On the validity of Bergmann's rule: *Journal of Biogeography*, v. 30, p. 331–351, doi:10.1046/j.1365-2699.2003.00837.x.
- Melnick, D., Rosenau, M., Folguera, A., and Echtler, H., 2006, Neogene tectonic evolution of the Neuquén Andes western flank (37–39°S), *in* Special Paper 407: Evolution of an Andean Margin: A Tectonic and Magmatic View from the Andes to the Neuquén Basin (35°–39°S lat), Geological Society of America, p. 73–95, doi:10.1130/2006.2407(04).
- Mendoza, M., Janis, C.M., and Palmqvist, P., 2006, Estimating the body mass of extinct ungulates: a study on the use of multiple regression: *Journal of Zoology*, v. 270, p. 90–101, doi:10.1111/j.1469-7998.2006.00094.x.
- Menéndez, I., Gómez Cano, A.R., García Yelo, B.A., Domingo, L., Domingo, M.S., Cantalapiedra, J.L., Blanco, F., and Hernández Fernández, M., 2017, Body-size structure of Central Iberian mammal fauna reveals semidesertic conditions during the middle Miocene Global Cooling Event (T. Smith, Ed.): *PLoS ONE*, v. 12, p. e0186762, doi:10.1371/journal.pone.0186762.
- Methner, K., Campani, M., Fiebig, J., Löffler, N., Kempf, O., and Mulch, A., 2020, Middle Miocene long-term continental temperature change in and out of pace with marine climate records: *Scientific Reports*, v. 10, p. 1–10, doi:10.1038/s41598-020-64743-5.
- Mitchell, M., Muftakhidinov, B., and Winchen, T., 2020, Engauge Digitizer Software Version 12.2.1:, doi:10.5281/zenodo.3941227.
- Mitchell, K.J., Scanferla, A., Soibelzon, E., Bonini, R., Ochoa, J., and Cooper, A., 2016, Ancient DNA from the extinct South American giant glyptodont *Doedicurus* sp. (Xenarthra: Glyptodontidae) reveals that glyptodonts evolved from Eocene armadillos: *Molecular Ecology*, v. 25, p. 3499–3508, doi:10.1111/mec.13695.
- Molnar, P., 2018, Simple concepts underlying the structure, support and growth of mountain ranges, high plateaus and other high terrain, *in* Hoorn, C., Perrigo, A., and Antonelli, A. eds.,

- Mountains, Climate and Biodiversity, Oxford, UK, p. 17–36.
- Molnar, P., and England, P., 1990, Late Cenozoic uplift of mountain ranges and global climate change: Chicken or egg? *Nature*, v. 346, p. 29–34, doi:10.1038/346029a0.
- Montoya-Sanhueza, G., Moreno, K., Bobe, R., Carrano, M.T., García, M., and Corgne, A., 2017, Peltephilidae and Mesotheriidae (Mammalia) from late Miocene strata of Northern Chilean Andes, Caragua: *Journal of South American Earth Sciences*, v. 75, p. 51–65, doi:10.1016/J.JSAMES.2017.01.009.
- Morrone, J.J., 2015, Track analysis beyond panbiogeography: *Journal of Biogeography*, v. 42, p. 413–425, doi:10.1111/jbi.12467.
- Muggeo, V.M.R., 2017, Interval estimation for the breakpoint in segmented regression: a smoothed score-based approach: *Australian & New Zealand Journal of Statistics*, v. 59, p. 311–322, doi:10.1111/anzs.12200.
- Mulch, A., 2016, Stable isotope paleoaltimetry and the evolution of landscapes and life: *Earth and Planetary Science Letters*, v. 433, p. 180–191, doi:10.1016/j.epsl.2015.10.034.
- Müller, R.D., Cannon, J., Qin, X., Watson, R.J., Gurnis, M., Williams, S., Pfaffelmoser, T., Seton, M., Russell, S.H.J., and Zahirovic, S., 2018, GPlates: Building a Virtual Earth Through Deep Time: *Geochemistry, Geophysics, Geosystems*, v. 19, p. 2243–2261, doi:10.1029/2018GC007584.
- Munizaga, F., 2020, Los peces óseos (Actinopterygii: Teleostei) del Mioceno de la Formación Cura-Mallín, en la zona de Lonquimay (38°27' S; 71°22' W, Provincia de Malleco) y sus implicaciones paleoambientales: Memoria de título, Departamento de Ciencias de la Tierra, Universidad de Concepción, 118 p.
- Muñoz-Ortiz, A., Velásquez-Álvarez, Á.A., Guarnizo, C.E., and Crawford, A.J., 2015, Of peaks and valleys: testing the roles of orogeny and habitat heterogeneity in driving allopatry in mid-elevation frogs (Aromobatidae: *Rheobates*) of the northern Andes (J. Stewart, Ed.): *Journal of Biogeography*, v. 42, p. 193–205, doi:10.1111/jbi.12409.
- Muñoz, J., and Niemeyer, H., 1984, Petrología de la formación Trapa-Trapa y consideraciones acerca del volcanismo mioceno entre los 36° y 39° lat. S (Cordillera Principal): *Revista geológica de Chile: An international journal on andean geology*, v. 23, p. 53–67.
- Naples, V.L., and McAfee, R.K., 2014, Chewing through the Miocene: An examination of the feeding musculature in the ground sloth *Hapalops* from South America (Mammalia: Pilosa): *F1000Research*, v. 3, doi:10.12688/f1000research.3282.1.
- Nasif, N.L., Musalem, S., and Cerdeño, E., 2000, A new toxodont from the late Miocene of Catamarca, Argentina, and a phylogenetic analysis of the Toxodontidae: *Journal of Vertebrate Paleontology*, v. 20, p. 591–600, doi:10.1671/0272-4634(2000)020[0591:ANTFTL]2.0.CO;2.
- Niemeyer, H.R., and Muñoz, J.B., 1983, Hoja Laguna de La Laja: Región del BioBío. Carta Geología de Chile 57, scale 1:250.000: Servicio Nacional de Geología y Minería, Santiago, Chile.
- Núñez-Flores, M., Solórzano, A., Hernández, C.E., and López-González, P.J., 2019, A latitudinal

- diversity gradient of shallow-water gorgonians (Cnidaria: Octocorallia: Alcyonacea) along the Tropical Eastern Pacific Ocean: testing for underlying mechanisms: *Marine Biodiversity*, v. 49, p. 2787–2800, doi:10.1007/s12526-019-01006-1.
- Ofstad, E.G., Herfindal, I., Solberg, E.J., and Sæther, B.E., 2016, Home ranges, habitat and body mass: simple correlates of home range size in ungulates: *Proceedings. Biological sciences*, v. 283, doi:10.1098/rspb.2016.1234.
- Ortiz-Jaureguizar, E., and Cladera, G.A., 2006, Paleoenvironmental evolution of southern South America during the Cenozoic: *Journal of Arid Environments*, v. 66, p. 498–532, doi:10.1016/J.JARIDENV.2006.01.007.
- Orts, D.L., Folguera, A., Encinas, A., Ramos, M., Tobal, J., and Ramos, V.A., 2012, Tectonic development of the North Patagonian Andes and their related Miocene foreland basin (41°30'–43°S): *Tectonics*, v. 31, p. n/a-n/a, doi:10.1029/2011TC003084.
- Palazzesi, L., and Barreda, V., 2012, Fossil pollen records reveal a late rise of open-habitat ecosystems in Patagonia: *Nature Communications*, v. 3, p. 1294, doi:10.1038/ncomms2299.
- Palazzesi, L., Barreda, V.D., Cuitiño, J.I., Guler, M.V., Tellería, M.C., and Ventura Santos, R., 2014, Fossil pollen records indicate that Patagonian desertification was not solely a consequence of Andean uplift: *Nature Communications*, v. 5, p. 3558, doi:10.1038/ncomms4558.
- Palma-Heldt, S., 1983, Estudio palinológico del Terciario sedimentario de Lonquimay, Provincia de Malleco, Chile: *Revista Geológica de Chile*, v. 18, p. 55–75.
- Palma-Heldt, S., and Rondanelli, M., 1990, Registro de improntas del Terciario del sector Cerro Rucañanco, Lonquimay, Chile, *in* Segundo Simposio sobre el Terciario de Chile, Concepción, Concepcion, Chile, p. 335–342.
- Pardiñas, U.F.J., 1991, Primer registro de Primates y otros vertebrados para la Formación Collon Cura (Mioceno Medio) del Neuquen, Argentina.: *Ameghiniana*, v. 28, p. 197–199.
- Parodiz, J., 1969, The Tertiary non-marine Mollusca of South America: *Annals of Carnegie Museum*, v. 40, p. 1–242.
- Pascual, R., and Jaureguizar, E.O., 1990, Evolving climates and mammal faunas in cenozoic South America: *Journal of Human Evolution*, v. 19, p. 23–60, doi:10.1016/0047-2484(90)90011-Y.
- Pascual, R., and Odreman-Rivas, O.E., 1971, Evolución de las comunidades de los Vertebrados del Terciario argentino. Los aspectos paleozoogeográficos y paleoclimáticos: *Ameghiniana*, v. 8, p. 372–412.
- Patterson, B., and Pascual, R., 1968, Evolution of Mammals in Southern Continents. V. Fossil Mammal Fauna of South America.: *The Quarterly Review of Biology*, v. 43, p. 409–451.
- Patton, J.L., Pardiñas, U.F.J., and D'Elía, G., 2015, *Mammals of South America. Volume 2, Rodents*: Chicago, The University of Chicago Press, 1336 p.
- Pedroza, V., Le Roux, J.P., Gutiérrez, N.M., and Vicencio, V.E., 2017, Stratigraphy, sedimentology, and geothermal reservoir potential of the volcanoclastic Cura-Mallín

- succession at Lonquimay, Chile: *Journal of South American Earth Sciences*, v. 77, p. 1–20, doi:10.1016/J.JSAMES.2017.04.011.
- Pérez, M.E., and Vucetich, M.G., 2012, A revision of the fossil genus *Phanomys* Ameghino, 1887 (Rodentia, Hystricognathi, Caviioidea) from the early Miocene of Patagonia (Argentina) and the acquisition of euhypsodonty in Caviioidea *sensu stricto*: *Paläontologische Zeitschrift*, v. 86, p. 187–204, doi:10.1007/s12542-011-0120-2.
- Pérez, M.E., Vucetich, M.G., and Kramarz, A.G., 2010, The first eocardiidae (Rodentia) in the Colhuehuapian (Early Miocene) of Bryn Gwyn (Northern Chubut, Argentina) and the early evolution of the peculiar cavioid rodents: *Journal of Vertebrate Paleontology*, v. 30, p. 528–534, doi:10.1080/02724631003618223.
- Peters, R.H., 1986, *The ecological implications of body size*: Cambridge University Press, 329 p.
- Picard, D., Sempere, T., and Plantard, O., 2008, Direction and timing of uplift propagation in the Peruvian Andes deduced from molecular phylogenetics of highland biotaxa: *Earth and Planetary Science Letters*, v. 271, p. 326–336, doi:10.1016/j.epsl.2008.04.024.
- Pinheiro, J., Bates, D., DebRoy, S., Sarkar, D., and R Core Team, 2020, nlme: Linear and Nonlinear Mixed Effects Models., <https://cran.r-project.org/package=nlme> (accessed August 2020).
- Piras, P. et al., 2018, Evolution of the sabertooth mandible: A deadly ecomorphological specialization: *Palaeogeography, Palaeoclimatology, Palaeoecology*, v. 496, p. 166–174, doi:10.1016/j.palaeo.2018.01.034.
- Prevosti, F.J., and Forasiepi, A.M., 2018a, Evolution of South American Mammalian Predators During the Cenozoic: Paleobiogeographic and Paleoenvironmental Contingencies: Springer, 155–196 p., doi:10.1007/978-3-319-03701-1_6.
- Prevosti, F.J., and Forasiepi, A.M., 2018b, South American endemic mammalian predators (order sparassodonta), *in* Prevosti, F.J. and Forasiepi, A.M. eds., Springer Geology, Cham, Switzerland, Springer, p. 39–84, doi:10.1007/978-3-319-03701-1_3.
- Prevosti, F.J., Forasiepi, A.M., Ercoli, M.D., and Turazzini, G.F., 2013, Paleocology of the mammalian carnivores (Metatheria, Sparassodonta) of the Santa Cruz Formation (late Early Miocene), *in* Early Miocene Paleobiology in Patagonia, Cambridge University Press, p. 173–193, doi:10.1017/cbo9780511667381.012.
- R Core Team, 2018, R: A Language and Environment for Statistical Computing. R Foundation for Statistical Computing. R Foundation for Statistical Computing:
- Radic, J.P., 2010, Las cuencas cenozoicas y su control en el volcanismo de los Complejos Nevados de Chillan y Copahue-Callaqui (Andes del Sur, 36-39°S): *Andean geology*, v. 37, p. 220–246, doi:10.4067/S0718-71062010000100009.
- Radic, J.P., Rojas, L., Carpinelli, A., and Zurita, E., 2002, Evolución tectónica de la cuenca terciaria de Cura-Mallín, región cordillerana chileno argentina (36 30'-39 00'S), *in* XV Congreso Geológico Argentino, El Calafate, Argentina, p. Vol. 15, 233-241.
- Rahbek, C. et al., 2019, Building mountain biodiversity: Geological and evolutionary processes: *Science*, v. 365, p. 1114–1119, doi:10.1126/science.aax0151.

- Raia, P., Carotenuto, F., Eronen, J.T., and Fortelius, M., 2011, Longer in the tooth, shorter in the record? The evolutionary correlates of hypsodonty in neogene ruminants: Proceedings of the Royal Society B: Biological Sciences, v. 278, p. 3474–3481, doi:10.1098/rspb.2011.0273.
- Raia, P., Carotenuto, F., Meloro, C., Piras, P., and Pushkina, D., 2010, The shape of contention: Adaptation, history, and contingency in ungulate mandibles: *Evolution*, v. 64, p. 1489–1503, doi:10.1111/j.1558-5646.2009.00921.x.
- Raigemborn, M.S., Matheos, S.D., Krapovickas, V., Vizcaíno, S.F., Bargo, M.S., Kay, R.F., Fernicola, J.C., and Zapata, L., 2015, Paleoenvironmental reconstruction of the coastal Monte León and Santa Cruz formations (Early Miocene) at Rincón del Buque, Southern Patagonia: A revisited locality: *Journal of South American Earth Sciences*, v. 60, p. 31–55, doi:10.1016/j.jsames.2015.03.001.
- Rambaut, A., Drummond, A.J., Xie, D., Baele, G., and Suchard, M.A., 2018, Posterior Summarization in Bayesian Phylogenetics Using Tracer 1.7 (E. Susko, Ed.): *Systematic biology*, v. 67, p. 901–904, doi:10.1093/sysbio/syy032.
- Ramos, V.A., 2009, Anatomy and global context of the Andes: Main geologic features and the Andean orogenic cycle, *in* *Memoir of the Geological Society of America*, Geological Society of America, v. 204, p. 31–65, doi:10.1130/2009.1204(02).
- Ramos, V.A., 2010, The tectonic regime along the Andes: Present-day and Mesozoic regimes: *Geological Journal*, v. 45, p. 2–25, doi:10.1002/gj.1193.
- Rasia, L.L., 2016, Los Chinchillidae (Rodentia, Caviomorpha) fósiles de la República Argentina: sistemática, historia evolutiva y biogeográfica, significado bioestratigráfico y paleoambiental: Ph. D. thesis, Universidad Nacional de La Plata.
- Rasia, L.L., and Candela, A.M., 2019, Upper molar morphology, homologies and evolutionary patterns of chinchilloid rodents (Mammalia, Caviomorpha): *Journal of Anatomy*, v. 234, p. 50–65, doi:10.1111/joa.12895.
- Reguero, M.A., Candela, A.M., and Cassini, G.H., 2010, Hypsodonty and body size in rodent-like notoungulates, *in* Madden, R.H., Carlini, A.A., Vucetich, M.G., and Kay, R.F. eds., *The paleontology of Gran Barranca: Evolution and Environmental Change through the Middle Cenozoic of Patagonia*, Cambridge University Press, p. 358–367.
- Reguero, M.A., Dozo, M.T., and Cerdeño, E., 2007, A poorly known rodentlike mammal (Pachyrhinae, Hegetotheriidae, Notoungulata) from the Deseadan (Late Oligocene) of Argentina. Paleocology, biogeography, and radiation of the rodentlike ungulates in South America: *Journal of Paleontology*, v. 81, p. 1301–1307, doi:10.1666/05-100.1.
- Reguero, M.A., and Prevosti, F.J., 2010, Rodent-like notoungulates (Typotheria) from Gran Barranca, Chubut Province, Argentina: phylogeny and systematics, *in* Madden, R.H., Carlini, A.A., Vucetich, M.G., and Kay, R.F. eds., *The paleontology of Gran Barranca: evolution and environmental change through the Middle Cenozoic of Patagonia*, Cambridge University Press, p. 152–162.
- Reguero, M.A., Ubilla, M., and Perea, D., 2003, A new species of *Eopachyrucos* (Mammalia,

- Notoungulata, Interatheriidae) from the Late Oligocene of Uruguay: *Journal of Vertebrate Paleontology*, v. 23, p. 445–457, doi:10.1671/0272-4634(2003)023[0445:ansoem]2.0.co;2.
- Rincón, A.D., Shockey, B.J., Anaya, F., and Solórzano, A., 2015, Palaeothentid Marsupials of the Salla Beds of Bolivia (Late Oligocene): Two New Species and Insights into the Post-Eocene Radiation of Palaeothentoids: *Journal of Mammalian Evolution*, v. 22, p. 455–471, doi:10.1007/s10914-015-9295-8.
- Rincón, A.D., Solórzano, A., Benammi, M., Vignaud, P., and Gregory McDonald, H., 2014, Cronología y geología de una asociación de mamíferos del Mioceno Temprano en el Norte de América del Sur, cerro La Cruz (Formación Castillo), Estado Lara, Venezuela: implicaciones para las hipótesis del ‘cambio del curso del río Orinoco’: *Andean Geology*, v. 41, p. 507–528, doi:10.5027/andgeoV41n3-a02.
- Rincón, A.D., Solórzano, A., Macsotay, O., McDonald, H.G., and Núñez-Flores, M., 2016, A new Miocene vertebrate assemblage from the Río Yuca Formation (Venezuela) and the northernmost record of typical Miocene mammals of high latitude (Patagonian) affinities in South America: *Geobios*, v. 49, p. 395–405, doi:10.1016/j.geobios.2016.06.005.
- Ripley, B., Venables, B., Bates, D., Hornik, K., Gebhardt, A., and Firth, D., 2020, Package “MASS”:, <ftp://192.218.129.11/pub/CRAN/web/packages/MASS/MASS.pdf> (accessed October 2020).
- Rojas Vera, E.A., Folguera, A., Zamora Valcarce, G., Bottesi, G., and Ramos, V.A., 2014, Structure and development of the Andean system between 36° and 39°S: *Journal of Geodynamics*, v. 73, p. 34–52, doi:10.1016/j.jog.2013.09.001.
- Rojas Vera, E.A., Mescua, J., Folguera, A., Becker, T.P., Sagripanti, L., Fennell, L., Orts, D., and Ramos, V.A., 2015, Evolution of the Chos Malal and Agrío fold and thrust belts, Andes of Neuquén: Insights from structural analysis and apatite fission track dating: *Journal of South American Earth Sciences*, v. 64, p. 418–433, doi:10.1016/j.jsames.2015.10.001.
- Rojas Vera, E.A., Orts, D.L., Folguera, A., Zamora Valcarce, G., Bottesi, G., Fennell, L., Chiachiarelli, F., and Ramos, V.A., 2016, The Transitional Zone Between the Southern Central and Northern Patagonian Andes (36–39°S), *in* Springer, Cham, p. 99–114, doi:10.1007/978-3-319-23060-3_5.
- Rosselot, E.A., Hurley, M., Sagripanti, L., Fennell, L., Iannelli, S., Orts, D., Encinas, A., Litvak, V., and Folguera, A., 2019a, Tectonics associated with the late Oligocene to early Miocene units of the High Andes (Cura Mallín Formation). A review of the geochronological, thermochronological and geochemical data, *in* Kietzmann, D. and Folguera, A. eds., *Opening and closure of the Neuquén Basin in the Southern Andes*, p. 431–448.
- Rosselot, E.A., Hurley, M., Sofia, I., Fennell, L., Astort, A., Orts, D., Encinas, A., and Folguera, A., 2018, Un análisis de las mecánicas de formación y sedimentación asociadas a la cuenca de Cura Mallín (Andes Centrales Australes), *in* XV Congreso Geológico Chileno, Concepcion, Chile, p. 1144.
- Rosselot, E.A., Hurley, M., Solórzano, A., Sagripanti, L., Fennell, L., Orts, D.L., Encinas, A., and Folguera, A., 2019b, Preliminary results on the tectonic genesis of the Cura Mallín Formation

- in the Southern Central Andes (36° - 39° S), *in* 8th International Symposium on Andean Geodynamics (ISAG).
- Le Roux, J.P., 2012, A review of Tertiary climate changes in southern South America and the Antarctic Peninsula. Part 2: continental conditions: *Sedimentary Geology*, v. 247–248, p. 21–38, doi:10.1016/J.SEDGEO.2011.12.001.
- Rubilar, A., 1994, Diversidad ictiológica en depósitos continentales miocenos de la Formación Cura-Mallín, Chile (37-39°S): implicancias paleogeográficas: *Andean Geology*, v. 21, p. 3–29, doi:10.5027/andgeov21n1-a01.
- Rubilar, A., and Abad, E., 1990, *Percichthys Sylvaniae* sp. nov. del terciario de los Andes Sur-Centrales de Chile (Pisces, Perciformes, Percichthyidae):, doi:10.5027/ANDGEOV17N2-A06.
- Rubilar, A., and Wall, R., 1990, Primer registro en Chile de siluriformes -pisces, ostariophysiformes procedente del mioceno de Lonquimay, *in* II Simposio sobre el Terciario de Chile, Concepción, p. 275–284.
- Saarinen, J., 2014, Ecometrics of large herbivorous land mammals in relation to climatic and environmental changes during the Pleistocene: Ph.d. Thesis, Faculty of Sciences. University of Helsinki, 42 p.
- Salinas, P., 1979, Geología del área Lolco - Lonquimay, Cordillera de los Andes, Alto Bio-Bio, IX Región, Chile: Undergraduate Thesis, University of Chile, 120 p.
- Scarano, A.C., Vera, B., and Reguero, M., 2021, Evolutionary Trends of Protypotherium (Interatheriidae, Notoungulata) Lineage throughout the Miocene of South America: *Journal of Mammalian Evolution*, p. 1–11, doi:10.1007/s10914-020-09534-5.
- Schmidt, G.I., 2015, Actualización sistemática y filogenia de los Protheroheriidae (Mammalia, Litopterna) del “Mesopotamiense” (Mioceno tardío) de Entre Ríos, Argentina: *Revista Brasileira de Paleontologia*, v. 18, p. 521–546, doi:10.4072/rbp.2015.3.14.
- Schmidt, G.I., 2013, Litopterna y Notoungulata (Mammalia) de la Formación Ituzzaingó (Mioceno tardío-Plioceno) de la Provincia de Entre Ríos: sistemática, bioestratigrafía y paleobiogeografía.: Phd thesis, Universidad Nacional de La Plata, La Plata, Argentina., 335 p p.
- Schmidt, G.I., and Ferrero, B.S., 2014, Taxonomic reinterpretation of *Theosodon hystatus* Cabrera and Kraglievich, 1931 (Litopterna, Macraucheniiidae) and phylogenetic relationships of the family: *Journal of Vertebrate Paleontology*, v. 34, p. 1231–1238, doi:10.1080/02724634.2014.837393.
- Schmidt, G.I., Hernández Del Pino, S., Muñoz, N.A., and Fernández, M., 2019, Litopterna (Mammalia) from the Santa Cruz Formation (Early-Middle Miocene) at the Río Santa Cruz, Southern Argentina: *Publicación Electrónica de la Asociación Paleontológica Argentina*, v. 19, p. 170–192, doi:10.5710/PEAPA.13.08.2019.290.
- Schrag, D.P., and Hoffman, P.F., 2001, Life, geology and snowball Earth: *Nature*, v. 409, p. 306–306, doi:10.1038/35053170.
- Scillato-Yané, G.J., 1977a, Notas sobre los Dasypodidae (Mammalia, Edentata) del Plioceno del

- territorio argentino I. Los restos de edad Chasiquense (Plioceno inferior) del sur de la Provincia de Buenos Aires: *Ameghiniana*, v. 14, p. 133–144.
- Scillato-Yané, G.J., 1977b, Sur quelques Glyptodontidae nouveaux (Mammalia, Edentata) du Déséadien (Oligocène inférieur) de Patagonie (Argentine): *Bulletin du Muséum National D'Histoire Naturelle*, v. 64, p. 249–262.
- Scillato-Yané, G.J., and Carlini, A.A., 1998, Nuevos Xenarthra del Friasense (Mioceno medio) de Argentina: *Studia Geologica Salmanticensia*, v. 34, p. 43–67, doi:[0211-8327 (1998) 34; 43-67].
- Scillato-Yané, G.J., Góis, F., Zurita, A.E., Carlini, A.A., Gonzáles, L.R., Krmpotic, C.M., Oliva, C., and Zamorano, M., 2013, Los Cingulata (Mammalia, Xenarthra) del “Conglomerado Osífero” (Mioceno Tardío) de la Formación Ituzaingó de Entre Ríos, Argentina, *in* Brandoni, D. and Noriega, J.I. eds., *El Neógeno de la Mesopotamia Argentina Asociación Paleontológica Argentina Publicación Especial*, Buenos Aires, Asociación Paleontológica Argentina, v. 14, p. 118–134.
- Scillato-Yané, G.J., Krmpotic, C.M., and Esteban, G.I., 2010, The species of genus *Chasicotatus* Scillato-Yané (Eutatini, Dasypodidae): *Revista Mexicana de Ciencias Geológicas*, v. 27, p. 43–55.
- Scott, W.B., 1905, Mammalia of the Santa Cruz beds, Part III., *in* Report of Princeton University Expedition to Patagonia, 1896-1899, v. 5, p. 1- 491 + Plates.
- Scott, W.B., 1910, Mammalia of the Santa Cruz Beds. Part I. Litopterna: Reports of the Princeton University Expedition to Patagonia (1896–1899), v. 7, p. 1–156.
- Scott, W.B., 1912, Part II: Toxodonta of the Santa Cruz beds, *in* Scott, W.B. ed., Report of Princeton University Expedition to Patagonia, Stuttgart, E. Schweizerbart'sche Verlagshandlung, p. 111–300.
- Semprebon, G.M., Rivals, F., and Janis, C.M., 2019, The role of grass vs. Exogenous abrasives in the paleodietary patterns of North American: *Frontiers in Ecology and Evolution*, v. 7, doi:10.3389/fevo.2019.00065.
- Seoane, F.D., and Cerdeño, E., 2019, Systematic revision of *Hegetotherium* and *Pachyrukhos* (Hegetotheriidae, Notoungulata) and a new phylogenetic analysis of Hegetotheriidae: *Journal of Systematic Palaeontology*, p. 1–29, doi:10.1080/14772019.2018.1545146.
- SERNAGEOMIN, 2003, Mapa geológico de Chile, versión digital, escala 1:1.000.000: Publicación Geológica Digital, Servicio Nacional de Geología y Minería, Chile, v. 4, p. 1–23.
- Shockey, B.J., Flynn, J.J., Croft, D.A., Gans, P.B., and Wyss, A.R., 2012, New leontiniid Notoungulata (Mammalia) from Chile and Argentina: comparative anatomy, character analysis, and phylogenetic hypotheses.: *American Museum novitates*, v. 3737, p. 1–64.
- Siler, N., Roe, G., and Durrán, D., 2012, On the Dynamical Causes of Variability in the Rain-Shadow Effect: A Case Study of the Washington Cascades: *Journal of Hydrometeorology*, v. 14, p. 122–139, doi:10.1175/jhm-d-12-045.1.
- Silvestro, D., Salamin, N., Antonelli, A., and Meyer, X., 2019a, Improved estimation of macroevolutionary rates from fossil data using a Bayesian framework: *Paleobiology*, v. 45,

- p. 546–570, doi:10.1017/pab.2019.23.
- Silvestro, D., Salamin, N., and Schnitzler, J., 2014a, PyRate: A new program to estimate speciation and extinction rates from incomplete fossil data: *Methods in Ecology and Evolution*, v. 5, p. 1126–1131, doi:10.1111/2041-210X.12263.
- Silvestro, D., and Schnitzler, J., 2018, Inferring macroevolutionary dynamics in mountain systems from fossils, *in* Hoorn, C., Perrigo, A., and Antonelli, A. eds., *Mountains, Climate and Biodiversity*, p. 217–230.
- Silvestro, D., Schnitzler, J., Liow, L.H., Antonelli, A., and Salamin, N., 2014b, Bayesian estimation of speciation and extinction from incomplete fossil occurrence data: *Systematic Biology*, v. 63, p. 349–367, doi:10.1093/sysbio/syu006.
- Silvestro, D., Tejedor, M.F., Serrano-Serrano, M.L., Loiseau, O., Rossier, V., Rolland, J., Zizka, A., Höhna, S., Antonelli, A., and Salamin, N., 2019b, Early Arrival and Climatically-Linked Geographic Expansion of New World Monkeys from Tiny African Ancestors: *Systematic Biology*, v. 68, p. 78–92, doi:10.1093/sysbio/syy046.
- Simpson, G.G., 1980, *Splendid isolation: the curious history of South American mammals.*: New Haven, Yale University Press, 275 p.
- Simpson, G.G., 1944, *Tempo and Mode in Evolution* -: New York, Columbia University Press, 237 p.
- Sinclair, W.J., 1908, The Santa Cruz Typotheria: *Proceedings of the American Philosophical Society*, v. 47, p. 64–78, doi:10.1016/S0016-0032(38)92229-X.
- Smith, F.A. et al., 2016, Body Size Evolution Across the Geozoic: *Annual Review of Earth and Planetary Sciences*, v. 44, p. 523–553, doi:10.1146/annurev-earth-060115-012147.
- Smith, F.A. et al., 2004, Similarity of mammalian body size across the taxonomic hierarchy and across space and time: *American Naturalist*, v. 163, p. 672–691, doi:10.1086/382898.
- Solórzano, A., Encinas, A., Bobe, R., Maximiliano, R., and Carrasco, G., 2019, The Early to late Middle Miocene mammalian assemblages from the Cura-Mallín Formation, at Lonquimay, southern Central Andes, Chile (~38°S): Biogeographical and paleoenvironmental implications: *Journal of South American Earth Sciences*, v. 96, p. 1–18, doi:10.1016/j.jsames.2019.102319.
- Solórzano, A., Encinas, A., Kramarz, A., Carrasco, G., Montoya-Sanhueza, G., and Bobe, R., 2021, Late early Miocene mammals from the Laguna del Laja, Cura-Mallín Formation, south-central Chile (~37°S) and their biogeographical, and paleoenvironmental significance: *Journal of South American Earth Sciences*,.
- Solórzano, A., Encinas, A., Kramarz, A.G., Carrasco, G., Montoya-Sanhueza, G., Reyes, M., and Bobe, R., 2020a, Late Early Miocene caviomorph rodents from the Laguna del Laja (~37° S), Cura-Mallín Formation, south central Chile: *Journal of South American Earth Sciences*, v. 102, p. 1–11, doi:10.1016/j.jsames.2020.102658.
- Solórzano, A., and Núñez-Flores, M., 2021, Evolutionary trends of body size and hypsodonty in notoungulates and their probable drivers: *Palaeogeography, Palaeoclimatology, Palaeoecology*, v. 568, p. 110306, doi:10.1016/j.palaeo.2021.110306.

- Solórzano, A., Núñez-Flores, M., Inostroza-Michael, O., and Hernández, C.E., 2020b, Biotic and abiotic factors driving the diversification dynamics of Crocodylia: *Palaeontology*, v. 63, p. 415–429, doi:10.1111/pala.12459.
- Soria, M., 1981, Los Liptoterna del Colhuehuapense (Oligoceno tardío) de la Argentina: *Revista del Museo Argentino de Ciencias Naturales "Bernardino Rivadavia, "Serie Paleontología"*, v. 3, p. 1–54.
- Soria, M., 2001, Los Protheroheriidae (Liptoterna, Mammalia), sistemática, origen y filogenia: *Monografías del Museo Argentino de Ciencias Naturales "Bernardino Rivadavia,"* v. 1, p. 1–167.
- Soria, M.F., and Hoffstetter, R., 1985, *Pternoconius tournoueri*, nueva especie de Macrauchenidae (Mammalia, Liptoterna) de edad Colhuehuapense (Oligoceno tardío, Provincia de Chubut, República Argentina: *Ameghiniana*, v. 22 (3–4), p. 149–158.
- Soto-Acuña, S., Alarcón, J., Yury-Yáñez, R.E., Otero, R.A., and Sallaberry, M., 2013, Nuevos materiales de *Meganhinga chilensis* (Suliformes: Anhingidae) del Mioceno temprano de Lonquimay, Región de la Araucanía, Chile Central, *in XXVII Jornadas Argentinas de Paleontología de Vertebrados*, p. 84.
- Spikings, R.A., Dungan, M., Foeken, J., Carter, A., Page, L., and Stuart, F., 2008, Tectonic response of the central Chilean margin (35–38 S) to the collision and subduction of heterogeneous oceanic crust: a thermochronological study: *Journal of the Geological Society*, v. 165, p. 941–953, doi:10.1144/0016-76492007-115.
- Strömberg, C.A.E., Dunn, R.E., Madden, R.H., Kohn, M.J., and Carlini, A.A., 2013, Decoupling the spread of grasslands from the evolution of grazer-type herbivores in South America: *Nature Communications*, v. 4, p. 1–8, doi:10.1038/ncomms2508.
- Suárez, M., and Emparan, G., 1997, Hoja Curacautín, Regiones de la Araucanía y del Bío-Bío, *Carta Geológica de Chile 71*, scale 1:250,000.:
- Suárez, M., and Emparan, C., 1995, The stratigraphy, geochronology and paleophysiology of a Miocene fresh-water interarc basin, southern Chile: *Journal of South American Earth Sciences*, v. 8, p. 17–31, doi:10.1016/0895-9811(94)00038-4.
- Suárez, M., Emparán, C., Wall, R., Salinas, P., Marshall, L.G., and Rubilar, A., 1990, Estratigrafía y vertebrados fósiles del Mioceno del Alto Biobío, Chile Central (38°-39°S), *in Actas del II Simposio sobre el terciario de Chile*, Concepcion, Chile, p. 311–324.
- Tassara, A., and Yáñez, G., 2003, Relación entre el espesor elástico de la litosfera y la segmentación tectónica del margen andino (15–47°S): *Revista Geologica de Chile*, v. 30, p. 159–186, doi:10.4067/s0716-02082003000200002.
- Tauber, A.A., 1996, Los representantes del genero *Protypotherium* (Mammalia, Notoungulata, Interatheriidae) del Mioceno temprano del sudeste de la Provincia de Santa Cruz, Republica Argentina: *Academia Nacional de Ciencias Cordoba*, v. 95, p. 1–30.
- Tejada-Lara, J. V., Salas-Gismondí, R., Pujos, F., Baby, P., Benammi, M., Brusset, S., De Franceschi, D., Espurt, N., Urbina, M., and Antoine, P.-O., 2015, Life in proto-Amazonia: Middle Miocene mammals from the Fitzcarrald Arch (Peruvian Amazonia): *Palaeontology*,

- v. 58, p. 341–378, doi:10.1111/pala.12147.
- Tejedor, M.F., 2003, New fossil primate from Chile: *Journal of Human Evolution*, v. 44, p. 515–520, doi:10.1016/S0047-2484(03)00026-5.
- Toriño, P., and Perea, D., 2018, New contributions to the systematics of the “Plohophorini” (Mammalia, Cingulata, Glyptodontidae) from Uruguay: *Journal of South American Earth Sciences*, v. 86, p. 410–430, doi:10.1016/j.jsames.2018.07.006.
- Townsend, K.E.B., and Croft, D.A., 2008, Diets of notoungulates from the Santa Cruz Formation, Argentina: new evidence from enamel microwear: *Journal of Vertebrate Paleontology*, v. 28, p. 37–41, doi:10.1671/0272-4634(2008)28[217:DONFTS]2.0.CO;2.
- Trayler, R.B., Kohn, M.J., Bargo, M.S., Cuitiño, J.I., Kay, R.F., Strömberg, C.A.E., and Vizcaíno, S.F., 2020, Patagonian Aridification at the Onset of the Mid-Miocene Climatic Optimum: *Paleoceanography and Paleoclimatology*, v. 35, p. e2020PA003956, doi:10.1029/2020PA003956.
- Trayler, R.B., Schmitz, M.D., Cuitiño, J.I., Kohn, M.J., Bargo, M.S., Kay, R.F., Strömberg, C.A.E., and Vizcaíno, S.F., 2019, An improved approach to age-modeling in deep time: Implications for the Santa Cruz Formation, Argentina: *GSA Bulletin*, doi:10.1130/b35203.1.
- Trumbull, R.B., Riller, U., Oncken, O., Scheuber, E., Munier, K., and Hongn, F., 2006, The Time-Space Distribution of Cenozoic Volcanism in the South-Central Andes: a New Data Compilation and Some Tectonic Implications, *in* *The Andes*, Springer Berlin Heidelberg, p. 29–43, doi:10.1007/978-3-540-48684-8_2.
- Upham, N., and Patterson, B.D., 2015, Evolution of caviomorph rodents: a complete phylogeny and timetree for living genera, *in* Vassallo, A.I. and Antenucci, D. eds., *Biology of Caviomorph Rodents: Diversity and Evolution*, Buenos Aires, SAREM Series A, p. 63–120.
- Utge, S., Folguera, A., Litvak, V., and Ramos, V.A., 2009, Geología del sector norte de la cuenca de Cura Mallín: zona de las Lagunas de Epulafquen (36°40'–50'S, 71°–71°10'O): *Revista de la Asociación Geológica Argentina*, v. 64, p. 231–248.
- Vera, B., González Ruiz, L., Novo, N., Martín, G., Reato, A., and Tejedor, M.F., 2019, The Interatheriinae (Mammalia, Notoungulata) of the Friasian *sensu stricto* and Mayoan (middle to late Miocene), and the fossils from Cerro Zeballos, Patagonia, Argentina: *Journal of Systematic Palaeontology*, v. 17, p. 923–943, doi:10.1080/14772019.2018.1511387.
- Vera, B., Reguero, M., and González Ruiz, L., 2017, The Interatheriinae notoungulates from the middle Miocene Collón Curá Formation in Argentina: *Acta Palaeontologica Polonica*, v. 62, p. 845–863, doi:10.4202/app.00373.2017.
- Vergés, J., Marzo, M., and Muñoz, J.A., 2002, Growth strata in foreland settings: *Sedimentary Geology*, v. 146, p. 1–9, doi:10.1016/S0037-0738(01)00162-2.
- Vizcaíno, S.F., Bargo, S., Cassini, G.H., and Toledo, N., 2016, Forma y función en paleobiología de vertebrados: La Plata, Argentina, Editorial de la Universidad Nacional de La Plata (EDULP), doi:10.35537/10915/55101.
- Vizcaíno, S.F., Cassini, G.H., Fernicola, J.C., and Susana Bargo, M., 2011, Evaluating habitats and feeding habits through ecomorphological features in glyptodonts (Mammalia,

- xenarthra): *Ameghiniana*, v. 48, p. 305–319, doi:10.5710/AMGH.v48i3(364).
- Vizcaíno, S.F., Fernicola, J.C., and Bargo, M.S., 2012, Paleobiology of Santacrucian glyptodonts and armadillos (*Xenarthra*, *Cingulata*), in Vizcaíno, S.F., Kay, R.F., and Bargo, M.S. eds., *Early Miocene Paleobiology in Patagonia*, Cambridge, Cambridge University Press, p. 194–215, doi:10.1017/CBO9780511667381.013.
- Voje, K.L., 2018, Assessing adequacy of models of phyletic evolution in the fossil record: Methods in *Ecology and Evolution*, v. 9, p. 2402–2413, doi:10.1111/2041-210X.13083.
- Vucetich, M.G., 1984, Los roedores de la edad Friasense (Mioceno medio) de Patagonia: *Revista del Museo de La Plata*, v. 8, p. 47–126.
- Vucetich, M.G., 1977, Un nuevo *Dasyproctidae* (Rodentia, *Caviomorpha*) de la edad Friasense (Mioceno tardío) de Patagonia: *Ameghiniana*, v. 14, p. 215–223.
- Vucetich, M.G., Arnal, M., Deschamps, C.M., Pérez, M.E., and Vieytes, E.C., 2015a, A brief history of caviomorph rodents as told by the fossil record, in Vassallo, A.I. and Antenucci, D. eds., *Biology of Caviomorph Rodents: Diversity and Evolution*, Buenos Aires, SAREM series A, p. 11–62.
- Vucetich, M.G., Dozo, M.T., Arnal, M., and Pérez, M.E., 2015b, New rodents (Mammalia) from the late Oligocene of Cabeza Blanca (Chubut) and the first rodent radiation in Patagonia: *Historical Biology*, v. 27, p. 236–257, doi:10.1080/08912963.2014.883506.
- Vucetich, M.G., and Kramarz, A.G., 2003, New Miocene rodents from Patagonia (Argentina) and their bearing on the early radiation of the Octodontoids (*Hystricognathi*): *Journal of Vertebrate Paleontology*, v. 23, p. 435–444, doi:10.1671/0272-4634(2003)023[0435:NMRFPA]2.0.CO;2.
- Vucetich, M.G., Kramarz, A.G., and Candela, A.M., 2010a, The Colhuehuapian rodents from Gran Barranca and other Patagonian localities: the state of the art, in Madden, R.H., Carlini, A.A., Vucetich, M.G., and Kay, R.F. eds., *The paleontology of Gran Barranca: Evolution and environmental change through the middle Cenozoic of Patagonia*, Cambridge University Press, p. 206–219.
- Vucetich, M.G., Mazzoni, M.M., and Pardiñas, U.F.J., 1993, Los roedores de la Formación Collón Curá (Mioceno medio), y la Ignimbrita Pilcaniyeu, Cañadón del Tordillo, Neuquén: *Ameghiniana*, v. 30, p. 361–381.
- Vucetich, M.G., Vieytes, E.C., Pérez, M.E., and Carlini, A.A., 2010b, The rodents from La Cantera and the early evolution of caviomorphs in South America, in Madden, R.H., Carlini, A.A., Vucetich, M.G., and Kay, R.F. eds., *The paleontology of Gran Barranca: evolution and environmental change through the middle Cenozoic of Patagonia*, Cambridge University Press, p. 189–201.
- Wang, Y., Wang, X., Xu, Y., Zhang, C., Li, Q., Tseng, Z.J., Takeuchi, G., Deng, T., and Elderfield, H., 2008, Stable isotopes in fossil mammals, fish and shells from Kunlun Pass Basin, Tibetan Plateau: Paleo-climatic and paleo-elevation implications:, doi:10.1016/j.epsl.2008.03.006.
- Welker, F. et al., 2015, Ancient proteins resolve the evolutionary history of Darwin's South

- American ungulates: *Nature*, v. 522, p. 81–84, doi:10.1038/nature14249.
- Wertheim, J.A., 2007, Fossil rodents from Laguna del Laja, Chile : a systematic, phylogenetic, and biochronologic study: PhD Thesis, University of California, Santa Barbara.
- Whipple, K.X., 2009, The influence of climate on the tectonic evolution of mountain belts: *Nature Geoscience*, v. 2, p. 97–104, doi:10.1038/ngeo413.
- Wood, A.E., and Patterson, B., 1959, The rodents of the deseadan Oligocene of Patagonia and the beginnings of south american rodent evolution: *Bulletin of the Museum of Comparative Zoology*, v. 120, p. 1–428.
- Woodburne, M.O., Goin, F.J., Bond, M., Carlini, A.A., Gelfo, J.N., López, G.M., Iglesias, A., and Zimicz, A.N., 2014, Paleogene Land Mammal Faunas of South America; a Response to Global Climatic Changes and Indigenous Floral Diversity: *Journal of Mammalian Evolution*, v. 21, p. 1–73, doi:10.1007/s10914-012-9222-1.
- Wyss, A.R., Flynn, J.J., and Croft, D.A., 2018, New Paleogene notoungulates and leontiniids (Toxodontia; Notoungulata; Mammalia) from the early Oligocene Tinguirica Fauna of the Andean Main Range, central Chile: *American Museum Novitates*, v. 3903, p. 1–42, doi:10.1206/3903.1.
- Zachos, J.C., Dickens, G.R., and Zeebe, R.E., 2008, An early Cenozoic perspective on greenhouse warming and carbon-cycle dynamics: *Nature*, v. 451, p. 279–283, doi:10.1038/nature06588.
- Zachos, J., Pagani, H., Sloan, L., Thomas, E., and Billups, K., 2001, Trends, rhythms, and aberrations in global climate 65 Ma to present: *Science*, v. 292, p. 686–693, doi:10.1126/science.1059412.
- Zhao, Y. et al., 2016, Detailed dynamic land cover mapping of Chile: Accuracy improvement by integrating multi-temporal data: *Remote Sensing of Environment*, v. 183, p. 170–185, doi:10.1016/J.RSE.2016.05.016.
- Zurita, A.E., González-Ruiz, L.R., Miño-Boilini, A.R., Herbst, R., Scillato-Yané, G.J., and Cuaranta, P., 2015, Paleogene Glyptodontidae Propalaehoplophorinae (Mammalia, Xenarthra) in extra-Patagonian areas: *Andean Geology*, v. 43, p. 127–136, doi:10.5027/andgeoV43n1-a07.

ANEXO 1. Publicaciones resultantes de esta tesis doctoral





Contents lists available at ScienceDirect

Journal of South American Earth Sciences

journal homepage: www.elsevier.com/locate/jsames

The Early to late Middle Miocene mammalian assemblages from the Cura-Mallín Formation, at Lonquimay, southern Central Andes, Chile (~38°S): Biogeographical and paleoenvironmental implications

Andrés Solórzano^{a,*}, Alfonso Encinas^b, René Bobe^c, Reyes Maximiliano^b, Gabriel Carrasco^d

^a Programa de Doctorado en Ciencias Geológicas, Facultad de Ciencias Químicas, Universidad de Concepción, Víctor Lamas, 1290, Concepción, Chile

^b Departamento de Ciencias de la Tierra, Facultad de Ciencias Químicas, Universidad de Concepción, Víctor Lamas, 1290, Concepción, Chile

^c School of Anthropology, University of Oxford, UK

^d Servicios Científicos Educativos y Turismo Científico Chile, Pedro León Ugalde 254, San Bernardo, Chile



ARTICLE INFO

Keywords:

Cura-Mallín Formation
Miocene
Fossils mammals
Rain-shadow effect
Protypotherium concepcionensis

ABSTRACT

The Cura-Mallín Formation consists of a series of upper Oligocene to Upper Miocene volcanic and sedimentary rocks deposited in continental settings that crop out in the Andean Cordillera in Chile and Argentina between ~37° and 39°S. Since the 1990s few fossil mammals have been recovered from this unit in the surroundings of Lonquimay, south-central Chile (38.5°S), and all of them were assigned to the Early Miocene. After a reassessment of the taxonomic affinities of the fauna so far recovered from the Cura-Mallín Formation in the Lonquimay area, and based on the radioisotopic ages of the fossil-bearing localities, here we recognized two chronological distinctive mammalian assemblages: one of Early Miocene age (probably Colhuehuapian–Santacrucian SALMA), which includes *Nesodon imbricatus* and *Parastrapotherium* sp.; and a second one of late Middle Miocene age (12.8–11.6 Ma; Serravallian; Mayoan SALMA), which includes glyptodonts (Glyptodontidae indeterminate), armadillos (*Eutatini* indeterminate), macraucheniids (*Theosodon* sp.), a new intertheriid species (*Protypotherium concepcionensis* sp. nov.), and a likely platyrrhine monkey. Therefore, in contrast with previous interpretations, the fauna from Lonquimay is not uniquely restricted to the Early Miocene. The fossil mammals and plants recognized from the area indicate the persistence of mostly temperate and forested habitats with permanent bodies of water during the Early to latest Middle Miocene. This suggests that this part of the Andean Cordillera (38°–39°S) did not reach enough paleoaltitudes (> 1000 m) to cause an important orographic rain shadow effect in the foreland basins at least after the late Middle Miocene (c. 12 Ma). However, the role of Neogene South Hemisphere climatic changes in triggering, or reinforcing, the foreland desertification along the south-central Andes is an additional factor that cannot be discarded.

1. Introduction

During the last decades our understanding of the extinct continental mammalian biodiversity from Chile has shown significant progress, with the discovery of many new localities and the description of several new taxa, especially from the late Paleogene and Neogene (Bertrand et al., 2012; Bostelmann et al., 2013; Canto et al., 2010; Charrier et al., 2015; Croft et al., 2008, 2007; Flynn et al., 2005, 2003; 2002a, 1995; Hitz et al., 2006; McKenna et al., 2006; Montoya-Sanhueza et al., 2017; Shockey et al., 2012; Wyss et al., 2018). Despite these efforts, the paleobiodiversity of Chilean mammals remains poorly known, as illustrated by the preliminary taxonomic reports from several of the most diverse localities with dozens of new undescribed taxa and/or taxa in

open nomenclature (Bostelmann et al., 2013; Charrier et al., 2015; Croft et al., 2007; Flynn et al., 2008, 2002a, 2002b). This makes it necessary to renew sampling efforts and to refine the taxonomy of poorly known faunas (Canto et al., 2010). The latter is needed for the mammalian remains reported from distinct localities of strata referred to the Cura-Mallín Formation (Flynn et al., 2008; Marshall et al., 1990; Suárez et al., 1990; Suárez and Emparan, 1995).

The Cura-Mallín Formation consists of a series of Upper Oligocene to Upper Miocene volcanic and sedimentary rocks deposited in continental settings that crop out in the Andean Cordillera in Chile and Argentina between 36° and 39°S (Burns et al., 2006; Flynn et al., 2008; Radic, 2010; Suárez and Emparan, 1995; Utge et al., 2009). In Chile, some of the best exposures of the Cura-Mallín Formation are located in

* Corresponding author.

E-mail address: solorzanoandres@gmail.com (A. Solórzano).

<https://doi.org/10.1016/j.jsames.2019.102319>

Received 28 May 2019; Received in revised form 14 August 2019; Accepted 14 August 2019

Available online 20 August 2019

0895-9811/ © 2019 Elsevier Ltd. All rights reserved.

the surroundings of Laguna del Laja (37–38°S) and Lonquimay (38–39°S) (Niemeyer and Muñoz, 1983; Pedroza et al., 2017; Suárez and Empanan, 1995, 1997). Miocene mammals have been reported from both localities (Croft et al., 2003; Flynn et al., 2008; Marshall et al., 1990; Shockey et al., 2012; Suárez et al., 1990). The first record of mammals from the Cura-Mallín Formation derives from geological and paleontological prospections carried out in 1988–1991 in multiple localities around the Lonquimay town (Marshall et al., 1990; Suárez et al., 1990). These initial works allowed for the recognition of *Astrapotherium* sp. (Astrapotheria; Marshall et al., 1990), an indeterminate Macraucheniiidae (Litopterna), cf. *Protypotherium* (Notoungulata: Interatheriidae), an indeterminate Glyptodontidae (Xenarthra: Cingulata), caviomorphs (Rodentia), and a possible mesotheriid (Notoungulata) (Suárez et al., 1990); which together were assigned to the Early Miocene (Santacrucian SALMA; Marshall et al., 1990; Suárez et al., 1990). Subsequent works dealing with the Lonquimay mammal fauna have refined or confirmed the taxonomic identity of some of these taxa, increased the number of taxa recognized, and provided a better chronostratigraphic context to this fauna. Croft et al. (2003) provided the first record of a large notoungulate from the Lonquimay area (Cerro Tallón locality) with the report of *Nesodon conspurcatus*, an age-diagnostic taxon of the Santacrucian SALMA (Croft et al., 2003). Though, the taxonomic validity of the last taxon has been questioned as its morphology falls within the range of variability of other *Nesodon* species (Cuitiño et al., 2019; Hernández Del Pino, 2018). Bostelmann et al. (2014) suggest that the astrapothere recovered by Marshall et al. (1990) from the Río Quepuca must be included in the genus *Parastrapotherium*, a taxon relatively common in the Late Oligocene and Early Miocene (Kramarz and Bond, 2010). Buldrini et al. (2015) and Buldrini and Bostelmann (2011) confirmed the presence of *Protypotherium* in the Cura-Mallín Formation after finding near the Puente Tucapel locality and suggested a lower Miocene age ('Pinturan' – Santacrucian SALMA) for the remains. However, excepting for *Parastrapotherium* and *Nesodon*, an Early Miocene age for the additional taxa reported from the Lonquimay surroundings are not well-supported by biochronological correlations nor geochronology data.

Recent stratigraphic work and U/Pb radiometric dates by Pedroza et al. (2017) and Rosselot et al. (2019b) in the Cura-Mallín Formation cropping out in the Lonquimay area have challenged some of the ages previous inferred for these taxa (Buldrini and Bostelmann, 2011; Marshall et al., 1990; Suárez et al., 1990). For example, the *Protypotherium* specimen recovered from Puente Tucapel must have a late Middle Miocene or younger age as detrital zircon dates indicate maximum ages of 12.5 and 12.7 Ma for this fossil-bearing stratigraphic section (Pedroza et al., 2017). This raised the question of how many temporally distinctive mammal assemblages are recorded in the Cura-Mallín Formation in the Lonquimay area. Moreover, according to Pedroza et al. (2017), the Macraucheniiidae remains (incorrectly identified as '*Macrauchenia litopterna*') also comes from the Puente Tucapel locality. However, Suárez et al. (1990) clearly stated that the Macraucheniiidae comes from the south bank of the BioBío river, at the NE foot of Cerro Rucañanco. These cases exemplify the uncertainties in the stratigraphic and geographic provenance of some of the mammalian fossils recovered from Lonquimay. This situation is further exacerbated as the fossils come from an area with discontinuous outcrops. Some of the reported materials have not been described in detail, and sometimes not even illustrated, limiting our understanding of the taxonomic diversity as well as the biochronological and paleoenvironmental significance of the fauna.

During the summers of 2017 and 2018 we conducted geological and paleontological prospections in the Lonquimay area, with special emphasis on the fossiliferous localities mentioned by previous authors (Pedroza et al., 2017; Rubilar, 1994; Suárez et al., 1990; Suárez and Empanan, 1995). Unfortunately, we did not find any new mammal specimens. In order to evaluate the significance of this fauna, here we review all the mammalian specimens recovered from the Cura-Mallín

Formation (in the traditional sense of Suárez and Empanan, 1995) in the Lonquimay area (38°S), now stored in the Museo Nacional de Historia Natural (MNHN in Santiago, Chile), and assess their biostratigraphic, biogeographical and paleoenvironmental significance. We also place our findings within the complex tectonostratigraphic framework of the Cura-Mallín Basin deposition.

2. Geological, paleontological and geographical background

The Cura-Mallín basin is part of a chain of basins that formed within the Andean volcanic arc and the foreland of Chile and Argentina between 33° and 43°S between the Upper Oligocene and Upper Miocene (Burns et al., 2006; Flynn et al., 2008; Jordan et al., 2001; Pedroza et al., 2017; Suárez and Empanan, 1995; Utge et al., 2009). The Cura-Mallín basin contains up to 4 km of volcanic and sedimentary rocks with three traditionally well-differentiated geological units, the Cura-Mallín, Trapa-Trapa, and Mitrauquén formations (Burns et al., 2006; Niemeyer and Muñoz, 1983; Suárez and Empanan, 1995, 1997). These geological units were deposited into several sub-basins (Rosselot et al., 2019a) whose lateral transitions are poorly understood because the original paleogeographic configuration was modified during the late Cenozoic deformation and uplift of the Andes, and some of the intervening zones are covered by younger volcanic rocks (Burns et al., 2006).

The Cura-Mallín Formation is the basal unit in the homonymous basin and it is characterized by a predominant volcanic member (with intercalations of sedimentary strata), and a predominant sedimentary member (with intercalations of volcanic strata), which generally overlies it and was deposited in alluvial, fluvial, lacustrine and deltaic environments (Burns et al., 2006; Pedroza et al., 2017; Radic, 2010; Suárez and Empanan, 1995). Different names have been applied locally to these members. Niemeyer and Muñoz (1983) defined the volcanic Río Queuco lower member and the sedimentary Malla-Malla upper member in the Laguna del Laja area. Suárez and Empanan (1995) defined the predominantly volcanic Guapitrio member and the sedimentary Río Pedregoso member in the Lonquimay region. Although traditionally, it has been considered that the sedimentary members of the Cura-Mallín Formation are younger than the volcanic ones (Utge et al., 2009), in the sector of Lonquimay it has been proposed that both members interdigitate and are partially coeval (Pedroza et al., 2017; Suárez and Empanan, 1995). The coeval sedimentation of lithological distinctive members has been also interpreted as the result of their dissimilar location respect to the Miocene main active volcanic sources (i.e., distal facies being predominantly clastic, and proximal facies being predominantly volcanic; Burns et al., 2006). However, Salinas (1979) had previously considered the sedimentary rocks present in the Guapitrio Member (*sensu* Suárez and Empanan, 1995), to be younger than the volcanic rocks and correlative with the Río Pedregoso Member (*sensu* Suárez and Empanan, 1995). Volcanic and sedimentary rocks included in the Cura-Mallín Formation typically crop out in separate areas, so their correlation has been inferred from their overlapping radiometric ages (Burns et al., 2006; Suárez and Empanan, 1995, 1997). However, some of these ages are dubious since they were obtained by the K-Ar method. Radiometric dates (K-Ar and U-Pb) suggest a Lower to earliest Upper Miocene age (22–10.7 Ma) for the Cura-Mallín Formation strata cropping out in the Lonquimay region (Pedroza et al., 2017; Rosselot et al., 2019b, 2019a; Suárez and Empanan, 1995). In particular, the Guapitrio Member was dated between 22 ± 0.9 and 10.7 ± 1.1 Ma, and the Río Pedregoso Member between 17.5 ± 0.6 and 11.64 ± 0.13 Ma (Pedroza et al., 2017; Rosselot et al., 2019a, 2019b; Suárez and Empanan, 1995, 1997). These geochronological data allow to partially correlate the Cura-Mallín Formation with the Farellones (32°–36° S) and the Ñirihuau (41°–47°S) formations (Bechis et al., 2014; Giambiagi et al., 2016). The units overlaying the Cura-Mallín Formation correspond to the Trapa-Trapa and Mitrauquén formations, which crop out in the Laguna del Laja, and Lonquimay areas,

respectively. Both formations are characterized predominantly by coarse-grained volcanoclastic deposits and volcanic rocks (Niemeyer and Muñoz, 1983; Pedroza et al., 2017; Suárez and Emparan, 1995, 1997). Radiometric dates (Ar-Ar and K-Ar) restrict both units to the Upper Miocene; 9.5 ± 2.8 and 8.0 ± 0.3 Ma for Mitrauquén Formation and 10.10 ± 0.20 and 8.9 ± 0.1 for Trapa-Trapa Formation (Flynn et al., 2008; Herriott, 2006; Suárez and Emparan, 1997). Both units are therefore correlative as proposed by Herriott (2006).

Pedroza et al. (2017) proposed a new stratigraphic scheme for the Cura-Mallín Formation in the Lonquimay area. They separated the traditionally recognized Cura-Mallín Formation (*sensu* Suárez and Emparan, 1995) into two units consisting of the mainly volcanic Guapitrío Formation (previously Guapitrío member), and the sedimentary Río Pedregoso Formation (previously Río Pedregoso member) that they divided (from base to top) in the Quilmahue, Rucañanco and Bío-Bío members. Pedroza et al. (2017) also proposed to use the term Cura-Mallín Group, which includes their Guapitrío and Río Pedregoso 'formations'. However, Pedroza et al.'s (2017) interpretations could be biased by the complex stratigraphic scenario exhibited by the study area and exacerbated by the lack of continuous outcrops. In this sense, while waiting for a comprehensive stratigraphic revision of the belonging to the Cura-Mallín Basin, and for the sake of simplicity, we will use the name Cura-Mallín Formation in the traditional sense of Suárez and Emparan (1995).

There is some controversy regarding the tectonic context in which the geological units included in the Cura-Mallín Basin were deposited. There is a consensus that the fluvial deposits of the Upper Miocene Mitrauquén Formation (and the coeval Trapa-Trapa Formation) are syntectonic deposits based on the occurrence of conglomeratic facies and growth strata in this unit (Melnick et al., 2006). Early authors suggested that the Cura-Mallín Formation was deposited in a pull-apart basin related to the Liqueñe-Oñqui system fault (Suárez and Emparan, 1995). Subsequent authors agree that the Cura-Mallín Formation was deposited during the Upper Oligocene to Lower Miocene under an extensional regimen, later subjected to a tectonic inversion (Burns et al., 2006; Jordan et al., 2001). However, the time in which the basin inversion begins has been a matter of discussion, with two opposing models: 1) the sedimentation of the Cura-Mallín Formation took place under extensional conditions and the first synorogenic facies occurred after 9–8 Ma, giving rise to deposition of the overlying Mitrauquén and Trapa-Trapa Formations (Burns et al., 2006; Jordan et al., 2001; Melnick et al., 2006; Radic, 2010); 2) only the lowest strata of the Cura-Mallín Formation are synextensional, while their upper beds, as well as their overlying units (Mitrauquén and Trapa-Trapa Formations) are synorogenic and were deposited in intermontane basins likely related with the rise of the Andes since ~19–18 Ma (Rosselot et al., 2018; Spikings et al., 2008; Utge et al., 2009). After a recent extensive review on the available geochronological, structural, geochemical, thermo-chronological and basin subsidence evidence (see Rosselot et al., 2019a for details), it is more likely that at least the upper part of the Cura-Mallín Formation is related to compressional rather than extensional conditions. The Early Miocene beginning of the compressional regime at these latitudes is consistent with observations north and south of the Cura-Mallín Formation outcrop area (Charrier et al., 2002; Cuitiño et al., 2016; Echaurren et al., 2016; Encinas et al., 2018; Folguera et al., 2018b, 2018a; Kay and Copeland, 2006).

As previously mentioned, several mammals have been recognized in distinct localities of the Cura-Mallín Formation in the Lonquimay region (Fig. 1) (Bostelmann et al., 2014; Buldrini et al., 2015; Buldrini and Bostelmann, 2011; Croft et al., 2003; Marshall et al., 1990; Suárez et al., 1990). Additional taxa recognized in the area includes a continental bird (*Megahinga chilensis*), an indeterminate Bufonidae (Anura), several plants (based in pollen and leaves) as well as freshwater fishes and invertebrates which are relatively common along the entire stratigraphic sequence (Alvarenga, 1995; Arratia, 2015; Azpelicueta Maria and Rubilar, 1997; Guevara et al., 2018; Palma-

Heldt, 1983; Palma-Heldt and Rondanelli, 1990; Pedroza et al., 2017; Rubilar, 1994; Salinas, 1979).

Recent radiometric ages have improved the understanding about the stratigraphic relationships of the distinct sequences of the Cura-Mallín Formation cropping out in the Lonquimay area (Pedroza et al., 2017; Rosselot et al., 2019b). An updated schematic stratigraphic arrangement of the mammal-bearing localities in this area is provided in Fig. 2. The main difference with the proposal of Pedroza et al. (2017) is in the location of the Piedra Parada succession (see details below). In the following lines, we provide a brief characterization of the Miocene mammal-bearing localities within the Lonquimay region.

2.1. Río Quepuca

The locality is along the Quepuca River, 50 km north of the Lonquimay town. It consists of a 14 m thick succession of crossbedded sandstones and black shales (Fig. 1; Marshall et al., 1990). The black shale and crossbedded sandstone association was interpreted as having been deposited in a meandering river system, adjacent to an active volcano (Marshall et al., 1990). This levels are comparable to sedimentary strata exposed along the Guapitrío River (where the Guapitrío member takes its name; Suárez and Emparan, 1995, 1997). Therefore, this locality is likely circumscribed to the Guapitrío member (Bostelmann et al., 2014). Although the Guapitrío Member yielded K/Ar ages between 22 and 10.7 Ma (Suárez and Emparan, 1995, 1997), radiometric ages are not available for the Río Quepuca locality. However, the fossil content (astropothere) has been referred to the Santacrucian (Marshall et al., 1990) or the Colhuehuapian SALMA (Bostelmann et al., 2014).

2.2. Cerro Tallón

The locality is 15 km to the southwestern of the Lonquimay town in the western edge of the Biobío River (Fig. 1). Deposits at the base of the Cerro Tallón in the banks of the Biobío river include shales and carbonaceous shales with a high content of fish scales and spines intercalated with fine-to medium-grained sandstones showing lower flow regime plane lamination, undulose stratification, and syndimentary folds (Pedroza et al., 2017). Fresh-water fishes and a large notoungulate have been reported from this locality (Croft et al., 2003; Pedroza et al., 2017; Rubilar, 1994). The last being recovered from 5 m thick succession of fine to coarse grain montmorillonite-rich sandstone with tuffaceous intercalations (Croft et al., 2003). A single radiometric K-Ar dates from a level overlaying the recovered mammal yields an age of 17.5 ± 0.6 Ma (Croft et al., 2003; Suárez and Emparan, 1995). In addition, the notoungulate recovered from this locality has been suggested as a taxon indicative of the Santacrucian SALMA (Croft et al., 2003). Therefore, both radiometric and biochronological evidence suggest a late Early Miocene (Santacrucian SALMA) age for the locality.

2.3. Piedra Parada

The locality is 13 km to the southwestern of the Lonquimay town, in the eastern edge of the Biobío River (Fig. 1). The stratigraphic succession is dominated by very fine-to medium-grained sandstones with numerous freshwater bivalve fossils, overlain by matrix-supported, polymictic conglomerates with poorly sorted, subrounded to angular clasts (Pedroza et al., 2017). Glyptodont osteoderms, fresh-water invertebrates, as well as wood and pollen have been recovered from this locality (Palma-Heldt, 1983; Pedroza et al., 2017; Suárez et al., 1990). Early K-Ar dates from the cliff of Piedra Parada indicated a Middle Miocene age (13 Ma) (Suárez and Emparan, 1995). Recent U-Pb dates in a volcanic tuff from the base of the Piedra Parada section indicates a late Middle Miocene age (12.8 Ma; Rosselot et al., 2019b). Pedroza et al. (2017) had assigned this section to the Early Miocene based on stratigraphic interpretations, but the cited radiometric ages indicate

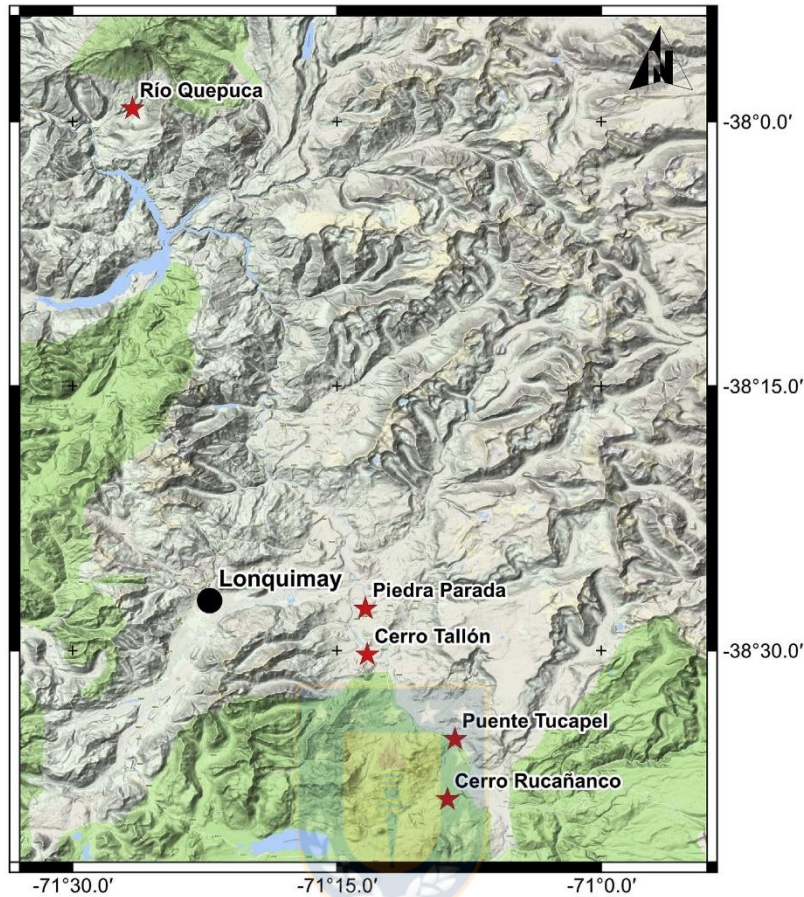


Fig. 1. Geographical settings of the fossil-bearing localities (star) mentioned in the text.

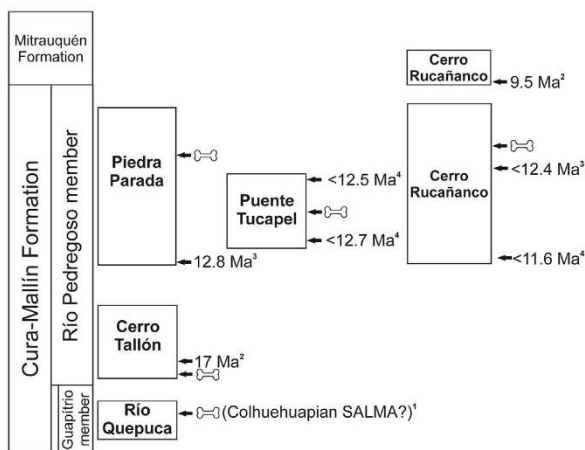


Fig. 2. Schematic (not in scale) chronostratigraphic framework of the fossil mammal-bearing localities among the Cura-Mallín Formation cropping out in the surroundings of Lonquimay, based on radiometric ages (⁴Pedroza et al., 2017; ³Rossetol et al., 2019b; ²Suárez and Emparan, 1995) and biochronologic correlation (Bostelmann et al., 2014; ¹Kramarz and Bond, 2010). The bone symbol represents the approximate location of the fossil-bearing levels along each stratigraphic sequence.

that this inference is erroneous.

2.4. Puente Tucapel

The 102 m thick succession crops out around 25 km to the southwestern of the Lonquimay town, in the eastern Biobío river margin (Fig. 1). The succession is dominated by sandstones with minor mudrocks and conglomerates, interpreted as deposited in deltaic and fluvial environments (Pedroza et al., 2017). An interatheriid has been reported in this locality, being referred without definitive evidence to the ‘Pinturan’–Santacrucian SALMAs (Buldrini et al., 2015; Buldrini and Bostelmann, 2011; Suárez et al., 1990). However, detrital zircons ages from the base and top of the Puente Tucapel succession yielded maximum ages of 12.7 ± 0.3 and 12.5 ± 0.3 Ma, respectively (Pedroza et al., 2017).

2.5. Cerro Rucañanco

The locality is 29 km to the southwestern of the Lonquimay town, in the western Biobío river margin. In this area, a 180 m thick succession of coarse-to-medium grained conglomerates, sandstones showing cross-bed stratification and inclined structures, with subordinate siltstones and channelized breccias, is exposed (Suárez and Emparan, 1995). The succession presents facies associations typical of Gilbert-type deltas according to Suárez and Emparan (1995) and Pedroza et al. (2017). The macraucheniid, bufonid, continental bird, as well as some freshwater

fishes and invertebrates come from this locality (Alvarenga, 1995; Guevara et al., 2018; Suárez et al., 1990). The coarse-grained succession of Cerro Rucañanco has been correlated with those of the Piedra Parada (Suárez and Emparan, 1995, Fig. 2). Recent U-Pb dating of detrital zircons from the middle section of the Cerro Rucañanco yielded a maximum depositional age of 12.4 Ma (Rossetol et al., 2019b). A sample obtained from beds located in another section located in the Biobío banks at the base of Cerro Rucañanco yielded a detrital zircons age of 11.64 Ma (Pedroza et al., 2017). Pedroza et al. (2017) considered that the Biobío section is stratigraphically above that of the Cerro Rucañanco. However, we concur with Suárez and Emparan (1995) that the Biobío section underlies the latter as it is located in a lower topographic position and strata in both sections are almost horizontal.

It is important to note that the Piedra Parada, Puente Tucapel, and Cerro Rucañanco sections show similar facies that, from base to top, consist of tuffs (only present at the base of the Piedra Parada section, dated in 12.8 Ma by Rossetol et al., 2019b), finely laminated lacustrine siltstones and sandstones, and coarse-grained sandstones and conglomerates. Therefore, these sections can be also correlated based on facies similarities (Fig. 2). The Mitrauquén Formation crops out at the top of the Cerro Rucañanco, overlying a covered area between this unit and the Cura-Mallín Formation. Therefore, the age of the Cura-Mallín Formation at the Puente Tucapel, Piedra Parada and Cerro Rucañanco sections is constraint between 12.8 Ma (late Middle Miocene, Serravallian; the age of the tuff at the base of the succession; Rossetol et al., 2019b) and 9.5 Ma (early Middle Miocene, Tortonian; the oldest age for the Mitrauquén Formation; Suárez and Emparan, 1997). However, the fossil-bearing sections of Piedra Parada, Puente Tucapel, and Cerro Rucañanco probably have ages close to 12.8–11.64 Ma (Serravallian; Fig. 2), because the available detrital zircons maximum ages could be interpreted as near-sedimentation ages. The similar age range for the radiometric dates (Pedroza et al., 2017; Rossetol et al., 2019b) is also consistent with this idea.

3. Material and methods

The original geographic provenance and collector labels for all the specimens deposited in the MNHN were reviewed in order to clarify this topic. All measurements are presented in millimeters (mm) and were made using a digital caliper. Dental terminology follows the convention of upper case for upper teeth (i.e., I, C, P, M) and lower case for lower teeth (i.e., i, c, p, m). For Cingulata osteoderm, we follow the nomenclature of Croft et al. (2007) and González-Ruiz (2010). For macraucheniids, and interatheriids, we follow the dental nomenclature of Soria and Hoffstetter (1985), and Reguero et al. (2003), respectively. Taxonomic nomenclature for higher categories follows McKenna and Bell (1997). However, we acknowledged the increasing body of literature (based in phylogenetic analyses on morphological and molecular data) highlighting different systematic hypothesis to those of McKenna and Bell (1997), especially regarding the arrangement within Cingulata (e.g. Delsuc et al., 2016; Gaudin and Wible, 2006; Mitchell et al., 2016).

The use of traditional (McKenna and Bell, 1997) over more recent systematic hypotheses do not affect our general conclusions. The specimens used for comparison are included in the Electronic Supplementary Materials (ESM_1).

3.1. Institutional abbreviations

SGO.PV, Museo Nacional de Historia Natural de Santiago, Santiago, Chile.

4. Systematic paleontology

MAMMALIA Linnaeus, 1758
 ASTRAPOTHERIA Lydekker, 1894
 ASTRAPOTHERIIDAE Ameghino, 1887
 PARASTRAPOTHERIUM Ameghino, 1895
Parastrapotherium sp.

Marshall et al. (1990): *Astrapotherium* sp.

Bostelmann et al. (2014): *Parastrapotherium* sp.

Revised materials. SGO. PV.4003; a fragment of right maxillary with P4–M3, and an isolated left M3, from a single individual.

Geographic and stratigraphic provenance. The specimen was collected by L. Marshall and P. Salinas in 1990 along the east bank of the Río Quepuca, southeast of Santa Bárbara, a tributary of the Biobío River, in Central Chile (38°3'2.38"S; 71°24'35.88"W). The specimen comes from fluvial and lacustrine facies resembling those exposed along the Guapitrió River (Marshall et al., 1990) and might belong to the Guapitrió member (*sensu* Suárez and Emparan, 1995). Based in biochronological correlation with Patagonian faunas and the known radiometric ages for the Cura-Mallín Formation, the age of this specimen is likely Early Miocene (Colhuehupian SALMA; Dunn et al., 2013; Kramarz and Bond, 2010, 2008).

Description. With half the size of M1, the P4 is the smallest of the preserved dental series (see ESM.2). The P4 has a single lingual cusp (protocone). Along the labial edge of the ectoloph there is a well-developed paracone fold and mesially directed parastyle (Fig. 3a). The last two structures are positioned more mesially than the protocone. The protoloph is transversely more developed than the metaloph (Fig. 3a), as in *Astrapotherium*, *Astrapothericulus*, *Parastrapotherium*, but unlike *Maddenia* (Kramarz, 2009; Kramarz and Bond, 2009, 2008). The mesiodistally oriented central valley is posterolingually closed (Fig. 3). In labial view, the P4 exhibit a labial fold broader at the base than in *Astrapotherium* and *Astrapothericulus* (Kramarz and Bond, 2010, 2008). The labial cingulum is absent at the base of the labial fold, while a well-developed mesiolingual cingulum is present in lingual view.

In occlusal view, the M1 and M2 are similar in shape, both are nearly trapezoidal with a wider labial edge and exhibits a clearly folded ectoloph. In M1 the protoloph and metaloph exhibit a rather similar transverse development (Fig. 3a) and the parastyle and paracone fold are slightly developed. The M2, larger than the M1, has a strongly folded ectoloph (parastyle and paracone fold are conspicuous), their



Fig. 3. *Parastrapotherium* sp. (SGO.PV.4003) from the Río Quepuca (Fig. 1), Río Guapitrió Member, Cura-Mallín Formation (Early Miocene), Chile. A fragment of right maxillary with P4–M3 in occlusal view (a); isolated left M3 in occlusal view (b). Scale bar = 20 mm [2-column fitting image].

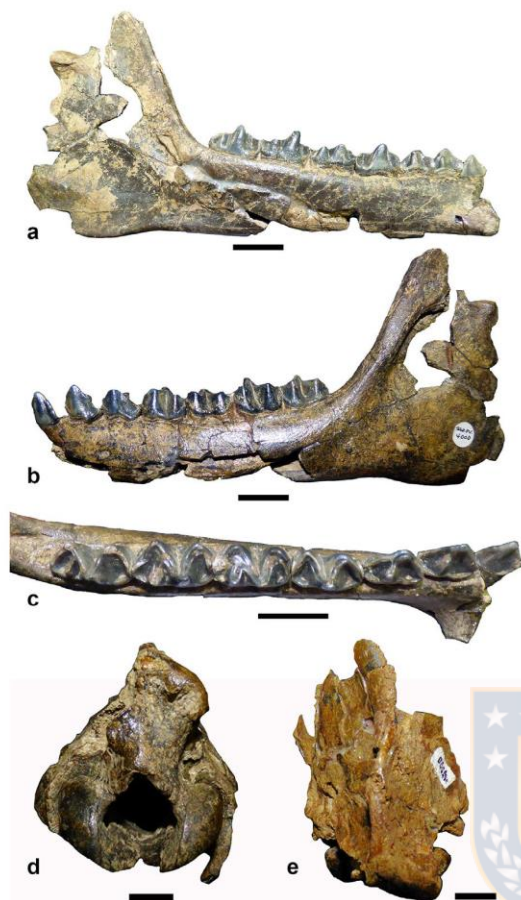


Fig. 4. *Theosodon* sp. (SGOP.4000) from the Cerro Rucañanco locality, Río Pedregoso Member, Cura-Mallín Formation (late Middle Miocene; Serravallian), Chile. Mandible in lingual (a), labial (b) and occlusal (c) views; a fragment of skull in posterior (d) and dorsal (e) views. Scale bar = 20 mm.

protoloph is transversely more developed than the metaloph, and the mesial portion of the parastyle overlaps the metaloph of M1 (Fig. 3a). In M1 and M2 a median fossette is absent (probably due to the advanced wear of the specimen), and the central valley is wide even in the advanced stages of wear of M1 (Fig. 3a). The M3 is rather subtriangular in occlusal view due to the reduction of the metaloph and the lack of a hypocone (Fig. 3b). The M3 also has a strongly folded ectoloph (conspicuous parastyle and paracone fold), and the mesial portion of the parastyle overlaps the metaloph of M2. Even considering the advanced wear, the central valley of the upper molars remains wide but isolated on M1 (Fig. 3a).

Remarks. The upper molar and premolars show an advanced stage of wear (Fig. 3), thus SGO. PV.4003 represents an adult individual. The specimen represents a large astrapotherium (like *Parastrapotherium*, *Astrapotherium*, *Xenastrapotherium*, and *Granastrapotherium*) as the M2 is larger than 40 mm long (Kramarz and Bond, 2009). The following character combination allows us to refer SGO. PV.4003 to the genus *Parastrapotherium*: upper premolars with labial fold broader at the base than in *Astrapotherium* and *Astrapothericulus*, upper molars without basal lingual cingulum, M3 hypocone absent (Kramarz and Bond, 2009, 2008). Thus, we agree with the interpretations of Bostelmann et al. (2014) about the taxonomic affinities of SGO. PV.4003.

In the genus *Parastrapotherium* there are circumscribed six valid

species, with four species in the Deseadan SALMA, *Parastrapotherium holmbergi* Ameghino, 1895, *Parastrapotherium martiale* Ameghino, 1901, *Parastrapotherium crassum* Ameghino, 1902, and *Parastrapotherium? voghtii* (Mercerat, 1891), and three species from the Colhuehuapian SALMA, *Parastrapotherium symmetrum* Ameghino, 1902, *Parastrapotherium herculeum* Ameghino, 1899, and *Parastrapotherium martiale* (also known from the Deseadan SALMA) (Kramarz and Bond, 2010, 2008). After the diagnosis of most of the species within *Parastrapotherium* are based on lower teeth and/or upper canines (Kramarz and Bond, 2010, 2008), we are unable to achieve a species level identification for the Río Quepuca specimen. All these species were recognized from Argentina (Kramarz and Bond, 2010, 2008), whereas SGO. PV.4003 represent the first evidence of the genus in Chile, and represents together with those of the Early Miocene of Cerro Banderas (Kramarz et al., 2005) the northern-most record of the genus (Bostelmann et al., 2014).

LITOPTERNA Ameghino (1889).

MACRAUCHENIIDAE Gervais, 1855

'CRAMAUCHENIINAE' Ameghino, 1902

THEOSODON Ameghino, 1887

Included species. *Theosodon lydekkeri* Ameghino, 1887 (type species), *Theosodon lallemani* Mercerat, 1891, *Theosodon fontanae* Ameghino, 1891, *Theosodon gracilis* Ameghino, 1891, *Theosodon patagonicum* Ameghino, 1891, *Theosodon karaikensis* Ameghino, 1904, *Theosodon garretorum* Scott (1910), *Theosodon pozzii* Kraglievich and Parodi, 1931, *Theosodon? Frenguelli* Soria, 1981, and *'Theosodon' arzuetai* McGrath et al. (2018).

Geographic and Stratigraphic Distribution. Early Miocene to late Middle Miocene (Colhuehuapian–Laventan? SALMAs) of Argentina (Sarmiento, Pinturas, Santa Cruz, and Collon Cura formations), Chile (Cura-Mallín, Pampa Castillo, Chucal, Río Negro, and Río Cisnes faunas), Bolivia (Quebrada Honda Fauna and Yecua Formation), Colombia (La Venta Fauna), and Peru (Fitzcarrald Arch) (Kramarz and Bond, 2005; McGrath et al., 2018).

Remarks. Several of the early species referred to this genus were based on fragmentary remains and/or ambiguous diagnoses (e.g. *T. fontanae*, *T. patagonicum* and *T. karaikensis*), hence the number of names proposed in the literature likely exceeds the actual number of taxa (Cifelli and Guerrero, 1997; McGrath et al., 2018). In addition, *T.? frenguelli* have a reduced m3 entolophid (Soria, 1981), unlike other *Theosodon* spp., hence this taxa is not clearly referred to the genus (Cifelli and Soria, 1983). As several authors (Cifelli and Guerrero, 1997; McGrath et al., 2018; Schmidt, 2013) have pointed out, *Theosodon* is in need of comprehensive systematic revision, which is out of the scope of the present work.

Theosodon sp.

Suárez et al. (1990): Macraucheniidae gen. et sp. indet.

Pedroza et al. (2017): '*Macrauchenia litopterna*'

Revised materials. SGO.PV.4000; a right hemimandible, with a portion of the symphyseal region, comprising the p1–m3, and an associated posterior fragment of skull.

Geographic and stratigraphic provenance. The specimen was collected by R. Wall in 1990 in the south bank of the BioBío river, at the northern foot of the Cerro Rucañanco in lacustrine facies of the Río Pedregoso Member (Suárez et al., 1990), late Middle Miocene (Serravallian) age (Pedroza et al., 2017; Rossetol et al., 2019b, Fig. 2).

Description. The mandible is relatively thin and gracile (mandible height of 25 mm below the m1 and 29.6 mm below the m3). The mandibular symphysis extends posteriorly to the level of the anterior edge of p2 (Fig. 4a and b). Posterior to the symphysis, the horizontal ramus is slightly thicker dorsoventrally (ca. 21 mm between p2 and p3, ca. 26 mm below the midpoint of m3). Although partially broken, in the labial side of the mandible is possible to recognize one mental foramina located below the anterior portion of the p3 (Fig. 4b). The angle and coronoid process of the mandible are partially broken, but them broadly resembles those of other macraucheniid (McGrath et al.,

2018). In the mandible, there is the p1–m3 series in situ. These teeth show little wear and the series does show deciduous teeth, indicating that the specimen is a young adult individual.

The p1–p3 are relatively simple (caniniform-like) with a single major cuspid (protoconid). The talonid and trigonid of p1–p3 are similar in size. The p1 is the smaller premolar, while the posterior ones progressively increasing in size and complexity. A small diastema separates the p1 and p2. In the posterolingual side of p2 and p3 are a columnar metaconid (absent in p1). The metaconid of p3 is larger than those of p2; p3 lacks a paraconid (unlike *Cramauchenia* and *Pternoconius*). The protocristid of p1–p3 is not completely aligned with the mandible axis (there are rather slightly imbricated), that is the reasons for why these premolars are partially overlapping in lateral and medial views (Fig. 4c). In p1–p3 the preprotocristid is rather straight and mesiolingually directed. A lingual cingulum is present in the mesiolingual margin of p1, and is relatively continuous along the lingual side of p2 and p3, being less-developed in the lingual portion of the metaconid. A labial cingulum is also present in the anterior-most side of the p3, less developed in p2, and absent in p1. The p4, larger than p3, is molariform with a selenodont and bicrescent pattern resembling most Macraucheniiidae (Soria and Hoffstetter, 1985). The p4 lacks entolophid and distinctive paraconid and entoconid (Fig. 4c). The hypolophulid is shorter than paralophid, unlike *Cramauchenia* (Schmidt, 2013; Schmidt and Ferrero, 2014). The trigonid is anteroposteriorly wider than the talonid, but in advances stages of wearing this feature likely disappear, generating a talonid-trigonid of a rather similar size. The metaconid is the higher cuspid in the lingual edge. In the labial edge, the hipoconid and protoconid are the most elevated cuspid. Both are mesiodistally separated by a wide and deep ectoflexid. In fact, the p4 ectoflexid is wider than those of m1 and m2, being comparable in width to the m3 (Fig. 4c).

The m1 is slightly larger than the p4, unlike *T. gracilis* and *T. frenguelli* in which the p4 is larger than the m1 (ESM_3). The m2 and m3 are of similar size. In m1 and m2 the trigonid is reduced with respect to the talonid, and the opposite occurs in the m3 (Fig. 4c). However, as previously mentioned this pattern probably is not observable in advances stages of wear. The lower molars (m1–m3) present a distinct entoconid, connected mesiolabially to the middle portion of the oblique cristid (anteriorly to the metaconid; Fig. 4c), forming a relatively long crest (entolophid). This large entolophid reaches the medial edge of the m1–m3 (Fig. 4c). In m1–m3 the paraconid and hypolophulid are indistinct and merged into the paralofid and hypolophulid, respectively. The hypolophulid is larger and better developed than the paralofid. In m1–m2 the paralophid reach the lingual side (Fig. 4c). In m3 the paralophid reach the lingual side. The entoconid of m1–m3 is large and mediolaterally opposed to the hypolophulid. In p4–m3 a labial cingulum is present in the paralophid and hypolophulid, but not in the ectoflexid, and two lingual cingula are present on either side of the metaconid. The p4–m3 series is mesiodistally aligned. The skull fragment is narrow, with a slender braincase and prominent sagittal crest clearly observed in dorsal view (Fig. 4d and e). In lateral view, the occipital condyles do not protrude at the level of the nuchal crest.

Remarks. Size is a relevant feature for distinguishing among Macraucheniiidae genera, and the Cura-Mallín specimen is more similar in size to several *Theosodon* species, being definitely larger than other 'Cramaucheniinae' (Cheme-Arriaga et al., 2016; Forasiepi et al., 2016; McGrath et al., 2018; Soria, 1981), and smaller than several Macraucheniiidae (Schmidt, 2013).

A well-developed m3 entolophid attached to the oblique crista is present in SGO. PV.4000, *Theosodon*, *Coniopternium*, *Scalabrinitherium*, *Paranauchenia*, differing from *Cramauchenia*, *Oxydontherium*, *Xenorhinotherium*, *Macrauchenia*, *Macrauchenopsis*, in which the m3 entolophid is absent (Cifelli and Soria, 1983; Forasiepi et al., 2016; Schmidt, 2013; Schmidt and Ferrero, 2014; Soria, 1981; Soria and Hoffstetter, 1985); *Cullinia*, *Promacrauchenia*, *Llullataruca*, in which the

m3 entolophid is reduced (Forasiepi et al., 2016; McGrath et al., 2018; Schmidt, 2013); and *Pternoconius* in which the m3 entolophid is attached to the hypoconulid (Soria and Hoffstetter, 1985). In SGO. PV.4000, *Coniopternium*, *Scalabrinitherium* and *Theosodon* the entoconid on m1–m2 reaches the lingual level of metaconid, while in *Paranauchenia* it does not (Forasiepi et al., 2016; Schmidt, 2013). In SGO. PV.4000, *Theosodon* and *Scalabrinitherium* the paralophid in m1–m2 is well-developed (terminates on the lingual side), while in *Coniopternium* it is less developed, terminating in an anterior medial position (Forasiepi et al., 2016; Schmidt, 2013; Schmidt and Ferrero, 2014). In dorsal view, the SGO. PV.4000 skull fragment shows a prominent sagittal crest (Fig. 4d), similar to those of *Theosodon* (Scott, 1910), but unlike *Scalabrinitherium* and others Macraucheniiidae (Forasiepi et al., 2016; Schmidt, 2013). This allows us to refer with confidence the Cura-Mallín macraucheniid to the *Theosodon* genus.

The Cura-Mallín *Theosodon* represents a young adult individual slightly smaller than others referred to Santacrucian (*T. lallemanti*, *T. gracilis*, *T. lydekkeri*, *T. garretorum*, *T. pozzii*, *T. patagonicus*) and Laventan (*T. arozquetai*, *Theosodon* sp.) species (Ameghino, 1897, 1889; Cifelli and Guerrero, 1997; McGrath et al., 2018; Scott, 1910; Soria, 1981; ESM_3). These size differences are especially evident by their reduced anteroposterior length of premolars and width of molar and premolars (ESM_3). SGO. PV.4000 is rather similar in size to *T. frenguelli* (Soria, 1981). Besides size differences, morphological traits also allow us to differentiate the Cura-Mallín specimen from some of the *Theosodon* spp. better known and illustrated. The specimen here described differs from the Colhuehuapian *T. frenguelli* in having a larger entolophid in m3, from *T. gracilis* in having a p4 smaller than the m1 (Scott, 1910; Soria, 1981; ESM_3), and from *T. lydekkeri* in having an m1 entolophid reaching the labial side (Ameghino, 1894). Despite these differences, and taking into account the uncertainty surrounding the taxonomic status of the putative species included in the genus, we prefer to use a conservative taxonomic approach and just refer the specimen from Lonquimay to the taxon *Theosodon* until a thorough revision of genus has been conducted.

Theosodon has been previously recorded in Chile in the Rio Cisnes Fauna ('Friasian' SALMA), as well from the Pampa Castillo (Colhuehuapian to 'Friasian' SALMAS) and Chucal faunas (Santacrucian SALMA) (Croft et al., 2004; Flynn et al., 2002a, 2002b). With a well-constrained late Middle Miocene age (Serravallian) SGO. PV.4000 represents the youngest record (ca. 12 Ma) of the genus in Chile, and the south of South America (see Discussion section).

NOTOUNGULATA Roth, 1903

TYPOTHERIA Zittel, 1893

INTERATHERIIDAE Ameghino 1887

INTERATHERIINAE Ameghino, 1887

PROTYPOTHERIUM Ameghino, 1885

Included species. *P. antiquum* Ameghino, 1885 (type species); *P. attenuatum* Ameghino, 1887a; *P. praeutilum* Ameghino, 1887a; *P. australe* Ameghino, 1887b; *P. diastematum* (Ameghino, 1891); *P. distinctum* Cabrera and Kraglievich, 1931; *P. minutus* Cabrera and Kraglievich, 1931; *P. sinclairi* Kramarz et al. (2015), *P. endiadys* (Roth, 1899), *P. colloncurensis* Vera et al. (2017) and *P. conceptionensis* sp. nov.

Geographic and Stratigraphic Distribution. Early to Late Miocene, Patagonia (Chile and Argentina), central Argentina, and Bolivia.

Remarks. According to recent phylogenetic analyses (Vera et al., 2018, 2017), the genus *Protypotherium* is not monophyletic.

Protypotherium conceptionensis sp. nov.

Suárez et al. (1990): cf. *Protypotherium* sp.

Buldrini and Bostelmann (2011): *Protypotherium* cf. *australe*

Buldrini et al. (2015): *Protypotherium* sp.

Holotype. SGO.PV.21000; well-preserved skull bearing all the teeth.

Referred materials. SGO.PV.4004; fragmented left dentary, with well-preserved p3, p4 and m1. SGO. PV.4005; anterior portion of the

mandibular symphysis, with fragmented portions of i1, i2, i3 and c, and partial p1.

Diagnosis. Large size interatherine (similar in size to *P. australe* and *P. colloncurensis*) with the following unique character combinations: I1 subequal in size to I2–I3; P1 does not overlap by P2 and C; P1 shape different from canine and P2; M1–M2 protocone more developed than hypocone and lingually protruding (especially in M1); deep parastylar sulcus on M1, but little evident parastylar sulcus in M2; single and vertical lingual sulcus on M1–2; upper molars imbricated and decrease in size from M1 to M3; lack of a posteriorly projected metastyle in the M3; moderately developed descending process of the maxilla; maxillary bone exposed along the laterodorsal surface of the skull and extended dorsally over the orbit; absence of a frontal-sliver anteriorly projected.

Etymology. In honor to the Universidad de Concepción (Concepción, Biobío region, Chile), an institution commemorating in 2019 its 100th foundation anniversary.

Type locality. The holotype (SGO.PV.21000) was collected in the surrounding of the Puente Tucapel locality, Araucanía Region, Chile (Fig. 1). The tentatively referred specimens SGO.PV.4004 and SGO.PV.4005 come from the east bank of the Biobío River, in outcrops located 1 km north of the Puente Tucapel, Araucanía Region, Chile.

Type horizon. Late Middle Miocene (Serravallian; Mayoan SALMA, see section 5.1. for details; Fig. 2), Rio Pedregoso member, Cura-Mallín Formation.

Description. The SGO.PV.21000 specimens is a nearly complete (but slightly deformed) skull with left and right I1–M3, but some of the incisors, canines, and premolars are partially damaged and/or covered by sediments (Fig. 5a,b,c). The jugals and the basioccipital bones are not preserved. The rostrum is relatively short (basicranium is much mesiodistally longer), with a high maxilla and wide nasals (Fig. 5b). The maxillary bone is exposed along the laterodorsal surface of the skull and largely extended dorsally over the orbit, as occurs in *P. endiadys*, but unlike *P. australe* (Vera et al., 2017). Besides, also resembling *P. endiadys* any anterior process of the frontal bone is observed between the nasals (Vera et al., 2017). The root of the zygomatic arch is well-expanded, as in *P. australe*. The sagittal crest is well-developed. The palate is rather curved (concave). In lateral view, the parietal is considerably elevated, therefore, the upper profile of the skull slopes forward and backward gradually. This feature, unlikely to be the result of post-mortem distortion, is much more marked in SGO.PV.21000 than in *P. endiadys* and *P. australe* (Sinclair, 1908; Vera et al., 2017). The antorbital foramen is large and circular and placed above the P4 (Fig. 5c).

The upper incisors are poorly preserved. However, several features can be distinguished. In occlusal view (Fig. 5a), the I1–I3 are rather similar in size (ESM₄), elongated, transversally flattened, and they appear to be slightly narrowing mesially. All the incisors are of similar mesiodistal length. The C is rather subtriangular, labiolingually compressed, with a wider mesial section. The P1 is wider than the C, and a diastema between both is lacking (Fig. 5a). The P1 is different in shape from canine and P2, as in *P. australe* and *P. endiadys* (Vera et al., 2018, 2017). P1 is longer than wide, with the longer axis mesiodistally oriented, lacks a parastyle, and does not overlaps with none P2 or C (Fig. 5a). The P2–P4 are completely differentiated from molars. As partially covered by sediment, details of the occlusal surface of P2–P4 are obscured, however, the broad outline of these premolars indicates that the P3 and P4 are rather similar in size (slightly wider than longer; ESM₄), while the P2 is nearly as long as wide (ESM₄). P2–4 have a folded ectoloph, which is more clearly marked in the P4 (Fig. 5a).

The upper tooth-row is gently curved. Upper molars are strongly imbricated (a feature clearly observed in P4–M2), lack permanent fosses, decrease in size markedly from M1 to M3 (ESM₄), and exhibit a single transversely straight and wide lingual sulcus dividing the lingual wall in anterior and posterior lobes. The M1 and M2 exhibit a more developed area of the protocone than area of the hypocone, and the area of the protocone is lingually protruding, especially in the M1 (Fig. 5a). M1 has a well-developed and forwardly extended parastyle

with a rather deep parastylar sulcus, unlike *P. australe* and *P. praerutilum* in which the parastyle is moderate and/or little evident (Sinclair, 1908; Vera et al., 2018). The M2 has a shallow parastylar sulcus (Fig. 5a). The M3 parastyle is much less developed than in M1 and M2. The M3 does not exhibit a posteriorly projected metastyle. Posteriorly, the parastyle and paracone fold become progressively less prominent than in premolars (Fig. 5a).

The two referred specimens likely represent a single individual. SGO.PV.4004 is a right fragment of the anterior region of the mandible preserving parts of the i1–p1 (see Buldrini et al., 2015, Fig. 2f–i). The i1–i3 display a similar oval shape, with the longer axis labiolingually oriented. The i1 lacks any groove, unlike *P. australe* in which the i1 is bifid (Vera et al., 2018). The incisors become distally larger (i.e., $i3 > i2 > i1$). The lower canine is larger than the i3. There is no space (diastema) among i3, c and p1. The p1 is oval in shape with the longer axis mesiodistally oriented and lacks a differentiated talonid (canine-form-like). SGO.PV.4005 is a fragment of the left mandible bearing the p3–m1 (Fig. 5d). The height of the mandible below the m1 is 18.7 mm. The p3–p4 are not molariform. Despite its poor preservation, premolars have a visible very shallow lingual and labial sulcus dividing the anterior (trigonid) and posterior (talonid) lobes (Fig. 5d). The p3 and p4 talonid are much more mesiodistally short and transversally narrower than the trigonid, giving to the teeth a pear-like shape. The m1 has two lobes separated by the hypoflexid and lingual fold, the anterior lobe is mesiodistally shorter and transversally wider than the posterior one. The m1 is larger than the premolars.

Remarks. The holotype and referred materials were recovered from the surroundings of the Puente Tucapel (Figs. 1 and 2), but they likely represent two different individuals. However, as the size of upper and lower teeth are rather congruent, we tentatively classify all these materials as belonging to the same new taxon. The presence of P/p3–P/p4 completely differentiated from molars, mesial sulcus on P/p3–4, and smaller talonid than trigonid on p3–4 supports their assignment to the genus *Protypotherium* (Schmidt, 2013; Vera et al., 2017).

Protypotherium concepcionensis differs from several of the species so far recognized; *P. attenuatum* has a highly curved upper tooth-row, and a shallow notch in the distal-most edge of the M3; *P. distictum* has upper molars with bifid lingual sulcus and a roughly equally developed area of the hypocone/protocone in M1–M2; *P. minutus* has upper molars with a single and mesially oriented lingual sulcus, and a posterior lobe of M3 with more triangular contour in occlusal view; *P. praerutilum* has a shallow notch in the distal-most edge of the M3; *P. endiadys* has nearly equally-sized upper molars and a well-developed parastylar sulcus in M2 (Tauber, 1996; Vera et al., 2017); *P. endiadys*, *P. praerutilum*, *P. attenuatum*, and *P. diastematum* are significant smaller than *P. concepcionensis* in tooth size (Sinclair, 1908; Tauber, 1996; Vera et al., 2017). Unlike *P. colloncurensis*, *P. concepcionensis* has a P1 different in size from canine and P2; P1 does not overlap with C or P2; P2–3 with a low length/width ratio; M1 with a deep parastylar sulcus; single and vertical lingual sulcus on M1–2. Previous work on the Lonquimay's protypotheres suggests close affinities with *P. australe* (Buldrini et al., 2015; Buldrini and Bostelmann, 2011). However, *P. concepcionensis* differs from the later in several features: I1 subequal in size to I2; M1–M2 with area of the protocone more developed than area of hypocone and lingually protruding; M1 with a deep parastylar sulcus; maxillary bone exposed along the laterodorsal surface of the skull and extended dorsally over the orbit; absence of a sliver of frontal anteriorly projected; and lack of a third lobe (posteriorly projected metastyle) in the M3. Few species within *Protypotherium* (*P. antiquum* and *P. sinclairi*) were described upon mandibular remains limiting comparisons with the skull SGO.PV.21000. The tentatively referred material (mandible fragment bearing the p3–m1; SGO.PV.4004; Fig. 5d) provides differences with these species. *Protypotherium sinclairi* (Colhuehuapian SALMA), a species similar in size to *P. australe* and SGO.PV.21000, has transversely larger talonids and deeper lingual and labial sulcus in p3–p4 (Kramarz et al., 2015); while *P. antiquum* (Huayquerian SALMA)

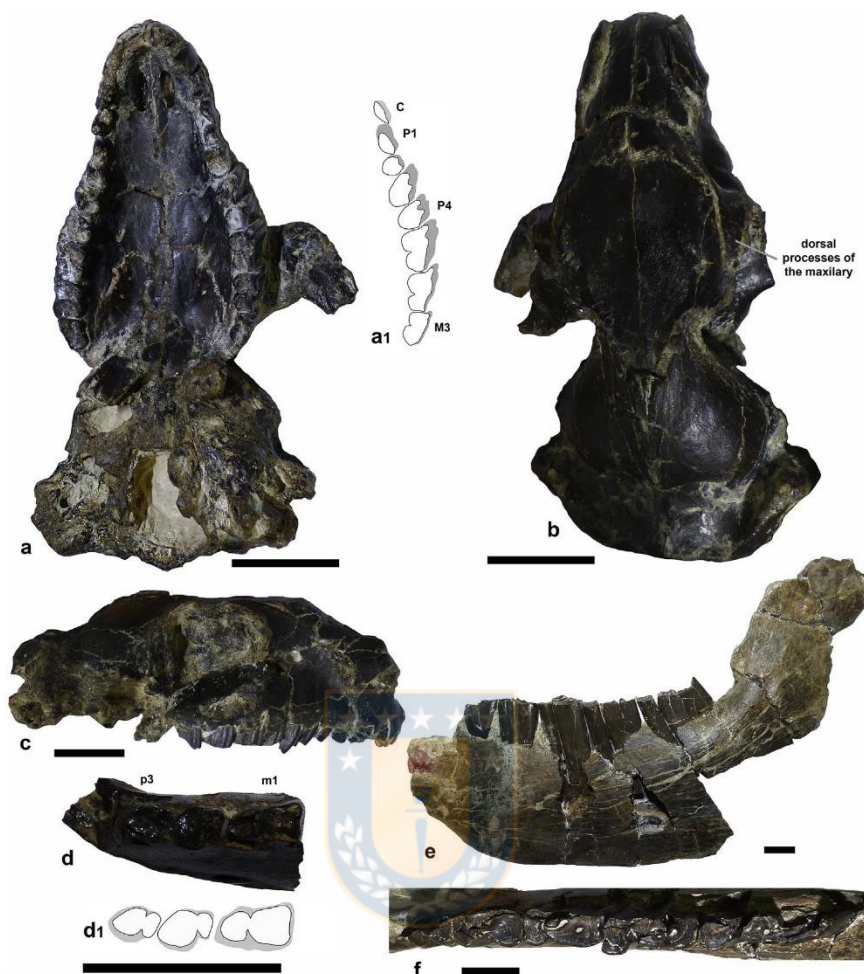


Fig. 5. Notoungulates from Cura-Mallín Formation (Río Pedregoso Member) recovered in the surroundings of Lonquimay, Chile. *Protypotherium concepcionensis* sp. nov. (Puente Tucape locality, late Middle Miocene; Serravallian): skull (SGO.PV.21000; holotype) in ventral (a), dorsal (b) and lateral (c) views, and mandible fragment (SGO.PV.4004; tentative referred material) in dorsal view (d). *Nesodon imbricatus* (Cerro Tallón, Early Miocene; Santacrucian SALMA), a partial left mandible (SGO.PV.5226) in lingual view (e) and a detail of the occlusal view (f). Scale bar = 20 mm.

exhibits a lingually displaced talonid in p4 (Fernández et al., 2018; Schmidt, 2013). Therefore, the unique character combination (mentioned in the diagnosis) of the holotype, as well those of the tentatively referred material, are distinct from those of other intherateriine species and warrants their attribution to a new species.

In Chile, *Protypotherium* remains appears to be common. It has been reported in Early Miocene localities of the Cura-Mallín Formation at Laguna del Laja (Flynn et al., 2008), and the Santa Cruz Formation, in Pampa Castillo, and Pampa Guadal (Buldrini et al., 2015); in early Middle Miocene of the Río Frías Formation in the upper Río Cisnes (Bostelmann et al., 2012; Encinas et al., 2016); and now in the late Middle Miocene of the Cura-Mallín Formation. Additional remains potentially referable to *Protypotherium* were collected at Río Oscuro, Aysén in Mayoan SALMA age strata (Buldrini et al., 2015).

TOXODONTIDAE Gervais, 1847

NESODONTINAE Murray, 1866

NESODON Owen 1846

Nesodon imbricatus Owen 1847

Croft et al. (2003): *Nesodon conspurcatus*

Revised materials. SGO.PV.5226; a partial left mandible preserving the base of the third incisor and nearly complete p3–m3, as well as

a portion of the coronoid process.

Geographic and stratigraphic provenance. The specimen was collected by J.P. Radic and E. Zurita toward the north of the Cerro Tallón locality, Río Pedregoso Member, in beds with an age slightly older than 17.5 Ma and younger than 20 Ma (Croft et al., 2003; Pedroza et al., 2017). Therefore, the specimen could be referred to the Early Miocene (Santacrucian SALMA; Fig. 2).

Description. The specimen SGO.PV.5226 was previously described in details by Croft et al. (2003).

Remarks. Based mostly on their size, SGO.PV.5226 was initially referred to *N. conspurcatus* (Croft et al., 2003). Nevertheless, after a recent review of the Santacrucian nesodontids, Hernández Del Pino (2018) suggested that *N. conspurcatus* is a junior synonym of *N. imbricatus*.

XENARTHRA Cope, 1889

CINGULATA Illiger, 1811

GLYPTODONTIDAE Gray, 1869

Glyptodontidae gen. et sp. indet.

Suárez et al. (1990): Glyptodontidae gen. et sp. indet.

Revised materials. SGO.PV.4006a, SGO.PV.4006b; two isolated (but associated) fixed osteoderms.

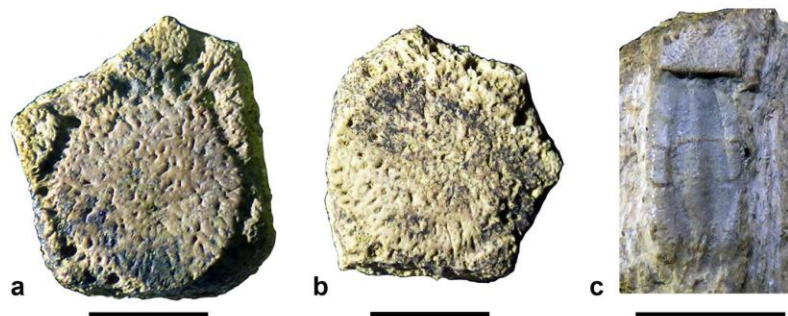


Fig. 6. Cingulata remains from the Cura-Mallín Formation (Río Pedregoso Member) in the surroundings of Lonquimay, Chile. Glyptodontidae gen. et sp. indet. (SGO.PV.4006a and SGO. PV.4006b), from the Piedra Parada locality (late Middle Miocene; Serravallian), osteoderm in dorsal view (a, and b respectively). Eutatini gen. et sp. indet. (SGO.PV.22476) from the Cerro Rucañanco locality (late Middle Miocene; Serravallian), osteoderm in dorsal view (c). Scale bar = 10 mm.

Geographic and stratigraphic provenance. The identification label of the MNHN indicates that the osteoderms were collected by L. Marshall and P. Salinas in 1989 at Piedra Parada locality, 2 km to the N-NE of Puente Lolén, BioBio river (Fig. 1), Río Pedregoso Member. However, the specimen was collected by one of us (GC) in the same locality. In the present work, we assign these specimens to the late Middle Miocene (Serravallian; see discussion below and Fig. 2).

Description. Fixed osteoderms of hexagonal contour and small size (SGO.PV.4006a = 19.4 × 20.8 mm; SGO.PV.4006b = 20 × 22.7 mm). They have an enlarged sub-circular principal figure positioned along the posterior edge of each osteoderm, occupying most of the dorsal surface of the osteoderm (Fig. 6a and b). The principal figure reaches the posterior edge of the osteoderm. There are four reduced peripheral figures located only in the anterior-most osteoderm edge; two to any peripheral figures in the lateral edges; lacking peripheral figures in the posterior edge (Fig. 6a). The principal and peripheral figures are separated by a shallow peripheral groove (U-shaped). Conspicuous dorsal foramina (=piliferous pits) occur at the intersections of the principal and peripheral figures. Dorsally the osteoderms are flat to gently convex, and the principal and peripheral figures are rather similar in height. The osteoderms are relatively thick (9–10 mm) in relation to their dorsal area. Dorsal osteoderm sculpturing is quite faint, as occurs in glyptatelines and propalaeophorines (Croft et al., 2007; González-Ruiz, 2010). The ventral portion of the osteoderm is much more sculpted, and there are several (2–5) pits.

Remarks. The most relevant features displayed by the Piedra Parada glyptodont are their large principal figure located close to the posterior edge of the osteoderm, without posterior peripheral figures and reduced lateral peripheral figures. These features are present in most portions of the carapace of glyptatelines and *Parapropalaeophorus septentrionalis* Croft et al. (2007), some dorsal osteoderm of *Eonacum colloncuranum* Scillato-Yané and Carlini (1998), the anterodorsal osteoderms of *Paraeucinepeltus raposeirasi* González-Ruiz et al. (2011), and in some lateral osteoderms of Propalaeophorinae and Hoplophorinae Hoplophorini (Croft et al., 2007; González-Ruiz, 2010; González-Ruiz et al., 2011; Scillato-Yané and Carlini, 1998). As the osteoderms from Cura-Mallín are rather hexagonal they likely represent dorsal ones (Ameghino, 1889; Croft et al., 2007). In this sense, their morphology appears to be more closely related with the Glyptatelines and the three Glyptodontidae *incertae sedis*, *Eonacum*, *Parapropalaeophorus*, and *Paraeucinepeltus*. The Piedra Parada glyptodont differs from the Glyptatelines (*Glyptatelus fractus*, *Glyptatelus tatusinus*, and *Clypeotherium magnum*) in which the principal and peripheral figures are convex and rounded (except in *Clypeotherium* where they are flat), and the grooves that delimit the figures are deep (Ameghino, 1897; Scillato-Yané, 1977b; Zurita et al., 2015). It differs from *Parapropalaeophorus* in its smaller size, because *Parapropalaeophorus* largest dorsal osteoderm is 42 mm long × 34 mm wide, but also by its more conspicuous piliferous pits (Croft et al., 2007). The anterodorsal osteoderms of *Paraeucinepeltus* are slightly

larger than those of the Cura-Mallín glyptodont, and have larger peripheral figures (González-Ruiz et al., 2011). *Eonacum* is a small size glyptodont (as SGO.PV.4006), but it shows a larger number and size of the peripheral figures than those observed in the Piedra Parada osteoderms (Scillato-Yané and Carlini, 1998). Glyptodont taxonomy is one of the most complex among fossil mammal groups in South America (e.g. González-Ruiz, 2010; Toriño and Perea, 2018). Further, the limited and fragmentary materials show some degree of erosion, which undoubtedly hinders the anatomical study of the material. Therefore, we are unable to perform any precise taxonomic arrangement of Piedra Parada glyptodont.

DASYPODOIDEA Gray, 1821

DASYPODIDAE Gray, 1821

EUPHRACTINAE Winge, 1923

EUTATINI Bordas, 1933

Eutatini gen. et sp. indet.

Revised materials. SGO.PV.22476; a moveable band osteoderm.

Geographic and stratigraphic provenance. The specimen was collected by L. Marshall in 1991, along the NE of Cerro Rucañanco, Río Pedregoso Member, Cura-Mallín Formation, late Middle Miocene (Serravallian; Pedroza et al., 2017; Rosselot et al., 2019b, Fig. 2).

Description. Rather small (20 mm length, 5 mm width) and smooth osteoderm composed of a principal figure separated by two wide and shallow transverse grooves from two lateral figures (Fig. 6c). The principal figure is broader toward the middle portion of the osteoderm (being wider than the lateral figures) and narrower toward the distal and proximal edges. The lateral figures are undivided by lateral grooves (Fig. 6c). The lateral and principal figures are of similar height (=elevation) along the entire osteoderm. Over the transversal groove (dorsal surface) there are few and inconspicuous piliferous pits. The caudal margin of the osteoderm is not well-preserved but appears to contain at least one large foramen. In the anterior-most osteoderm edge, there is the quadrangular region for the overlap between moveable band osteoderms.

Remarks. The moveable band osteoderm SGO.PV.22476 lacks distinctive pits on its dorsal surface, as occurs in the tribe Eutatini (Croft et al., 2007; Scillato-Yané, 1977a; Scillato-Yané et al., 2010). Members of Eutatini also display a row of three-four large piliferous pits along the caudal margin of moveable band osteoderms (Ciancio et al., 2017; Croft et al., 2007). Yet, due to the poor preservation of the osteoderm caudal margin, we are unable to confirm whether this last feature is present in the Cura-Mallín material.

At least 11 genera, ranging from ?late Eocene to the late Pleistocene, are grouped within Eutatini (Croft et al., 2007; McKenna and Bell, 1997). During the Neogene, several Eutatini genera could be recognized (Croft et al., 2007; González-Ruiz, 2010; Scillato-Yané et al., 2010; Scott, 1903). Many of them (e.g. *Proeutatus*, *Paraeutatus*, *Doellotatus* and *Paraeutatus*) are characterized by moveable band osteoderms with a lageniform central figure (Ciancio and Carlini, 2016; Dozo et al., 2014; González-Ruiz, 2010; Scillato-Yané et al., 2010), unlike that of

SGO.PV.22476 (Fig. 6c). In this sense, the Cura-Mallín Eutatini mostly resembles *Stenotatus*, a late Oligocene to Middle Miocene genus that includes five named species, as well as two potentially undescribed species (Croft et al., 2009, 2007; González-Ruiz, 2010). The specimen SGO.PV.22476 is in the range of size of *Stenotatus patagonicus* Ameghino, 1887, and *S. planus* Scillato-Yané and Carlini (1998) (Croft et al., 2009; González-Ruiz, 2010; Scott, 1903). However, taking into account the scarcity of available material, we are unable to achieve a reliable genus level identification for the Cura-Mallín armadillo.

5. Discussion

The few specimens so far collected from the Lonquimay area (38° S) allow us to recognize at least six taxa including a primitive toxodont (*Nesodon imbricatus*), astrapotheres (*Parastrapotherium* sp.), glyptodonts (Glyptodontidae indeterminate), armadillos (Eutatini indeterminate), macraucheniiids (*Theosodon* sp.), and new interatheriine species (*Protypotherium conceptionensis* sp. nov.). The last three taxa are for the first time recognized in the area. Contrasting with previous interpretations (Marshall et al., 1990), after our surveys of the MNHN collections, we are unable to recognize any specimen referable to mesotheriid nor caviomorph. Thus, their record from the Lonquimay area could not be confirmed, albeit it does not mean that they did not exist there. We acknowledge the presence of a seventh taxon, which likely corresponds to a small Platyrrhini monkey represented by a worn lower molar (SGO.PV.22204; Fig. 7) recovered from the Cerro Rucañanco locality (late Middle Miocene, Serravallian; Cura-Mallín Formation; Fig. 2), but whose taxonomic status is still under study. Whether their taxonomic assignment is confirmed the specimen SGO. PV.22204 could correspond to the first record of a monkey in the Cura-Mallín Formation.

5.1. A reassess of the biochronological affinities of the Lonquimay Neogene mammals

The Cura-Mallín mammalian assemblages found in the surroundings of Lonquimay town were initially assigned to the Early Miocene (Marshall et al., 1990; Suárez et al., 1990). Successive works (Bostelmann et al., 2014; Buldrini et al., 2015; Croft et al., 2003) re-inforced an Early Miocene age for this fauna. The *Nesodon* indicated a Santacrucian (~18.2 to ~15.6 Ma *sensu* Cuitiño et al., 2016) SALMA (Croft et al., 2003), the *Protypotherium* was tentatively assigned to the 'Pinturan' (19.0–18.0 Ma *sensu* Cuitiño et al., 2016)– Santacrucian SALMA (Buldrini and Bostelmann, 2011), whereas the *Parastrapotherium* was referred to the Colhuehuapian (20–21 Ma *sensu* Dunn et al., 2013) SALMA (Bostelmann et al., 2014). At the genus levels, these interpretations were considered reliable because these notoungulates as well as the macraucheniid genera are typical (although not exclusive) from the Santacrucian SALMA (e.g. Cassini et al., 2012),

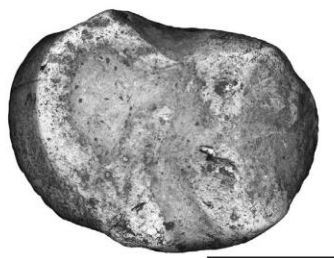


Fig. 7. Scanning electron microscopy photograph of the lower molar (SGO.PV.22204; in occlusal view) of the putative Platyrrhini monkey recovered from the Cerro Rucañanco locality (late Middle Miocene, Serravallian; Río Pedregoso Member; Cura-Mallín Formation). Scale bar = 2mm.

and *Parastrapotherium* is known from the Deseadan to the Colhuehuapian SALMA (Kramarz and Bond, 2010, 2008). However, new stratigraphic information and U-Pb dating have challenged some of these ideas (Pedroza et al., 2017; Rosselot et al., 2019b), with the *Protypotherium* recovered from the Puente Tucapel being referred to the Laventan SALMA (13.5–11.8 Ma; Pedroza et al., 2017). These contradictions illustrate the need of a reassessment of the biochronological affinities of the Lonquimay Neogene mammals.

A review of the stratigraphic interpretations, published radiometric dates, the original geographic provenance of the fossil specimens (Pedroza et al., 2017; Rosselot et al., 2019b; Suárez et al., 1990; Suárez and Emparan, 1995, Fig. 2), as well as preliminary field observations, allows us to recognize two distinctive chronological mammalian assemblages in the Lonquimay area of Early Miocene (likely Colhuehuapian–Santacrucian SALMA), and late Middle Miocene (Serravallian) ages. The former includes the mammals recovered from Cerro Tallón and Río Quepuca localities, while the latter contains those recovered from Piedra Parada, Cerro Rucañanco, and Puente Tucapel localities (Table 1; Figs. 1 and 2). Although the maximum depositional ages from Puente Tucapel and Cerro Rucañanco localities (Pedroza et al., 2017; Rosselot et al., 2019b) might be interpreted as near-sedimentation ages, slightly younger (early Late Miocene; Tortonian) ages for these localities are also plausible and cannot be completely discarded.

The Early Miocene assemblage includes the large taxa *Nesodon* and *Parastrapotherium*. As previously mentioned, *Parastrapotherium* is a taxon so far only known from the Deseadan–Colhuehuapian SALMAS (Kramarz and Bond, 2010, 2008). However, due to the lack of radiometric data in the sampling locality, we cannot definitively assign an age for this specimen rather than likely Early Miocene (likely Colhuehuapian SALMA) based on biostratigraphic correlation. On the other hand, *N. imbricatus* comes from the Cerro Tallón locality from which K-Ar radioisotopic dating yields an age of 17.5 ± 0.6 Ma (Croft et al., 2003; Suárez and Emparan, 1995, Fig. 2). Yet, the K-Ar method has limited accuracy and the age must be taken with caution. In spite of this, the age is broadly consistent with those of *N. imbricatus* in Early Miocene (Santacrucian SALMA) faunas from the Santa Cruz Formation, where this taxon is very common and abundant (Cassini et al., 2012; Hernández Del Pino, 2018).

The late Middle Miocene assemblage is the more diverse and includes the protypothere, macraucheniid, armadillo, glyptodont, and the presumable platyrrhini. The *Protypotherium* specimens from Lonquimay were found in loose blocks on the Puente Tucapel hillside, making their geochronological assignment doubtful (Suárez et al., 1990). However, a nearly-autochthonous provenance is inferred. Recent U-Pb dates of detrital zircons from the base and top of Puente Tucapel section yielded maximum ages of 12.7 ± 0.3 and 12.5 ± 0.3 Ma (late Middle Miocene; Pedroza et al., 2017). Hence, the new taxon *Protypotherium conceptionensis* must be of late Middle Miocene age (Fig. 2). The armadillo, macraucheniid and putative platyrrhini were recovered from the Cerro Rucañanco surroundings (Fig. 2). There are recent U-Pb dating of detrital zircons from the basal (?) and middle sections of this locality that yielded maximum depositional ages of 11.64 and 12.4 Ma respectively (Pedroza et al., 2017; Rosselot et al., 2019b). In this sense, the putative Platyrrhini from the Cerro Rucañanco would be one of the younger records of monkeys in the south of South America, likely indicating continuous presence of the clade in Chile from the Early to late Middle Miocene (after *Chilecebus* and Río Cisnes Platyrrhini) (Bobé et al., 2015; Flynn et al., 1995; Tejedor, 2003). The presence of *Theosodon* in the late Middle Miocene is of particular interest because most of *Theosodon* specimens and all named species come from the Early Miocene (McGrath et al., 2018; Scott, 1910). While the younger (Serravallian) records of the genus are restricted to low and middle latitudes in La Venta (Colombia), Quebrada Honda (Bolivia) and Fitzcarrald (Peru) (Cifelli and Guerrero, 1997; McGrath et al., 2018; Tejada-Lara et al., 2015). Therefore, here we illustrate the persistence of

Table 1

Summary of the age and mammals from each of the recognized mammal-bearing localities from the Cura-Mallín Formation at the Lonquimay area (Chile). References from ages: ^aRosset et al. (2019b), ^bPedroza et al. (2017), ^cSuárez and Emparan (1995), ^dKramarz and Bond (2008).

Locality	Age (Ma)	Epoch	Dating method	Mammals recovered
Cerro Rucañanco	12.4 ^a – 11.64 ^b	late Middle Miocene	U/Pb in detrital zircons (maximum age)	Platirini indet., Eutatini indet. <i>Theosodon</i> sp.
Puente Tucapel	12.5–12.7 ^b	late Middle Miocene	U/Pb in detrital zircons (maximum age)	<i>P. conceptionensis</i> sp. nov.
Piedra Parada	13.0 ^c	late Middle Miocene	K-Ar (whole-rock) in brecciated andesite	Glyptodontidae indet.
	12.8 ^a	late Middle Miocene	U/Pb in detrital zircons	
Río Quepuca	–	Early Miocene ^d	Biochronological correlation	<i>Paratrypaetherium</i> sp.
Cerro Tallón	17.5 ^c	Early Miocene	K-Ar (biotite) tuff	<i>Nesodon imbricatus</i>

Theosodon in the Chilean Andes until ca. 12 Ma.

The glyptodont was recovered from Piedra Parada outcrops (Figs. 1 and 2). Early K-Ar dates from the cliff of Piedra Parada hill indicated a Middle Miocene age (13 Ma) (Suárez and Emparan, 1995). Nonetheless, based on stratigraphical interpretations this locality was later referred to the Early Miocene (22–17 Ma; *sensu* Pedroza et al., 2017). Recent U-Pb dating of a volcanic tuff at the base of the Piedra Parada section indicates an age of 12.8 Ma (Rosset et al., 2019a) confirming a late Middle Miocene (Serravallian) age for this locality. These findings also raise the question about the general reliability of Pedroza et al.'s (2017) interpretations, and reinforce the idea of a complex stratigraphic scenario in the area exacerbated by the lack of continuous outcrops. In any case, the age of the glyptodont from Lonquimay must be slightly younger than 12.8 Ma (late Middle Miocene; Fig. 2) because it was recovered from a bed overlying the dated tuff.

As previously mentioned, Pedroza et al. (2017) assign the *Protypotherium* remains from Puente Tucapel locality to the Laventan SALMA. The U-Pb radiometric ages of 12.8 to 11.6 Ma (Fig. 2; Table 1) indicate a late Middle Miocene age for the upper mammal assemblages from the Cura-Mallín Formation, and agrees with the proposed interval of the Laventan SALMA (13.5–11.8 Ma) which was erected based on the locality of La Venta (~3°N) in Colombia (Madden et al., 1997). However, recent faunal comparison between localities coeval with La Venta, as Quebrada Honda (~22°S, Bolivia) for example, demonstrates the relative paucity of taxa shared between them. Therefore SALMAS may not be useful for biocorrelation between low-latitude faunas and those from elsewhere in South America as previously proposed by Croft (2007). Here, we argued that the age range (12.8–11.6 Ma) of the upper mammalian assemblage of the Cura-Mallín Formation is also consistent with the Mayoan SALMA. Fossils considered Mayoan comes typically from the Río Mayo Formation a continental sequence mainly characterized by sandstones, tuffs, tuffites, pelites and conglomerates, which crops out in several localities in south-western Chubut and northwestern Santa Cruz provinces, Argentina (Dal Molin et al., 1998; De Iuliis et al., 2008; González Ruiz et al., 2017; Vera et al., 2018). Additional Mayoan fossils also have been recovered in the underlying El Portezuelo and El Pedregoso formations (De Iuliis et al., 2008; Folguera et al., 2018a; Scillato-Yané and Carlini, 1998). Early works suggested, without the aid of radiometric ages, an early Late Miocene age (10.0–11.8 Ma) for the Mayoan fauna (Flynn and Swisher, 1995). However, recent radiometric data acquired from the El Pedregoso, El Portezuelo, and Río Mayo formations (with faunas typically ascribed to the Mayoan) indicates ages between 13.5 and 11.8 Ma (De Iuliis et al., 2008; Folguera et al., 2018a; Vera et al., 2018). Consequently, the updated chronostratigraphic framework indicates that the Mayoan SALMA (defined in the high latitudes, ~46°S) is, at least partially (González Ruiz et al., 2017), temporally superposed with the Laventan SALMA (defined in low latitudes, ~3°N; Madden et al., 1997). Thus, the differences between both Laventan and Mayoan faunas are probably linked to different environmental and ecological conditions in both regions of South America rather than to temporally distinctive evolutionary stages, and deserve further scrutiny as discussed in the present contribution. New fossil collections under strict stratigraphic control will be necessary to corroborate and/or refine the validity and position

of the Mayoan mammal association (González Ruiz et al., 2017). Despite the fauna analyzed here does not bear typical 'Mayoan' taxa, we tentatively correlate the upper mammalian assemblage from the Cura-Mallín Formation cropping out in Lonquimay with the Mayoan SALMA based in geochronological correlations.

5.2. Paleobiogeographical considerations

Some of the specimens analyzed here could not be identified at the species level due to their fragmentary state of preservation, limited sampling, and the uncertainty surrounding the taxonomy of some genera (e.g., *Theosodon* needing taxonomic revision). However, it is possible to establish the broad biogeographical relationships of the Lonquimay mammal assemblages with those from other coeval localities.

The Lonquimay fauna encompasses one of the few well-documented occurrences of *Nesodon imbricatus* outside of high latitude localities (e.g. Croft et al., 2004, 2003), as well as the unique report of *Paratrypaetherium* from Chile (Bostelmann et al., 2014). Both indicated Early Miocene biogeographic connections with the classic high latitude Patagonian faunas (~50°S) in both Argentina and Chile (Bostelmann et al., 2013; Cassini et al., 2012; Hernández Del Pino, 2018; Kramarz and Bond, 2010, 2008). Before the present work, the geographic distribution of *Theosodon* during the late Middle Miocene (Serravallian) was limited to La Venta (3°N; Colombia), and to Quebrada Honda (22°S; Bolivia) (Cifelli and Guerrero, 1997; McGrath et al., 2018). Consequently, our work corroborates a significant southern extension of the geographic distribution of this taxon during the late Middle Miocene, extending from the cited localities to the Lonquimay area (38°S). *Protypotherium conceptionensis* (Cura-Mallín Formation, Chile) contributed to increase the biodiversity of the genus in the Serravallian. Two additional late Middle Miocene taxa are known, *P. colloncurensis* (Collon Cura, ~41°S and Río Mayo, ~46°S formations, Argentina), and *P. endiadydys* (Collon Cura formation, ~41°S). Both are recognized in the Colloncuran SALMA and likely in younger Mayoan SALMA beds (Vera et al., 2018, 2017). This suggests that protypotheres were more widespread along the late Middle Miocene (Serravallian) intra-arc and foreland basins in the south-central Andes than previously thought.

Considering the limited sampling of mammals so far recorded from the Lonquimay region, taxonomic comparison with relatively close geographic paleontological localities in both Chile and Argentina must be considered preliminary. Three taxa (*Nesodon*, *Theosodon*, and *Protypotherium*) are shared with the Early Miocene Pampa Castillo fauna (~47°S), and that of the early Middle Miocene Río Frías Formation (~45°S) in southern Chile (Bostelmann et al., 2012; Charrier et al., 2015; Encinas et al., 2016; Flynn et al., 2002b), and also with the Santa Cruz Formation (~51°S) in Argentina (Cassini et al., 2012). Two taxa (*Nesodon* and *Theosodon*) are shared with the early Miocene Chucal fauna, Chile (~19°S; Charrier et al., 2015; Croft et al., 2004). One genus (*Protypotherium*) is shared with the early Miocene Cerro Bandera fauna of Neuquen, Argentina (Kramarz et al., 2005). So far no taxon is shared with the early to middle Miocene fauna from the Aisol Formation, Argentina (~34.5°S; Forasiepi et al., 2015, 2011), nor with the late Miocene of Caragua, Chile (~18°S; Bostelmann et al., 2018).

It is necessary to note the paucity of shared taxa between the two mammalian faunas of the Cura-Mallín Formation in Chile, Lonquimay (38°S) and Laguna del Laja (~37.5°S). This could be due to the combination of several factors including poor taxonomic resolution, few fossil findings, and differences in age. The lower mammalian assemblage from Lonquimay might temporally correlate with the Tcm₁ (19.8–18 Ma) and Tcm₃ (17.8–16.4 Ma) levels of the Laguna del Laja, cropping out in the Estero Trapa-Trapa (Flynn et al., 2008; Herriott, 2006), but none shared taxa between both have been so far reported. The upper mammalian assemblage from Lonquimay area might temporally correlate with the fossil-bearing horizons reported from the Trapa-Trapa Formation (cropping out in the Laguna del Laja area), which appears to be mid-late Miocene, possibly Colloncuran or Mayoan SALMA, in age (Flynn et al., 2008). The Trapa-Trapa Formation only include a record of an interatheriid referred to cf. *Interatherium* sp. (Flynn et al., 2008). The upper mammalian assemblage from Lonquimay also include an interatheriid, but included in the *Protypotherium* genus (Fig. 5). Indeterminate *Protypotherium* remains have also been reported from Early Miocene (Tcm₁ and Tcm₃) levels in the Laguna del Laja (Flynn et al., 2008; Herriott, 2006). Therefore, *Protypotherium* is the only taxa shared between the Lonquimay and Laguna del Laja faunas so far. Future studies dealing with the taxonomy and systematics of the Laguna del Laja fauna, as well as increasing sampling efforts, could certainly provide a better framework for further comparisons between these two geographically close localities within the Cura-Mallín Basin.

5.3. Paleoenvironmental significance

Even though the Lonquimay taxa described here may not have necessarily coexisted, as they were recovered from different outcrops (Fig. 2), they provide ecological information about the depositional environment of the study area. The macraucheniid *Theosodon* would likely have inhabited mainly closed-canopy habitats, with the larger species having more mixed-feeding habits than the smaller ones, which would have had more browsing habits (Cassini et al., 2012). Several lines of evidence, including paleobiology (Cassini, 2013; Cassini et al., 2012), taphonomy (common occurrence in stream-channel sediments or associated with aquatic fauna), and microanatomical features (Houssaye et al., 2016), are consistent with the astrapothere specialization for graviportal, semi-aquatic, and closed-habitat foraging. Using a microwear approach, Townsend and Croft (2008) described *Nesodon imbricatus* as a leaf browser focused more on hard browsing, and *Protypotherium* as a browser on both soft browse and soft fruits. However, other authors used paleobiological evidence to indicate that *Nesodon* was a taxon adapted to foraging on grass and leaves depending on the availability in mixed habitats (Cassini, 2013; Cassini et al., 2012). *Protypotherium* has been interpreted as a generalized terrestrial mammal tending toward cursoriality (Croft and Anderson, 2007) living in open habitats and foraging on grass (Cassini, 2013; Cassini et al., 2012). The armadillos, essentially fossorial and occupants of burrows, naturally avoid the environments in which these can be overflown (Scillato-Yané et al., 2013). Due to their small size, both the armadillo and glyptodont from the Lonquimay area likely inhabited mixed to closed habitats (Vizcaíno et al., 2012, 2011). The platyrrhine monkey would suggest forested environments, as modern platyrrhines are mostly adapted to such habitats in tropical to subtropical conditions (Lynch Alfaro et al., 2015; Silvestro et al., 2019), and the same has been acknowledged for some Miocene platyrrhines (Kay et al., 2012a).

The knowledge about taxonomic diversity of the mammals from the Lonquimay area is low, and micromammals are likely underrepresented due to the scarce fossiliferous content of the Cura-Mallín Formation in the area. Then, additional lines of evidence must be necessary for a more reliable paleoenvironmental reconstruction (Kay et al., 2012b). Previous work dealing with the fossil pollen and leaves imprints recovered from the CMF in the Lonquimay area allows for the recognition

of a diverse flora suitable to complement the paleoenvironmental reconstruction based on mammals. For example, Palma-Heldt and Rondanelli (1990) report the presence of *Nothofagus pumillo*, *Nothofagus antarctica* and *Boquilla trifoliolata* from the Cerro Rucañanco section (late Middle Miocene). These *Nothofagus* species are indeed extant ones and indicate (if a niche conservatism is accepted) a microthermal climate with a mean annual temperature of ~7 °C (11.6–2.5 °C), and mean of annual precipitation of ~1200 mm (Hinojosa et al., 2016). Salinas (1979) reports Myrtaceae leaves, a family with extant representatives in Chile commonly found in humid rainforests or flooded environments (Kausel, 1944), from the Lolco Formation (a former name for the Guapitrio Member) at the Estero Los Azules (38°14'30.49"S; 71°26'13.16"W). On the other hand, palynomorphs recovered from several stratigraphic levels along Lonquimay area, including the older (Early Miocene) levels of the Cura-Mallín Formation at Paso Rahue area and the younger levels outcropping in Cerro Rucañanco, suggest the persistence of humid and partly marshy forests in temperate to cold temperatures (Palma-Heldt, 1983). The freshwater fishes and invertebrates commonly found in along the Rio Pedregoso member advocate fluviolacustrine environments (Rubilar, 1994). Finally, the presence of serrasalmid remains in the Cerro Rucañanco (Rubilar, 1994) is indicative of tropical affinities, as they are common in ichthyological assemblages from Neotropics (Freeman et al., 2007). However, additional work is necessary in order to refine the taxonomic affinities of those serrasalmids remains.

Putting all this paleoecological information into a temporal framework (Table 1; Fig. 2) it is possible to recognize an Early Miocene environment mainly characterized by the existence of semi-aquatic and forested habitats, and a late Middle Miocene environment with a microthermal climate with closed canopy and permanent bodies of water. Yet, the presence of *Protypotherium* in the last assemblage might advocate the existence of open habitats in their surroundings. In any case, though restricted, the information provided by the fossil biota (mammals, freshwater-fishes, and flora) reveals a rather homogeneous forested, humid and temperate environment during the deposition of the Cura-Mallín Formation (Early to late Middle Miocene).

Today, the Andean Cordillera exhibits a lower topography (up to 3500 m) between the 37°–39°S than in northern parts of this range (Rojas Vera et al., 2016). Even though, these relatively low altitudes constitute a topographic barrier to atmospheric circulation, and causes a 'rain-shadow effect'—the sharp decline in precipitation often observed on the leeward side of mountain ranges—(Hijmans et al., 2005; Siler et al., 2012). Based on regional scale land cover and global annual mean precipitation data are possible to characterize the present-day broad-scale setting of the Andes Cordillera around the 37°–39°S (Hijmans et al., 2005; Zhao et al., 2016). The western-most (windward side) portion of the Andes has high precipitation rates (> 1500 mm/year), with the dominance of forested environments (Fig. 8). In the eastern portion of the Andes (leeward side), where the Lonquimay fossiliferous localities are located, there is a progressive decrease in the precipitation rates (reaching ~1000 mm/year), and a progressive dominance of grasslands and shrublands toward the east (Fig. 8). Finally, the foreland (east of the Andean Cordillera) exhibits a very low mean annual precipitation rate (< 500 mm/year), with predominant grassland and barren land (Fig. 8). Therefore, at the latitudes of our work (37°–39°S) the foreland is strongly affected by the rain-shadow effect, but the intermontane basins emplaced in the eastern portion of the Andes main Cordillera also exhibit a rain-shadow effect, even if not extreme. The combination of Andean uplift (and the subsequent rain-shadow effect in the foreland) and global climatic oscillations cause a significant impact on the southern South American Neogene biota (Horton, 2018; Ortiz-Jaureguizar and Cladera, 2006; Palazzesi and Barreda, 2012; Zachos et al., 2001). Neogene mammals exhibit a pattern of progressive reduction of browsers and frugivorous taxa, which were abundant in the Early Miocene and successive less common in the Late Miocene, with grazers showing the inverse pattern (Ortiz-

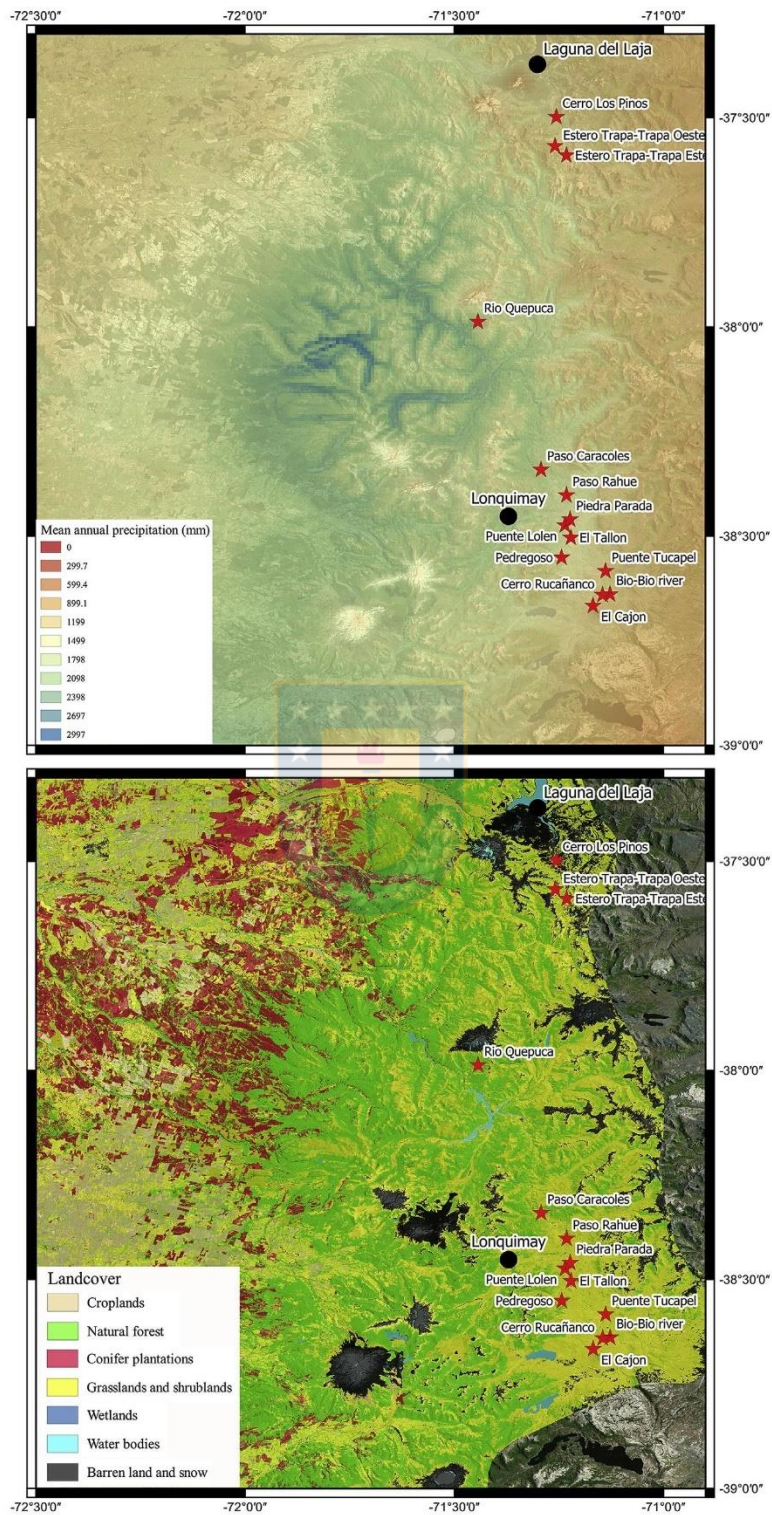


Fig. 8. The present-day global annual mean of precipitation (upper) and land cover (lower) setting of the Andes Cordillera around the 37°–39°S. Based on Hijmans et al. (2005) and Zhao et al. (2016). The red stars indicated the localities in which fossil mammals from the Cura-Mallín Formation have been recovered (Flynn et al., 2008; Marshall et al., 1990; Pedroza et al., 2017; Suárez et al., 1990). (For interpretation of the references to colour in this figure legend, the reader is referred to the Web version of this article.)

Jaureguizar and Cladera, 2006). The Patagonian (46°–50°S) floral change from an Early Miocene highly diverse forested ecosystem to a markedly different community of lower diversity dominated by arid-adapted shrubs by Late Miocene (Barreda and Palazzesi, 2014; Palazzesi and Barreda, 2012). But the possible existence of environmental changes during the Miocene related to the rain-shadow effect is not well-documented at the 38°–39°S latitude.

The rather homogenous paleoenvironmental conditions suggested by the fossil biota of the Cura-Mallín Formation recovered from the Lonquimay area indicate that during the late Middle Miocene forested, temperate and humid conditions persist at this latitude. These environmental interpretations contrast with the present-day setting of the Lonquimay area, where is noted the predominance of grasslands and shrublands (Fig. 8). Therefore, even when contractional conditions in the CMB could be established since the Early Miocene (Rosset et al., 2019a), we suggest that this portion of the Andes did not reach sufficient paleoaltitudes (> 1000 m) to cause an important orographic rain shadow effect, with the subsequent increase in the aridity in the eastern foreland, at least until after the late Middle Miocene (ca. 12 Ma). This scenario is consistent with previous works at the latitude of our study area (~38°–39°S), because after the Late Miocene there is a significant increase in crustal shortening (Rojas Vera et al., 2014), exhumation rates (Spikings et al., 2008), the occurrence of synorogenic deposits (Melnick et al., 2006), and seasonally wet and dry conditions in the foreland (Le Roux, 2012). Our interpretation is also consistent with the diverse, humid and forested vertebrate fauna reported in the Middle Miocene (Langhian) Collon Cura Formation (37°–40°S), which also includes platyrrhine monkeys (Pardiñas, 1991; Vucetich et al., 1993). However, we acknowledge that in similar time spans (~12 Ma) the southern extra-Andean Patagonia regions already exhibited vegetational, and faunal changes toward cooler and more arid climate likely driven by an important orographic rain shadow effects due to the uplift of the Patagonian Andes (45–47°S) (Blisniuk et al., 2005; Folguera et al., 2018a; Ortiz-Jaureguizar and Cladera, 2006; Palazzesi and Barreda, 2012). On the another hand, it has been argued that the Neogene Andean uplift (and the associated rain shadow effect) may not be the sole determinant force for Patagonian desertification, because global climatic changes affecting the Southern Hemisphere could be another important factor (Palazzesi et al., 2014; Trayler et al., 2019). Thus, an alternative climatically driven scenario is also plausible, because both (tectonic and climatic) triggers are virtually indistinguishable with the available data. Future paleoecological analysis of the still poorly known Early to Late Miocene mammalian assemblages cropping out in the Laguna del Laja area (Cura-Mallín and Trapa-Trapa Formations; Flynn et al., 2008) certainly could shed more light in this regard.

6. Conclusions

The review of the taxonomic and chronological affinities of the Lonquimay fauna (Cura-Mallín Formation) allows us to recognize two chronological distinctive mammalian assemblages (Table 1). The lower assemblage is Early Miocene (likely Colhuehuapian–Santacrucian SALMA) in age, and includes *Nesodon imbricatus* and *Parastrapotherium* sp.; while the upper assemblage is late Middle Miocene in age (12.8–11.6 Ma) and includes glyptodonts (Glyptodontidae indeterminate), armadillos (Eutani indeterminate), macraucheniiids (*Theosodon* sp.), a new protypothere species (*Protypotherium conceptionensis* sp. nov.) and likely a platyrrhini monkey. In this sense, contrasting with previous interpretations (Alvarenga, 1995; Bostelmann et al., 2013; Buldrini et al., 2015; Buldrini and Bostelmann, 2011; Diederle, 2015; Marshall et al., 1990; Suárez et al., 1990) the fauna from Lonquimay is not uniquely confined to the Early Miocene. As a consequence, the continental bird *Meganhinga chilensis* from the Cerro Rucañanco (Alvarenga, 1995) must be of late Middle Miocene age.

Despite their very low species richness, and only based in the age of

their sediment-bearing fauna, the upper levels from the Cura-Mallín Formation in Lonquimay area must be putatively assigned to the Mayoan SALMA. Biogeographically, the lower Lonquimay fauna (Early Miocene) is clearly of Patagonian affinities. At the genus level *Theosodon* is shared with other coeval localities in Colombia, and Bolivia, highlighting the wider geographic late Middle Miocene (Serravallian) distribution of this macraucheniid along the Andes.

Even when limited, the information provided by the fossil biota (mammals, freshwater-fishes and flora) recovered from the Lonquimay area reveals a rather homogeneous environment during the deposition of the Cura-Mallín Formation along the Early to late Middle (Fig. 2), with a predominance of rather temperate, humid and forested habitats with permanent bodies of water. At the time, our finding suggests that the Andean Cordillera of south-central Chile (38°S) did not reach a sufficient elevation to cause an important orographic rain-shadow effect in late Middle Miocene, and the increased aridity in the eastern foreland basins was likely developed at this latitude only after c. 12 Ma. However, considering the contrasting degrees of Neogene crustal shortening and exhumation noted in the immediately northern latitudes (Rojas Vera et al., 2016, 2014; Spikings et al., 2008), we prefer not to generalize our interpretations to the entire Cura-Mallín basin. Given the scarcity of fossils mammals in the area, future studies involving independent proxies such as oxygen isotopic analyses of fish tooth/bone bioapatite and mollusk shells (Wang et al., 2008) undoubtedly will provide valuable information to test our paleoenvironmental interpretations.

Acknowledgments

We wish to thank the Consejo de Monumentos Nacionales (CMN, Chile) the authorization for fossil prospecting and to the Corporación Nacional Forestal (CONAF). To David Rubilar (MNHN), Marcelo Reguero (MLP) and Laura Chornogubsky (MACN) for granting access to the vertebrate paleontological collections under his care, and Yuanyan Zhao (Tsinghua University, China) for providing access to the land cover original data. We thank to Andres Folguera, Alejandro Kramarz, and an anonymous reviewer for valuable suggestions and comments that greatly improved the manuscript. This research was funded by Conicyt, Fondecyt project n°1151146 (AE); and Conicyt-PCHA/Doctorado Nacional/2018–21180471(AS).

Appendix A. Supplementary data

Supplementary data to this article can be found online at <https://doi.org/10.1016/j.jsames.2019.102319>.

References

- Alvarenga, H.M.F., 1995. A large and probably flightless aninga from the Miocene of Chile. *Cour. Forschungsinst. Senckenberg* 181, 149–161.
- Ameghino, F., 1897. Mammifères crétaqués de l'Argentine. 1. *Boletín del Inst. Geol. Argent.* 18, 406–521.
- Ameghino, F., 1894. Enumeration Synoptique des especes de mammifères fossiles des formations Eocenes de Patagonie. 13:259–452. *Bol. la Acad. Nac. Ciencias en Cordoba (Republica Argentina)* 13, 259–452. <https://doi.org/10.5962/bhl.title.77348>.
- Ameghino, F., 1889. Contribución al conocimiento de los mamíferos fósiles de la República Argentina. *Actas la Acad. Nac. Ciencias en Córdoba* 6, 1–1027.
- Arratia, G., 2015. Los peces osteictios fósiles de Chile y su importancia en los contextos paleobiogeográfico y evolutivo. *Publicación Ocas. del Mus. Nac. Hist. Nat. Chile* 63, 35–83.
- Azpelicueta Maria, de las Mercedes, Rubilar, A., 1997. A fossil siluriform spine (Teleostei, Ostariophysi) from the Miocene of Chile. *Andean Geol.* 24, 109–113. <https://doi.org/10.5027/andgeov24n1-a07>.
- Barreda, V.D., Palazzesi, L., 2014. Response of plant diversity to Miocene forcing events: the case of Patagonia. In: Stevens, W.D., Montiel, O.M., Raven, P.H. (Eds.), *Paleobotany and Biogeography: A Festschrift for Alan Graham in His 80th Year*. Missouri Botanical Garden Press, pp. 1–25.
- Bechis, F., Encinas, A., Concheyro, A., Litvak, V.D., Aguirre-Urreta, B., Ramos, V.A., 2014. New age constraints for the Cenozoic marine transgressions of northwestern Patagonia, Argentina (41°–43° S): paleogeographic and tectonic implications. *J. South Am. Earth Sci.* 52, 72–93. <https://doi.org/10.1016/j.jsames.2014.02.003>.

- Bertrand, O.C., Flynn, John J., Joseph, John, Croft, D.A., Wyss, A.R., 2012. Two new taxa (Caviomorpha, Rodentia) from the early oligocene Tinguiririca fauna (Chile). *Am. Mus. Novit.* 3750, 1–36 1955-.
- Blisniuk, P.M., Stern, L.A., Chamberlain, C.P., Idelman, B., Zeitler, P.K., 2005. Climatic and ecologic changes during miocene surface uplift in the southern patagonian Andes. *Earth Planet. Sci. Lett.* 230, 125–142. <https://doi.org/10.1016/J.EPSL.2004.11.015>.
- Bohe, R., Bostelmann, E., Tejedor, M.F., Carrasco, G., Mancuso, A.C., Alloway, B.V., Bellosi, E., Ugalde, R., Buldrini, K.E., 2015. Primates del Mioceno de Río Cisnes, Patagonia Chilena. In: V Congreso Latinoamericano de Paleontología de Vertebrados. Colonia del Sacramento, Uruguay, pp. 36.
- Bostelmann, E., Bohe, R., Carrasco, G., Alloway, B.V., Santi-Malnis, P., Mancuso, A., Agüero, B., Allemsged, Z., Godoy, Y., 2012. The Alto Río Cisnes fossil fauna (Río Frías Formation, early Middle Miocene, Fríasian SALMA): a keystone and paradigmatic vertebrate assemblage of the South American fossil record. In: III Simposio Paleontología En Chile, pp. 42–45 Punta Arenas, Chile.
- Bostelmann, E., Buldrini, K.E., Kramarz, A.G., 2014. A new generic assignment for the Quepuca River astrapothere (Mammalia, Astrapotheria). In: IV Simposio Paleontología En Chile. Universidad Austral de Chile, Valdivia.
- Bostelmann, E., Le Roux, J.P., Vásquez, A., Gutiérrez, N.M., Oyarzún, J.L., Carreño, C., Torres, T., Otero, R., Llanos, A., Fanning, C.M., Hervé, F., 2013. Burdigalian deposits of the Santa Cruz Formation in the sierra Baguales, austral (Magallanes) basin: age, depositional environment and vertebrate fossils. *Andean Geol.* 40, 458–489. <https://doi.org/10.5027/andgeoV40n3-a04>.
- Bostelmann, E.J., Castro, N., Moreno, K., García, M., Fosdick, J., Campos-Medina, J., Croft, D.A., Montoya-Sanhueza, G., 2018. Stratigraphy and paleontology of Caragua, Arica and Parinacota regions, Chile, part 2: biostratigraphy and geochronology of the late Miocene sedimentary sequence. In: XV Congreso Geológico Chileno. Concepción, Chile, pp. 1321.
- Buldrini, K.E., Bostelmann, E., 2011. A well preserved skull of *Protypotherium* CF. P. australe Ameghino 1887, (mammalia, notoungulata, Interatheriidae) from the early miocene of Chile. *Ameghiniana* 48, R-149.
- Buldrini, K.E., Bostelmann, E., Soto Acuña, S., 2015. Taxonomic identity of the Interatheriidae SGO.PV.4004 and SGO.PV.4005, and rectification of collection numbering of Caraguatypotherium muñozii (Notoungulata; Mesotheriidae). In: XIV Congreso Geológico Chileno, La Serena, Chile, pp. 702–705.
- Burns, W.M., Jordan, T.E., Copeland, P., Kelley, S.A., 2006. The case for extensional tectonics in the Oligocene-Miocene Southern Andes as recorded in the Cura Mallín basin (36°–38°S). In: Special Paper 407: Evolution of an Andean Margin: A Tectonic and Magmatic View from the Andes to the Neuquén Basin (35°–39°S Lat). Geological Society of America, pp. 163–184. <https://doi.org/10.1130/2006.2407.08>.
- Canto, J., Yáñez, J., Rovira, J., Rovira, J., 2010. Estado actual del conocimiento de los mamíferos fósiles de Chile. *Estud. Geol.* 66, 255–284. <https://doi.org/10.3989/egool.39778.055>.
- Cassini, G.H., 2013. Skull geometric morphometrics and paleoecology of santacrucian (late early miocene; Patagonia) native ungulates (astrapotheria, litopterna, and notoungulata). *Ameghiniana* 50, 193–216. <https://doi.org/10.5710/AMGH.7.04.2013.606>.
- Cassini, G.H., Cerdeño, E., Villafañe, A.L., Muñoz, N.A., 2012. Paleobiology of santacrucian native ungulates (Meridiungulata: astrapotheria, litopterna and notoungulata). In: Vizcaíno, S.F., Kay, R.F., Bargo, M.S. (Eds.), Early Miocene Paleobiology in Patagonia. Cambridge University Press, Cambridge, pp. 243–286. <https://doi.org/10.1017/CBO9780511667381.015>.
- Charrier, R., Baeza, O., Elgueta, S., Flynn, J., Gans, P., Kay, S., Muñoz, N., Wyss, A., Zurita, E., 2002. Evidence for Cenozoic extensional basin development and tectonic inversion south of the flat-slab segment, southern Central Andes, Chile (33°–36°S.L.). *J. South Am. Earth Sci.* 15, 117–139. [https://doi.org/10.1016/S0895-9811\(02\)00009-3](https://doi.org/10.1016/S0895-9811(02)00009-3).
- Charrier, R., Flynn, J.J., Wyss, A.R., Croft, D.A., 2015. Marco Geológico-tectónico, contenido fosilífero y cronología de los yacimientos cenozoicos pre-pleistocénicos de Mamíferos terrestres fósiles de Chile. *Publicación Ocas. del Mus. Nac. Hist. Nat. Chile* 63, 293–338.
- Cheme-Arriaga, L., Dozo, M.T., Gelfo, J.N., 2016. A new Cramaucheniinae (litopterna, Macraucheniiidae) from the early miocene of Patagonia, Argentina. *J. Vertebr. Paleontol.* 36, e1229672. <https://doi.org/10.1080/02724634.2017.1229672>.
- Ciancio, M.R., Carlini, A.A., 2016. Identification of type specimens of Dasypodidae (mammalia , xenarthra) of the paleogene of Argentina. *Rev. del Mus. Argentino Ciencias Nat. nueva Ser.* 10, 221–237.
- Ciancio, M.R., Krmptovic, C.M., Scarano, A.C., Epele, M.B., 2017. Internal morphology of osteoderms of extinct armadillos and its relationship with environmental conditions. *J. Mamm. Evol.* 1–13. <https://doi.org/10.1007/s10914-017-9404-y>.
- Cifelli, R., Guerrero, J., 1997. Litopterns. In: Kay, R., Madden, R.H., Cifelli, R., Flynn, J. (Eds.), *Vertebrate Paleontology in the Neotropics: the Miocene Fauna of La Venta, Colombia*. Smithsonian Institution Press, Washington, D.C., pp. 289–302.
- Cifelli, R.L., Soria, M.F., 1983. Notes on Deseadan Macraucheniiidae. *Ameghiniana* 20, 141–153.
- Croft, D. a. Flynn, J.J., Wyss, A.R., 2004. Notoungulata and litopterna of the early miocene Chucal fauna , northern Chile notoungulata and litopterna of the early miocene Chucal fauna, northern Chile. *Fieldiana Geol.* 50, 1–52. <https://doi.org/10.5962/bhl.title.5228>.
- Croft, D.A., 2007. The middle miocene (Laventan) Quebrada Honda fauna, southern Bolivia and a description of its notoungulates. *Palaentology* 50, 277–303. <https://doi.org/10.1111/j.1475-4983.2006.00610.x>.
- Croft, D.A., Anaya, F., Auerbach, D., Garzone, C., MacFadden, B.J., 2009. New data on miocene Neotropical provinciality from Cerdas, Bolivia. *J. Mamm. Evol.* 16, 175–198. <https://doi.org/10.1007/s10914-009-9115-0>.
- Croft, D.A., Anderson, L.C., 2007. Locomotion in the extinct notoungulate *Protypotherium*. *Palaentol. Electron.* 11, 1–20. http://paleo-electronica.org/2008_1/138/index.html.
- Croft, D.A., Flynn, J.J., Wyss, A.R., 2008. The Tinguiririca fauna of Chile and the early stages of “Modernization” of south American mammal fauna 1. *Arq. do Mus. Nac.* 1, 191–211.
- Croft, D.A., Flynn, J.J., Wyss, A.R., 2007. A new basal glyptodontid and other Xenarthra of the early Miocene Chucal Fauna, Northern Chile. *J. Vertebr. Paleontol.* 27, 781–797. [https://doi.org/10.1671/0272-4634\(2007\)27\[781:ANBGAO\]2.0.CO;2](https://doi.org/10.1671/0272-4634(2007)27[781:ANBGAO]2.0.CO;2).
- Croft, D.A., Radic, J.P., Zurita, E., Charrier, R., Flynn, J.J., Wyss, A.R., 2003. A miocene toxodontid (mammalia: notoungulata) from the sedimentary series of the Cura-Mallín Formation, Lonquimay, Chile. *Rev. Geol. Chile* 30, 285–298. <https://doi.org/10.4067/S0716-02082003000200008>.
- Cuitiño, J.I., Fernicola, J.C., Kohn, M.J., Traylor, R., Naipauer, M., Bargo, M.S., Kay, R.F., Vizcaíno, S.F., 2016. U-Pb geochronology of the Santa Cruz Formation (early miocene) at the Río Bote and Río Santa Cruz (southernmost Patagonia, Argentina): implications for the correlation of fossil vertebrate localities. *J. South Am. Earth Sci.* 70, 198–210. <https://doi.org/10.1016/J.JSAMES.2016.05.007>.
- Cuitiño, J.I., Vizcaíno, S.F., Bargo, M.S., Aramendía, I., 2019. Sedimentology and fossil vertebrates of the Santa Cruz Formation (early miocene) in Lago Posadas, south-western Patagonia, Argentina. *Andean Geol.* 46, 383–420. <https://doi.org/10.5027/andgeoV46n2-3128>.
- Dal Molin, C., Márquez, M., Maisonabe, B., 1998. Hoja Geológica 4571-IV Alto Río Senguerr, provincia del Chubut. 1. Escala: 250000. SEGEMAR, pp. 1–34.
- De Iuliis, G., Brandoni, D., Scillato-Yané, G.J., 2008. New remains of *Megatheriulus* patagonicus Ameghino, 1904 (Xenarthra, Megatheriidae): information on primitive features of megatheriines. *J. Vertebr. Paleontol.* 28, 181–196. [https://doi.org/10.1671/0272-4634\(2008\)28\[181:nrompa\]2.0.co;2](https://doi.org/10.1671/0272-4634(2008)28[181:nrompa]2.0.co;2).
- Delsuc, F., Gibb, G.C., Kuch, M., Billet, G., Hautier, L., Southon, J., Rouillard, J.-M., Fernicola, J.C., Vizcaíno, S.F., MacPhee, R.D.E., Poinar, H.N., 2016. The phylogenetic affinities of the extinct glyptodonts. *Curr. Biol.* 26, R155–R156. <https://doi.org/10.1016/J.CUB.2016.01.039>.
- Diederle, J.M., 2015. Los Anhingidae (Aves: Suliformes) del Neógeno de América del Sur: sistemática, filogenia y paleobiología. Phd. Thesis. Universidad de la Plata.
- Dozo, M.T., Ciancio, M., Bouza, P., Martínez, G., 2014. Nueva asociación de mamíferos del Paleógeno en el este de la Patagonia (provincia de Chubut, Argentina): implicancias biocronológicas y paleobiogeográficas. *Andean Geol.* 41, 224–247. <https://doi.org/10.5027/andgeoV41n1-a09>.
- Dunn, R.E., Madden, R.H., Kohn, M.J., Schmitz, M.D., Stromberg, C.A.E., Carlini, A.A., Re, G.H., Crowley, J., 2013. A new chronology for middle Eocene-early miocene south American land mammal ages. *Geol. Soc. Am. Bull.* 125, 539–555. <https://doi.org/10.1130/B30660.1>.
- Echaurren, A., Folguera, A., Gianni, G., Orts, D., Tassara, A., Encinas, A., Giménez, M., Valencia, V., 2016. Tectonic evolution of the North Patagonian Andes (41°–44° S) through recognition of syntectonic strata. *Tectonophysics* 677–678, 99–114. <https://doi.org/10.1016/J.TECTO.2016.04.009>.
- Encinas, A., Folguera, A., Bechis, F., Finger, K.L., Zambrano, P., Pérez, F., Bernabé, P., Tapia, F., Riffó, R., Buatois, L., Orts, D., Nielsen, S.N., Valencia, V.V., Cuitiño, J., Oliveros, V., De Girolamo Del Mauro, L., Ramos, V.A., 2018. The Late Oligocene–Early Miocene Marine Transgression of Patagonia. *Springer, Cham*, pp. 443–474. https://doi.org/10.1007/978-3-319-67774-3_18.
- Encinas, A., Folguera, A., Litvak, V.D., Echaurren, A., Gianni, G., Fernández Paz, F., Bohe, R., Valencia, V., 2016. New age constraints for the Cenozoic deposits of the patagonian Andes and the sierra de San Bernardo between 43° and 46°S. In: *Primer Simposio de Tectónica Sudamericana*, pp. 140 Santiago, Chile.
- Fernández, M., Fernicola, J.C., Cerdeño, E., Reguero, M.A., 2018. Identification of type materials of the species of *Protypotherium* Ameghino, 1885 and *Patriarchus* Ameghino, 1889 (notoungulata: Interatheriidae) erected by Florentino Ameghino. *Zootaxa* 4387, 473. <https://doi.org/10.11646/zootaxa.4387.3.4>.
- Flynn, J.J., Charrier, R., Croft, D.A., Gans, P.B., Herriott, T.M., Wertheim, J.A., Wyss, A.R., 2008. Chronologic implications of new Miocene mammals from the Cura-Mallín and Trapa Trapa formations, Laguna del Laja area, south central Chile. *J. South Am. Earth Sci.* 26, 412–423. <https://doi.org/10.1016/J.JSAMES.2008.05.006>.
- Flynn, J.J., Croft, D.A., Charrier, R., Hérail, G., Wyss, A.R., 2002a. The first Cenozoic mammal fauna from the Chilean Altiplano. *J. Vertebr. Paleontol.* 22, 200–206. <https://doi.org/10.1017/S0016756897007061>.
- Flynn, J.J., Croft, D.A., Wyss, A.R., Hérail, G., García, M., 2005. New Mesotheriidae (mammalia, notoungulata, Typotheria), geochronology and tectonics of the Caragua area, northernmost Chile. *J. South Am. Earth Sci.* 19, 55–74. <https://doi.org/10.1016/J.JSAMES.2004.06.007>.
- Flynn, J.J., Novacek, M.J., Dodson, H.E., Frassinetti, D., McKenna, M.C., Norell, M.A., Sears, K.E., Swisher, C.C., Wyss, A.R., 2002b. A new fossil mammal assemblage from the southern Chilean Andes: implications for geology, geochronology, and tectonics. *J. South Am. Earth Sci.* 15, 285–302. [https://doi.org/10.1016/S0895-9811\(02\)00043-3](https://doi.org/10.1016/S0895-9811(02)00043-3).
- Flynn, J.J., Swisher, C.C., 1995. Cenozoic south American land mammal ages: correlation to global geochronologies. In: *Geochronology, Time Scales, and Global Stratigraphic Correlation*. SEPM (Society for Sedimentary Geology), pp. 317–333. <https://doi.org/10.2110/pec.95.04.0317>.
- Flynn, J.J., Wyss, A.R., Charrier, R., Swisher, C.C., 1995. An early miocene anthropoid skull from the Chilean Andes. *Nature* 373, 603–607. <https://doi.org/10.1038/373603a0>.
- Flynn, J.J., Wyss, A.R., Croft, D.A., Charrier, R., 2003. The Tinguiririca fauna, Chile: biochronology, paleoecology, biogeography, and a new early oligocene south American land mammal age. *Palaeoogeogr. Palaoclimatol. Palaeoecol.* 195, 229–259. [https://doi.org/10.1016/S0031-0182\(03\)00360-2](https://doi.org/10.1016/S0031-0182(03)00360-2).

- Folguera, A., Encinas, A., Echaurren, A., Gianni, G., Orts, D., Valencia, V., Carrasco, G., 2018a. Constraints on the Neogene growth of the central Patagonian Andes at the latitude of the Chile triple junction (45–47°S) using U/Pb geochronology in synorogenic strata. *Tectonophysics* 744, 134–154. <https://doi.org/10.1016/J.TECTO.2018.06.011>.
- Folguera, A., Gianni, G.M., Encinas, A., Álvarez, O., Orts, D., Echaurren, A., Litvak, V.D., Navarrete, C.R., Sellés, D., Tobal, J., Ramos, M.E., Fennell, L., Fernández Paz, I., Giménez, M., Martínez, P., Ruiz, F., Iannelli, S.B., 2018b. Neogene Growth of the Patagonian Andes. Springer, Cham, pp. 475–501. https://doi.org/10.1007/978-3-319-67774-3_19.
- Forasiepi, A.M., Cerdeño, E., Bond, M., Schmidt, G.I., Naipauer, M., Straehel, F.R., Martinelli, A.G., Garrido, A.C., Schmitz, M.D., Crowley, J.L., 2015. New toxodontid (notoungulata) from the early miocene of Mendoza, Argentina. *Paläontol. Z.* <https://doi.org/10.1007/s12542-014-0233-5>.
- Forasiepi, A.M., MacPhee, R.D.E., Del Pino, S.H., Schmidt, G.I., Amson, E., Grohé, C., 2016. Exceptional skull of Huayqueriana (mammalia, litopterna, Macraucheniiidae) from the late miocene of Argentina: anatomy, systematics, and paleobiological implications. *Bull. Am. Mus. Nat. Hist.* 404, 1–76. <https://doi.org/10.1206/0003-0090-404.1.1>.
- Forasiepi, A.M., Martinelli, A.G., de la Fuente, M.S., Dieguez, S., Bond, M., 2011. Paleontology and stratigraphy of the Aisol (Neogene), san Rafael, Mendoza. *Cenozoic Geology of the Central Andes of Argentina*. pp. 135–154.
- Freeman, B., Nico, L.G., Osenetoski, M., Jelks, H.L., Collins, T.M., 2007. Molecular systematics of Serrasalmidae: Deciphering the identities of piranha species and unraveling their evolutionary histories. *Zootaxa* 1484, 1–38. <https://doi.org/10.11646/zootaxa.1484.1.1>.
- Gaudin, T.J., Wible, J.R., 2006. The phylogeny of living and extinct armadillos (mammalia, xenarthra, Cingulata): a Craniodental analysis. In: Carrano, M.T., Gaudin, T.J., Blob, R., Wible, J.R. (Eds.), *Amniote Paleobiology: Perspectives on the Evolution of Mammals, Birds, and Reptiles*. University of Chicago Press, pp. 153–198.
- Giambiagi, L., Mescua, J., Bechis, F., Hoke, G., Suriano, J., Spagnotto, S., Moreira, S.M., Lössada, A., Mazzitelli, M., Dapozo, R.T., Folguera, A., Mardonez, D., Pagano, D.S., 2016. Cenozoic Orogenic evolution of the southern central Andes (32–36°S). In: Folguera, A., Naipauer, M., Sagripanti, L., Ghiglione, Matías C., Orts, D.L., Giambiagi, L. (Eds.), *Growth of the Southern Andes*. Springer, Cham, pp. 63–98. https://doi.org/10.1007/978-3-319-23060-3_4.
- González-Ruiz, L.R., 2010. Los Cingulata (Mammalia, Xenarthra) del Mioceno temprano y medio de Patagonia (edades Santacrucense y “Friasense”). Revisión sistemática y consideraciones bioestratigráficas. Phd thesis. Universidad Nacional de La Plata, La Plata, Argentina.
- González-Ruiz, L.R., Zurita, A.E., Scillato-Yané, G.J., Zamorano, M., Tejedor, M.F., 2011. Un nuevo Glyptodontidae (Mammalia, Xenarthra, Cingulata) del Mioceno de Patagonia (Argentina) y comentarios acerca de la sistemática de los gliptodontes “friasenses”. *Rev. Mex. Ciencias Geol.* 28, 566–579.
- González Ruiz, L., Reato, A., Cano, M., Martínez, O., 2017. Old and new specimens of a poorly known glyptodont from the Miocene of Patagonia and their biochronological implications. *Acta Paleontol. Pol.* 62. <https://doi.org/10.4202/app.00280.2016>.
- Guevara, J.P., Alarcón-Muñoz, J., Soto-Acuña, S., Lara, F.S., Buldrini, K.E., Rubilar-Rogers, D., Sallaberry, M., 2018. Primer registro de un Anuro fósil en el Neógeno de Chile. In: *Resúmenes Del I Congreso Paleontológico Chileno*, pp. 313–316 Punta Arenas, Chile.
- Hernández Del Pino, S., 2018. Anatomía y sistemática de los Toxodontidae (Notoungulata) de la Formación Santa Cruz, Mioceno temprano, Argentina. Universidad de La Plata, Facultad de Ciencias Naturales y Museo.
- Herriott, T.M., 2006. Stratigraphy, structure, and 40Ar/39Ar geochronology of the southeastern Laguna de Laja area: Implications for the mid-late Cenozoic evolution of the Andes near 37.5°S, Chile 2. Master's Thesis. Department of Earth Science, University of California, Santa Barbara.
- Hijmans, R.J., Cameron, S.E., Parra, J.L., Jones, P.G., Jarvis, A., 2005. Very high resolution interpolated climate surfaces for global land areas. *Int. J. Climatol.* 25, 1965–1978. <https://doi.org/10.1002/joc.1276>.
- Hinojosa, L.F., Gaxiola, A., Pérez, M.F., Carvajal, F., Campano, M.F., Quattrocchio, M., Nishida, H., Uemura, K., Yabe, A., Bustamante, R., Arroyo, M.T.K., 2016. Non-congruent fossil and phylogenetic evidence on the evolution of climatic niche in the Gondwana genus *Nothofagus*. *J. Biogeogr.* 43, 555–567. <https://doi.org/10.1111/jbi.12650>.
- Hitz, R.B., Flynn, J.J., Wyss, A.R., 2006. New basal Interatheriidae (Tyotheria, notoungulata, mammalia) from the paleogene of central Chile. *Am. Mus. Novit.* 3520, 1–32.
- Horton, B.K., 2018. Sedimentary record of Andean mountain building. *Earth Sci. Rev.* 178, 279–309. <https://doi.org/10.1016/J.EARSCIREV.2017.11.025>.
- Houssaye, A., Fernandez, V., Billet, G., 2016. Hyperspecialization in some south American Endemic ungulates revealed by long bone Microstructure. *J. Mamm. Evol.* 23, 221–235. <https://doi.org/10.1007/s10914-015-9312-y>.
- Jordan, T.E., Burns, W.M., Veiga, R., Pángaro, F., Copeland, P., Kelley, S., Mpodzis, C., 2001. Extension and basin formation in the southern Andes caused by increased convergence rate: a mid-Cenozoic trigger for the Andes. *Tectonics* 20, 308–324. <https://doi.org/10.1029/1999TC001181>.
- Kausel, E., 1944. Contribución al estudio de las Mirtáceas chilenas. *Rev. Argent. Agron.* 11, 320–327.
- Kay, R.F., Perry, J.M.G., Malinzak, M., Allen, K.L., Kirk, E.C., Plavcan, J.M., Fleagle, J.G., 2012a. Paleobiology of santacrucian primates. In: Vizcaino, S.F., Kay, R.F., Bargo, M.S. (Eds.), *Early Miocene Paleobiology in Patagonia*. Cambridge University Press, Cambridge, pp. 306–330. <https://doi.org/10.1017/CBO9780511667381.017>.
- Kay, R.F., Vizcaino, S.F., Bargo, M.S., 2012b. A review of the paleoenvironment and paleoecology of the miocene Santa Cruz Formation. In: Vizcaino, S.F., Kay, R.F., Bargo, M.S. (Eds.), *Early Miocene Paleobiology in Patagonia*. Cambridge University Press, Cambridge, pp. 331–365. <https://doi.org/10.1017/cbo9780511667381.018>.
- Kay, S.M., Copeland, P., 2006. Early to middle Miocene backarc magmas of the Neuquén Basin: geochemical consequences of slab shallowing and the westward drift of South America. In: *Special Paper 407: Evolution of an Andean Margin: A Tectonic and Magmatic View from the Andes to the Neuquén Basin (35°–39°S Lat)*. Geological Society of America, pp. 185–213. <https://doi.org/10.1130/2006.2407.09>.
- Kramarz, A., Forasiepi, A., Garrido, A., Bond, M., Tambussi, C., 2005. Stratigraphy and vertebrates (Aves and mammalia) from the Cerro Bandera formation, early miocene of Neuquén province, Argentina. *Rev. Geol. Chile* 32, 273–291. <https://doi.org/10.4067/S0716-02082005000200006>.
- Kramarz, A.G., 2009. Additions to the knowledge of Astrapotheriidae (mammalia, astrapotheria): Craniodental anatomy, diversity and distribution. *Rev. Bras. Palaontol.* 12, 55–66. <https://doi.org/10.4072/rbp.2009.1.05>.
- Kramarz, A.G., Bond, M., 2010. Colhuehuapian Astrapotheriidae (mammalia) from gran Barranca south of lake Colhue-Huapi. In: Madden, R.H., Carlini, A.A., Vucetich, M.G., Kay, R.F. (Eds.), *The Paleontology of Gran Barranca: Evolution and Environmental Change through the Middle Cenozoic of Patagonia*. Cambridge University Press, Cambridge, pp. 182–192.
- Kramarz, A.G., Bond, M., 2009. A new oligocene astrapother (Mammalia, Meridiungulata) from Patagonia and a new appraisal of astrapother phylogeny. *J. Syst. Palaontol.* 7, 117–128. <https://doi.org/10.1017/S147720190800268X>.
- Kramarz, A.G., Bond, M., 2008. Revision of Parastrapotherium (mammalia, astrapotheria) and other Deseadan astrapotheres of Patagonia. *Ameghiniana* 45, 537–551.
- Kramarz, A.G., Bond, M., 2005. Los litopterna (mammalia) de la Formación Pinturas, Mioceno temprano-medio de Patagonia. *Ameghiniana* 42, 611–625.
- Kramarz, A.G., Bond, M., Arnal, M., 2015. Systematic description of three new mammals (notoungulata and Rodentia) from the early miocene Cerro Bandera formation, northern Patagonia, Argentina. *Ameghiniana* 52, 585–597.
- Le Roux, J.P., 2012. A review of Tertiary climate changes in southern South America and the Antarctic Peninsula. Part 2: continental conditions. *Sediment. Geol.* 247–248, 21–38. <https://doi.org/10.1016/J.SEDGEO.2011.12.001>.
- Lynch Alfaro, J.W., Cortés-Ortiz, L., Di Fiore, A., Boulbi, J.P., 2015. Special issue: comparative biogeography of Neotropical primates. *Mol. Phylogenetics Evol.* 82, 518–529. <https://doi.org/10.1016/j.ympev.2014.09.027>.
- Madden, R.H., Guerrero, J., Kay, R.F., Flynn, J.J., Swisher III, C.C., Walton, A.H., 1997. The Laventan stage and age. In: Kay, R.F., Madden, R.H., Cifelli, R.L., Flynn, J.J. (Eds.), *Vertebrate Paleontology in the Neotropics: the Miocene Fauna of La Venta, Colombia*. Smithsonian Institution Press, Washington, D.C. pp. 499–519.
- Marshall, L.G., Salinas, P., Suarez, M., 1990. Astrapotherium sp. (mammalia, Astrapotheriidae) from miocene strata along the Quepuca River, central Chile. *Rev. Geol. Chile* 17, 215–223.
- McGrath, A.J., Anaya, F., Croft, D.A., 2018. Two new macraucheniiids (mammalia: litopterna) from the late middle miocene (Laventan south American land mammal age) of Quebrada Honda, Bolivia. *J. Vertebr. Paleontol.* 38, e1461632. <https://doi.org/10.1080/02724634.2018.1461632>.
- McKenna, M.C., Bell, S.K., 1997. Classification of Mammals: above the Species Level. Columbia University Press, New York.
- McKenna, M.C., Wyss, A.R., Flynn, J.J., 2006. Paleogene Pseudoglyptodont Xenarthrans from Central Chile and Argentine Patagonia. *Am. Mus. Novit.* 3536, 1–18. [https://doi.org/10.1206/0003-0082\(2006\)3536\[1:PPXFCJ\]2.0.CO;2](https://doi.org/10.1206/0003-0082(2006)3536[1:PPXFCJ]2.0.CO;2).
- Melnick, D., Rosenau, M., Folguera, A., Echter, H., 2006. Neogene tectonic evolution of the Neuquén Andes western flank (37–39°S). In: *Special Paper 407: Evolution of an Andean Margin: A Tectonic and Magmatic View from the Andes to the Neuquén Basin (35°–39°S Lat)*. Geological Society of America, pp. 73–95. <https://doi.org/10.1130/2006.2407.04>.
- Mitchell, K.J., Scanferla, A., Soibelzon, E., Bonini, R., Ochoa, J., Cooper, A., 2016. Ancient DNA from the extinct South American giant glyptodont *Doedicurus* sp. (Xenarthra: Glyptodontidae) reveals that glyptodonts evolved from Eocene armadillos. *Mol. Ecol.* 25, 3499–3508. <https://doi.org/10.1111/mec.13695>.
- Montoya-Sanhueza, G., Moreno, K., Bobe, R., Carrano, M.T., García, M., Corgne, A., 2017. Peltephilidae and Mesotheriidae (mammalia) from late miocene strata of northern Chilean Andes, Caragua. *J. South Am. Earth Sci.* 75, 51–65. <https://doi.org/10.1016/J.JSAMES.2017.01.009>.
- Niemeyer, H.R., Muñoz, J.B., 1983. Hoja Laguna de La Laja: Region del Bio Bio. Carta Geológica de Chile, vol. 57 Servicio Nacional de Geología y Minería, Santiago, Chile scale 1:250.000.
- Ortiz-Jaureguizar, E., Cladera, G.A., 2006. Paleoenvironmental evolution of southern South America during the Cenozoic. *J. Arid Environ.* 66, 498–532. <https://doi.org/10.1016/J.JARIDENV.2006.01.007>.
- Palazzesi, L., Barreda, V., 2012. Fossil pollen records reveal a late rise of open-habitat ecosystems in Patagonia. *Nat. Commun.* 3, 1294. <https://doi.org/10.1038/ncomms2299>.
- Palazzesi, L., Barreda, V.D., Cuitiño, J.I., Guler, M.V., Tellería, M.C., Ventura Santos, R., 2014. Fossil pollen records indicate that Patagonian desertification was not solely a consequence of Andean uplift. *Nat. Commun.* 5, 3558. <https://doi.org/10.1038/ncomms4558>.
- Palma-Heldt, S., 1983. Estudio palinológico del Terciario sedimentario de Lonquimay, Provincia de Malleco, Chile. *Rev. Geol. Chile* 18, 55–75.
- Palma-Heldt, S., Rondanelli, M., 1990. Registro de improntas del Terciario del sector Cerro Rucañanco, Lonquimay, Chile. In: *Segundo Simposio Sobre El Terciario de Chile*, Concepción, Chile, pp. 335–342.
- Pardiñas, U.F.J., 1991. Primer registro de Primates y otros vertebrados para la Formación Colón Cura (Mioceno Medio) del Neuquén, Argentina. *Ameghiniana* 28, 197–199.
- Pedroza, V., Le Roux, J.P., Gutiérrez, N.M., Vicencio, V.E., 2017. Stratigraphy, sedimentology, and geothermal reservoir potential of the volcanoclastic Cura-Mallín

- succession at Lonquimay, Chile. *J. South Am. Earth Sci.* 77, 1–20. <https://doi.org/10.1016/j.jsames.2017.04.011>.
- Radic, J.P., 2010. Las cuencas cenozoicas y su control en el volcanismo de los Complejos Nevados de Chillan y Copahue-Callaqui (Andes del Sur, 36°–39°S). *Andean Geol.* 37, 220–246. <https://doi.org/10.4067/S0718-71062010000100009>.
- Reguero, M.A., Ubilla, M., Perera, D., 2003. A new species of *Epachyrucos* (mammalia, notoungulata, Interatheriidae) from the late oligocene of Uruguay. *J. Vertebr. Paleontol.* 23, 445–457. [https://doi.org/10.1671/0272-4634\(2003\)023\[0445:ansoem\]2.0.co;2](https://doi.org/10.1671/0272-4634(2003)023[0445:ansoem]2.0.co;2).
- Rojas Vera, E.A., Folguera, A., Zamora Valcarce, G., Bottesi, G., Ramos, V.A., 2014. Structure and development of the Andean system between 36° and 39°S. *J. Geodyn.* 73, 34–52. <https://doi.org/10.1016/j.jog.2013.09.001>.
- Rojas Vera, E.A., Orts, D.L., Folguera, A., Zamora Valcarce, G., Bottesi, G., Fennell, L., Chiachiarrelli, F., Ramos, V.A., 2016. The Transitional Zone between the Southern Central and Northern Patagonian Andes (36°–39°S). Springer, Cham, pp. 99–114. https://doi.org/10.1007/978-3-319-23060-3_5.
- Rosselot, E.A., Hurley, M., Sagripanti, L., Fennell, L., Iannelli, S., Orts, D., Encinas, A., Litvak, V., Folguera, A., 2019a. Tectonics associated with the late Oligocene to early Miocene units of the High Andes (Cura Mallín Formation). A review of the geochronological, thermochronological and geochemical data. In: Kietzmann, D., Folguera, A. (Eds.), *Opening and Closure of the Neuquén Basin in the Southern Andes*.
- Rosselot, E.A., Hurley, M., Sofia, I., Fennell, L., Astort, A., Orts, D., Encinas, A., Folguera, A., 2018. Un análisis de las mecánicas de formación y sedimentación asociadas a la cuenca de Cura Mallín (Andes Centrales Australes). In: XV Congreso Geológico Chileno. Concepcion, Chile, pp. 1144.
- Rosselot, E.A., Hurley, M., Solórzano, A., Sagripanti, L., Fennell, L., Orts, D.L., Encinas, A., Folguera, A., 2019b. Preliminary results on the tectonic genesis of the Cura Mallín Formation in the southern central Andes (36°–39°S). In: 8th International Symposium on Andean Geodynamics (ISAG).
- Rubilar, A., 1994. Diversidad ictiológica en depósitos continentales miocenos de la Formación Cura-Mallín, Chile (37°–39°S): implicancias paleogeográficas. *Andean Geol.* 21, 3–29. <https://doi.org/10.5027/andgeoV21n1-a01>.
- Salinas, P., 1979. Geología del área Lolco - Lonquimay, Cordillera de los Andes, Alto Bio-Bio, IX Región, Chile. Undergraduate Thesis, University of Chile.
- Schmidt, G.I., 2013. Litopterna y Notoungulata (Mammalia) de la Formación Ituzaingó (Mioceno tardío-Plioceno) de la Provincia de Entre Ríos: sistemática, bioestratigrafía y paleobiogeografía. Phd thesis, Universidad Nacional de La Plata, La Plata, Argentina.
- Schmidt, G.I., Ferrero, B.S., 2014. Taxonomic reinterpretation of *Theosodon hystatus* Cabrera and Kraglievich, 1931 (litopterna, Macrauchenidae) and phylogenetic relationships of the family. *J. Vertebr. Paleontol.* 34, 1231–1238. <https://doi.org/10.1080/02724634.2014.837393>.
- Scillato-Yané, G.J., 1977a. Sur quelques Glyptodontidae nouveaux (mammalia, Edentata) du Déséadien (Oligocène inférieur) de Patagonie (Argentine). *Bull. du Mus. Natl. D'Hist. Nat.* 64, 249–262.
- Scillato-Yané, G.J., 1977b. Notas sobre los Dasypodidae (Mammalia, Edentata) del Plioceno del territorio argentino I. Los restos de edad Chasicuense (Plioceno inferior) del sur de la Provincia de Buenos Aires. *Ameghiniana* 14, 133–144.
- Scillato-Yané, G.J., Carlini, A.A., 1998. Nuevos Xenarthra del Friasense (Mioceno medio) de Argentina. *Stud. Geol. Salmant.* 34, 43–67 [0211-8327].
- Scillato-Yané, G.J., Góis, F., Zurita, A.E., Carlini, A.A., Gonzáles, L.R., Krmptovic, C.M., Oliva, C., Zamorano, M., 2013. Los Cingulata (Mammalia, Xenarthra) del “Conglomerado Osífero” (Mioceno Tardío) de la Formación Ituzaingó de Entre Ríos, Argentina. In: Brandoni, D., Noriega, J.I. (Eds.), *El Neógeno de La Mesopotamia Argentina Asociación Paleontológica Argentina Publicación Especial. Asociación Paleontológica Argentina, Buenos Aires*, pp. 118–134.
- Scillato-Yané, G.J., Krmptovic, C.M., Esteban, G.I., 2010. The species of genus *Chasicotatus* Scillato-Yané (Eutaini, Dasypodidae). *Rev. Mex. Ciencias Geol.* 27, 43–55.
- Scott, W.B., 1910. Mammalia of the Santa Cruz beds. Part I. Litopterna. *Reports Princet. Univ. Exped. Patagon* 7, 1–156.
- Scott, W.B., 1903. Mammalia of the Santa Cruz beds, parts I, II and III. In: Report of Princeton University Expedition to Patagonia, pp. 1–491 (+ Plates).
- Shockey, B.J., Flynn, J.J., Croft, D.A., Gans, P.B., Wyss, A.R., 2012. New leontiniid Notoungulata (Mammalia) from Chile and Argentina: comparative anatomy, character analysis, and phylogenetic hypotheses. *Am. Mus. Novit.* 3737, 1–64.
- Siler, N., Roe, G., Durran, D., 2012. On the Dynamical causes of variability in the rain-shadow effect: a case study of the Washington Cascades. *J. Hydrometeorol.* 14, 122–139. <https://doi.org/10.1175/jhm-d-12-045.1>.
- Silvestro, D., Tejedor, M.F., Serrano-Serrano, M.L., Loiseau, O., Rossier, V., Rolland, J., Zizka, A., Höhna, S., Antonelli, A., Salamin, N., 2019. Early Arrival and climatically-linked geographic Expansion of new world monkeys from Tiny African Ancestors. *Syst. Biol.* 68, 78–92. <https://doi.org/10.1093/sysbio/syy046>.
- Sinclair, W.J., 1908. The Santa Cruz Tytotheria. *Proc. Am. Philos. Soc.* 47, 64–78. [https://doi.org/10.1016/S0016-0032\(38\)92229-X](https://doi.org/10.1016/S0016-0032(38)92229-X).
- Soria, M., 1981. Los Litopterna del Colhuehuapense (Oligoceno tardío) de la Argentina. *Rev. del Mus. Argentino Ciencias Nat.* “Bernardino Rivadavia. Ser. Paleontol.” 3, 1–54.
- Soria, M.F., Hoffstetter, R., 1985. *Pteronotus tourmoueri*, nueva especie de Macrauchenidae (mammalia, Litopterna) de edad Colhuehuapense (oligoceno tardío, pcia de chubut, republia Argentina. *Ameghiniana* 22 (3–4), 149–158.
- Spikings, R.A., Dungan, M., Foeken, J., Carter, A., Page, L., Stuart, F., 2008. Tectonic response of the central Chilean margin (35–38 S) to the collision and subduction of heterogeneous oceanic crust: a thermochronological study. *J. Geol. Soc. Lond.* 165, 941–953. <https://doi.org/10.1144/0016-76492007-115>.
- Suárez, M., Emparan, C., 1995. The stratigraphy, geochronology and paleogeography of a Miocene fresh-water interarc basin, southern Chile. *J. South Am. Earth Sci.* 8, 17–31. [https://doi.org/10.1016/0895-9811\(94\)00038-4](https://doi.org/10.1016/0895-9811(94)00038-4).
- Suárez, M., Emparán, C., Wall, R., Salinas, P., Marshall, L.G., Rubilar, A., 1990. Estratigrafía y vertebrados fósiles del Mioceno del Alto Biobío, Chile Central (38°–39°S). In: *Actas Del II Simposio Sobre El Terciario de Chile*. Concepcion, Chile, pp. 311–324.
- Suárez, M., Emparan, G., 1997. Hoja Curacautín, Regiones de la Araucanía y del Bio-Bío, Carta Geológica de Chile 71. scale 1:250,000.
- Tauber, A.A., 1996. Los representantes del genero *Protypotherium* (Mammalia, Notoungulata, Interatheriidae) del Mioceno temprano del sudeste de la Provincia de Santa Cruz, Republica Argentina. *Acad. Nac. Cienc. Cordoba* 95, 1–30.
- Tejada-Lara, J.V., Salas-Gismondi, R., Pujos, F., Baby, P., Benammi, M., Brusset, S., De Franceschi, D., Espurt, N., Urbina, M., Antoine, P.-O., 2015. Life in proto-Amazonia: middle miocene mammals from the Fitzcarrald arch (Peruvian Amazonia). *Palaeontology* 58, 341–378. <https://doi.org/10.1111/pala.12147>.
- Tejedor, M.F., 2003. New fossil primate from Chile. *J. Hum. Evol.* 44, 515–520. [https://doi.org/10.1016/S0047-2484\(03\)00026-5](https://doi.org/10.1016/S0047-2484(03)00026-5).
- Toriño, P., Perea, D., 2018. New contributions to the systematics of the “Plohophorini” (mammalia, Cingulata, Glyptodontidae) from Uruguay. *J. South Am. Earth Sci.* 86, 410–430. <https://doi.org/10.1016/j.jsames.2018.07.006>.
- Townsend, K.E.B., Croft, D.A., 2008. Diets of notoungulates of the Santa Cruz Formation, Argentina: new evidence from enamel microwear. *J. Vertebr. Paleontol.* 28, 37–41. [https://doi.org/10.1671/0272-4634\(2008\)28\[217:DONFTS\]2.0.CO;2](https://doi.org/10.1671/0272-4634(2008)28[217:DONFTS]2.0.CO;2).
- Traylor, R.B., Schmitz, M.D., Cuitiño, J.I., Kohn, M.J., Bargo, M.S., Kay, R.F., Strömberg, C.A.E., Vizcaíno, S.F., 2019. An Improved Approach to Age-Modeling in Deep Time: Implications for the Santa Cruz Formation, Argentina. *GSA Bull.* <https://doi.org/10.1130/b35203.1>.
- Utge, S., Folguera, A., Litvak, V., Ramos, V.A., 2009. Geología del sector norte de la cuenca de Cura Mallín: zona de las Lagunas de Epulafuen (36°40'–50'S, 71°–71°10'O). *Rev. la Asoc. Geol. Argent.* 64, 231–248.
- Vera, B., González Ruiz, L., Novo, N., Martín, G., Reato, A., Tejedor, M.F., 2018. The Interatheriinae (mammalia, notoungulata) of the Friasian *sensu stricto* and Mayoan (middle to late miocene), and the fossils from Cerro Zeballos, Patagonia, Argentina. *J. Syst. Paleontol.* 1–21. <https://doi.org/10.1080/14772019.2018.1511387>.
- Vera, B., Reguero, M., González Ruiz, L., 2017. The Interatheriinae notoungulates from the middle miocene Collón Curá formation in Argentina. *Acta Paleontol. Pol.* 62. <https://doi.org/10.4202/app.00373.2017>.
- Vizcaíno, S.F., Cassini, G.H., Fernicola, J.C., Susana Bargo, M., 2011. Evaluating habitats and feeding habits through ecomorphological features in glyptodonts (Mammalia, xenarthra). *Ameghiniana* 48, 305–319. [https://doi.org/10.5710/AMGH.v48i3\(364](https://doi.org/10.5710/AMGH.v48i3(364).
- Vizcaíno, S.F., Fernicola, J.C., Bargo, M.S., 2012. Paleobiology of santacrucian glyptodonts and armadillos (xenarthra, Cingulata). In: Vizcaíno, S.F., Kay, R.F., Bargo, M.S. (Eds.), *Early Miocene Paleobiology in Patagonia*. Cambridge University Press, Cambridge, pp. 194–215. <https://doi.org/10.1017/CBO9780511667381.013>.
- Vucetich, M.G., Mazzoni, M.M., Pardiñas, U.F.J., 1993. Los roedores de la Formación Collon Cura (Mioceno Medio), y la Ignimbrita Pilcaniyeu, Cañadon del Tordillo, Neuquen. *Ameghiniana* 30, 361–381.
- Wang, Y., Wang, X., Xu, Y., Zhang, C., Li, Q., Tseng, Z.J., Takeuchi, G., Deng, T., Elderfield, H., 2008. Stable isotopes in fossil mammals, fish and shells from Kunlun Pass Basin, Tibetan Plateau: paleo-climatic and paleo-elevation implications. <https://doi.org/10.1016/j.epsl.2008.03.006>.
- Wyss, A.R., Flynn, J.J., Croft, D.A., 2018. New paleogene nothippids and leontiniids (Toxodontia; notoungulata; mammalia) from the early oligocene Tinguirica fauna of the Andean main range, central Chile. *Am. Mus. Novit.* 3903, 1–42. <https://doi.org/10.1206/3903.1>.
- Zachos, J., Pagani, H., Sloan, L., Thomas, E., Billups, K., 2001. Trends, rhythms, and aberrations in global climate 65 Ma to present. *Science* 80. <https://doi.org/10.1126/science.1059412>.
- Zhao, Y., Feng, D., Yu, L., Wang, X., Chen, Y., Bai, Y., Hernández, H.J., Galleguillos, M., Estades, C., Biging, G.S., Radke, J.D., Gong, P., 2016. Detailed dynamic land cover mapping of Chile: accuracy improvement by integrating multi-temporal data. *Remote Sens. Environ.* 183, 170–185. <https://doi.org/10.1016/j.rse.2016.05.016>.
- Zurita, A.E., González-Ruiz, L.R., Miño-Boilini, A.R., Herbst, R., Scillato-Yané, G.J., Cuarenta, P., 2015. Paleogene Glyptodontidae Propalaeohoplophorinae (mammalia, xenarthra) in extra-Patagonian areas. *Andean Geol.* 43, 127–136. <https://doi.org/10.5027/andgeoV43n1-a07>.



Contents lists available at ScienceDirect

Journal of South American Earth Sciences

journal homepage: www.elsevier.com/locate/jsames

Late early Miocene caviomorph rodents from Laguna del Laja (~37° S), Cura-Mallín Formation, south-central Chile

Andrés Solórzano^{a,*}, Alfonso Encinas^b, Alejandro Kramarz^c, Gabriel Carrasco^d, Germán Montoya-Sanhueza^e, René Bobe^f

^a Programa de Doctorado en Ciencias Geológicas, Facultad de Ciencias Químicas, Universidad de Concepción, Víctor Lamas, 1290, Concepción, Chile

^b Departamento de Ciencias de la Tierra, Facultad de Ciencias Químicas, Universidad de Concepción, Víctor Lamas, 1290, Concepción, Chile

^c Sección Paleontología de Vertebrados, Museo Argentino de Ciencias Naturales Bernardino Rivadavia, Av. Ángel Gallardo 470 (C1405DJR), Ciudad Autónoma de Buenos Aires, Argentina

^d Servicios Científicos Educativos y Turismo Científico Chile, Pedro León Ugalde 254, San Bernardo, Chile

^e Department of Biological Sciences, University of Cape Town, Cape Town, South Africa

^f School of Anthropology, University of Oxford, UK



ARTICLE INFO

Keywords:

Santacrucian SALMA
Neogene fossils rodents
Echimyids
Dasyproctids
"Eocardiids"
Lagostomines
Early Miocene paleoenvironments

ABSTRACT

Despite recent efforts, the paleodiversity of the Neogene mammals in Chile remains poorly known, with several putative new species awaiting description. For example, previous studies suggest that the early to late Miocene mammalian assemblages from the Laguna del Laja fossiliferous locality (Cura-Mallín and Trapa-Trapa formations), which crop out in the Andean Cordillera of Chile (~37°), comprise dozens of undescribed taxa. A better understanding of the taxonomic affinities of the Laguna del Laja faunas is needed, as it represents one of the few faunas known from the early to late Miocene of the south-central Andean main range. Several specimens of caviomorphs recently recovered in late early Miocene beds of the Cura-Mallín Formation at Laguna del Laja are here described in detail, and a brief discussion of their chronological, biogeographical, and paleoenvironmental significance is also provided. Based on fragments of mandible, maxilla and isolated teeth five taxa were recognized, *Phanomys mixtus* Ameghino, *Prolagostomus* sp., *Neoreomys* sp., *Maruchito* nov. sp., and *Luantus sompallwei* nov. sp. The radiometric ages of the fossil-bearing horizons, constrained between 17.7 and 16.4 Ma, as well as the common species (*P. mixtus*) and genera (*Prolagostomus* and *Neoreomys*) indicate that the fauna here reported belongs to the Santacrucian SALMA. Finally, our finding preliminary suggests the predominance of rather open habitats in the Cura-Mallín Formation during this time, but also a widely distributed late Early Miocene caviomorph fauna along the southern Andes, in both intra-arc and foreland basins.

1. Introduction

Caviomorpha is a taxonomically and ecomorphologically diverse clade of hystricognath rodents endemic to the Americas and Caribbean islands that comprises nearly 250 extant species distributed among 52 genera and 10 families (Álvarez et al., 2011; Patton et al., 2015; Upham and Patterson, 2015). Caviomorphs have a long evolutionary history, and their representation in the South American fossil record begins in the late middle Eocene deposits of Contamana, Peru (Antoine et al., 2012; Boivin et al., 2017). Slightly younger assemblages indicate an early diversification of the group since the late Eocene and early Oligocene as exemplified by the Santa Rosa (Peru), Tinguiririca (Chile) and La Cantera (Argentina) faunas (Álvarez et al., 2017; Arnal et al., 2019a; Bertrand et al., 2012; Frailey and Campbell Jr, 2004; Vucetich

et al., 2010b). Early Miocene caviomorphs were also diverse with 36 genera recognized in the Colhuehuapian and Santacrucian SALMA faunas, mostly recognized in several localities in the Argentinean Patagonia (Ameghino, 1889, 1894; Arnal et al., 2019b; Kramarz et al., 2010; Kramarz and Bellosi, 2005; Scott, 1905; Vucetich et al., 2010a, 2015). However, in contrast with neighboring geographical areas such as Argentina, work focused on Chilean caviomorph paleodiversity is still scarce. Recent findings indicate the presence of several distinctive early Miocene rodent assemblages in Chile (Bostelmann et al., 2013, 2012; Charrier et al., 2015; Croft et al., 2008; Flynn et al., 2002b, 2002a), but some of them are poorly studied. This is the case of the rodent assemblages of the Cura-Mallín Formation in south-central Chile.

The Cura-Mallín Formation consists of a series of upper Oligocene to

* Corresponding author.

E-mail address: solorzanoandres@gmail.com (A. Solórzano).

<https://doi.org/10.1016/j.jsames.2020.102658>

Received 14 February 2020; Received in revised form 15 May 2020; Accepted 19 May 2020

Available online 31 May 2020

0895-9811/ © 2020 Elsevier Ltd. All rights reserved.

middle Miocene volcanic and sedimentary rocks deposited in continental settings that crop out in the Andean Cordillera of Chile and Argentina between 36° and 39°S (Burns et al., 2006; Flynn et al., 2008; Pedroza et al., 2017; Radic, 2010; Solórzano et al., 2019; Suárez and Emparan, 1995; Utge et al., 2009). In Chile, some of the best exposures of the Cura-Mallín Formation are located near Laguna del Laja (37–38°S) and Lonquimay (38–39°S) (Flynn et al., 2008; Pedroza et al., 2017; Solórzano et al., 2019; Suárez et al., 1990). Miocene mammals including caviomorphs have been reported from both localities. Suárez et al. (1990) reported an indeterminate rodent in the Lonquimay area in putative early Miocene beds. However, the only specimen stored in the collections of the Museo Nacional de Historia Natural in Santiago (Chile) labeled as “Rodentia” likely belongs to a platyrrhine monkey of late middle Miocene age (Solórzano et al., 2019). Therefore, the presence of caviomorph rodents in the Cura-Mallín Formation at Lonquimay could not be confirmed (Solórzano et al., 2019).

Flynn et al. (2008) reported multiple fossiliferous horizons of the Cura-Mallín and Trapa-Trapa formations cropping out in the surroundings of Laguna del Laja, with ages ranging from early to late Miocene. The preliminary faunal lists provided indicates that these faunas are dominated, in terms of diversity, by caviomorph rodents and notoungulates (Flynn et al., 2008; Shockey et al., 2012). Interestingly, the former group appears to include several undescribed species of octodontids, dinomyids, dasyproctids, “eocardiids”, lagostomines, and echimyids (Flynn et al., 2008). Some of these forms show affinities with Patagonian taxa at the genus level, but most likely represent new genera and species (Flynn et al., 2008). In this sense, the Laguna del Laja rodents may be distinct from their Patagonian contemporaries in Argentina (Flynn et al., 2008). This is noteworthy given the geographic location of Laguna del Laja in the northern edge of modern Patagonia (Flynn et al., 2008). This proposed uniqueness could be related to habitat heterogeneity and environmental fragmentation caused by the surrounding volcanoes, geographic isolation probably linked to Andean uplift, and differences in age with contemporaneous faunas (Flynn et al., 2008). In any case, as none of these putative new caviomorph rodent taxa have been formally described, the relatively high endemism could not be assessed and confirmed. Therefore, a better understanding of the taxonomic affinities of the Laguna del Laja faunas is needed, as it represents one of the few early to late Miocene faunas from the south-central Andean main range (Charrier et al., 2015).

Recent paleontological surveys of the lower beds of the Cura-Mallín Formation south of Laguna del Laja (Chile) allowed us to collect few informative new rodent specimens within a relatively well-constrained chronostratigraphic framework (Flynn et al., 2008; Herriott, 2006). The main goal of this work is to describe these specimens, which include a new taxon, and to discuss the chronological and biogeographical affinities of the assemblage.

2. Geological and geographical settings

The Cura-Mallín Formation is the basal unit in the homonymous basin and is characterized by a predominant volcanic member (with intercalations of sedimentary strata), and a sedimentary member, which generally overlies it and was deposited in alluvial, fluvial, lacustrine and deltaic environments (Burns et al., 2006; Pedroza et al., 2017; Radic, 2010; Suárez and Emparan, 1995). Different names have been applied locally to these members. Niemeyer and Muñoz (1983) defined the volcanic Río Queuco lower member and the sedimentary Malla-Malla upper member in the Laguna del Laja area (Chile). Suárez and Emparan (1995) defined the volcanic Guapitrio member and the sedimentary Río Pedregoso member in the Lonquimay region (Chile) but considered both members to be coeval. However, based on lithostratigraphic data, Herriott (2006) and Flynn et al. (2008) could not recognize the volcanic (Río Queuco) and sedimentary (Malla-Malla) members within the southeast of Laguna del Laja.

In contrast, they subdivided the southeast the Laguna del Laja area

into five mappable units: Tcm₁, Tcm₂, Tcm₃, Tcm₄, and Tcm₅. The Tcm₁, Tcm₃, and Tcm₅ are volcanoclastic sandstone and mudstone, with Tcm₅ having a greater component of fine-grained strata; the Tcm₂ is an ignimbrite that separates the lithologically similar Tcm₁ and Tcm₃ strata, being considered a well-marker bed; Tcm₄ is lithologically distinctive in containing pebble-sized clasts of granitoid and quartzite (Herriott, 2006). Herriott (2006) and Flynn et al. (2008) also provides Ar/Ar radiometric dates for the rock cropping out in Laguna del Laja and indicates that deposition of the Cura-Mallín Formation in this area started in 19.80 Ma and continued until at least 14.50 Ma. The bracket age of the defined mappable units is 18–19.8 Ma for Tcm₁, 17.84–18 Ma for Tcm₂, ~16–17.84 Ma for Tcm₃, 14.5–~16 Ma for Tcm₄ and younger than 14.5 Ma and older than 10 Ma for Tcm₅ (Flynn et al., 2008; Herriott, 2006; Shockey et al., 2012). In the Laguna del Laja, the predominantly volcanic conglomerates and breccias, intermediate to mafic lavas, and rare to minor beds of finer-grained volcanoclastic deposits of the late Miocene (8.9 ± 0.1 and 10.10 ± 0.20 Ma) Trapa-Trapa Formation overly the Cura-Mallín Formation (Flynn et al., 2008; Herriott, 2006; Niemeyer and Muñoz, 1983).

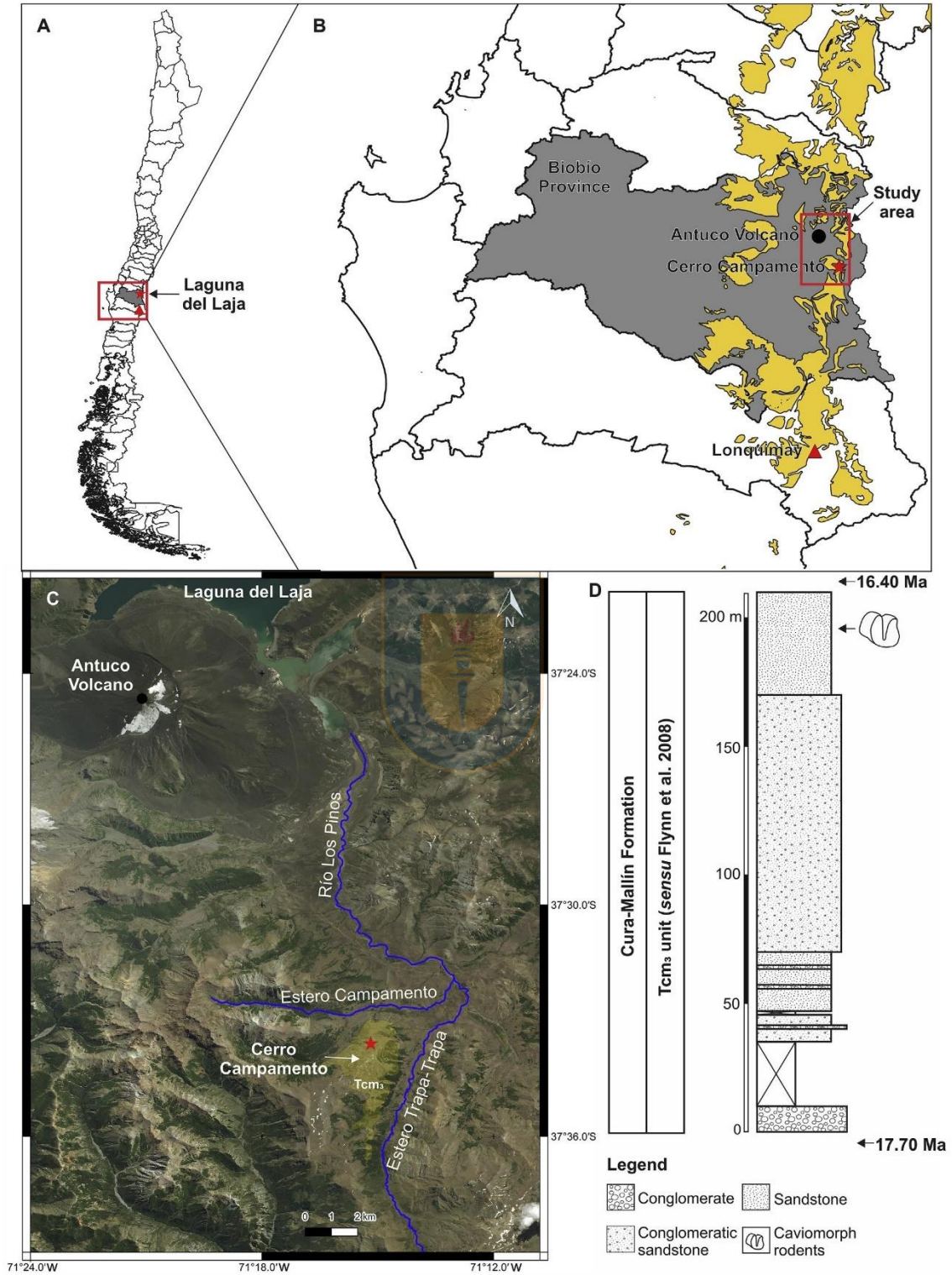
In the present work, we follow the lithostratigraphic framework previously described (Flynn et al., 2008; Herriott, 2006; Shockey et al., 2012). The rodents here reported were recovered from surface picking along few subhorizontal volcanoclastic grey sandstones cropping out at the top of the Cerro Campamento, at the west of the Estero Trapa-Trapa, south of the Laguna del Laja (Biobío Province, Chile; Fig. 1). Volcanoclastic sandstone and conglomerate are the dominant lithologies over the upper section of the Cerro Campamento, which belongs to the Tcm₃ unit (Flynn et al., 2008). The age of these fossil-bearing horizons is constrained to the late early Miocene, between 17.70 and 16.40 Ma (Fig. 1).

3. Brief paleontological background

Flynn et al. (2008) provide a preliminary faunal list for the distinct localities and stratigraphic levels cropping out in the Laguna del Laja area. The mammals so far reported from the early Miocene Tcm₁–Tcm₃ levels include notoungulates (*Paedotherium minor*, *Colpodon antucoensis*, cf. *Protyotherium* sp., *?Hegetotherium* sp., Toxodontidae indet., Tytopheria indet. and Interatheriinae indet.), caviomorph rodents (*?Neoreomys* sp., *Maruchito* sp. nov., *Protacaremys* sp. nov., *Prostichomys* sp. nov. I, *Prostichomys* sp. nov. II, *Luantus* sp. nov., *Acarechimy* sp. nov., *Scleromys* sp. nov., *Prolagostomus* sp. nov., gen. et sp. nov. aff. *Prostichomys*, gen. et sp. nov. aff. *Protacaremys*, gen. et sp. nov. aff. *Incamys*, gen. et sp. nov. aff. *Maruchito*, gen. et sp. nov. aff. *Prospaniomys* and gen. et sp. nov. aff. *Alloiomys*), marsupials (*Sipalocoyon* sp. and *Abderitidae* indet.), astraprotheres (*Astraprotheriidae* indet.), armadillos (*Dasypodidae* indet.), and sloths (*Nematherium* cf. *N. angulatum* or sp. nov.) (Flynn et al., 2008; Shockey et al., 2012). However, just few of these taxa have been illustrated (Flynn et al., 2008), and excepting *Colpodon antucoensis* (Shockey et al., 2012), none of them have been described. Therefore, the Laguna del Laja paleodiversity remains poorly known.

4. Material and methods

The specimens described here are housed at the Museo de Historia Natural de Concepción, Concepción, and the Museo Nacional de Historia Natural de Santiago, Chile. All measurements are in millimeters and were taken with a digital caliper. Comparisons of taxa described here are mainly with closely related taxa in Argentina (see Electronic Supplementary Material 1). Nomenclature of the lower and upper cheek teeth of caviomorph rodents follows Boivin and Marivaux (2018), Marivaux et al. (2004) and Rasia and Candela (2019).



(caption on next page)

Fig. 1. Geographic and stratigraphic provenance of the caviomorph remains described in the present study from the Laguna del Laja region (late early Miocene of the Cura-Mallín Formation; Cerro Campamento, west of the Estero Trapa-Trapa; Biobío Province, south-central Chile). A and B) geographic location of the study area; C) aerial view of the Laguna del Laja region showing details about the location of the fossiliferous sampled levels (denoted by a red star); D) generalized stratigraphic profile of the Cerro Campamento. The grey region in A and B, denotes the location of the Biobío Province, Chile. The yellow polygons in B indicate the geographic extension of the Oligocene to Miocene volcano-sedimentary units, which must mainly correspond (at this latitudes) with the units included in the Cura-Mallín Basin (SERNAGEOMIN, 2003). The pale-yellow polygon in C, denotes the extension of the Tcm₃ unit over the Cerro Campamento (west of the Estero Trapa-Trapa). The geographic and chronological extension of Tcm₃ unit is based on Flynn et al. (2008) and Herriott (2006). (For interpretation of the references to colour in this figure legend, the reader is referred to the Web version of this article).

4.1. Abbreviations

Upper case letters are used for the upper dentition (P: for premolar, M: for molar) and lower case letters for the lower dentition (p: for premolar, m: for molar); dP/dp: deciduous premolar, SALMA, South American Land Mammal Age; APL, anteroposterior length; AW, anterior width; PW, posterior width.

4.2. Institutional abbreviations

SGOPV, Museo Nacional de Historia Natural de Santiago, Santiago, Chile; MHNC, Museo de Historia Natural de Concepción, Concepción, Chile; MACN, Museo Argentino de Ciencias Naturales “Bernardino Rivadavia”, Buenos Aires, Argentina; MLP, Museo de La Plata, La Plata, Argentina.

5. Systematic paleontology

Order RODENTIA Bowdich, 1821
Suborder HYSTRICOGNATHI Tullberg, 1899
Superfamily OCTODONTOIDEA Waterhouse, 1839
Family ECHIMYIDAE Gray, 1825
Genus *MARUCHITO* Vucetich et al. (1993)

Type and only species. *Maruchito trilofodonte* Vucetich et al. (1993).

Geographic and Stratigraphic Distribution. Late early Miocene, Cura-Mallín Formation, Biobío Province, Chile, and middle Miocene, Collón Curá Formation, Neuquén Province, Argentina (Flynn et al., 2008; Vucetich et al., 1993).

Maruchito nov. sp.?

Fig. 2

Referred material. SGO.PV.1400, a fragment of left maxilla with dP4-M3.

Geographic and stratigraphic provenance. Estero Trapa-Trapa west, Laguna del Laja (Chile), Tcm₃ unit, Cura-Mallín Formation, early Miocene.

Description. The tooth row is straight and preserves rectangular, mesodont (crown height/anteroposterior length on M3 = 0.60), and tetralophodont upper molariforms (dP4-M3), with crests broader than flexi (Fig. 2), and cusps entirely subsumed in their associated crests. The enamel layers are relatively narrow and surround the entire molariforms. The mesiodistal length of the dP4-M3 series is 13.32 mm.

The dP4, slightly (4%) larger than the M1 (Table 1), has a short anteroloph (not reaching the labial end of the protoloph, suggesting that the labial end of the anteroloph is located more lingual than the paracone and metacone areas), while the other crests (protoloph, metaloph and posteroloph) are similar in length (Fig. 2A). The crests are oblique, forming around 60° with the mesiodistal tooth axis, with labial ends broadly pointed (this feature is better exemplified in the protoloph; Fig. 2A). Labial flexi of approximately similar length, but paraflexus is the most penetrating one. The hypoflexus is relatively short (reaching less than half of the occlusal surface), transverse (forming around 90° with the lingual tooth wall), and slightly mesiodistally wider than the labial flexi. The mesiolingual angle is typically obtuse (~110°); the distal teeth wall is broadly concave.

The upper molars are broadly similar to the dP4. The major differences are in the obliquity of the crests and flexi (Fig. 2A), with a

progressive reduction in the obliquity from M1 to M3: in M1 the crest forms an angle around 60° with the mesiodistal tooth axis, 75° in M2, and nearly 90° in the M3. The mesiolingual angle is nearly 90° (this feature is especially clear in the M3; Fig. 2A). In M1, the protoloph and mesolophule have a similar labial extension; while in the M2 and M3, the protoloph extends more labially than the remaining crests, suggesting that the paracone area is located more labial than the metacone area and the labial end of the anteroloph. The hypoflexus in the M1–M3 series is transverse and persistently reaches less than half of the occlusal surface. In M1 and M2 the paraflexus is the most penetrating labial flexus (Fig. 2A). The M2 is the largest tooth of the series, being slightly (~5%) larger than the M1 and M3 (Table 1). In M2, the mesolophule and posteroloph are connected in the lingual margin, enclosing the posterior-most fossette (Fig. 2A). In M3, the posteroloph is transversally shorter than in M1 or M2 (Fig. 2A), the area of the protocone appears to be mesiodistally shorter than the area of the hypocone (unlike other upper molariforms), the paraflexus is less penetrating with respect to M2, being the posteroflexus the most penetrating labial flexus, but, it does not reach the lingual margin. The wear trajectory of the upper molars suggests that the posteroloph becomes less penetrating in advanced stages of wear, while the paraflexus becomes more penetrating with wear (Fig. 2A).

A direct examination of the labial wall of the molars of the specimen was not possible (Fig. 2A). However, in the dP4 and M1 the metastria must be deeper than in M2, because the metastria persists even with greater wear (Fig. 2A). The labial ends of dP4-M3 crest are acuminate (Fig. 2A). In lingual view, variable depth of the hypostria was noted likely suggesting differences in wear (Fig. 2B): hypostria becomes progressively deeper distally (i.e., in the dP4 the hypostria did not reach the base of the tooth, while in the M3 the hypostria almost reach the 95% of the tooth base).

Remarks. The material from Laguna del Laja (SGO.PV.1400) shares several dental characters with the middle Miocene echimyid *M. trilofodonte*, including size, crown height, rather narrow and straight hypoflexus, and transverse crests and labial flexi in some of the upper molars (Vucetich et al., 1993). These similarities suggest that they might belong to the same genus.

A preliminary revision of a sample of upper molariforms referred to *M. trilofodonte* (from the Collón Curá Formation, Argentina; see Electronic Supplementary Material 1) indicates the wide ontogenetic variability of this taxon. In this sense, an assessment of this variability is in need. Unlike SGO.PV.1400, *M. trilofodonte* has dP4 with a marked rectangular outline (mesiodistal length >> transverse length) in most stages of wear (e.g. MLP 91-IX-1-33, MLP 91-IX-1-23), upper molars with a transversely more penetrating posterior-most fossette (even in a very advanced stage of wear), and acuminate labial ends of crest only in early stages of wear, which become rounded and thicker with wear. Considering the limited sample of *Maruchito* from Laguna del Laja, as well as the unclear ontogenetic variability of the type species, the identity of SGO.PV.1400 cannot be determined with certainty. Based on the differences previously mentioned, SGO.PV.1400 could represent a new species of *Maruchito* as previously proposed (Flynn et al., 2008). Nevertheless, additional materials, especially lower molars, are necessary to refine its taxonomic affinities.

Superfamily CAVIOIDEA (Fischer von Waldheim, 1817)

Family “EOCARDIIDAE” Ameghino, 1891

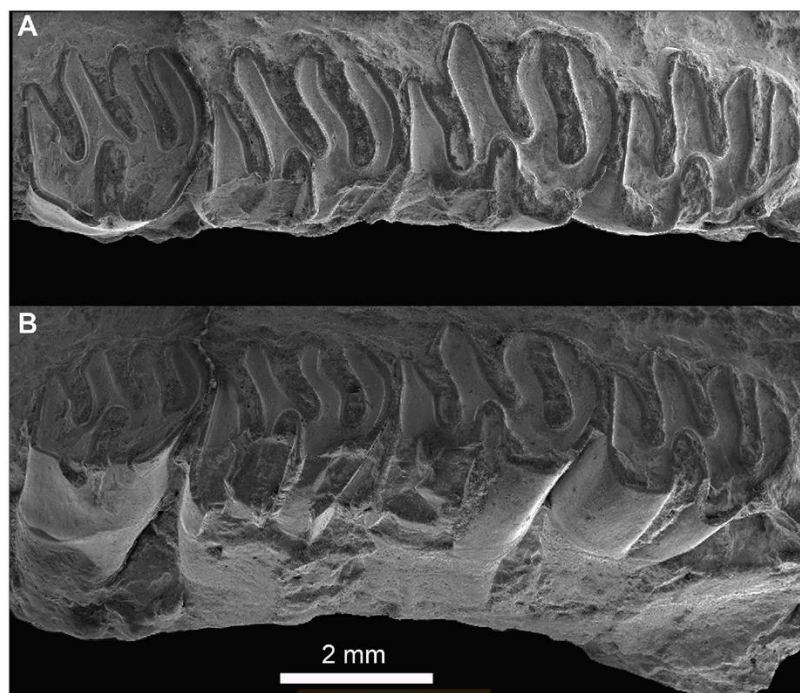


Fig. 2. *Maruchito* sp. nov? (SGO.PV.1400) from late early Miocene beds of the Cura-Mallín Formation, Laguna del Laja, Chile; left maxilla with dP4-M3 in occlusal (A) and lingual (B) views.

Genus *LUANTUS* Ameghino, 1899

Included species. *Luantus propheticus* Ameghino, 1899 (type species), *Luantus initialis* Ameghino, 1902, *Luantus toldensis* Kramarz, 2006, *Luantus minor* Pérez et al. (2010) and *Luantus sompallwei* nov. sp.

Geographic and Stratigraphic Distribution. Early Miocene (Colhuehuapian SALMA) of the Sarmiento Formation (Colhue Huapi Member), Chubut Province, Argentina; early Miocene (Santacrucean SALMA) of Pinturas (Santa Cruz Province, Argentina), Santa Cruz (Santa Cruz Province, Argentina) and Cura-Mallín formations (Biobío Province, Chile) (Flynn et al., 2008; Kramarz, 2006a; Kramarz and Bellosi, 2005; Pérez et al., 2010).

Luantus sompallwei nov. sp.

Fig. 3A–F

Holotype. SGO.PV.1401, a fragment of right mandible with the base of incisor, incompletely erupted unworn p4, and moderately worn m1.

Tentatively referred material. SGO.PV.1402, isolated m1 or m2.

Diagnosis. Similar in size to *L. propheticus*, and *L. toldensis*, but 20% larger than *L. minor* (based in dental measurements, Table 1). Cheek teeth lower crowned than *L. initialis*, but higher crowned than in *L. propheticus*, with large discontinuities of the enamel covering on the base of the cheek teeth (resembling *L. toldensis*). Differs from *L. propheticus*, and *L. toldensis* in having a p4 with a persistent (even in advance stage of wear) and well-developed mesially projected lophid (“anteroconid”) attached to the metaconid area, and two ephermal

Table 1

Measurements (in mm) of the materials collected in the late early Miocene of the Cura-Mallín Formation at Laguna del Laja, Chile. Abbreviations: MDL, mesiodistal length; MW, mesial width; DW, distal width; W, width.

Lower tooth																	
Taxa	Specimen	p4			m1			m2			m3			m1 or m2			
		MDL	MW	DW	MDL	MW	DW	MDL	MW	DW	MDL	MW	DW	MDL	MW	DW	
<i>L. sompallwei</i> sp. nov.	SGO.PV.1401 (holotype)	4.51	2.98	3.23	4.26	3.59	3.73	–	–	–	–	–	–	–	–	–	
<i>L. sompallwei</i> sp. nov.	SGO.PV.1402	–	–	–	–	–	–	–	–	–	–	–	–	–	4.55	3.80	3.75
<i>Prolagostomus</i> sp.	MHNC 38.0041	–	–	–	–	–	–	2.5	3.2	3	2.43	3.3	3	–	–	–	
Upper tooth																	
Taxa	Specimen	P4		dP4		M1		M2		M3		M1 or M2					
		MDL	W	MDL	W	MDL	W	MDL	W	MDL	W	MDL	AW	PW			
<i>Maruchito</i> sp. nov.?	SGO.PV.1400	–	–	3.24	2.98	3.12	2.95	3.34	3.15	3.15	3.02	–	–	–			
<i>Phanomys mixtus</i>	MHNC 38.0038	–	–	–	–	–	–	–	–	–	–	4.39	4.50	4.37			
<i>Phanomys mixtus</i>	MHNC 38.0037	–	–	–	–	–	–	–	–	–	–	4.35	4.55	4.41			
<i>Neoreomys</i> sp.	MHNC 38.0039	4.76	4.84	–	–	–	–	–	–	–	–	–	–	–			
<i>Prolagostomus</i> sp.	MHNC 38.0040	–	–	–	–	2.38	3.00	2.20	2.95	–	–	–	–	–			

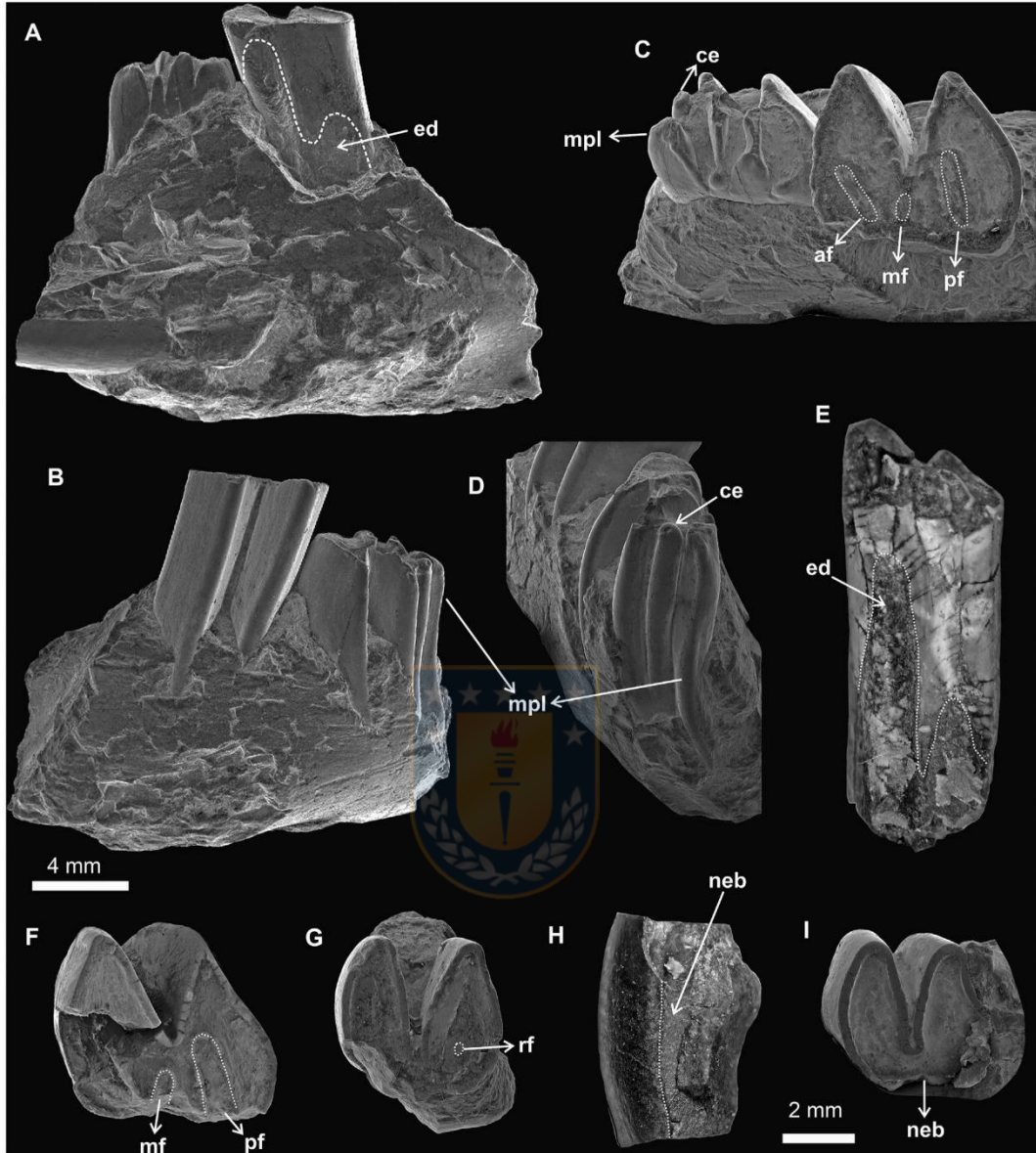


Fig. 3. Cavioid rodents from late early Miocene beds of the Cura-Mallín Formation, Laguna del Laja, Chile. A–F, *Luantus sompallwei* sp. nov.: fragment of right dentary bearing the p4, m1 and the base of the lower incisor (Holotype: SGO.PV.1401) in lingual (A), labial (B), occlusal (C) and mesial (D) views; isolated m1 or m2 (SGO.PV.1402) in lingual (E) and (F) occlusal views. G–I, *Phanomys mixtus*: right isolated upper M1 or M2 (MHNC 38.0038) in occlusal (G) and distolabial (H) views; right isolated M1 or M2 (MHNC 38.0037) in occlusal view (I). Note the lack of enamel in the lingual face of the tooth in G. A and B are in the same scale (4 mm); C–I are in the same scale (2 mm). Abbreviations: ed, exposed dentine; neb, no enamel band; af, anterofossette; mf, mesofossette; pf, posterior-most fossette; mpl, mesially projected lophid (= “anteroconid”); ce, columnar element on mesial p4 wall; rf, relictual fossette.

flexids on the mesial wall in early stages of wear, which are lost in later stages.

Etymology. *Sompallwe*, refers a mermaid shaped mythological entities of the Mapuche cosmovision which inhabit and protect their lakes, as the Laguna del Laja.

Geographic and stratigraphic provenance. Estero Trapa-Trapa west, Laguna del Laja, Chile, Tcm₃ unit, Cura-Mallín Formation, late early Miocene (Santacrucian SALMA).

Description and comparison. The mandible of the holotype is poorly preserved and shows no relevant characters. The incisor extends

posteriorly beyond the m1. The base of the incisor is rather transversally compressed, at least in the exposed portion above the m1 (Fig. 3A and B). The cheek teeth are high crowned but rooted (protohypsodont).

The unworn, and not fully erupted, p4 has two asymmetrical lobes with the mesial being mesiodistally larger and transversely narrower than the distal (Fig. 3C). These lobes are labially separated by the rather sub-triangular hypoflexid, which is located opposite to the mesofossettid, extends more than half of the tooth width, and lacks cement (at least in this stage of wear). The p4 also exhibits three lingual flexids forming a tetralophodont (molariform-like) occlusal pattern. Two

flexids (anteroflexid and mesoflexid) are located in the mesial lobe, while the metaflexid is on the distal one. The anteroflexid and mesoflexid open lingually, with the former being labiolingually larger and mesiodistally narrower than the latter. The metaconid area is well-developed and has a mesially projected lophid, that could be equivalent to the element described as “anteroconid” in premolars of other caviomorphs with lower crowned cheek teeth (e.g. *Cephalomys*; see Wood and Patterson, 1959). The last feature is retained even in advanced stages of wear because it persists toward the base of the tooth (Fig. 3D). In occlusal view, there is a columnar element on the mesial wall of the tooth, between the metaconid and protoconid areas, likely derived from the metalophulid I. The flexids separating this column from the adjacent cusps are ephemeral, and thus the column becomes indistinct in advanced stages of wear, and the labial edge of the “anteroconid” would form a roughly right angle with the mesiolabial aspect of the tooth (metalophulid I). The second transverse lophid (metalophulid II?) connects the lingual aspect of the protoconid area with the small cuspid in the lingual margin of the tooth between the metaconid and the entoconid areas. The marginal cuspid (mesostylid?) is smaller than the adjacent cusps, and would become indistinct with moderate wear. The posterior lobe of the tooth is rather triangular, with a very large, labiolingually elongate, and lingually open metaflexid separating the hypolophid from the posterolophid (Fig. 3C). The protoconid area is slightly lingually positioned with respect to the hypoconid area, and thus the trigonid is distinctly narrower than the talonid.

The m1 of the holotype is bilobed, with a lingual wall straight, and wide, transversally elongated, and persistent fossettid (Fig. 3C). The mesial lobe has two fossettids: the anterofossettid and the mesofossettid. The former is labiolingually elongate and distolingually oblique, while the latter is smaller, transverse, more posteriorly placed, and opposite the hypoflexid (Fig. 3C). The distal lobe is slightly transversally larger than the mesial one and exhibits a very labiolingually elongate metafossettid. The posterolophid occupies more than 50% of the occlusal surface of the distal lobe (Fig. 3C). The hypoflexid is triangular, with “V” shaped apex extending more than halfway the crown width, and lacks cement (at least in this stage of wear). The enamel is rather continuous along the occlusal surface of the tooth but appears to be thinner toward the lingual margin and in the mesiolingual and distolingual corners. Two vertical bands of exposed dentine are present on the lingual wall, reaching more than half of the preserved crown height (Fig. 3A).

The isolated m1 or m2 (SGO.PV.1402) (Fig. 3E and F) is almost identical to the m1 of the holotype, although it is slightly larger (Table 1). In this molar, two vertical bands of exposed dentine are also present on the lingual wall, reaching 75% the preserved height of the crown (Fig. 3E).

Remarks. The specimens described here show the diagnostics feature of the genus *Luantus*, e.g. protohypsodont cheek teeth, hypoflexid with triangular contour, large and transversally elongated fossettids which persist in at least moderate ontogenetic stages (Kramarz, 2006a; Pérez et al., 2010). The Laguna del Laja specimens differ from the Colluhueapian *L. initialis* in having higher crowned teeth and more molarized p4 (Kramarz, 2006a; Vucetich et al., 2010b), and from *L. minor* (Colluhueapian) by their larger size and more penetrating hypoflexids (Pérez et al., 2010).

The configuration of the p4 from the Laguna del Laja specimen differs from those observed in named *Luantus* species in which this tooth is known (Kramarz, 2006a; Pérez et al., 2010). After a revision of a large sample of *L. propheticus*, Kramarz (2006a) reports intraspecific variability within the mesial lobe of p4, particularly the varying presence and degree of development of a mesial projection of the metaconid (which likely might include an “anteroconid”) and an ephemeral flexid on the anterior wall. However, when present the mesial projection of the metaconid of *L. propheticus* (e.g. MACN- PV SC3617; MACN- Pv SC2235) is much less developed and persistent than in the Laguna del Laja specimen (Fig. 3D). The p4 of *L. toldensis* has a comparatively

larger mesiodistal diameter than in *L. propheticus*, and the anterolingual projection of the tooth is more pronounced than in the former (Kramarz, 2006a). Unlike *L. sompallwei*, the p4 of *L. toldensis* has a simpler trigonid with a rather straight mesial wall or with a single and more superficial mesial flexid (Kramarz, 2006a). After a revision of several isolated p4 from the Pinturas Formation referred to *L. toldensis*, we conclude that the distinctive p4 morphology of SGO.PV.1401 exceeds the known range of intraspecific variability of *L. toldensis*, reinforcing the notion that both represent distinct species. Moreover, although the specimens from Laguna del Laja exhibits an unique trait combination (mentioned in the diagnosis) they appear to be closely related to *L. toldensis*, because both share relatively high crowned tooth and vertical bands of exposed dentine (in the lingual wall) that reach nearly half the height of the tooth crown (Kramarz, 2006a).

PHANOMYS Ameghino, 1887

Included species. *Phanomys mixtus* Ameghino, 1887 (type species), and *Phanomys vetulus* Ameghino, 1891.

Geographic and chronological distribution. Late early Miocene of Pinturas, Jeinemení and Santa Cruz formations (Santacrucian SALMA), Santa Cruz Province, Argentina, and Cura-Mallín Formation (Santacrucian SALMA), Biobío Province, Chile (Kramarz, 2006a; Pérez and Vucetich, 2012).

Phanomys mixtus Ameghino, 1887b

Fig. 3G–I

Referred materials. MHNC 38.0038, right isolated M1 or M2; MHNC 38.0037, right isolated M1 or M2.

Geographic and stratigraphic provenance. Estero Trapa-Trapa west, Laguna del Laja (Chile), Tcm₃ unit, Cura-Mallín Formation, early Miocene (Santacrucian SALMA).

Description. The specimens represent isolated upper molars (M1 or M2). These molars are high crown (protohypsodont) and deeply bilobed, with the mesial lobe slightly labiolingually narrower than the distal one. In the distal lobe of MHNC 38.0038 (Fig. 3G) there is a relicual fossette, while MHNC 38.0037 lacks fossettes over the occlusal surface (Fig. 3I). The hypoflexus is roughly funnel-shaped, with a “U” shaped apex, extends transversely more than the half of the tooth, and shows cement in its more labial portion. Most of the labial wall of the teeth lack enamel, while the remaining walls of the teeth show a relatively thick enamel coverage (Fig. 3H and I).

Remarks. The specimens display all the recognized diagnostics features of the genus *Phanomys*, as protohypsodont molariforms; enamel interrupted along labial walls of the upper teeth; fossettes less persistent during ontogeny than in any other protohypsodont species of Cavioidae; hypoflexus narrow, extending transversely more than half of the crown and bearing cement since early ontogenetic stages (Pérez and Vucetich, 2012). There are only two species recognized within the genus, *P. mixtus* and *P. vetulus*, and size is the main difference between both taxa, with the former being larger than the latter (Pérez and Vucetich, 2012). The size of the molars recovered from the Laguna del Laja falls into the range size reported for *P. mixtus*, and is decidedly larger than those known for *P. vetulus* (Pérez and Vucetich, 2012). Therefore, Laguna del Laja specimens can be referred to *P. mixtus*. The genus *Phanomys*, was previously recognized only in southern Argentina (Pérez and Vucetich, 2012). Therefore, *Phanomys* is reported here for the first time in Chile.

Family DASYPROCTIDAE Smith, 1842

Genus *NEOREOMYS* Ameghino, 1887

Included species. *Neoreomys australis* Ameghino, 1887 (type species), *Neoreomys huilensis* Fields (1957) and *Neoreomys pinturensis* Kramarz (2006b).

Geographic and chronological distribution. Late early Miocene of Pinturas Formation and Santa Cruz formations, Santa Cruz and Chubut provinces, Argentina; late early Miocene of Cura-Mallín Formation, Biobío Province, Chile; middle Miocene (Colloncuran SALMA) of Collón Curá Formation, Río Negro and Neuquén provinces, Argentina; late middle Miocene (Laventan SALMA) of La Victoria Formation, Colombia

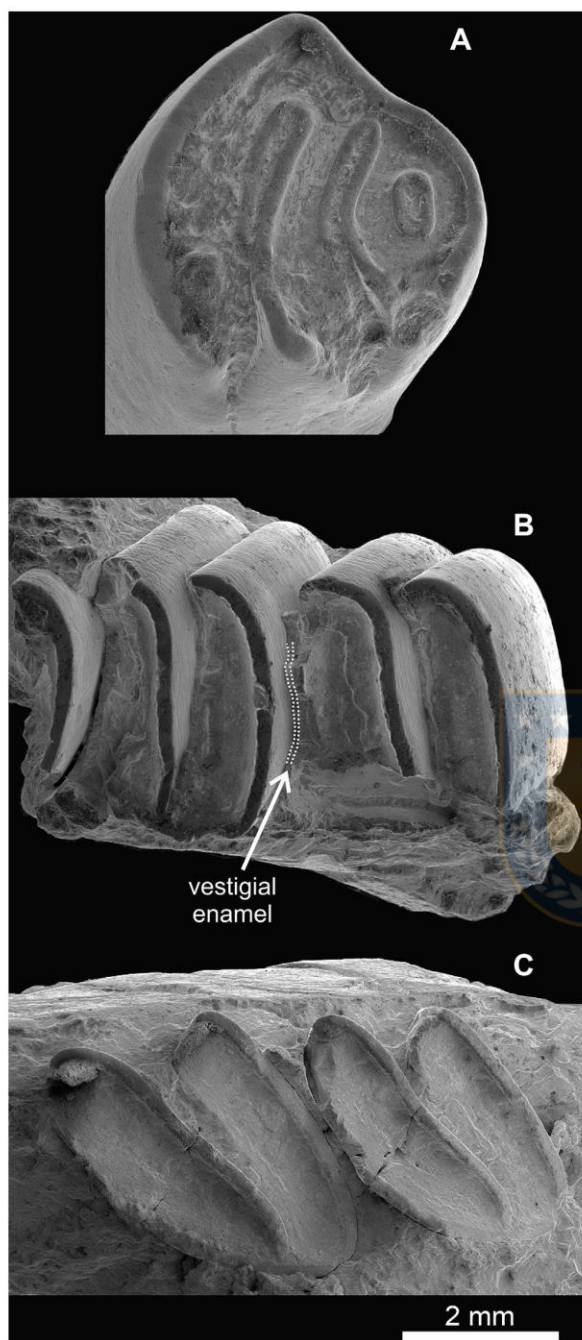


Fig. 4. Dasyproctid and chinchillid rodents from late early Miocene beds of the Cura-Mallín Formation, Laguna del Laja, Chile. *Neoreomys* sp.: isolated P4 (MHNC 38.0039) in occlusal view (A). *Prolagostomus* sp.: left maxillary fragment with M1, M2 and a mesial portion of the M3; MHNC 38.0040 in occlusal view (B), right mandibular fragment with m2 and m3 (MHNC 38.0041) in occlusal view (C).

(Fields, 1957).

Neoreomys sp.

Fig. 4A

Revised specimen. MHNC 38.0039; isolated right P4.

Geographic and stratigraphic provenance. Estero Trapa-Trapa west, Laguna del Laja, Chile, Tcm₃ unit, Cura-Mallín Formation, early Miocene.

Description. Tetralophodont and protohypsodont upper premolar, with a distinctive bell-shape crown outline (in occlusal view), wide crests and thick enamel layers. The tooth is slightly wider than long (Fig. 4A). The paraflexus and mesoflexus are very narrow. The paraflexus is rather straight and subparallel to the mesial edge of the tooth (Fig. 4A). The mesoflexus is distally more penetrating than the paraflexus and curved along the occlusal tooth surface. The posteroloph and mesolophule enclosed a short and elliptical posterior-most fossette. While the most lingual portion of protoloph is almost parallel to the paraflexus, the protoloph becomes markedly curved distally toward the central surface of the tooth (Fig. 4A). Hypoflexus absent.

Remarks. Among Miocene taxa referred to Dasyproctidae, the absence of a hypoflexus over the lingual side of the P4 plus a wide enamel layer is known in *Neoreomys*, *Alloiomys*, and *Australoprocta* (Kramarz, 1998). The upper premolar from Laguna del Laja rather resembles the general morphology of the former. It differs from *Australoprocta* in being much larger and higher crowned and in having a more simplified occlusal pattern by lacking a distinctive mesoloph (Kramarz, 2006b, 1998); while the P4 of *Alloiomys* has a rather subtriangular contour, and has only three transverse lophs (at least in a similar stage of wear) (Vucetich, 1977). The P4 from Laguna del Laja is in the size range of the *N. australis* (Santacrucian) and is decidedly larger than *N. huilensis* (Laventan) (Fields, 1957; Kramarz, 2006b). Even when the P4 of *N. pinturensis* is unknown, this taxon differs from *N. australis* by their lower crowned cheek teeth (Kramarz, 2006b). However, as the only P4 available from Laguna del Laja is broken toward its base the crown height cannot be estimated, making it unreliable to provide more details at the species level and its affinities with other species.

Superfamily CHINCHILLOIDEA Bennett, 1833

Family CHINCHILLIDAE Bennett, 1833

Subfamily LAGOSTOMINAE Pocock, 1922

Genus *PROLAGOSTOMUS* Ameghino, 1887

Included species. *Prolagostomus pusillus* Ameghino, 1887 (type species), *Prolagostomus divisus* Ameghino, 1887; *Prolagostomus profluens* Ameghino, 1887; *Prolagostomus imperialis* Ameghino, 1887; *Prolagostomus lateralis* (Ameghino, 1889); *Prolagostomus primigenius* (Ameghino, 1889); *Prolagostomus obliquidens* Scott (1905) and *Prolagostomus rosendoi* Vucetich (1984).

Geographic and chronological record. Late early to late middle Miocene of Pinturas and Santa Cruz formations (Santacrucian SALMA), south of Patagonia, Argentina, Collón Curá Formation (Colloncuran SALMA), north of Patagonia, Argentina, Cerro Boleadoras Formation (Santacrucian SALMA), Patagonia, Argentina, Rio Frias Formation ("Friasian" SALMA), Western Patagonia, Chile, Cura-Mallín Formation (Laguna del Laja; Santacrucian to Laventan? SALMA) South Central Chile, Galera Formation (Pampa Castillo; Santacrucian to "Frisian"), South of Chile, and Honda Group (Quebrada Honda; Laventan SALMA), Bolivia (Croft et al., 2011; Kramarz, 2002).

Prolagostomus sp.

Fig. 4B,C

Referred materials. MHNC 38.0040, a fragment of left maxilla with M1-M2 and the mesial-most edge of M3; MHNC 38.0042, right isolated M1 or M2, with portions of the maxillary; MHNC 38.0041, a fragment of right mandible with m2 and m3.

Geographic and stratigraphic provenance. Estero Trapa-Trapa west, Laguna del Laja, Chile, Tcm₃ unit, Cura-Mallín Formation, early Miocene.

Description. The M1 and M2 are euhyposodont and bilaminated (formed by two laminae connected by a narrow labial isthmus). The mesial and distal laminae has an enamel layer in its mesial and lingual walls (Fig. 4B). However, a vestigial enamel layer on the backside of the M1 is present, but it is not clearly observed in the partially eroded M2 (Fig. 4B). The M1 and M2 are quite similar, with the mesial lamina

slightly labially projected. In the distal lamina, the labial wall is mesiodistally more elongated than the lingual wall. The mesial wall is slightly curved, and the distal wall is straight. The hypoflexus is very narrow and penetrating (almost reaching the labial edge), slightly sinuous, and filled with cementum. The laminae are slightly oblique (the labial and mesial wall form an angle of around 80°).

The lower molars have two oblique laminae. The boundary between lingual and mesial walls is curved, forming a 120° angle (Fig. 4C). The distal lamina is mesiodistally wider than the mesial. The mesial lamina wedges toward the lingual wall, while the distal one is rather rectangular (Fig. 4C). The enamel covers the mesiolingual and distal wall of the anterior lamina and distal wall of the distal lamina (Fig. 4C).

Remarks. The specimens here described display the diagnostic features of the genus *Prolagostomus* (Vucetich, 1984), and differ from *Lagostomus* and *Pliolagostomus* in having rounded molariform walls (Croft et al., 2011). *Prolagostomus* is the most common taxon found in the sampled beds of the Tcm₃ unit on the Estero Trapa-Trapa west. Contrasting with previous findings (Flynn et al., 2008), *Prolagostomus* remains are the most common rodent in the analyzed stratigraphic levels.

Several species have been historically assigned to *Prolagostomus*, and some of them are mostly recognized by size differences (Croft et al., 2011; Kramarz, 2002; Scott, 1905; Vucetich, 1984). However, the actual number of valid species is likely overestimated because it is unclear how to confidently distinguish among ontogenetic, intraspecific, and interspecific variation (Croft et al., 2011; Kramarz, 2002). The rather distinctive feature of the Laguna del Laja *Prolagostomus* is the presence of a vestigial enamel layer in the distal wall of the upper molars. This feature is absent in other *Prolagostomus* species recognized on upper molars (e.g. *P. pusillus*, *P. divisus* and *P. profuens*) (Kramarz, 2002). However, several *Prolagostomus* specimens recovered from the middle and upper levels of the Pinturas Formation (Argentina), appears to display the same putative ancestral feature and may represent an unnamed taxon (Kramarz, 2002). In this sense, even when we agree with the complex taxonomic status of some species within *Prolagostomus*, the Laguna del Laja specimens are likely more closely related to forms from the upper beds (Santacrucian SALMA) of the Pinturas Formation (Kramarz and Bellosi, 2005).

6. Discussion

The study of a restricted collection of mandibular and maxillary fragments, and isolated teeth of caviomorph rodents recovered from beds of relatively well-constrained late early Miocene age from the Laguna del Laja region (Cura-Mallín Formation) allows to the recognizing of five taxa, *Phanomys mixtus*, *Prolagostomus* sp., *Neoreomys* sp., *Luantus sompallwei* nov. sp., and *Maruchito* nov. sp.? One of these taxa is new to science and increases the paleodiversity of Miocene mammals in southern South America. The early to middle Miocene has been regarded as the time period with the highest known mammal paleodiversity in Chile with more than 54 taxa (Canto et al., 2010). However, the available preliminary taxonomic lists from the most diverse localities in the country reporting dozens of new undescribed taxa and/or taxa in open nomenclature (Bostelmann et al., 2013; Charrier et al., 2015; Flynn et al., 2008, 2002a, 2002b), indicate that much more work is necessary to assess the ancient diversity of the Miocene of Chile. Therefore, our study provides a new step in this regard.

The Tcm₁ and Tcm₃ units are the most prolific source of fossils in the Laguna del Laja area (Flynn et al., 2008). The five rodent taxa here reported come from the middle section of the Tcm₃ unit (*sensu* Flynn et al., 2008), with a relatively well-constrained ⁴⁰Ar/³⁹Ar ages of 17.70–16.40 Ma. Flynn et al. (2008) suggested that the successive faunas from the Laguna del Laja, which include materials recovered from the Cura-Mallín and Trapa-Trapa formations, might represent as many as six SALMAs, including the Colhuehuapian, Santacrucian, Colloncuran, Laventan, Mayoan, and Chasicooan. Other authors

(Kramarz et al., 2010), suggested that the Laguna del Laja fauna could be referred, at least in part, to the “Pinturan” fauna (likely representing the earliest part of the Santacrucian SALMA) due to the presence of the octodontoid rodent *Prostichomys* (Flynn et al., 2008). In fact, there are two putative and undescribed new species of *Prostichomys* from Laguna del Laja, both recovered from the lower-most Tcm₃ levels with a ⁴⁰Ar/³⁹Ar radiometric age of ~17.9 Ma (Flynn et al., 2008). These remains are therefore broadly consistent with the age of the “Pinturan” faunas (19.0–18.0 Ma) in Argentina (Cuitiño et al., 2016). However, the incomplete taxonomic record of the successive mammalian faunas of Laguna del Laja limits our attempts to use biochronologic correlations. The rodent assemblage here reported comes from levels with radiometric ages consistent with the late early Miocene Santacrucian SALMA (Cuitiño et al., 2016). The presence of the exclusive Santacrucian species (e.g. *Phanomys mixtus*) associated with typical (but not exclusive) Santacrucian genera (*Prolagostomus*, *Neoreomys*), also support that the fauna reported here belongs to this SALMA (e.g. Arnal et al., 2019b).

Prolagostomus was a widespread taxon during the early to middle Miocene, with records in Argentina, Chile, and Bolivia (Croft et al., 2011; Vucetich, 1984). In two Chilean localities the genus has been reported, Pampa Castillo (Santacrucian to “Friasian” (Flynn et al., 2002b)), and Laguna del Laja (Flynn et al., 2008). *Neoreomys* is also a widely distributed taxon being known in the late early Miocene faunas of Pinturas and Santa Cruz formations (Santacrucian SALMA), the Early Miocene Pampa Castillo fauna, Chile, as well as in the middle Miocene Collón Curá (Colloncuran SALMA; Río Negro and Neuquén provinces) and La Victoria (Laventan SALMA) formations in Argentina and Colombia (Cuitiño et al., 2019; Fields, 1957; Flynn et al., 2008, 2002b; Kramarz, 2006b). *Luantus* was recognized in the Sarmiento Formation (43°–46°S; Colhuehuapian SALMA), Chubut Province, the lower, middle and upper beds of the Pinturas Formation (47°–51°S; Santacrucian SALMA), and the late Early Miocene of the Cura-Mallín Formation at Laguna del Laja (Flynn et al., 2008; Kramarz, 2006a; Pérez et al., 2010). *Phanomys* was previously known only from the Santa Cruz, Río Jeinemení and Pinturas formations (Pérez and Vucetich, 2012), but here its geographic distribution is extended to the east, thus representing a shared taxon between the Santacrucian faunas of Laguna del Laja and Patagonia.

The *Prolagostomus* and *Luantus* forms from the Laguna del Laja are likely closely related to forms from upper levels of the Pinturas Formation which bear mammals with Santacrucian SALMA affinities (Kramarz, 2002; Kramarz and Bellosi, 2005). *Phanomys mixtus* and *Neoreomys* are also present in the upper levels of the Pinturas Formation (Kramarz and Bellosi, 2005). Therefore, the rodent assemblage here reported is closely allied with the western Santacrucian faunas of the upper levels of the Pinturas Formation.

Previous to the present work, the only confirmed records of *Maruchito* comes from the Collón Curá Formation (40°S; Colloncuran SALMA) (Vucetich et al., 1993). Here, we confirm the presence of *Maruchito* into the late early Miocene of the Cura-Mallín Formation at Laguna del Laja, representing the unequivocal oldest record of the genus, and expanding its biochron from the late early (Santacrucian) to middle Miocene (Colloncuran) in southern Andean Cordillera (Vucetich et al., 1993). In addition, a species closely related to *M. trilofodonte*, yet undescribed, has been recognized in the Río Frías Formation (44°S; “Friasian” SALMA) (Vucetich et al., 1993). Nevertheless, it should be noted that we could not confirm the presence of *Maruchito*, or some related form nearby, in the Río Frías Collection at MLP. The Collón Curá and Río Frías formations are slightly younger than classic deposits of the Santa Cruz Formation in Southern Patagonia (Folguera et al., 2018). However, radiometric ages in the Santa Cruz Formation suggest some chronological overlap with the base of the formers formations (Cuitiño et al., 2016), with several taxa shared among these faunas (e.g. Marshall, 1990). That is why some authors have been advised that taxonomic differences within Santacrucian, Colloncuran and “Friasian” faunas might reflect ecological or geographic, rather than temporal,

differences (Cuitiño et al., 2016). Despite this situation, which deserves further scrutiny (and is out of the scope of the present contribution), the presence of a putative new species of *Maruchito* in early Miocene levels of the Cura-Mallín Formation tentatively suggests their relationships with early middle Miocene western Patagonian localities (e.g. Collón Curá and Río Frías formations). Therefore, the rodents described here consist of a mosaic of taxa, which indicates a widely distributed late early Miocene caviomorph fauna along the south of the Andes, in both intra-arc and foreland basins.

The paleoenvironmental affinities of the fauna described here are difficult to assess, mostly because several aspects of their paleobiology based on postcranial elements, areas of origin and insertion of masticatory muscles and locomotor modes are barely known for most of the present taxa, even at the genus levels. *Neoreomys*, a common and abundant Miocene rodent with protohypsodont teeth, has been interpreted as a cursorial taxon that probably inhabited relatively warm forested areas, probably associated with water bodies (Candela et al., 2013b; Kramarz and Bellosi, 2005). In their type locality, *Maruchito* inhabit relatively warm and humid environments (Vucetich et al., 1993). *Luantus* and *Phanomys* have protohypsodont cheek teeth, which may indicate abrasive diets and/or living in more open habitats such as grassland (Eronen et al., 2010). However, it must be noted that some euhypsodont Miocene caviomorph could be mixed feeders (Candela et al., 2013a). This is likely the case for the euhypsodont *Prolagostomys* which has been interpreted as a mixed feeder, depending on food availability (Rasia, 2016). Based on the limited available evidence the late early Miocene rodent fauna of the Laguna del Laja tentatively advocates the occurrence of warm and rather open habitats. This generalized paleoenvironmental interpretation disagrees with the temperate and forested habitats with permanent bodies of water inferred for the Lonquimay fauna (also belonging to the Cura-Mallín Formation) during the late early Miocene (Solórzano et al., 2019). However, considering the limited studied taxa, this paleoenvironmental interpretation fauna must be taken with caution. Additional sampling efforts and future taxonomic assessments on the Laguna del Laja Neogene mammals will provide a better framework to evaluate this hypothesis.

The multiple fossiliferous horizons previously reported from the Laguna del Laja (early to late Miocene), appears to include several putative undescribed species of octodontids, dinomyids, dasyproctids, "eocardiids", lagostomines and echimyids, suggesting an important distinctiveness of the Laguna del Laja rodents relative to Patagonian contemporaries deposits (*sensu* Flynn et al., 2008). Several potential explanations have been mentioned to account for the proposed uniqueness of the Laguna del Laja rodents, including unusual environments or elevation, topographic or other geographic barriers, and/or temporal distinctions (Flynn et al., 2008). One (but probably two) of the five taxa reported here represent new taxa, supporting, in part, the apparent uniqueness of the late early Miocene fauna of Laguna del Laja. Nevertheless, given the limited sample of the caviomorph rodents described, the proposed pronounced local endemism must remain in question until additional materials from Laguna del Laja will be collected and properly described.

7. Conclusions

The study of a restricted collection of rodents from late early Miocene beds of the Cura-Mallín Formation at the Laguna del Laja area allowed us to illustrate the presence of five taxa belonging to echimyids, dasyproctids, "eocardiids", and lagostomines, including a new taxon, *Luantus sompallwei* nov. sp. Additionally, *Phanomys mixtus* is reported in Chile for the first time, while the presence of *Maruchito* (likely represented by a new species) into the late early Miocene (Santacrucian) is confirmed, representing the unequivocal oldest record of the genus. This fauna has biostratigraphical and geochronological affinities with the Santacrucian SALMA formations of Argentina and especially resembles that reported in the temporal equivalent beds of upper levels of

the Pinturas Formation. Our findings support a widely distributed late early Miocene caviomorph fauna along the south of South America, and suggest the predominance of warm and open habitats in the Cura-Mallín Formation during this time period, yet the recovery of additional Laguna del Laja early Miocene mammals will provide a better framework to evaluate this hypothesis.

Declaration of competing interest

The authors declare that they have no conflict of interest.

Acknowledgments

We wish to thank the Consejo de Monumentos Nacionales (CMN, Chile) and the Corporación Nacional Forestal (CONAF) for the authorization of paleontological prospections in the Laguna del Laja area. To David Rubilar (MNHN), Katherine Cisterna (MHNC), Laura Chornogubsky (MACN), Martín Ezcurra (MACN) and Marcelo Reguero (MLP) for granting access to the vertebrate paleontological collections under their care; to Mónica Núñez-Flores, Maximiliano Reyes, Paz Butikofer, Francisca Riffo, Gabriel Arriagada, Hernán Arriagada and Aníbal Anavalón for their help and camaraderie during the field trips at Laguna del Laja; and to Paul San Martín (CMA Biobío), and Verónica Oliveros (Udec) for their assistance and support in obtaining pictures of the studied materials. We thank to María Encarnación Pérez (Museo Paleontológico Egidio Feruglio) and an anonymous reviewer for their valuable comments and suggestions that greatly improved the early version of the manuscript. This research was funded by Conicyt, Fondecyt project n°1151146 (AE), and Conicyt-PCHA/Doctorado Nacional/2018–21180471 (AS).

Appendix A. Supplementary data

Supplementary data to this article can be found online at <https://doi.org/10.1016/j.jsames.2020.102658>.

References

- Álvarez, A., Arévalo, R.L.M., Verzi, D.H., 2017. Diversification patterns and size evolution in caviomorph rodents. *Biol. J. Linn. Soc.* 121, 907–922. <https://doi.org/10.1093/biolinnean/blx026>.
- Álvarez, A., Pérez, S.I., Verzi, D.H., 2011. Ecological and phylogenetic influence on mandible shape variation of South American caviomorph rodents (Rodentia: Hystricomorpha). *Biol. J. Linn. Soc.* 102, 828–837. <https://doi.org/10.1111/j.1095-8312.2011.01622.x>.
- Ameghino, F., 1894. Enumération Synoptique des espèces de mammifères fossiles des formations Éocènes de Patagonie. *Bol. Acad. Nac.* 13, 259–452. <https://doi.org/10.5962/bhl.title.77348>. Ciencias en Córdoba (República Argentina).
- Ameghino, F., 1889. Contribución al conocimiento de los mamíferos fósiles de la República Argentina. *Actas Acad. Nac. Ciencias en Córdoba* 6, 1–1027.
- Antoine, P.-O., Marivaux, L., Croft, D.A., Billet, G., Ganerod, M., Jaramillo, C., Martin, T., Orliac, M.J., Tejada, J., Altamirano, A.J., Duranthon, F., Fanjat, G., Rousse, S., Gismondi, R.S., 2012. Middle Eocene rodents from Peruvian Amazonia reveal the pattern and timing of caviomorph origins and biogeography. *Proc. Roy. Soc. B Biol. Sci.* 279, 1319–1326. <https://doi.org/10.1098/rspb.2011.1732>.
- Arnal, M., Kramarz, A.G., Vucetich, M.G., Frailey, C.D., Campbell, K.E., 2019a. New Palaeogene caviomorphs (Rodentia, Hystricomorpha) from Santa Rosa, Peru: systematics, biochronology, biogeography and early evolutionary trends. *Pap. Palaeontol.* 1–24. <https://doi.org/10.1002/spp2.1264>.
- Arnal, M., Pérez, M.E., Deschamps, C.M., 2019b. Revision of the Miocene caviomorph rodents from the Río Santa Cruz (Argentinean Patagonia). *Publicación Electrónica la Asoc. Paleontológica Argentina* 19, 193–229. <https://doi.org/10.5710/PEAPA.25.09.2019.299>.
- Bertrand, O.C., Flynn, J.J., Croft, D.A., Wyss, A.R., 2012. Two new taxa (Caviomorpha, Rodentia) from the early Oligocene Tinguiririca fauna (Chile). *Am. Mus. Novit.* 3750, 1–36.
- Boivin, M., Marivaux, L., 2018. Dental homologies and evolutionary transformations in Caviomorpha (Hystricomorpha, Rodentia): new data from the Paleogene of Peruvian Amazonia. *Hist. Biol.* 1–27. <https://doi.org/10.1080/08912963.2018.1506778>.
- Boivin, M., Marivaux, L., Orliac, M., Pujos, F., Salas-Gismondi, R., Tejada-Lara, J., Antoine, P.-O., 2017. In: Late Middle Eocene Caviomorph Rodents from Contamana. Peruvian Amazonia. <https://doi.org/10.26879/742>. *Pap. Palaeontol. Electron.*
- Bostelmann, E., Bobe, R., Carrasco, G., Alloway, B.V., Santi-Malnis, P., Mancuso, A., Aguero, B., Alleseneged, Z., Godoy, Y., 2012. The Alto Río Cisnes fossil fauna (Río Frías Formation, early Middle Miocene, Friasian SALMA): a keystone and paradigmatic vertebrate assemblage of the South American fossil record. In: III Simposio

- Paleontología En Chile. Punta Arenas, Chile, pp. 42–45.
- Bostelmann, E., Le Roux, J.P., Vásquez, A., Gutiérrez, N.M., Oyarzún, J.L., Carreño, C., Torres, T., Otero, R., Llanos, A., Fanning, C.M., Hervé, F., 2013. Burdigalian deposits of the Santa Cruz formation in the Sierra Baguales, austral (Magallanes) basin: age, depositional environment and vertebrate fossils. *Andean Geol.* 40, 458–489. <https://doi.org/10.5027/andgeov40n3-a04>.
- Burns, W.M., Jordan, T.E., Copeland, P., Kelley, S.A., 2006. The case for extensional tectonics in the Oligocene-Miocene Southern Andes as recorded in the Cura Mallín basin (36°–38°S). In: Special Paper 407: Evolution of an Andean Margin: A Tectonic and Magmatic View from the Andes to the Neuquén Basin (35°–39°S Lat). Geological Society of America, pp. 163–184. <https://doi.org/10.1130/2006.2407.08>.
- Candela, A.M., Cassini, G.H., Nasif, N.L., 2013a. Fractal dimension and cheek teeth crown complexity in the giant rodent *Eumegamys paranensis*. *Lethaia* 46, 369–377. <https://doi.org/10.1111/let.12015>.
- Candela, A.M., Rasia, L.L., Pérez, M.E., 2013b. Paleobiology of Santacrucian caviomorph rodents: a morphofunctional approach. In: Vizcaíno, S.F., Kay, R.F., Bargo, S. (Eds.), Early Miocene Paleobiology in Patagonia. Cambridge University Press, pp. 287–305. <https://doi.org/10.1017/cbo9780511667381.016>.
- Canto, J., Yáñez, J., Rovira, J., 2010. Estado actual del conocimiento de los mamíferos fósiles de Chile. *Estud. Geol.* 66, 255–284. <https://doi.org/10.3989/egol.39778.055>.
- Charrier, R., Flynn, J.J., Wyss, A.R., Croft, D.A., 2015. Marco Geológico-tectónico, contenido fosilífero y cronología de los yacimientos cenozoicos pre-pleistocénicos de Mamíferos terrestres fósiles de Chile. Publicación Ocas. del Mus. Nac. Hist. Nat. Chile 63, 293–338.
- Croft, D.A., Chick, J.M.H., Anaya, F., 2011. New middle Miocene caviomorph rodents from Quebrada Honda, Bolivia. *J. Mamm. Evol.* 18, 245–268. <https://doi.org/10.1007/s10914-011-9164-z>.
- Croft, D.A., Flynn, J.J., Wyss, A.R., 2008. The Tinguiririca fauna of Chile and the early stages of “modernization” of South American mammal faunas 1. *Arq. Mus. Nac.* 1, 191–211.
- Cuitiño, J.I., Fernicola, J.C., Kohn, M.J., Traylor, R., Naipauer, M., Bargo, M.S., Kay, R.F., Vizcaíno, S.F., 2016. U-Pb geochronology of the Santa Cruz formation (early Miocene) at the Río Bote and Río Santa Cruz (southernmost Patagonia, Argentina): implications for the correlation of fossil vertebrate localities. *J. S. Am. Earth Sci.* 70, 198–210. <https://doi.org/10.1016/j.jsames.2016.05.007>.
- Cuitiño, J.I., Vizcaíno, S.F., Bargo, M.S., Aramendía, I., 2019. Sedimentology and fossil vertebrates of the Santa Cruz formation (early Miocene) in Lago Posadas, southwestern Patagonia, Argentina. *Andean Geol.* 46, 383–420. <https://doi.org/10.5027/andgeov46n2-3128>.
- Eronen, J.T., Puolamäki, K., Liu, L., Lintulaakso, K., Damuth, J., Janis, C., Fortelius, M., 2010. Precipitation and large herbivorous mammals II: Application to fossil data. *Evol. Ecol. Res.* 12, 235–248.
- Fields, R.W., 1957. Hystricomorph Rodents from the Late Miocene of Colombia, South America, vol. 273 A Contrib. from Univ. Calif. Museum Paleontol.
- Fischer von Waldheim, G., 1817. *Adversaria zoologica. Mémoires de la Société impériale des naturalistes de Moscou* 5, 357–472.
- Flynn, J.J., Charrier, R., Croft, D.A., Gans, P.B., Herriott, T.M., Wertheim, J.A., Wyss, A.R., 2008. Chronologic implications of new Miocene mammals from the Cura-Mallín and Trapa Trapa formations, Laguna del Laja area, south central Chile. *J. S. Am. Earth Sci.* 26, 412–423. <https://doi.org/10.1016/j.jsames.2008.05.006>.
- Flynn, J.J., Croft, D.A., Charrier, R., Hérail, G., Wyss, A.R., 2002a. The first Cenozoic mammal fauna from the Chilean Altiplano. *J. Vertebr. Paleontol.* 22, 200–206. <https://doi.org/10.1017/S0016756897007061>.
- Flynn, J.J., Novacek, M.J., Dodson, H.E., Frassinetti, D., McKenna, M.C., Norell, M.A., Sears, K.E., Swisher, C.C., Wyss, A.R., 2002b. A new fossil mammal assemblage from the southern Chilean Andes: implications for geology, geochronology, and tectonics. *J. S. Am. Earth Sci.* 15, 285–302. [https://doi.org/10.1016/S0895-9811\(02\)00043-3](https://doi.org/10.1016/S0895-9811(02)00043-3).
- Folguera, A., Encinas, A., Echaurren, A., Gianni, G., Orts, D., Valencia, V., Carrasco, G., 2018. Constraints on the Neogene growth of the central Patagonian Andes at the latitude of the Chile triple junction (45–47°S) using U/Pb geochronology in synorogenic strata. *Tectonophysics* 744, 134–154. <https://doi.org/10.1016/j.tecto.2018.06.011>.
- Frailey, C.D., Campbell Jr., K.E., 2004. Paleogene rodents from Amazonian Peru: the Santa Rosa local fauna. In: In: Campbell, K.E. (Ed.), The Paleogene Mammalian Fauna of Santa Rosa, Amazonian Peru. Natural History Museum of Los Angeles County, Science Series, vol. 40, pp. 71–130.
- Herriott, T.M., 2006. Stratigraphy, structure, and 40Ar/39Ar geochronology of the southeastern Laguna del Laja area: Implications for the mid-late Cenozoic evolution of the Andes near 37.5°S, Chile. Unpublished Master's Thesis. Department of Earth Science, University of California, Santa Barbara.
- Kramarz, A.G., 2006a. Eocardiids (Rodentia, Hystricognathi) from the Pinturas formation, late early Miocene of Patagonia, Argentina. *J. Vertebr. Paleontol.* 26, 770–778. [https://doi.org/10.1671/0272-4634\(2006\)26\[770:ERHFTP\]2.0.CO;2](https://doi.org/10.1671/0272-4634(2006)26[770:ERHFTP]2.0.CO;2).
- Kramarz, A.G., 2006b. *Neoreomys* and *Scleromys* (Rodentia, Hystricognathi) from the Pinturas formation, late early Miocene of Patagonia, Argentina. *Rev. Mus. Argent. Ciencias Nat.* 8, 53–62. <https://doi.org/10.22179/revmacn.8.356>.
- Kramarz, A.G., 2002. Roedores chinchilloideos (Hystricognathi) de la Formación Pinturas, Mioceno temprano-medio de la provincia de Santa Cruz, Argentina. *Rev. del Mus. Argent. Ciencias Nat. Nueva Ser.* 4, 167–180.
- Kramarz, A.G., 1998. Un nuevo Dasyproctidae (Rodentia, Caviomorpha) del Mioceno inferior de Patagonia. *Ameghiniana* 35, 181–192.
- Kramarz, A.G., Bellosi, E.S., 2005. Hystricognath rodents from the Pinturas formation, early–middle Miocene of Patagonia, biostratigraphic and paleoenvironmental implications. *J. S. Am. Earth Sci.* 18, 199–212. <https://doi.org/10.1016/j.jsames.2004.10.005>.
- Kramarz, A.G., Vucetich, M., María Guiomar, Carlini, Alfredo Armando, Ciancio, M.R., Abello, M.A., Deschamps, C.M., Gelfo, J.N., Madden, R.H., Kay, R.F., 2010. A new mammal fauna at the top of the Gran Barranca sequence and its biochronological significance. In: Madden, R.H., Carlini, A.A., Vucetich, M.G., Kay, R. (Eds.), The Paleontology of Gran Barranca: Evolution and Environmental Change Through the Middle Cenozoic of Patagonia, pp. 260–273 Cambridge.
- Marivaux, L., Vianey-Liaud, M., Jaeger, J.J., 2004. High-level phylogeny of early Tertiary rodents: dental evidence. *Zool. J. Linn. Soc.* 142, 105–134. <https://doi.org/10.1111/j.1096-3642.2004.00131.x>.
- Marshall, L.G., 1990. Fossil marsupials from the type friasian Land mammal age (Miocene), Alto Río Cisnes, Aisen, Chile. *Andean Geol.* 17, 19–55. <https://doi.org/10.5027/andgeov17n1-a02>.
- Niemeyer, H.R., Muñoz, J.B., 1983. Hoja Laguna de La Laja: Región del Biobío. Carta Geológica de Chile 57, scale 1:250.000. Servicio Nacional de Geología y Minería, Santiago, Chile.
- Patton, J.L., Pardiñas, U.F.J., DeIlla, G., 2015. Mammals of South America, vol. 2 Rodents. The University of Chicago Press, Chicago.
- Pedroza, V., Le Roux, J.P., Gutiérrez, N.M., Vicencio, V.E., 2017. Stratigraphy, sedimentology, and geothermal reservoir potential of the volcanoclastic Cura-Mallín succession at Lonquimay, Chile. *J. S. Am. Earth Sci.* 77, 1–20. <https://doi.org/10.1016/j.jsames.2017.04.011>.
- Pérez, M.E., Vucetich, M.G., 2012. A revision of the fossil genus *Phanomys* Ameghino, 1887 (Rodentia, Hystricognathi, Caviodea) from the early Miocene of Patagonia (Argentina) and the acquisition of euhyposodonty in Caviodea *sensu stricto*. *Paläontol. Z.* 86, 187–204. <https://doi.org/10.1007/s12542-011-0120-2>.
- Pérez, M.E., Vucetich, M.G., Kramarz, A.G., 2010. The first eocardiidae (Rodentia) in the Colhuehuapian (early Miocene) of Bryn Gwyn (northern Chubut, Argentina) and the early evolution of the peculiar cavioid rodents. *J. Vertebr. Paleontol.* 30, 528–534. <https://doi.org/10.1080/02724631003618223>.
- Radic, J.P., 2010. Las cuencas cenozoicas y su control en el volcanismo de los Complejos Nevados de Chillan y Copahue-Callaqui (Andes del Sur, 36°–39°S). *Andean Geol.* 37, 220–246. <https://doi.org/10.4067/S0718-1062010000100009>.
- Rasia, L.L., 2016. Los Chinchillidae (Rodentia, Caviomorpha) fósiles de la República Argentina: sistemática, historia evolutiva y biogeográfica, significado bioestratigráfico y paleoambiental. Ph. D. thesis. Universidad Nacional de La Plata.
- Rasia, L.L., Candela, A.M., 2019. Upper molar morphology, homologies and evolutionary patterns of chinchilloid rodents (Mammalia, Caviomorpha). *J. Anat.* 234, 50–65. <https://doi.org/10.1111/joa.12895>.
- Scott, W.B., 1905. Mammalia of the Santa Cruz beds, Part III. In: Report of Princeton University Expedition to Patagonia, 1896–1899, 1–491 + Plates.
- SERNAGEOMIN, 2003. Mapa geológico de Chile, versión digital, escala 1:1.000.000. Publicación Geológica Digit. Serv. Nac. Geol. Minería, Chile 4, 1–23.
- Shockey, B.J., Flynn, J.J., Croft, D.A., Gans, P.B., Wyss, A.R., 2012. New leontiniid Notoungulata (Mammalia) from Chile and Argentina: comparative anatomy, character analysis, and phylogenetic hypotheses. *Am. Mus. Novit.* 3737, 1–64.
- Solórzano, A., Encinas, A., Bobe, R., Reyes, M., Carrasco, G., 2019. The early to late middle Miocene mammalian assemblages from the Cura-Mallín formation, at Lonquimay, southern central Andes, Chile (–38°S): biogeographical and paleoenvironmental implications. *J. S. Am. Earth Sci.* 96, 102319. <https://doi.org/10.1016/j.jsames.2019.102319>.
- Suárez, M., Empanan, C., 1995. The stratigraphy, geochronology and paleogeography of a Miocene fresh-water interarc basin, southern Chile. *J. S. Am. Earth Sci.* 8, 17–31. [https://doi.org/10.1016/0895-9811\(94\)00038-4](https://doi.org/10.1016/0895-9811(94)00038-4).
- Suárez, M., Empanan, C., Wall, R., Salinas, P., Marshall, L., Rubilar, A., 1990. Estratigrafía y vertebrados fósiles del Mioceno del Alto Biobío, Chile Central (38°–39°S). In: Actas, II Simposio Sobre El Terciario de Chile. Concepción, pp. 311–324.
- Upham, N., Patterson, B.D., 2015. Evolution of caviomorph rodents: a complete phylogeny and timetree for living genera. In: Vassallo, A.I., Antenucci, D. (Eds.), Biology of Caviomorph Rodents: Diversity and Evolution. SAREM Series A, Buenos Aires, pp. 63–120.
- Utge, S., Folguera, A., Litvak, V., Ramos, V.A., 2009. Geología del sector norte de la cuenca de Cura Mallín: zona de las Lagunas de Epulafquen (36°40'–50'S, 71°–71'10'O). *Rev. Asoc. Geol. Argent.* 64, 231–248.
- Vucetich, M.G., 1984. Los roedores de la edad Friasense (Mioceno medio) de Patagonia. *Rev. Mus. La Plata* 8, 47–126.
- Vucetich, M.G., 1977. Un nuevo Dasyproctidae (Rodentia, Caviomorpha) de la edad Friasense (Mioceno tardío) de Patagonia. *Ameghiniana* 14, 215–223.
- Vucetich, M.G., Arnal, M., Deschamps, C.M., Pérez, M.E., Vieytes, E.C., 2015. A brief history of caviomorph rodents as told by the fossil record. In: Vassallo, A.I., Antenucci, D. (Eds.), Biology of Caviomorph Rodents: Diversity and Evolution. SAREM series A, Buenos Aires, pp. 11–62.
- Vucetich, M.G., Kramarz, A.G., Candela, A.M., 2010a. The Colhuehuapian rodents from Gran Barranca and other Patagonian localities: the state of the art. In: Madden, R.H., Carlini, A.A., Vucetich, M.G., Kay, R.F. (Eds.), The Paleontology of Gran Barranca: Evolution and Environmental Change through the Middle Cenozoic of Patagonia. Cambridge University Press, pp. 206–219.
- Vucetich, M.G., Mazzoni, M.M., Pardiñas, U.F.J., 1993. Los roedores de la Formación Collón Curá (Mioceno medio), y la Ignimbrita Pilcaniyeh, Cañadón del Tordillo, Neuquén. *Ameghiniana* 30, 361–381.
- Vucetich, M.G., Guiomar, María, Vieytes, E.C., Pérez, M.E., Carlini, A.A., 2010b. The rodents from La Cantera and the early evolution of caviomorphs in South America. In: Madden, R.H., Carlini, A.A., Vucetich, M.G., Kay, R.F. (Eds.), The Paleontology of Gran Barranca: Evolution and Environmental Change through the Middle Cenozoic of Patagonia. Cambridge University Press, pp. 189–201.
- Wood, A.E., Patterson, B., 1959. The rodents of the desecated Oligocene of Patagonia and the beginnings of south american rodent evolution. *Bull. Mus. Comp. Zool.* 120, 1–428.



Contents lists available at ScienceDirect

Palaeogeography, Palaeoclimatology, Palaeoecology

journal homepage: www.elsevier.com/locate/palaeo

Evolutionary trends of body size and hypsodonty in notoungulates and their probable drivers

Andrés Solórzano^{a,*}, Mónica Núñez-Flores^{b,c}^a Programa de Doctorado en Ciencias Geológicas, Facultad de Ciencias Químicas, Universidad de Concepción, Concepción, Chile^b Programa de Doctorado en Sistemática y Biodiversidad, Facultad de Ciencias Naturales y Oceanográficas, Universidad de Concepción, Concepción, Chile^c Programa de Doctorado en Biología Integrada, Facultad de Biología, Universidad de Sevilla, Sevilla, Spain

ARTICLE INFO

Keywords:
 Macroevolution
 Species sorting
 Typotheria
 Toxodontia
 South America

ABSTRACT

Members of the Order Notoungulata are among the most diverse and common mammals in South America during the Cenozoic. Several lineages within notoungulates (e.g., suborders Typotheria and Toxodontia) show a tendency for increased body sizes and hypsodonty during the last 50 Myr. However, the timing, evolutionary mode, and drivers of such tendencies are not entirely understood. In this paper, we use an extensive database of notoungulate fossil occurrences and body mass and hypsodonty estimates to characterize the evolutionary mode of these two phenotypic traits over time, test the extent to which several factors (e.g., development of open environments in the south of South America) have influenced it through time, and investigate whether large trait values were selected through elevated origination or reduced extinction rates. Our results demonstrate that most of the major notoungulate clades evolved toward larger body sizes (up to 1500 kg) and higher tooth crown, from a small and low-crowned tooth ancestor, in a punctuated mode. We also show that body mass and the hypsodonty in typotherians and toxodonts had a coupled evolutionary history. Species sorting was a relevant macroevolutionary process in some notoungulate clades, as taxa with high teeth crown and body mass had lower extinction rates. Finally, the development of the hypsodonty in notoungulates must reflect repeated and quick instances of adaptive responses to the increased availability of volcanic or other terrigenous particles, within the broad context of the SSA Cenozoic Andean mountain building.

1. Introduction

During most of the Cenozoic, South America (SA) witnessed the evolution of several groups of mammals in relative geographic isolation (Simpson, 1980). One of the most diverse and common Cenozoic mammal groups that evolved was the notoungulates (Order Notoungulata), achieving an impressive taxonomic diversity (at least 154 genera so far recognized, but now extinct) and morphologic disparity, and filling a wide variety of ecological niches (Croft et al., 2020; Reguero et al., 2010; Reguero and Prevosti, 2010; Scarano et al., 2021). Their relationships within placental mammals remained elusive for more than a century, but recent ancient collagen and protein analyses have identified notoungulates, together with other South American native ungulates like litopterns (Order Litopterna), as the sister taxon of Perissodactyla (Buckley, 2015; Welker et al., 2015). Phylogenetic relationships within notoungulates have supported monophyly and the existence of two relatively well-defined suborders, Toxodontia and

Typotheria, and two early-diverging families, Henricosborniidae and Notostylopidae (Billet, 2011; Croft et al., 2020).

High-crowned (hypsodont) teeth are widely found among extant and extinct mammalian herbivores (Damuth and Janis, 2011; Janis and Fortelius, 1988; Kaiser et al., 2013). Notoungulata is one of the clades of SA mammals that evolved high-crowned or hypsodont teeth (Croft et al., 2020; Madden, 2014; Ortiz-Jaureguizar and Cladera, 2006). The development of such kinds of tooth in SA appears precocious compared to other continents (Pascual and Odreman-Rivas, 1971; Patterson and Pascual, 1968). This precocity was first evident as early as the end of the Paleocene. Independent of body size, it was during the Late Oligocene when many families of notoungulates acquired protohypsodont to hypselodont cheek-teeth (Ortiz-Jaureguizar and Cladera, 2006; Pascual and Jaureguizar, 1990; Pascual and Odreman-Rivas, 1971), and the Tinguirirican (Early Oligocene) fauna of SA is the world's oldest fauna dominated by hypsodont herbivores (Flynn et al., 2003). Recent evidence suggests the existence of several periods of relatively intense

* Corresponding author.

E-mail address: solorzanoandres@gmail.com (A. Solórzano).<https://doi.org/10.1016/j.palaeo.2021.110306>

Received 4 November 2020; Received in revised form 11 February 2021; Accepted 12 February 2021

Available online 18 February 2021

0031-0182/© 2021 Elsevier B.V. All rights reserved.

evolutionary change in hypsodonty in South American mammals (Madden, 2014; Strömberg et al., 2013), and a general trend for an increased hypsodonty throughout the last 40 Myr has been noted in several notoungulates clades (Reguero et al., 2010; Strömberg et al., 2013). Increased hypsodonty appears to be synchronous across several lineages of tyotherians by the Tinguirirican South American Land Mammals Age (SALMA) (Reguero et al., 2010). In contrast, hypselodont (i.e., ever-growing teeth) appears to have originated among notoungulates in two pulses: Divisaderan SALMA (late Eocene) in hegetotheriids and mesotheriids and Deseadan SALMA (late Oligocene) in interatheriids and toxodontids (Reguero et al., 2007). Nevertheless, some authors have noted that relatively large errors in hypsodonty estimates are present, and consequently, a potential bias in some of the estimated temporal trends cannot be ruled out (Dunn et al., 2015).

The causes of the development of a precocious hypsodonty in SA notoungulates are not entirely understood and they might be very complex (Dunn et al., 2015; Madden, 2014; Reguero et al., 2010; Strömberg et al., 2013). Its development was initially linked to adaptive shifts given grassland/open habitats expansion (Flynn et al., 2003), consistent with the idea that most modern ungulate clades developed hypsodont teeth in drier and more open habitats (Damuth and Janis, 2011; Janis, 1990; Raia et al., 2010). However, recent works found that grasses only became common in SA after the Miocene, being relatively rare during the Eocene, making it unclear whether hypsodonty evolved in forested or in open but grass-free habitats (Dunn et al., 2015; Raia et al., 2010; Strömberg et al., 2013). In any case, the relevance of exogenous grit or soil's ingestion has driven the necessity to deal with tooth abrasion has been claimed and now are considered a plausible mechanism for hypsodonty evolution in ungulates (Damuth and Janis, 2011; Dunn et al., 2015; Madden, 2014; Semprebon et al., 2019; Strömberg et al., 2013). Indeed, the current view is that hypsodonty represents an adaptation to a worn effect that comprises both diet (e.g., phytoliths in grasses) and environment (dust or grit related to volcanism and erosion) (Damuth and Janis, 2011; Kaiser et al., 2013).

On the other hand, there are possible feedbacks among traits related to hypsodonty. For instance, hypsodont species could be larger-sized than non-hypsodont taxa because the resource that hypsodonty makes available to herbivores is a physiologically demanding one (Raia et al., 2011). Notoungulates show high hypsodonty (brachyodont to hypselodont) and body size (~1–1000 kg) disparity, which likely increases over time (Croft et al., 2020). Body size is one of the essential quantitative traits under evolutionary scrutiny because it influences nearly every aspect of an organism's biology (Peters, 1986). Body size exhibits prominent general trends in both space and time, as the tendency to evolve larger body sizes over evolutionary time (i.e., Cope's rule), or the pattern in which body size among closely related endothermic taxa tends to increase toward colder geographical regions (i.e., Berman's rule) (Ashton et al., 2000; Heim et al., 2015; Hone and Benton, 2005; McNab, 2010; Meiri and Dayan, 2003; Smith et al., 2016). However, none of these trends has been shown to apply generally across taxa (Ashton et al., 2000; Heim et al., 2015; Meiri and Dayan, 2003; Smith et al., 2016). The body size of organisms is often under selection pressure because it provides a direct way to adapt to several different environmental regimes (Kingsolver and Pfennig, 2004; Lyons and Smith, 2010; Smith et al., 2016). Thus, it seems likely that changes in the physical environment should exert a strong influence on the nature and directionality of body size evolution and other phenotypic traits (Clavel and Morlon, 2017; Hunt et al., 2015, 2010; Hunt and Roy, 2006). In general, both clade's biology and environment must be considered to understand trait evolution fully, and in general, macroevolutionary patterns. Accordingly, characterizing first-order patterns is essential for understanding the potential underlying causes that have shaped traits, like body size or hypsodonty, over evolutionary time (Hunt et al., 2015; Hunt and Roy, 2006; Smith et al., 2016). Characterizing the mode and tempo of the evolutionary change is a major theme in macroevolution since Simpson's earliest days (Simpson, 1944). Nowadays, it is possible

to characterize trait evolution based on the fossil record, as each mode of evolution can be expressed as a statistical model (Hunt, 2006a). Three general models have become standard in attempts to understand the nature of evolutionary divergence in fossil lineages: directional change, unbiased random walk, and stasis, and although simplified, these modes of change are useful abstractions that distinguish fundamentally different kinds of evolutionary dynamics (Hunt, 2007, 2006a; Hunt et al., 2015; Hunt and Rabosky, 2014).

Even though the unique hypsodonty patterns exhibited by several lineages of notoungulates, to our knowledge, studies dealing with their evolutionary mode of trait evolution are still lacking, and the same situation is uncovered for the body size. Two primary drivers for evolutionary patterns of hypsodonty in notoungulates have been proposed, the tectonic evolution of the Andean orogen (as well as their concomitant complex volcanic history) and the development of open habitats through changes in the disposal of exogenous grit or soil (Gomes Rodrigues et al., 2017; Kohn et al., 2015; Madden, 2014). However, the few studies explicitly testing them have focused on the effects of the availability of open habitats over notoungulate hypsodonty (Strömberg et al., 2013). On the other hand, it has been recently argued that the evolutionary patterns of body size in *Protypotherium*, a diverse genus of tyotherians, could be correlated with global temperature trends (Scarano et al., 2021). Therefore, the potential drivers of the evolutionary change of body mass and hypsodonty through time appear to be mostly related to abiotic or environmental changes. In contrast, additional potential drivers, including feedbacks among own-clade traits, have not been considered, and to our knowledge, no studies have examined multiple hypotheses simultaneously. The last is in need, given the complex interactions of biotic and abiotic factors driving long-term evolutionary patterns (Fraser et al., 2020; Lehtonen et al., 2017; Solórzano et al., 2020).

In the present work, we compiled a comprehensive database of notoungulate fossil species occurrences, dental measurements (as a way to estimate the body mass of each species), and hypsodonty categories from the literature. Within a statistical framework, we analyzed these data to characterize the mode of evolution of phenotypic traits (body size and hypsodonty) over time. The more considerable diversity of notoungulates concentrates toward the south of South America. Therefore, we also test the extent to which assorted environmental factors (e.g., paleobotanical changes) have influenced these traits (body size and hypsodonty). Given that both traits could fluctuate in both space and time, we also test the correlation between body size, hypsodonty, and geography (e.g., latitude, longitude as predictive variables). Moreover, although previous works have advocated an apparent increase of body size and hypsodonty in notoungulates through time (Madden, 2014; Reguero et al., 2010; Strömberg et al., 2013), it is necessary to distinguish whether these general trends are generated by a non-directional diffusive process or by an active directional evolutionary process due to selection for large body size or hypselodont species (Huang et al., 2017; McShea, 1994). Therefore, we also investigate whether large trait values (body size or hypsodonty) were selected through differential origination or extinction rates (Jablonski, 2008).

2. Methods

2.1. Fossil occurrence database

We collected data on fossil species occurrences over the entire evolutionary history of the Order Notoungulata, using mainly information in the Paleobiology Database (PBDB; <https://paleobiodb.org>). The data from the PBDB was taxonomically standardized by removing junior synonyms, outdated combinations, and *nomina dubia*. Some taxa were manually added to the dataset as they were absent from the PBDB. Each taxon's age was confirmed with the faunal list of the more diverse fossiliferous localities and updated accordingly to the recent advances in SALMAS (Croft et al., 2020; Dunn et al., 2013; Prevosti and Forasiepi,

2018; Reguero and Prevosti, 2010). Each taxon was assigned to one of the traditionally recognized families. The final database comprises 1098 fossil occurrences representing 260 taxa (Supplementary File Table S1).

2.2. Body mass estimations in notoungulates

Several linear regression models have been developed to predict the body mass (hereafter BM) of extinct ungulates based on dental, cranial, and postcranial morphometric and body mass data from extant ungulates (e.g., Janis, 1990; Mendoza et al., 2006). Three of the most widely employed, and also feasible to recover in the fossil record, dental measurements for body mass estimations in notoungulates are the lower molar series length (LMRL), second lower molar length (SLML), and second upper molar length (SUML) (Elissamburu, 2012; Reguero et al., 2010). After an extensive survey of the literature, we recover LMRL, SLML, SUML measurements for most (~90%) of the notoungulates species in our dataset (Supplementary File Tables S2, S3).

Craniodental body mass estimates appear to be inaccurate for large notoungulates, in part due to their relatively large head with ever-growing molars that are not closely similar to any extant ungulate (Croft et al., 2020). Therefore, body mass estimations in relatively large notoungulates based on ungulate craniodental variables (as LMRL, SLML, SUML) might result in overestimations (Croft et al., 2020). To circumvent this potential issue, we first use the database of LMRL, SLML, and SUML dental measurements (in mm) and body mass (in kg) of extant ungulates ($n = 138$) from Mendoza et al. (2006) (Supplementary File Table S4). After, regression models with segmented relationships (= piecewise linear regression) between the response (BM) and explanatory variables (LMRL, SLML, and SUML) were fitted using the package *segmented* (Muggeo, 2017) in the R environment (R Core Team, 2018). These allow us to find breaking points in the slope between the response and each of the explanatory variables at the following values: LMRL = 73.9, FLML = 19.2, and SUML = 20. The data of taxa in the dataset with lower values than these breakpoints ($n = 68$; BM ranging between 2 and 78.4 kg) was used to fit natural log-log ordinary linear regression (OLS) between the response (BM) and explanatory variables (LMRL, SLML, and SUML). For these models, we estimated their slope, interception, r^2 , Mean Absolute Error (MAE), percent Sum of Squares Error (%SSE), and percent Predicted Error (%PE). As tyotherians and other basal notoungulates include taxa smaller than 100 kg (Elissamburu, 2012; Reguero et al., 2010), we believe that estimations based on these new equations will provide an adequate approximation to their body mass.

Given that relatively large notoungulates (i.e., members of Toxodontia) appear to have a relatively large head compared to extant ungulates, their BM estimations may be severely biased. To reduce this bias, we use the above-resulting equations and estimate the 95% prediction intervals (which reflects the uncertainty around a single value) for the BM given each of the predictive variables (LMRL, SLML, SUML) in large notoungulates. Based on these prediction intervals, the lower BM values obtained for each taxon, even when more than a single dental measurement was available, was regarded as the most conservative BM estimation for members of the suborder Toxodontia and used in downstream analyses. In cases in which more than a single dental measurement was available, we calculated these values' mean as a proxy of the BM in each taxon. Additionally, a summary of the BM calculations and their Log10 frequency of distribution for all notoungulates and subordinate clades was provided. The last allows us to categorize the body size of notoungulates based on their BM (as well as their Log10 BM) as follows: very small (<1 kg, or < 0 in Log10 space), small (BM between 1 and 10 kg, or 0–1 in Log10 space), medium (BM between 10 and 100 kg, or 1–2 in Log10 space), large (BM between 100 and 320 kg, or 2–2.5 in Log10 space), very large (BM between 320 and 1000 kg, or 2.5–3 in Log10 space) and giant taxa (BM >1000 kg, or > 3 in Log10 space). Finally, we also estimate the body mass disparity (a measure of the range of morphologic variation in a sample of organisms) in each notoungulate family and suborder. While different methods and metrics for

quantifying morphological disparity have been proposed (Erwin, 2007), the disparity was represented by the BM's standard deviation (in kg).

2.3. Hypsodonty in notoungulates

Notoungulate taxa are hypsodont when a tooth crown's height exceeds its anteroposterior length, i.e., when hypsodonty index (hereafter HI), the ratio of first (or second) upper molar enamel crown height to anteroposterior or ectoloph length, is over 1. The crown height in this group has been discussed in different ways (e.g., Madden, 2014). One approach is to express crown height measurements in individual taxa as a hypsodonty index, which is generally measured on the best-preserved and least worn adult specimen available for each species, and the same value is assigned to the species (Madden, 2014). The last is a plausible measurement, as within an extant species, wear rates may not significantly differ among populations because individuals may vary little in dietary and habitat preferences (Damuth and Janis, 2011). Despite possible concerns regarding, among others, whether HI taken from upper or lower molars systematically differ or not (Madden, 2014), this measurement it is available for several notoungulates taxa (e.g., Reguero et al., 2010). A second approach is to express hypsodonty as an average of HI among the species, within a particular time-bin, at the family-level clade allowing the establishment of temporal evolutionary patterns of hypsodonty for each clade (Madden, 2014; Reguero et al., 2010; Strömberg et al., 2013). A third approach is to measure the percentage of faunal hypsodonty (i.e., the rate of herbivorous species with HI > 1). The last allows establishing the relative predominance of hypsodont taxa in different time-intervals (Dunn et al., 2015; Madden, 2014).

On the other hand, several categories could represent the distinct hypsodonty stages observed in herbivores molars, including brachyodont (HI < 1), mesodont (HI ~1), hypsodont (HI ≥ 1–2.5), and hypselodont (i.e., ever-growing teeth; HI > 2.5). We initially retrieved, from the literature, HI face values for 92 of the 260 notoungulate spp. (Supplementary File Tables S2, S3). Given the limited sample of HI values, as well as the apparent variability of ways in which it has been estimated (e.g., HI measured on upper vs. lower molars), we codify most of the studied taxa (259 spp.) in one of the hypsodonty stages above mentioned, following information from the literature. Specifically, taxa with brachyodont, mesodont, hypsodont, and hypselodont dentition were coded as 0, 1, 2, and 3, respectively. These values were used in downstream analyses (Supplementary File Tables S2, S3). We argue that this data can capture the long-term evolutionary dynamics of hypsodonty in notoungulates. Finally, it is noteworthy that we are interested in determining relative hypsodonty changes through time rather than their absolute amount of change.

2.4. Dealing with potential bias in the lifespan of individual species

The first and last appearances of a species in the fossil record are likely to underestimate the true extent of its life span (Liow and Stenseth, 2007). We envisioned that this could be an issue with South American mammals, as they are mainly known within the SALMAs framework which has critical temporal gaps. Therefore, we estimate the speciation and extinction times for each lineage in our dataset considering the uncertainties of the preservation process. For this task, we used the hierarchical Bayesian framework implemented in the software PyRate v2.0 (Silvestro et al., 2019, 2014a, 2014b). From our original dataset, we randomly resampled the ages of each fossil occurrence to generated ten datasets and ran the analyses on all replicates. To assess which of the preservation models implemented in PyRate (Non-homogeneous Poisson process of preservation (NHPP), Homogeneous Poisson process (HPP), or Time-variable Poisson process (TPP)) is best supported by our data, a maximum likelihood test was run in PyRate (Silvestro et al., 2019). For the TPP model of preservation, we use the times that delimit the last stages of the International Chronostratigraphic Chart (v2020/03) with a duration of more than 2 Myr (Cohen et al., 2013). We

ran 10,000,000 Reversible Jump Markov Chain Monte Carlo (RJMCMC) generations (sampling every 10,000), assuming a Gamma model to assess the heterogeneity in the preservation rate and the best-supported preservation model to estimate the expected number of fossil occurrences per lineage/Myr (Silvestro et al., 2019). We inspected RJMCMC convergence ($ESS > 200$) using Tracer software (Rambaut et al., 2018) and discarded the initial 10% iterations as burn-in. Finally, posterior estimates across replicates were summarized, and the higher and lower 95% HPD times in speciation (TS) and extinction (TE), respectively, were obtained representing a plausible lifespan of each taxon.

2.5. Correlations between body size and hypsodonty with origination and extinction rates

PyRate also implements birth-death models in which speciation and extinction rates change in a lineage-specific fashion as a function of an estimated correlation with continuous or discrete traits (*covar* model) (Piras et al., 2018; Silvestro et al., 2014a). Therefore, we use this model to test whether large body size and hypsodonty were selected, at the suborder level, through elevated origination rate or reduced extinction rate. Our original dataset was split in two, focusing on the fossil occurrences of the Toxodontia and Typotheria suborders. We randomly resampled the ages of each fossil occurrence to generated ten datasets and ran the analyses on all replicates. For each trait, using the *covar* model (setting *-mCov* 5), we ran 10,000,000 MCMC generations (sampling every 1000), inspect MCMC convergence and discard the initial 10% iterations as burn-in. The correlations were considered statistically significant when 0 was not included within the 95% credibility interval for $\alpha_{\text{speciation}}$ and $\alpha_{\text{extinction}}$ parameters, while the correlation was interpreted as positive or negative depending on whether $\alpha > 0$ or $\alpha < 0$, respectively (Silvestro et al., 2014a; Solórzano et al., 2020).

2.6. Body mass and hypsodonty evolution through time

The lifespan (previously inferred) and the traits (BM and hypsodonty) calculated for each species were used to compute the mean and standard deviation of these traits values in 1 Myr time bins using the *paleoTS* package (Hunt, 2006b) implemented in the R environment (R Core Team, 2018). We used the “joint” parameterization of the *paleoTS* package to examine support across different simple statistical models of trait evolution: random walk (URW), directional evolution (GRW), Ornstein-Uhlenbeck (OU) model, and stasis (see model details in Hunt, 2008, 2006a). More complex models, implying punctuations (number of punctuations ranging from 1 to 5) and changes among some of the simple models above mentioned (e.g., stasis to GRW), were also tested considering the minimum number of samples (= time-bins) within a segment as 6 ($\text{minb} = 6$). Some of the samples (= time-bins) could have very low N, and their variances are likely estimated imprecisely. Therefore, we replace the low N samples' variances with the estimated pooled variance (Hunt, 2006b). The BM analyses were based on their natural logarithm, therefore considering the rate of proportional, rather than absolute, change and reducing the potential bias regarding trait estimations (Cooper and Purvis, 2010; Lyons and Smith, 2010).

Model support for the fitted evolutionary models was assessed by using the bias-corrected Akaike Information Criterion (AICc), which balances the goodness of fit (log-likelihood) with model complexity (the number of model parameters). For each trait, the model with the lowest AICc value and higher Akaike weights is the best supported. However, AICc cannot reject all candidate models even when they represent poor descriptions of the observed trait dynamics (Voje, 2018). Tests of model adequacy may help us avoid making meaningless interpretations of model parameters that do not describe the data well (Voje, 2018). Therefore, we use the model adequacy tests for the best phyletic models implemented in the R package *adePEM* (Voje, 2018) to test whether the simple statistical models of trait evolution fitted in *paleoTs* describe the data well. The trait evolution analyses first were performed considering

all Notoungulates and repeated at the suborder and family levels when possible (i.e., number of time bins > 20). Finally, we are interested in identifying whether BM and hypsodonty increase or not with time. Therefore, we performed generalized least squares (GLS), as those described below, to identify possible correlations among mean, minimum, and maximum BM and hypsodonty with time and evaluate the relationship significance using the *p* values for the slope coefficient.

2.7. Potential mechanisms driving the historical dynamics of body size and hypsodonty in notoungulates in the south of South America

The larger diversity of notoungulates (250 of 260 spp. in our dataset) concentrates toward the south of South America (hereafter SSA, and defined as the area located south of the 15°S (Ortiz-Jaureguizar and Cladera, 2006)), making this region suitable to test whether regional or global environmental factors could be driving the evolution of body sizes and hypsodonty in notoungulates. To this task, we use four time-continuous global and regional (SSA) factors, including global mean temperature based on $\delta^{18}\text{O}$ values of deep-sea benthic fauna (Zachos et al., 2001), temporal patterns on the relative abundance of open habitats in SSA (Dunn et al., 2015; Palazzesi and Barreda, 2012), vegetation openness index in SSA (Dunn et al., 2015), and feedbacks among BM and hypsodonty in notoungulates.

To obtain a proxy on the broad paleobotanical changes in the SSA, we also use the Engauge Digitizer software (Mitchell et al., 2020) to digitalize the data of Palazzesi and Barreda (2012), which summarized the evolution of the wet-demanding (e.g., rainforest trees) and the arid-adapted (e.g., steppe elements) plants groups during the last 26 Ma in Patagonia, based on pollen records. We also compiled the data from Strömberg et al. (2013), which provides a high-resolution temporal succession of phytolith assemblages in Patagonia between 43 and 18 Ma. Even when the last works deals with different types of data (pollen vs. phytolith), we combined these two datasets to provide a broad approximation to the temporal patterns on the relative abundance of forest and open habitats in SSA. Besides, Dunn et al. (2015) developed the leaf area index (LAI) as a proxy for vegetation openness. We use the Engauge Digitizer software (Mitchell et al., 2020) to digitalize the data LAI values reported in SSA for a period restricted between 49 and 10 Ma (Dunn et al., 2015).

Correlations between our mean of BM (in natural log scale) and hypsodonty data through time and the proxies of the different factors mentioned above were implemented using generalized least squares (GLS) regressions with a first-order autoregressive model incorporated to avoid potential inflation of correlation coefficients created by temporal autocorrelation (Hunt et al., 2005; Mannion et al., 2015). To determinate the best combinations of explanatory variables explaining our data, stepwise regressions and the Akaike information criterion (AICc) were employed. The best model was the one with lower AICc values and few numbers of explanatory variables. We use the time-weighted mean of all the variables mentioned above for data points that fall within each time bin of 1 Myr (Table S9). As these explanatory variables are in distinct units, they were rescaled to have zero mean and unit variance before the analyses. GLS and model selection analyses were implemented in R (R Core Team, 2018) with the packages *nlme*, *MASS*, *rr2*, and *MuMIn* (Barton, 2020; Ives, 2019; Pinheiro et al., 2020; Ripley et al., 2020). The analyses were focused on a time-period restricted between 10 and 49 Ma because the factors investigated are well represented in this period, and were implemented first in Notoungulates and repeated at the suborder level.

2.8. Spatial patterns of body size and hypsodonty in notoungulates

The significant role of volcanic particles in drives the evolution of high tooth crowns in notoungulates has been previously suggested (Madden, 2014; Strömberg et al., 2013). Therefore, we expect a prevalence of hypsodonty taxa toward the western's longitudes associated

with the Andean volcanic belt, as this is the only portion of the continent with an active tectonic margin in SA during the Cenozoic. On the other hand, it is also plausible to expect a positive relationship between body size and latitude (i.e., Bergman Rule) as this pattern appears to be general for mammals, even when it has not been extensively studied in extinct taxa. For these reasons, we test for possible correlation between the BM, hypsodonty, and geography (e.g., latitude, longitude as predictive variables) using ordinary least squares (OLS) regressions and evaluating the relationship significance using the *p* values for the slope coefficient. Data from paleogeographic coordinates were mostly retrieved from the PBDB. For fossil occurrence not included in PBDB, modern latitude and longitude of fossil collection were introduced in the GPlates portal (Müller et al., 2018) to estimate their ancient latitude and longitude (paleocoordinates) considering the mean lifespan age of each taxon. Recent work has claimed that paleoclimatic information obtained from a particular location might require accurate knowledge of its paleolatitude defined relative to the Earth's spin-axis (de Groot et al., 2015). As ancient latitude is essential for the hypotheses here tested, we additionally estimated a second proxy for the paleolatitude (namely paleolatitude 2) relative to the Earth's spin-axis of each taxa considering the centroid of their current geographic coordinates of fossil collection and the mean of their lifespan, using the webpage <http://www.paleolatitude.org/> version 2.1 (de Groot et al., 2015). For taxa with more than a single fossil occurrence, the centroid of their reported geographic distribution was estimated and used for the analyses. The OLS analyses were performed in R (R Core Team, 2018) and were implemented first with all the SSA notoungulates and repeated at the suborder level (only including SSA taxa).

2.9. Abbreviations

SALMA, South American Land Mammals Age; Myr, millions of years (as time interval); Ma, millions of years ago; SA, South America; BM, body mass; HI; hypsodonty index; LMRL, lower molar series length; SLML, second lower molar length; SUML, second upper molar length.

3. Results

3.1. Body mass in notoungulates

Table S5 (Supplementary File) summarized the results of the log-

transformed bivariate ordinary least-squares regressions performed on LMRL, SLML, and SUML and BM of extant ungulates with a body mass lower than 79 kg. The resulting equations had, in general, low error values (i.e., low %PE, %SEE, and MAE), which indicate an adequate power for predictive accuracy. The LMRL variable had low errors, and consequently, it is likely the best predictor of the BM in extinct taxa. However, the additional predictors (SLML and SUML) also displayed relatively low errors (Table S5) and can even predict the BM in extinct taxa. Based on these equations, we estimated the body mass of notoungulates. The full set of body mass estimations is available in the Supplementary File (Table S6), but a summary is presented in Table 1 and Fig. 1a, b. As previously mentioned, craniodental body mass estimates appear to be inaccurate for large notoungulates (e.g., Toxodontia) because of their relatively large head and/or longer limbs compared with extant ungulates (Croft et al., 2020). For this reason, body mass estimations of Toxodontia were based on the lower value of 95% prediction intervals for each of the variables.

Most of the earliest notoungulates were relatively small (BM between 1 and 10 kg) animals (Fig. 1a), but their body masses increased rapidly with time, especially in Toxodontia, during the Casamayoran SALMA. In this time, the first medium (BM between 10 and 100 kg) and large (BM between 100 and 320) sized taxa (Fig. 1a) evolved for the first time. The two main clades within Notoungulata, Typotheria, and Toxodontia achieve different body masses during the Casamayoran (Fig. 1a, b), with the former being smaller than the latter. Toxodonts attain huge sizes, especially since the Miocene and at least three taxa probably achieve more than 1000 kg in weight during the last 10 Myr (late Miocene to late Pleistocene). In contrast, larger-sized typotherians were present during the Oligocene (Desedeian) and especially in the late Miocene (Chapadmalalan, Montehermosan, and Huayquerian SALMAs) (Fig. 1a).

The basal notoungulates, mainly included in the Henricosborniidae and Notostylopidae families, diverge each other in body mass. Henricosborniidae, represented by 13 taxa, has a mean body mass of ~13 kg (ranging from 1 to 109 kg) and a high body mass disparity (SD = 29). However, henricosborniids were predominantly (76%) small-sized animals (BM: 1–10 kg). On the other hand, notostylopidae, represented by 11 taxa, were mainly (63%) medium-sized taxa (BM: 10–100 kg) with a mean body mass of ~16 kg and a much lower body mass disparity than henricosborniids (SD = 12; Table 1).

The body mass of typotherians could range between 0.36 and 155 kg (mean BM = 15 kg), with *Punapithecus minor* and *Typotheriopsis internum*

Table 1

Summary of BM and HI values estimated for each of the clades analyzed (families and suborder as a whole). The largest and smaller taxon in each clade is also provided. Abbreviations: n, number of species in each clade; Min, minimum; Max, maximum; SD, standard deviation of the trait. Note that SD is considered a measure of morphological disparity.

Clade	# spp.	Body mass (kg)				Hypsodonty				Largest taxa	Smaller taxa
		Mean	Min	Max	SD	Mean	Min	Max	SD		
Basal notoungulate	26	14	1.15	109.8	22.6	0	0	0	0	<i>Acamana ambiguus</i>	<i>Peripantostylops minutus</i>
Henricosborniidae	13	13.3	1.15	109.8	29.6	0	0	0	0	<i>Acamana ambiguus</i>	<i>Peripantostylops minutus</i>
Notostylopidae	11	15.9	1.67	43.6	12.2	0	0	0	0	<i>Edvardotrouessartia sola</i>	<i>Homalostylops atavus</i>
Other basal notoungulates	2	2.3	2.33	2.3	-	0	0	0	0	-	-
Toxodontia	111	216.8	2.65	1464.1	281.9	1.45	0	3	1.26	<i>Piaulhytherium capivarae</i>	<i>Pampahippus secundus</i>
Homalodtheriidae	5	300.7	135.43	476	137.7	0.80	0	2	1.10	<i>Chasicotherium rothi</i>	<i>Trigonolophodon elegans</i>
Isotemnidae	19	82.1	6.72	468.7	109.5	0	0	0	0	<i>Periphragus circumflexus</i>	<i>Isotennus ctalego</i>
Leontiniidae	18	216.9	52.55	565.4	150.3	0.67	0	1	0.49	<i>Leontinia gaudryi</i>	<i>Termasterium flacoensis</i>
Notohippidae	29	34.1	2.65	80	25.3	1.14	0	2	0.95	<i>Rhynchippus equinus</i>	<i>Pampahippus secundus</i>
Toxodontidae	40	402.9	15.1	1464.1	369.2	2.80	0	3	0.56	<i>Piaulhytherium capivarae</i>	<i>Hypsitherium bolivianum</i>
Typotheria	123	15	0.36	155.2	27.9	1.69	0	3	1.06	<i>Typotheriopsis internum</i>	<i>Punapithecus minor</i>
Archaeohyracidae	14	10.4	1.7	23.8	6.8	1.93	0	3	0.62	<i>Archaeotypotherium propheticus</i>	<i>Protarchaeohyrax minor</i>
Archaeopithecidae	2	1.7	1.35	2.1	0.5	0	0	0	0	<i>Archaeopithecus rogeri</i>	<i>Teratopithecus elpidophorus</i>
Hegetheriidae	25	5.5	0.92	27.9	5.6	2.64	2	3	0.49	<i>Hemihegetotherium achataleptum</i>	<i>Tremacyllus impressus</i>
Intertheriidae	41	4.1	0.36	11.5	3.3	1.78	0	3	0.97	<i>Prototypotherium australe</i>	<i>Punapithecus minor</i>
Mesotheriidae	21	60.1	12.96	155.2	45.2	2.00	2	2	0	<i>Typotheriopsis internum</i>	<i>Rusconitherium mendocense</i>
Oldfieldthomasiidae	13	5.1	1.06	8.3	2.5	0.00	0	0	0	<i>Oldfieldthomasia anfractuosa</i>	<i>Itaboratherium atavum</i>
Basal Typotheria	7	7.9	1.67	27.4	9.7	0	0	0	0	<i>Acoelohyrax complicatissimus</i>	<i>Campanorco inauguralis</i>
All notoungulates	260	101.4	0.36	1464.1	210.6	1.42	0	3	1.20	<i>Piaulhytherium capivarae</i>	<i>Punapithecus minor</i>

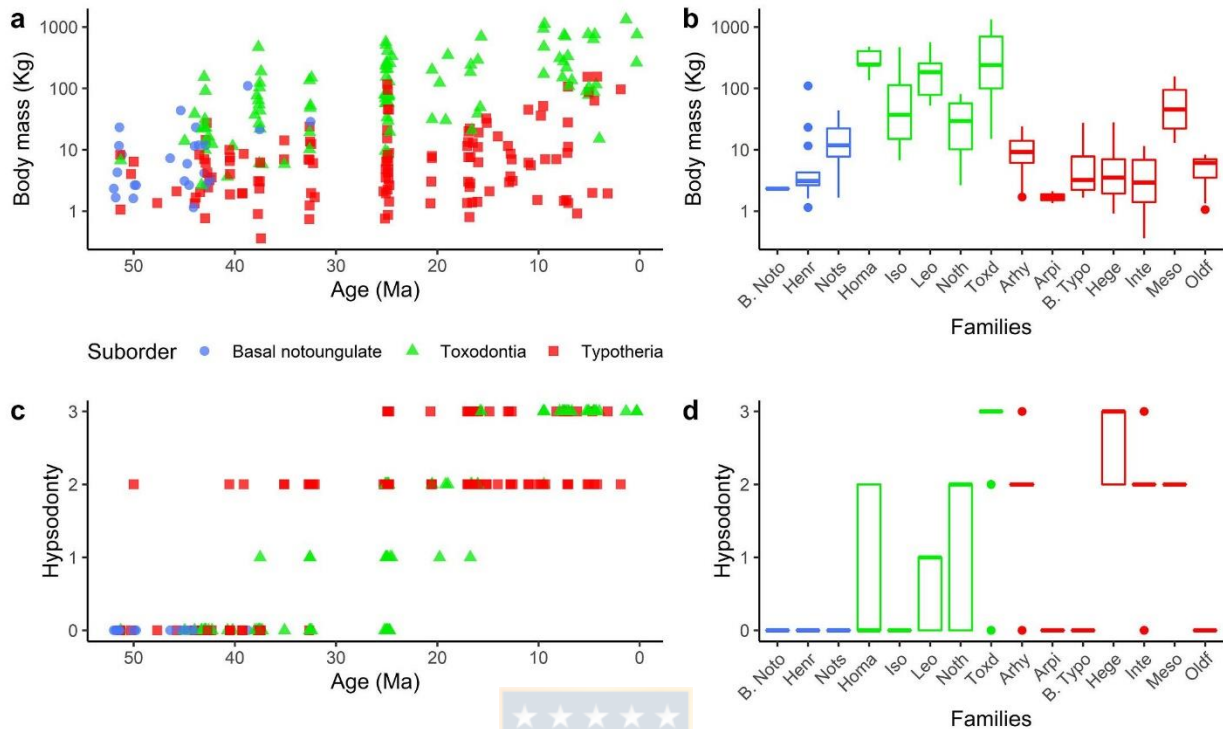


Fig. 1. Body mass and hypsodonty in Notoungulates. a, Notoungulate BM (in kg) through time (in log10 scale); b, Box plot showing median (dark line), ranges (box range), and outliers (points) of BM for major notoungulate families; c, Notoungulate hypsodonty through time; d, Box plot showing median (dark line), ranges (box range), and outliers (points) of hypsodonty for major notoungulate families. Colors in b and d represent suborders as in a and c. Abbreviations: Arhy, Archaeohyracidae; Arpi, Archaeopithecidae; B. Noto: basal notoungulate; B. Typo, basal typotherians; Hege, Hegetotheriidae; Henr, Henricosborniidae; Homa, Homalodtheriidae; Inte, Interatheriidae; Iso, Isotemnidae; Leo, Leontiniidae; Meso, Mesotheriidae; Noth, Notohippidae; Nots, Notostylopidae; Oldf, Oldfieldthomasiidae; Toxd, Toxodontidae.

representing the smaller and largest taxon, respectively (Table 1). Regarding the frequency distribution of the body mass, it is clear that most (64%) typotherians were of small size (BM between 1 and 10 kg) and in a lower proportion medium (BM between 10 and 100 kg; 26%), very small (BM < 1 kg; 7%) or large (BM between 100 and 320 kg; 3%) sized taxa (Fig. 2a). Most of the families within typotherians (Interatheriidae, Hegetotheriidae, Oldfieldthomasiidae, basal typotherians, Archaeopithecidae) are mainly composed of small taxa, displaying body masses with a mean around 5 kg (Table 1). However, members of “Archaeohyracidae” and especially mesotheriids are in the upper range of the typotherians size (Fig. 1b; Table 1). The only typotherians with estimated body masses over 100 kg (= large taxa) are from the Mesotheriidae family. Except for mesotheriids, the BM disparity of most of the families within typotherians appears to be relatively low (SD between 0.5 and 10) (Table 1).

On the other hand, members of Toxodontia had a body mass ranging between 2.6 and 1464 kg (mean BM = 217 kg), with *Pampahippus secundus* and *Piauhitherium capivarae* representing the smaller and largest taxon, respectively. Regarding the frequency distribution of the body mass, it is clear that most toxodonts were of medium size (BM between 10 and 100 kg; 42%), but with a high proportion of large (BM between 100 and 320 kg; 27%) to very large (BM between 320 and 1000 kg; 20%) sizes (Fig. 2b). In contrast, only a few members of Toxodontia were of small or giant size (8 and 3%, respectively) (Fig. 2b). Notohippidae, represented by 29 spp., is the family with the lower mean BM (34 kg) as well BM disparity of the suborder, and groups predominantly (75%) medium-sized animals reaching up to 80 kg (Table 1; Fig. 1b). Isotemnidae, represented by 19 spp., exhibits a wide BM disparity (SD

= 110) and includes predominantly (57%) medium-sized taxa (yet small to very large taxa were noted), with a mean BM of 82 kg. Homalodtheriidae is a family with five large to very large representatives (mean BM of 300 kg), showing a large BM disparity (SD = 138) and reaching sizes up to 476 kg. Leontiniidae, represented by 18 spp., exhibits a wide BM disparity (SD = 150), as includes predominantly (50%) large-sized taxa (yet small to very large taxa were noted), with a mean BM of 217 kg, and up to 565 kg. Toxodontidae is the family with the high species richness (40 spp.) and exhibits the larger body mass disparity (SD = 369) within notoungulates (i.e., the largest toxodontid has a BM one hundred times than those of the smaller one). They were predominantly very large (38%) and large (30%) animals (mean BM of 403 kg; reaching up to 1460 kg), and includes the largest known notoungulates, as *Piauhitherium capivarae* or *Toxodon platensis* (Table 1; Fig. 1a,b). In fact, over time, the family Toxodontidae has ranged over three orders of magnitude in size.

3.2. Hypsodonty in notoungulates

The full set of HI values recovered from the literature (at face value) or even inferred based on hypsodonty degree categories (e.g., brachydont, mesodont, and hypsodont) from each notoungulate is available in the Supplementary File (Table S6). However, a summary of this information is presented in Table 1 and Fig. 1c, d. Taken together, our results illustrate the temporal (Fig. 1c) and within-clade (Fig. 1d) hypsodonty variations in notoungulates. The notoungulate families and suborders show unique hypsodonty patterns. However, there is a general trend of increased hypsodonty with time in Typotheria, and Toxodontia. Besides, all the basal notoungulates have low crown heights (HI < 1;

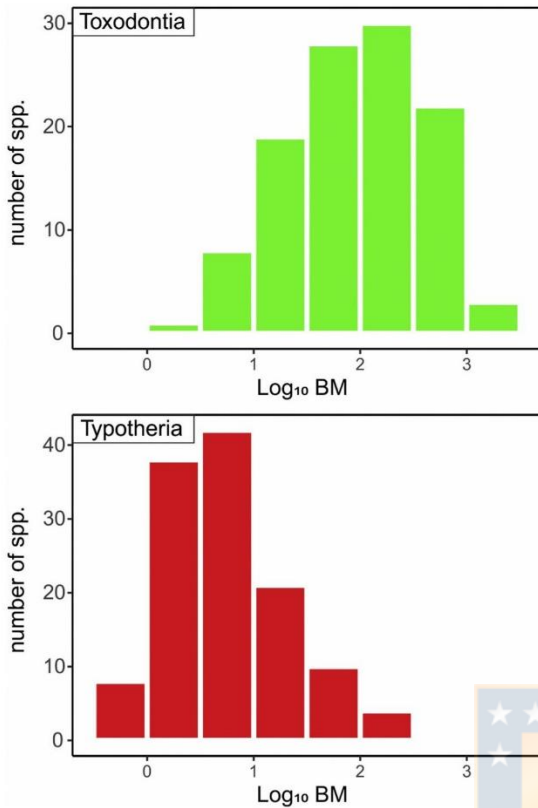


Fig. 2. Distribution of frequency of the Log_{10} of the body mass of toxodonts and typotherians. Note the predominance of relatively small to medium-sized typotherians and medium to very large-sized toxodonts (see further details in Fig. 1).

brachydont).

3.3. Lifespan of individual species

The maximum likelihood test results indicate that our data best supported the Time-variable Poisson process (TPP). The TPP model of preservation assumes that preservation rates are constant within a predefined time frame but can vary across time frames (e.g., geological epochs). The PyRate results are summarized in the Supplementary File (Table S6). The older species of notoungulate described (so far) appears to date from the early Eocene (~ 55 Ma), and the younger species go extinct at the end of the Pleistocene (or even the early Holocene). The mean lifespan of notoungulates species is ~5.4 Myr.

3.4. Correlation between traits and speciation/extinction rates

Neither speciation nor extinction rates were significantly correlated with body mass in typotherians. In toxodonts, higher body mass appears to be correlated with low extinction rates (mean $\alpha_{\text{extinction}} = -0.41$; 95% HPD interval = -1.10 to 0.26) although the credible interval's upper bound falls slightly above zero. In another hand, higher crown teeth were significantly associated with very low extinction rates in typotherians (mean $\alpha_{\text{extinction}} = -0.47$; 95% HPD interval = -0.84 to -0.19) and toxodonts (mean $\alpha_{\text{extinction}} = -0.290$; 95% HPD interval = -0.69 to -0.09). Finally, either of the suborders showed a significant correlation between the traits examined (body mass and hypsodonty) and preservation rate.

3.5. Describing the body size and hypsodonty macroevolutionary patterns in notoungulates

3.5.1. Body mass

The results of the mode of body mass evolution across notoungulates and lower taxonomic hierarchies are in the Supplementary File (Table S7), but a summary is presented in Table 2.

When all notoungulates were analyzed, the directional evolution (GRW) outperforms other simple models and pass the adequacy tests (Table 2). This directionality is positive ($\mu_{\text{step}} = 0.054$; $\sigma^2_{\text{step}} = 0.020$), suggesting a relatively constant increase of BM in notoungulates through

Table 2

Summary of the best mode of trait (BM and hypsodonty) evolution in notoungulates and lower taxonomic hierarchies. The complete results of the model comparisons are in the Supplementary File. Together with the best model of evolution in each analyzed trait, we provide the age(s) of the change(s) in the complex models' evolutionary regimen. Abbreviations: BM, body mass; Hyp, hypsodonty; Punc-*i*, punctuational mode of evolution with *i* changes; GRW, directional evolution; URW, random walk, μ_i , mean of the *i* period; σ^2_{step} , variance of slope (for GRW models); μ_{step} , slope (for GRW models). In cases in which any of the simple evolutionary modes (e.g., GRW) were not the best model based on the AICc, but pass the adequacy test, they were also reported and denoted in parenthesis.

Clade	Time bins	The best model of trait evolution (PaleoTs)			
		BM _{Best} model	BM _{Parameters} best model	Hyp _{Best} model	Hyp _{Parameters} best model
Notoungulata	51	Punc-4: 40, 30, 19, 11 Ma (GRW)	$\mu_1 = 1.95$, $\mu_2 = 2.38$, $\mu_3 = 3.36$, $\mu_4 = 2.84$, $\mu_5 = 3.92$ ($\mu_{\text{step}} = 0.054$; $\sigma^2_{\text{step}} = 0.020$)	Punc-5: 25, 16, 9 Ma (GRW)	$\mu_1 = 0.05$, $\mu_2 = 0.18$, $\mu_3 = 1.37$, $\mu_4 = 1.65$, $\mu_5 = 2.32$, $\mu_6 = 2.76$ ($\mu_{\text{step}} = 0.055$; $\sigma^2_{\text{step}} = 0.008$)
Typotheria	54	GRW	$\mu_{\text{step}} = 0.020$; $\sigma^2_{\text{step}} = 0$	Punc-4: 37, 31, 25, 16 Ma (GRW)	$\mu_1 = 0.13$, $\mu_2 = 0.36$, $\mu_3 = 1.92$, $\mu_4 = 2.18$, $\mu_5 = 2.47$ ($\mu_{\text{step}} = 0.05$; $\sigma^2_{\text{step}} = 0.01$)
Archaeohyracidae	23	Punc-1: 30 Ma	$\mu_1 = 2.03$, $\mu_2 = 2.89$	GRW	$\mu_{\text{step}} = 0.05$, $\sigma^2_{\text{step}} = 0$
Hegetotheriidae	27	Punc-1: 6 Ma	$\mu_1 = 1.42$, $\mu_2 = 0.60$	Punc-1: 19 Ma	$\mu_1 = 2.13$, $\mu_2 = 3$
Intertheriidae	37	GRW	$\mu_{\text{step}} = 0.037$; $\sigma^2_{\text{step}} = 0$	URW-30 Ma (GRW)	$\sigma^2_{\text{step}} = 0.11$, $\mu = 2.29$ ($\mu_{\text{step}} = 0.06$, $\sigma^2_{\text{step}} = 0.04$)
Mesotheriidae	27	Punc-2: 20, 13 Ma	$\mu_1 = 4.27$, $\mu_2 = 2.99$, $\mu_3 = 4.26$	-	-
Toxodontia	49	Punc-4: 40, 30, 14, 8 Ma (GRW)	$\mu_1 = 2.99$, $\mu_2 = 3.51$, $\mu_3 = 4.62$, $\mu_4 = 5.79$, $\mu_5 = 5.04$ ($\mu_{\text{step}} = 0.062$; $\sigma^2_{\text{step}} = 0.016$)	Punc-3: 30, 20, 10 Ma (GRW)	$\mu_1 = 0.06$, $\mu_2 = 1.22$, $\mu_3 = 2.31$, $\mu_4 = 2.98$ ($\mu_{\text{step}} = 0.07$; $\sigma^2_{\text{step}} = 0.01$)
Notohippidae	31	Punc-1: 31 Ma	$\mu_1 = 2.41$, $\mu_2 = 3.76$	Punc-1: 30 Ma	$\mu_1 = 0.16$, $\mu_2 = 1.85$
Toxodontidae	29	GRW-10 Ma	$\mu_{\text{step}} = 0.12$, $\sigma^2_{\text{step}} = 0$; $\mu_1 = 5.45$	Punc-2: 20, 13 Ma (GRW)	$\mu_1 = 1.18$, $\mu_2 = 2.47$, $\mu_3 = 3$ ($\mu_{\text{step}} = 0.08$, $\sigma^2_{\text{step}} = 0.01$)

time. However, even when directional evolution might describe the data well, the more complex model with four punctuations (Punc-4) has a much better fit ($dAICc = 13.21$; Table 2 and S7). The last model indicates several periods exhibiting stasis around one mean, which instantaneously shifts to stasis around a different mean. Notably, our data favored a scenario with four punctuations occurred in 40 (end of the Casamayoran), 30 (beginning of Deseadan SALMA), 19 (beginning of Santacrucian SALMA), and 11 Ma (Mayoan SALMA), which delimited five time periods (55–40 Ma, 40–30 Ma, 30–19 Ma, 19–11 Ma and 11–0.001 Ma) with dissimilar means BM values ($\mu_1 = 1.95$, $\mu_2 = 2.38$, $\mu_3 = 3.36$, $\mu_4 = 2.84$ and $\mu_5 = 3.92$, respectively in Log space; Fig. 3). Interestingly, the Punc-4 model indicates that during the early to late Miocene (19–11 Ma), the mean body mass of notoungulates decreases ($\mu_4 = 2.84$) compared with the immediately early interval ($\mu_3 = 3.36$). The early to middle Eocene and late Miocene to late Pleistocene time intervals show the lowest ($\mu_1 = 1.95$) and the highest ($\mu_5 = 3.92$) mean BM values, respectively. The last results must indicate a general trend of the BM increase in notoungulates with time, yet this increase is not monotonic and was given in four main punctuations (Fig. 3). On the other hand, the evolutionary mode analyses at distinct taxonomic hierarchies (suborders and family levels) are summarized in Table 2 (see details in the Supplementary File S7) and illustrated in Figs. 3 and 4. These results reveal distinct ways of body mass evolution among the notoungulates clades (Table 2).

The better-supported model of the body-size evolution of typotherians is the directional evolution (GRW), with a positive ($\mu_{step} = 0.020$; $\sigma_{step}^2 = 0$) trend suggesting a relatively constant increase through time (Table 2). The slope of the BM increase in typotherians is 2.7 times

lower than those exhibited by all notoungulates. However, none of the simple models (included the GRW) pass the adequacy tests (Table S7). Within Typotheria the only families with enough data to implement the evolutionary models above described were Interatheriidae, Hegetotheriidae, Mesotheriidae, and Archaeohyracidae (Fig. 3; Table 2). The BM evolution of interatheriids fits better with a directional evolution (GRW), with a BM increase with time ($\mu_{step} = 0.037$; $\sigma_{step}^2 = 0$). The better-fitted model for the hegetotheriids BM evolution is one with a single punctuation that occurred at the end of the Miocene (~ 6 Ma) and delimited two broad periods (30–6 Ma, 6–0.001 Ma) with distinct mean BM values ($\mu_1 = 1.42$, $\mu_2 = 0.60$, respectively; in Log space). The last indicated that the mean BM of hegetotheriids was somewhat similar among the earliest forms and during a large portion of their evolutionary history (30–5 Ma) but much lower in younger (5–0.001 Ma) representatives. The best model describing the BM evolution of archaeohyracids is one with single punctuation, which occurred at 30 Ma, delineating two broad periods (43–30 Ma, 29–30 Ma) with dissimilar mean BM values ($\mu_1 = 2.03$, $\mu_2 = 2.89$, respectively; in Log space). The best model of mesotheriids BM evolution is those with two punctuations that occurred at the end Colhuehuapian (20 Ma) and the Laventan SALMAS (13 Ma), which delimited three broad periods (29–20 Ma, 20–13 Ma, and 13–2 Ma) with dissimilar means BM values ($\mu_1 = 4.27$, $\mu_2 = 2.99$, $\mu_3 = 4.26$, respectively; in Log space). Mesotheriids show a significant decrease of the mean BM during the early to middle Miocene (Fig. 3), with a progressive BM increase in younger taxa.

The better-supported model of body-size evolution of toxodonts is a complex one with four punctuations (Punc-4), occurred during at 40, 30, 14, and 8 Ma, delimiting five periods (50–40, 40–30, 30–14, 14–8 and

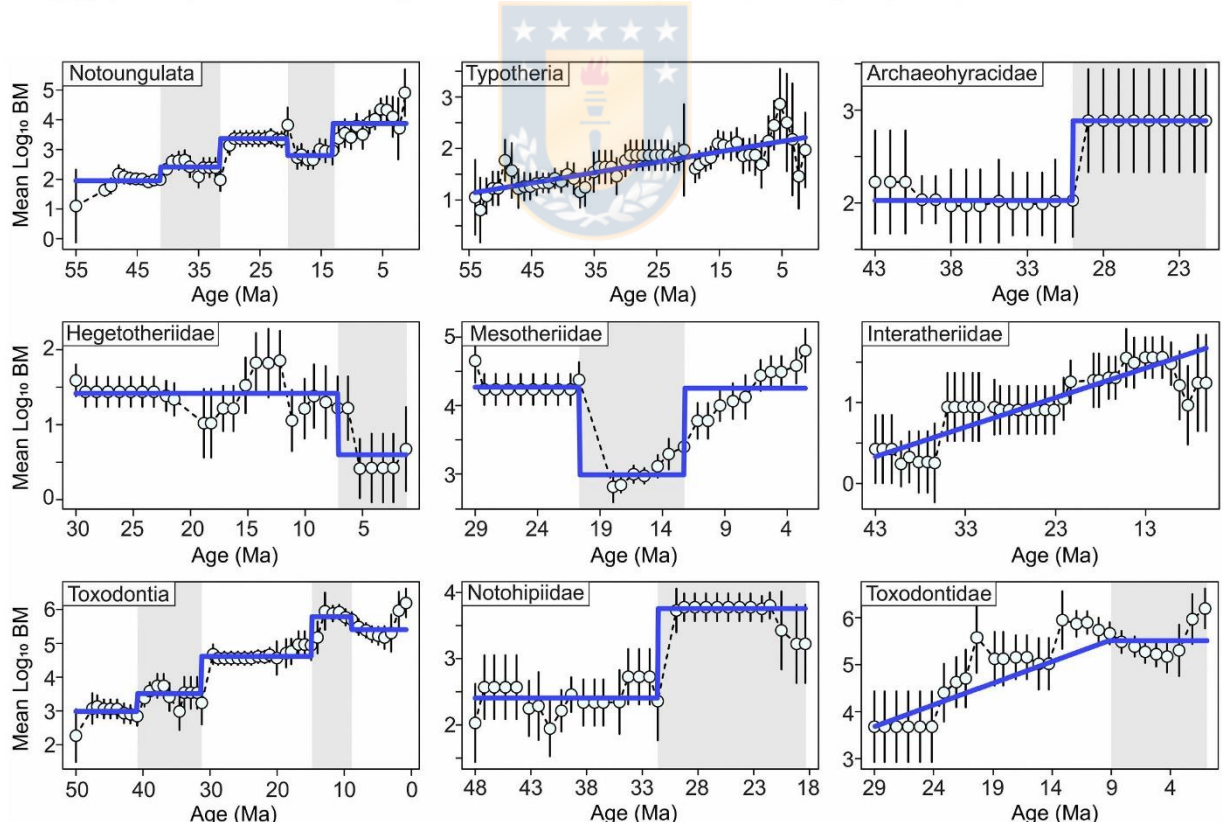


Fig. 3. Temporal patterns of body size evolution in notoungulates and subordinate clades. The blue line denotes the best model parameters based on the trait evolution results performed with the *PaleoTs* package. The circles represent the mean value in each time bin (1 Myr), and their associated vertical lines denote the variance around the mean. Time is in Ma. Note the predominance of punctuated changes in most clades. (For interpretation of the references to colour in this figure legend, the reader is referred to the web version of this article.)

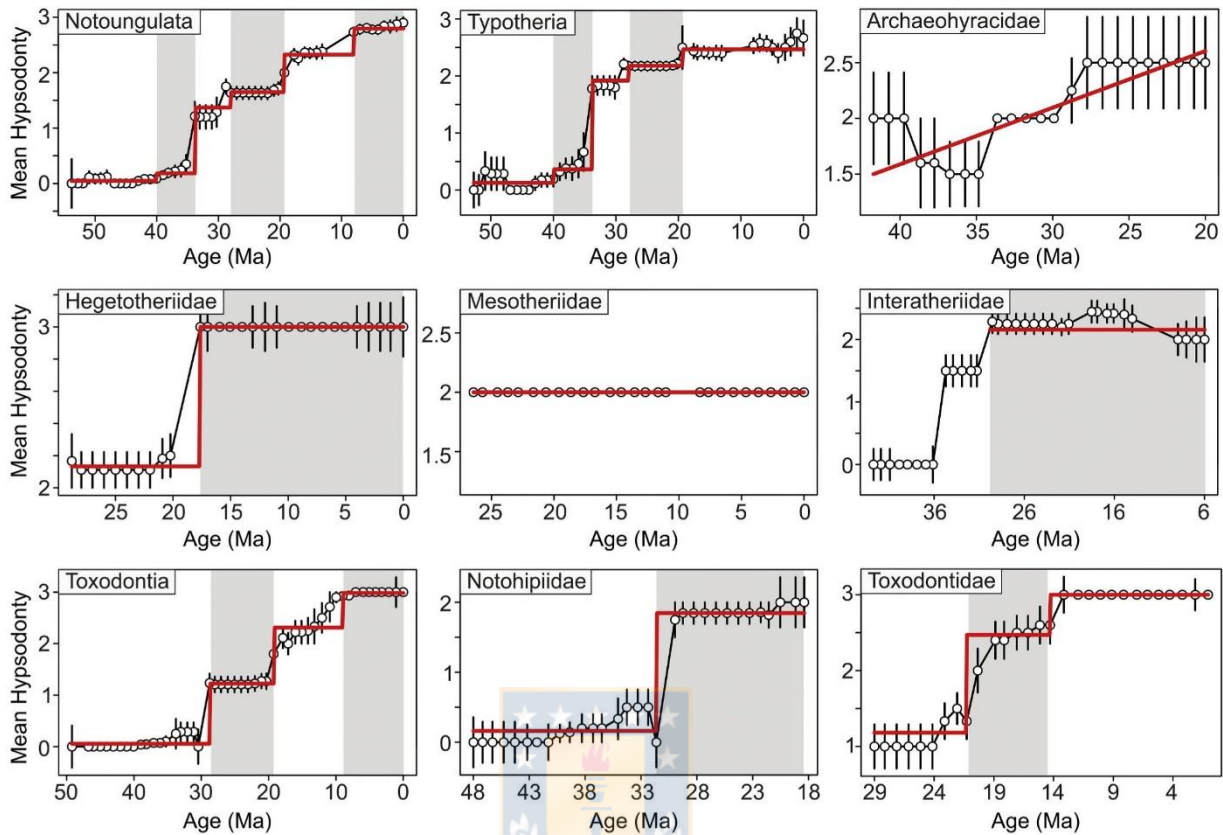


Fig. 4. Temporal patterns of hypsodonty evolution in notoungulates and subordinate clades. The red line denotes the best model parameters based on the trait evolution results performed with the *PaleoTS* package. The circles represent the mean value in each time bin (1 Myr), and their associated vertical lines denote the variance around the mean. Time is in Ma. Note the predominance of punctuated changes in most clades. (For interpretation of the references to colour in this figure legend, the reader is referred to the web version of this article.)

8–0.001 Ma) of relative stasis with different means ($\mu_1 = 2.99$, $\mu_2 = 3.51$, $\mu_3 = 4.62$, $\mu_4 = 5.79$, $\mu_5 = 5.04$, respectively; in Log space). However, as occurs when all notoungulates were analyzed, the directional evolution (GRW) ($\mu_{\text{step}} = 0.062$; $\sigma_{\text{step}}^2 = 0.016$) outperforms other simple models and is the only one passing the adequacy tests (Table S7). Therefore, it is evident a general trend of toxodont BM increases with time, but this increase occurs in four pulses. Within Toxodontia the families with enough data to implement the evolutionary models (above described) were Notohippiidae, and Toxodontidae (Table 2). For toxodontids, the best fit model of BM evolution is one complex with an early phase (29–10 Ma) of sustained positive directional evolution (GRW; $\mu_{\text{step}} = 0.12$; $\sigma_{\text{step}}^2 = 0$), followed by a period (10–0.001 Ma) of relative stasis ($\mu = 5.45$, in Log space). The best BM evolution model for notohippids is one with a single punctuation at 31 Ma, which separates two relative BM stasis periods. The first period (48–31 Ma) with somewhat lower BM values ($\mu_1 = 2.41$, in Log space) and a second one (31–17 Ma) with much larger values ($\mu_2 = 3.76$, in Log space).

In typotherians, the minimum BM show a slightly yet non-significant increase with time (slope = -0.011 ; $p > 0.05$), while the mean and maximum BM significantly increase with time (slope = -0.01839 ; $p < 0.01$ and slope = -0.039 ; $p < 0.01$, respectively). In toxodonts, the minimum, maximum, and mean BM increase significantly with time (slopes varying between -0.061 to -0.0707 ; $p < 0.01$). Note that a negative slope implies an increase of body size toward the recent.

3.5.2. Hypsodonty

The results of the mode of hypsodonty evolution across notoungulates and lower taxonomic hierarchies are in the Supplementary File (Table S8), but a summary is presented in Table 2 and Fig. 4. The directional evolution (GRW) outperforms other simple models and passes the adequacy tests when all notoungulates were analyzed (Table 2). This directionality is positive ($\mu_{\text{step}} = 0.06$; $\sigma_{\text{step}}^2 = 0.01$), suggesting a relatively constant hypsodonty increase through time. However, even when directional evolution might describe well the data, a more complex model with five punctuations (Punc-5) has a much better fit (dAICc = 6.53; Table S8), indicating the existence of six periods exhibiting stasis around one mean which instantaneously shifts to stasis around a different mean. Remarkably, our data favored a scenario with five punctuations occurred in 37, 31, 25, 16 and 9 Ma, which delimited five time periods (55–37, 37–31, 31–25, 25–16, 16–9 and 9–0.001 Ma) with dissimilar means hypsodonty values ($\mu_1 = 0.05$, $\mu_2 = 0.18$, $\mu_3 = 1.37$, $\mu_4 = 1.65$, $\mu_5 = 2.32$, and $\mu_6 = 2.76$, respectively; Fig. 4). Therefore, our results must indicate a general trend of the hypsodonty increase in notoungulates with time, with monotonic increases given in five main punctuations (Fig. 4). The most significant increase in hypsodonty appears to occur at 31 Ma, during the Tinguirirican SALMA, when hypsodont taxa are dominant within the Order for the first time. The hypsodonty analyses at distinct taxonomic hierarchies (suborders and family levels) were summarized in Table 2, revealing different ways of hypsodonty evolution among the clades within notoungulates (Fig. 4).

The best model describing the hypsodonty evolution of typotherians

is one of four punctuations (Punc-4, at 37, 31, 25 and 16 Ma), denoting five-time periods with dissimilar means hypsodonty values ($\mu_1 = 0.13$, $\mu_2 = 0.36$, $\mu_3 = 1.92$, $\mu_4 = 2.18$ and $\mu_5 = 2.47$, respectively; Fig. 4). However, the GRW ($\mu_{step} = 0.05$; $\sigma^2_{step} = 0.01$) also appears to be an adequate model to explain our data. For archaohyracids, the directional evolution (GRW; $\mu_{step} = 0.05$, $\sigma^2_{step} = 0$) is the best model for the hypsodonty evolution. However, this model fails the adequacy test. A single punctuation model (Punc-1) better explains the evolutionary mode of hegetotheriids. The punctuation occurred at 19 Ma (Early Miocene), and separate two time periods (30–19 and 19–0.001 Ma) of relatively modest hypsodonty change ($\mu_1 = 2.13$, $\mu_2 = 3$). Nevertheless, the GRW ($\mu_{step} = 0.03$, $\sigma^2_{step} = 0.01$) also appears to be an adequate model explaining the hegetotheriid data. For interatheriids, the better fitter model of hypsodonty evolution is a complex one (URW-Stasis) with an initial phase of random walk ($\sigma^2_{step} = 0.11$), which changes at 30 Ma to a stasis model ($\mu = 2.29$). Nevertheless, the GRW ($\mu_{step} = 0.06$, $\sigma^2_{step} = 0.04$) also appears to be an adequate model. Finally, the hypsodonty in mesotheriids did not vary significantly with time (Fig. 4).

The best model describing the hypsodonty evolution of toxodonts is one of three punctuations (Punc-3), occurred at 30, 20, and 10 Ma, and indicating the presence of four-time intervals (50–30, 30–20, 20–12, and 10–0.01 Ma) with relative stasis around a mean hypsodonty value ($\mu_1 = 0.06$, $\mu_2 = 1.22$, $\mu_3 = 2.31$, and $\mu_4 = 2.98$, respectively). Nonetheless, the GRW ($\mu_{step} = 0.01$; $\sigma^2_{step} = 0.01$) also appears to be an adequate model to explain the toxodont data (Table 2). The hypsodonty evolution of notohippids fit better to a single punctuation model at 30 Ma, indicating the presence of two-time intervals (48–30, and 30–17 Ma) of relative stasis around means of $\mu_1 = 0.16$ (predominantly brachyodont), and $\mu_2 = 1.85$ (predominantly hypsodont), respectively. For toxodontids, the better model of BM evolution is one complex two punctuations occurred at 20 and 13 Ma, indicating the presence of three-time intervals (29–20, 20–13, and 13–0.01 Ma) of relative stasis around means of $\mu_1 = 1.18$, $\mu_2 = 2.47$, and $\mu_3 = 3$, respectively (Fig. 4). While the GRW ($\mu_{step} = 0.08$, $\sigma^2_{step} = 0.01$) could be also an adequate model for explain the data. Finally, the minimum, maximum, and mean hypsodonty increase significantly ($p < 0.01$) with time in both typotherians and toxodonts.

3.6. Potential mechanisms driving the historical dynamics of body size and hypsodonty in SSA

The GLS model fitting results show that when all notoungulates were considered, their mean body mass is positive and significantly correlated with the availability of open habitats, while none of the studied factors tracks, in a significant way, their mean hypsodonty patterns (Table 3). In typotherians, the best GLS model indicates that the mean body mass tracks the self-clade hypsodonty (and vice versa), with positive and significant relationship between both variables, and explaining a large portion of the data variance ($R^2_{BM} = 0.78$; $R^2_{Hyp} = 0.96$; Table 3). For

toxodonts, the best GLS model reveals that a combination of global mean temperature and self-clade hypsodonty are the best predictor for the mean body mass evolution ($R^2_{Hyp} = 0.92$). Both factors had positive and significant effects on the response trait. Finally, the self-clade body mass is the single best predictor on the mean hypsodonty in toxodonts ($R^2_{Hyp} = 0.96$), having positive effects (Table 3). Therefore, the coupled evolution of the body mass and hypsodonty in typotherians and toxodonts (Table 3) is well supported.

3.7. Body size and hypsodonty in through space and time

The OLS analyses performed between the body mass, hypsodonty, and ancient latitude and longitude, with all SSA notoungulates, suggest that (Table 4): 1) the body mass significantly increase with latitude, but only when the “paleolatitude 2” proxy is employed ($p < 0.01$), and therefore it is not completely clear the generality of this trend; 2) the body mass shows a negative, yet non-significant ($p > 0.05$), relationships to longitude; 3) the hypsodonty significantly increase ($p < 0.01$) to western longitudes and lower latitudes.

4. Discussion

4.1. Body mass estimations in notoungulates

Previous work has claimed that craniodental and postcranial based body mass estimations appear to be inaccurate for large notoungulates because the use of these kinds of data might result in overestimations (Croft et al., 2020). The likely explanation is that notoungulates might have relatively large-heads, as well as short and stocky limbs, unlikely most extant ungulates (Croft et al., 2020). *Nesodon*, an early Miocene notoungulate, can help us to illustrate the claimed body mass overestimations. The body mass of this taxon has previously been estimated based on craniodental measurements and limb bone dimensions as ranging between 500 and 800 kg (Cassini et al., 2012; Elissamburu, 2012). However, these estimations contrast with those obtained on different proxies (e.g., head-body length) considered more reliable (Croft et al., 2020). Using the non-selenodont head-body length equation (Janis, 1990) and a head-body length estimate of 1.75 m (Scott, 1912), the body mass of this taxon was recently estimated as 247 kg (Croft et al., 2020), less than half that previously calculated. Based on available dental measurements of *Nesodon imbricatus* and the equations and methodology here developed, our body mass estimation on this taxon is 289 kg, in close agreement with those of Croft et al. (2020). Table 5 shows a sample of BM estimations of selected notoungulate taxa taken from the literature. Noteworthy, our BM estimations appear to be within the range of body mass values obtained by previous authors (Cassini et al., 2012; Elissamburu, 2012; Fernández-Monescillo et al., 2019; Gomes Rodrigues et al., 2017; Reguero et al., 2010). Even when our BM estimations appear to be reliable, given the above-described concerns regarding the potential dissimilarity between teeth and limb proportions of notoungulates relative to extant ungulates, we highlight it should be considered as provisional and consequently taken with some caution. The best way to circumvent the claimed problems in the notoungulate body mass estimation will be to use volumetric BM estimation methods based on whole articulated skeletons (Brassey, 2017).

Table 3
Summary of best-fitting GLS multiple regression models for predicting mean body mass (BM in natural log scale) and hypsodonty in notoungulates, typotherians, and toxodonts considering an autocorrelation structure for age parameter. R^2 is a measure of the variance explained by each model (Ives, 2019). Note that the GLS models were fitted with data from 49 to 10 Ma.

Clade	Response	Parameters	Slope	p-value	R^2
Notoungulates	Body mass	Open habitats	0.25	<0.01	0.73
	Hypsodonty	–	–	–	–
Typotheria	Body mass	Self-clade Hypsodonty	0.25	<0.01	0.78
	Hypsodonty	Self-clade body mass	0.63	<0.01	0.96
Toxodontia	Body mass	Global temperature	0.39	<0.01	0.92
		Self-clade Hypsodonty	0.81	<0.01	–
	Hypsodonty	Self-clade body mass	0.38	<0.01	0.96

Table 4
Results of the OLS analyses dealing with the spatial patterns of the body mass (BM in kg) and hypsodonty in the SSA notoungulates.

Response	Parameters	Slope	SE	p-value
BM	Paleolongitude	–1.31	2.21	>0.05
	Paleolatitude	2.25	1.17	>0.05
	Paleolatitude 2	3.08	1.08	<0.01
HI	Paleolongitude	–0.09	0.01	<0.01
	Paleolatitude	0.02	0.01	<0.01
	Paleolatitude 2	0.04	0.01	<0.01

Table 5

Comparisons among the body mass reported in the literature from a selected sampled of notoungulates, and those estimated by us in the present contribution. Data from: I^(Ellsamburni, 2012), II^(Cassini et al., 2012), III^(Reguero et al., 2010), IV^(Gomes Rodrigues et al., 2017), and others^{(Fernández-Monescillo et al., 2019)* and (Scarano et al., 2011)**}.

Taxa	BM (kg)					Present work
	I	II	III	IV	Others	
<i>Asmodeus osborni</i>	–	–	–	400.70	–	406.21
<i>Asmodeus</i>	1785.70	–	–	–	–	325
<i>Adinotherium ovinum</i>	–	100.30	–	61.40	33.75–119.45*	31.4
<i>Adinotherium</i>	119.45	113.27	–	–	–	31.4
<i>Rhynchippus equinus</i>	99.67	–	–	–	77.87–99.67*	80.02
<i>Rhynchippus punilus</i>	21.83	–	–	–	–	9
<i>Morphippus imbricatus</i>	97.80	–	–	31	–	57.2
<i>Nesodon imbricatus</i>	587.90	637.51	–	197	170.13–637.51*	289.42
<i>Interatherium robustum</i>	–	2.38	–	–	0.4–3.5*	1.42
<i>Interatherium</i>	3.33	–	–	–	–	1.64
<i>Protyotherium attenuatum</i>	–	3.80	–	–	2.59–3.1**	2.85
<i>Protyotherium australe</i>	–	7.30	2.82	–	2.81–7.73*; 3.79–7.39**	11.02
<i>Protyotherium praeutilum</i>	–	4.50	–	–	3.87–5.80**	7.58
<i>Protyotherium</i>	6.74	–	–	–	–	6.6
<i>Hegetotherium mirabile</i>	–	7.71	2.19	2.20	–	6.28
<i>Hegetotherium</i>	9.69	–	–	–	–	5.5
<i>Pachyrukhos moyani</i>	–	2.13	0.46	–	–	1.38
<i>Pachyrukhos</i>	1.77	–	–	–	–	1.36
<i>Trachytherus speggazzinianus</i>	–	–	40.75	29.50	136–408*	116.61
<i>Trachytherus alloxus</i>	–	–	–	21.70	18.56–120.45*	94.62
<i>Trachytherus</i>	408	–	–	–	–	–
<i>Plesiomyotherium achirensis</i>	–	–	20.359	–	5.40–138*	35.91

Of course, the application of such methods to the notoungulate fossil record could be limited by the paucity of well-preserved specimens.

4.2. The evolution of the body size in notoungulates

Our results illustrate that notoungulates had a large body size disparity because they include very small taxa of a rodent size (hundreds of grams) to large creatures of a rhino size (achieving nearly up to 1.5 tons; Table 1; Fig. 1). It is also possible to state that since a small-sized ancestor, notoungulates increased their body mass through time, ranging over 3.5 orders of magnitude in size (Table 1; Fig. 1a). Nevertheless, when analyzed at lower taxonomic levels, each clade's body mass is distinctive, and it is noticeable that the two main suborders display different size ranges and unique evolutionary trends.

Toxodonts display a relatively active body mass increase during the last 50 Myr (McShea, 1994), as the mean BM increase is coupled with an increase in minimum and maximum BM of descendants (Fig. 1a). Their body size trends were likely generated by species sorting for large bodies (McShea, 1994), as claimed for late Cenozoic artiodactyls and perissodactyls (Huang et al., 2017). The finding of correlations of body size with extinction rate (negatively) in toxodonts further supports the idea of a driven evolution toward larger body sizes through species sorting (McShea, 1994). Besides, the pattern exhibited by toxodonts is consistent with the expectations of the Cope's rule, a trend widely supported by the mammalian fossil record (Huang et al., 2017; Smith et al., 2016, 2004) but, to our knowledge, for the first time invoked for any extinct native south American mammal clade. In contrast, the body mass evolution in tyotherians is best explained by a passive trend where the temporal pattern should mimic a diffusive process, perhaps asymmetrically bounded by a limit on the minimum size viable animal body (likely around 350 g). This passive process increases the maximum BM, and after enough time, it increases the mean body size but without raising the minimum (Huang et al., 2017; McShea, 1994; Smith et al., 2016).

Once we have supported the prevalence of distinct macroevolutionary processes generating the increasing body size through time observed in the two suborders within notoungulates (species sorting and diffusive process), it becomes necessary to characterize their predominant evolutionary modes. The likelihood-based models of evolution implemented (Hunt, 2008, 2006a; Hunt et al., 2015) allow us to

recognize the prevalence of the directional (GRW) and punctuated (Punc) evolutionary modes as the best fitting models among both, the traits under scrutiny and taxonomic groups (Table 2, Fig. 3). Interestingly, these models are not the most commonly supported by the fossil record (Hunt et al., 2015). Further, the predominance of complex punctuational models over the simple GRW model illustrates a stepwise, rather than gradual, evolution of the body size in most clades but also how the evolutionary reality is likely more complex than represented by simplified (though useful) models of trait change (Hunt et al., 2015; Hunt and Rabosky, 2014). These punctuational explanations exemplified intervals of accelerated evolution that differ qualitatively from "normal" evolutionary dynamics, and even when numerous mechanisms have been proposed to account for these two regimes of punctuation and stasis, what matters is that punctuations represent evolutionary changes governed by a different set of rules than those operating during stasis (Hunt, 2008). However, the causes of such punctuation are difficult to assess without further analyses, as ecophenotypic responses to environmental change and condensed stratigraphic intervals can produce patterns that mirror punctuated evolution within a lineage (Hunt, 2008). In any case, the variation in the timing of shifts in evolutionary dynamics emphasizes the complex nature of the trait evolution here documented (Fig. 3).

In toxodonts, there are a few time-intervals in which most of the rapid, and in several cases repeated, instances of evolutionary change of the body mass appears to occur (Table 2): middle Eocene (Bartonian; Barrancan; 40 Ma), early Oligocene (Rupelian; Deseadan; 30 Ma), and middle (Langhian; 14 Ma) and late Miocene (Tortonian; 8 Ma). The Bartonian is when the global temperature begins to decrease and coincides with the earliest stages of the Drake Passage opening (Zachos et al., 2008). Besides, an anomalously low $\delta^{13}\text{C}$ cluster in the Barrancan at ~39 Ma might represent a brief (c. 200 ka) interval of enhanced precipitation and wetter climates in Patagonia (Kohn et al., 2015). The analyses of $\delta^{18}\text{O}$ on teeth and bone reveals a dramatic drop in temperature, likely around 7–10 °C, between 30 and 28 Ma (Deseadan) in high latitudes (~45°S) of South America, representing a short interval of drier climates in Patagonia likely due to regional (e.g., the uplift of the Patagonian Andes) rather than global reasons (Kohn et al., 2010). Besides, during the Early Oligocene, the Patagonian mammal fauna had experienced a significant turnover associated with global climate

cooling (Goin et al., 2010). Finally, the middle and late Miocene abrupt changes of the toxodonts BM coincides with the beginning of the middle Miocene Climatic Transition marked by the cooling of high and low latitudes and the stabilization of Antarctic ice sheets (Flower and Kennett, 1994), and with the enhanced seasonality, and restructuring of terrestrial plant and animal communities around the world (Herbert et al., 2016; Palazzesi and Barreda, 2012), respectively. Moreover, during the middle and late Miocene also essential environmental changes occurred in South America related to Andean uplift (e.g., reduced seasonal precipitation on the leeward side of the Andes mountains), impacting, among others, the trophic diversity of the mammalian communities in South America (e.g., Hoorn et al., 2010; Ortiz-Jaureguizar and Cladera, 2006).

In summary, the abrupt changes in toxodonts BM appear to be likely a response related to the high extinction rate affecting small-sized species more strongly than large ones in the face of rapid changes in the regional environmental settings (Kohn et al., 2015). Attaching such large bodies sizes can contribute to resisting the extinction of toxodonts in several ways, including the increased capability of find suitable conditions due to longer dispersal distance and more extensive geographical ranges, providing a larger volume-to-surface ratio for preserving energy, and reducing the relative energy requirements (Huang et al., 2017; Ofstad et al., 2016; Peters, 1986). While on the other hand, the overall body size trend of typotherians was generated by a bounded diffusive process rather than selecting large bodies (McShea, 1994). However, similar environmental drivers might also impact their passive trend of size increase over time.

4.3. The evolution of the hypsodonty in notoungulates

Notoungulates displayed a wide range of hypsodonty degrees, including brachyodont to hypselodont taxa, with high crown forms (hypsodont and hypselodont) being increasingly common since the late Eocene (Dunn et al., 2015; Strömberg et al., 2013). Even when having a higher tooth crown represents different mechanisms that generated ecological and evolutionary advantages (Madden, 2014), the increased hypsodonty is shared by typotherians and toxodonts. Both suborders display an active trend of increased hypsodonty through time (including mean, minimum, and maximum). Therefore, it is also possible to hypothesize that the hypsodonty's long-term evolution was also driven by species sorting (Jablonski, 2008; McShea, 1994). Our results support that species sorting favored high-crown lineages within Toxodontia and Typotheria increase their survivorship during changes in the regional temperature or tectonic settings (Goin et al., 2010; Ortiz-Jaureguizar and Cladera, 2006; Pascual and Jaureguizar, 1990). These results are somewhat consistent with those observed in insular mammals, in which the acquisition of increased hypsodonty allowed them to delay senescence, extend reproductive lifespan, and increase fitness under environments with resource limitations (Jordana et al., 2012).

The current fossil record of notoungulates, and subordinate suborders, indicates that hypsodonty did not evolve gradually. Instead, we found rapid and repeated evolutionary change instances toward higher tooth crowns (Table 2), in broad agreement with previous interpretations (Kohn et al., 2015). When all notoungulates were considered, five main four punctuations were identified (at 37, 31, 25, 16, and 9 Ma), separating successive intervals of relative stasis (Table 2). Typotherians and toxodonts also display rapid and repeated evolutionary change instances toward higher tooth crowns, but with four and three punctuations, respectively (Table 2). The first punctuational increase in the mean hypsodonty occurs early in typotherians (at 37 Ma; Mustersan SALMA), but it was modest. In fact, since ~30 Ma (likely the earliest Deseadan) were the toxodonts, which achieves for the first time mean hypsodonty values over 1. Besides, along with the Miocene distinct episodes of rapid hypsodonty increases in both typotherians and toxodonts were recognized (Table 2). However, as mentioned above, the causes of such punctuations are difficult to assess without further

analyses (Hunt, 2008) (but see details below).

4.4. Drivers of the body size and hypsodonty evolution in SSA notoungulates

Several GLS models were fitted to estimate the influence of some likely important variables on the mean evolution of the body mass and hypsodonty in SSA notoungulates using a maximum likelihood approach (Table 3). Our results supported that biotic (i.e., feedback among traits) and in less degree abiotic (global temperature) factors were important in driving the body mass and hypsodonty's temporal trends notoungulates, typotherians, and toxodonts. However, as described above, the analyzed traits and suborders showed somewhat independent evolutionary histories. Therefore, let begin first with the main drivers in the evolution of their hypsodonty.

Previous works have hypothesized that increased hypsodonty in notoungulates must be related to the evolution of structural enhancements to prolong the functional longevity of the dentition given landscape changes associated with the spread of grasslands, the climatic history of South America, and the tectonic evolution of the Andean orogen (and their concomitant complex volcanic history) (Dunn et al., 2015; Flynn et al., 2003; Kohn et al., 2015; Madden, 2014; Strömberg et al., 2013). Now, we examined each of these potential drivers in a separate way focusing in the SSA notoungulates.

The initial expansion of open herbaceous communities in SSA begins in the Middle Eocene (~45 Ma), while the appearance of grassy habitats' likely occurs during the greenhouse to icehouse transition at the Eocene/Oligocene boundary (Bellosi and Krause, 2014). Although open-habitat grasses existed in southern South America since the middle Eocene, they were rather minor floral components in predominantly forested habitats until the early Miocene (Strömberg et al., 2013). Other authors have estimated a leaf area index (LAI) for the SSA extinct plant communities as a proxy of vegetation openness during the Eocene-late Miocene (Dunn et al., 2015). These authors suggested that the development of hypsodonty in notoungulates agrees relatively well with the increased availability of open habitats (Dunn et al., 2015). Nevertheless, when the proportion of grasses and LAI were included as explanatory variables in our GLS analyses, none of these were significantly correlated with the mean hypsodonty evolution in notoungulates, and neither toxodonts nor typotherians ($p > 0.05$). Therefore, the hypotheses that the development of grasses or the increased open environments drive the long-term hypsodonty's evolution in notoungulates and subordinate suborders (Dunn et al., 2015; Strömberg et al., 2013) lacks statistical support.

South America's climatic history must respond to the tectonic changes in the subcontinent and global climate trends (e.g., Goin et al., 2010; Ortiz-Jaureguizar and Cladera, 2006). It has been suggested that the high tooth crowns in notoungulates likely evolved slowly and progressively over 20 Ma after the apparition of relatively dry environments through natural selection in response to dust ingestion favored by a cooled gradient of temperature and increases wind speeds across Patagonia (Kohn et al., 2015). While a proxy for wind speeds along the Cenozoic is lacking, we explicitly test whether global temperatures drive hypsodonty changes using GLS regressions. We found that the global climate (Zachos et al., 2001) is not statistically correlated ($p > 0.05$) with the trends of hypsodonty in notoungulates and subordinate suborders. Denoting that significant changes in global temperature by himself did not drive the long-term trends in the evolution of this trait. Nevertheless, the global climate might be important in the evolution of some notoungulates lineages (Scarano et al., 2021).

The building of the Andes mountains can drove evolutionary changes in the Cenozoic mammals of South America in several ways. Mountain building creates topographic heterogeneity and new habitats where species evolve, but also can provide nutrients to surrounding lowlands, increases sediment delivery (including volcanic particles) and heterogeneity of soil types, modified drainage patterns, and even alter the

regional climate, generating climatic gradients along their slopes (Antonelli et al., 2018; Ehlers and Poulsen, 2009; Hoorn et al., 2010; Huang et al., 2019; Silvestro and Schnitzler, 2018). However, a proxy for the broad patterns in Cenozoic Andean uplift is not yet available. Mainly because their growth has been complex, involving fluctuations over time among three different tectonic regimes (shortening, extension, and neutral conditions, each of one reflecting contrasting degrees of mechanical coupling along the plate boundary between South America and the subducting oceanic slab), and along-strike variability in deformation and crustal thickening (Horton, 2018; Ramos, 2010). Therefore, it is likely that the SSA Andes' uplift was heterogeneous in both time and space. For these reasons, we cannot include an SSA tectonic proxy in our analyses and cannot reject it as a potential driver for the hypsodonty's evolutionary patterns in notoungulates.

By fitting models describing the impact of several environmental factors driven macroevolution of the hypsodonty on our data, we can examine their relative importance, mainly because they are likely multicausal (Madden, 2014). For this reason, we fit GLS models looking for the best combination (if any) of variables explaining the evolution of the traits under scrutiny. Interestingly, our findings support that in tyotherians and toxodonts the body mass and the hypsodonty might have a coupled evolutionary history, unlike previous interpretations (Gomes Rodrigues et al., 2017). Challenging the view in which the main evolutionary changes in the hypsodonty in notoungulates were driven by environmental factors (Dunn et al., 2015; Kohn et al., 2015; Strömberg et al., 2013). In any case, it remains unclear which of these traits (body mass and hypsodonty) were explanatory or response, although our data show that body mass increases in notoungulates predate increases in hypsodonty (Figs. 3 and 4).

On the other hand, the main driver of the SSA notoungulates (as a whole) body size evolution is the availability of savanna grassland vegetation in this region (Palazzesi and Barreda, 2012; Strömberg et al., 2013), the single variable with a better fit to our data (Table 3). However, at the suborder level, this factor appears to be unrelated. The increase of the body size through time in toxodonts is best explained by a combination of increased global temperature (Zachos et al., 2001) and hypsodonty in the clade. This finding partially supports the coupling between global temperatures and species body sizes generally observed in some mammals (Lovegrove and Mowoe, 2013; Martin et al., 2018). While the BM evolution of tyotherians is compatible with purely passive explanations for trends through time (McShea, 1994; Smith et al., 2016), the availability of savanna grassland vegetation and global temperatures are unlike drivers of their long-term mean fluctuations.

4.5. Spatial patterns in notoungulate body size and hypsodonty

Previous works have focused on the temporal patterns in the body mass and hypsodonty evolution in notoungulates (Dunn et al., 2015; Madden, 2014; Reguero et al., 2010; Strömberg et al., 2013). However, much less attention has been given to the spatial patterns of these traits. Today, the dominant mountain range of South America, located toward western longitudes, positively influence hypsodonty prevalence, and herbivores in the Andes are consistently more hypsodont (Madden, 2014). Here, we demonstrate a similar pattern in the fossil record, as there is a significant increase of hypsodonty in notoungulates toward the west of South America, close to the Andean mountains. This finding is highly congruent with the relevance of the Andean growth and its associated generation of volcanoclastic particles in potentially drove the development of high crown tooth in notoungulates and supports previous interpretations (Madden, 2014; Strömberg et al., 2013). Therefore, it is likely that the surface processes related to the Andean orogen in South America drive the long-term evolution of some traits, like hypsodonty, in native mammal's lineages.

On the other hand, our results also indicate an increase of BM toward tropical regions, contrasting with Bergman's Rule's expectations (Ash-ton et al., 2000). The spatial patterns in notoungulate body size did not

trace the temperature (latitude), but whether it tracks other ecological important factors, as net primary production (Huston and Wolverton, 2011) or the availability and quality of resources (McNab, 2010; Saari-nen, 2014), although likely, are not distinguishable with the available data. Nevertheless, these results may also be an artifact of fewer small-bodied species where species richness is low, as at lower latitudes (Fig. 5).

Inferring the macroevolutionary dynamics of completely extinct clades is challenging, mostly due to the fragmentary, distorted, and even biased nature of their fossil remains (e.g., Solórzano et al., 2020). At present, the fossil record of notoungulates certainly reflects the absence or paucity of sampling from particular time intervals and geographic regions (Fig. 5) (Croft et al., 2020). For example, the record of notoungulates is very poorly known in the neotropical area, as before the middle Miocene there is a lack of species reported in tropical regions (latitudes $<15^{\circ}\text{S}$), as well as a lack of notoungulates in higher latitudes ($>40^{\circ}\text{S}$) (Fig. 5). Besides, it is also possible to note that these spatial biases might be related to BM, as there are just a few small-sized notoungulates in latitudes lower than 20°S (Fig. 5). Whether this represents an absence of ecological opportunities for small-sized notoungulates or a sampling bias needs to be further explored. However, we argue that further sampling effort for fossil data is unlikely to modify the broad patterns here described, as our analyses found neither body size nor hypsodonty associated with lower preservation rates in any of our suborders. Spatial heterogeneity in sampling is among the most pervasive biases of fossil data and might bias macroevolutionary analyses (Holland, 2016), and here we acknowledge that this kind of bias should be present in our data. Subsequently, our results might be improved or even challenged after the development of new proxies for the Cenozoic Andean building's timing, and after further advances in sampling efforts (especially toward lower latitudes) and taxonomy will be achieved.

5. Conclusions

We have compiled and analyzed a large dataset of notoungulates body mass and hypsodonty (>250 spp.) within statistical frameworks to determine the broad evolutionary patterns of these traits through space and time and how environmental changes (at a global and regional SSA scale) and trait feedbacks have driven these patterns. Our results illuminate how these traits have emerged, providing further advances in understanding the long-term evolution of this intriguing and pervasive group of extinct South American mammals. Notoungulates, and most low taxonomic hierarchies, have mainly evolved from relatively small and lower-crowned ancestral forms after one or more abrupt positive and punctuated evolutionary changes in body mass and hypsodonty, denoting the complex nature of the evolution of these traits. Furthermore, species sorting appears to be a crucial process in the macroevolutionary trends of the hypsodonty in notoungulates, and body mass in toxodonts, primarily through extinction selectivity.

Here, we demonstrate for the first time that notoungulates have consistently evolved toward larger sizes and higher tooth crowns in a coupled way. Moreover, these increases were punctuated rather than gradual in most of the analyzed clades. The increases in hypsodonty must reflect repeated and quick instances of adaptive responses to the increase in volcanic and other terrigenous particles' availability to the removed or transported, within the broad context of the SSA Cenozoic Andean mountain building. The significant increase in hypsodonty toward the west of South America supports the last notion. Therefore, the Andean growth must be regarded as a more likely driver for the long-term hypsodonty evolution in notoungulates than the development of grasses, the increased availability of open environments, or even the global temperature. Nevertheless, rapid and punctuated body mass and hypsodonty changes may have been induced by short-term periods of high aridity, resource limitations, or volcanic activity. Whether the Andes growth and short-term environmental changes associated had a similar role in developing the hypsodonty (or other key traits) in other

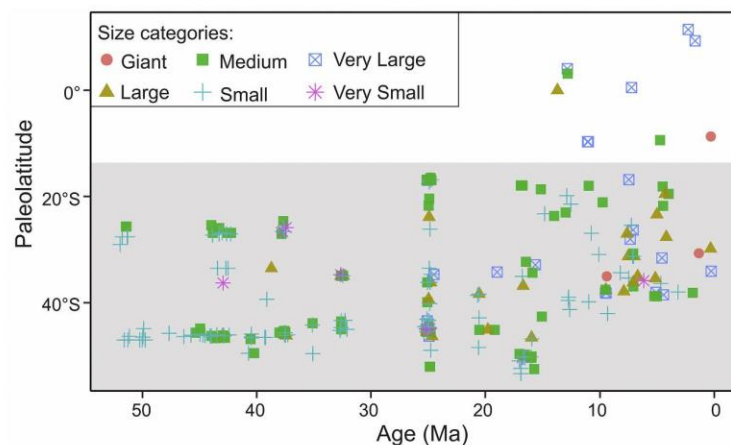


Fig. 5. Paleolatitudinal distribution of notoungulates through time grouped according to body size classifications described in the main text. In grey is highlighted the location of taxa inhabiting the SSA.

groups of South American mammals needs to be tested.

Declaration of Competing Interest

The authors declare that they have no known competing financial interests or personal relationships that could have influenced the work reported in this paper.

Acknowledgments

We want to express our gratitude to John Alroy and the entire PBDB team for their outstanding efforts in compiling and maintaining this database. We also thank Darin Croft, Howard Falcon-Lang, and an anonymous reviewer for valuable comments and suggestions in an earlier manuscript version. The authors acknowledge partial support from ANID-PCHA/Doctorado Nacional/2018–21180471 (to AS) and 2017–21170438 (to NFM).

Appendix A. Supplementary data

Supplementary data to this article can be found online at <https://doi.org/10.1016/j.palaeo.2021.110306>.

References

- Antonelli, A., Kissling, W.D., Flantua, S.G.A., Bermúdez, M.A., Mulch, A., Muellner-Riehl, A.N., Kreft, H., Linder, H.P., Badgley, C., Fjeldsá, J., Fritz, S.A., Rahbek, C., Herman, F., Hooghiemstra, H., Hooim, C., 2018. Geological and climatic influences on mountain biodiversity. *Nat. Geosci.* <https://doi.org/10.1038/s41561-018-0236-z>.
- Ashton, K.G., Tracy, M.C., De Queiroz, A., 2000. Is Bergmann's rule valid for mammals? *Am. Nat.* 156, 390–415. <https://doi.org/10.1086/303400>.
- Barton, K., 2020. MuMIn: Multi model inference. In: R Package Version 1.43, p. 17.
- Belloso, E.S., Krause, J.M., 2014. Onset of the Middle Eocene global cooling and expansion of open-vegetation habitats in Central Patagonia. *Andean Geol.* 41, 29–48. <https://doi.org/10.5027/andgeoV41n1-a02>.
- Billet, G., 2011. Phylogeny of the Notoungulata (Mammalia) based on cranial and dental characters. *J. Syst. Palaeontol.* 9, 481–497. <https://doi.org/10.1080/14772019.2010.528456>.
- Brassey, C.A., 2017. Body-mass estimation in paleontology: a review of volumetric techniques. *Paleontol. Soc. Pap.* 22, 133–156. <https://doi.org/10.1017/scs.2017.12>.
- Buckley, M., 2015. Ancient collagen reveals evolutionary history of the endemic south american 'ungulates'. *Proc. R. Soc. B Biol. Sci.* 282 <https://doi.org/10.1098/rspb.2014.2671>.
- Cassini, G.H., Cerdeño, E., Villafañe, A.L., Muñoz, N.A., 2012. Paleobiology of Santacrucian native ungulates (Meridiungulata: Astrapotheria, Litopterna and Notoungulata). In: Vizcaino, S.F., Kay, R.F., Bargo, M.S. (Eds.), *Early Miocene Paleobiology in Patagonia*. Cambridge University Press, Cambridge, pp. 243–286. <https://doi.org/10.1017/CBO9780511667381.015>.
- Clavel, J., Morlon, H., 2017. Accelerated body size evolution during cold climatic periods in the Cenozoic. *Proc. Natl. Acad. Sci. U. S. A.* 114, 4183–4188. <https://doi.org/10.1073/pnas.1606868114>.
- Cohen, K.M., Finney, S.C., Gibbard, P.L., Fan, J.X., 2013. The ICS international chronostratigraphic chart. *Episodes* 36, 199–204. <https://doi.org/10.18814/epiiugs/2013/v36i3/002>.
- Cooper, N., Purvis, A., 2010. Body size evolution in mammals: complexity in tempo and mode. *Am. Nat.* 175, 727–738. <https://doi.org/10.1086/652466>.
- Core Team, R., 2018. R: A Language and Environment for Statistical Computing. R Foundation for Statistical Computing. R Foundation for Statistical Computing.
- Croft, D.A., Gelfo, J.N., López, G.M., 2020. Splendid innovation: the extinct South American native ungulates. *Annu. Rev. Earth Planet. Sci.* 48, 259–290. <https://doi.org/10.1146/annurev-earth-072619-060126>.
- Damuth, J., Janis, C.M., 2011. On the relationship between hypsodonty and feeding ecology in ungulate mammals, and its utility in palaeoecology. *Biol. Rev.* 86, 733–758. <https://doi.org/10.1111/j.1469-185X.2011.00176.x>.
- Dunn, R.E., Madden, R.H., Kohn, M.J., Schmitz, M.D., Strömberg, C.A.E., Carlini, A.A., Re, G.H., Crowley, J., 2013. A new chronology for middle Eocene-early Miocene South American land mammal ages. *Geol. Soc. Am. Bull.* 125, 539–555. <https://doi.org/10.1130/B30660.1>.
- Dunn, R.E., Strömberg, C.A.E., Madden, R.H., Kohn, M.J., Carlini, A.A., 2015. Linked canopy, climate, and faunal change in the Cenozoic of Patagonia. *Science* 347(347), 258–261. <https://doi.org/10.1126/science.1260947>.
- Ehlers, T.A., Poulsen, C.J., 2009. Influence of Andean uplift on climate and paleoaltimetry estimates. *Earth Planet. Sci. Lett.* 281, 238–248. <https://doi.org/10.1016/j.epsl.2009.02.026>.
- Elissamburu, A., 2012. Estimación de la masa corporal en géneros del orden Notoungulata. *Estud. Geol.* 68, 91–111. <https://doi.org/10.3989/eegeol.40336.133>.
- Erwin, D.H., 2007. Disparity: Morphological pattern and developmental context. In: *Palaeontology*. John Wiley & Sons, Ltd, pp. 57–73. <https://doi.org/10.1111/j.1475-4983.2006.00614.x> (10.1111).
- Fernández-Monescillo, M., Antoine, P.O., Pujos, F., Gomes Rodrigues, H., Mamani Quispe, B., Orliac, M., 2019. Virtual endocast morphology of mesotheriidae (Mammalia, Notoungulata, Typotheria): new insights and implications on notoungulate encephalization and brain evolution. *J. Mammi. Evol.* 26, 85–100. <https://doi.org/10.1007/s10914-017-9416-7>.
- Flower, B.P., Kennett, J.P., 1994. The middle Miocene climatic transition: East Antarctic ice sheet development, deep ocean circulation and global carbon cycling. *Palaeogeogr. Palaeoclimatol. Palaeoecol.* 108, 537–555. [https://doi.org/10.1016/0031-0182\(94\)90251-8](https://doi.org/10.1016/0031-0182(94)90251-8).
- Flynn, J.J., Wyss, A.R., Croft, D.A., Charrier, R., 2003. The Tinguiririca Fauna, Chile: biochronology, paleoecology, biogeography, and a new earliest Oligocene South American Land Mammal 'Age'. *Palaeogeogr. Palaeoclimatol. Palaeoecol.* 195, 229–259. [https://doi.org/10.1016/S0031-0182\(03\)00360-2](https://doi.org/10.1016/S0031-0182(03)00360-2).
- Fraser, D., Soul, L.C., Tóth, A.B., Balk, M.A., Eronen, J.T., Pineda-Munoz, S., Shupinski, A.B., Villaseñor, A., Barr, W.A., Behrensmeier, A.K., Du, A., Faith, J.T., Gotelli, N.J., Graves, G.R., Jukar, A.M., Looy, C.V., Miller, J.H., Potts, R., Lyons, S.K., 2020. Investigating biotic interactions in deep time. *Trends Ecol. Evol.* 17 <https://doi.org/10.1016/j.tree.2020.09.001>.
- Goin, F.J., Abello, M.A., Chornogubsky, L., 2010. Middle Tertiary marsupials from Central Patagonia (early Oligocene of Gran Barranca): Understanding South America's Grande Coupure. In: Madden, R.H., Carlini, A.A., Vucetich, M.G., Kay, R. F. (Eds.), *The Paleontology of Gran Barranca: Evolution and Environmental Change through the Middle Cenozoic of Patagonia*. Cambridge University Press, Cambridge, Massachusetts, pp. 69–105.
- Gomes Rodrigues, H., Herrel, A., Billet, G., 2017. Ontogenetic and life history trait changes associated with convergent ecological specializations in extinct ungulate

- mammals. *Proc. Natl. Acad. Sci. U. S. A.* 114, 1069–1074. <https://doi.org/10.1073/pnas.1614029114>.
- Heim, N.A., Knope, M.L., Schaaf, E.K., Wang, S.C., Payne, J.L., 2015. Cope's rule in the evolution of marine animals. *Science* 80 (347), 867–870. <https://doi.org/10.1126/science.1260065>.
- Herbert, T.D., Lawrence, K.T., Tzanova, A., Peterson, L.C., Caballero-Gill, R., Kelly, C.S., 2016. Late Miocene global cooling and the rise of modern ecosystems. *Nat. Geosci.* 9, 843–847. <https://doi.org/10.1038/ngeo2813>.
- van Hinsbergen, D.J.J., de Groot, L.V., van Schaik, S.J., Spakman, W., Bijl, P.K., Sluijs, A., Langereis, C.G., Brinkhuis, H., 2015. A paleolatitude calculator for paleoclimate studies. *PLoS One* 10, e0126946. <https://doi.org/10.1371/journal.pone.0126946>.
- Holland, S.M., 2016. The non-uniformity of fossil preservation. *Philos. Trans. R. Soc. B Biol. Sci.* <https://doi.org/10.1098/rstb.2015.0130>.
- Hone, D.W.E., Benton, M.J., 2005. The evolution of large size: how does Cope's Rule work? *Trends Ecol. Evol.* <https://doi.org/10.1016/j.tree.2004.10.012>.
- Hoorn, C., Wesselingh, F.P., ter Steege, H., Bermudez, M.A., Mora, A., Sevink, J., Sanmartín, I., Sanchez-Meseguer, A., Anderson, C.L., Figueiredo, J.P., Jaramillo, C., Riff, D., Negri, F.R., Hooghiemstra, H., Lundberg, J., Stadler, T., Sárkinen, T., Antonelli, A., 2010. Amazonia through time: andean uplift, climate change, landscape evolution, and biodiversity. *Science* 330, 927–931. <https://doi.org/10.1126/science.1194585>.
- Horton, B.K., 2018. Tectonic regimes of the Central and Southern Andes: responses to variations in plate coupling during subduction. *Tectonics* 37, 402–429. <https://doi.org/10.1002/2017TC004624>.
- Huang, S., Eronen, J.T., Janis, C.M., Saarinen, J.J., Silvestro, D., Fritz, S.A., 2017. Mammal body size evolution in North America and Europe over 20 Myr: similar trends generated by different processes. *Proc. R. Soc. B Biol. Sci.* 284 <https://doi.org/10.1098/rspb.2016.2361>.
- Huang, S., Meijers, M.J.M., Eyres, A., Mulch, A., Fritz, S.A., 2019. Unravelling the history of biodiversity in mountain ranges through integrating geology and biogeography. *J. Biogeogr.* 46, 1777–1791. <https://doi.org/10.1111/jbi.13622>.
- Hunt, G., 2006a. Fitting and comparing models of phyletic evolution: random walks and beyond. *Paleobiology* 32, 578–601. <https://doi.org/10.1666/05070.1>.
- Hunt, G., 2006b. *paleoTS: Modeling Evolution in Paleontological Time-Series*, Version 0.1–2.
- Hunt, G., 2007. The relative importance of directional change, random walks, and stasis in the evolution of fossil lineages. *Proc. Natl. Acad. Sci. U. S. A.* 104, 18404–18408. <https://doi.org/10.1073/pnas.0704088104>.
- Hunt, G., 2008. Gradual or pulsed evolution: when should punctuational explanations be preferred? *Paleobiology* 34, 360–377. <https://doi.org/10.1666/07073.1>.
- Hunt, G., Rabosky, D.L., 2014. Phenotypic evolution in fossil species: pattern and process. *Annu. Rev. Earth Planet. Sci.* 42, 421–441. <https://doi.org/10.1146/annurev-earth.040809-152524>.
- Hunt, G., Roy, K., 2006. Climate change, body size evolution, and Cope's Rule deep sea ostracodes. *Proc. Natl. Acad. Sci. U. S. A.* 103, 1347–1352. <https://doi.org/10.1073/pnas.0510550103>.
- Hunt, G., Cronin, T.M., Roy, K., 2005. Species-energy relationship in the deep sea: a test using the Quaternary fossil record. *Ecol. Lett.* 8, 739–747. <https://doi.org/10.1111/j.1461-0248.2005.00778.x>.
- Hunt, G., Wicaksono, S.A., Brown, J.E., Macleod, K.G., 2010. Climate driven body-size trends in the ostracod fauna of the deep Indian Ocean. *Palaeontology* 53, 1255–1268. <https://doi.org/10.1111/j.1475-4983.2010.01007.x>.
- Hunt, G., Hopkins, M.J., Lidgard, S., 2015. Simple versus complex models of trait evolution and stasis as a response to environmental change. *Proc. Natl. Acad. Sci. U. S. A.* 112, 4885–4890. <https://doi.org/10.1073/pnas.1403662111>.
- Huston, M.A., Wolvertson, S., 2011. Regulation of animal size by eNPP, Bergmann's rule, and related phenomena. *Ecol. Monogr.* 81, 349–405. <https://doi.org/10.1890/10-1523.1>.
- Ives, A.R., 2019. R 2 s for Correlated Data: Phylogenetic Models, LMMs, and GLMMs. *Syst. Biol.* 68, 234–251. <https://doi.org/10.1093/sysbio/syy060>.
- Jablonski, D., 2008. Species selection: theory and data. *Annu. Rev. Ecol. Syst.* 39, 501–524. <https://doi.org/10.1146/annurev.ecolsys.39.110707.173510>.
- Janis, C.M., 1990. Correlation of cranial and dental variables with dietary preferences in mammals: A comparison of macropodoids and ungulates. In: Danuth, J., Mac Fadden, B.J. (Eds.), *Body Size in Mammalian Paleobiology: Estimation and Biological Implications*. Cambridge University Press, pp. 255–299.
- Janis, C.M., Fortelius, M., 1988. On the means whereby mammals achieve increased functional durability of their dentitions, with special reference to limiting factors. *Biol. Rev. Camb. Philos. Soc.* <https://doi.org/10.1111/j.1469-185x.1988.tb00630.x>.
- Jordana, X., Marín-Moratalla, N., de Miguel, D., Kaiser, T.M., Köhler, M., 2012. Evidence of correlated evolution of hypsodonty and exceptional longevity in endemic insular mammals. *Proc. R. Soc. B Biol. Sci.* 279, 3339–3346. <https://doi.org/10.1098/rspb.2012.0689>.
- Kaiser, T.M., Müller, D.W.H., Fortelius, M., Schulz, E., Codron, D., Clauss, M., 2013. Hypsodonty and tooth facet development in relation to diet and habitat in herbivorous ungulates: implications for understanding tooth wear. *Mammal Rev.* 43, 34–46. <https://doi.org/10.1111/j.1365-2907.2011.00203.x>.
- Kingsolver, J.G., Pfennig, D.W., 2004. Individual-level selection as a cause of cope's rule of phyletic size increase. *Evolution (N. Y.)* 58, 1608–1612. <https://doi.org/10.1111/j.0014-3820.2004.tb01740.x>.
- Kohn, M.J., Zanazzi, A., Josef, J.A., 2010. Stable isotopes of fossil teeth and bones at Gran Barranca as monitors of climate change and tectonics. In: Madden, R.H., Carlini, A.A., Vucetich, M.G., Kay, R.F. (Eds.), *The Paleontology of Gran Barranca: Evolution and Environmental Change through the Middle Cenozoic of Patagonia*. Cambridge University Press, Cambridge, Massachusetts, pp. 341–361.
- Kohn, M.J., Strömberg, C.A.E., Madden, R.H., Dunn, R.E., Evans, S., Palacios, A., Carlini, A.A., 2015. Quasi-static Eocene-Oligocene climate in Patagonia promotes slow faunal evolution and mid-Cenozoic global cooling. *Palaeogeogr. Palaeoclimatol. Palaeoecol.* 435, 24–37. <https://doi.org/10.1016/j.palaeo.2015.05.028>.
- Lehtonen, S., Silvestro, D., Karger, D.N., Scotese, C., Tuomisto, H., Kessler, M., Peña, C., Wahlberg, N., Antonelli, A., 2017. Environmentally driven extinction and opportunistic origination explain fern diversification patterns. *Sci. Rep.* 7, 4831. <https://doi.org/10.1038/s41598-017-05263-7>.
- Liow, L.H., Stenseth, N.C., 2007. The rise and fall of species: implications for macroevolutionary and macroecological studies. *Proc. R. Soc. B Biol. Sci.* 274, 2745–2752. <https://doi.org/10.1098/rspb.2007.1006>.
- Lovegrove, B.G., Mowoe, M.O., 2013. The evolution of mammal body sizes: responses to Cenozoic climate change in North American mammals. *J. Evol. Biol.* 26, 1317–1329. <https://doi.org/10.1111/jeb.12138>.
- Lyons, S.K., Smith, F.A., 2010. Using macroecological approach to study geographic range, abundance and body size in the fossil record. *Paleontol. Soc. Pap.* 16, 117–141.
- Madden, R.H., 2014. *Hypsodonty in Mammals: Evolution, Geomorphology and the Role of Earth Surface Processes*. Cambridge University Press, Cambridge and New York.
- Mannion, P.D., Benson, R.B.J., Carrano, M.T., Tennant, J.P., Judd, J., Butler, R.J., 2015. Climate constrains the evolutionary history and biodiversity of crocodylians. *Nat. Commun.* 6, 8438. <https://doi.org/10.1038/ncomms9438>.
- Martin, J.M., Mead, J.L., Barboza, P.S., 2018. Bison body size and climate change. *Ecol. Evol.* 8, 4564–4574. <https://doi.org/10.1002/ece3.4019>.
- McNab, B.K., 2010. Geographic and temporal correlations of mammalian size reconsidered: a resource rule. *Oecologia*. <https://doi.org/10.1007/s00442-010-1621-5>.
- McShea, D.W., 1994. Mechanisms of large-scale evolutionary trends. *Evolution (N. Y.)* 48, 1747–1763. <https://doi.org/10.1111/j.1558-5646.1994.tb02211.x>.
- Meiri, S., Dayan, T., 2003. On the validity of Bergmann's rule. *J. Biogeogr.* 30, 331–351. <https://doi.org/10.1046/j.1365-2699.2003.00837.x>.
- Mendoza, M., Janis, C.M., Palmqvist, P., 2006. Estimating the body mass of extinct ungulates: a study on the use of multiple regression. *J. Zool.* 270, 90–101. <https://doi.org/10.1111/j.1469-7998.2006.00094.x>.
- Mitchell, M., Muftakhidinov, B., Winchen, T., 2020. Engauge Digitizer Software Version 12.2.1. <https://doi.org/10.5281/zenodo.3941227>.
- Muggeo, V.M.R., 2017. Interval estimation for the breakpoint in segmented regression: a smoothed score-based approach. *Aust. N. Z. J. Stat.* 59, 311–322. <https://doi.org/10.1111/anvs.12200>.
- Müller, R.D., Cannon, J., Qin, X., Watson, R.J., Gurnis, M., Williams, S., Pfaffelmoser, T., Seton, M., Russell, S.H.J., Zahirovic, S., 2018. GPlates: building a virtual earth through deep time. *Geochem. Geophys. Geosyst.* 19, 2243–2261. <https://doi.org/10.1029/2018GC007584>.
- Ofstad, E.G., Herfindal, I., Solberg, E.J., Sæther, B.E., 2016. Home ranges, habitat and body mass: simple correlates of home range size in ungulates. *Proc. Biol. Sci.* 283 <https://doi.org/10.1098/rspb.2016.1234>.
- Ortiz-Jaureguizar, E., Cladera, G.A., 2006. Paleoenvironmental evolution of southern South America during the Cenozoic. *J. Arid Environ.* 66, 498–532. <https://doi.org/10.1016/j.jaridenv.2006.01.007>.
- Palazzesi, L., Barreda, V., 2012. Fossil pollen records reveal a late rise of open-habitat ecosystems in Patagonia. *Nat. Commun.* 3, 1294. <https://doi.org/10.1038/ncomms2299>.
- Pascual, R., Jaureguizar, E.O., 1990. Evolving climates and mammal faunas in cenozoic South America. *J. Hum. Evol.* 19, 23–60. [https://doi.org/10.1016/0047-2484\(90\)90011-Y](https://doi.org/10.1016/0047-2484(90)90011-Y).
- Pascual, R., Odreman-Rivas, O.E., 1971. Evolución de las comunidades de los Vertebrados del Terciario argentino. Los aspectos paleozooecográficos y paleoclimáticos. *Ameghiniana* 8, 372–412.
- Patterson, B., Pascual, R., 1968. Evolution of mammals in Southern Continents. V. Fossil Mammal Fauna of South America. *Q. Rev. Biol.* 43, 409–451.
- Peters, R.H., 1986. *The Ecological Implications of Body Size*. Cambridge University Press.
- Pinheiro, J., Bates, D., DebRoy, S., Sarkar, D., R Core Team, 2020. *nlme: Linear and Nonlinear Mixed Effects Models*.
- Piras, P., Silvestro, D., Carotenuto, F., Castiglione, S., Kotsakis, A., Maiorino, L., Melchionna, M., Mondanaro, A., Sansalone, G., Serio, C., Vero, V.A., Raia, P., 2018. Evolution of the sabertooth mandible: a deadly ecomorphological specialization. *Palaeogeogr. Palaeoclimatol. Palaeoecol.* 496, 166–174. <https://doi.org/10.1016/j.palaeo.2018.01.034>.
- Prevosti, F.J., Forasiepi, A.M., 2018. South American endemic mammalian predators (order sparrow-donta). In: *Springer Geology*. Springer, pp. 39–84. https://doi.org/10.1007/978-3-319-03701-1_3.
- Raia, P., Carotenuto, F., Meloro, C., Piras, P., Pushkina, D., 2010. The shape of contention: Adaptation, history, and contingency in ungulate mandibles. *Evolution (N. Y.)* 64, 1489–1503. <https://doi.org/10.1111/j.1558-5646.2009.00921.x>.
- Raia, P., Carotenuto, F., Eronen, J.T., Fortelius, M., 2011. Longer in the tooth, shorter in the record? The evolutionary correlates of hypsodonty in neogene ruminants. *Proc. R. Soc. B Biol. Sci.* 278, 3474–3481. <https://doi.org/10.1098/rspb.2011.0273>.
- Rambaut, A., Drummond, A.J., Xie, D., Baele, G., Suchard, M.A., 2018. Posterior summarization in bayesian phylogenetics using tracer 1.7. *Syst. Biol.* 67, 901–904. <https://doi.org/10.1093/sysbio/syy032>.
- Ramos, V.A., 2010. The tectonic regime along the Andes: present-day and Mesozoic regimes. *Geol. J.* 45, 2–25. <https://doi.org/10.1002/gj.1193>.

- Reguero, M.A., Prevosti, F.J., 2010. Rodent-like notoungulates (Typrotheria) from Gran Barranca, Chubut Province, Argentina: Phylogeny and systematics. In: Madden, R.H., Carlini, A.A., Vucetich, M.G., Kay, R.F. (Eds.), *The Paleontology of Gran Barranca: Evolution and Environmental Change through the Middle Cenozoic of Patagonia*. Cambridge University Press, pp. 152–162.
- Reguero, M.A., Dozo, M.T., Cerdano, E., 2007. A poorly known rodentlike mammal (Pachyrukhinae, Hegetotheriidae, Notoungulata) from the Deseadan (Late Oligocene) of Argentina. *Paleoecology, biogeography, and radiation of the rodentlike ungulates in South America*. *J. Paleontol.* 81, 1301–1307. <https://doi.org/10.1666/05-100.1>.
- Reguero, M.A., Candela, A.M., Cassini, G.H., 2010. Hipsodonty and body size in rodent-like notoungulates. In: Madden, R.H., Carlini, A.A., Vucetich, M.G., Kay, R.F. (Eds.), *The Paleontology of Gran Barranca: Evolution and Environmental Change through the Middle Cenozoic of Patagonia*. Cambridge University Press, pp. 358–367.
- Ripley, B., Venables, B., Bates, D., Hornik, K., Gebhardt, A., Firth, D., 2020. Package “MASS.”.
- Saarinen, J., 2014. *Econometrics of Large Herbivorous Land Mammals in Relation to Climatic and Environmental Changes during the Pleistocene*. Department of Geosciences and Geography.
- Scarano, A.C., Carlini, A.A., Illius, A.W., 2011. Interatheriidae (Typrotheria; Notoungulata), body size and paleoecology characterization. *Mamm. Biol.* 76, 109–114. <https://doi.org/10.1016/j.mambio.2010.08.001>.
- Scarano, A.C., Vera, B., Reguero, M., 2021. Evolutionary Trends of Prototyprotherium (Interatheriidae, Notoungulata) Lineage throughout the Miocene of South America. *J. Mamm. Evol.* 1–11. <https://doi.org/10.1007/s10914-020-09534-5>.
- Scott, W.B., 1912. Part II: Toxodontia of the Santa Cruz beds. In: Scott, W.B. (Ed.), *Report of Princeton University Expedition to Patagonia*. E. Schweizerbart'sche Verlagshandlung, Stuttgart, pp. 111–300.
- Semprebon, G.M., Rivals, F., Janis, C.M., 2019. The role of grass vs. Exogenous abrasives in the paleodietary patterns of North American. *Front. Ecol. Evol.* 7. <https://doi.org/10.3389/fevo.2019.00065>.
- Silvestro, D., Schnitzler, J., 2018. Inferring macroevolutionary dynamics in mountain systems from fossils. In: Hoom, C., Perrigo, A., Antonelli, A. (Eds.), *Mountains, Climate and Biodiversity*, pp. 217–230.
- Silvestro, D., Salamin, N., Schnitzler, J., 2014a. PyRate: a new program to estimate speciation and extinction rates from incomplete fossil data. *Methods Ecol. Evol.* 5, 1126–1131. <https://doi.org/10.1111/2041-210X.12263>.
- Silvestro, D., Schnitzler, J., Liow, L.H., Antonelli, A., Salamin, N., 2014b. Bayesian estimation of speciation and extinction from incomplete fossil occurrence data. *Syst. Biol.* 63, 349–367. <https://doi.org/10.1093/sysbio/syu006>.
- Silvestro, D., Salamin, N., Antonelli, A., Meyer, X., 2019. Improved estimation of macroevolutionary rates from fossil data using a Bayesian framework. *Paleobiology* 45, 546–570. <https://doi.org/10.1017/pab.2019.23>.
- Simpson, G.G., 1944. *Tempo and Mode in Evolution*. Columbia University Press, New York.
- Simpson, G.G., 1980. *Splendid Isolation: The Curious History of South American Mammals*. Yale University Press, New Haven.
- Smith, F.A., Brown, J.H., Haskell, J.P., Lyons, S.K., Alroy, J., Charnov, E.L., Dayan, T., Enquist, B.J., Ernest, S.K.M., Hadly, E.A., Jones, K.E., Kaufman, D.M., Marquet, P.A., Maurer, B.A., Niklas, K.J., Porter, W.P., Tiffney, B., Willig, M.R., 2004. Similarity of mammalian body size across the taxonomic hierarchy and across space and time. *Am. Nat.* 163, 672–691. <https://doi.org/10.1086/382898>.
- Smith, F.A., Payne, J.L., Heim, N.A., Balk, M.A., Finnegan, S., Kowalewski, M., Lyons, S.K., McClain, C.R., McShea, D.W., Novack-Gottshall, P.M., Anich, P.S., Wang, S.C., 2016. Body size evolution across the geozoic. *Annu. Rev. Earth Planet. Sci.* 44, 523–553. <https://doi.org/10.1146/annurev-earth-060115-012147>.
- Solórzano, A., Núñez Flores, M., Inostroza Michael, O., Hernández, C.E., 2020. Biotic and abiotic factors driving the diversification dynamics of Crocodylia. *Palaeontology* 63, 415–429. <https://doi.org/10.1111/pala.12459>.
- Strömberg, C.A.E., Dunn, R.E., Madden, R.H., Kohn, M.J., Carlini, A.A., 2013. Decoupling the spread of grasslands from the evolution of grazer-type herbivores in South America. *Nat. Commun.* 4, 1–8. <https://doi.org/10.1038/ncomms2508>.
- Voje, K.L., 2018. Assessing adequacy of models of phyletic evolution in the fossil record. *Methods Ecol. Evol.* 9, 2402–2413. <https://doi.org/10.1111/2041-210X.13083>.
- Welker, F., Collins, M.J., Thomas, J.A., Wadsley, M., Brace, S., Cappellini, E., Turvey, S.T., Reguero, M., Gelfo, J.N., Kramarz, A., Burger, J., Thomas Oates, J., Ashford, D.A., Ashton, P.D., Rowsell, K., Porter, D.M., Kessler, B., Fischer, R., Baessmann, C., Kaspar, S., Olsen, J.V., Kiley, P., Elliott, J.A., Kelstrup, C.D., Mullin, V., Hofreiter, M., Willerslev, E., Hublin, J.J., Orlando, L., Barnes, I., Macphree, R.D.E., 2015. Ancient proteins resolve the evolutionary history of Darwin's South American ungulates. *Nature* 522, 81–84. <https://doi.org/10.1038/nature14249>.
- Zachos, J., Pagani, H., Sloan, L., Thomas, E., Billups, K., 2001. Trends, rhythms, and aberrations in global climate 65 Ma to present. *Science* 80. <https://doi.org/10.1126/science.1059412>.
- Zachos, J.C., Dickens, G.R., Zeebe, R.E., 2008. An early Cenozoic perspective on greenhouse warming and carbon cycle dynamics. *Nature*. <https://doi.org/10.1038/nature06588>.



ANEXO 2. Materiales suplementarios asociados a cada una de las publicaciones resultantes de esta tesis doctoral



Electronic supplementary materials for: The Early to late Middle Miocene mammalian assemblages from the Cura-Mallín Formation, at Lonquimay, southern Central Andes, Chile (~38°S): biogeographical and paleoenvironmental implications

Contents:

ESM_1. List of materials used for comparisons.

ESM_2. Dental measurements of *Parastrapotherium* sp.

ESM_3. Dental measurements of *Theosodon* sp.

ESM_4. Dental measurements of *Protypotherium conceptionensis*

ESM_1. List of materials used for comparisons. *Institutional abbreviations:* **MLP**, Museo de La Plata, La Plata, Argentina; **MACN**, Museo Argentino de Ciencias Naturales, Buenos Aires, Argentina; **ZMK**, Zoological Museum of the University of Copenhagen, Quaternary Zoology Collections, Copenhagen, Denmark; **PVPH**, Colección Paleontología de Vertebrados, Museo Municipal Carmen Funes, Plaza Huincul, Neuquén, Argentina; **AMNH**, American Museum of Natural History, New York, USA.

Protypotherium endiadys. MLP 12-2886 (holotype)

Protypotherium praerutilum. MACN-A 1081–1083

Protypotherium colloncurensis. MLP 91-IX-4-26 (holotype)

Protypotherium australe. MACN-A-3883, MACN-A-3884, MACN-A-533, MACN-A-530, MACN-A-531, MACN-A-529

Protypotherium minutus. MLP-12-2177

Protypotherium attenuatum. MACN-A-627, MACN-A-630, MACN-A-628

Protypotherium antiquum. ZMK 21/1877

Protypotherium sinclairi. PVPH 352 (holotype)

Parastrapotherium martiale. MACN A 52-604 (holotype)

?*Theosodon frenguelli*. MLP-52-IX-30-63

T. lydekkeri. MACN-A 2487-90, MACN-A 9269-88

T. gracilis. AMNH 9230, MACN A-9297

ESM_2. Dental measurements (in mm) of *Parastrapotherium* sp. (SGO.PV.4003) recovered from the Cura-Mallín Formation outcrops in the surrounding of Lonquimay, Chile. Abbreviations: W=transverse width, L=mesiodistal length.

Specimen	M1		M2		M3	
	L	W	L	W	L	W
SGO.PV.4003	44.39	42.80	59.98	45.00	52.08	45.47

ESM_3. Dental measurements (in mm) of *Theosodon* sp. (SGOP.4000) from the Cura-Mallín Formation (Chile), and other *Theosodon* spp. Data based on Cifelli and Guerrero (1997), Cifelli and Soria (1983), and Scott (1910). Abbreviations: W=transverse width, L=mesiodistal length.

Taxa	p1		p2		p3		p4		m1		m2		m3	
	L	W	L	W	L	W	L	W	L	W	L	W	L	W
<i>Theosodon</i> sp. (SGOP.4000)	10,8	6,5	14,3	7,3	14,4	7,5	17,2	8,8	17,7	9,9	20	10,5	19,9	10
<i>T. lallemanti</i> (Scott, 1910)	-	-	-	-	-	-	-	-	21,5–22,6	-	23–24	-	22–25	-
<i>T. garretorum</i> (YPV-VPPU 15164)	15	9	18	9,5	21	12	22	13,5	22,5	15	23	19	23	15
<i>T. gracilis</i> (AMNH 9230)	14	10,5	17	1	19	11	21	13	20	13	22	-	-	12
<i>T. gracilis</i> (MACN A-9297)	-	-	-	-	22	11,7	23	12	21	12,8	22,5	13,8	22,8	12,8
<i>T.?</i> <i>frenquellii</i> (MLP-52-IX-30-63)	-	-	16	7,5	16,3	8	19	10	18,2	11	22,2	12,8	19	11
<i>Theosodon</i> sp. (IGM183498)	-	-	-	-	-	-	-	-	22,1	11,5	-	-	-	-

SM_4. Dental measurements (in mm) of the holotype (SGO.PV.21000 (right side)) and referred materials (SGO.PV.4005) of *Protyotherium concepcionensis*. These remains were recovered in the late Middle Miocene Puente Tucapel locality, Cura-Mallín Formation, in the surrounding of Lonquimay, Chile. Abbreviations: W=transverse width, L=mesiodistal length.

Tooth		SGO.PV.21000	SGO.PV.4005
p3	L	-	5.06
	W	-	3.36
p4	L	-	5.42
	W	-	3.80
m1	L	-	7.19
	W	-	3.37
I1	L	4.95	-
	W	1.8	-
I2	L	5	-
	W	2	-
I3	L	5.02	-
	W	2.2	-
C	L	4.8	-
	W	2.5	-
P1	L	4.05	-
	W	3	-
P2	L	4.15	-
	W	4.20	-
P3	L	4.66	-
	W	5.08	-
P4	L	4.60	-
	W	5.13	-
M1	L	9.50	-
	W	6.41	-
M2	L	8.12	-
	W	5.44	-
M3	L	7.46	-
	W	3.87	-

References

- Cifelli, R., Guerrero, J., 1997. Litopterns, in: Kay, R., Madden, R.H., Cifelli, R., Flynn, J. (Eds.), *Vertebrate Paleontology in the Neotropics: The Miocene Fauna of La Venta, Colombia*. Smithsonian Institution Press, Washington, D.C, pp. 289–302.
- Cifelli, R.L., Soria, M.F., 1983. Notes on Deseadan Macraucheniidae. *Ameghiniana* 20, 141–153.
- Scott, W.B., 1910. *Mammalia of the Santa Cruz Beds. Part I. Litopterna*. Reports Prinet. Univ. Exped. to Patagon. 7, 1–156.

Electronic supplementary materials for: Late early Miocene caviomorph rodents from Laguna del Laja (~37° S), Cura-Mallín Formation, south-central Chile.

ESM_1. List of the materials used for comparisons.

Luantus toldensis. MACN Pv SC2574 (Holotype), lower molar; MACN Pv SC4033, isolated p4.

Luantus propheticus. MACN A 2018 (Holotype), mandible with p4-m3; MACN Pv SC2072, isolated p4; MACN Pv SC2235, isolated p4; MACN Pv SC2871, isolated p4; MACN Pv SC3617, a fragment of mandible bearing p4-m3.

Phanomys mixtus. MACN A 11302 (Lectotype), maxillary fragment with P4-M2; MACN A 2022 (Neosyntype), nine isolated cheek teeth; MACN Pv SC3450, maxillary fragment with P4-M3.

Phanomys vetulus. MACN A 2024 (Syntype), nine isolated molariforms.

Scleromys quadrangulatus. MACN Pv SC2224, m3; MACN Pv SC3433, mandibular fragment with p4-m3; MACN Pv SC3972, mandibular fragment with p4-m2.

Scleromys osbornianus. MACN Pv SC2771, mandibular fragment with m3; MACN Pv SC3434, mandibular fragment with p4-m2; MACN Pv SC3439, mandibular fragment with p4-m1; MACN Pv SC3440, mandibular fragment with p4-m2; MACN-A-10121; partial skull with left P4-M3 series.

Neoreomys australis. MACN-A-4349, a deformed skull with both P4-M3 series; MACN-A-4345-4350; mandibular and maxillary fragments bearing partial or completed p4-m3 and P4-M3 series in distinct ontogenetic stages; MACN-A-4320; partial skull with both P4-M3 series; MACN A 4318, a skull with complete dentition.

Prolagostomus pusillus. MLP-15-136, right maxillary with P4-M3;

Prolagostomus divisus. MLP-15-152, palates with both maxillaries bearing P4-M3; MLP-15-129, isolated upper molar.

Prolagostomus profluens. MLP-15-88, left mandibular fragment with p4-m3 series; MLP-15-65, right mandibular fragment with p4-m2.

Prolagostomus rosendoi. MLP-76-VIII-30-3, skull fragment with left P4-M3 and right P4-M2 series.

Alloiomys friasensis. MLP-15-416, almost complete skull with both P4-M3 series.

Maruchito trilofodonte. MLP 91-IV-1-29, MLP 91-IV-1-25, MLP 91-IV-1-26, MLP 91-1V-1-31, MLP 91-IX-1-33, MLP 91-IX-1-32, MLP 91-IX-1-23, and MLP 91-IX-1-25, isolated molariforms (some of them illustrated in Vucetich et al., 1993).

Electronic supplementary materials for: Late early Miocene mammals from the Laguna del Laja, Cura-Mallín Formation, south-central Chile (~37°S) and their biogeographical and paleoenvironmental significance

Supplementary File 1. List of the materials used for comparisons.

Luantus toldensis. MACN Pv SC2574 (Holotype), lower molar; MACN Pv SC4033, isolated p4.

Luantus propheticus. MACN A 2018 (Holotype), mandible with p4-m3; MACN Pv SC2072, isolated p4; MACN Pv SC2235, isolated p4; MACN Pv SC2871, isolated p4; MACN Pv SC3617, a fragment of mandible bearing p4-m3.

Galileomys antelucanus. MLP 82-V-2-105 (Holotype), left partial mandible with i and p4-m2.

Galileomys eurygnathus. MACN Pv SC2163 (Holotype), left mandibular fragment with p4-m2.

Phanomys mixtus. MACN A 11302 (Lectotype), maxillary fragment with P4-M2; MACN A 2022 (Neosyntype), nine isolated cheek teeth; MACN Pv SC3450, maxillary fragment with P4-M3.

Phanomys vetulus. MACN A 2024 (Syntype), nine isolated molariforms.

Neoreomys australis. MACN-A-4349, a deformed skull with both P4-M3 series; MACN-A-4345-4350; mandibular and maxillary fragments bearing partial or completed p4-m3 and P4-M3 series in distinct ontogenetic stages; MACN-A-4320; partial skull with both P4-M3 series; MACN A 4318, a skull with complete dentition.

Prolagostomus pusillus. MLP-15-136, right maxillary with P4-M3;

Prolagostomus divisus. MLP-15-152, palates with both maxillaries bearing P4-M3; MLP-15-129, isolated upper molar.

Prolagostomus profluens. MLP-15-88, left mandibular fragment with p4-m3 series; MLP-15-65, right mandibular fragment with p4-m2.

Prolagostomus rosendoi. MLP-76-VIII-30-3, skull fragment with left P4-M3 and right P4-M2 series.

Alloiomys friasensis. MLP-15-416, almost complete skull with both P4-M3 series.

Maruchito trilofodonte. MLP 91-IV-1-29, MLP 91-IV-1-25, MLP 91-IV-1-26, MLP 91-IV-1-31, MLP 91-IX-1-33, MLP 91-IX-1-32, MLP 91-IX-1-23, and MLP 91-IX-1-25, isolated molariforms (some of them illustrated in Vucetich et al., 1993).

Diadiaphorus majusculus. MLP 12-333, mandible.

Diadiaphorus? caniadensis. MACN Pv SC4241, mandible with m1–m3.

Lambdaconus lacerum. MACN A 52-247, mandible fragment with p3–m3.

Adinotherium ovinum. MACN A 5352 53, skull and mandible; MACN SC 4355, skull and mandible; MACN A 5353, mandible.

Nesodon imbricatus. MACN A 772, skull; MACN A 773, fragment of mandible; MACN A 774, skull; MACN A 775, mandible; MLP 12-3, skull and mandible; MLP 12-15, skull and mandible.

Hegetotherium mirabile. MACN A 631–632, Associated remains including right maxilla preserving I1–M3, where I1–2–3 and P1 are broken, and fragment of left I1; and partial left dentary bearing p2–m3; MLP 90-XII-24-35, mandibular fragment with m1–m3.

Hegetotherium novum. MACN Pv 11749, skull with right fragmented I1 and I3–M3 and left I2.

Pachyrukhos politus. MACN A 52-438. mandibular fragment with p2–m3; MACN A 52-439 mandibular fragment with p2–m2.

Pachyrukhos moyani. MACN-A 279 (holotype), upper molars P2–M3; MACN-A 276, upper molars P2-M3; MACN A 3314–3317, five mandibular rami.

Protypotherium sinclairi. PVPH 352 (holotype), partial right mandibular ramus with i2–m2; MLP 75-II-5-8, mandible with p3–m2.

Protypotherium australe. MACN-A-3884 (type), a mandibular symphysis and its right mandibular ramus.

Protherotherium attenuatum. MACN-A 524, left maxilla with P2–M3; MACN-A 628, right fragmented mandible with alveoli of i1–3 and the c (broken)–m1 series.

Protypotherium praerutilum. MACN-A 1081 (holotype), partial skull; MACN-A 1082, partial mandible bearing right i1-m3; MACN-A 1083, mandible bearing m1-3.

Protypotherium colloncurensis. MLP 91-IX-4-26 (holotype), skull fragmented in several pieces: hemipalates with right and left M1–3, part of basicranium and posterodorsal fragment of vault.

Protypotherium concepcionensis. SGO.PV.21000 ((holotype), well-preserved skull bearing all the teeth.

Protypotherium endiadys. MLP 12-2886 (holotype), skull with left I1–M3 and right P2–M3.

Protypotherium minutus. MLP-12-2176, incomplete maxillary and mandibles.

Protypotherium antiquum. ZMK 21/1877 (lectotype), right mandibular fragment with p4-m3.



Supplementary File 2. Dental measurements (in mm) of the upper and lower teeth of the taxa recovered from the Laguna del Laja and described in the main text. Bold letter indicates approximate values.

Taxon	Specimen	P3		P4		M1		M2		M3		p3		p4		m1/mf1		m2/mf2		m3/mf4		m4/mf4	
		L	W	L	W	L	W	L	W	L	W	L	W	L	W	L	W	L	W	L	W	L	W
<i>cf. Sipalocyon sp.</i>	MHNCCL PALEO-CS 65	-	-	-	-	-	-	-	-	-	-	-	-	-	-	3.9	-	-	-	-	-	-	-
<i>Palaeotheres intermedius</i>	MHNCCL PALEO-CS 66	-	-	-	-	-	-	-	-	-	-	-	-	1.9	-	3.7	1.9	2.2	-	1.9	-	1.6	-
<i>Galileomys antelucanus</i>	MHNCCL PALEO-CS 67	-	-	-	-	-	-	-	-	-	-	-	-	-	-	2.2	2	2.4	2.1	-	-	-	-
<i>Diadiaphorus majusculus</i>	MHNCCL PALEO-CS 68	-	-	-	-	-	-	-	-	-	-	-	-	14.7	8.2	-	-	-	-	18.4	8	-	-
<i>Diadiaphorus majusculus</i>	MHNCCL PALEO-CS 69	-	-	-	-	-	-	-	-	-	-	-	-	-	-	-	11.1	-	11.2	-	-	-	-
<i>Nesodon sp.</i>	MHNCCL PALEO-CS 71a	-	-	-	-	27.2	16.5	27.5	16.7	26.7	17.2	-	-	-	-	25.6	9.4	23	9.8	-	-	-	-
<i>Adinotherium sp.</i>	MHNCCL PALEO-CS 70	-	-	-	-	-	-	-	-	-	-	-	-	-	13.3	8	15.7	8	-	-	-	-	-
<i>Pachyrukhos sp. nov.?</i>	MHNCCL PALEO-CS 72	4.1	2.3	4.5	3.2	5.6	3.3	4.2	2.9	4.1	2.6	-	-	-	-	-	-	-	-	-	-	-	-
<i>Pachyrukhos sp. nov.?</i>	MHNCCL PALEO-CS 73	-	-	-	-	5.8	3.4	4.8	2.9	4.5	2.5	-	-	-	-	-	-	-	-	-	-	-	-
<i>Pachyrukhos sp. nov.?</i>	MHNCCL PALEO-CS 74	-	-	-	-	-	-	-	-	-	-	3.2	1.9	3.8	2.3	-	-	-	-	-	-	-	-
<i>Pachyrukhos sp. nov.?</i>	MHNCCL PALEO-CS 75	-	-	-	-	-	-	-	-	-	-	-	-	-	-	-	-	-	-	5.3	2.2	-	-
<i>Pachyrukhos sp. nov.?</i>	MHNCCL PALEO-CS 76	-	-	-	-	-	-	-	-	-	-	-	-	-	-	4.5	2	-	-	-	-	-	-
<i>Pachyrukhos sp. nov.?</i>	MHNCCL PALEO-CS 77	3.6	2.2	-	-	-	-	-	-	-	-	-	-	-	-	-	-	-	-	-	-	-	-
<i>Pachyrukhos sp. nov.?</i>	MHNCCL PALEO-CS 78	-	-	-	-	5.6	2.9	-	-	-	-	-	-	-	-	-	-	-	-	-	-	-	-
<i>Pachyrukhos sp. nov.?</i>	MHNCCL PALEO-CS 79	-	-	4.1	2.4	4.9	3	-	-	-	-	-	-	-	-	-	-	-	-	-	-	-	-
<i>Pachyrukhos sp. nov.?</i>	MHNCCL PALEO-CS 80	-	-	-	-	5.9	3.2	4.8	3	4.3	2.6	-	-	-	-	-	-	-	-	-	-	-	-
<i>Protypotherium cf. sinclairi</i>	MHNCCL PALEO-CS 81	-	-	-	-	-	-	-	-	-	-	4.3	2.5	4.3	2.5	5.8	3.6	6.2	2.9	-	-	-	-
<i>Protypotherium sp.</i>	MHNCCL PALEO-CS 82	-	-	-	-	-	-	-	-	-	-	4.7	3.1	-	-	6.8	3.3	6.5	3.4	7.6	3.4	-	-

<i>Protypotherium</i> sp.	MHNCCL PALEO-CS 83	-	-	-	-	-	-	9.1	5.1	-	-	-	-	-	-	-	-	-	-	-	-	-
<i>Protypotherium</i> sp.	MHNCCL PALEO-CS 84	-	-	-	-	-	-	-	-	-	-	-	-	-	-	-	6.9	3.1	-	-	-	-
<i>Protypotherium</i> sp.	MHNCCL PALEO-CS 85	-	-	-	-	-	-	-	-	-	3.4	1.7	4	-	5.5	-	-	-	-	-	-	-
<i>Hapalops</i> sp.	MHNCCL PALEO-CS 86	-	-	-	-	-	-	-	-	-	-	-	-	-	6.6	7.2	-	-	6.6	7.6	-	-



Electronic supplementary materials for: Evolutionary trends of body size and hypsodonty in notoungulates (Mammalia: Notoungulata) and its probable drivers.

Contents:

Table S1. Database for notoungulate fossil occurrences, mainly based on the PBDB⁵.

Table S2. Data on Toxodontia LMRL, SLML, and SUML measurements, body mass estimations and HI from the literature.

Table S3. Data on Typotheria LMRL, SLML, and SUML measurements, body mass estimations and HI from the literature.

Table S4. Database of LMRL, SLML, and SUML dental measurements (in mm) and body mass (in kg) of extant ungulates (n=138) from Mendoza et al. (2006).

Table S5. Results of the log-transformed bivariate ordinary least-squares (OLS) regressions performed on LMRL, SLML, and SUML (predictive variables) dental measurements and BM (response variable) of extant ungulates with a body mass lower than 75 kg (n=68) taken from the Mendoza et al. (2006) dataset.

Table S6. Summary of the data recovered from the literature and estimated using the methods described in the main text, including the taxonomic arrangement, body mass (BM) in Kg, natural logarithm of the BM (Log_{BM}), times of speciation (TS) and extinction (TE), hypsodonty categories (HI), paleocoordinates (P_Lng, P_Lat, P_Lat_2), and size category (Size) of each taxon. Abbreviations: Arhy, Archaeohyracidae; Arpi, Archaeopithecidae; B. Noto: basal notoungulate; B. Typo, basal typotheres; Hege, Hegetotheriidae; Henr, Henricosborniidae; Homa, Homalodtheriidae; Inte, Interatheriidae; Iso, Isotemnidae; Leo, Leontiniidae; Meso, Mesotheriidae; Noth, Notohippidae; Nots, Notostylopidae; Oldf, Oldfieldthomasiidae; Toxd, Toxodontidae; B, brachiodont, H, hypsodont; M, mesodont; EU, euhypsodont; VS, very small-sized; S, small-sized; M, medium-sized; L, large-sized; VL, very large-sized; G, giant-sized.

Table S7. Results of the evolutionary modes of BM performed with the package *PaleoTs* in different notoungulates clades.

Table S8. Results of the evolutionary modes of HI performed with the package *PaleoTs* in different notoungulates clades.

Table S9. Data used for GLS and model selection analyses (based on SSA taxa).

⁵Ver detalles de esta tabla en <https://doi.org/10.1016/j.palaeo.2021.110306>

Table S2. Data on Toxodontia LMRL, SLML, and SUML measurements, body mass estimations and HI from the literature.

Suborder	Family	Genus	Species	SALMA	LMRL	SUML	FLML	Source Measurements	BM (g) literature	Source BM	Hypsodonty index (HI)	Source HI	Hypsodonty	Hypsodonty values
Basal notoungulate	Basal notoungulate	<i>Perutherium</i>	<i>Perutherium altiplanense</i>	Itaboraian									brachiodont	0
Basal notoungulate	Basal notoungulate	<i>Satshatemnus</i>	<i>Satshatemnus bonapartei</i>	Itaborian	-	5.8	-	Soria, 1989					brachiodont	0
Basal notoungulate	Henricosborniidae	<i>Acamana</i>	<i>Acamana ambiguus</i>	Divisaderan									brachiodont	0
Basal notoungulate	Henricosborniidae	<i>Henricosbornia</i>	<i>Henricosbornia ampla</i>	Casamayoran				similar to <i>H. lophodonta</i> (Simpson 1948)					brachiodont	0
Basal notoungulate	Henricosborniidae	<i>Henricosbornia</i>	<i>Henricosbornia lophodonta</i>	Paso del Sapo/Casamayoran	18.6	5.5	5.6	Simpson 1948	0.4	Gomes Rodrigues et al., 2017			brachiodont	0
Basal notoungulate	Henricosborniidae	<i>Henricosbornia</i>	<i>Henricosbornia minuta</i>	Riochican				similar to <i>H. lophodonta</i> (Simpson 1948)					brachiodont	0
Basal notoungulate	Henricosborniidae	<i>Henricosbornia</i>	<i>Henricosbornia waitehor</i>	Riochican				similar to <i>H. lophodonta</i> (Simpson 1948)					brachiodont	0
Basal notoungulate	Henricosborniidae	<i>Orome</i>	<i>Orome deepi</i>	Itaboraian	-	7.16	-	Bauzá et al. 2019					brachiodont	0
Basal notoungulate	Henricosborniidae	<i>Othnielmarsha</i>	<i>Othnielmarsha curvicrista</i>	Casamayoran			5.6	Simpson 1948					brachiodont	0
Basal notoungulate	Henricosborniidae	<i>Othnielmarsha</i>	<i>Othnielmarsha lacunifera</i>	Paso del Sapo/Casamayoran	-	6.4	-	Simpson 1948					brachiodont	0
Basal notoungulate	Henricosborniidae	<i>Othnielmarsha</i>	<i>Othnielmarsha reflexa</i>	Casamayoran		7.1		Simpson 1948					brachiodont	0
Basal notoungulate	Henricosborniidae	<i>Peripantostyl</i>	<i>Peripantostyl ops minutus</i>	Vacan	13.7	4.4	4.1	Simpson 1948					brachiodont	0

Basal notoungulate	Henricosborniidae	<i>Peripantostyl ops</i>	<i>Peripantostyl ops orehor</i>	Riochican		5.1			Simpson 1948					brachiodont	0
Basal notoungulate	Henricosborniidae	<i>Simpsonotus</i>	<i>Simpsonotus major</i>	Itaboraian					comparable to Orome Bauzá et al. 2019					brachiodont	0
Basal notoungulate	Henricosborniidae	<i>Simpsonotus</i>	<i>Simpsonotus praecursor</i>	Itaboraian					double that S. praecursor (Pascual et al. 1978)	0.6	Gomez-Rodriguez et al. 2017			brachiodont	0
Toxodontia	Homalodtheriidae	<i>Asmodeus</i>	<i>Asmodeus osborni</i>	Deseadan		44.4			Gomez-Rodriguez et al. 2017	1785	Elissamburu 2012			brachiodont	0
Toxodontia	Homalodtheriidae	<i>Asmodeus</i>	<i>Asmodeus petrasnerus</i>	Deseadan					40% smaller than A. osborni (Hernández del Pino et al. 2017)	1785	Elissamburu 2012			brachiodont	0
Toxodontia	Homalodtheriidae	<i>Chasicotherium</i>	<i>Chasicotherium rothi</i>	Chasicoan		47	38		de Ringuélet, 1957					hypodont	2
Toxodontia	Homalodtheriidae	<i>Homalodotherium</i>	<i>Homalodotherium cunninghami</i>	Santacrucian	118	52.5	34		Scott 1912	1171.6	Elissamburu 2012			hypodont	2
Toxodontia	Homalodtheriidae	<i>Trigonolophodon</i>	<i>Trigonolophodon elegans</i>	Tinguirirican		30*			Estimated	1637	Elissamburu 2012			brachiodont	0
Toxodontia	Isotemnidae	<i>Anisotemnus</i>	<i>Anisotemnus distentus</i>	Casamayoran	40.9	24	23.2		Simpson 1967					brachiodont	0
Toxodontia	Isotemnidae	<i>Distylophorus</i>	<i>Distylophorus alouatinus</i>	Mustersan	68	-	19		Simpson 1967					brachiodont	0
Toxodontia	Isotemnidae	<i>Isotemnus</i>	<i>Isotemnus ctalego</i>	Itaborian		10.5			Simpson 1967					brachiodont	0
Toxodontia	Isotemnidae	<i>Isotemnus</i>	<i>Isotemnus haugi</i>	Riochican		13.5			Simpson 1967					brachiodont	0
Toxodontia	Isotemnidae	<i>Isotemnus</i>	<i>Isotemnus latidens</i>	Casamayoran		12	13		Simpson 1967					brachiodont	0
Toxodontia	Isotemnidae	<i>Isotemnus</i>	<i>Isotemnus primitivus</i>	Casamayoran		16	15.5		Simpson 1967					brachiodont	0
Toxodontia	Isotemnidae	<i>Pampatemnus</i>	<i>Pampatemnus deuterus</i>	Casamayoran	39.6	17.4	11		Vucetich and Bond 1982					brachiodont	0
Toxodontia	Isotemnidae	<i>Pampatemnus</i>	<i>Pampatemnus infernalis</i>	Casamayoran	43.7	17.25	12.4		Vucetich and Bond 1982					brachiodont	0

Toxodontia	Isotemnidae	<i>Periphragnis</i>	<i>Periphragnis circumflexus</i>	Mustersan			36.5	Simpson 1967	352	Elissamburu 2012			brachiodont	0
Toxodontia	Isotemnidae	<i>Periphragnis</i>	<i>Periphragnis exauctus</i>	Mustersan			26.8	Simpson 1967	352	Elissamburu 2012			brachiodont	0
Toxodontia	Isotemnidae	<i>Periphragnis</i>	<i>Periphragnis harmeri</i>	Mustersan	86	29.3	25.5	Simpson 1967	352	Elissamburu 2012			brachiodont	0
Toxodontia	Isotemnidae	<i>Periphragnis</i>	<i>Periphragnis palmeri</i>	Mustersan		29		Simpson 1967	352	Elissamburu 2012			brachiodont	0
Toxodontia	Isotemnidae	<i>Periphragnis</i>	<i>Periphragnis vicentei</i>	Tingirirican		31		Bradham et al., 2015	352	Elissamburu 2012			brachiodont	0
Toxodontia	Isotemnidae	<i>Pleurostylodon</i>	<i>Pleurostylodon modicus</i>	Casamayoran	-	18	13.3	Simpson 1967	53.47	Elissamburu 2012			brachiodont	0
Toxodontia	Isotemnidae	<i>Pleurostylodon</i>	<i>Pleurostylodon similis</i>	Casamayoran		17.9	15	Simpson 1967	53.47	Elissamburu 2012			brachiodont	0
Toxodontia	Isotemnidae	<i>Rhyphodon</i>	<i>Rhyphodon angusticephalus</i>	Mustersan		19		Simpson 1967					brachiodont	0
Toxodontia	Isotemnidae	<i>Rhyphodon</i>	<i>Rhyphodon lankesteri</i>	Mustersan	62.5	24	19	Simpson 1967					brachiodont	0
Toxodontia	Isotemnidae	<i>Thomashuxleya</i>	<i>Thomashuxleya externa</i>	Casamayoran	87	28.5	21	Simpson 1967	337.84	Elissamburu 2012			brachiodont	0
Toxodontia	Isotemnidae	<i>Thomashuxleya</i>	<i>Thomashuxleya rostrata</i>	Casamayoran	99.6	33	26	Simpson 1967	337.84	Elissamburu 2012			brachiodont	0
Toxodontia	Leontiniidae	<i>Anayatherium</i>	<i>Anayatherium ekacoa</i>	Deseadan	-	34.7		Shockey 2005					mesodont	1
Toxodontia	Leontiniidae	<i>Anayatherium</i>	<i>Anayatherium fortis</i>	Deseadan	-	48.2		Shockey 2005					mesodont	1
Toxodontia	Leontiniidae	<i>Ancylocoelus</i>	<i>Ancylocoelus frequens</i>	Deseadan	-		25.1	Similar size to <i>Anayatherium ekacoa</i> (shockey 2005)	443	Elissamburu 2012			mesodont	1
Toxodontia	Leontiniidae	<i>Colpodon</i>	<i>Colpodon antucoensis</i>	Santacruccian		34.4	26.6	Shockey et al. 2012	48.3; 316.62	Gomez PNAS; Elissamburu 2012			mesodont	1

Toxodontia	Leontiniidae	<i>Colpodon</i>	<i>Colpodon distinctus</i>	Colhuehuapian		29		Estimated	316.62	Elissamburu 2012			mesodont	1
Toxodontia	Leontiniidae	<i>Coquenia</i>	<i>Coquenia bondi</i>	Mustersan	86.6	27.6	19.8	Deraco et al. 2008					brachiodont	0
Toxodontia	Leontiniidae	<i>Elmerriggsia</i>	<i>Elmerriggsia fieldia</i>	Deseadan		37.6		Shockey et al. 2012					mesodont	1
Toxodontia	Leontiniidae	<i>Gualta</i>	<i>Gualta cuyana</i>	Deseadan	93.6	47.1	38.6	Cerdeño and Vera, 2015					brachiodont	0
Toxodontia	Leontiniidae	<i>Henricofilhola</i>	<i>Henricofilhola lustrata</i>	Deseadan				similar in size to <i>H. vucetichia</i> (Ribeiro et al. 2010)					brachiodont	0
Toxodontia	Leontiniidae	<i>Henricofilhola</i>	<i>Henricofilhola vucetichia</i>	Deseadan			20						brachiodont	0
Toxodontia	Leontiniidae	<i>Huilatherium</i>	<i>Huilatherium pluripicatum</i>	Laventan	140	54	44	Villaroel and Colwell 1997					mesodont	1
Toxodontia	Leontiniidae	<i>Leontinia</i>	<i>Leontinia gaudryi</i>	Deseadan		50		Ribeiro, 2015	285.1; 558.2	Gomes Rodriguez et al. 2017; Elissamburu 2012			mesodont	1
Toxodontia	Leontiniidae	<i>Martinmiguella</i>	<i>Martinmiguella fernandezi</i>	Mustersan		23		Bond y Lopez 1995					brachiodont	0
Toxodontia	Leontiniidae	<i>Scarrittia</i>	<i>Scarrittia barranquensis</i>	Deseadan	-	-	28.84031503	Ribeiro et al. 2010	1404.4	Elissamburu 2012			mesodont	1
Toxodontia	Leontiniidae	<i>Scarrittia</i>	<i>Scarrittia canquelensis</i>	Deseadan	121.9	-	36.4	Ubilla et al. 1994	1404.4	Elissamburu 2012			mesodont	1
Toxodontia	Leontiniidae	<i>Scarrittia</i>	<i>Scarrittia robusta</i>	Deseadan	133.4	-	35.2	Ubilla et al. 1994	1404.4	Elissamburu 2012			mesodont	1
Toxodontia	Leontiniidae	<i>Taubatherium</i>	<i>Taubatherium paulacoutoi</i>	Deseadan		35		Ribeiro, 2015					mesodont	1
Toxodontia	Leontiniidae	<i>Termastherium</i>	<i>Termastherium flacoensis</i>	Tingirirican	-	24.7	17.5	Wyss et al. 2018					brachiodont	0
Toxodontia	Notohippidae	<i>Argyrohippus</i>	<i>Argyrohippus boulei</i>	Colhuehuapian				similar to others spp. In genus	90.12	Elissamburu 2012	2.55	Madde n 2014	hypodont	2
Toxodontia	Notohippidae	<i>Argyrohippus</i>	<i>Argyrohippus fraterculus</i>	Colhuehuapian	56.8	17.9	15.4	Hernández Del Pino et al. 2019	22.21	Gomez PNAS	2.55	Shockey 1997	hypodont	2
Toxodontia	Notohippidae	<i>Argyrohippus</i>	<i>Argyrohippus praecox</i>	Deseadan	54.75	17.5	15.5	Patterson 1935	90.12	Elissamburu 2012	2.55	Madde n 2014	hypodont	2
Toxodontia	Notohippidae	<i>Coelostylodon</i>	<i>Coelostylodon</i>	Barrancan	-	8.5	-	Simpson 1970					brachiodont	0

			<i>caroloameghinoides</i>																
Toxodontia	Notohippidae	<i>Coelostylops</i>	<i>Coelostylops florentinoameghinoides</i>	Barrancan	-	12.6	-	Simpson 1970										brachiodont	0
Toxodontia	Notohippidae	<i>Coresodon</i>	<i>Coresodon scalpridens</i>	Deseadan	57	-	18	Lomis 1914										hypsodont	2
Toxodontia	Notohippidae	<i>Eomorphippus</i>	<i>Eomorphippus bondi</i>	Tinguirirican	70.4	20.8	20.4	Wyss et al. 2018	83.83	Elissamburu 2012								mesodont	1
Toxodontia	Notohippidae	<i>Eomorphippus</i>	<i>Eomorphippus neilopydykei</i>	Tinguirirican	-	-	10.2	Wyss et al. 2018	83.83	Elissamburu 2012								mesodont	1
Toxodontia	Notohippidae	<i>Eomorphippus</i>	<i>Eomorphippus obscurus</i>	Mustersan	-	16.3	13.1	Simpson 1967	83.83	Elissamburu 2012	1	Shockey 1997						mesodont	1
Toxodontia	Notohippidae	<i>Eurygenium</i>	<i>Eurygenium latirostris</i>	Deseadan	-	24.1	-	Marani and Dozo 2008			1.7	Madde n 2014						hypsodont	2
Toxodontia	Notohippidae	<i>Eurygenium</i>	<i>Eurygenium pacegnum</i>	Deseadan	-	23.6	-	Shockey 1997			1.8	Shockey 1997						hypsodont	2
Toxodontia	Notohippidae	<i>Mendozahippus</i>	<i>Mendozahippus fierensis</i>	Deseadan		22.1		Cerdeño and Vera 2010										brachiodont	0
Toxodontia	Notohippidae	<i>Moqueguahippus</i>	<i>Moqueguahippus glycisma</i>	Deseadan				slightly larger than <i>E. pacegnum</i> (shockey et al. 2006)										hypsodont	2
Toxodontia	Notohippidae	<i>Morphippus</i>	<i>Morphippus imbricatus</i>	Deseadan				similar in size to <i>Patagonhippus canterensis</i> (Lopez et al. 2010)	31; 97.8	Gomez PNAS; Elissamburu 2012	1.17	Madde n 2014						hypsodont	2
Toxodontia	Notohippidae	<i>Notohippus</i>	<i>Notohippus toxodontoides</i>	Santacruccian	51	17.2	12.9	Hernández Del Pino et al. 2019										hypsodont	2
Toxodontia	Notohippidae	<i>Pampahippus</i>	<i>Pampahippus arenalesi</i>	Casamayoran				de tamaño similar a <i>E. obscurus</i> (Bond and Lopez 1993)			0.54	Shockey 1997						brachiodont	0
Toxodontia	Notohippidae	<i>Pampahippus</i>	<i>Pampahippus powelli</i>	Casamayoran	70.19	19.23	21.1	García-López et al. 2018										brachiodont	0

Toxodontia	Notohippidae	<i>Pampahippus</i>	<i>Pampahippus secundus</i>	Casamayoran		11.9	6.6	Deraco and García-Lopez, 2016					brachiodont	0
Toxodontia	Notohippidae	<i>Pascualihippus</i>	<i>Pascualihippus boliviensis</i>	Deseadan		24.1		Shockey 1997			1.53	Shockey 1997	Hypsodont	2
Toxodontia	Notohippidae	<i>Patagonhippus</i>	<i>Patagonhippus canterensis</i>	Oligocene		24.3	18	Lopez et al. 2010			1.56	Madde n 2014	Hypsodont	2
Toxodontia	Notohippidae	<i>Patagonhippus</i>	<i>Patagonhippus dukei</i>	Oligocene			10	Lopez et al. 2010			1.56	Madde n 2014	Hypsodont	2
Toxodontia	Notohippidae	<i>Puelia</i>	<i>Puelia coarctatus</i>	Mustersan		11.5	8.5	Simpson 1967			0.86	Madde n 2014	brachiodont	0
Toxodontia	Notohippidae	<i>Puelia</i>	<i>Puelia plicata</i>	Mustersan/Tinguirirican		10		Simpson 1967			0.75	Madde n 2014	brachiodont	0
Toxodontia	Notohippidae	<i>Puelia</i>	<i>Puelia sigma</i>	Mustersan			8.6	Simpson 1967			0.86	Madde n 2014	brachiodont	0
Toxodontia	Notohippidae	<i>Rhynchippus</i>	<i>Rhynchippus brasiliensis</i>	Deseadan				25% más pequeño que R. equinus			1.4	Shockey 1997	hypsodont	2
Toxodontia	Notohippidae	<i>Rhynchippus</i>	<i>Rhynchippus equinus</i>	Deseadan		24.9		Martínez et al. 2016	99.67	Elissam buru 2012	1.56	Madde n 2014	hypsodont	2
Toxodontia	Notohippidae	<i>Rhynchippus</i>	<i>Rhynchippus pumilus</i>	Deseadan	38.8	14.8	9.8	Chaffee and Simpson, 1952	21.83	Elissam buru 2012	1.65	Shockey 1997	hypsodont	2
Toxodontia	Notohippidae	<i>Rosendo</i>	<i>Rosendo pascuali</i>	Tinguirirican	49.1	15.1	14.3	Wyss et al. 2018			0.72	Madde n 2014	brachiodont	0
Toxodontia	Notohippidae	<i>Trimerostephanos</i>	<i>Trimerostephanos coalitus</i>	Mustersan			14	Simpson 1967					brachiodont	0
Basal notoungulate	Notostylopidae	<i>Boreastylops</i>	<i>Boreastylops lumbrerensis</i>	Vacan	37.7	13.4	10.8	Vucetich 1980					brachiodont	0
Basal notoungulate	Notostylopidae	<i>Brandmayria</i>	<i>Brandmayria simpsoni</i>	Riochican									brachiodont	0
Basal notoungulate	Notostylopidae	<i>Chilestylops</i>	<i>Chilestylops davidsoni</i>	Tinguirirican		13.8		Bradham et al., 2015					brachiodont	0
Basal notoungulate	Notostylopidae	<i>Edvardotrouessartia</i>	<i>Edvardotrouessartia sola</i>	Paso del Sapó/Vacan			13.1	Simpson 1948					brachiodont	0
Basal notoungulate	Notostylopidae	<i>Homalostylops</i>	<i>Homalostylops atavus</i>	Itaborian	16		4.4	PAULA COUTO 1954	4.9	Elissam buru 2012			brachiodont	0
Basal notoungulate	Notostylopidae	<i>Homalostylops</i>	<i>Homalostylops parvus</i>	Paso del Sapó/Vacan		7.5	7.2	Simpson 1948	4.9	Elissam buru 2012	0.7	Stromberg et	brachiodont	0

Basal notoungulate	Notostylopidae	<i>Notostylops</i>	<i>Notostylops appressus</i>	Riochican/Vacan	-	7.3	Simpson 1948	11.9	Elissamburu 2012	0.5	al., 2013 estimated	brachiodont	0
Basal notoungulate	Notostylopidae	<i>Notostylops</i>	<i>Notostylops murinus</i>	Casamayoran	10	8.7	Simpson 1948	11.9	Elissamburu 2012	0.53	Stromberg et al., 2013	brachiodont	0
Basal notoungulate	Notostylopidae	<i>Notostylops</i>	<i>Notostylops pendens</i>	Vacan	10.6	8	Simpson 1948	11.9	Elissamburu 2012	0.61	Simpson 1948	brachiodont	0
Basal notoungulate	Notostylopidae	<i>Notostylops</i>	<i>Notostylops pigafettai</i>	Casamayoran			About the size of <i>N. murinus</i> . Simpson 1948	11.9	Elissamburu 2012	0.5	estimated	brachiodont	0
Basal notoungulate	Notostylopidae	<i>Otonia</i>	<i>Otonia muehlbergi</i>	Mustersan		12.5	Simpson 1948					brachiodont	0
Toxodontia	Toxodontidae	<i>Adinotherium</i>	<i>Adinotherium ovinum</i>	Santacrucian/Colloncuran	60	22	16	Scott 1912	100	Cassini et al. 2012		hypsodont	2
Toxodontia	Toxodontidae	<i>Alitoxodon</i>	<i>Alitoxodon vetustum</i>	Montehermosan	77.5	-	27	Roveretto 1914				euhypsodont	3
Toxodontia	Toxodontidae	<i>Calchaquitherium</i>	<i>Calchaquitherium mixtum</i>	Huayquerian	133.1	-	41	Nasif et al. 2000				euhypsodont	3
Toxodontia	Toxodontidae	<i>Dinotoxodon</i>	<i>Dinotoxodon paranensis</i>	Huayquerian	123.6	64.8	36.4	Schmidt 2013				euhypsodont	3
Toxodontia	Toxodontidae	<i>Falcontoxodon</i>	<i>Falcontoxodon aguilerai</i>	Late Pliocene/Early Pleistocene	146	51	43	Carrillo et al. 2018	796	Carrillo et al. 2018		euhypsodont	3
Toxodontia	Toxodontidae	<i>Gyrinodon</i>	<i>Gyrinodon quassus</i>	Huayquerian	142	55	39.5	Schmidt 2013				euhypsodont	3
Toxodontia	Toxodontidae	<i>Haplodontherium</i>	<i>Haplodontherium wildei</i>	Huayquerian	175.3	78	53	Schmidt 2013				euhypsodont	3
Toxodontia	Toxodontidae	<i>Hemixotodon</i>	<i>Hemixotodon chasicoensis</i>	Chasicoan		48.4	26	Sostillo 2019				euhypsodont	3
Toxodontia	Toxodontidae	<i>Hoffstetterius</i>	<i>Hoffstetterius imperator</i>	Huayquerian		55		Schmidt 2013				euhypsodont	3
Toxodontia	Toxodontidae	<i>Hyperoxotodon</i>	<i>Hyperoxotodon speciosus</i>	Santacrucian/Colloncuran	-	21		Schmidt 2013				euhypsodont	3
Toxodontia	Toxodontidae	<i>Hypsitherium</i>	<i>Hypsitherium bolivianum</i>	Chapadmalalan		14.5	11.6	Anaya and MacFadden 1995				euhypsodont	3

Toxodontia	Toxodontidae	<i>Mixotoxodon</i>	<i>Mixotoxodon larensis</i>	Pleistocene	177.2		53.7	Rincon 2011	3797	Elissamburu 2012				euhyposodont	3
Toxodontia	Toxodontidae	<i>Neotrigodon</i>	<i>Neotrigodon utoquineae</i>	Tortonian		50		Estimated after Spillman 1949						euhyposodont	3
Toxodontia	Toxodontidae	<i>Nesodon</i>	<i>Nesodon imbricatus</i>	Santacrucian/Colloncuran		46	31	Scott 1912	657-197	Cassini et al., 2012; Gomez PNAS	2.2	Croft et al. 2003		hypsodont	2
Toxodontia	Toxodontidae	<i>Nesodon</i>	<i>Nesodon taweretus</i>	Colhuehuapian/Santacrucian		42.6	33	Forasiepi et al. 2014						hypsodont	2
Toxodontia	Toxodontidae	<i>Nonotherium</i>	<i>Nonotherium hennigi</i>	Early Pliocene		52		Castellanos 1942						euhyposodont	3
Toxodontia	Toxodontidae	<i>Ocnerotherium</i>	<i>Ocnerotherium intermedium</i>	Chasicosan		64		Schmidt 2013						euhyposodont	3
Toxodontia	Toxodontidae	<i>Palyeidodon</i>	<i>Palyeidodon obtusum</i>	Santacrucian/Colloncuran		53.9		Schmidt 2013						euhyposodont	3
Toxodontia	Toxodontidae	<i>Paratrigodon</i>	<i>Paratrigodon euguii</i>	Chasicosan		60		Schmidt 2013						euhyposodont	3
Toxodontia	Toxodontidae	<i>Pericotoxodon</i>	<i>Pericotoxodon platignathus</i>	Laventan	110.7	53.3	32.4	Madden 1997						euhyposodont	3
Toxodontia	Toxodontidae	<i>Piauhyaerium</i>	<i>Piauhyaerium capivarae</i>	Late Pleistocene		70.5	54	Guérin and Faure 2013						euhyposodont	3
Toxodontia	Toxodontidae	<i>Pisanodon</i>	<i>Pisanodon nazari</i>	Chasicosan		40.2	1	Sostillo 2019						euhyposodont	3
Toxodontia	Toxodontidae	<i>Plesiotoxodon</i>	<i>Plesiotoxodon amazonensis</i>	Tortonian		44		Ribeiro et al. 2013						euhyposodont	3
Toxodontia	Toxodontidae	<i>Posnanskytherium</i>	<i>Posnanskytherium desaguaderoi</i>	Chapadmalalan	80.8	33	23.9	Anaya and MacFadden 1995						euhyposodont	3
Toxodontia	Toxodontidae	<i>Posnanskytherium</i>	<i>Posnanskytherium inchasense</i>	Chapadmalalan	89.7	41.8	26.7	Anaya and MacFadden 1995						euhyposodont	3
Toxodontia	Toxodontidae	<i>Proadinothierium</i>	<i>Proadinothierium leptognathus</i>	Deseadan		25		Lomis 1914	103.7	Elissamburu 2012	1.98	Wilson et al. 2012		hypsodont	2
Toxodontia	Toxodontidae	<i>Proadinothierium</i>	<i>Proadinothierium muensteri</i>	Colhuehuapian		34.5		Hernández Del Pino, 2018	103.7	Elissamburu 2012	3.67	Wilson et al. 2012		hypsodont	2
Toxodontia	Toxodontidae	<i>Proadinothierium</i>	<i>Proadinothierium saltoni</i>	Deseadan	52.5	-	12.6	Shockley and Anaya 2008	103.7	Elissamburu 2012				brachiodont	0

Toxodontia	Toxodontidae	<i>Stenotephanos</i>	<i>Stenotephanos plicidens</i>	Huayquerian	-	39.5	28.14	Schmidt 2013					euhypsodont	3
Toxodontia	Toxodontidae	<i>Toxodon</i>	<i>Toxodon burmeisteri</i>	Lujanian				similar a otros toxodon	1790	Elissamburu 2012			euhypsodont	3
Toxodontia	Toxodontidae	<i>Toxodon</i>	<i>Toxodon chapalmalensis</i>	Montehermosan				similar a otros toxodon	1790	Elissamburu 2012			euhypsodont	3
Toxodontia	Toxodontidae	<i>Toxodon</i>	<i>Toxodon gracilis</i>	Late Pleistocene			30	Ameguino 1887	1790	Elissamburu 2012			euhypsodont	3
Toxodontia	Toxodontidae	<i>Toxodon</i>	<i>Toxodon platensis</i>	Lujanian		73.5	52	Guérin and Faure 2013	1790	Elissamburu 2012			euhypsodont	3
Toxodontia	Toxodontidae	<i>Trigodon</i>	<i>Trigodon gaudryi</i>	Montehermosan	181		58	Ameguino 1887	600-800	Croft, 2016			euhypsodont	3
Toxodontia	Toxodontidae	<i>Trigodon</i>	<i>Trigodonops lopesi</i>	Tortonian		32.8	18	Mendoza 2007	1809	Elissamburu 2012			euhypsodont	3
Toxodontia	Toxodontidae	<i>Xotodon</i>	<i>Xotodon ambrosetti</i>	Montehermosan	81.7		24.64	Armella et al. 2018	625	Elissamburu 2012			euhypsodont	3
Toxodontia	Toxodontidae	<i>Xotodon</i>	<i>Xotodon caravela</i>	Late Miocene	98.74	38.7	30.6	Armella et al. 2018	625	Elissamburu 2012			euhypsodont	3
Toxodontia	Toxodontidae	<i>Xotodon</i>	<i>Xotodon doellojuradoi</i>	Huayquerian	87.6		26.75	Armella et al. 2018	625	Elissamburu 2012			euhypsodont	3
Toxodontia	Toxodontidae	<i>Xotodon</i>	<i>Xotodon foricurvatus</i>	Huayquerian	94.9	30.89	26.65	Armella et al. 2018	625	Elissamburu 2012			euhypsodont	3
Toxodontia	Toxodontidae	<i>Xotodon</i>	<i>Xotodon maimarensis</i>	Montehermosan	86.2		25.7	Armella et al. 2018	625	Elissamburu 2012			euhypsodont	3

Table S3. Data on Typotheria LMRL, SLML, and SUML measurements, body mass estimations and HI from the literature.

Sub order	Family	Genus	Species	SALMA	LMRL	SUML	FLML	Source Measurements	BM (g) literature	Source BM	HI	Source HI	Hypsodonty	Hypsodonty values
Typotheria	Basal Typotheria	<i>Acoelohyrax</i>	<i>Acoelohyrax complicatissimus</i>	Casamayoran		13.6		Simpson 1967					brachiodont	0
Typotheria	Basal Typotheria	<i>Acoelohyrax</i>	<i>Acoelohyrax coronatus</i>	Casamayoran		10.9		Simpson 1967					brachiodont	0
Typotheria	Unnamed family	<i>Allalmeia</i>	<i>Allalmeia atalaensis</i>	Vacambarrancan	-	7	5.1	Lorente et al. 2014	2786	Lorente et al. 2014			brachiodont	0
Typotheria	Mesotheriidae	<i>Altitypothierium</i>	<i>Altitypothierium chucalensis</i>	Santacrucian	34.4	12.9	10.4	Croft et al. 2004					Hypsodont	2
Typotheria	Mesotheriidae	<i>Altitypothierium</i>	<i>Altitypothierium paucidens</i>	Santacrucian	38	12.8	10.8	Croft et al. 2004					Hypsodont	2
Typotheria	Interatheriidae	<i>Antepithecus</i>	<i>Antepithecus brachystephanus</i>	Barrancan	15.9	5.6	4.6	Vera and Cerdeño 2014			0.45	Stromberg et al., 2013	brachiodont	0
Typotheria	Interatheriidae	<i>Antofagastia</i>	<i>Antofagastia turneri</i>	Mustersan	-	4.17	-	García-López and Babot 2015	-	-	-	-	brachiodont	0
Typotheria	Archaeohyracidae	<i>Archaeohyrax</i>	<i>Archaeohyrax patagonicus</i>	Deseadan	36.1	13.3	10.2	Reguero 1998	2.817	Reguero et al. 2010	2.74	Reguero et al. 2010	hypselenodont	3
Typotheria	Archaeohyracidae	<i>Archaeohyrax</i>	<i>Archaeohyrax suniensis</i>	Deseadan	34.6	11.1	9.4	Billet et al. 2009	-	-	2.5	Reguero et al. 2010	Hypsodont	2
Typotheria	Interatheriidae	<i>Archaeophylus</i>	<i>Archaeophylus patrius</i>	Deseadan	-	4.2	3.6	Vera et al. 2017			2.1	Reguero et al. 2010	Hypsodont	2
Typotheria	Archaeopitheciidae	<i>Archaeopithecus</i>	<i>Archaeopithecus rogeri</i>	Riochican-Mustersan (ACTUALIZAR)	16.1	5.7	5	Vera 2017					brachiodont	0
Typotheria	Archaeohyracidae	<i>Archaeotypotherium</i>	<i>Archaeotypotherium pattersoni</i>	Tinguirirican	32	10.3	8.8	Croft et al. 2003	-	-	1.5	Croft et al. 2003	Hypsodont	2
Typotheria	Archaeohyracidae	<i>Archaeotypotherium</i>	<i>Archaeotypotherium propheticus</i>	Tinguirirican	38.1	12.2	11.8	Croft et al. 2003	4.285	Reguero et al. 2010	1.5	Reguero et al. 2010	Hypsodont	2

Typotheria	Archaeohyracidae	<i>Archaeotypotherium</i>	<i>Archaeotypotherium tinguiriricaense</i>	Tinguirirican	32.1	10.6	9.3	Croft et al. 2003	-	-	1.5	Stromberg et al., 2013	Hypsodont	2
Typotheria	Interatheriidae	<i>Argyrohyrax</i>	<i>Argyrohyrax proavus</i>	Deseadan	20.5	7.2	7.1	Vera et al. 2017	-	-	2.1	Stromberg et al., 2013	Hypsodont	2
Typotheria	Unnamed family	<i>Brachystephanus</i>	<i>Brachystephanus postremus</i>	Vacant-Barrancan	15.6	6	4.7	Simpson et al. 1962	-	-			brachiodont	0
Typotheria	Interatheriidae	<i>Brucemacfadden</i>	<i>Brucemacfaddenia boliviensis</i>	Deseadan	19.4	7.1	6.7	Hitz et al. 2008	-	-	-	-	hypselodont	3
Typotheria	Interatheriidae	<i>Caenophilus</i>	<i>Caenophilus tripartitus</i>	Colloncuran-Laventan?	-	-	6.7	Vera et al. 2019	-	-	-	-	NA	NA
Typotheria	Basal Typotheria	<i>Campanorco</i>	<i>Campanorco inauguralis</i>	Vacant	-	-	-	-	1.665	Reguero et al. 2010	0.75	Reguero et al. 2010	brachiodont	0
Typotheria	Mesotheriidae	<i>Caraguatypotherium</i>	<i>Caraguatypotherium munozii</i>	Tortonian	46.3	16.1	14.3	Flynn et al. 2005					Hypsodont	2
Typotheria	Interatheriidae	<i>Cochilius</i>	<i>Cochilius fumensis</i>	Deseadan	15.8	5.6	4.8	Reguero 1998			2.3	* estimated after Simpson 1932	Hypsodont	2
Typotheria	Interatheriidae	<i>Cochilius</i>	<i>Cochilius volvens</i>	Colhuehuapian	-	-	5.5	Wilson et al. 2012	2.437	Wilson et al. 2012	2.49	Reguero et al. 2010	Hypsodont	2
Typotheria	Oldfieldthomasiidae	<i>Colbertia</i>	<i>Colbertia lumbrense</i>	Casamayoran	-	8.5	-	Simpson 1967 (ESTIMATED)					brachiodont	0
Typotheria	Oldfieldthomasiidae	<i>Colbertia</i>	<i>Colbertia magellanica</i>	Itaboraian	-	9	7.6	Paula Couto 1952					brachiodont	0
Typotheria	Oldfieldthomasiidae	<i>Dolichostylodon</i>	<i>Dolichostylodon saltensis</i>	Vacant-Barrancan	-	7.05	5.45	García López and Powell 2009					brachiodont	0
Typotheria	Archaeohyracidae	<i>Eohyrax</i>	<i>Eohyrax isotemnoides</i>	Barrancan	30.8	9	8.3	Reguero et al. 2008	2100	Gomes Rodrigues et al. 2017 (PNAS)	1.28	Stromberg et al., 2013	Hypsodont	2
Typotheria	Archaeohyracidae	<i>Eohyrax</i>	<i>Eohyrax praeustus</i>	Riochican	-	-	7	Simpson 1967	1400	Gomes Rodrigues et al. 2017 (PNAS)	1.2	Croft et al. 2003	Hypsodont	2
Typotheria	Archaeohyracidae	<i>Eohyrax</i>	<i>Eohyrax rusticus</i>	Barrancan-Mustersan	-	-	7.7	Simpson 1967	-	-	1.25	Stromberg et al., 2013	Hypsodont	2

Typotheriina	Interatheriidae	<i>Eopachyrucos</i>	<i>Eopachyrucos pliciformis</i>	Tinguirirican	-	-	4.1	Reguero 1998	-	-	1.58	Reguero et al. 2003	Hypodont	2
Typotheriina	Interatheriidae	<i>Eopachyrucos</i>	<i>Eopachyrucos ranchoverdensis</i>	Deseadan	23.7*	-	8.7	Reguero et al. 2003	-	-	1.25	Reguero et al. 2003	Hypodont	2
Typotheriina	Mesotheriidae	<i>Eotypotherium</i>	<i>Eotypotherium chico</i>	Santacrucian	-	9.6	9.6	Croft et al. 2004			2	Reguero et al. 2010	Hypodont	2
Typotheriina	Hegetotheriidae	<i>Ethegotherium</i>	<i>Ethegotherium careiiei</i>	Santacrucian	18	-	5.1	Lopez 2002; López and Manassero, 2008					hypodont	3
Typotheriina	Mesotheriidae	<i>Eutrachytherus</i>	<i>Eutrachytherus modestus</i>	Santacrucian-Colloncuran	-	12	-	Garrido et al. 2014					Hypodont	2
Typotheriina	Mesotheriidae	<i>Eutypotherium</i>	<i>Eutypotherium lehmannitschei</i>	Friasiense o Colloncurense	-	-	11.25	Fernández García 2018			2.03	Reguero et al. 2010	Hypodont	2
Typotheriina	Interatheriidae	<i>Federicoanaya</i>	<i>Federicoanaya sallaensis</i>	Deseadan	18.3	6	5.3	Hitz et al. 2008	-	-	-	-	hypselodont	3
Typotheriina	Basal Typotheriina	<i>Griphotherion</i>	<i>Griphotherion peiranoi</i>	Vacan-Barrancan	18.1	6.56	4.34	García López & Powell 2011					brachiodont	0
Typotheriina	Interatheriidae	<i>Guilielmoscottia</i>	<i>Guilielmoscottia plicifera</i>	Paso del Sapo (ACTUALIZAR)	18.7	5.9	6	Vera 2013			0.86	Stromberg et al., 2013	brachiodont	0
Typotheriina	Hegetotheriidae	<i>Hegetotheriopsis</i>	<i>Hegetotheriopsis sulcatus</i>	Colhuehuapian-Deseadean	23.2	8.2	7.6	Kramarz and Paz 2013	-	-	3	Kramarz and Paz 2013	hypselodont	3
Typotheriina	Hegetotheriidae	<i>Hegetotherium</i>	<i>Hegetotherium cerdasensis</i>	Colloncuran-Tortonian?	18	-	5.7	Croft et al. 2016	-	-	-	-	Hypodont	3
Typotheriina	Hegetotheriidae	<i>Hegetotherium</i>	<i>Hegetotherium mirabile</i>	Santacrucian-Colloncuran	24.4	7.3	7.7	Seoane and Cerdeño 2019	2190	Reguero et al. 2010	2.42	Reguero et al. 2010	Hypodont	3
Typotheriina	Hegetotheriidae	<i>Hegetotherium</i>	<i>Hegetotherium novum</i>	Colhuehuapian	-	8.6	-	Seoane and Cerdeño 2019	-	-	-	-	Hypodont	2
Typotheriina	Hegetotheriidae	<i>Hemihegetotherium</i>	<i>Hemihegetotherium achataleptum</i>	Huayquerian	40		12	Vera 2019	13681	Reguero et al. 2010	1.81	Reguero et al. 2010	Hypodont	3
Typotheriina	Hegetotheriidae	<i>Hemihegetotherium</i>	<i>Hemihegetotherium lazai</i>	Huayquerian	-	-	8.4	Vera 2019	-	-	-	-	hypselodont	3

Typotheria	Hegetotheriidae	<i>Hemihegetotherium</i>	<i>Hemihegetotherium tantillum</i>	Colloncuran-Mayoan	24.8	8.6	7.4	Vera 2019	-	-	-	-	hypselodont	3
Typotheria	Hegetotheriidae	<i>Hemihegetotherium</i>	<i>Hemihegetotherium torresi</i>	Chasicoan-Huayquerian	-	8.5	-	Vera 2019	-	-	3.61	Reguero et al. 2010	hypselodont	3
Typotheria	Hegetotheriidae	<i>Hemihegetotherium</i>	<i>Hemihegetotherium trilobus</i>	Laventan	30.1	9.9	8.9	Vera 2019	-	-	-	-	hypselodont	3
Typotheria	Interatheriidae	<i>Ignigena</i>	<i>Ignigena minisculus</i>	Casamayoran	-	3.95	-	Hitz et al. 2006	-	-	0.79	Hitz et al. 2006	brachiodont	0
Typotheria	Interatheriidae	<i>Interatherium</i>	<i>Interatherium excavatum</i>	Santacrucian	-	4	-	Sinclair 1909					hypselodont	3
Typotheria	Interatheriidae	<i>Interatherium</i>	<i>Interatherium extensum</i>	Santacrucian	-	4.8	-	Sinclair 1909					hypselodont	3
Typotheria	Interatheriidae	<i>Interatherium</i>	<i>Interatherium robustum</i>	Santacrucian	-	4.6	4.5	Sinclair 1909					hypselodont	3
Typotheria	Interatheriidae	<i>Interatherium</i>	<i>Interatherium rodens</i>	Santacrucian	23	-	4	Sinclair 1909			2.94		hypselodont	3
Typotheria	Oldfieldthomasiidae	<i>Itaboraitherium</i>	<i>Itaboraitherium atavum</i>	Itaborian	-	-	3.9	Line and Bergqvist 2005					brachiodont	0
Typotheria	Interatheriidae	<i>Johnbell</i>	<i>Johnbell hatcheri</i>	Tinguirirican	-	3.83	3.53	Hitz et al. 2006	-	-	0.86	Hitz et al. 2006	brachiodont	0
Typotheria	Interatheriidae	<i>Juchuysillu</i>	<i>Juchuysillu arenalesensis</i>	Langhian	15.6	4.9	5.6	Croft and Anaya 2020	-	-	-	-	hypselodont	3
Typotheria	Oldfieldthomasiidae	<i>Kibenikhoria</i>	<i>Kibenikhoria get</i>	Riochican	-	7	-	Simpson 1967 (ESTIMATED)					brachiodont	0
Typotheria	Oldfieldthomasiidae	<i>Maxschlosseria</i>	<i>Maxschlosseria praeterita</i>	Casamayoran-Vacan	-	8.1	-	Simpson 1967			0.67	Madden 2014	brachiodont	0
Typotheria	Hegetotheriidae	<i>Medistylus</i>	<i>Medistylus dorsatus</i>	Deseadan	-	5.6	-	Reguero et al. 2007	-	-	2.41	Reguero et al. 2007	Hypodont	2
Typotheria	Mesotheriidae	<i>Mesotherium</i>	<i>Mesotherium cristatum</i>	Ensenadan	-	23.3	14.7	Fernández García 2018			2.02	Reguero et al. 2010	Hypodont	2

Typotheriina	Mesotheriidae	<i>Microtypotherium</i>	<i>Microtypotherium choquecotense</i>	Colloncuran-Friasian	-	14.4	-	Fernández García 2018			2.2	Reguero et al. 2010	Hypodont	2
Typotheriina	Interatheriidae	<i>Miocochilius</i>	<i>Miocochilius anomopodus</i>	Laventan	28	-	8.75	Wilson et al. 2012	10621.003	Wilson et al. 2012	2.47	Reguero et al. 2010	Hypodont	2
Typotheriina	Interatheriidae	<i>Miocochilius</i>	<i>Miocochilius federicoi</i>	Laventan	-	6.4	-	Croft 2007			2.3	Croft 2007	Hypodont	2
Typotheriina	Interatheriidae	<i>Munizia</i>	<i>Munizia paranensis</i>	Huayquerian	-	4.8	-	Schmidt 2013					hypodont	2
Typotheriina	Interatheriidae	<i>Notopithecus</i>	<i>Notopithecus adapinus</i>	Barrancan	16.4	5	5.1	Vera 2013			0.69	Wilson et al. 2012	brachiodont	0
Typotheriina	Oldfieldthomasiidae	<i>Oldfieldthomasia</i>	<i>Oldfieldthomasia anfractuosa</i>	Casamayoran	-	9	-	Simpson 1967			0.4	Reguero et al. 2010	brachiodont	0
Typotheriina	Oldfieldthomasiidae	<i>Oldfieldthomasia</i>	<i>Oldfieldthomasia debilitata</i>	Casamayoran	-	8.3	-	Simpson 1967			0.4	Reguero et al. 2010	brachiodont	0
Typotheriina	Oldfieldthomasiidae	<i>Oldfieldthomasia</i>	<i>Oldfieldthomasia parvidens</i>	Casamayoran	-	7	-	Simpson 1967			0.4	Reguero et al. 2010	brachiodont	0
Typotheriina	Hegetotheriidae	<i>Pachyrukhos</i>	<i>Pachyrukhos moyani</i>	Santacrucian-Colloncuran	14.1	4.5	4.6	Seoane and Cerdeño 2019	1770	Elissamburu 2012	3.52	Reguero et al. 2007	hypsodont	3
Typotheriina	Hegetotheriidae	<i>Pachyrukhos</i>	<i>Pachyrukhos politus</i>	Colhuehuapian	14	-	4.3	Seoane and Cerdeño 2019	-	-	3.5	Estimated	hypsodont	3
Typotheriina	Hegetotheriidae	<i>Paedotherium</i>	<i>Paedotherium bonaerense</i>	Montehermosa n-Marplatan	15	5.07	5.3	Cerdeño and Bond 1999	2030	Elissamburu 2012	4.1	Reguero et al. 2015	hypsodont	3
Typotheriina	Hegetotheriidae	<i>Paedotherium</i>	<i>Paedotherium kakai</i>	Huayquerian	14.8	-	4.43	Reguero et al. 2015	-	-	2.61	Reguero et al. 2015	hypsodont	3
Typotheriina	Hegetotheriidae	<i>Paedotherium</i>	<i>Paedotherium minor</i>	Chasicoan-Huayquerian	14	5.31	4.24	Cerdeño and Bond 1999	-	-	4	Estimated	hypsodont	3
Typotheriina	Hegetotheriidae	<i>Paedotherium</i>	<i>Paedotherium typicum</i>	Montehermosa n-Marplatan	14.6	5.98	4.82	Cerdeño and Bond 1999	1820	-	4.06	Reguero et al. 2015	hypsodont	3
Typotheriina	Oldfieldthomasiidae	<i>Paginula</i>	<i>Paginula parca</i>	Vacan	-	-	4.2	Simpson 1967					brachiodont	0

Typotheriina	Interatheriidae	<i>Patriarchus</i>	<i>Patriarchus palmidens</i>	Santacrucean				slightly smaller (ca. 15%) than <i>Miocochilius</i> , but slightly larger than <i>Protypotherium</i> (ca. 10% compared with <i>P. australe</i>)			-		Hypodont	2
Typotheriina	Mesotheriidae	<i>Plesiotypotherium</i>	<i>Plesiotypotherium achirensense</i>	Mayoan-Chasicooan	-	16.4	10.9	Fernández García 2018	72.42	Fernández García 2018	2.12	Reguero et al. 2010	Hypodont	2
Typotheriina	Mesotheriidae	<i>Pseudotypotherium</i>	<i>Plesiotypotherium casirensense</i>	Montehermosana	-	20	13	Fernández García 2018					Hypodont	2
Typotheriina	Mesotheriidae	<i>Plesiotypotherium</i>	<i>Plesiotypotherium minus</i>	Friasian Laventan	-	12.8	8.1	Fernández García 2018					Hypodont	2
Typotheriina	Interatheriidae	<i>Proargyrohyrax</i>	<i>Proargyrohyrax curanderensis</i>	Tinguirirican	-	7.9	7.6	Hitz et al. 2000			1.2	Stromberg et al., 2013	Hypodont	2
Typotheriina	Interatheriidae	<i>Progaleopithecus</i>	<i>Progaleopithecus fissurellatus</i>	Deseadan	-	-	3.5	Vera et al. 2017b	-	-	-	-	Hypodont	2
Typotheriina	Interatheriidae	<i>Progaleopithecus</i>	<i>Progaleopithecus tournoueri</i>	Deseadan	16.7	5.4	5.4	Vera et al. 2017b	-	-	1.9	Stromberg et al., 2013	Hypodont	2
Typotheriina	Hegetotheriidae	<i>Prohegetotherium</i>	<i>Prohegetotherium malalhuense</i>	Deseadan	18.8	5.5	6.5	Cerdeño and Reguero 2015	-	-	-	-	Hypodont	2
Typotheriina	Hegetotheriidae	<i>Prohegetotherium</i>	<i>Prohegetotherium schiaffinoi</i>	Deseadan	19.1	7.7	6.9	Reguero and Cerdeño 2005	1178	Reguero et al. 2010	2.2	Reguero et al. 2010	Hypodont	2
Typotheriina	Hegetotheriidae	<i>Prohegetotherium</i>	<i>Prohegetotherium sculptum</i>	Deseadan	24.4	8.2	8	Reguero and Cerdeño 2005	-	-	2.23	Reguero et al. 2007	Hypodont	2
Typotheriina	Hegetotheriidae	<i>Propachyrucos</i>	<i>Propachyrucos crassus</i>	Deseadan	-	-	7	Reguero 1998	-	-	-	-	Hypodont	2
Typotheriina	Hegetotheriidae	<i>Propachyrucos</i>	<i>Propachyrucos smithwoodwardii</i>	Deseadan	13.4	-	4.6	Seoane et al. 2019	-	-	2.5	Reguero et al. 2007	Hypodont	2
Typotheriina	Hegetotheriidae	<i>Prosotherium</i>	<i>Prosotherium garzoni</i>	Deseadan	19	6.2	6.4	Seoane et al. 2019	1980	Elissamburu 2012	2.72	Reguero et al. 2007	Hypodont	2
Typotheriina	Archaeohyracidae	<i>Protarchaeohyrax</i>	<i>Protarchaeohyrax gracilis</i>	Tinguirirican-La Cantera	20.7	7.5	8	Reguero et al. 2003	1125	Reguero et al. 2010	1.73	Reguero et al. 2010	Hypodont	2

Typotheria	Archaeohyracidae	<i>Protarchaeohyrax</i>	<i>Protarchaeohyrax intermedium</i>	Tinguirirican	17	5.4	4.7	Reguero et al. 2003	-	-	1.7	Stromberg et al., 2013	Hypodont	2
Typotheria	Archaeohyracidae	<i>Protarchaeohyrax</i>	<i>Protarchaeohyrax minor</i>	Tinguirirican	-	5.2	-	Reguero et al. 2003	-	-	1.7	Stromberg et al., 2013	Hypodont	2
Typotheria	Interatheriidae	<i>Protypotherium</i>	<i>Protypotherium antiquum</i>	Huayquerian	-	-	7.8	Wilson et al. 2012					Hypodont	2
Typotheria	Interatheriidae	<i>Protypotherium</i>	<i>Protypotherium attenuatum</i>	Santacrucian	17.2	6	5.9	MACN 627,628,630			2.34	Estimated	Hypodont	2
Typotheria	Interatheriidae	<i>Protypotherium</i>	<i>Protypotherium australe</i>	Santacrucian	24.4	-	9.5	Wilson et al. 2012	2817	Reguero et al. 2010	2.34	Reguero et al. 2010	Hypodont	2
Typotheria	Interatheriidae	<i>Protypotherium</i>	<i>Protypotherium colloncurensis</i>	Colloncuran	28.2	8.1	8.4	Vera et al. 2017					Hypodont	2
Typotheria	Interatheriidae	<i>Protypotherium</i>	<i>Protypotherium concepcionensis</i>	Mayoan	-	8.1	-	Solórzano et al. 2019					Hypodont	2
Typotheria	Interatheriidae	<i>Protypotherium</i>	<i>Protypotherium diastematum</i>	Santacrucian	-	-	7.4	equal in size to P. Praerutilum sensu Scot 1912					Hypodont	2
Typotheria	Interatheriidae	<i>Protypotherium</i>	<i>Protypotherium distinctum</i>	Chasicooan	-	8.5	-	Vera et al. 2017					Hypodont	2
Typotheria	Interatheriidae	<i>Protypotherium</i>	<i>Protypotherium endiadyds</i>	Colloncuran	19.7	6.3	6.4	Vera et al. 2017					Hypodont	2
Typotheria	Interatheriidae	<i>Protypotherium</i>	<i>Protypotherium minutum</i>	Chasicooan	-	5	-	Vera et al. 2017					Hypodont	2
Typotheria	Interatheriidae	<i>Protypotherium</i>	<i>Protypotherium praerutilum</i>	Santacrucian	-	-	7.4	Wilson et al. 2012			2.34	Estimated	Hypodont	2
Typotheria	Interatheriidae	<i>Protypotherium</i>	<i>Protypotherium sinclairi</i>	Colhuehuapian	-	-	7.5	Kramarz et al. 2015					Hypodont	2
Typotheria	Archaeohyracidae	<i>Pseudhyrax</i>	<i>Pseudhyrax eutrachytheroideus</i>	Mustersan/Tinguirirican	33.5	10.8	9.21	Croft et al. 2003; Reguero et al. 2008	3825	Reguero et al. 2010	1.6	Reguero et al. 2010	Hypodont	2
Typotheria	Archaeohyracidae	<i>Pseudhyrax</i>	<i>Pseudhyrax strangulatus</i>	Mustersan/Tinguirirican	-	-	7.2	Croft et al. 2003	-	-	1.6	Stromberg et al., 2013	Hypodont	2

Typotheria	Mesotheriidae	<i>Pseudotyoptherium</i>	<i>Pseudotyoptherium insigne</i>	Montehermosa n	-	-	19.8	Fernández García 2018						Hypodont	2
Typotheria	Mesotheriidae	<i>Pseudotyoptherium</i>	<i>Pseudotyoptherium maendrum</i>	Montehermosa n	-	22.7	14.1	Fernández García 2018	93.8	Fernández García 2018	2.1	Reguero et al. 2010		Hypodont	2
Typotheria	Mesotheriidae	<i>Pseudotyoptherium</i>	<i>Pseudotyoptherium subinsigne</i>	Huayquerian	-	23.7	15.8	Fernández García 2018						Hypodont	2
Typotheria	Archaeohyracidae	<i>Punahyrax</i>	<i>Punahyrax bondesioi</i>	Mustersan	20*	5	6.2	Reguero et al. 2008	453	Reguero et al. 2010	0.88	Reguero et al. 2010		brachiodont	0
Typotheria	Interatheriidae	<i>Punapithecus</i>	<i>Punapithecus minor</i>	Mustersan	-	3.04	-	García-López and Babot 2015	-		0.61	Hitz et al. 2006		brachiodont	0
Typotheria	Mesotheriidae	<i>Rusconitherium</i>	<i>Rusconitherium mendocense</i>	Santacrucian	30.1	11	9	Cerdeño et al. 2018						Hypodont	2
Typotheria	Hegetotheriidae	<i>Sallatherium</i>	<i>Sallatherium altiplanense</i>	Deseadan	25	8	8.8	Reguero and Cerdeño 2005	-	-	2.3	Reguero et al. 2010		Hypodont	2
Typotheria	Interatheriidae	<i>Santiagorothia</i>	<i>Santiagorothia chiliensis</i>	Tinguirirican	>20	8.7	6.9	Hitz et al. 2000			1.2	Reguero et al. 2010		Hypodont	2
Typotheria	Oldfieldthomasiidae	<i>Suniodon</i>	<i>Suniodon catamarcensis</i>	Mustersan	-	5.8	-	Lopez 1995						brachiodont	0
Typotheria	Archaeopithecidae	<i>Teratopithecus</i>	<i>Teratopithecus elpidophoros</i>	Itaboraian Vacan	-	4.8	-	Lopez 2020						brachiodont	0
Typotheria	Mesotheriidae	<i>Trachytherus</i>	<i>Trachytherus alloxus</i>	Deseadan	58.4	23	16.9	Billet et al. 2008	45200	Fernández García 2018				Hypodont	2
Typotheria	Mesotheriidae	<i>Trachytherus</i>	<i>Trachytherus ramirezi</i>	Deseadan	49.8	19.3	10.2	Shockey et al. 2016						Hypodont	2
Typotheria	Mesotheriidae	<i>Trachytherus</i>	<i>Trachytherus spegazzinianus</i>	Deseadan	63.2	25.5	17.3	Billet et al. 2008	139000	Fernández García 2018	2.32	Wilson et al. 2012		Hypodont	2
Typotheria	Mesotheriidae	<i>Trachytherus</i>	<i>Trachytherus subandinus</i>	Deseadan	-	16.2	-	Villaroel et al. 1994						Hypodont	2
Typotheria	Interatheriidae	<i>Transpithecus</i>	<i>Transpithecus obtentus</i>	Barrancan	16.5	5.6	4.6	Vera 2012			0.73	Wilson et al. 2012		brachiodont	0

Typotheria	Hegetotheriidae	<i>Tremacyllus</i>	<i>Tremacyllus impressus</i>	Huayquerian-Marplatan	-	4.1	3.81	Cerdeño and Bond 1999	1190	Elissamburu 2012	3.23	Reguero et al. 2007	hypsodont	3
Typotheria	Oldfieldthomasiidae	<i>Tsamnichoria</i>	<i>Tsamnichoria cabrerai</i>	Mustersan	22.7	8.9	6.8	Simpson 1967					brachiodont	0
Typotheria	Mesotheriidae	<i>Typotheriopsis</i>	<i>Typotheriopsis chasicoensis</i>	Chasicoan-Huayquerian-Pliocene	-	18.2	12.7	Fernández García 2018			1.93	Reguero et al. 2010	Hypsodont	2
Typotheria	Mesotheriidae	<i>Typotheriopsis</i>	<i>Typotheriopsis internum</i>	Chapadmalense	-	24.7	19.9	Fernández García 2018			1.93	Reguero et al. 2010	Hypsodont	2
Typotheria	Oldfieldthomasiidae	<i>Ultrapiethecus</i>	<i>Ultrapiethecus rutilans</i>	Barrancan	-	8.7	-	Simpson 1967			0.78	Madden 2014	brachiodont	0
Typotheria	Unnamed family	<i>Xenostephanus</i>	<i>Xenostephanus chiottii</i>	Vacan-Barrancan	20	6.5	6.9	Simpson 1962		-			brachiodont	0



Table S4. Database of LMRL, SLML, and SUML dental measurements (in mm) and body mass (in kg) of extant ungulates (n=138) from Mendoza et al. (2006).

SP	FAMILY	in cm and Kg				in mm and Kg			
		BM	LMRL	FLML	SUML	BM	LMRL	FLML	SUML
<i>Heterohyrax brucei</i>	Procaviidae	2	1.67	0.56	0.61	2	16.7	5.6	6.1
<i>Tragulus javanicus</i>	Tragulidae	3	2.23	0.58	0.7	3	22.3	5.8	7
<i>Procavia capensis</i>	Procaviidae	3.8	2.09	0.64	0.81	3.8	20.9	6.4	8.1
<i>Dendrohyrax dorsalis</i>	Procaviidae	4	1.86	0.62	0.67	4	18.6	6.2	6.7
<i>Tragulus meminna</i>	Tragulidae	4	2.53	0.7	0.78	4	25.3	7	7.8
<i>Madoqua guentheri</i>	Bovidae	4	2.4	0.73	0.78	4	24	7.3	7.8
<i>Neotragus pygmaeus</i>	Bovidae	4	2.43	0.54	0.82	4	24.3	5.4	8.2
<i>Madoqua kirki</i>	Bovidae	5	2.31	0.72	0.75	5	23.1	7.2	7.5
<i>Neotragus moschatus</i>	Bovidae	5	2.24	0.71	0.84	5	22.4	7.1	8.4
<i>Tragulus napu</i>	Tragulidae	6	2.43	0.62	0.72	6	24.3	6.2	7.2
<i>Cephalophus monticolor</i>	Bovidae	6	2.37	0.62	0.8	6	23.7	6.2	8
<i>Pudu mephistopheles</i>	Cervidae	9	2.82	0.82	0.89	9	28.2	8.2	8.9
<i>Dorcatragus megalotis</i>	Bovidae	9	3.26	0.92	1.08	9	32.6	9.2	10.8
<i>Raphicerus melanotis</i>	Bovidae	10.6	2.73	0.73	0.84	10.6	27.3	7.3	8.4
<i>Hyemoschus aquaticus</i>	Tragulidae	10.8	3.35	0.93	0.97	10.8	33.5	9.3	9.7
<i>Pudu pudu</i>	Cervidae	11	3.18	0.9	1.03	11	31.8	9	10.3
<i>Sylvicapra grimmia</i>	Bovidae	11	3.4	0.91	1.19	11	34	9.1	11.9
<i>Raphicerus campestris</i>	Bovidae	11.8	3.11	0.84	0.98	11.8	31.1	8.4	9.8
<i>Hydropotes inermis</i>	Cervidae	12.6	3.35	0.95	1.06	12.6	33.5	9.5	10.6
<i>Oreotragus oreotragus</i>	Bovidae	12.8	3.4	0.98	1.01	12.8	34	9.8	10.1
<i>Ourebia ourebi</i>	Bovidae	13	3.4	0.85	1.19	13	34	8.5	11.9
<i>Moschus moschiferus</i>	Moschidae	13.5	3.21	0.84	1.01	13.5	32.1	8.4	10.1
<i>Muntiacus reevesi</i>	Cervidae	13.5	3.48	0.94	1.1	13.5	34.8	9.4	11
<i>Elaphodus cephalophus</i>	Cervidae	18	3.76	1.08	1.25	18	37.6	10.8	12.5
<i>Gazella dorcas</i>	Bovidae	19	3.69	0.86	1.14	19	36.9	8.6	11.4
<i>Gazella thomsoni</i>	Bovidae	19.3	4.28	1.06	1.35	19.3	42.8	10.6	13.5
<i>Tayassu tajacu</i>	Tayassuidae	20	4.4	1.2	1.33	20	44	12	13.3
<i>Cephalophus dorsalis</i>	Bovidae	21	3.92	0.96	1.23	21	39.2	9.6	12.3
<i>Tetraceras quadricornis</i>	Bovidae	22.7	3.95	0.97	1.28	22.7	39.5	9.7	12.8
<i>Mazama mazama</i>	Cervidae	22.8	3.87	1.05	1.2	22.8	38.7	10.5	12
<i>Pelea capreolus</i>	Bovidae	23	4.52	1.23	1.38	23	45.2	12.3	13.8
<i>Capreolus capreolus</i>	Cervidae	23.4	4.46	1.19	1.38	23.4	44.6	11.9	13.8
<i>Muntiacus muntjak vaginalis</i>	Cervidae	25	4.27	1.13	1.3	25	42.7	11.3	13
<i>Redunca fulvorufula</i>	Bovidae	26	4.06	1.03	1.28	26	40.6	10.3	12.8
<i>Ammodorcas clarkei</i>	Bovidae	28	3.73	0.91	1.17	28	37.3	9.1	11.7
<i>Procapra gutterosa</i>	Bovidae	30	5.33	1.31	1.68	30	53.3	13.1	16.8
<i>Tayassu pecari</i>	Tayassuidae	31	5.2	1.38	1.53	31	52	13.8	15.3
<i>Nemorhaedus goral</i>	Bovidae	32	4.49	1.17	1.44	32	44.9	11.7	14.4
<i>Litocranius walleri</i>	Bovidae	34.7	3.46	0.92	1.03	34.7	34.6	9.2	10.3
<i>Antilope cervicapra</i>	Bovidae	35.3	4.87	1.19	1.37	35.3	48.7	11.9	13.7
<i>Catagonous wagneri</i>	Suidae	36	6.28	1.73	2.08	36	62.8	17.3	20.8

<i>Rupicapra rupicapra</i>	Bovidae	36.4	4.22	1.08	1.32	36.4	42.2	10.8	13.2
<i>Saiga tatarica</i>	Bovidae	36.4	5.51	1.41	1.77	36.4	55.1	14.1	17.7
<i>Pantheops hodgsoni</i>	Bovidae	36.5	4.65	1	1.54	36.5	46.5	10	15.4
<i>Axis porcinus</i>	Cervidae	37.4	4.99	1.32	1.58	37.4	49.9	13.2	15.8
<i>Ozotoceras bezoarticus</i>	Cervidae	38	4.85	1.36	1.51	38	48.5	13.6	15.1
<i>Antidorcas marsupialis</i>	Bovidae	39.1	5.16	1.34	1.64	39.1	51.6	13.4	16.4
<i>Vicugna vicugna</i>	Camelidae	45	5.52	1.41	1.83	45	55.2	14.1	18.3
<i>Tragelaphus scriptus</i>	Bovidae	48	4.14	1.09	1.3	48	41.4	10.9	13
<i>Antilocapra americana</i>	Antilocapridae	50	5.94	1.19	1.45	50	59.4	11.9	14.5
<i>Gazella granti</i>	Bovidae	50	5.58	1.37	1.75	50	55.8	13.7	17.5
<i>Cervus nippon</i>	Cervidae	53	4.94	1.29	1.64	53	49.4	12.9	16.4
<i>Aepyceros melampus</i>	Bovidae	53	5.61	1.41	2.01	53	56.1	14.1	20.1
<i>Babryrousa babryrousa</i>	Suidae	54.2	5.58	1.33	1.76	54.2	55.8	13.3	17.6
<i>Dama dama</i>	Cervidae	55	5.55	1.51	1.79	55	55.5	15.1	17.9
<i>Axis axis</i>	Cervidae	55	5.58	1.52	1.8	55	55.8	15.2	18
<i>Ovis dalli</i>	Bovidae	56	5.66	1.44	1.84	56	56.6	14.4	18.4
<i>Cephalophus spadix</i>	Bovidae	57	4.42	1.26	1.38	57	44.2	12.6	13.8
<i>Kobus kob</i>	Bovidae	58	4.96	1.28	1.53	58	49.6	12.8	15.3
<i>Pseudois nayeur</i>	Bovidae	59	5.25	1.29	1.62	59	52.5	12.9	16.2
<i>Ovis Canadensis nelsoni</i>	Bovidae	59	6.4	1.5	1.99	59	64	15	19.9
<i>Odocoileus virginianus</i>	Cervidae	62	5.16	1.39	1.62	62	51.6	13.9	16.2
<i>Redunca arundinum</i>	Bovidae	62	5.85	1.49	1.83	62	58.5	14.9	18.3
<i>Damaliscus dorcas</i>	Bovidae	64	5.74	1.59	1.88	64	57.4	15.9	18.8
<i>Hippocamelus bisulcus</i>	Cervidae	65	5.67	1.51	1.63	65	56.7	15.1	16.3
<i>Cephalophus silvicultor</i>	Bovidae	65.4	5.96	1.48	1.91	65.4	59.6	14.8	19.1
<i>Kobus vardonii</i>	Bovidae	70	5.2	1.42	1.55	70	52	14.2	15.5
<i>Tragelaphus spekei</i>	Bovidae	74	5.5	1.39	1.65	74	55	13.9	16.5
<i>Odocoileus hemionus</i>	Cervidae	74	5.59	1.47	1.75	74	55.9	14.7	17.5
<i>Lama pacos</i>	Camelidae	75	6.57	1.69	2.26	75	65.7	16.9	22.6
<i>Potamochoerus porcus</i>	Suidae	78	6.92	1.73	2.21	78	69.2	17.3	22.1
<i>Oreamnus americanus</i>	Bovidae	78.4	5.26	1.36	1.85	78.4	52.6	13.6	18.5
<i>Hemitragus jehmlahicus</i>	Bovidae	80	5.75	1.31	1.75	80	57.5	13.1	17.5
<i>Sus scroca cristatus</i>	Suidae	80	8.04	1.57	2.34	80	80.4	15.7	23.4
<i>Ammotragus lervia</i>	Bovidae	86	6.17	1.42	2.03	86	61.7	14.2	20.3
<i>Kobus lechwe</i>	Bovidae	87	5.26	1.36	1.62	87	52.6	13.6	16.2
<i>Capra ibex</i>	Bovidae	87	5.89	1.33	1.91	87	58.9	13.3	19.1
<i>Phacochoerus aethiopicus</i>	Suidae	90	7.61	1.38	1.93	90	76.1	13.8	19.3
<i>Tragelaphus imberbis</i>	Bovidae	91.5	6.11	1.51	1.95	91.5	61.1	15.1	19.5
<i>Tragelaphus angasi</i>	Bovidae	93.3	5.63	1.37	1.8	93.3	56.3	13.7	18
<i>Blastocerus dichotomus</i>	Cervidae	96	5.49	1.49	1.73	96	54.9	14.9	17.3
<i>Capricornis sumatrensis</i>	Bovidae	102	6.01	1.49	1.86	102	60.1	14.9	18.6
<i>Lama guanicoe</i>	Camelidae	110	5.73	1.58	2.12	110	57.3	15.8	21.2
<i>Addax nasomacultus</i>	Bovidae	111	7.39	1.68	2.64	111	73.9	16.8	26.4
<i>Damaliscus hunteri</i>	Bovidae	124	6.81	1.63	3.13	124	68.1	16.3	31.3

<i>Alcelaphus buselaphus</i>	Bovidae	136	6.77	1.82	2.14	136	67.7	18.2	21.4
<i>Hylochoerus meinertzhageni</i>	Suidae	140	8.42	1.82	2.7	140	84.2	18.2	27
<i>Rangifer tarandus</i>	Cervidae	145	6.04	1.81	1.86	145	60.4	18.1	18.6
<i>Bubalus depressicornis</i>	Bovidae	150	5.52	1.53	1.7	150	55.2	15.3	17
<i>Damaliscus lunatus</i>	Bovidae	150	6.71	1.8	2.12	150	67.1	18	21.2
<i>Connochaetes gnou</i>	Bovidae	150	7.2	1.75	2.56	150	72	17.5	25.6
<i>Cervus Elaphus scottius</i>	Cervidae	153	6.86	1.86	2.16	153	68.6	18.6	21.6
<i>Kobus ellipsiprymnus</i>	Bovidae	160.5	7.44	2.19	2.5	160.5	74.4	21.9	25
<i>Elaphurus davidianus</i>	Cervidae	175	7.74	2.2	2.53	175	77.4	22	25.3
<i>Hippotragus niger</i>	Bovidae	181	7.2	1.88	2.36	181	72	18.8	23.6
<i>Tragelaphus buxtoni</i>	Bovidae	183	6.82	1.7	2.1	183	68.2	17	21
<i>Cervus duvaucelli</i>	Cervidae	183	7.1	1.78	2.22	183	71	17.8	22.2
<i>Cervus Unicolor</i>	Cervidae	188	7.19	1.83	2.37	188	71.9	18.3	23.7
<i>Tragelaphus strepciceros</i>	Bovidae	196	8.08	2	2.54	196	80.8	20	25.4
<i>Boselaphus tragocamelus</i>	Bovidae	200	8.09	1.8	2.46	200	80.9	18	24.6
<i>Oryx gazalla</i>	Bovidae	200	8.46	1.99	2.83	200	84.6	19.9	28.3
<i>Tragelaphus euryceros</i>	Bovidae	205	8.03	2.06	2.5	205	80.3	20.6	25
<i>Connochaetus taurinus</i>	Bovidae	216	7.32	1.81	2.56	216	73.2	18.1	25.6
<i>Equus asinus</i>	Equidae	220	7.13	2.25	2.22	220	71.3	22.5	22.2
<i>Choeropsis liberiensis</i>	Hippopotamidae	235	7.98	2.2	2.77	235	79.8	22	27.7
<i>Tapirus terrestris</i>	Tapiridae	240	6.89	2.16	2.41	240	68.9	21.6	24.1
<i>Hippotragus equinus</i>	Bovidae	241	8.18	2.27	2.58	241	81.8	22.7	25.8
<i>Equus burchelli</i>	Equidae	250	7.42	2.28	2.19	250	74.2	22.8	21.9
<i>Tapirus pinchaque</i>	Tapiridae	250	6.78	2.18	2.34	250	67.8	21.8	23.4
<i>Budorcas taxicolor</i>	Bovidae	250	8.45	1.89	2.68	250	84.5	18.9	26.8
<i>Equus hemionus</i>	Equidae	260	7.57	2.21	2.26	260	75.7	22.1	22.6
<i>Okapia johnstoni</i>	Giraffidae	263	8.56	2.49	2.58	263	85.6	24.9	25.8
<i>Tapirus bairdii</i>	Tapiridae	275	6.77	2.23	2.41	275	67.7	22.3	24.1
<i>Equus zebra</i>	Equidae	281	7.83	2.35	2.44	281	78.3	23.5	24.4
<i>Equus kiang</i>	Equidae	300	7.85	2.54	2.31	300	78.5	25.4	23.1
<i>Ovibos moschatus</i>	Bovidae	305	9.68	2.44	3.21	305	96.8	24.4	32.1
<i>Tapirus indicus</i>	Tapiridae	317	7.99	2.51	2.86	317	79.9	25.1	28.6
<i>Cervus canadensis</i>	Cervidae	325	9.1	2.3	3	325	91	23	30
<i>Equus przewalski</i>	Equidae	350	9.24	2.96	2.84	350	92.4	29.6	28.4
<i>Equus grevyi</i>	Equidae	400	8.85	2.56	2.68	400	88.5	25.6	26.8
<i>Alces alces</i>	Cervidae	400.5	9.73	2.65	3.07	400.5	97.3	26.5	30.7
<i>Camelus dromedarius</i>	Camelidae	415	11.52	3.03	4.01	415	115.2	30.3	40.1
<i>Syncerus caffer</i>	Bovidae	496	9.57	2.4	2.79	496	95.7	24	27.9
<i>Bos javanicus</i>	Bovidae	500	8.66	2.34	2.75	500	86.6	23.4	27.5
<i>Taurotragus oryx</i>	Bovidae	511	9.59	2.3	3.17	511	95.9	23	31.7
<i>Camelus bactrianus</i>	Camelidae	550	13.48	3.06	4.39	550	134.8	30.6	43.9
<i>Bos indicus</i>	Bovidae	600	9.72	2.34	2.96	600	97.2	23.4	29.6
<i>Bison bison</i>	Bovidae	611	9.98	2.4	3.24	611	99.8	24	32.4
<i>Bison bonasus</i>	Bovidae	625	10.03	2.46	2.89	625	100.3	24.6	28.9
<i>Bubalis bubalis</i>	Bovidae	725	11.57	3	3.6	725	115.7	30	36
<i>Bos gaurus</i>	Bovidae	755	9.89	2.5	2.84	755	98.9	25	28.4

<i>Giraffa camelopardalis</i>	Giraffidae	800	10.57	2.92	2.97	800	105.7	29.2	29.7
<i>Dicerorhinus sumatrensis</i>	Rhinocerotidae	800	11.72	3.49	4.86	800	117.2	34.9	48.6
<i>Diceros bicornis</i>	Rhinocerotidae	1100	15.96	4.89	6.12	1100	159.6	48.9	61.2
<i>Rhinoceros sondaicus</i>	Rhinocerotidae	1400	12.67	3.88	5.04	1400	126.7	38.8	50.4
<i>Hippopotamus amphibius</i>	Hippopotamidae	1430	16.56	4.04	5.01	1430	165.6	40.4	50.1
<i>Rhinoceros unicornis</i>	Rhinocerotidae	1557.5	15.16	3.91	5.72	1557.5	151.6	39.1	57.2
<i>Ceratotherium simum</i>	Rhinocerotidae	1600	16.26	4.69	6.33	1600	162.6	46.9	63.3



Table S5. Results of the log-transformed bivariate ordinary least-squares (OLS) regressions performed on LMRL, SLML, and SUML (predictive variables) dental measurements and BM (response variable) of extant ungulates with a body mass lower than 75 kg (n=68) taken from the Mendoza et al. (2006) dataset.

Index	Slope	Intercept	p	r²	%PE	%SEE	MAE
LMRL	2.77	-7.12	<0.001	0.91	3.77	7.81	6.82
SUML	2.95	-4.37	<0.001	0.89	4.82	10.08	7.87
FLML	3.08	-4.16	<0.001	0.88	5.46	11.16	7.92



Table S6. Summary of the data recovered from the literature and estimated using the methods described in the main text, including the taxonomic arrangement, body mass (BM) in Kg, natural logarithm of the BM (Log_BM), times of speciation (TS) and extinction (TE), hypsodonty categories (HI), paleocoordinates (P_Lng, P_Lat, P_Lat_2), and size category (Size) of each taxon. Abbreviations: Arhy, Archaeohyracidae; Arpi, Archaeopithecidae; B. Noto: basal notoungulate; B. Typo, basal typotheres; Hege, Hegetotheriidae; Henr, Henricosborniidae; Homa, Homalodtheriidae; Inte, Interatheriidae; Iso, Isotemnidae; Leo, Leontiniidae; Meso, Mesotheriidae; Noth, Notohippidae; Nots, Notostylopidae; Oldf, Oldfieldthomasiidae; Toxd, Toxodontidae; B, brachiodont, H, hypsodont; M, mesodont; EU, euhypsodont; VS, very small-sized; S, small-sized; M, medium-sized; L, large-sized; VL, very large-sized; G, giant-sized.

Suborder	Family	Taxa	BM	Log_BM	TS	TE	Hypsodonty	Hypsodonty values	P_Lng	P_Lat	P_Lat_2	Size
Basal notoungulate	Henr	<i>Acamana ambiguus</i>	109.83	4.699	41.28	36.16	brachiodont	0	-59.71	-33.52	-41.23	L
Typotheria	B. Typo	<i>Acoelohyrax complicatissimus</i>	27.36	3.309	48.48	37.08	brachiodont	0	-60.37	-46.6	-54.09	M
Typotheria	B. Typo	<i>Acoelohyrax coronatus</i>	14.43	2.669	48.74	37.01	brachiodont	0	-60.74	-46.43	-54.09	M
Toxodontia	Toxd	<i>Adinotherium ovinum</i>	38.8	3.659	18.28	13.74	hypsodont	2	-67.1	-50.36	-54.96	M
Toxodontia	Toxd	<i>Alitoxodon vetustum</i>	77.86	4.355	6.17	3.97	hypselenodont	3	-60.8	-38.78	-40.77	M
Typotheria	B. Typo	<i>Allalmeia atalaensis</i>	3.22	1.169	45.21	39.82	brachiodont	0	-59.71	-33.52	-41.31	S
Typotheria	Meso	<i>Altityotherium chucalensis</i>	19.94	2.993	18.1	15.71	Hypsodont	2	-65.05	-17.94	-22.75	M
Typotheria	Meso	<i>Altityotherium paucidens</i>	22.2	3.1	18.13	15.42	Hypsodont	2	-65.05	-17.94	-22.75	M
Toxodontia	Leo	<i>Anayatherium ekacoa</i>	203.89	5.318	29.3	20.79	mesodont	1	-61.08	-16.94	-23.08	L
Toxodontia	Leo	<i>Anayatherium fortis</i>	510.58	6.236	29.74	20.38	mesodont	1	-61.08	-16.94	-23.08	VL
Toxodontia	Leo	<i>Ancylocoelus frequens</i>	154.7	5.041	29.31	20.74	mesodont	1	-62.99	-45.48	-51.65	L
Toxodontia	Iso	<i>Anisotemnus distentus</i>	13.57	2.608	47.32	38.55	brachiodont	0	-60.06	-46.21	-53.76	M
Typotheria	Inte	<i>Antepithecus brachystephanus</i>	1.88	0.631	42.41	38.53	brachiodont	0	-60.2	-45.9	-53.52	S
Typotheria	Inte	<i>Antofagastia turneri</i>	0.9	-0.107	39.35	36.09	brachiodont	0	-58.29	-26.61	-34.27	VS
Typotheria	Arhy	<i>Archaeohyrax patagonicus</i>	20.95	3.042	29.38	20.53	hypselenodont	3	-63.32	-44.49	-50.64	M
Typotheria	Arhy	<i>Archaeohyrax suniensis</i>	15.35	2.731	29.38	20.52	Hypsodont	2	-61.9	-21.72	-27.89	M
Typotheria	Inte	<i>Archaeophylus patrius</i>	0.87	-0.134	29.24	20.47	Hypsodont	2	-63.41	-44.87	-51.06	VS
Typotheria	Arpi	<i>Archaeopithecus rogeri</i>	2.11	0.746	56.08	35.42	brachiodont	0	-59.71	-46.12	-53.43	S

Typotheria	Arhy	<i>Archaeotypotherium pattersoni</i>	12.43	2.52	33.71	31.17	Hypsodont	2	-63.44	-34.93	-42.13	M
Typotheria	Arhy	<i>Archaeotypotherium propheticus</i>	23.77	3.168	34.49	30.72	Hypsodont	2	-62.79	-45	-52.64	M
Typotheria	Arhy	<i>Archaeotypotherium tinguiriricaense</i>	13.61	2.611	33.86	31.28	Hypsodont	2	-63.44	-34.93	-42.64	M
Toxodontia	Noth	<i>Argyrohippus boulei</i>	30.3	3.411	20.95	17.39	hypsodont	2	-65.57	-45.09	-50.35	M
Toxodontia	Noth	<i>Argyrohippus fraterculus</i>	31.28	3.443	21.07	19.96	hypsodont	2	-65.57	-45.09	-50.77	M
Toxodontia	Noth	<i>Argyrohippus praecox</i>	29.32	3.378	28.79	20.92	hypsodont	2	-64.12	-52.06	-54.64	M
Typotheria	Inte	<i>Argyrohyrax proavus</i>	4.86	1.582	29.48	20.72	Hypsodont	2	-63.31	-44.33	-50.51	S
Toxodontia	Homa	<i>Asmodeus osborni</i>	406.21	6.007	29.31	20.54	brachiodont	0	-62.47	-46.31	-52.47	VL
Toxodontia	Homa	<i>Asmodeus petrasnerus</i>	243.72	5.496	28.84	21.12	brachiodont	0	-64.38	-36.17	-42.4	L
Basal notoungulate	Nots	<i>Boreastylops lumbreensis</i>	23.15	3.142	47.16	40.53	brachiodont	0	-54.46	-26.83	-34.08	M
Typotheria	B. Typo	<i>Brachystephanus postremus</i>	2.04	0.715	46.26	40.6	brachiodont	0	-59.71	-33.52	-41.31	S
Basal notoungulate	Nots	<i>Brandmayria simpsoni</i>	8.3	2.116	52.79	49.51	brachiodont	0	-59.63	-46.32	-53.32	S
Typotheria	Inte	<i>Brucemacfaddenia boliviensis</i>	4.28	1.453	29.39	20.37	hypselenodont	3	-61.11	-17.28	-23.41	S
Typotheria	Inte	<i>Caenophilus tripartitus</i>	5.59	1.721	12.06	9.47	NA	NA	-57.23	-26.92	-30.31	S
Toxodontia	Toxd	<i>Calchaquitherium mixtum</i>	334.59	5.813	8.87	5.34	hypselenodont	3	-64.39	-26.31	-28.72	VL
Typotheria	B. Typo	<i>Campanorco inauguralis</i>	1.67	0.51	46.2	41.54	brachiodont	0	-54.57	-27.26	-34.5	S
Typotheria	Meso	<i>Caraguatypotherium munozi</i>	45.08	3.808	12.16	9.83	Hypsodont	2	-67.44	-17.98	-21.08	M
Toxodontia	Homa	<i>Chasicotherium rothi</i>	475.99	6.165	10.63	8.32	hypsodont	2	-61.48	-38.2	-41.33	VL
Basal notoungulate	Nots	<i>Chilestylops davidsoni</i>	28.54	3.351	34.06	30.97	brachiodont	0	-63.44	-34.93	-42.64	M
Typotheria	Inte	<i>Cochilius fumensis</i>	1.95	0.669	28.96	21.18	Hypsodont	2	-64.5	-45.4	-51.63	S
Typotheria	Inte	<i>Cochilius volvens</i>	3.05	1.116	21.08	20.08	Hypsodont	2	-64.11	-48.43	-50.83	S
Toxodontia	Noth	<i>Coelostylodon caroloameghinoi</i>	3.63	1.288	42.1	39.35	brachiodont	0	-58.64	-49.5	-53.99	S
Toxodontia	Noth	<i>Coelostylodon florentinoameghinoi</i>	11.4	2.433	41.62	38.82	brachiodont	0	-58.64	-49.5	-54.04	M
Typotheria	Oldf	<i>Colbertia lumbreense</i>	7.03	1.951	45.65	40.4	brachiodont	0	-54.46	-26.83	-34.08	S
Typotheria	Oldf	<i>Colbertia magellanica</i>	8.26	2.111	53.26	49.41	brachiodont	0	-28.11	-27.58	-32.39	S
Toxodontia	Leo	<i>Colpodon antucoensis</i>	183.85	5.214	17.82	15.65	mesodont	1	-67.27	-36.83	-41.64	L
Toxodontia	Leo	<i>Colpodon distinctus</i>	123.1	4.813	22.08	17.46	mesodont	1	-65.6	-45.08	-50.53	L
Toxodontia	Leo	<i>Coquenia bondi</i>	76.16	4.333	39.27	36.37	brachiodont	0	-54.35	-27.04	-33.94	M
Toxodontia	Noth	<i>Coresodon scalpridens</i>	33.73	3.518	28.79	21.12	hypsodont	2	-62.94	-44.95	-51.12	M
Toxodontia	Toxd	<i>Dinotoxodon paranensis</i>	274.32	5.614	10.03	5.04	hypselenodont	3	-58.44	-31.26	-34.27	L
Toxodontia	Iso	<i>Distylophorus alouatinus</i>	54.58	4	39.9	35.3	brachiodont	0	-61.72	-45.9	-53.71	M

Typotheria	Oldf	<i>Dolichostylodon saltensis</i>	3.53	1.262	44.65	39.91	brachiodont	0	-54.35	-27.04	-34.29	S
Basal notoungulate	Nots	<i>Edvardotrouessartia sola</i>	43.61	3.775	50.58	40.1	brachiodont	0	-59.94	-45.64	-52.91	M
Toxodontia	Leo	<i>Elmerriggisia fieldia</i>	255.32	5.543	28.23	21.08	mesodont	1	-63.95	-46.34	-52.56	L
Typotheria	Arhy	<i>Eohyrax isotemnoides</i>	10	2.303	42.99	38.1	Hypsodont	2	-60.09	-46.84	-54.38	M
Typotheria	Arhy	<i>Eohyrax praerusticus</i>	6.39	1.855	51.93	48.01	Hypsodont	2	-60	-46.46	-53.67	S
Typotheria	Arhy	<i>Eohyrax rusticus</i>	8.56	2.147	43.01	35.22	Hypsodont	2	-56.78	-39.35	-46.47	S
Toxodontia	Noth	<i>Eomorphippus bondi</i>	48.01	3.871	33.83	31.29	mesodont	1	-63.44	-34.93	-42.64	M
Toxodontia	Noth	<i>Eomorphippus neilopydyei</i>	10.18	2.32	34.04	31.19	mesodont	1	-63.44	-34.93	-42.64	M
Toxodontia	Noth	<i>Eomorphippus obscurus</i>	21.87	3.085	39.46	35.54	mesodont	1	-62.15	-45.5	-53.46	M
Typotheria	Inte	<i>Eopachyrucos pliciformis</i>	1.24	0.216	34.39	30.83	Hypsodont	2	-62.31	-44.7	-52.33	S
Typotheria	Inte	<i>Eopachyrucos ranchoverdensis</i>	8.88	2.183	29.33	20.18	Hypsodont	2	-50.69	-34.64	-40.27	S
Typotheria	Meso	<i>Eotypotherium chico</i>	13.41	2.596	18.03	15.84	Hypsodont	2	-65.05	-17.94	-22.75	M
Typotheria	Hege	<i>Ethegotherium careiiei</i>	2.46	0.898	18.06	15.55	hypsodont	3	-65.66	-35.04	-37.1	S
Toxodontia	Noth	<i>Eurygenium latirostris</i>	72.95	4.29	28.65	21.1	hypsodont	2	-62.94	-44.95	-51.12	M
Toxodontia	Noth	<i>Eurygenium pacegnum</i>	68.74	4.23	29.55	20.72	hypsodont	2	-61.08	-16.94	-23.08	M
Typotheria	Meso	<i>Eutrachytherus modestus</i>	19.05	2.947	17.76	14.07	Hypsodont	2	-64.63	-34.34	-38.9	M
Typotheria	Meso	<i>Eutypotherium lehmannitschei</i>	27.35	3.309	16.47	13.72	Hypsodont	2	-67	-42.62	-44.45	M
Toxodontia	Toxd	<i>Falcontoxodon aguilerai</i>	428.64	6.061	4.33	0.23	hypselodont	3	-69.7	11.44	10	VL
Typotheria	Inte	<i>Federicoanaya sallaensis</i>	2.63	0.968	29.03	20.4	hypselodont	3	-60.76	-16.87	-22.99	S
Typotheria	B. Typo	<i>Griphotherion peiranoi</i>	2.44	0.893	45.74	39.54	brachiodont	0	-54.35	-27.04	-34.08	S
Toxodontia	Leo	<i>Gualta cuyana</i>	129.77	4.866	28.68	20.85	brachiodont	0	-64.38	-36.17	-42.4	L
Typotheria	Inte	<i>Guiliemoscottia plicifera</i>	3.07	1.12	39.72	35.31	brachiodont	0	-61.15	-45.64	-53.09	S
Toxodontia	Toxd	<i>Gyrinodon quassus</i>	397.93	5.986	9.86	4.62	hypselodont	3	-67.42	0.51	-1.86	VL
Toxodontia	Toxd	<i>Haplodontherium wildei</i>	698.57	6.549	9.86	4.86	hypselodont	3	-59.31	-28.03	-30.49	VL
Typotheria	Hege	<i>Hegetotheriopsis sulcatus</i>	6.52	1.875	29.93	19.77	hypselodont	3	-63.91	-40.17	-46.51	S
Typotheria	Hege	<i>Hegetotherium cerdasensis</i>	2.95	1.081	16.77	9.05	Hypsodont	3	-64.18	-19.84	-23.67	S
Typotheria	Hege	<i>Hegetotherium mirabile</i>	6.28	1.838	18.25	13.68	Hypsodont	3	-67.01	-46.8	-51.39	S
Typotheria	Hege	<i>Hegetotherium novum</i>	7.28	1.985	21.01	20.07	Hypsodont	2	-62.13	-42.85	-48.48	S
Typotheria	Hege	<i>Hemihegetotherium achataleptum</i>	27.91	3.329	9.11	5.09	Hypsodont	3	-67.68	-30.75	-33.15	M
Typotheria	Hege	<i>Hemihegetotherium lazai</i>	11.17	2.413	8.92	5.25	hypselodont	3	-61.89	-36.93	-39.36	M
Typotheria	Hege	<i>Hemihegetotherium tantillum</i>	6.96	1.94	16.75	8.56	hypselodont	3	-68.21	-41.28	-45.1	S

Typotheria	Hege	<i>Hemihegetotherium torresi</i>	7.03	1.951	11.25	5.2	hypselodont	3	-63.48	-34.36	-37.07	S
Typotheria	Hege	<i>Hemihegetotherium trilobus</i>	11.51	2.443	14.31	11.71	hypselodont	3	-63.68	-23	-24.79	M
Toxodontia	Toxd	<i>Hemixotodon chasicoensis</i>	171.79	5.146	10.98	8	hypselodont	3	-62.7	-37.56	-40.71	L
Toxodontia	Leo	<i>Henricofilholia lustrata</i>	78.49	4.363	29.15	21.29	brachiodont	0	-63.93	-45.37	-51.54	M
Toxodontia	Leo	<i>Henricofilholia vucetichia</i>	78.49	4.363	28.73	20.81	brachiodont	0	-63.48	-45.48	-51.54	M
Basal notoungulate	Henr	<i>Henricosbornia ampla</i>	2.65	0.974	47.22	38.51	brachiodont	0	-59.29	-46.22	-53.58	S
Basal notoungulate	Henr	<i>Henricosbornia lophodonta</i>	2.65	0.974	50.02	39.02	brachiodont	0	-60.09	-46.17	-53.57	S
Basal notoungulate	Henr	<i>Henricosbornia minuta</i>	2.65	0.975	51.47	48.33	brachiodont	0	-55.96	-44.87	-51.73	S
Basal notoungulate	Henr	<i>Henricosbornia waitehor</i>	2.65	0.975	51.24	48.28	brachiodont	0	-57.92	-47.01	-53.6	S
Toxodontia	Toxd	<i>Hoffstetterius imperator</i>	736.69	6.602	9.37	5.58	hypselodont	3	-66.89	-16.83	-19.22	VL
Toxodontia	Homa	<i>Homalodotherium cunninghami</i>	242.2	5.49	18.57	14.8	hypodont	2	-67.07	-50.26	-55.08	L
Basal notoungulate	Nots	<i>Homalostylops atavus</i>	1.67	0.513	53.3	50.24	brachiodont	0	-28.11	-27.58	-32.33	S
Basal notoungulate	Nots	<i>Homalostylops parvus</i>	5.93	1.78	50.57	38.84	brachiodont	0	-60.58	-46.07	-53.52	S
Toxodontia	Leo	<i>Huilatherium pluripicatum</i>	383.1	5.948	14.69	11.04	mesodont	1	-71.56	4.05	0.13	VL
Toxodontia	Toxd	<i>Hyperoxotodon speciosus</i>	49.34	3.899	18.43	13.1	hypselodont	3	-66.53	-52.49	-54.55	M
Toxodontia	Toxd	<i>Hypsitherium bolivianum</i>	15.1	2.714	5.28	2.71	hypselodont	3	-64.57	-19.52	-21.25	M
Typotheria	Inte	<i>Ignigena minisculus</i>	0.77	-0.264	46.15	39.74	brachiodont	0	-58.56	-36.28	-43.2	VS
Typotheria	Inte	<i>Interatherium excavatum</i>	0.8	-0.227	18.01	15.62	hypselodont	3	-66.95	-50.32	-55.14	VS
Typotheria	Inte	<i>Interatherium extensum</i>	1.35	0.299	18.18	15.93	hypselodont	3	-67.04	-50.95	-55.77	S
Typotheria	Inte	<i>Interatherium robustum</i>	1.42	0.352	18.38	13.69	hypselodont	3	-67.25	-50.21	-55.11	S
Typotheria	Inte	<i>Interatherium rodens</i>	3.02	1.105	18.18	15.68	hypselodont	3	-66.13	-52.36	-54.38	S
Toxodontia	Iso	<i>Isotemnus ctalego</i>	6.72	1.905	52.91	49.65	brachiodont	0	-57.92	-47.01	-53.38	S
Toxodontia	Iso	<i>Isotemnus haugi</i>	13.91	2.633	49.91	40	brachiodont	0	-55.96	-44.87	-51.79	M
Toxodontia	Iso	<i>Isotemnus latidens</i>	9.9	2.292	47.08	38.77	brachiodont	0	-60.22	-46.12	-53.62	S
Toxodontia	Iso	<i>Isotemnus primitivus</i>	22.68	3.122	46.95	38.95	brachiodont	0	-59.94	-46.52	-53.96	M
Typotheria	Oldf	<i>Itaboraitherium atavum</i>	1.06	0.062	52.66	49.94	brachiodont	0	-28.11	-27.58	-32.39	S
Typotheria	Inte	<i>Johnbell hatcheri</i>	0.74	-0.297	34.77	30.52	brachiodont	0	-63.56	-34.72	-42.44	VS
Typotheria	Inte	<i>Juchuisillu arenalesensis</i>	2.11	0.747	16.46	13.23	hypselodont	3	-62.8	-23.26	-25.25	S
Typotheria	Oldf	<i>Kibenikhorja get</i>	4.01	1.39	51.63	48.87	brachiodont	0	-57.92	-47.01	-53.6	S
Toxodontia	Leo	<i>Leontinia gaudryi</i>	565.39	6.338	29.78	20.39	mesodont	1	-60.58	-43.41	-49.45	VL
Toxodontia	Leo	<i>Martinmiguelia fernandesi</i>	63.9	4.157	39.04	36.3	brachiodont	0	-54.26	-24.64	-31.54	M

Typotheria	Oldf	<i>Maxschlosseria praeterita</i>	6.12	1.811	46.86	38.88	brachiodont	0	-59.65	-46.23	-53.66	S
Typotheria	Hege	<i>Medistylus dorsatus</i>	2.11	0.745	30.01	20.6	Hypsodont	2	-63.08	-44.53	-50.72	S
Toxodontia	Noth	<i>Mendozahippus fierensis</i>	57.05	4.044	29.36	20.78	brachiodont	0	-64.38	-36.17	-42.4	M
Typotheria	Meso	<i>Mesotherium cristatum</i>	95.86	4.563	3.55	0.22	Hypsodont	2	-57.57	-38.14	-39.48	M
Typotheria	Meso	<i>Microtypotherium choquecotense</i>	32.27	3.474	16.92	13.43	Hypsodont	2	-64.23	-18.64	-22.93	M
Typotheria	Inte	<i>Miocochilius anomopodus</i>	10.54	2.355	14.62	11.05	Hypsodont	2	-71.47	3.14	-0.77	M
Typotheria	Inte	<i>Miocochilius federicoi</i>	3.1	1.131	13.73	11.37	Hypsodont	2	-62.62	-21.44	-25.33	S
Toxodontia	Toxd	<i>Mixotoxodon larensis</i>	718.94	6.578	3.35	0	hypselodont	3	-78.07	9.3	8.46	VL
Toxodontia	Noth	<i>Moqueguahippus glycisima</i>	75.61	4.326	29.22	20.38	hypselodont	2	-64.69	-16.78	-23.06	M
Toxodontia	Noth	<i>Morphippus imbricatus</i>	57.2	4.047	28.72	20.94	hypselodont	2	-64.12	-52.06	-54.64	M
Typotheria	Inte	<i>Munizia paranensis</i>	1.35	0.299	9.06	5.06	hypselodont	2	-58.44	-31.26	-33.69	S
Toxodontia	Toxd	<i>Neotrigodon utoquineae</i>	565.39	6.338	11.91	10.15	hypselodont	3	-64.57	-9.7	-13.01	VL
Toxodontia	Toxd	<i>Nesodon imbricatus</i>	289.42	5.668	18.3	13.68	hypselodont	2	-67.08	-46.57	-51.17	L
Toxodontia	Toxd	<i>Nesodon taweretus</i>	348.15	5.853	22.89	15.02	hypselodont	2	-64.93	-34.23	-39.5	VL
Toxodontia	Toxd	<i>Nonotherium hennigi</i>	630.48	6.446	5.92	3.24	hypselodont	3	-64	-31.58	-33.54	VL
Toxodontia	Noth	<i>Notohippus toxodontoides</i>	20.87	3.038	18.5	14.69	hypselodont	2	-69.71	-49.77	-54.6	M
Typotheria	Inte	<i>Notopithecus adapinus</i>	1.95	0.67	42.4	36.03	brachiodont	0	-60.19	-46.52	-53.96	S
Basal notoungulate	Nots	<i>Notostylops appressus</i>	7.27	1.983	52.47	40.3	brachiodont	0	-59.44	-46.37	-53.71	S
Basal notoungulate	Nots	<i>Notostylops murinus</i>	11.85	2.472	46.66	39.08	brachiodont	0	-60.27	-46.54	-54.04	M
Basal notoungulate	Nots	<i>Notostylops pendens</i>	11.47	2.44	46.85	41.08	brachiodont	0	-59.49	-46.24	-53.65	M
Basal notoungulate	Nots	<i>Notostylops pigafettai</i>	11.85	2.472	45.85	41.31	brachiodont	0	-60.72	-46.67	-54.13	M
Toxodontia	Toxd	<i>Ocnerotherium intermedium</i>	1120.82	7.022	10.81	8.01	hypselodont	3	-63.49	-35.02	-38.04	G
Typotheria	Oldf	<i>Oldfieldthomasia anfractuosa</i>	8.3	2.116	50.61	36.37	brachiodont	0	-60.62	-46.03	-53.53	S
Typotheria	Oldf	<i>Oldfieldthomasia debilitata</i>	6.57	1.882	42.44	38.53	brachiodont	0	-60.3	-46.46	-54.06	S
Typotheria	Oldf	<i>Oldfieldthomasia parvidens</i>	4.01	1.39	43.29	37.65	brachiodont	0	-60.37	-46.6	-54.21	S
Basal notoungulate	Henr	<i>Orome deepi</i>	4.28	1.455	54.12	49.09	brachiodont	0	-57.98	-47.02	-53.09	S
Basal notoungulate	Henr	<i>Othnielmarshia curvicrista</i>	3.23	1.171	45.61	39.22	brachiodont	0	-60.03	-46.07	-53.58	S
Basal notoungulate	Henr	<i>Othnielmarshia lacunifera</i>	3.1	1.131	50.64	39.29	brachiodont	0	-59.49	-45.93	-53.19	S
Basal notoungulate	Henr	<i>Othnielmarshia reflexa</i>	4.18	1.431	46.42	39.61	brachiodont	0	-60.03	-46.07	-53.55	S
Basal notoungulate	Nots	<i>Otonia muehlbergi</i>	21.44	3.065	39.67	35.42	brachiodont	0	-61.92	-45.87	-53.69	M
Typotheria	Hege	<i>Pachyrukhos moyani</i>	1.38	0.325	18.47	14.65	hypselodont	3	-67.47	-50.4	-55.23	S

Typotheria	Hege	<i>Pachyrukhos politus</i>	1.34	0.293	21.17	20.18	hypselodont	3	-64.15	-38.59	-44.26	S
Typotheria	Hege	<i>Paedotherium bonaerense</i>	1.94	0.661	6.35	0	hypselodont	3	-60.65	-37.98	-39.58	S
Typotheria	Hege	<i>Paedotherium kakai</i>	1.51	0.413	9.04	5.47	hypselodont	3	-64.22	-25.43	-27.84	S
Typotheria	Hege	<i>Paedotherium minor</i>	1.48	0.389	10.77	4.2	hypselodont	3	-62.32	-35.35	-37.81	S
Typotheria	Hege	<i>Paedotherium typicum</i>	1.99	0.69	9.37	0	hypselodont	3	-61.42	-36.38	-38.34	S
Typotheria	Oldf	<i>Paginula parca</i>	1.34	0.289	47.26	40.67	brachiodont	0	-59.94	-46.31	-53.73	S
Toxodontia	Toxd	<i>Palyeidodon obtusum</i>	696.53	6.546	18.34	12.99	hypselodont	3	-65.4	-32.86	-37.44	VL
Toxodontia	Noth	<i>Pampahippus arenalesi</i>	21.87	3.085	47.82	38.76	brachiodont	0	-54.37	-25.95	-33.19	M
Toxodontia	Noth	<i>Pampahippus powelli</i>	38.39	3.648	46.32	41.64	brachiodont	0	-54.93	-25.39	-32.66	M
Toxodontia	Noth	<i>Pampahippus secundus</i>	2.65	0.974	47.02	39.57	brachiodont	0	-54.35	-27.04	-34.28	S
Toxodontia	Iso	<i>Pampatemnus deuterus</i>	12.41	2.519	45.15	39.35	brachiodont	0	-54.46	-26.83	-34.08	M
Toxodontia	Iso	<i>Pampatemnus infernalis</i>	16.28	2.79	45.75	39.41	brachiodont	0	-54.46	-26.83	-34.08	M
Toxodontia	Toxd	<i>Paratrigodon euguii</i>	937.55	6.843	11.02	8.03	hypselodont	3	-61.93	-38.1	-41.25	VL
Toxodontia	Noth	<i>Pascualhippus boliviensis</i>	72.95	4.29	29.26	20.46	Hypsodont	2	-61.07	-16.94	-23.08	M
Toxodontia	Noth	<i>Patagonhippus canterensis</i>	57.2	4.047	28.96	21.3	Hypsodont	2	-63.48	-45.48	-51.54	M
Toxodontia	Noth	<i>Patagonhippus dukei</i>	9.58	2.26	29.18	21.08	Hypsodont	2	-63.48	-45.48	-51.54	S
Typotheria	Inte	<i>Patriarchus palmidens</i>	11.5	2.442	18.18	15.91	Hypsodont	2	-69.49	-49.64	-54.47	M
Toxodontia	Toxd	<i>Pericotoxodon platignathus</i>	203.99	5.318	16.26	11.19	hypselodont	3	-71.13	0	-4.14	L
Basal notoungulate	Henr	<i>Peripantostylops minutus</i>	1.15	0.143	47.27	40.9	brachiodont	0	-59.57	-46.23	-53.62	S
Basal notoungulate	Henr	<i>Peripantostylops orehor</i>	1.61	0.475	51.52	48.53	brachiodont	0	-57.92	-47.01	-53.6	S
Toxodontia	Iso	<i>Periphragis circumflexus</i>	468.65	6.15	39.26	36.1	brachiodont	0	-59.61	-45.63	-52.7	VL
Toxodontia	Iso	<i>Periphragis exauctus</i>	187.98	5.236	39.51	35.3	brachiodont	0	-61.44	-46.2	-53.71	L
Toxodontia	Iso	<i>Periphragis harmeri</i>	103.22	4.637	39.55	35.56	brachiodont	0	-61.5	-45.75	-53.46	L
Toxodontia	Iso	<i>Periphragis palmeri</i>	123.1	4.813	39.79	35.27	brachiodont	0	-61.79	-45.61	-53.42	L
Toxodontia	Iso	<i>Periphragis vicentei</i>	148.53	5.001	33.88	30.94	brachiodont	0	-63.44	-34.93	-42.13	L
Basal notoungulate	B. Noto	<i>Perutherium altiplanense</i>	NA	NA	53.28	50.25	brachiodont	0	-54.92	-17.48	-23.51	NA
Toxodontia	Toxd	<i>Piauhytherium capivarae</i>	1464.07	7.289	0.6	0	hypselodont	3	-42.61	-8.7	-42.61	G
Toxodontia	Toxd	<i>Pisanodon nazari</i>	308.03	5.73	11.12	4.71	hypselodont	3	-61.59	-37.88	-40.61	L
Toxodontia	Toxd	<i>Plesiotoxodon amazonensis</i>	396.09	5.982	12.02	10.17	hypselodont	3	-64.57	-9.7	-13.01	VL
Typotheria	Meso	<i>Plesiotypotherium achirensense</i>	35.91	3.581	14.84	4.7	Hypsodont	2	-64.83	-21.1	-24.22	M
Typotheria	Meso	<i>Plesiotypotherium casirensense</i>	62.99	4.143	5.91	3.04	Hypsodont	2	-64.66	-21.78	-23.54	M

Typotheria	Meso	<i>Plesiotypotherium minus</i>	16.48	2.802	15.66	12.38	Hypsodont	2	-62.91	-23.67	-25.56	M
Toxodontia	Iso	<i>Pleurostylodon modicus</i>	22.9	3.131	46.7	39.02	brachiodont	0	-60.3	-46.5	-54.03	M
Toxodontia	Iso	<i>Pleurostylodon similis</i>	31.28	3.443	47.14	38.77	brachiodont	0	-59.88	-46.18	-53.64	M
Toxodontia	Toxd	<i>Posnanskytherium desaguaderoi</i>	87.18	4.468	6.58	2.46	hypselenodont	3	-65.94	-18.13	-20.04	M
Toxodontia	Toxd	<i>Posnanskytherium inchasense</i>	115.67	4.751	5.61	2.99	hypselenodont	3	-64.57	-19.52	-21.25	L
Toxodontia	Toxd	<i>Proadinothierium leptognathus</i>	80.94	4.394	28.86	21.27	hypsodont	2	-62.94	-44.95	-51.12	M
Toxodontia	Toxd	<i>Proadinothierium muensteri</i>	200.61	5.301	21.21	19.84	hypsodont	2	-65.95	-38.35	-44.04	L
Toxodontia	Toxd	<i>Proadinothierium saltoni</i>	19.43	2.967	28.58	20.82	brachiodont	0	-61.07	-16.94	-23.08	M
Typotheria	Inte	<i>Proargyrohyrax curanderensis</i>	6.96	1.94	34.72	30.7	Hypsodont	2	-60.9	-45.21	-52.78	S
Typotheria	Inte	<i>Progaleopithecus fissurellatus</i>	0.76	-0.269	29.06	21.26	Hypsodont	2	-62.94	-44.95	-51.12	VS
Typotheria	Inte	<i>Progaleopithecus tournoueri</i>	2.27	0.819	29.41	20.39	Hypsodont	2	-63.02	-44.63	-50.85	S
Typotheria	Hege	<i>Prohegetotherium malalhuense</i>	3.3	1.194	28.73	20.92	Hypsodont	2	-64.38	-36.17	-42.4	S
Typotheria	Hege	<i>Prohegetotherium schiaffinoi</i>	4.78	1.564	29.35	20.32	Hypsodont	2	-59.16	-26.15	-32.21	S
Typotheria	Hege	<i>Prohegetotherium sculptum</i>	7.24	1.98	29.39	20.5	Hypsodont	2	-63.74	-43.36	-49.57	S
Typotheria	Hege	<i>Propachyrucos crassus</i>	6.39	1.855	28.95	21.14	Hypsodont	2	-64.38	-36.17	-42.4	S
Typotheria	Hege	<i>Propachyrucos smithwoodwardii</i>	1.43	0.361	28.71	20.82	Hypsodont	2	-62.91	-48.96	-51.59	S
Typotheria	Hege	<i>Prosotherium garzoni</i>	3.52	1.259	29.59	20.61	Hypsodont	2	-63.54	-43.07	-49.28	S
Typotheria	Arhy	<i>Protarchaeohyrax gracilis</i>	6.06	1.802	34.83	29.71	Hypsodont	2	-62.78	-43.33	-50.47	S
Typotheria	Arhy	<i>Protarchaeohyrax intermedium</i>	1.97	0.678	33.87	31.04	Hypsodont	2	-63.44	-34.93	-42.13	S
Typotheria	Arhy	<i>Protarchaeohyrax minor</i>	1.7	0.531	34.54	29.66	Hypsodont	2	-62.99	-45.01	-52.25	S
Typotheria	Inte	<i>Protypotherium antiquum</i>	8.9	2.186	9.01	5.29	Hypsodont	2	-58.44	-31.26	-33.69	S
Typotheria	Inte	<i>Protypotherium attenuatum</i>	2.85	1.047	18.32	15.17	Hypsodont	2	-67.08	-50.22	-55.04	S
Typotheria	Inte	<i>Protypotherium australe</i>	11.02	2.4	18.34	13.64	Hypsodont	2	-67.32	-50.12	-54.71	M
Typotheria	Inte	<i>Protypotherium colloncurensis</i>	8.62	2.154	16.36	9.14	Hypsodont	2	-65.85	-38.97	-42.45	S
Typotheria	Inte	<i>Protypotherium concepcionensis</i>	6.12	1.811	12.31	9.66	Hypsodont	2	-69.38	-39.84	-41.27	S
Typotheria	Inte	<i>Protypotherium diastematum</i>	7.58	2.025	18.17	15.68	Hypsodont	2	-65.51	-53.36	-55.4	S
Typotheria	Inte	<i>Protypotherium distinctum</i>	7.03	1.951	10.43	8.24	Hypsodont	2	-64.39	-42.04	-43.47	S
Typotheria	Inte	<i>Protypotherium endiadys</i>	3.67	1.3	16.13	9.44	Hypsodont	2	-67.25	-39.57	-44.74	S
Typotheria	Inte	<i>Protypotherium minutum</i>	1.52	0.417	12.55	7.67	Hypsodont	2	-63.93	-30.93	-34.05	S
Typotheria	Inte	<i>Protypotherium praerutilum</i>	7.58	2.025	18.27	15.15	Hypsodont	2	-67.14	-50.19	-55.02	S
Typotheria	Inte	<i>Protypotherium sinclairi</i>	7.89	2.066	21.23	19.85	Hypsodont	2	-65.98	-38.37	-44.06	S

Typotheria	Arhy	<i>Pseudhyrax eutrachytheroides</i>	14.22	2.655	39.66	30.57	Hypsodont	2	-61.74	-43.86	-51.13	M
Typotheria	Arhy	<i>Pseudhyrax strangulatus</i>	6.97	1.941	39.73	30.52	Hypsodont	2	-61.93	-44.19	-51.51	S
Typotheria	Meso	<i>Pseudotypotherium insigne</i>	154.63	5.041	6.24	4.08	Hypsodont	2	-63.22	-35.41	-37.42	L
Typotheria	Meso	<i>Pseudotypotherium maendrum</i>	87.43	4.471	6.07	4.01	Hypsodont	2	-60.78	-38.8	-40.79	M
Typotheria	Meso	<i>Pseudotypotherium subinsigne</i>	106.81	4.671	9.48	4.7	Hypsodont	2	-62.56	-36.17	-38.59	L
Toxodontia	Noth	<i>Puelia coarctatus</i>	5.81	1.759	38.64	35.93	brachiodont	0	-61.69	-46.05	-53.7	S
Toxodontia	Noth	<i>Puelia plicata</i>	5.83	1.763	39.52	30.66	brachiodont	0	-60.09	-49.58	-53.27	S
Toxodontia	Noth	<i>Puelia sigma</i>	6.02	1.795	39.75	35.39	brachiodont	0	-61.16	-46.04	-53.59	S
Typotheria	Arhy	<i>Punahyrax bondesioi</i>	3.08	1.126	39.76	35.64	brachiodont	0	-57.82	-25.86	-33.5	S
Typotheria	Inte	<i>Punapithecus minor</i>	0.36	-1.021	39.69	35.17	brachiodont	0	-57.82	-25.86	-33.32	VS
Toxodontia	Noth	<i>Rhynchippus brasiliensis</i>	60.02	4.095	29.23	20.58	hypsodont	2	-50.19	-20.4	-26.05	M
Toxodontia	Noth	<i>Rhynchippus equinus</i>	80.02	4.382	29.56	20.58	hypsodont	2	-62.66	-39.91	-45.93	M
Toxodontia	Noth	<i>Rhynchippus pumilus</i>	9	2.198	29.2	20.59	hypsodont	2	-62.63	-33.51	-39.64	S
Toxodontia	Iso	<i>Rhyphodon angusticephalus</i>	37.09	3.613	39.4	36.63	brachiodont	0	-59.61	-45.63	-52.7	M
Toxodontia	Iso	<i>Rhyphodon lankesteri</i>	43.38	3.77	39.56	35.46	brachiodont	0	-61.83	-45.7	-53.51	M
Toxodontia	Noth	<i>Rosendo pascuali</i>	19.21	2.955	34.54	30.67	brachiodont	0	-62.81	-43.55	-51.18	M
Typotheria	Meso	<i>Rusconitherium mendocense</i>	12.96	2.562	18.51	14.47	Hypsodont	2	-65.55	-32.29	-36.88	M
Typotheria	Hege	<i>Sallatherium altiplanense</i>	8.31	2.118	29.3	20.48	Hypsodont	2	-60.76	-16.87	-22.99	S
Typotheria	Inte	<i>Santiagorothia chiliensis</i>	6.82	1.92	34.48	30.72	Hypsodont	2	-62.79	-43.36	-51.05	S
Basal notoungulate	B. Noto	<i>Satshatemnus bonapartei</i>	2.33	0.846	53.41	50.51	brachiodont	0	-50.85	-29.04	-34.8	S
Toxodontia	Leo	<i>Scarrittia barranquensis</i>	235.14	5.46	29.51	20.67	mesodont	1	-63.71	-45.43	-51.54	L
Toxodontia	Leo	<i>Scarrittia canquelensis</i>	264.31	5.577	29.4	20.62	mesodont	1	-63.87	-44.85	-51.04	L
Toxodontia	Leo	<i>Scarrittia robusta</i>	336.62	5.819	28.22	20.76	mesodont	1	-50.73	-34.69	-40.16	VL
Basal notoungulate	Henr	<i>Simpsonotus major</i>	23.16	3.142	53.87	48.93	brachiodont	0	-50.3	-25.66	-31.49	M
Basal notoungulate	Henr	<i>Simpsonotus praecursor</i>	11.58	2.449	53.21	49.68	brachiodont	0	-50.3	-25.66	-31.49	M
Toxodontia	Toxd	<i>Stenotephanos plicidens</i>	217.28	5.381	10.07	4.41	hypselenodont	3	-58.44	-31.26	-30.88	L
Typotheria	Oldf	<i>Suniodon catamarcensis</i>	2.33	0.846	39.26	35.9	brachiodont	0	-58.29	-26.61	-34.27	S
Toxodontia	Leo	<i>Taubatherium paulacoutoi</i>	208.87	5.342	29.35	20.48	mesodont	1	-39.3	-23.86	-28.77	L
Typotheria	Arpi	<i>Teratopithecus elpidophoros</i>	1.35	0.299	53.42	41.92	brachiodont	0	-58.72	-45.75	-52.62	S
Toxodontia	Leo	<i>Termastherium flacoensis</i>	52.55	3.962	33.97	31.1	brachiodont	0	-63.44	-34.93	-42.64	M
Toxodontia	Iso	<i>Thomashuxleya externa</i>	90.84	4.509	47.07	38.75	brachiodont	0	-59.76	-46.33	-53.81	M

Toxodontia	Iso	<i>Thomashuxleya rostrata</i>	153.46	5.033	47.5	38.57	brachiodont	0	-60.51	-46.47	-54	L
Toxodontia	Toxd	<i>Toxodon burmeisteri</i>	750	6.62	0.54	0	hypselodont	3	-57.13	-34.07	-34.07	VL
Toxodontia	Toxd	<i>Toxodon chapalmalensis</i>	750	6.62	6.66	2.22	hypselodont	3	-59.55	-38.52	-40.31	VL
Toxodontia	Toxd	<i>Toxodon gracilis</i>	262.66	5.571	0.64	0	hypselodont	3	-62.49	-29.83	-29.83	L
Toxodontia	Toxd	<i>Toxodon platensis</i>	1322.53	7.187	2.7	0	hypselodont	3	-59.12	-30.69	-32.6	G
Typotheria	Meso	<i>Trachytherus alloxus</i>	94.62	4.55	29.25	20.48	Hypsodont	2	-61.08	-16.94	-23.08	M
Typotheria	Meso	<i>Trachytherus ramirezi</i>	45.54	3.819	28.86	20.9	Hypsodont	2	-64.45	-16.8	-23.04	M
Typotheria	Meso	<i>Trachytherus spegazzinianus</i>	116.61	4.759	29.34	20.57	Hypsodont	2	-62.52	-39.33	-45.49	L
Typotheria	Meso	<i>Trachytherus subandinus</i>	45.36	3.815	28.49	21.07	Hypsodont	2	-59.47	-16.5	-22.59	M
Typotheria	Inte	<i>Transpithecus obtentus</i>	1.94	0.664	42.73	35.87	brachiodont	0	-59.98	-46.52	-53.95	S
Typotheria	Hege	<i>Tremacyllus impressus</i>	0.92	-0.08	10.74	1.61	hypselodont	3	-62.78	-35.84	-38.04	VS
Toxodontia	Toxd	<i>Trigodon gaudryi</i>	760.76	6.634	6.44	3.76	hypselodont	3	-60.29	-38.04	-40.04	VL
Toxodontia	Toxd	<i>Trigodonops lopesi</i>	57.2	4.047	9.49	0	hypselodont	3	-51.32	-9.39	-11.56	M
Toxodontia	Homa	<i>Trigonolophodon elegans</i>	135.43	4.908	34.06	31.2	brachiodont	0	-63.44	-34.93	-42.64	L
Toxodontia	Noth	<i>Trimerostephanos coalitus</i>	26.76	3.287	39.93	35.28	brachiodont	0	-62.09	-45.29	-53.28	M
Typotheria	Oldf	<i>Tsamnichoria cabrerai</i>	6.2	1.824	38.98	35.99	brachiodont	0	-62.04	-46.13	-53.79	S
Typotheria	Meso	<i>Typotheriopsis chasiccoensis</i>	51.57	3.943	11.01	8.03	Hypsodont	2	-62.69	-37.55	-40.7	M
Typotheria	Meso	<i>Typotheriopsis internum</i>	155.25	5.045	5.56	2.84	Hypsodont	2	-66.26	-27.64	-28.64	L
Typotheria	Oldf	<i>Ultrapihcus rutilans</i>	7.52	2.018	42.68	38.26	brachiodont	0	-60.44	-46.49	-54.17	S
Typotheria	B. Typo	<i>Xenostephanus chiotii</i>	4.23	1.442	45.69	39.71	brachiodont	0	-59.71	-33.52	-41.31	S
Toxodontia	Toxd	<i>Xotodon ambrosetti</i>	89.83	4.498	6.38	4.14	hypselodont	3	-60.8	-38.78	-40.77	M
Toxodontia	Toxd	<i>Xotodon caravela</i>	149.91	5.01	11.47	3.79	hypselodont	3	-63.77	-27	-29.81	L
Toxodontia	Toxd	<i>Xotodon doellojuradoi</i>	108.5	4.687	8.89	5.11	hypselodont	3	-58.44	-31.26	-33.69	L
Toxodontia	Toxd	<i>Xotodon foricurvatus</i>	134.7	4.903	9.88	3.53	hypselodont	3	-59.62	-35.02	-37.43	L
Toxodontia	Toxd	<i>Xotodon maimarensis</i>	103.87	4.643	6.06	3.98	hypselodont	3	-64.27	-23.39	-25.34	L

Table S7. Results of the evolutionary modes of BM performed with the package PaleoTs in different notoungulates clades.

All notoungulates (n=51)						
Model	logL	K	AICc	dAICc	Akaike.wt	Adequacy test
GRW	-15.07247	3	36.66	13.21	0.00	Passed
URW	-17.72	2	39.69	16.25	0	Failed
Stasis	-58.67	2	121.60	98.15	0	Failed
OU	-14.36	4	37.59	14.14	0.00	Failed
Punc-1	-22.86	4	54.59	31.15	0	-
Punc-2	-11.54	6	36.99	13.55	0.00	-
Punc-3	-3.77	8	26.97	3.53	0.10	-
Punc-4	1.03	10	23.44	0.00	0.61	-
Punc-5	3.63	12	24.96	1.51	0.29	-
GRW-Stasis	-11.95	6	37.81	14.37	0	-
URW-Stasis	-13.44	5	38.22	14.78	0	-
Stasis-GRW	-14.79	5	40.91	17.47	0	-
Stasis-URW	-17.04	4	42.96	19.51	0	-
Typotheria (n=54)						
GRW	1.2	3	4.07	0	0.57	Failed
URW	-4.6	2	13.43	9.35	0.01	Failed
Stasis	-19.81	2	★43.86★	★39.79	0	Failed
OU	1.38	4	★6.06★	1.99	0.21	Failed
Punc-1	0.21	4	8.4	4.33	0.07	-
Punc-2	2.43	6	8.93	4.85	0.05	-
Punc-3	3.13	8	12.94	8.87	0.01	-
Punc-4	3.49	10	18.14	14.06	0	-
Punc-5	3.73	12	24.16	20.08	0	-
GRW-Stasis	1.56	6	10.66	6.59	0.02	-
URW-Stasis	0.21	5	10.83	6.76	0.02	-
Stasis-GRW	1.04	5	9.16	5.09	0.05	-
Stasis-URW	-3.35	4	15.51	11.44	0	-
Intertheriidae (n=37)						
GRW	0.57	3	5.59	0	0.55	Failed
URW	-4.87	2	14.09	8.5	0.008	Failed
Stasis	-20.03	2	44.42	38.83	0	Failed
OU	0.99	4	7.28	1.69	0.24	Failed
Punc-1	-4.47	4	18.19	12.6	0	-
Punc-2	3.13	6	8.55	2.96	0.13	-
Punc-3	3.58	8	13.98	8.38	0.008	-
Punc-4	3.59	10	21.29	15.7	0	-
Punc-5	1.94	12	33.13	27.54	0	-
GRW-Stasis	1.78	6	11.23	5.64	0.03	-
URW-Stasis	-1.99	5	15.91	10.32	0	-
Stasis-GRW	0.36	5	11.22	5.63	0.03	-
Hegetotheriidae (n=27)						
GRW	-2.68	3	12.33	3.86	0.07	Failed

URW	-5.33	2	15.11	6.64	0.02	Failed
Stasis	-8.46	2	21.38	12.9	0	Failed
OU	-2.69	4	15.05	6.58	0.02	Failed
Punc-1	0.6	4	8.47	0	0.5	-
Punc-2	0.98	6	13.85	5.38	0.03	-
Punc-3	1.56	8	20.07	11.6	0	-
GRW-Stasis	0.86	6	14.1	5.63	0.03	-
URW-Stasis	0.6	5	11.42	2.94	0.11	-
Stasis-GRW	0.92	5	10.76	2.29	0.16	-
Stasis-URW	-1.52	4	12.71	4.23	0.06	-
Mesotheriidae (n=27)						
GRW	-5.94	3	18.92	9.04	0.01	Failed
URW	-5.96	2	16.42	6.54	0.03	Failed
Stasis	-24.25	2	53	43.13	0	Failed
OU	-5.52	4	20.85	10.98	0	Failed
Punc-1	-20.75	4	51.32	41.45	0	-
Punc-2	3.16	6	9.87	0	0.81	-
Punc-3	-5.35	8	34.7	24.83	0	-
GRW-Stasis	-3.64	6	23.48	13.61	0	-
URW-Stasis	-3.72	5	20.29	10.41	0	-
Stasis-GRW	-1.88	5	16.62	6.75	0.03	-
Stasis-URW	-1.95	4	13.71	3.83	0.12	-
Archaeohyracidae (n = 23)						
GRW	-6.6	3	20.47	4.25	0.08	Failed
URW	-8.95	2	22.5	6.29	0.03	Failed
Stasis	-11.4	2	27.4	11.19	0	Failed
OU	-6.62	4	23.45	7.24	0.02	Failed
Punc-1	-3	4	16.21	0	0.66	-
Punc-2	-2.93	6	23.11	6.9	0.02	-
GRW-Stasis	-2.92	6	23.09	6.87	0.02	-
URW-Stasis	-3	5	19.52	3.31	0.13	-
Stasis-GRW	-4.4	5	22.34	6.12	0.03	-
Stasis-URW	-6.66	4	23.53	7.32	0.02	-
Toxodontia (n=49)						
GRW	-13	3	32.54	13.49	0	Passed
URW	-16.4	2	37.05	18	0	Failed
Stasis	-70.46	2	145.18	126.14	0	Failed
OU	-13	4	34.91	15.87	0	Failed
Punc-1	-33.17	4	75.25	56.21	0	-
Punc-2	-5.64	6	25.28	6.24	0.02	-
Punc-3	0	8	19.6	0.55	0.4	-
Punc-4	3.37	10	19.05	0	0.53	-
Punc-5	4.42	12	23.82	4.77	0.05	-
GRW-Stasis	-10.02	6	34.05	15	0	-
URW-Stasis	-11.72	5	34.84	15.79	0	-
Stasis-GRW	-9.58	5	30.56	11.51	0	-

Stasis-URW	-15.48	4	39.86	20.81	0	-
Toxodontidae (n=29)						
GRW	-15.98	3	38.92	2.38	0.1	Failed
URW	-17.84	2	40.14	3.6	0.06	Failed
Stasis	-30.66	2	65.78	29.24	0	Failed
OU	-13.6	4	36.86	0.32	0.28	Failed
Punc-1	-14.67	4	39	2.46	0.1	-
Punc-2	-11.8	6	39.42	2.89	0.08	-
Punc-3	-9.46	8	42.11	5.57	0.02	-
GRW-Stasis	-10.36	6	36.54	0	0.33	-
URW-Stasis	-14.67	5	41.94	5.4	0.02	-
Stasis-GRW	-16.02	5	44.64	8.11	0.01	-
Stasis-URW	-17.51	4	44.68	8.15	0.01	-
Notohippidae (n=31)						
GRW	-9.88	3	26.65	18.19	0	Passed
URW	-10.95	2	26.34	17.88	0	Failed
Stasis	-32.16	2	68.76	60.3	0	Failed
OU	-9.63	4	28.8	20.34	0	Failed
Punc-1	0.54	4	8.46	0	0.72	-
Punc-2	1	6	13.5	5.04	0.06	-
Punc-3	1.17	8	20.21	11.76	0	-
Punc-4	1.22	10	28.55	20.1	0	-
GRW-Stasis	0.77	6	13.96	5.5	0.05	-
URW-Stasis	0.54	5	11.32	2.86	0.17	-
Stasis-GRW	-7.32	5	27.03	18.58	0	-
Stasis-URW	-8.43	4	26.4	17.94	0	-

Table S8. Results of the evolutionary modes of HI performed with the package PaleotTs in different notoungulates clades.

All notoungulates (n=51)						
Model	logL	K	AICc	dAICc	Akaike.wt	Adequacy test
GRW	30.20	3	-53.90	6.53	0.016	Pass
URW	22.91	2	-41.56	18.86	0	Failed
Stasis	-75.90	2	156.04	216.47	0	Failed
OU	30.35	4	-51.83	8.59	0.01	Failed
Punc-1	-33.01	4	74.89	135.32	0	-
Punc-2	14.16	6	-14.41	46.01	0	-
Punc-3	33.08	8	-46.72	13.70	0	-
Punc-4	42.84	10	-60.19	0.24	0.37	-
Punc-5	46.32	12	-60.42	0	0.42	-
GRW-Stasis	36.35	6	-58.79	1.63	0.18	-
URW-Stasis	31.44	5	-51.55	8.87	0.01	-
Stasis-GRW	25.81	5	-40.28	20.15	0	-
Stasis-URW	20.48	4	-32.09	28.33	0	-
Typotheria (n=50)						
GRW	12.69	3.00	-18.85	27.80	0	Passed
URW	6.38	2.00	-8.50	38.15	0	Failed
Stasis	-72.63	2.00	149.52	196.18	0	Failed
OU	12.68	4.00	-16.47	30.19	0	Failed
Punc-1	3.71	4.00	1.46	48.12	0	-
Punc-2	23.75	6.00	-33.55	13.10	0	-
Punc-3	30.30	8.00	-41.09	5.57	0.04	-
Punc-4	36.15	10.00	-46.65	0.00	0.58	-
Punc-5	37.54	12.00	-42.65	4.00	0.08	-
GRW-Stasis	29.66	6.00	-45.37	1.29	0	-
URW-Stasis	23.71	5.00	-36.06	10.60	0	-
Stasis-GRW	15.44	5.00	-19.51	27.14	0.00	-
Stasis-URW	12.67	4	-16.46	30.20	0	-
Interatheriidae (n=33)						
GRW	-4.32	3	15.47	22.34	0	Passed
URW	-5.65	2	15.70	22.57	0	Failed
Stasis	-44.78	2	93.95	100.82	0	Failed
OU	-4.33	4	18.08	24.95	0	Failed
Punc-1	-11.82	4	33.07	39.94	0	-
Punc-2	-9.26	6	33.74	40.61	0	-
GRW-Stasis	9.88	6	-4.53	2.34	0.23	-
URW-Stasis	9.55	5	-6.87	0	0.73	-
Stasis-GRW	6.25	5	-0.28	6.59	0.03	-
Stasis-URW	4.26	4	0.90	7.77	0.02	-
Hegetotheriidae (n=27)						
GRW	16.55	3	-26.14	33.68	0	Passed
URW	15.18	2	-25.90	33.93	0	Failed
Stasis	-15.75	2	35.96	95.79	0	Failed
OU	16.56	4	-23.45	36.37	0	Failed

Punc-1	34.74	4	-59.82	0	0.76	-
Punc-2	34.74	6	-53.67	6.15	0.04	-
Punc-3	34.74	8	-46.29	13.53	0.00	-
GRW-Stasis	34.74	6	-53.67	6.15	0.04	-
URW-Stasis	34.74	5	-56.88	2.94	0.17	-
Stasis-GRW	24.57	5	-36.52	23.30	0	-
Stasis-URW	23.15	4	-36.64	23.18	0	-
Archaeohyrcidae (n = 23)						
GRW	2.32	3	2.62	0	0.46	Failed
URW	-0.69	2	5.97	3.36	0.09	Failed
Stasis	-9.47	2	23.54	20.92	0	Failed
OU	2.64	4	4.94	2.32	0.14	Failed
Punc-1	1.93	4	6.35	3.73	0.07	-
Punc-2	6.01	6	5.24	2.62	0.12	-
GRW-Stasis	5.33	6	6.59	3.98	0.06	-
URW-Stasis	2.12	5	9.29	6.67	0.02	-
Stasis-GRW	2.26	5	9.02	6.40	0.02	-
Stasis-URW	0.42	4	9.38	6.76	0.02	-
Toxodontia (n=49)						
GRW	11.99	3	-17.45	18.72	0	Pass
URW	6.43	2	-8.61	27.57	0	Failed
Stasis	-77.53	2	159.31	195.48	0	Failed
OU	12.34	4	-15.77	20.40	0	Failed
Punc-1	-36.15	4	81.21	117.38	0	-
Punc-2	1.40	6	11.21	47.38	0.00	-
Punc-3	27.89	8	-36.17	0	0.79	-
Punc-4	23.56	10	-38.55	2.38	0.09	-
Punc-5	30.15	12	-40.56	4.39	0.02	-
GRW-Stasis	22.80	6	-31.59	4.58	0.09	-
URW-Stasis	18.99	5	-26.58	9.59	0.01	-
Stasis-GRW	15.80	5	-20.20	15.97	0	-
Stasis-URW	10.33	4	-11.75	24.42	0	-
Toxodontidae (n=29)						
GRW	11.09	3	-15.22	17.68	0	Pass
URW	7.17	2	-9.88	23.02	0	Failed
Stasis	-35.17	2	74.80	107.69	0	Failed
OU	13.07	4	-16.48	16.41	0	Failed
Punc-1	-2.04	4	13.75	46.64	0	-
Punc-2	24.36	6	-32.89	0	0.58	-
Punc-3	24.36	8	-25.51	7.38	0.01	-
GRW-Stasis	23.80	6	-31.78	1.11	0.33	-
URW-Stasis	20.74	5	-28.86	4.03	0.08	-
Stasis-GRW	12.58	5	-12.55	20.34	0	-
Stasis-URW	8.92	4	-8.17	24.73	0	-
Notohippidae (n=31)						
GRW	-3.33	3	13.54	29.01	0	Failed
URW	-5.55	2	15.52	30.98	0	Failed
Stasis	-39.41	2	83.26	98.72	0	Failed

OU	-3.03	4	15.59	31.05	0	Failed
Punc-1	12.50	4	-15.46	0	0.58	-
Punc-2	14.61	6	-13.73	1.74	0.25	-
GRW-Stasis	12.61	6	-9.72	5.74	0.03	-
URW-Stasis	12.50	5	-12.60	2.86	0.14	-
Stasis-GRW	2.69	5	7.03	22.49	0	-
Stasis-URW	1.09	4	7.35	22.82	0	-



Table S9. Data used for GLS and model selection analyses (based on SSA taxa).

Time averaged predictive variables				BM			HI		
Age	P_open	O18	rLAI	BM_Noto	BM_Tx	BM_Ty	HI_Noto	HI_Tx	HI_Ty
0	90.08	4.06	NA	4.215	6.459	1.971	2.833	3.000	2.667
1	87.98	3.78	NA	2.604	5.853	1.459	2.800	3.000	2.750
2	98.73	3.55	NA	3.541	5.247	2.176	2.778	3.000	2.600
3	86.67	3.13	NA	4.098	5.054	2.504	2.813	3.000	2.500
4	59.59	3.04	NA	4.221	5.193	2.861	2.750	3.000	2.400
5	41.29	2.96	NA	3.959	5.301	2.450	2.765	3.000	2.500
6	44.68	2.85	NA	3.846	5.434	2.144	2.793	3.000	2.571
7	59.56	2.79	NA	3.359	5.588	1.688	2.762	3.000	2.583
8	69.78	2.84	NA	3.699	5.805	1.873	2.714	2.923	2.533
9	70.85	2.73	NA	3.307	5.906	1.878	2.660	2.909	2.512
10	68.84	2.60	1.867	3.313	5.864	1.855	2.606	2.875	2.491
11	61.31	2.54	2.025	2.728	5.861	1.945	2.552	3.000	2.470
12	25.18	2.43	2.178	2.364	5.402	2.016	2.498	2.750	2.450
13	14.42	2.22	2.283	2.685	4.943	2.039	2.444	2.500	2.429
14	6.68	1.79	3.056	2.798	4.717	2.078	2.409	2.333	2.438
15	9.20	1.74	2.992	2.573	4.921	1.821	2.333	2.125	2.400
16	3.20	1.69	2.104	2.566	4.921	1.781	2.344	2.125	2.417
17	7.15	1.93	1.427	2.827	4.759	1.690	2.259	2.000	2.412
18	2.70	1.93	0.810	2.726	4.709	1.611	2.320	2.111	2.438
19	18.89	2.03	1.079	3.823	4.564	1.971	2.000	1.800	2.500
20	13.99	2.10	1.998	3.336	4.659	1.840	1.714	1.269	2.217
21	20.36	2.00	0.376	3.334	4.595	1.793	1.683	1.273	2.185
22	15.86	1.85	0.610	3.441	4.610	1.867	1.630	1.226	2.174
23	16.67	2.00	1.728	3.369	4.560	1.867	1.635	1.207	2.174
24	17.25	1.64	1.837	3.369	4.560	1.867	1.635	1.207	2.174
25	17.50	1.90	1.719	3.369	4.560	1.867	1.635	1.207	2.174
26	2.60	2.68	1.650	3.369	4.560	1.867	1.635	1.207	2.174
27	0.45	2.75	1.593	3.369	4.560	1.867	1.635	1.207	2.174
28	0.3	2.64	1.528	3.369	4.560	1.867	1.635	1.207	2.174
29	0.15	2.66	1.444	3.141	4.677	1.766	1.750	1.235	2.211
30	0	2.63	1.331	1.978	3.240	1.462	1.286	0.000	1.800
31	1.07	2.50	1.178	2.391	3.540	1.640	1.200	0.286	1.833
32	2.12	2.58	0.981	2.391	3.540	1.640	1.200	0.286	1.833
33	3.2	2.46	0.741	2.391	3.540	1.640	1.200	0.286	1.833
34	0.44	1.77	0.426	2.084	2.987	1.542	1.214	0.250	1.778
35	1.05	1.80	0.570	2.372	3.415	1.136	0.350	0.100	0.667
36	4.4	1.77	1.218	2.582	3.743	1.133	0.241	0.071	0.462
37	8.0	1.62	1.780	2.571	3.743	1.381	0.219	0.071	0.375
38	7.6	1.49	0.704	2.557	3.587	1.464	0.191	0.045	0.381
39	6.6	1.35	2.062	2.316	3.379	1.337	0.150	0.038	0.320
40	0.4	1.24	0.879	1.986	2.847	1.420	0.085	0.000	0.190
41	0.4	1.00	1.172	1.975	2.901	1.331	0.077	0.000	0.174
42	0.4	0.97	1.460	1.912	2.934	1.331	0.080	0.000	0.174
43	0	0.95	2.030	2.003	3.061	1.321	0.047	0.000	0.118
44	0	1.05	1.802	2.014	3.061	1.261	0.000	0.000	0.000

45	0	0.86	1.799	2.033	3.061	1.261	0.000	0.000	0.000
46	0	0.58	1.970	2.091	3.134	1.220	0.000	0.000	0.000
47	0	0.32	2.191	2.178	3.072	1.571	0.000	0.000	0.000
48	0	0.13	2.439	1.778	1.769	1.769	0.118	0.000	0.286
49	0	0.09	2.694	1.636	1.226	1.226	0.095	0.000	0.286

References for the Supplementary material

- Ameghino, F., 1887. Observaciones generales sobre el orden de mamíferos estinguidos sudamericanos llamados toxodontes (Toxodontia) y sinopsis de los géneros y especies hasta ahora conocidos. *Anales del Museo de La Plata* 1, 1–66.
- Anaya, F., MacFadden, B. J., 1995. Pliocene mammals from Inchasi, Bolivia: The endemic fauna just before the Great American Interchange. *Bulletin of the Florida Museum of Natural History* 39(3), 87–140.
- Armella, M.A., García-López, D.A., Dominguez, L., 2018. A new species of *Xotodon* (Notoungulata, Toxodontidae) from northwestern Argentina. *Journal of Vertebrate Paleontology*, 38(1), e1425882.
- Bauzá, N., Gelfo, J.N., López, G. M., 2019. Early steps in the radiation of notoungulate mammals in southern South America: A new henricosborniid from the Eocene of Patagonia. *Acta Palaeontologica Polonica* 64(3), 597–603.
- Billet, G., De Muizon, C., Mamani Quispe, B., 2008. Late Oligocene mesotheriids (Mammalia, Notoungulata) from Salla and Lacayani (Bolivia): implications for basal mesotheriid phylogeny and distribution. *Zoological Journal of the Linnean Society* 152(1), 153–200.
- Billet, G., Patterson, B., De Muizon, C., 2009. Craniodental anatomy of late Oligocene archaeohyracids (Notoungulata, Mammalia) from Bolivia and Argentina and new phylogenetic hypotheses. *Zoological Journal of the Linnean Society* 155(2), 458–509.
- Bond, M., López, G., 1993. El primer Nothohippidae (Mammalia, Notoungulata) de la Formación Lumbrera (Grupo Salta) del Noroeste argentino. *Consideraciones sobre la sistemática de la familia Notohippidae*. *Ameghiniana* 30(1), 59–68.
- Bond, M., López, G., 1995. Los mamíferos de la Formación Casa Grande (Eoceno) de la provincia de Jujuy. *Argentina*. *Ameghiniana* 32(3), 301–309.
- Bradham, J., Flynn, J.J., Croft, D.A., Wyss, A.R., 2015. New notoungulates (Notostylopidae and basal toxodontians) from the early Oligocene Tinguiririca Fauna of the Andean Main Range, central Chile. *American Museum Novitates* (3841), 1–24.
- Carrillo, J.D., Amson, E., Jaramillo, C., Sánchez, R., Quiroz, L., Cuartas, C., et al., 2018. The Neogene record of northern South American native ungulates. Washington: Smithsonian Institution Scholarly Press.
- Cassini, G.H., Cerdeño, E., Villafañe, A.L., Muñoz, N.A., 2012. Paleobiology of Santacrucian native ungulates (Meridiungulata: Astrapotheria, Litopterna and Notoungulata), in: Vizcaino, S.F., Kay, R.F., Bargo, M.S. (Eds.), *Early Miocene Paleobiology in Patagonia*. Cambridge University Press, Cambridge, 243–286.

- Castellanos, A., 1942. Los sedimentos prepampeanos del Valle de Nono (Sierra de Córdoba) Argentina. Publicaciones del Instituto de Fisiografía y Geología de la Universidad Nacional del Litoral 4, 1–63.
- Cerdeño, E., Bond, M., 1998. Taxonomic revision and phylogeny of *Paedotherium* and *Tremacyllus* (Pachyrukhinae, Hegetotheriidae, Notoungulata) from the Late Miocene to the Pleistocene of Argentina. *Journal of Vertebrate Paleontology* 18(4), 799–811.
- Cerdeño, E., Reguero, M., 2015. The Hegetotheriidae (Mammalia, Notoungulata) assemblage from the late Oligocene of Mendoza, central-western Argentina. *Journal of Vertebrate Paleontology*, 35(2), e907173.
- Cerdeño, E., Vera, B., 2010. *Mendozahippus fierensis*, gen. et sp. nov., new Notohippidae (Notoungulata) from the Late Oligocene of Mendoza (Argentina). *Journal of Vertebrate Paleontology* 30(6), 1805–1817.
- Cerdeño, E., Vera, B., 2015. A new Leontiniidae (Notoungulata) from the late Oligocene beds of Mendoza Province, Argentina. *Journal of Systematic Palaeontology* 13(11), 943–962.
- Cerdeño, E., Vera, B., Combina, A.M., 2018. A new early Miocene Mesotheriidae (Notoungulata) from the Mariño Formation (Argentina): Taxonomic and biostratigraphic implications. *Journal of South American Earth Sciences* 88, 118–131.
- Chaffee, R.G., Simpson, G.G., 1952. The Deseadan vertebrate fauna of the Scarritt Pocket, Patagonia. *Bulletin of the AMNH*, v. 98, 6.
- Croft, D.A., 2007. The middle Miocene (Laventan) Quebrada Honda fauna, southern Bolivia and a description of its notoungulates. *Palaeontology* 50(1), 277–303.
- Croft, D.A., 2016. Horned armadillos and rafting monkeys: the fascinating fossil mammals of South America. Indiana University Press.
- Croft, D.A., Anaya, F., 2020. A new tyotherine notoungulate (Mammalia: Interatheriidae), from the Miocene Nazareno Formation of southern Bolivia. *Ameghiniana* 57(2), 189–208.
- Croft, D.A., Bond, M., Flynn, J.J., Reguero, M., Wyss, A.R., 2003. Large archaeohyracids (Tyotheria, Notoungulata) from central Chile and Patagonia: including a revision of *Archaeotyotherium*. *Fieldiana Geology* 49, 1–38.
- Croft, D.A., Carlini, A.A., Ciancio, M.R., Brandoni, D., Drew, N.E., Engelman, R.K., Anaya, F., 2016. New mammal faunal data from Cerdas, Bolivia, a middle-latitude Neotropical site that chronicles the end of the Middle Miocene Climatic Optimum in South America. *Journal of Vertebrate Paleontology* 36(5), e1163574.
- Croft, D.A., Flynn, J.J., Wyss, A.R., 2004. Notoungulata and Litopterna of the early Miocene Chucal fauna, northern Chile. *Fieldiana Geology* (50), 1–52.
- de Ringelet, A.B., 1957. Estudio del género *Chasicotherium* Cabrera y Kraglievich 1931 (Notoungulata-Homalotheriidae). *Ameghiniana* 1(1–2), 7–14.
- Deraco, M.V., Powell, J.E., Guillermo, L., 2008. First leontiniid (Mammalia, Notoungulata) from the Lumbrera Formation (Santa Barbara Subgroup, Salta Group-Paleogene) of northwestern Argentina. *Ameghiniana* 45(1), 83–91.

- Deraco, V., García-López, D.A., 2016. A new Eocene Toxodontia (Mammalia, Notoungulata) from northwestern Argentina. *Journal of Vertebrate Paleontology*, 36(1), e1037884.
- Elissamburu, A., 2012. Estimation of the body mass in the Notoungulata Order. *Estudios Geológicos*, 68(1), 91–111.
- Fernández García, M. (2018). Descripción dentaria y osteológica, anatomía funcional, paleoneurología, sistemática y filogenia de la familia Mesotheriidae (Mammalia, Notoungulata). Tesis doctoral, Universidad Nacional de Cuyo, Argentina.
- Flynn, J.J., Croft, D.A., Charrier, R., Wyss, A.R., Hérail, G., García, M., 2005. New Mesotheriidae (Mammalia, Notoungulata, Typotheria), geochronology and tectonics of the Caragua area, northernmost Chile. *Journal of South American Earth Sciences* 19(1), 55–74.
- Forasiepi, A.M., Cerdano, E., Bond, M., Schmidt, G.I., Naipauer, M., Straehl, F.R., et al., 2015. New toxodontid (Notoungulata) from the early Miocene of Mendoza, Argentina. *Paläontologische Zeitschrift* 89(3), 611–634.
- García López, D.A., Powell, J.E., 2011. *Griphotherion peiranoi*, gen. et sp. nov., a new Eocene Notoungulata (Mammalia, Meridiungulata) from northwestern Argentina. *Journal of Vertebrate Paleontology*, 31(5), 1117–1130.
- García-López, D.A., Babot, M.J., 2015. Notoungulate faunas of north-western Argentina: new findings of early-diverging forms from the Eocene Geste Formation. *Journal of Systematic Palaeontology* 13(7), 557–579.
- García-López, D.A., Deraco, V., del Papa, C., 2018. Fossil mammals of the Quebrada de los Colorados Formation (late middle Eocene) at the locality of La Poma, Salta Province, Argentina. *Historical Biology*, 30(4), 507–517.
- Garrido, A.C., Turazzini, G.F., Bond, M., Aguirrezabala, G., Forasiepi, A.M., 2014. Estratigrafía, vertebrados fósiles y evolución tectosedimentaria de los depósitos neógenos del Bloque de San Rafael (Mioceno-Plioceno), Mendoza, Argentina. *Acta geológica lilloana*, 26.
- Gomes Rodrigues, H., Herrel, A., Billet, G., 2017. Ontogenetic and life history trait changes associated with convergent ecological specializations in extinct ungulate mammals. *Proc. Natl. Acad. Sci. U. S. A.* 114, 1069–1074.
- Guérin, C., Faure, M., 2013. Un nouveau Toxodontidae (mammalia, Notoungulata) du Pléistocène supérieur du Nordeste du Brésil. *Geodiversitas* 35(1), 155–205.
- Hernández Del Pino, S., 2018. Anatomía y sistemática de los Toxodontidae (Notoungulata) de la Formación Santa Cruz, Mioceno temprano, Argentina. Doctoral dissertation, Universidad Nacional de La Plata.
- Hernández Del Pino, S., Fernández, M., Cerdeño, E., Fernicola, J.C., 2019. Anatomy and Systematics of *Notohippus toxodontoides* Ameghino, 1891 (Mammalia, Notoungulata), from the Miocene of Santa Cruz Province, Argentina. *Journal of Vertebrate Paleontology*, 39(1), e1577870.
- Hernández Del Pino, S., Seoane, F.D., Cerdeño, E., 2017. New postcranial remains of large toxodontian notoungulates from the late Oligocene of Mendoza, Argentina and their systematic implications. *Acta Palaeontologica Polonica* 62(1), 195–210.

- Hitz, R.B., Billet, G., Derryberry, D., 2008. New interatheres (Mammalia, Notoungulata) from the late Oligocene Salla beds of Bolivia. *Journal of Paleontology* 82(3), 447–469.
- Hitz, R.B., Flynn, J.J., Wyss, A.R., 2006. New basal Interatheriidae (Typotheria, Notoungulata, Mammalia) from the Paleogene of central Chile. *American Museum Novitates* 2006(3520), 1–32.
- Hitz, R.B., Reguero, M.A., Wyss, A.R., Flynn, J., 2000. New interatheriines (Interatheriidae, Notoungulata) from the Paleogene of central Chile and southern Argentina. *Fieldiana Geology* 42, 1–26.
- Kramarz, A.G., Bond, M., Arnal, M., 2015. Systematic description of three new mammals (Notoungulata and Rodentia) from the early Miocene Cerro Bandera Formation, northern Patagonia, Argentina. *Ameghiniana* 52(6), 585–597.
- Kramarz, A.G., Paz, E.R., 2013. Un Hegetotheriidae (Mammalia, Notoungulata) basal del Mioceno temprano de Patagonia. *Revista mexicana de ciencias geológicas* 30(1), 186–195.
- Line, S.R.P., Bergqvist, L.P., 2005. Enamel structure of Paleocene mammals of the São José de Itaboraí basin, Brazil 'Condylarthra', Litopterna, Notoungulata, Xenungulata, and Astrapotheria. *Journal of Vertebrate Paleontology* 25(4), 924–928.
- Loomis, F.B., 1914. *The Deseado Formation of Patagonia*. Rumford Press, 1–232.
- López, D.G., Powell, J.E., 2009. Un nuevo Oldfieldthomasiidae (Mammalia: Notoungulata) del Paleógeno de la provincia de Salta, Argentina. *Ameghiniana* 46(1), 153–164.
- López, G., 2002. Redescrición de *Ethegotherium carettei* (Notoungulata, Hegetotheriidae) de la Formación Divisadero Largo de la provincia de Mendoza, Argentina. *Ameghiniana* 39(3), 295–306.
- López, G., Manassero, M., 2008. Revision of the stratigraphic provenance of *Ethegotherium carettei* (Notoungulata, Hegetotheriidae) by sedimentary petrography. *Neues Jahrbuch für Geologie und Paläontologie Abhandlungen*, 248(1), 1–9.
- López, G.M., 1995. *Suniodon catamarcensis* gen. et sp. nov. y otros Oldfieldthomasiidae (Notoungulata, Typotheria) del Eoceno de Antofagasta de la Sierra, Catamarca, Argentina. *Trelew*, *Actas*, 167–172.
- López, G.M., Gelfo, J.N., Bauzá, N., Bond, M., Tejedor, M.F., 2020. Biochron and diversity of Archaeopithecidae (mammalia, notoungulata) and a new genus and species from the Eocene of Patagonia, Argentina. *Ameghiniana* 57(2), 103–116.
- López, G.M., Ribeiro, A.M., Bond, M., 2010. The Notohippidae (Mammalia, Notoungulata) from Gran Barranca: preliminary considerations. In R. H. Madden, A. A. Carlini, M. G. Vucetich, R. F. Kay (eds.), *The Paleontology of Gran Barranca: Evolution and Environmental Change through the Middle Cenozoic of Patagonia*, 143–151.
- Lorente, M., Gelfo, J.N., López, G.M., 2014. Postcranial anatomy of the early notoungulate *Allalmeia atalaensis* from the Eocene of Argentina. *Alcheringa*, 38(3), 398–411.
- Madden, A., 1997. A new Toxodontid Notoungulate. In R. F. Kay, R. H. Madden, J. J. Flynn. (eds.), *Vertebrate Paleontology in the Neotropics. The Miocene fauna of La Venta, Colombia*, 335–354.
- Madden, R. H. (2014). *Hypsodonty in mammals*. Cambridge University Press.

- Marani, H., Dozo, M.T., 2013. El cráneo más completo de *Eurygenium latirostris* Ameghino, 1895 (Mammalia, Notoungulata), un Notohippidae del Deseadense (Oligoceno Tardío) de la Patagonia, Argentina. *Ameghiniana* 45(3), 619–626.
- Martínez, G., Dozo, M.T., Gelfo, J.N., Marani, H., 2016. Cranial morphology of the Late Oligocene Patagonian notohippid *Rhynchippus equinus* Ameghino, 1897 (Mammalia, Notoungulata) with emphases in basicranial and auditory region. *Plos one* 11(5), e0156558.
- Mendoza, M., Janis, C.M., and Palmqvist, P., 2006, Estimating the body mass of extinct ungulates: a study on the use of multiple regression: *Journal of Zoology*, v. 270, p. 90–101.
- Mendonza, R., 2007. Revisão dos toxodontes pleistocênicos brasileiros e considerações sobre *Trigodonops lopesi* (Roxo, 1921) (Notoungulata, Toxodontidae). Master Thesis, Instituto de Biociências da Universidade de São Paulo.
- Nasif, N.L., Musalem, S., Cerdeño, E., 2000. A new toxodont from the Late Miocene of Catamarca, Argentina, and a phylogenetic analysis of the Toxodontidae. *Journal of Vertebrate Paleontology*, 20(3), 591–600.
- Pascual, R., Vucetich, M.G., Fernández, J., 1978. Henricosborniidae de la Formación Mealla (Grupo Salta, Subgrupo Santa Barbara), sus implicancias filogeneticas, taxonomicas y cronologicas. *Ameghiniana* 15(3-4), 366–390.
- Patterson, B., 1935. A new *Argyrohippus* from the Deseado Beds of Patagonia. *Field Museum of Natural History, Geological Series* 6:161–166.
- Paula Couto, C. d., 1954. On a Notostylopid from the Paleocene of Itaborai, Brazil. *American Museum Novitates* 1693, 1–5.
- Paula Couto, C.D., 1952. Fossil mammals from the beginning of the Cenozoic in Brazil. Notoungulata. *American Museum Novitates* 1568:1–16.
- Reguero, M.A., 1998. El problema de las relaciones sistemáticas y filogenéticas de los Typotheria y Hegetotheria (Mammalia, + Notoungulata): análisis de los taxones de Patagonia de la edad-mamífero Deseadense (Oligoceno). Tesis doctoral, Facultad de Ciencias Exactas y Naturales. Universidad de Buenos Aires.
- Reguero, M.A., Candela, A.M., Cassini, G.H., 2010. Hypsodonty and body size in rodent-like notoungulates, in: Madden, R.H., Carlini, A.A., Vucetich, M.G., Kay, R.F. (Eds.), *The Paleontology of Gran Barranca: Evolution and Environmental Change through the Middle Cenozoic of Patagonia*. Cambridge University Press, pp. 358–367.
- Reguero, M.A., Candela, A.M., Galli, C.I., Bonini, R., Voglino, D., 2015. A new hypsodont notoungulate (Hegetotheriidae, Pachyrukhinae) from the late Miocene of the Eastern Cordillera, Salta province, northwest of Argentina. *Andean Geology* 42(1), 56–70.
- Reguero, M.A., Cerdeño, E., 2005. New late Oligocene Hegetotheriidae (Mammalia, Notoungulata) from Salla, Bolivia. *Journal of Vertebrate Paleontology*, 25(3), 674–684.
- Reguero, M.A., Croft, D.C., López, G.M., Alonso, R.N., 2008. Eocene archaeohyracids (Mammalia: Notoungulata: Hegetotheria) from the Puna, northwest Argentina. *Journal of South American Earth Sciences* 26(2), 225–233.

- Reguero, M.A., Dozo, M.T., Cerdeño, E., 2007. A poorly known rodentlike mammal (Pachyrukhinae, Hegetotheriidae, Notoungulata) from the Deseadan (late Oligocene) of Argentina. *Paleoecology, biogeography, and radiation of the rodentlike ungulates in South America. Journal of Paleontology* 81(6), 1301–1307.
- Reguero, M.A., Ubilla, M., Perea, D., 2003. A new species of *Eopachyrucos* (Mammalia, Notoungulata, Interatheriidae) from the late Oligocene of Uruguay. *Journal of Vertebrate Paleontology* 23(2), 445–457.
- Ribeiro, A.M., López, G.M., Bond, M., 2010. The Leontiniidae (Mammalia, Notoungulata) from the Sarmiento Formation at Gran Barranca, Chubut Province, Argentina. In R. H. Madden, A. A. Carlini, M. G. Vucetich, R. F. Kay (eds.), *The Paleontology of Gran Barranca: Evolution and Environmental Change through the Middle Cenozoic of Patagonia*, 170–181.
- Ribeiro, A.M., Madden, R.H., Negri, F.R., Kerber, L., Hsiou, A.S., Rodrigues, A., 2013. Mamíferos fósiles y biocronología en el suroeste de la Amazonia, Brasil. *Publicación Electrónica de la Asociación Paleontológica Argentina* 14(1), 207–221.
- Ribeiro, G.D.C., 2015. Osteología de *Taubatherium paulacoutoi* Soria & Alvarenga, 1989 (Notoungulata, Leontiniidae) e de um novo Pyrotheria: dois mamíferos fósseis da Formação Tremembé, Brasil (SALMA Deseadense-Oligoceno Superior). Doctoral dissertation, Universidade de São Paulo.
- Rincón, A.D., 2011. New remains of *Mixotoxodon larensis* Van Frank 1957 (Mammalia: Notoungulata) from mene de inciarte tar pit, north-western Venezuela. *Interciencia* 36(12), 894–899.
- Rovereto, C., 1914. Los estratos araucanos y sus fósiles. *Anal. Mus. Nac. Hist. Nat. Buenos Aires*, 25, 1–249.
- Schmidt, G.I. 2013. Litopterna y Notoungulata (Mammalia) de la Formación Ituzaingó (Mioceno tardío) de la provincia de Entre Ríos: Sistemática, Bioestratigrafía y Paleobiogeografía. Tesis Doctoral. Facultad de Ciencias Naturales y Museo, Universidad Nacional de La Plata, La Plata, 423 p.
- Scott, W.B., 1912. Palaeontology. II, Toxodonta of the Santa Cruz beds. *Reports of the Princeton University Expeditions to Patagonia 1896–1899* 6, 111–238.
- Seoane, F.D., Cerdeño, E., 2019. Systematic revision of *Hegetotherium* and *Pachyrukhos* (Hegetotheriidae, Notoungulata) and a new phylogenetic analysis of Hegetotheriidae. *Journal of Systematic Palaeontology* 17(19), 1635–1663.
- Shockey, B. J., 1997. Two new notoungulates (Family Notohippidae) from the Salla Beds of Bolivia (Deseadan: Late Oligocene): systematics and functional morphology. *Journal of Vertebrate Paleontology* 17(3), 584–599.
- Shockey, B. J., Billet, G., & Salas-Gismondi, R. (2016). A new species of *Trachytherus* (Notoungulata: Mesotheriidae) from the late Oligocene (Deseadan) of Southern Peru and the middle latitude diversification of early diverging mesotheriids. *Zootaxa* 4111(5), 565–583.
- Shockey, B.J., 2005. New leontiniids (Class Mammalia, Order Notoungulata, Family Leontiniidae) from the Salla Beds of Bolivia (Deseadan, late Oligocene). *Bulletin of the Florida Museum of Natural History* 45(4), 249–260.

- Shockey, B.J., Anaya, F., 2008. Postcranial osteology of mammals from Salla, Bolivia (late Oligocene): form, function, and phylogenetic implications. In *Mammalian Evolutionary Morphology* (pp. 135–157). Springer, Dordrecht.
- Shockey, B.J., Flynn, J.J., Croft, D.A., Gans, P., Wyss, A.R., 2012. New leontiniid Notoungulata (Mammalia) from Chile and Argentina: comparative anatomy, character analysis, and phylogenetic hypotheses. *American Museum Novitates* (3737), 1–64.
- Shockey, B.J., Salas, R., Quispe, R., Flores, A., Sargis, E. J., Acosta, J., Pino, A., Jarica, N.J., Urbina, M., 2006. Discovery of Deseadan fossils in the upper Moquegua Formation (late Oligocene - ?early Miocene) of southern Peru. *Journal of Vertebrate Paleontology* 26(1), 205–208.
- Simpson, G. G., 1967. The beginning of the age of mammals in South America. Part 2, Systematics: Notoungulata, concluded (Typotheria, Hegetotheria, Toxodonta, Notoungulata incertae sedis), Astrapotheria, Trigonostylopoidea, Pyrotheria, Xenungulata, Mammalia incertae sedis. *Bulletin of the AMNH*, 137, 1–260.
- Simpson, G.G., 1932. *Cochilius volvens* from the Colpodon beds of Patagonia. *American Museum novitates*, 577, 1–14.
- Simpson, G.G., 1948. The beginning of the age of mammals in South America. Part I. *Bulletin of the American Museum of Natural History* 91, 1–232.
- Simpson, G.G., 1970. Mammals from the early Cenozoic of Chubut, Argentina. *Breviora* 360, 1–13.
- Simpson, G.G., Minoprio, J.L., Patterson, B., 1962. The mammalian fauna of the Divisadero Largo Formation, Mendoza, Argentina. *Bulletin of the Museum of Comparative Zoology* 127(4), 239–293.
- Sinclair, W.J., 1909. Mammalia of the Santa Cruz beds. I. Typotheria. *Reports of the Princeton University Expeditions to Patagonia 1896–1899* 6, 1–110.
- Solórzano, A., Encinas, A., Bobe, R., Maximiliano, R., Carrasco, G., 2019. The early to late middle Miocene mammalian assemblages from the Cura-Mallín Formation, at Lonquimay, southern Central Andes, Chile (~ 38 S): Biogeographical and paleoenvironmental implications. *Journal of South American Earth Sciences*, 96, 102319.
- Soria, M.F., 1989. El primer Notoungulata de la Formación Rio Loro (Paleoceno medio), Provincia de Tucumán, República Argentina. *Ameghiniana* 26(3–4), 145–151.
- Sostillo, R., Montalvo, C.I., Cerdeño, E., Schmidt, G.I., Folguera, A., Cardonatto, M.C., 2019. Updated knowledge on the Notoungulata (Mammalia) from the late Miocene Cerro Azul Formation, La Pampa Province, Argentina. *Historical Biology*, 1–19.
- Spillman, F., 1949. Contribución a la Paleontología del Peru, Una mamifaua fosil de la región del río Ucayali. *Publicaciones del Museo de Historia Natural “Javier Prado”* 1, 1–39.
- Strömberg, C.A., Dunn, R.E., Madden, R.H., Kohn, M.J., Carlini, A.A., 2013. Decoupling the spread of grasslands from the evolution of grazer-type herbivores in South America. *Nature communications* 4(1), 1–8.
- Ubilla, M., Perea, D., Bond, M., 1994. The deseadan land mammal age in Uruguay and the report of *Scarrittia robusta* nov. sp.(Leontiniidae, Notoungulata) in the Fray Bentos Formation (Oligocene-? Lower miocene). *Geobios* 27(1), 95–102.

- Vera, B., 2012. Revisión del género *Transpithecus* Ameghino, 1901 (Notoungulata, Interatheriidae) del Eoceno medio de Patagonia, Argentina. *Ameghiniana* 49(1), 60–74.
- Vera, B., 2013. Sistemática, filogenia y paleoecología de los Notopithecinae (Interatheriidae, Notoungulata) del Paleógeno de Argentina. Tesis doctoral, Universidad de Buenos Aires, Argentina.
- Vera, B., 2017. Patagonian Eocene Archaeopithecidae Ameghino, 1897 (Notoungulata): systematic revision, phylogeny and biostratigraphy. *Journal of Paleontology* 91(6), 1272–1295.
- Vera, B., 2019. A new species and the record of *Hemihegetotherium* (Notoungulata, Hegetotheriidae) in the Middle to Late Miocene of Patagonia, Argentina. *Journal of South American Earth Sciences* 93, 23–35.
- Vera, B., Cerdano, E., 2014. Systematic revision of *Antepithecus brachystephanus* Ameghino, 1901, and dental eruption sequence in Eocene “notopithecines”(Notoungulata) from Patagonia. *Geobios* 47(3), 165–181.
- Vera, B., Cerdeño, E., Reguero, M., 2017. The Interatheriinae from the late Oligocene of Mendoza (Argentina), with comments on some Deseadan Interatheriidae. *Historical Biology* 29(5), 607–626.
- Vera, B., González Ruiz, L., Novo, N., Martín, G., Reato, A., Tejedor, M.F., 2019. The Interatheriinae (Mammalia, Notoungulata) of the Friasian *sensu stricto* and Mayoan (middle to late Miocene), and the fossils from Cerro Zeballos, Patagonia, Argentina. *Journal of Systematic Palaeontology* 17(13), 1143–1163.
- Villarroel C., Colwell, J., 1997. New Leontiniid Notoungulate. In R. F. Kay, R. H. Madden, J. J. Flynn. (eds.), *Vertebrate Paleontology in the Neotropics. The Miocene fauna of La Venta, Colombia*, 303–318.
- Villarroel, C., Sempéré, T., Marshall, L.G., 1994. Un nuevo *Trachytherus* (Notoungulata, Mammalia) en el Terciario de la faja subandina norte de Bolivia. *Memorias del XI Congreso Geológico de Bolivia*, 28–32.
- Vucetich, M. G., 1980. Un nuevo Notostylopidae (Mammalia, Notoungulata) proveniente de la Formación Lumbrera (Grupo Salta) del noroeste argentino. *Ameghiniana* 17:363–372.
- Vucetich, M.G., Bond, M., 1982. Los primeros Isotemnidae (Mammalia, Notoungulata) registrados en la Formación Lumbrera (Grupo Salta), del noroeste argentino. *Ameghiniana* 19(1–2), 7–18.
- Wilson, L.A., Sánchez-Villagra, M.R., Madden, R.H., Kay, R.F., 2012. Testing a developmental model in the fossil record: molar proportions in South American ungulates. *Paleobiology* 38(2), 308–321.
- Wyss, A.R., Flynn, J.J., Croft, D.A., 2018. New Paleogene Notohippids and Leontiniids (Toxodontia; Notoungulata; Mammalia) from the Early Oligocene Tinguiririca Fauna of the Andean Main Range, Central Chile. *American Museum Novitates* 2018(3903), 1–42.